



The University of
Nottingham

UNITED KINGDOM · CHINA · MALAYSIA

Clare, Constance E (2021) One-carbon metabolism and epigenetic programming of mammalian development. PhD thesis, University of Nottingham.

Access from the University of Nottingham repository:

<http://eprints.nottingham.ac.uk/64521/1/Constance%20Emily%20Clare%20PhD%20Thesis%20submission.pdf>

Copyright and reuse:

The Nottingham ePrints service makes this work by researchers of the University of Nottingham available open access under the following conditions.

This article is made available under the Creative Commons Attribution licence and may be reused according to the conditions of the licence. For more details see: <http://creativecommons.org/licenses/by/2.5/>

For more information, please contact eprints@nottingham.ac.uk

One-carbon metabolism and epigenetic programming of mammalian development

Constance Emily Clare

BSc (Hons)

Thesis submitted in fulfilment of the requirements for the degree of

Doctor of Philosophy (PhD)

September 2020



The University of
Nottingham

UNITED KINGDOM · CHINA · MALAYSIA

School of Biosciences

Sutton Bonington Campus

Loughborough

Leicestershire

LE12 5RD

I dedicate this work to my parents.

Without your unconditional love, support and guidance,

I would not have been able to achieve my successes.

Thank you.

Declaration

I hereby declare that this thesis is my own and the work herein has not been submitted for any other degree or award. Other sources of information and assistance given to me during the preparation of this thesis have been acknowledged.

Constance Emily Clare

Publications associated with this thesis

Clare CE, Brassington AH, Kwong WY and Sinclair KD (2019) One-Carbon Metabolism: Linking Nutritional Biochemistry to Epigenetic Programming of Long-Term Development. *Annu Rev Anim Biosci.* 7: 263-87

Xu J, Clare CE, Brassington AH, Sinclair KD and Barrett DA (2020) Comprehensive and quantitative profiling of B vitamins. *J. Chromatogr. B.* 1136: 121884

Clare CE, Pestinger V, Kwong WY, Tutt DAR, Xu J, Byrne HM, Barrett DA, Emes RD and Sinclair KD (2021) Interspecific variation in one-carbon metabolism within the ovarian follicle, oocyte and pre-implantation embryo: consequences for epigenetic programming of DNA methylation. *International Journal of Molecular Sciences.* In press.

Publications associated with BBSRC-funded PIPS

Clare C, Cruz M, Papadopoulou E, Savage J, Teperek M, Wang Y, Witowska I and Yeomans J (2019) Engaging Researchers with Data Management: The Cookbook. Open Book Publishers. doi: 10.11647/OBP.0185

C Clare (2019) The Real World of Research Data. Zenodo. <http://doi.org/10.5281/zenodo.3584373>

C Clare (2020) Sound bytes: sightless coding. *Nature.* 581(230). doi: 10.1038/d41586-020-01369-7

Conference abstracts associated with PhD

Clare CE, Tutt D, Kwong WY and Sinclair KD (2019) Methionine, one-carbon metabolism and bovine preimplantation embryo development. 12th International Conference on One Carbon Metabolism, B Vitamins and Homocysteine. *Understanding their role in health and disease from the womb to old age.* Southern Catalonia, Spain. June 2019

Clare CE, Tutt D, Kwong WY and Sinclair KD (2020) Methionine, one-carbon metabolism and bovine preimplantation embryo development. *Fertility 2020.* Society for Reproduction and Fertility, Edinburgh, UK. January 2020

Acknowledgements

I would like to express my gratitude to my supervisors, Prof. Kevin Sinclair, Prof. David Barrett and Prof. Ramiro Alberio.

Kevin, thank you for your unrelenting support, guidance and philosophical discussion over the past four years, and particularly during the current pandemic. You've taught me 'the importance of stupidity in scientific research' and how to become resilient to overcome the many hurdles and knockbacks. I won't forget your words of wisdom, and will try to get my 'ducks in a row' and 'keep my powder dry' in the future.

David, your patience, kindness and positive mentoring made learning mass spectrometry a little easier in the early days. Thanks to you and **Cath Ortori** for offering your technical expertise during my time working in the School of Pharmacy.

Ramiro, thank you for your scientific input with the embryology work. You lead by example and have been an inspiration to me.

My sincere appreciation goes to my colleagues at the University of Nottingham who have made this work possible.

Lydia Kwong, thank you for sharing your knowledge and for assisting with the molecular research, particularly the RRBS and qPCR. On a side note, your birthday cakes are spectacular and I will miss them greatly.

Des Tutt, it has been a pleasure to have you as a colleague and more importantly as a friend. Thank you for always finding time to help me, no matter how busy your schedule, and for the deep and meaningful chats over coffee - Long may they continue!

Richard Emes, thank you for your help with the bioinformatic analyses. Analysing the DNA methylation data became one of the most enjoyable aspects of my PhD. I think I could be converted to a computational biologist after all.

To the technical specialists; **Dongfang Li**, **Doris Klisch** and **Kamila Derecka**, thank you all for your help and education in the lab. **Ralph Hourd**, thank you for waking up at the crack of dawn and travelling miles to the abattoir to collect cattle ovaries – this work would not have been possible without you! Also, thanks to **Leigh Silvester** and **Chris Alford** for coming to the rescue with IT support on numerous occasions.

To the good friends I have made during my time at UoN; **Amey Brassington**, **Laura Tennant**, **Sarah Withey**, **Judith Gómez-Martínez**, **Haitham Alhilfi**, **Qifan Zhu**, **Gizem Guven Ates**, **Stuart Bagley**, **Pardeep Pabla**, **James Gillis**, **Chloe Geoghegan**, **Lucy Ross**, **Eleni Papagianni**, **Chloe Sargent** and **Lorrita Chinwendu**, thank you for the laughs and good times (and for keeping me sane!)

I would also like to thank **George Mann** for being a friend and mentor since 2014. Thank you for building my confidence during my undergraduate degree at UoN, and for allowing me to believe that studying for a PhD was even possible for me.

To my colleagues and friends at TU Delft, thank you for welcoming me to the Netherlands and for making me feel like a valued member of your team during my BBSRC-funded internship. I'm excited to join forces with you all again soon.

Finally, thank you to my family for believing in me. Without your love and support I would not have come this far. To my fiancé, **Alex**, thank you for loving and caring for me, for sharing the highs and lows of this journey, and for always giving me courage to pursue my dreams.

Abstract

One-carbon (1C) metabolism comprises a series of integrated metabolic pathways, including the linked methionine-folate cycles, that provide methyl groups for the synthesis of biomolecules and the epigenetic regulation of gene expression via chromatin methylation. Most of the research investigating the function of 1C metabolism pertains to studies undertaken in the rodent liver. Comparatively little is known about the function of 1C metabolism in reproductive and embryonic cells, particularly in domestic ruminant species. Periconceptional dietary deficiencies in 1C substrates and cofactors are known to lead to epigenetic alterations in DNA methylation in genes that regulate key developmental processes in the embryo. Such modifications can have negative implications on the subsequent development, metabolism and health of offspring. This thesis sought to improve current understanding of the regulation of 1C metabolism in the ruminant liver, ovary and preimplantation embryo through *in vivo* and *in vitro* nutritional supplementation experiments coupled with metabolomic, transcriptomic and epigenetic analyses.

The first part of this thesis (Chapter 2) assessed the metabolic consequences of dietary methyl deficiency using novel mass spectrometry-based methods that were developed for the quantification of B vitamins, folates and 1C-related amines in sheep liver. This study provided the first comparison of the relative abundance of bioactive 1C metabolites in liver harvested from methyl deficient sheep relative to a control study population of abattoir derived sheep. Relevant reductions in dietary methyl availability led to significant alterations in hepatic 1C metabolite concentrations. Large natural variations in the hepatic concentrations of individual metabolites in both sheep study populations reflected the dietary and genetic variation in our chosen outbred model species. These metabolomics platforms will be useful for investigating 1C metabolism and linked biochemical pathways in order to facilitate future dietary and genetic studies of metabolic health and epigenetic regulation of gene expression.

Based on the absence of methionine cycle enzyme transcripts (e.g. *MAT1A* and *BHMT*) in the bovine ovary and preimplantation embryo, the second part of this thesis (Chapter 3 and Chapter 4) addressed the hypothesis that ruminant reproductive and embryonic cells are highly sensitive to methyl group availability and, therefore, epigenetic programming during the periconceptional period. Transcript analyses confirmed *MAT2A* expression in the bovine liver, ovary and at each stage of preimplantation embryo development assessed to Day 8.

Transcripts for *BHMT* isoforms (*BHMT* and *BHMT2*) were detected in the bovine ovary but were weak or absent in embryos, highlighting a key difference in methionine metabolism between hepatic and reproductive cells.

Bovine embryos were produced *in vitro* using custom-made media containing 0 (nonphysiological), 10 (low physiological), 50 (high physiological), and 500 $\mu\text{mol/L}$ (supraphysiological) added methionine (Chapter 3). Gross morphological assessments of embryo stage, grade, cell lineage allocation and primary sex ratio revealed that culture in non- and supraphysiological methionine concentrations was detrimental for embryo development, whilst culture in the high physiological concentration appeared to be best. Reduced representation bisulphite sequencing (RRBS) of inner cell mass (ICM) and trophectoderm (TE) cells immunodissected from Day 8 blastocysts demonstrated that culturing embryos in low physiological methionine led to global hypomethylation within both cell lineages. Bioinformatic analyses of differentially methylated genes included gene set enrichment analyses (GSEA). Gene Ontology (GO) terms and Kyoto Encyclopedia of Genes and Genomes (KEGG) pathways that were enriched within the ICM were associated with protein catabolism and autophagy, and significant terms and pathways enriched within the TE were associated with cellular transport. Of particular biological interest was the loss of methylation within regulatory region (DMR2) of the paternally imprinted gene, *IGF2R*, in the TE following culture in low physiological methionine. Transcript analysis found no significant effect of methionine concentration on the expression of *IGF2R* or the antisense transcript, *AIRN*, in the primary cell lineages of the Day 8 bovine preimplantation embryo. Hypomethylation of *IGF2R* DMR2 has been associated with aberrant *IGF2R* expression and large offspring syndrome (LOS) in cattle and sheep that were subjected to embryo manipulation during assisted reproductive technology (ART) procedures, such as somatic cell nuclear transfer (SCNT) or non-physiological *in vitro* embryo culture environments.

Chapter 5 sought to evaluate the effect of somatic donor cell type on epigenetic reprogramming via DNA methylation in hepatocytes isolated from cloned sheep. RRBS facilitated the comparison of methylation reprogramming between Finn Dorset (D) clone hepatocytes and their mammary epithelial (OP5) donor cell line; and, Lleyn (L) clone hepatocytes and their Lleyn fetal fibroblast (LFF4) donor cell line. Methylation was most closely correlated between D and L clone hepatocytes than between clones and their respective donor cell lines. In

general, hepatocytes were hypomethylated relative to their somatic donor cell nuclei. GSEA identified genes that encoded transcription factor proteins enriched within the 'Sequence-specific DNA binding' term (GO:0043565) as differentially methylated between clone hepatocytes and their donor cell lines. In addition, imprinted genes, including *IGF2R*, were differentially methylated in clone hepatocytes relative to somatic cell nuclei.

In summary, this thesis promotes and supports the importance of an optimal methyl balance to support periconceptual development in mammals. The experiments detailed herein provide an insight into the metabolic consequences of dietary methyl deficiency (and excess) in outbred populations of domestic ruminants, with a specific focus on the liver, ovary and preimplantation embryo. The results demonstrate that tissue- and species-specific features of 1C metabolism render ruminant embryonic cells sensitive to methionine inputs within a physiological range. The observation that *in vitro* embryo culture and manipulation techniques, such as somatic cell nuclear transfer, can cause epigenetic alterations to DNA methylation during preimplantation development provides a basis for further study into the safety and efficacy of emerging assisted reproductive technologies.

Table of contents

General Introduction.....	1
Chapter 1 One-carbon metabolism and epigenetic regulation of periconceptual development	6
1.1 Maternal nutrition, 1C metabolism and pregnancy outcome	7
1.1.1 The periconceptual period	7
1.1.1.1 Epigenetic reprogramming.....	7
1.1.1.2 Epigenetic effect of diet on periconceptual development..	9
1.2 One-carbon (1C) metabolism and related pathways	12
1.2.1 Methionine-folate cycles	12
1.2.2 <i>Transsulphuration</i> pathway.....	15
1.2.3 Propionate pathway.....	15
1.2.4 Polyamine pathway	16
1.2.5 Phosphatidylcholine pathway	17
1.2.6 Nucleotide biosynthesis.....	18
1.3 Genetics of 1C metabolism.....	20
1.3.1 Hyperhomocysteinemia (HHcy)	20
1.3.1.1 HHcy and epigenetics.....	21
1.4 Regulation of 1C metabolism in the mammalian embryo	22
1.5 Epigenetics and methylation.....	23
1.5.1 Genomic DNA (gDNA) methylation.....	23
1.5.1.1 CpG methylation.....	24
1.5.1.2 Non-CpG methylation	24
1.5.2 Mitochondrial DNA (mtDNA) methylation.....	25
1.5.3 Histone modifications	26
1.5.4 RNA methylation	26
1.5.5 Demethylation machinery	27
1.5.5.1 Cytosine hydroxymethylation (5hmC)	27

1.6	DNA methylation analysis.....	28
1.6.1	DNA methylation analysis of preimplantation embryos	31
1.7	Assisted reproductive technology (ART) and epigenetics	32
1.7.1	1C metabolites in <i>in vitro</i> embryo production (IVP) media.....	33
1.7.2	Methionine and epigenetic programming.....	35
1.8	Working hypothesis	37
Chapter 2 Quantification of folates, B vitamins and 1C-related metabolites in ovine liver by HILIC-MS/MS.....		39
2.1	Introduction.....	40
2.2	Materials and methods	42
2.2.1	Animals, treatments and tissue collection	42
2.2.1.1	Methyl deficient (MD) cohort.....	42
2.2.1.2	Tissue collection.....	44
2.2.1.3	Blood analysis	44
2.2.1.3.1	Vitamin B ₁₂	44
2.2.1.3.2	Homocysteine (Hcy)	45
2.2.1.3.3	Methylmalonic acid (MMA)	45
2.2.2	Liver 1C metabolite quantification.....	46
2.2.2.1	HILIC-MS/MS	46
2.2.2.1.1	Analytical grade reagents	46
2.2.2.1.2	Standard preparation and calibration.....	50
2.2.2.1.3	Sample extraction.....	50
2.2.2.1.4	LC-MS/MS analysis.....	51
2.2.2.1.5	Method validation	54
2.2.2.1.6	Statistical data analysis	56
2.3	Results and Discussion	56
2.3.1	Blood biomarkers.....	56
2.3.2	Liver metabolites	57

2.3.2.1	Vitamin B ₁₂	57
2.3.2.2	Vitamin B ₆	59
2.3.2.3	Vitamin B ₂	61
2.3.2.4	Vitamin B ₁	63
2.3.2.5	Vitamin B ₉ (folates)	65
2.3.2.6	Methionine cycle metabolites.....	68
2.3.2.7	1C-related amino acids and derivatives	69
2.3.2.8	Polyamine metabolites	72
2.3.2.9	Propionate metabolites.....	74
2.4	Concluding remarks.....	75
Chapter 3 Methionine, 1C metabolism and bovine preimplantation embryo development.....		
3.1	Introduction.....	79
3.2	Materials and methods	83
3.2.1	Methionine cycle enzyme transcripts.....	83
3.2.1.1	Sample collection	83
3.2.1.1.1	Liver (positive control)	83
3.2.1.1.2	Germinal vesicle (GV) oocytes	83
3.2.1.1.3	Cumulus cells (CC)	84
3.2.1.1.4	Granulosa cells (GC).....	85
3.2.1.2	<i>In vitro</i> embryo production (IVP)	85
3.2.1.2.1	Metaphase II (MII) oocytes, zygotes and embryos.....	85
3.2.1.3	RNA extraction	86
3.2.1.3.1	Liver and granulosa cells.....	86
3.2.1.3.2	Cumulus cells, oocytes and blastocysts	87
3.2.1.4	Reverse transcription (RT).....	88
3.2.1.5	Polymerase chain reaction (RT-PCR).....	88
3.2.1.5.1	Primer design.....	88

3.2.1.5.2	Transcript expression	89
3.2.2	Methionine and embryo development during culture.....	89
3.2.2.1	High performance liquid chromatography (HPLC)	90
3.2.2.1.1	Analytical grade reagents	90
3.2.2.1.2	Standard preparation and calibration.....	90
3.2.2.1.3	Method validation	91
3.2.2.1.4	Follicular fluid collection.....	91
3.2.2.1.5	IVP media and follicular fluid sample extraction.....	92
3.2.2.2	Methionine-adjusted <i>in vitro</i> embryo production (IVP).....	93
3.2.2.2.1	Whole-mount immunofluorescence	93
3.2.2.2.2	Embryo sexing by polymerase chain reaction (PCR).....	94
3.2.2.2.3	Statistical data analysis	95
3.3	Results and Discussion	95
3.3.1	Methionine cycle enzyme transcripts	95
3.3.2	Methionine and embryo development during culture.....	98
3.3.2.1	Methionine composition of custom-made IVP media	98
3.3.2.2	Amino acid composition of custom-made IVP media	98
3.3.2.3	Amino acid composition of bovine follicular fluid	101
3.3.2.4	<i>In vitro</i> embryo production with added methionine.....	105
3.3.2.4.1	Gross morphology	105
3.3.2.4.2	Cell lineage specification	110
3.3.2.4.3	Primary sex ratio	112
3.4	Concluding remarks.....	114
Chapter 4	Methionine and epigenetic programming of the bovine preimplantation embryo	116
4.1	Introduction.....	117
4.2	Materials and methods	119
4.2.1	<i>In vitro</i> embryo production	119

4.2.2	Immunodissection of bovine blastocysts.....	119
4.2.3	Validation of cell lineage purity	120
4.2.3.1	RNA extraction and cDNA synthesis	120
4.2.3.2	Primer design	121
4.2.3.3	Quantitative real-time PCR	122
4.2.4	DNA methylation analysis.....	122
4.2.4.1	Reagents.....	122
4.2.4.2	Reduced Representation Bisulphite Sequencing (RRBS)	123
4.2.4.2.1	gDNA purification	123
4.2.4.2.2	Restriction enzyme (Msp1) digestion.....	123
4.2.4.2.3	End-repair and dA tailing	124
4.2.4.2.4	Adapter ligation	124
4.2.4.2.5	Bisulphite conversion	124
4.2.4.3	Library quality control (QC).....	125
4.2.4.3.1	Multiplex sequencing.....	125
4.2.4.4	Bioinformatic Data Analysis	126
4.2.4.4.1	Gene set enrichment analysis (GSEA)	127
4.2.5	<i>IGF2R</i> and <i>AIRN</i> transcript expression.....	129
4.2.5.1	RNA extraction and cDNA synthesis	129
4.2.5.2	Quantitative real-time PCR	129
4.2.6	Statistical data analysis	130
4.3	Results and Discussion	131
4.3.1	Validation of cell lineage purity	131
4.3.2	DNA methylation analyses by RRBS	132
4.3.2.1	Mean methylation (%).....	132
4.3.2.2	Directional methylation	135
4.3.2.3	Distribution of DMS.....	136
4.3.2.4	Enriched pathways and genes.....	140

4.3.2.5	Imprinted genes.....	150
4.3.2.6	<i>Insulin-like growth factor 2 receptor (IGF2R)</i>	155
4.3.2.6.1	Regulation of <i>IGF2R</i> imprinting	156
4.3.2.6.2	Loss of methylation in DMR2.....	158
4.3.2.6.3	<i>IGF2R</i> and <i>AIRN</i> transcript expression.....	161
4.4	Concluding remarks.....	162
Chapter 5 Donor cell type and epigenetic reprogramming of cloned sheep hepatocytes		165
5.1	Introduction.....	166
5.2	Materials and methods	168
5.2.1	Animals, treatments and tissue collection	168
5.2.1.1	Donor cell culture	168
5.2.1.2	Somatic cell nuclear transfer (SCNT)	169
5.2.1.3	Isolation of hepatocytes.....	169
5.2.2	DNA methylation analysis.....	170
5.2.2.1	Library quality control (QC).....	170
5.2.2.2	Multiplex sequencing.....	170
5.2.2.3	Bioinformatic Data Analysis	171
5.2.2.3.1	Gene set enrichment analysis (GSEA)	172
5.2.3	Statistical data analysis	172
5.3	Results and Discussion	173
5.3.1	Overall CpG methylation.....	173
5.3.2	Directional methylation	175
5.3.3	Distribution of DMS.....	176
5.3.4	Enriched pathways and genes.....	177
5.3.4.1	Mammary-specific genes.....	180
5.3.4.2	Fetal fibroblast-specific genes	181
5.3.4.3	Liver-specific genes.....	182

5.3.5	Imprinted genes.....	190
5.3.5.1	<i>Delta-like 1 (DLK1) and Growth factor receptor bound protein 10 (GRB10)</i>	192
5.3.5.2	<i>Insulin-like growth factor 2 receptor (IGF2R)</i>	194
5.4	Concluding remarks.....	197
Chapter 6 Discussion and Conclusion		199
6.1	General discussion	200
6.2	Summary of key findings	201
6.3	Clinical impact	204
6.4	General conclusions and future research	209
References		215
Appendices.....		1
Appendix Chapter 1		2
Appendix Chapter 2.....		13
Appendix 2.1 Sheep blood plasma trace-element analysis by ICP-MS.....		15
Appendix 2.2 Sheep liver amino acid analysis by HPLC.....		15
Appendix 2.3 Sheep liver polyamine analysis by HPLC.....		17
Appendix 2.4 Liver propionate metabolites by GC-MS		18
Appendix Chapter 3.....		21
Appendix 3.1 Bovine COC grade and morphological description.....		22
Appendix 3.2 <i>In vitro</i> embryo production (IVP) media.....		23
Appendix 3.3 Bovine embryo stage and morphological description		26
Appendix 3.4 Sperm preparation by swim-up method		27
Appendix 3.5 <i>BHMT</i> and <i>BHMT2</i> multiple sequence alignment.....		28
Appendix 3.6 Minus reverse transcription (-RT) for <i>β-Actin (ACTB)</i>		29
Appendix 3.7 Amplicon purification for sequencing		29
Appendix 3.8 Custom-made IVP formulations and methionine stock solutions		
31		
Appendix Chapter 4.....		33

Appendix 4.1 Calibration standard curves for qPCR.....	33
Appendix 4.2 Reference gene selection using geNorm	34
Appendix 4.3 Stock and working solutions for RRBS analysis.....	36
Appendix 4.4 Differentially methylated genes in bovine ICM and TE	39
Appendix 4.5 GO terms enriched in bovine ICM and TE	46
Appendix 4.6 <i>IGF2R</i> and <i>AIRN</i> primer test by RT-PCR.....	53
Appendix 4.7 <i>IGF2R/AIRN</i> amplicon sequencing	54
Appendix 4.8 Calibration standard curves for qPCR (liver)	56
Appendix 4.9 Calibration standard curves for qPCR (blastocysts).....	57
Appendix 4.10 Position and methylation (%) of each DMS within <i>IGF2R</i> intron 2 DMR.....	58
Appendix 4.11 ClustalW2 multiple sequence alignment: <i>IGF2R</i> nucleotide sequence homology (%) between species.	59
Appendix 4.12 Multiple sequence alignment of <i>IGF2R</i> DMR2 clusters	60
Appendix Chapter 5	63
Appendix 5.1 Working solutions and methodology for RRBS	63
Appendix 5.2 GO terms enriched in DvOP5 and LvLFF4	66
Appendix 5.3 Enriched 'Sequence-specific DNA binding' GO term	72
PIPS Reflective Statement.....	76
Appendix references.....	78

List of tables

Table 1.1 Methyl supplementation in maternal diet and epigenetic programming of periconceptual development.	9
Table 1.2 Methyl deficiency in maternal diet and epigenetic programming of periconceptual development.	10
Table 1.3 Methods for profiling whole genome DNA methylation.	29
Table 1.4 Methods for profiling differentially methylated regions (DMRs).	30
Table 1.5 1C metabolites in commercial cell and embryo culture media.	34
Table 1.6 Epigenetic effects of methionine on mammalian cells and embryos.	36
Table 2.1 Macro and micro mineral composition of methyl deficient (MD) concentrate diet and cobalt (Co) deficient hay.	43
Table 2.2 B vitamin and 1C-related amine analytes measured by HILIC-MS/MS.	48
Table 2.3 Folate and methionine cycle analytes measured by HILIC-MS/MS.	49
Table 2.4 Mass spectrometer parameters for identification of B vitamins and 1C-related amines. Adapted from Xu <i>et al.</i> (2020).	53
Table 2.5 Mass spectrometer parameters for identification of folates and methionine cycle metabolites.	53
Table 2.6 Validation data for quantification of B vitamins and 1C-related amines in sheep liver.	55
Table 2.7 Validation data for quantification of folates and methionine cycle metabolites in sheep liver.	55
Table 3.1 Methionine concentrations in culture media can be >10-fold higher than those found in physiological fluids.	79
Table 3.2 Primers used for methionine cycle enzyme transcript expression.	89
Table 3.3 Validation data for quantification of amino acids in IVP media and ovarian follicular fluid.	91
Table 3.4 Primers used for sex determination of Day 8 bovine blastocysts.	95

Table 4.1 Immunodissected inner cell mass (ICM) and trophectoderm (TE) cells isolated from Day 8 bovine blastocysts were pooled ($n=5$) by lineage for DNA methylation analysis.	120
Table 4.2. Primers used for the detection of trophectoderm-specific marker, <i>GATA3</i> , and reference genes in bovine blastocysts and immunodissected embryonic cell samples.	121
Table 4.3 Summary of Bismark final alignment report.	126
Table 4.4 Primers used for the detection of <i>IGF2R</i> and <i>AIRN</i> in bovine blastocysts and immunodissected embryonic cell samples.	130
Table 4.5 A count of differentially methylated sites (DMS), genes and transcripts, and directional methylation for each experimental combination (%).	135
Table 4.6 Distribution and direction of differentially methylated sites (DMS) for each experimental combination (%).	139
Table 4.7 Top five enriched Biological Process (A) and Cellular Component (B) Gene Ontology (GO) terms ranked by number of differentially methylated genes of interest.	147
Table 4.8 Top five enriched Molecular Function Gene Ontology (GO) terms (A) and KEGG Pathways (B) ranked by number of differentially methylated genes of interest.	148
Table 4.9 Genes of interest (GOI) with the highest number of differentially methylated sites (DMS) selected from the first Gene Ontology (GO) term and KEGG Pathway.	149
Table 4.10 Monoallelically expressed genes in cattle.	151
Table 5.1 Summary of Bismark final alignment report.	171
Table 5.2 A count of differentially methylated sites (DMS) and genes, and directional methylation for each experimental combination (%).	175
Table 5.3 Distribution of differentially methylated sites (DMS) for each experimental combination (%).	176
Table 5.4 Top five enriched Gene Ontology (GO) terms ranked by number of differentially methylated genes of interest (GOI).	179

Table 5.5 Imprinted genes in sheep and/or cattle that were differentially methylated between clone hepatocytes and donor cell lines.....190

Table 6.1 Experimental design for methyl supplementation study.....211

List of figures

Figure 1.1 One-carbon (1C) metabolism includes the linked methionine-folate cycle and <i>transsulphuration</i> pathway. Adapted from Clare et al. (2019)	13
Figure 1.2 One-carbon (1C) substrates and cofactors serve as key intermediates of propionate and energy metabolism. Adapted from Clare et al. (2019)	16
Figure 1.3 Polyamine synthesis and the methionine salvage pathway requires decarboxylated SAM as an aminopropyl donor. Adapted from Clare et al. (2019)	17
Figure 1.4 Phosphatidylcholine can be synthesised by choline or via the cytidine diphosphate (CDP)-choline pathway. Adapted from Clare et al. (2019)	18
Figure 1.5 One-carbon (1C) metabolism provides purines (adenine and guanine), and pyrimidine, thymine, for nucleotide biosynthesis. Adapted from Clare et al. (2019)	19
Figure 2.1 HILIC-MS/MS MRM chromatograms for 1C metabolites quantified in sheep liver.	54
Figure 2.2 Plasma homocysteine (Hcy) and methylmalonic acid (MMA) concentrations increase as a result of Vitamin B ₁₂ deficiency in Texel lambs.	57
Figure 2.3 Vitamin B ₁₂ species are decreased in methyl deficient sheep liver.	58
Figure 2.4 Vitamin B ₆ species are decreased in methyl deficient sheep liver..	61
Figure 2.5 Vitamin B ₂ species are decreased in methyl deficient sheep liver.	62
Figure 2.6 Vitamin B ₁ (thiamine) is decreased in methyl deficient sheep liver.	64
Figure 2.7 5-methyltetrahydrofolate accumulates in methyl deficient sheep liver.	66
Figure 2.8 Concentrations of methionine cycle metabolites are altered in methyl deficient sheep liver.	68
Figure 2.9 Amino acids drive folate metabolism and <i>transsulphuration</i> in sheep liver.....	70
Figure 2.10 Amino acids facilitate the remethylation of homocysteine (Hcy) to methionine (Met) in sheep liver.	72

Figure 2.11 Polyamines increase in methyl deficient sheep liver.....	73
Figure 2.12 The propionate metabolome is altered in methyl deficient sheep liver.....	74
Figure 3.1 Developmental stages and epigenetic events in bovine preimplantation embryos.....	81
Figure 3.2. Methionine concentrations added during <i>in vitro</i> production of bovine blastocysts.....	83
Figure 3.3 Ovarian follicular fluid volume increases with follicular dominance.	92
Figure 3.4 <i>MAT2A</i> , <i>BHMT</i> and <i>BHMT2</i> transcript expression in bovine ovarian cells, oocytes and preimplantation embryos.....	96
Figure 3.5 Concentrations of methionine in custom-made <i>in vitro</i> embryo production media formulations.	98
Figure 3.6 Amino acid profile of <i>in vitro</i> maturation (IVM) media (A) and <i>in vitro</i> culture (IVC) media (B).	99
Figure 3.7 Amino acid composition of bovine follicular fluid by follicular size.	102
Figure 3.8 A study comparison of the amino acid profile in bovine follicular fluid aspirated from non-dominant (2 to 6 mm) and dominant (6 to >15 mm) ovarian follicles.....	103
Figure 3.9 A comparison of amino acids in custom-made TCM199 IVM formulation and preovulatory ovarian follicular fluid.....	104
Figure 3.10 Methionine concentration during bovine IVP had no effect on the proportion of inseminated oocytes that cleaved by Day 2 ($P=0.147$).....	105
Figure 3.11 Added methionine increases ($P<0.001$) the proportion of blastocysts by Day 7.....	106
Figure 3.12 Physiological (10 and 50 $\mu\text{mol/L}$) methionine increases the proportion ($P<0.05$) of advanced transferable blastocysts.	108
Figure 3.13 Blastocyst cell number increases ($P<0.001$) in a dose-dependent manner with methionine.....	111
Figure 3.14 Non-physiological (0 $\mu\text{mol/L}$) methionine concentration reduces ($P=0.022$) the proportion of male blastocysts.....	113

Figure 4.1 Reference gene stability plot using Reference Gene Selector Tool in CFX Maestro™ software.....	122
Figure 4.2 UpSet R plot demonstrates intersection size between the numbers of differentially methylated sites (DMS) across experimental combinations.	128
Figure 4.3 Enrichment of bovine embryonic cell populations following immunodissection.	131
Figure 4.4 Low methionine significantly reduced mean cytosine methylation (%) in inner cell mass (ICM) and trophectoderm (TE).....	134
Figure 4.5 Distribution of differentially methylated sites (DMS) across genomic regions for each experimental combination.....	137
Figure 4.6 Top 10 significantly enriched Biological Process (A) and Cellular Component (B) Gene Ontology (GO) terms in the bovine inner cell mass (ICM) when methionine concentration is reduced within physiological range during IVP.	141
Figure 4.7 Top 10 significantly enriched Molecular Function Gene Ontology (GO) terms (A) and KEGG Pathways (B) in the bovine inner cell mass (ICM) when methionine concentration is reduced within physiological range during IVP.	142
Figure 4.8 Top 10 significantly enriched Biological Process (A) and Cellular Component (B) Gene Ontology (GO) terms in the bovine trophectoderm (TE) when methionine concentration is reduced within physiological range during IVP.	143
Figure 4.9 Top 10 significantly enriched Molecular Function Gene Ontology (GO) terms (A) and KEGG Pathways (B) in the bovine trophectoderm (TE) when methionine concentration is reduced within physiological range during IVP.	144
Figure 4.10 Low physiological methionine concentration during culture decreases CpG methylation of six imprinted genes within the primary cell lineages of the Day 8 bovine preimplantation embryo.....	152
Figure 4.11 Mean methylation (%) of six differentially methylated imprinted genes in bovine inner cell mass (ICM) and trophectoderm (TE) following culture in physiologically high (50 µmol/L) and low (10 µmol/L) methionine.....	154
Figure 4.12 Bovine <i>IGF2R</i> gene is imprinted by antisense transcript, <i>AIRN</i>	157

Figure 4.13 Two clusters of DMS were hypomethylated within DMR2 of the <i>IGF2R</i> gene in the trophectoderm (TE) lineage following bovine embryo culture in low physiological methionine (50 v 10 μ mol/L).	160
Figure 4.14 Relative transcript expression of <i>IGF2R</i> (A) and antisense transcript, <i>AIRN</i> (B) in Day 8 bovine blastocysts cultured at physiologically high and low methionine concentrations.	161
Figure 5.1 Procedure and potential applications of somatic cell nuclear transfer (SCNT).	166
Figure 5.2 Distribution of methylated CpGs across hepatocyte cell samples derived from cloned Finn Dorset (D) and Lleyrn (L) sheep, and their respective somatic donor cell lines.	173
Figure 5.3 Correlation of CpG methylation (%) between cell samples ($n=11$).	174
Figure 5.4 Flowchart of the methodology used to select differentially methylated tissue-specific genes ($n=9$) between donor cell lines and clone hepatocytes.	177
Figure 5.5 Differential methylation of mammary-specific genes ($n=4$) between clone sheep hepatocytes and their somatic donor cell lines.	184
Figure 5.6 Clusters of differentially methylated sites (DMS) in the <i>POU5F1</i> gene are hypermethylated in somatic donor cell line (OP5 and LFF4) relative to clone hepatocyte (D and L).	185
Figure 5.7 Differential methylation of fetal fibroblast-specific genes ($n=2$) between clone sheep hepatocytes and their somatic donor cell lines.	186
Figure 5.8 Clusters of differentially methylated sites (DMS) in the <i>PITX1</i> gene are hypermethylated in somatic donor cell line (OP5 and LFF4) relative to clone hepatocyte (D and L).	187
Figure 5.9 Differential methylation of liver-specific genes ($n=3$) between clone sheep hepatocytes and their somatic donor cell lines.	188
Figure 5.10 Clusters of differentially methylated sites (DMS) in the <i>FOXA2</i> gene are hypomethylated in somatic donor cell line (OP5 and LFF4) relative to clone hepatocyte (D and L).	189

Figure 5.11 CpG methylation levels of imprinted genes ($n=16$) differ between the OP5 donor cell line and D clone hepatocytes (A), and between the LFF4 donor cell line and L clone hepatocytes (B). 191

Figure 5.12 Differential methylation of imprinted genes, *DLK1* and *GRB10*, between clone sheep hepatocytes and their somatic donor cell lines. 193

Figure 5.13 Differential methylation of *IGF2R* gene between clone sheep hepatocytes and their somatic donor cell lines. 194

Figure 5.14 Clusters of differentially methylated sites (DMS) in the *IGF2R* gene between somatic donor cell line (OP5 and LFF4) and clone hepatocyte (D and L). 196

List of Abbreviations

1C	One-carbon
5hmC	5-hydroxymethylcytosine
5mC	5-methylcytosine
8-Br-cAMP	8-bromoadenosine 3',5'-cyclic monophosphate
Ab	Abattoir
ACN	Acetonitrile
ANOVA	Analysis of variance
ART	Assisted reproduction technology
ATP	Adenosine triphosphate
<i>A^{vy}</i>	Viable yellow agouti
B ₁ - ¹³ C ₃	Thiamine- ¹³ C ₃
BF	Scottish Blackface
BLAST	Basic Local Alignment Search Tool
BME	Basal Medium Eagle
bp	Base pair
BS	Bisulphite sequencing
BSA	Bovine serum albumin
BWS	Beckwith-Wiedemann syndrome
CC	Cumulus cells
cDNA	Complementary deoxyribonucleic acid
CGI	CpG island
CH ₃	Methyl
Co	Cobalt
CO ₂	Carbon dioxide
COC	Cumulus oocyte complex
CpG	Cytosine-phosphate-guanosine
CV	Coefficient of variation
D	Finn-Dorset
dH ₂ O	Distilled water
DM	Dry matter
DMR	Differentially methylated region
DMS	Differentially methylated site
DNA	Deoxyribonucleic acid
DNMT	DNA methyltransferase
DOHaD	Developmental origins of adult health and disease
EAA	Essential amino acid
EGA	Embryonic genome activation
Epi	Epiblast

ESC	Embryonic stem cell
EtBr	Ethidium bromide
FA	Folic acid
FCS	Fetal calf serum
FDR	False discovery rate
GC	Granulosa cells
GC-MS	Gas chromatography-mass spectrometry
gDNA	Genomic DNA
GO	Gene Ontology
GOI	Gene of interest
GSEA	Gene set enrichment analysis
GV	Germinal vesicle
HCl	Hydrochloric acid
HDAC	Histone deacetylase
HHcy	Hyperhomocysteinemia
HIF	Hog intrinsic factor
HILIC	Hydrophilic interaction liquid chromatography
hpi	Hours post-insemination
HPLC	High performance liquid chromatography
Hz	Hertz
IAP	Intracisternal A particle
ICM	Inner cell mass
IETS	International Embryo Technology Society
IS	Internal standard
IVC	<i>In vitro</i> culture
IVF	<i>In vitro</i> fertilisation
IVM	<i>In vitro</i> maturation
IVP	<i>In vitro</i> embryo production
kb	Kilobase
kDa	Kilodalton
KEGG	Kyoto Encyclopedia of Genes and Genomes
K_m	Michaelis-Menten constant
L	Lleyn
LC-MS/MS	Liquid chromatography-mass spectrometry
lcrRNA	Long non-coding RNA
LFF4	Lleyn fetal fibroblast cell line
LINE	Long interspersed element
LLOQ	Lower limit of quantification
LOD	Limit of detection
LOI	Loss of imprinting

LOQ	Limit of quantification
LOS	Large offspring syndrome
LPD	Low protein diet
LTR	Long terminal repeat
m/z	Mass/charge
m ⁶ A	N ⁶ -methyladenosine
MCE	2-mecaptoethanol
MD	Methyl deficient
MEM	Minimum Essential Medium
MII	Metaphase II
mRNA	Messenger RNA
mtDNA	Mitochondrial DNA
MTX	Methotrexate
NaOH	Sodium hydroxide
NCBI	National Center for Biotechnology Information
NEAA	Non-essential amino acid
NTD	Neural tube defect
NVA	Norvaline
O ₂	Oxygen
°C	Celsius
OP5	Mammary epithelial cell line
PBS	Phosphate buffered saline
PCR	Polymerase chain reaction
PE	Primitive endoderm
PN-d ₃	Pyridoxine hydrochloride methyl-D ₃
PVP	Polyvinylpyrrolidone
Q	Quality score
QC	Quality control
qPCR	Quantitative real-time polymerase chain reaction
REML	Residual maximum likelihood
RNA	Ribonucleic acid
RRBS	Reduced representation bisulphite sequencing
RSD	Relative standard deviation
RT	Reverse transcription
RT-PCR	Reverse transcription polymerase chain reaction
S	Sulphur
S/N	Signal to noise
SAH-d ₄	S-adenosylhomocysteine-d ₄
SCNT	Somatic cell nuclear transfer
SEM	Standard error of mean

SMM	S-methylmethionine
SNP	Single nucleotide polymorphism
SOF	Synthetic oviductal fluid
SSA	5-sulphosalicylic acid
T	Texel
TCM	Tissue culture media
TE	Trophectoderm
tRNA	Transfer ribonucleic acid
UV	Ultraviolet
v/v	Volume to volume
w/v	Weight to volume
xg	Gravitational force

General Introduction

Evidence from epidemiological cohort studies in humans and mechanistic studies in animals demonstrates that altering key developmental processes *in utero* can predispose offspring to adult-onset non-communicable diseases, such as cancer, dyslipidaemia, type II diabetes and cardiovascular disease (Barker, 1995; McMillen and Robinson, 2005; Sinclair *et al.*, 2016b). These and related observations, originally advanced by David Barker and colleagues at the University of Southampton over thirty years ago (Barker and Osmond, 1986; Barker and Osmond, 1988; Barker *et al.*, 1989), became known as 'The Barker Hypothesis' but are now commonly referred to as the 'Developmental Origins of Health and Disease' (DOHaD) hypothesis (Wadhwa *et al.*, 2009). This theory postulates that environmental factors, such as parental diet or embryo culture media used during assisted reproduction technologies (ART), can act during critical stages of mammalian embryo development to programme physiological and metabolic functions in the fetus, thereby determining its susceptibility to adverse health outcomes in later life (Stephenson *et al.*, 2018; Fleming *et al.*, 2018).

Studies of human cohorts exposed to maternal undernutrition at various stages of pregnancy during the Dutch Hunger Winter of 1944-45 (a famine that took place in the German-occupied Netherlands) revealed that people exposed to famine during early gestation were more likely to develop cardiometabolic disease, such as obesity, compared to those who had been exposed to famine in late gestation (Ravelli *et al.*, 1976; Stein *et al.*, 2007). Hence, two important conclusions were drawn from these cohort studies: i) intrauterine exposures can have long-lasting effects on adult health; and, ii) the timing of the exposure is critical for the programming of adult health (Schulz, 2010).

Much of the evidence underpinning DOHaD has since been obtained during direct intervention studies using animal models. The effects of nutrient deprivation (i.e. gross caloric restriction or protein deficiency) in the maternal diet during pregnancy have been well-documented in rodents and sheep (Langley-Evans, 2006; Sinclair and Singh, 2007). By way of example, feeding rats a maternal low protein diet (LPD) causes a range of sex-specific molecular, metabolic, neuroendocrine and physiological adaptations in offspring that lead to adverse adult health-related phenotypes, such as obesity and hypertension (Kwong *et al.*, 2000; Kwong *et al.*, 2006; Kwong *et al.*, 2007; Watkins *et al.*,

2008). Similar observations have been also reported in sheep (Edwards and McMillen, 2002; Dunford *et al.*, 2014; Lan *et al.*, 2013).

Whilst animal models confirm that long-term health can be compromised by nutrient deprivation *in utero*, little is known about the effects of specific dietary nutrients and the mechanistic basis underpinning the metabolic programming of development (Sinclair and Singh, 2007). In recent years, B vitamins and methyl (CH₃) donating metabolites that serve as key substrates and cofactors of one-carbon (1C) metabolism have been identified as molecular mediators responsible for developmental programming (Sinclair *et al.*, 2007; Maloney *et al.*, 2011; Kalhan, 2016). Since 1C metabolic pathways provide a biochemical conduit between parental diet and epigenetic regulation of early development (Clare *et al.*, 2019), it follows that fluctuations in dietary methyl group availability can alter epigenetic regulation of gene expression via biological methylation reactions during critical periods of mammalian development, thereby modifying adult health-related phenotypes in offspring (Maloney *et al.*, 2011; Araújo *et al.*, 2013).

The periconceptual period is the stage of mammalian development considered most environmentally sensitive to perturbations in 1C metabolism and epigenetic programming. This period can be broadly defined as the time before and immediately following conception wherein a diverse range of key biological and molecular processes take place (discussed in Section 1.1.1) (Sinclair *et al.*, 2007; Louis *et al.*, 2008; Maloney *et al.*, 2011; Steegers-Theunissen *et al.*, 2013; Padhee *et al.*, 2015).

The observation that offspring health is programmed by maternal diet during the earliest stages of development emphasises the importance of adequate nutritional status amongst women of reproductive age and, particularly, expectant mothers (Louis *et al.*, 2008; Hambidge *et al.*, 2014; Young *et al.*, 2018). Health surveys demonstrate that the nutritional intake of the general population is suboptimal. According to a recent review of European National Dietary Surveys, World Health Organisation (WHO) Recommended Nutrient Intakes (RNIs) are most notably lacking in women (Rippin *et al.*, 2017). It follows that suboptimal nutritional intakes are likely to prevail in women planning for pregnancy and who are pregnant (Hammiche *et al.*, 2011; Gernand *et al.*, 2016). Since 44% of pregnancies worldwide are unplanned (Bearak *et al.*, 2018), with many women unaware that they are pregnant until the fifth week of pregnancy (Temel *et al.*, 2014), women experiencing unplanned pregnancy are unlikely to

intentionally initiate nutritional health care behaviours to address perinatal risk factors and, therefore, may lack essential vitamin, mineral and micronutrient intakes during their first trimester of pregnancy (Kuroki *et al.*, 2008). Consequently, birth outcomes for unintended pregnancies may place the newborn at increased risk of preterm birth, low weight, congenital abnormalities, and neonatal death (Kost *et al.*, 1998; Gernand *et al.*, 2016).

Worldwide efforts are being undertaken to reduce such adverse pregnancy outcomes with an increasing focus on periconceptional care (Dunlop *et al.*, 2007; Temel *et al.*, 2014). A case in point refers to the public recommendation of periconceptional maternal folic acid (FA) supplementation (400 µg/d) as a dietary intervention to reduce adverse birth outcomes, primarily neural tube defects (NTDs; De-Regil *et al.*, 2010). It is well recognised that maternal folate status is critical for normal neural tube closure and the prevention of NTDs up to day 28 post-conception (McNulty *et al.*, 2000).

With an aim to reduce the incidence of NTDs, the United States and Canada introduced a policy of mandatory fortification of enriched cereal grain products with FA. Since its implementation in 1998, this policy has witnessed a 19-32% decline in the prevalence of NTDs (Crider *et al.*, 2011). Fortification programmes have now been implemented in >81 countries (Wald *et al.*, 2018) and studies have shown a clear reduction in NTDs (Honein *et al.*, 2001; De Wals *et al.*, 2007; Hertrampf and Cortés, 2008). However, there is general resistance to implementation of this within Europe and mandatory FA fortification remains a topic of contention. Concerns revolve around putative adverse effects of unmetabolised FA in the systemic circulation, cognitive decline in the elderly, increased risk of cancer, and masking or exacerbating the effects of vitamin B₁₂ deficiency (Smith and Refsum, 2016; Field and Stover, 2018).

Unfortunately, dietary inadequacies of 1C metabolites prevail in Europe (Gilsing *et al.*, 2010) and pose considerable risk to women of reproductive age (Gernand *et al.*, 2016; Obeid *et al.*, 2016; Ferraro *et al.*, 2017; Table 1). Most of the scientific literature has focused on the association between folate and B vitamin deficiency, and adverse reproductive outcomes in humans (Dasarthy *et al.*, 2010), however, the effect of methionine deficiency on reproductive health is an important line of enquiry. Methionine is often the first rate-limiting amino acid for protein synthesis in animal and human diets (Laurichesse *et al.*, 1998; Schwab and Broderick, 2017). In humans, vegetarians and vegans are at increased risk

of methionine deficiency, since plant proteins tend to be lower in methionine than animal proteins ([McCarty et al., 2009](#); [Kim et al., 2018](#)).

Table 1. Effect of maternal dietary deficiency of 1C metabolites during the periconceptual period in humans.

Dietary 1C metabolite deficiency		Reproductive outcome	Reference(s)
Folate	B9	NTDs Megaloblastic anaemia	Lucock (2000) Beaudin and Stover (2009) Cooper and Lowenstein (1966)
Vitamin B₁₂	B12	Infertility Recurrent abortion NTDs Pre-term birth Megaloblastic anaemia	Pront et al. (2009) Reznikoff-Etiévant et al. (2002) Lucock (2000) Beaudin and Stover (2009) Cooper and Lowenstein (1966)
Vitamin B₆	B6	Reduced conception rate	Reznikoff-Etiévant et al. (2002) Ronnberg et al. (2007)
Vitamin B₂	B2	Preeclampsia	Wacker et al. (2000)
Choline	Chol	NTDs	Shaw et al. (2004)
Betaine	TMG	NTDs	Shaw et al. (2004)
Methionine	Met	NTDs	Kalhan (2009) Shoob et al. (2001) Shaw et al. (2004)

Abbreviation(s): NTDs, neural tube defects; TMG, trimethylglycine.

A 5-year, population-based case-control study of 439 women reported a 30-55% lower NTD risk among women whose average daily dietary intake of methionine was greater than the lowest quartile of intake (>1580 mg/d; [Shoob et al., 2001](#)). Risks were also lowest for women whose diets were rich in other methionine cycle metabolites, specifically choline and betaine (TMG; [Shaw et al., 2004](#)).

It follows that the availability of methionine and other 1C metabolites during critical periods of mammalian development is essential to supply methyl groups for methylation reactions, particularly those that support high rates of maternal and fetal tissue synthesis and deposition during pregnancy and early life ([Rees et al., 2006](#); [Kurpad et al., 2014](#)). As important is the balance of methionine relative to other metabolites in the maternal diet as fetal growth and development can be retarded by methionine deficiency and excess ([Rees et al., 2006](#)).

With accumulating evidence to indicate that dietary imbalances in 1C metabolites are detrimental to health ([Stegers-Theunissen et al., 2013](#); [Obeid](#)

et al., 2017), there is a need for further investigation. Set against this general background is the need to improve our understanding of how 1C metabolism functions within the somatic cells of the mammalian ovary, oocyte and pre-implantation embryo. Extensive research investigating the function of 1C metabolism has been conducted in rodent liver (Balaghi *et al.*, 1993) with the help of mathematical models (Finkelstein and Martin, 1986; Finkelstein, 1990; Caudill *et al.*, 2001; Reed *et al.*, 2004; Korendyaseva *et al.*, 2008) but there is limited knowledge of how this series of interlinked metabolic pathways functions within reproductive tissues. Aside tissue-specific differences, there are species-specific differences in 1C metabolism between ruminants and non-ruminants that cannot be disregarded (Xue and Snoswell, 1985; Snoswell and Xue, 1987; Lambert *et al.*, 2002).

Knowledge of the function of 1C metabolism in ruminants is of particular agricultural and economic importance. Cattle and sheep have a low dietary intake of methyl donors in the post-ruminant state (the developmental stage when the rumen becomes fully functional for microbial fermentation and digestion of food) and are, therefore, sensitive to impairments to 1C metabolic pathways (Snoswell and Xue, 1987). As the liver is the major site of 1C metabolism (Lu and Mato, 2012; da Silva *et al.*, 2020), it seems insightful to begin by investigating the function of these pathways in this metabolically active tissue.

Previous studies from our laboratory suggest that methionine metabolism is likely to function differently in reproductive tissues than in the liver as transcripts encoding key methionine cycle enzymes were either absent or expressed at low levels in bovine ovarian cells, oocytes and early embryos (Kwong *et al.*, 2010). The metabolic implications of this, regarding the provision of dietary 1C substrates and cofactors, together with consequences of polymorphic variances in genes encoding 1C enzymes are not fully understood but are the subject of ongoing investigations. Hence, the broad aims and objectives of this thesis are to enhance our current understanding of the regulation of 1C metabolism in the ruminant liver, ovary and preimplantation embryo, with a specific focus on methionine metabolism and epigenetic programming of mammalian development.

Chapter 1

One-carbon metabolism and epigenetic regulation of periconceptual development

This chapter provides an overview of the interaction between maternal nutrition, one-carbon (1C) metabolism and epigenetic programming during mammalian embryo development. A detailed description of the biochemistry of hepatic 1C metabolism and related pathways is presented, followed by a summary of what is currently known about the regulation of 1C metabolism in the ovary and early embryo. Thereafter, the review focuses on methionine metabolism and DNA methylation within the preimplantation embryo, culminating in a working hypothesis.

1.1 Maternal nutrition, 1C metabolism and pregnancy outcome

One-carbon metabolism serves as a biochemical conduit between external environment and epigenetic regulation of early development ([Clare *et al.*, 2019](#)). It is now generally recognised that reproductive failures and problems associated with epigenetic programming of offspring health are due in no small measure to dietary disturbances in 1C pathways during the periconceptual period.

1.1.1 The periconceptual period

In women, this can be defined as a 5 to 6-month period that encompasses oocyte growth, fertilisation and embryonic development to week 10 of gestation (a stage which coincides with the closure of the secondary palate). The analogous phase in men encompasses the spermatogenic cycle which lasts approximately 75 days ([Steegers-Theunissen *et al.*, 2013](#)). Animal models use different timings around conception to define the periconceptual period according to gestation length, however, this stage of development typically includes gametogenesis, pre- and post-implantation embryogenesis and placentation for all model species ([Spencer *et al.*, 2004](#); [Padhee *et al.*, 2015](#)).

1.1.1.1 Epigenetic reprogramming

Two critical epigenetic reprogramming events take place during mammalian development. The first ensues after fertilisation when the gametic marks are erased and replaced with embryonic marks important for early embryo development ([Morgan *et al.*, 2005](#)). The paternal genome undergoes dynamic epigenetic reprogramming that involves the exchange of protamines for histones, the acquisition of histone modifications (i.e. histone code) and active

demethylation of DNA. In contrast, the maternal genome undergoes passive demethylation via DNA replication during subsequent cleavage stages to the morula stage (Santos *et al.*, 2002; Guo *et al.*, 2014). The embryo remains in a state of transcriptional quiescence that is maintained until a species-specific stage (2-cell in the mouse, 4-cell in the pig, and 8-16 cell in the cow and human) when transcription resumes during a process known as embryonic genome activation (EGA; Morgan *et al.*, 2005). Following EGA, a wave of *de novo* methylation aids the establishment of epigenetic programmes that give rise to the primary cell lineages of the blastocyst; the inner cell mass (ICM) and trophectoderm (TE). These embryonic and extraembryonic cell lineages acquire distinct epigenetic marks required for totipotency and correct initiation of embryonic gene expression patterns required for differentiation (Morgan *et al.*, 2005).

DNA methylation regulates chromatin structure and gene expression during early developmental processes, including X chromosome inactivation and genomic imprinting (Li, 2002). The former phenomenon requires that only one X chromosome is active in each somatic nucleus in females to regulate chromosome dosage relative to males (Barakat and Gribnau, 2012). The latter phenomenon requires that certain genes are monoallelically expressed in a parent-of-origin dependent manner (Barlow and Bartolomei, 2014). Genomic imprints originate in sperm and oocytes and are required for normal fetal and placental development (Peters, 2014). Whilst imprints are generally protected from the first genome-wide epigenetic reprogramming event that occurs during early embryogenesis, they are erased during the second epigenetic reprogramming event that occurs midgestation (Morgan *et al.*, 2005). Extensive demethylation of fetal primordial germ cells restores totipotency in preparation for sex-specific *de novo* methylation that takes place during gametogenesis (Morgan *et al.*, 2005; Zeng and Chen, 2019). As oogenesis takes place during gestation, female mammals are born with the maximum number of oocytes they will have in their lifetime. With respect to maternal diet, oogenesis represents a time when nutritional insults may impact germline reprogramming and ultimately a granddaughter's reproductive health via transgenerational inheritance of epigenetic marks (Padhee *et al.*, 2015).

1.1.1.2 Epigenetic effect of diet on periconceptual development

Significant epigenetic modifications to chromatin correspond with abnormal periconceptual development irrespective of the species. Subtle variations in 1C metabolism, including dietary imbalances in 1C metabolites, have been shown to perturb key methylation events that contribute to reproductive failure and poor pregnancy outcomes. A number of studies have identified epigenetic changes associated with dietary methyl supplementation (Table 1.1) or depletion (Table 1.2) during periconceptual development in a number of mammalian species.

Table 1.1 Methyl supplementation in maternal diet and epigenetic programming of periconceptual development.

Species	↑ 1C metabolite	Offspring phenotype	Epigenetic changes	Reference(s)
Mouse (Agouti)	Methionine, Folate, B12, Choline, Betaine	Altered coat colour (yellow → brown) ↓ obesity	↑ Methylation <i>A^{vy}</i> LTR sequence	Wolff et al. (1998) Cooney et al. (2002) Waterland & Jirtle (2003)
Mouse	Methionine, B12, Choline, Betaine	↓ Tail kinking in axin fused mutants	↑ Methylation <i>Axin</i> (Fu)	Waterland et al. (2006)
Rat	Choline	Altered histone methyltransferase <i>G9a</i> and <i>Suv39h1</i>	↑ H3K9me2, H3K27me3 (repressed chromatin) ↑ Methylation <i>G9a</i> <i>Suv39h1</i> liver and brain	Davison et al. (2009)
Pig	Betaine	↑ Glucocorticoid receptor mRNA in hippocampus	↑ miR-130b, miR-181a, miR-181d ↑ Methylation <i>GR</i> promoter	Sun et al. (2016)
Cow	B vitamins	↑ Blastocyst development, ↑ Day 8 hatching ↓ Carcinogenesis	↑ H3K27me3 <i>TXNIP</i> promoter, ↓ <i>Txnip</i> stress biomarker	Ikeda et al. (2018)
Human	Folate	↓ Carcinogenesis	↓ Methylation, ↑ miR-203, miR-375 in cervical cancer cell line	Hao et al. (2016)
Human	Folate	Altered DNA methylation	↑ Methylation at <i>ZFP57</i> DNA methylation regulator in CD4(+) immune cells	Amarasekera et al. (2014)
Human	Folate	Altered imprinting (genomic imprint)	↓ Methylation <i>H19/IGF2</i> in blood	Hoyo et al. (2011)
Human	Folate	Altered imprinting (genomic imprint)	↑ Methylation <i>IGF2</i> , ↓ <i>PEG3</i> , <i>LINE-1</i> in blood	Steegers-Theunissen et al. (2009) Haggarty et al. (2013) Jiang et al. (2012)
Human	Choline	Altered fetal HPA axis, cortisol-regulation	↑ Methylation <i>CRH</i> , <i>NR3C1</i> , ↑ H3K9me2 in placenta	Jiang et al. (2012)
Human	B6	↑ Birth weight (male offspring)	↑ Methylation <i>MEG</i> in blood	McCullough et al. (2016)

Arrows: ↑ increase, ↓ decrease. Abbreviation(s): 1C, one-carbon; *A^{vy}*, agouti viable yellow; *Axin*(Fu), axin-fused; B12, vitamin B₁₂; B6, vitamin B₆; CD4(+), cluster of differentiation 4; CRH, corticotropin-releasing hormone; GR, glucocorticoid receptor; H19, imprinted maternally expressed transcript; HPA, hypothalamic-pituitary-adrenal axis; IGF2, insulin like growth factor 2; LINE-1, long interspersed nuclear element 1; LTR, long terminal repeat; MEG3, maternally expressed 3; MiR, micro RNA; NR3C1, nuclear receptor subfamily 3 group C member 1; PEG3, paternally expressed 3; TXNIP, thioredoxin interacting protein; ZFP57, zinc finger protein 57 homolog.

Table 1.2 Methyl deficiency in maternal diet and epigenetic programming of periconceptual development.

Species	↓ 1C metabolite	Offspring phenotype	Epigenetic changes	Reference(s)
Mouse	Methionine, Folate, Choline	↑ Insulin resistance (male offspring)	-	Maloney <i>et al.</i> (2011)
Mouse	Methionine, Folate, B12, Choline	Altered imprinting (genomic imprint)	↑ <i>Igf2</i> DMR2 in kidney	Waterland <i>et al.</i> (2006b)
Mouse	Methionine	Altered amino acid metabolism	↓ H3K4me3, H3K27me3, H3K4me2 in liver	Mentch <i>et al.</i> (2015)
Mouse	Folate	↓ Plasma glucose, ↑ TAG	↓ Methylation <i>Slc39a4</i> fetal gut zinc transporter gene	McKay <i>et al.</i> (2011) McKay <i>et al.</i> (2014)
Mouse	Folate	-	↑ Methylation <i>Mthfr</i> in liver and brain	Lévesque <i>et al.</i> (2016)
Mouse	Choline	Altered cell cycle	↓ Methylation <i>Cdkn3</i> in brain	Niculescu <i>et al.</i> (2006)
Mouse	Choline	↓ Neural progenitor cell proliferation in hippocampus	↓ H3K9 methylation <i>calbindin 1</i> promoter in brain	Mehedint <i>et al.</i> (2010)
Mouse	Choline, B2	↑ Delayed, small embryos; ↑ cardiac defects	-	Chan <i>et al.</i> (2010)
Rat	Methionine, Choline	Altered DNA methylation	↓ Global methylation in liver	Wilson <i>et al.</i> (1984)
Rat	Choline	Altered DNA methylation and genomic imprinting	↑ <i>Igf2</i> DMR2, ↓ Methylation <i>Dnmt1</i> in liver	Kovacheva <i>et al.</i> (2007)
Sheep	Methionine, Folate, B12	↑ Adiposity, ↑ insulin resistance, altered immune function, hypertension	↓ Methylation of 4% CGIs (>50% affected loci specific to males)	Sinclair <i>et al.</i> (2007)

Arrows: ↑ increase, ↓ decrease. Abbreviation(s): 1C, one-carbon; B12, vitamin B₁₂; B2, vitamin B₂; Cdkn3, cyclin-dependent kinase inhibitor 3; CGIs, CpG islands; DMR2, differentially methylated region 2; Dnmt1, DNA methyltransferase 1; *Igf2*, insulin like growth factor 2; *Mthfr*, methyltetrahydrofolate reductase; *Slc39a4*, solute carrier family 39 member 4; TAG, triacylglyceride.

The relationships between dietary methyl donors and epigenetic modifications became apparent in studies using methylation indicator-mouse models in which changes in DNA methylation give rise to visible, long-lasting offspring phenotypes (Ideraabdullah and Zeisel, 2018). For example, the viable yellow agouti (*A^{vy}*) mouse is an epigenetic biosensor for nutritional alterations to the fetal epigenome (Dolinoy, 2008). Agouti mice harbour a metastable epiallele resulting from the insertion of an intracisternal A particle (IAP) retrotransposon upstream of the *Agouti* gene transcription start site. A ‘retrotransposon’ is a widespread mobile genetic element that replicates through reverse transcription of RNA and integrates the product DNA into the host genome (Cordaux and Batzer, 2009). The IAP retrotransposon is epigenetically regulated. When hypomethylated, the *A^{vy}* gene is expressed and mice possess a yellow coat colour, obesity, hyperinsulinemia and increased susceptibility to tumours (Morgan *et al.*, 1999). When hypermethylated, the *A^{vy}* gene is repressed and mice are brown in colour with a lean body composition (Wolff *et al.*, 1998).

Methyl donor supplementation to an already nutritionally adequate diet fed to pregnant yellow agouti mice permanently increased DNA methylation and altered the body composition and metabolism of their offspring (Wolff *et al.*, 1998; Waterland and Jirtle, 2003; Table 1.1).

The agouti mouse model provided the first evidence that dietary excesses of 1C metabolites during early development can alter the epigenome and metabolic phenotype of offspring. As discussed above, these epigenetic modifications appear to be transgenerationally heritable due to their incomplete erasure during germline reprogramming meaning epigenetic gene regulation may persist transgenerationally despite lack of continued exposure in subsequent generations (Waterland and Jirtle, 2003). This is of particular importance considering the aforementioned issues raised by mandatory fortification of human diets with folic acid (FA) and the detrimental effects of imbalances 1C metabolites. Moreover, putative metastable epialleles have since been identified in humans and they are correlated with seasonal fluctuation in maternal nutrition around the time of conception (Waterland *et al.*, 2010; Dominguez-Salas *et al.*, 2014).

According to Maloney *et al.* (2011), diets containing an excess of methyl groups are unlikely to be encountered outside an experimental setting other than when taking supplements, such as 400 µg FA. Human diets, especially vegetarian and vegan diets, are more likely to be deficient in methionine and vitamin B₁₂ leading to a low availability of methyl groups (McCarty *et al.*, 2009; Kim *et al.*, 2018). The Pune Maternal Nutritional Study showed that ~67% of expectant mothers had B12 deficiency whilst folate deficiency affected only one study participant. The offspring of mothers with a combination of high folate and low vitamin B12 concentrations were the most insulin resistant and, therefore, at increased risk of developing type II diabetes (Yajnik *et al.*, 2008). These findings highlight concerns about the masking of B12 deficiency by folate and raise questions regarding suitable dietary intakes of both nutrients to ensure a safe balance between the two is established during pregnancy.

Methyl deficient (MD) diets, in conjunction with single nucleotide polymorphisms (SNPs) in 1C metabolism genes, can lead to epigenetic alterations in DNA and histone methylation that regulate key developmental processes (Xu and Sinclair, 2015). In turn, this can lead to wide-spread metabolic alterations in protein, lipid and carbohydrate metabolism due to the complex relationship

between 1C metabolism and related pathways (Maloney *et al.*, 2007; McNeil *et al.*, 2008; Maloney *et al.*, 2011).

1.2 One-carbon (1C) metabolism and related pathways

One-carbon (1C) metabolism comprises the linked methionine-folate cycle and *transsulphuration* pathway (Figure 1.1; Xu and Sinclair, 2015; Clare *et al.*, 2019). This complex metabolic network facilitates 1C transfer in the form of methenyl, formyl and methyl moieties, required for essential cellular processes within the cytoplasm, nucleus and mitochondria (Stover, 2009; Stover and Field, 2011). Such processes include molecular biosynthesis (e.g. nucleotides, proteins, polyamines, phospholipids and creatine); epigenetic regulation of gene expression via methylation of DNA, RNA and histones; and redox defence (Lucock, 2000; Ducker and Rabinowitz, 2017). Dietary constituents such as methionine, folate (vitamin B9), B vitamins (B12, B6, B2) and choline (betaine) are essential 1C enzyme substrates or cofactors (Mason, 2003).

1.2.1 Methionine-folate cycles

The linked methionine-folate cycles facilitate transmethylation reactions, including chromatin methylation which plays a pivotal role in epigenetic regulation of gene expression (Razin and Cedar, 1991). Methionine is adenylated by methionine adenosyltransferase (MAT; EC 2.5.1.6) to S-adenosylmethionine (SAM), a universal methyl donor involved in >200 downstream cellular transmethylation reactions (Roje, 2006; Figure 1.1). During methyl (CH₃) transfer, SAM is converted to S-adenosylhomocysteine (SAH) (Ulrey *et al.*, 2005), which is hydrolysed to homocysteine (Hcy) and adenosine through a reversible reaction catalysed by S-adenosylhomocysteine hydrolase (AHCY; EC 3.3.1.1; Caudill *et al.*, 2001).

Folate-dependent remethylation of Hcy to methionine is catalysed by B12-dependent methionine synthase (MTR; EC 2.1.1.13) to complete the methionine cycle (Škovierová *et al.*, 2016). Methionine synthase reductase (MTRR; EC 1.16.1.8) restores MTR activity by catalysing the reductive methylation of cob(II)alamin to methylcob(III)alamin to maintain adequate levels of bioactive B12 cofactor for Hcy remethylation (Gaughan *et al.*, 2001; Ho *et al.*, 2013). Reductive methylation of cob(II)alamin for MTR restoration is an example of SAM-dependent transmethylation (Ho *et al.*, 2013).

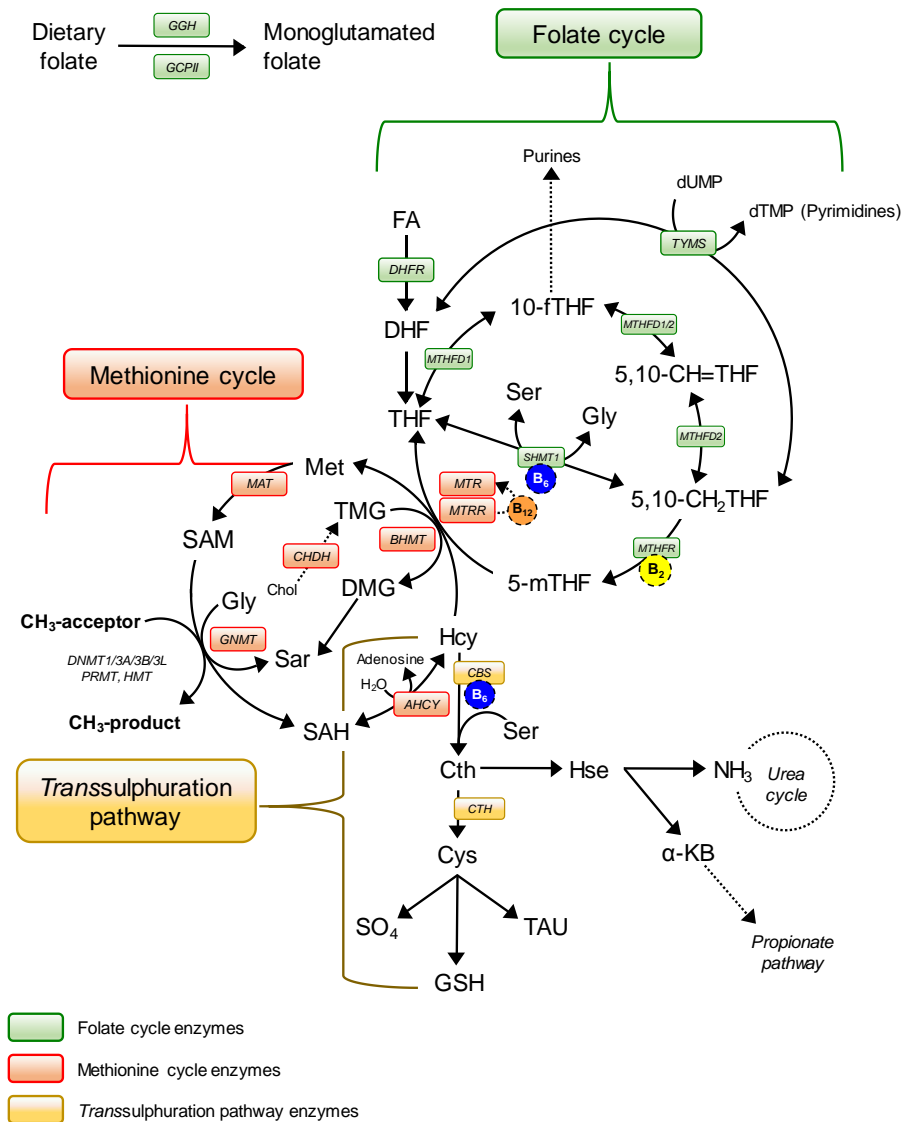


Figure 1.1 One-carbon (1C) metabolism includes the linked methionine-folate cycle and *transsulphuration* pathway. Adapted from [Clare et al. \(2019\)](#).

Folate cycle enzymes (green boxes): DHFR, dihydrofolate reductase; GCPII, glutamate carboxypeptidase; GGH, γ -glutamyl hydrolase; MTHFD1/2, methylenetetrahydrofolate dehydrogenase; MTHFR, 5,10-methylenetetrahydrofolate reductase; SHMT, serine hydroxymethyltransferase; TYMS, thymidylate synthase. Methionine cycle enzymes (red boxes): AHCY; S-adenosyl-L-homocysteine hydrolase; BHMT, betaine-homocysteine S-methyltransferase; CHDH, choline dehydrogenase; GNMT, glycine N-methyltransferase; MATI/III, methionine adenosyltransferase; MTR, methionine synthase; MTRR, methionine synthase reductase. Transsulphuration pathway enzymes (yellow boxes): CBS, cystathionine β -synthase; CTH, cystathionine γ -lyase. Key methyltransferase enzymes: DNMT1/3A/3B/3L, *de novo* and maintenance DNA methyltransferases; HMT, histone methyltransferase; PRMT, protein arginine methyltransferase. Enzyme cofactors (coloured circles): vitamin B₂, B₆, and B₁₂. Substrates: 5,10-CH=THF, 5,10-methylenetetrahydrofolate; 5,10-CH₂THF, 5,10-methylenetetrahydrofolate; 5-mTHF, 5-methyltetrahydrofolate; 10-fTHF, 10-formyltetrahydrofolate; α -KB, α -ketobutyrate; Chol, choline; Cth, cystathionine; Cys, cysteine; DHF, dihydrofolate; DMG, dimethylglycine; dTMP, thymidine monophosphate; dUMP, deoxyuridine monophosphate; FA, folic acid; Gly, glycine; GSH, glutathione; Hcy, homocysteine; Hse, homoserine; Met, methionine; NH₃, ammonia; SAH, S-adenosylhomocysteine; SAM, S-adenosylmethionine; Sar, sarcosine; Ser, serine; SO₄, sulphate; TAU, taurine; THF, tetrahydrofolate; TMG, trimethylglycine/betaine.

A parallel folate-independent pathway, catalysed by B6-dependent enzyme, betaine-homocysteine S-methyltransferase (BHMT; EC 2.1.1.5; [Finkelstein and Martin, 1984](#)), involves the transfer of a methyl group from trimethylglycine (TMG), otherwise known as betaine, to generate dimethylglycine (DMG) and methionine ([Li et al., 2008](#)). Whilst it is uncertain why animals have two independent pathways for Hcy remethylation, BHMT accounts for up to 50% Hcy remethylation to methionine ([McKeever et al., 1991](#); [Garrow, 1996](#); [Chadwick et al., 2000](#); [Yamashita et al., 2000](#)), emphasising the importance of this pathway in the liver.

Folates (B9) are a family of enzyme cofactors that function as versatile methyl donors in 1C metabolism ([Stover, 2009](#)). Unlike bacteria, animals cannot endogenously synthesise folates, therefore, requirements must be met entirely from dietary sources ([Garratt et al., 2005](#)). Due to their hydrophilic nature, folate absorption requires functionally diverse transport mechanisms within the proximal small intestine ([Visentin et al., 2014](#)). Such mechanisms involve the reduced folate carrier (RC), proton-coupled folate transporter (PCFT) and folate receptor (FR). Folates are hydrolysed into their monoglutamated forms in the intestinal mucosa by γ -glutamyl hydrolase (GGH; EC 3.4.19.9) and glutamate carboxypeptidase II (GCP II; EC 3.4.17.21) to facilitate absorption ([Zhao et al., 2009](#); Figure 1.1).

Upon reaching systemic tissues, folate monoglutamates are converted to 5-methyltetrahydrofolate (5-mTHF); the predominant species in non-hepatic cells and are subsequently polyglutamated for cellular retention and 1C coenzyme function ([Xu and Sinclair, 2015](#)). Folic acid (FA), the synthetic folate supplement, is fully oxidised not a bioactive coenzyme ([Shane, 2008](#)). Folic acid is reduced to dihydrofolate (DHF) and then to the bioactive form, tetrahydrofolate (THF) by dihydrofolate reductase (DHFR; EC 1.5.1.3), before entering the folate cycle ([Ducker and Rabinowitz, 2017](#)). Subsequently, THF is converted to 5,10-methylenetetrahydrofolate (5,10-CH₂THF) by B6-dependent enzyme, serine hydroxymethyltransferase (SHMT; EC 2.1.2.1) and then irreversibly reduced to 5-mTHF by B2-dependent methylenetetrahydrofolate reductase (MTHFR; EC 1.5.1.20). Alternatively, THF can be converted to 10-formyltetrahydrofolate (10-fTHF) through consecutive reactions catalysed by methylenetetrahydrofolate dehydrogenase enzymes (MTHFD; EC 1.5.1.5). Demethylation of 5-mTHF completes the folate cycle as 1C is donated for remethylation of Hcy to methionine ([Mentch and Locasale, 2016](#)).

1.2.2 *Transsulphuration pathway*

When methionine and folate levels are adequate, SAM allosterically regulates Hcy catabolism via a two-step *transsulphuration* pathway that requires the bioactive B6 cofactor (Figure 1.1). SAM coordinates *transsulphuration* by inhibiting MTHFR and activating cystathionine β -synthase (CBS; EC 4.2.1.22; Selhub, 1999; Lucock, 2000), the primary enzyme in the *transsulphuration* pathway that catalyses condensation of serine (Ser) with Hcy to produce cystathionine (Cth). The secondary enzyme, cystathionine γ -lyase (CTH; EC 4.4.1.1), yields cysteine (Cys); a precursor for glutathione (GSH) which is a major endogenous antioxidant in cells (Ebisch *et al.*, 2006; Aquilano *et al.*, 2014).

1.2.3 Propionate pathway

Cystathionine (Cth) hydrolysis also yields α -ketobutyrate (α -KB), an intermediate that is transformed to propionyl CoA by the branched chain α -ketoacid dehydrogenase complex (BCKDC; EC 1.2.4.4; EC 2.3.1.168; EC 1.8.1.4; Figure 1.2). Amino acids, such as methionine, threonine (Thr), isoleucine (Ile), valine (Val); odd-chain fatty acids (OCFA), cholesterol and propionate (PPA) are also catabolised to produce propionyl-CoA (Tretter *et al.*, 2016). In the mitochondria, propionyl-CoA is carboxylated to D-methylmalonyl-CoA by propionyl-CoA carboxylase (PCCA/B; EC 6.4.1.3), an enzyme that requires biotin as a cofactor (Ballhausen *et al.*, 2009).

D-methylmalonyl-CoA is epimerised to L-stereoisomer by methylmalonyl-CoA epimerase (MCEE; EC 5.1.99.1) before undergoing an intramolecular rearrangement catalysed by B12-dependent methylmalonyl-CoA mutase (MUT; EC 5.4.99.2) to produce succinyl-CoA, an intermediate of the tricarboxylic acid (TCA) cycle (De Vadder *et al.*, 2016). When vitamin B₁₂ is absent, L-methylmalonyl-CoA forms methylmalonic acid (MMA), a reliable biomarker of B12 status and 1C metabolic function (Mendonça *et al.*, 2017).

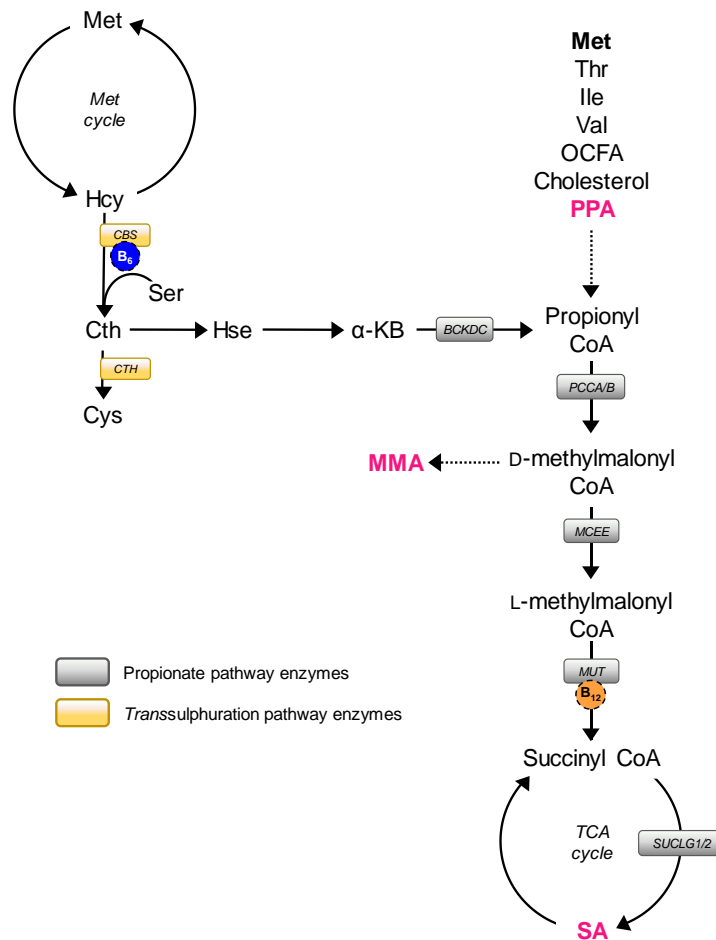


Figure 1.2 One-carbon (1C) substrates and cofactors serve as key intermediates of propionate and energy metabolism. Adapted from [Clare et al. \(2019\)](#).

Propionate metabolism enzymes (grey boxes): BCKDC, α -keto acid dehydrogenase; MCEE, methylmalonyl-CoA epimerase; MUT, methylmalonyl-CoA mutase; PCCA/B, propionyl-CoA carboxylase; SUCLG1/2, succinate CoA ligase. Transsulphuration pathway enzymes (yellow boxes): CBS, cystathionine β -synthase; CTH, cystathionine γ -lyase. Enzyme cofactors (coloured circles): vitamin B6 and B12. Substrates: α -KB, α -ketobutyrate; Cth, cystathionine; Hcy, homocysteine; Hse, homoserine; Ile, isoleucine; Met, methionine; MMA, methylmalonic acid; OCFA, odd-chain fatty acids; Ser, serine; Thr, threonine; Val, valine.

1.2.4 Polyamine pathway

Ornithine (Orn) is decarboxylated to the primary polyamine, putrescine (Put), by B6-dependent enzyme, ornithine decarboxylase (ODC; EC 4.1.1.17; [Pegg, 2006](#); Figure 1.3). Putrescine is further processed to produce the more abundant polyamines, spermidine (Spd) and spermine (Spm), by aminopropyltransferases, spermidine synthase (SRM; EC 2.5.1.16) and spermine synthase (SMS; EC 2.5.1.22), respectively ([Gamble et al., 2012](#)). After Put production, the second rate-limiting factor for higher polyamine

synthesis is the decarboxylation of SAM to provide the aminopropyl donor, dSAM, required for Spd and Spm synthesis (Pegg, 2016).

Polyamine biosynthesis is linked to the methionine salvage pathway. Sulphur-containing metabolites, such as 5'-methylthioadenosine (MTA), are recycled back to methionine, demonstrating an additional pathway for methionine regulation (Albers *et al.*, 2009; Chou *et al.*, 2014).

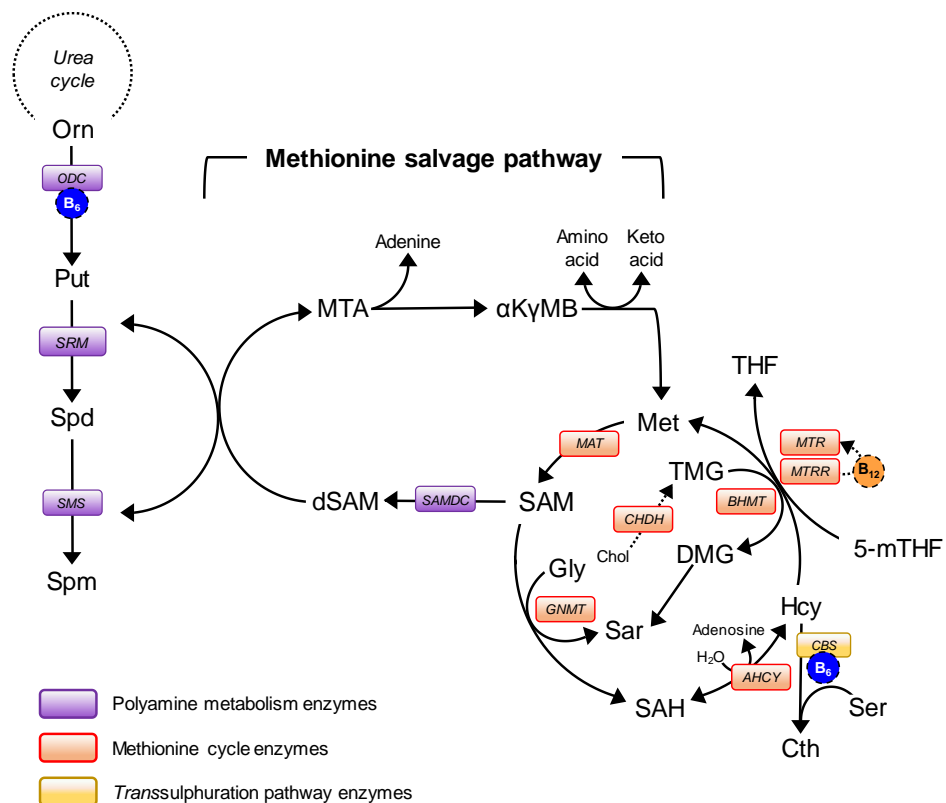


Figure 1.3 Polyamine synthesis and the methionine salvage pathway requires decarboxylated SAM as an aminopropyl donor. Adapted from Clare *et al.* (2019).

Polyamine metabolism enzymes (purple boxes): ODC, ornithine decarboxylase; SAMDC, S-adenosylmethionine decarboxylase; SMS, spermine synthase; SRM, spermidine synthase. Methionine cycle enzymes (red boxes): AHCY, S-adenosyl-L-homocysteine hydrolase; BHMT, betaine-homocysteine S-methyltransferase; CHDH, choline dehydrogenase; GNMT, glycine N-methyltransferase; MATI/III, methionine adenosyltransferase; MTR, methionine synthase; MTRR, methionine synthase reductase. Enzyme cofactors (coloured circles): vitamin B6 and B12. Substrates: α KyMB, α -keto- γ -methiolbutyrate; Chol, choline; DMG, dimethylglycine; Gly, glycine; Hcy, homocysteine; Met, methionine; MTA, 5'-methylthioadenosine; Orn, ornithine; Put, putrescine; SAH, S-adenosylhomocysteine; SAM, S-adenosylmethionine; Sar, sarcosine; Spd, spermidine; Spm, spermine; TMG, trimethylglycine/betaine.

1.2.5 Phosphatidylcholine pathway

S-adenosylmethionine (SAM) donates three methyl groups to phosphatidylethanolamine (PE) to synthesise phosphatidylcholine (PC), an abundant glycerophospholipid constituent of cell membranes that facilitates lipid

transport in mammalian tissues (Wright *et al.*, 2004; Figure 1.4). This reaction is catalysed by phosphatidylethanolamine methyltransferase (PEMT; EC 2.1.1.17), an enzyme predominantly expressed in the liver (Kanno *et al.*, 2007; Vance *et al.*, 2013). Alternatively, PC can be synthesised from choline via the cytidine diphosphate (CDP)-choline pathway (Cole *et al.*, 2012).

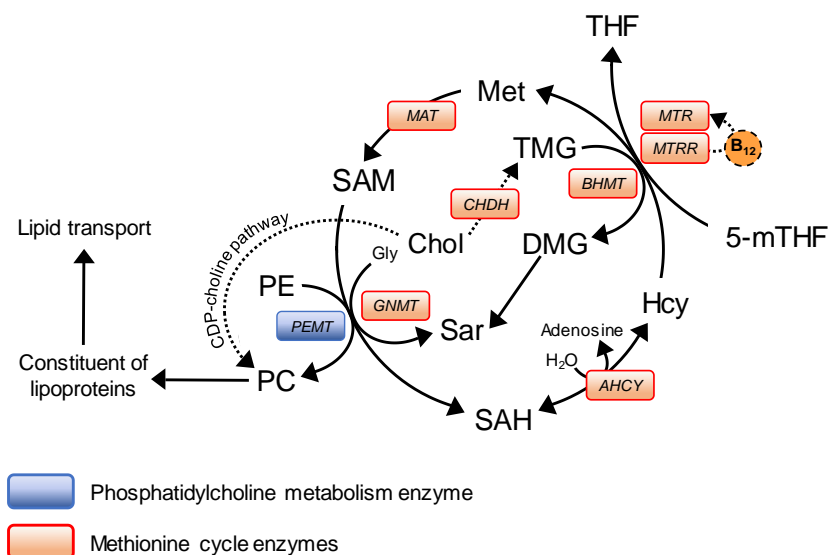


Figure 1.4 Phosphatidylcholine can be synthesised by choline or via the cytidine diphosphate (CDP)-choline pathway. Adapted from Clare *et al.* (2019).

Phosphatidylcholine metabolism enzyme (blue box): PEMT, phosphatidylethanolamine methyltransferase. Methionine cycle enzymes (red boxes): AHCY, S-adenosyl-L-homocysteine hydrolase; BHMT, betaine-homocysteine S-methyltransferase; CHDH, choline dehydrogenase; GNMT, glycine N-methyltransferase; MATI/III, methionine adenosyltransferase. Enzyme cofactor (orange circle): vitamin B12. Substrates: Chol, choline; DMG, dimethylglycine; Gly, glycine; Hcy, homocysteine; Met, methionine; PC, phosphatidylcholine; PE, phosphatidylethanolamine; SAH, S-adenosylhomocysteine; SAM, S-adenosylmethionine; TMG, trimethylglycine/betaine.

1.2.6 Nucleotide biosynthesis

Inosine-monophosphate (IMP) is the central intermediate for the *de novo* synthesis of purine nucleotides (Shuvalov *et al.*, 2017). Generation of IMP from phosphoribosyl pyrophosphate (PRPP) requires the sequential organisation of several multifunctional enzymes (Pedley and Benkovic, 2017). Phosphoribosylglycinamide formyltransferase (GART; EC 2.1.2.2) and phosphoribosylamidazolecarboxamide formyltransferase (ATIC; EC 2.1.2.3) provide C2 and C8 atoms for purine ring synthesis using 10-fTHF as a 1C donor. Next, IMP is oxidised to xanthine monophosphate (XMP), a precursor for adenine and guanine nucleotides (Pedley and Benkovic, 2017). The precursor for pyrimidine synthesis, uridine monophosphate (UMP), does not require 1C

cofactors. Conversion of UMP to deoxyuridine monophosphate (dUMP) is catalysed by nucleoside diphosphate kinase (NME; EC 2.7.4.6). In a reaction catalysed by thymidylate synthase (TYMS; EC 2.1.45), 5,10-CH₂-THF donates 1C to convert dUMP to thymidine monophosphate (dTMP) and becomes oxidised to DHF in the process. Subsequently, DHF is reduced to THF to enclose the metabolic loop (Shuvalov *et al.*, 2017; Figure 1.5).

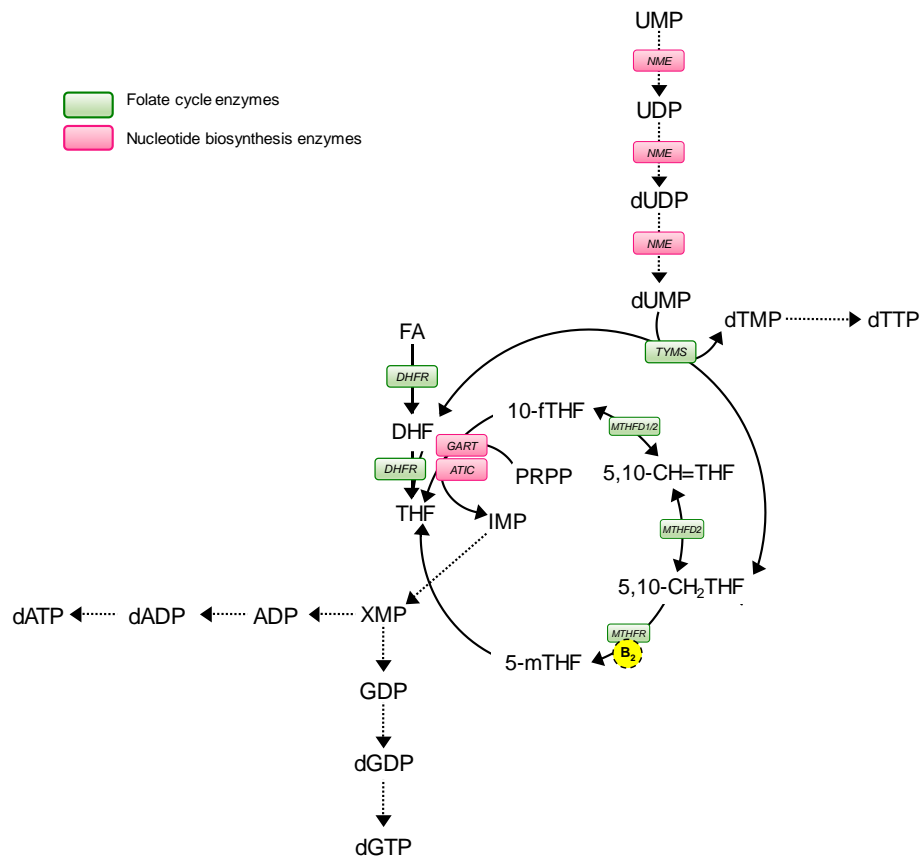


Figure 1.5 One-carbon (1C) metabolism provides purines (adenine and guanine), and pyrimidine, thymine, for nucleotide biosynthesis. Adapted from [Clare *et al.* \(2019\)](#).

Nucleotide biosynthesis enzymes (pink boxes): ATIC, phosphoribosylaminoimidazole-carboxamide formyltransferase; GART, phosphoribosylglycinamide formyltransferase; NME, nucleoside diphosphate kinase. Folate cycle enzymes (green boxes): DHFR, dihydrofolate reductase; MTHFD1/2, methylenetetrahydrofolate dehydrogenase; TYMS, thymidylate synthase. Enzyme cofactor (yellow circle): vitamin B₁₂. Substrates: 5,10-CH=THF, 5,10-methenyl-tetrahydrofolate; 5,10-CH₂THF, 5,10-methylenetetrahydrofolate; 10-fTHF, 10-formyl-tetrahydrofolate; ADP, adenosine diphosphate; dADP, deoxyadenosine diphosphate; dATP, deoxyadenosine triphosphate; dGDP, deoxyguanosine diphosphate; dGTP, deoxyguanosine triphosphate; DHF, dihydrofolate; dTMP, thymidine monophosphate; dTTP, thymidine triphosphate; dUDP, deoxyuridine diphosphate; dUMP, deoxyuridine monophosphate; GDP, guanosine diphosphate; IMP, inosine monophosphate; PRPP, phosphoribosyl pyrophosphate; THF, tetrahydrofolate; UDP, uridine diphosphate; UMP, uridine monophosphate; XMP, xanthine monophosphate.

1.3 Genetics of 1C metabolism

Inter-individual and ethnic variability in epigenetic regulation of gene expression may arise due to single nucleotide polymorphisms (SNPs) within 1C metabolism and epigenetic regulator genes, and differentially methylated target DNA sequences (Clare *et al.*, 2019). Polymorphic variants can act synergistically with nutritional deficiencies to magnify imbalances which may, in turn, affect methyl donor synthesis and epigenetic regulation of gene expression causing a wide range of reproductive and developmental outcomes in humans (Appendix Table 1.1).

Insight into the function of key 1C enzymes, particularly during periconceptual development, can be obtained from targeted or complete deletions of specific enzymes in the pathways using animal models (Appendix Table 1.2). Whilst gene deletion (or inhibition) does not recapitulate the effect of a SNP, they still offer valuable mechanistic insight into enzyme function and downstream metabolic and developmental consequences.

1.3.1 Hyperhomocysteinemia (HHcy)

Single nucleotide polymorphisms and gene deletions that impair 1C metabolic pathways often lead to hyperhomocysteinemia (HHcy), a condition characterised by elevated Hcy concentrations (Figure 1.1) in plasma. Mild hyperhomocysteinemia is prevalent in subjects polymorphic for a number of enzymes involved in 1C metabolism (Midttun *et al.*, 2007; Tsitsiou *et al.*, 2009; Appendix Table 1.1). In humans, the reference range of Hcy for healthy adults is 5-15 $\mu\text{mol/L}$ (Jacobsen, 1998). Mild, moderate and severe HHcy conditions are characterised by plasma concentrations of 15-25 $\mu\text{mol/L}$, 25-50 $\mu\text{mol/L}$ and >50 $\mu\text{mol/L}$, respectively (Brustolin *et al.*, 2010).

Homocysteine is a sensitive biomarker of aberrant 1C metabolic function and an independent risk factor for various diseases, including cancer, cardiovascular disease, and neurological and reproductive disorders (Škovierová *et al.*, 2016). Elevated plasma Hcy has been associated with reduced placental weight, placental abruption, preeclampsia, recurrent pregnancy loss, NTDs, oral clefts, Down's syndrome and small for gestational age babies (Hague, 2003; Brustolin *et al.*, 2010; Bergen *et al.*, 2012; Ganu *et al.*, 2013; Cavallé-Busquets *et al.*, 2020). High concentrations of Hcy in follicular fluid can have a detrimental effect on oocyte and embryo quality (Ebisch *et al.*,

2006), leading to poor *in vitro* fertilisation (IVF) outcomes as reflected by decreased pregnancy and implantation rates in affected patients (Pachiarotti *et al.*, 2007). Consequently, concentrations in follicular fluid or embryo culture media can provide a useful metabolic profiling marker of fertilisation rate, embryo quality and pregnancy outcome in patients undergoing assisted reproduction technology (ART) procedures (Berker *et al.*, 2009; Boyama *et al.*, 2016).

1.3.1.1 HHcy and epigenetics

Several lines of evidence implicate that epigenetic mechanisms underpin Hcy-related pathologies (Škovierová *et al.*, 2016). The bidirectional reaction catalysed by AHCY (Figure 1.1) has a dynamic equilibrium that strongly favours SAH synthesis over hydrolysis (Castro *et al.*, 2003). A rise in Hcy can, therefore, cause accumulation of SAH which is a potent inhibitor of DNA methyltransferase enzymes (DNMTs; Chen *et al.*, 2010). A decreased SAM:SAH ratio is predictive of global DNA hypomethylation with consequences for epigenetic programming (Caudill *et al.*, 2001). Thus, Hcy must be metabolised effectively to prevent SAH accumulation and to normalise 1C metabolic flux (Blom and Smulders, 2011).

Since HHcy is often diagnosed in conjunction with decreased plasma folate and B12 in infertile patients (Dhillon *et al.*, 2007), it may not seem surprising that Hcy concentrations are responsive to dietary intakes of specific 1C nutrients. Plasma Hcy concentrations can be lowered by supplementation with FA, B12 (cobalamin) and B6 (pyridoxine; Malinow *et al.*, 1999; Boxmeer *et al.*, 2008; Boxmeer *et al.*, 2009), whereas methionine supplementation can increase concentrations (Ditscheid *et al.*, 2005). Accordingly, dietary methionine restriction is a potential treatment for patients with Mudd's disease who suffer methionine adenosyltransferase (MAT) deficiency and who exhibit elevated methionine and Hcy concentrations (Chien *et al.*, 2015; Appendix Table 1.1).

The foregoing discussion is further complicated by the fact that 1C metabolism genes are epigenetically regulated by DNA methylation in their own right (Uekawa *et al.*, 2009; Dobbs *et al.*, 2013; Ho *et al.*, 2015). Excluding studies concerned with cancer (Huidobro *et al.*, 2013), there is limited information about the precise nature and clinical significance of such interactions. The extent to which methyl deficiency may affect 1C gene expression warrants further investigation.

1.4 Regulation of 1C metabolism in the mammalian embryo

Most of the detailed research concerning the regulation of 1C metabolism is restricted to the mammalian liver (Okuyama *et al.*, 1976; Balaghi *et al.*, 1993; Shibata *et al.*, 2013; Zhang, 2018) with comparatively little research conducted on reproductive cells and embryos (Sinclair and Singh, 2007; Kwong *et al.*, 2010). This is surprising given the importance attached to FA supplementation in the diet of intending mothers to prevent congenital abnormalities (Lucock, 2000; McNulty *et al.*, 2000; Beaudin and Stover, 2009; De-Regil *et al.*, 2010) and the compelling evidence that dietary methyl group availability during periconceptual development can have long-lasting metabolic and developmental health consequences for offspring.

Transcripts for 1C metabolic enzymes have been detected in human embryonic stem cells (hESCs; Steele *et al.*, 2005), human and bovine germinal vesicle oocytes, and bovine preimplantation embryos (Bhenkhalifa *et al.*, 2010; Ikeda *et al.*, 2010; Kwong *et al.*, 2010). However, the absence of *methionine adenosyltransferase 1A (MAT1A)* and *betaine homocysteine S-methyltransferase (BHMT)* transcripts within the bovine follicle-enclosed oocyte and preimplantation embryo indicates that the methionine cycle operates differently in reproductive cells to hepatocytes, perhaps rendering oocytes and embryos more sensitive to methyl availability (Kwong *et al.*, 2010; Ikeda *et al.*, 2010). The metabolic implications of these tissue-specific transcriptional differences remain unknown.

Aside tissue-specific differences, there are species-specific differences in methionine cycle transcript expression. To contrast observations in cattle, *Bhmt* is transiently expressed within the ICM of the mouse blastocyst (Lee *et al.*, 2012). *Bhmt* mRNA expression was first detected in morula but protein levels and enzyme activity were not detected until the blastocyst stage. Deletion of *Bhmt* reduced ICM cell number, decreased DNA methylation within the ICM, and increased fetal resorption following embryo transfer (Lee *et al.*, 2012). Detrimental consequences of *Bhmt* deletion were independently rescued by exogenous methionine and SAM supplementation (200 $\mu\text{mol/L}$; Lee *et al.*, 2012; Zhang *et al.*, 2015). Collectively, these findings identify an indispensable role of BHMT in the provision of methyl groups for the establishment of methylation patterns within the murine preimplantation embryo.

1.5 Epigenetics and methylation

The three main epigenetic mechanisms that regulate gene expression are DNA methylation, post-translational histone modifications (histone code) and non-coding RNAs (Xu and Sinclair, 2015). Together, these non-genetic covalent modifications to chromatin affect transcription and readout of DNA. This allows genetically identical cells to differ phenotypically within and between cell lineages (Canovas and Ross, 2016; Maldonado *et al.*, 2019). Such epigenetic processes are critical for interpretation of the genome in response to physiological factors and environmental stimuli. Together with other regulatory elements, epigenetic mechanisms contribute to lineage- and tissue-specific gene expression that contributes toward mammalian preimplantation embryo development and differentiation (Hemberger *et al.*, 2009).

1.5.1 Genomic DNA (gDNA) methylation

The most extensively studied mechanism of epigenetic gene regulation is genomic DNA (gDNA) methylation (Anderson *et al.*, 2012), a repressive epigenetic modification associated with stable gene silencing (Lande-Diner *et al.*, 2007). DNA methylation depends upon the availability of methyl groups transferred from SAM (Murín *et al.*, 2017; Figure 1.1). SAM-dependent transmethylation of DNA, RNA and proteins (e.g. histones) is catalysed by a family of DNA methyltransferase enzymes (DNMTs; EC 2.1.1.37). DNA methyltransferase 1 (DNMT1) recognises hemimethylated DNA and maintains DNA methylation during mitosis by methylating the unmethylated strand (Leonhardt *et al.*, 1992). Conversely, DNMT3A and DNMT3B do not distinguish between methylated substrates and are responsible for *de novo* methylation (Jurkowska *et al.*, 2011; Jin and Robertson, 2013). DNA methyltransferase-like protein (DNMT3L) lacks the conserved catalytic domain common to DNMTs and, therefore, lacks inherent methyltransferase activity. However, through allosteric cooperation with DNMT3 family enzymes, DNMT3L facilitates germline DNA methylation and specifically genomic imprinting during gametogenesis (Chédin *et al.*, 2002; Hata *et al.*, 2002). DNMT2 also lacks DNA methyltransferase activity but catalyses transfer RNA (tRNA) methylation (Goll *et al.*, 2006; Kaiser *et al.*, 2017).

1.5.1.1 CpG methylation

In mammals, the primary site of DNA methylation is the covalent attachment of a methyl (CH₃) group at the fifth carbon position of the pyrimidine ring of cytosine to form 5-methylcytosine (5mC). Cytosine methylation predominantly occurs at the 5'-CpG-3' dinucleotide in mammalian cells, whereby cytosine is linked to guanine by a phosphate bond (Lim and Maher, 2010; Deaton and Bird, 2011). However, in certain cell types, such as embryonic stem cells (ESCs), 5mC also occurs at CHG and CHH sites, where 'H' represents a cytosine (C), thymine (T) or adenine (A) (Feng *et al.*, 2010).

Approximately 60-80% of CpG dinucleotides in the human genome are methylated, whereas <10% are unmethylated and clustered together within short interspersed GC-rich DNA sequences (i.e. 500-2000 base pairs) known as CpG islands (CGIs; Lim and Maher, 2010; Zeng and Chen, 2019). The human genome contains ~30,000 CGIs (Jeziorska *et al.*, 2017), around half of which contain transcription start sites since they are found at the promoters of virtually all protein coding genes, including housekeeping, tissue-specific and developmental regulator genes (Deaton and Bird, 2011). While the majority of CGIs associated with promoters are unmethylated, repetitive sequences (i.e. retrotransposons), centromeric and pericentromeric repeats, and intragenic regions (i.e. gene bodies) are methylated during development. The epigenetic mechanisms by which some CGIs become differentially methylated under such circumstances are not yet understood (Jeziorska *et al.*, 2017; Zeng and Chen, 2019). It follows that 5mC is involved in almost all processes during preimplantation embryo development, including transcriptional regulation, silencing of retrotransposons, X-chromosome inactivation and genomic imprinting (Hochberg *et al.*, 2011; Smith and Meissner, 2013; Messerchmidt *et al.*, 2014).

1.5.1.2 Non-CpG methylation

Non-CpG methylation involves the methylation of cytosine followed by adenine (CpA), cytosine (CpC), and thymine (CpT). Like CpG methylation, non-CpG methylation is distributed throughout the genome and catalysed by DNMTs. These methylation marks are restricted to specific cell types, such as ESCs, oocytes, neurones and glial cells, however, knowledge of their cell-specific

function remains incomplete (Patil *et al.*, 2014; Jang *et al.*, 2017; Lee *et al.*, 2017).

Jiang and colleagues (2018) measured detectable levels of non-CpG methylation in early bovine embryos. Non-CpG methylation followed a similar enrichment pattern to CpG methylation and was located within CGIs in and around gene bodies. It is postulated that the co-existence of non-CpG and CpG methylation reflects a state of *de novo* DNMT hyperactivity (Ziller *et al.*, 2011; Smith and Meissner, 2013). Others argue that non-CpG methylation is an important mechanism of controlling gene expression wherein high levels of non-CpG methylation at gene promoters facilitate transcription factor binding and transcriptional repression (Barrès *et al.*, 2009; Patil *et al.*, 2014; Zhang *et al.*, 2017).

1.5.2 Mitochondrial DNA (mtDNA) methylation

The presence of mitochondrial CpG methylation went undetected in mammalian cells and tissues for many years (Groot and Kroon, 1979; Maekawa *et al.*, 2004). Although not completely characterised, mounting evidence has emerged to support the role of methylation in mitochondrial gene expression and replication (Bellizzi *et al.*, 2013; Castegna *et al.*, 2015; van der Wijst *et al.*, 2017). Firstly, the expression of a mitochondrial *DNMT1* transcript variant alludes to a plausible mechanism by which mtDNA methylation patterns are established (Shock *et al.*, 2011). Secondly, differential CpG and non-CpG mtDNA methylation across cell types reaffirms the notion of cell-specific methylation patterns (Bellizzi *et al.*, 2013). Thirdly, there is a link between mtDNA methylation, and human ageing and disease (van der Wijst *et al.* 2017).

A recent study comparing mtDNA methylation in reproductive tissues found that mtDNA methylation patterns were more conserved in oocytes and blastocysts than in ovarian granulosa cells (Sirard, 2019). This is not surprising given that mitochondria are inherited from oocytes with no paternal transmission (Luo *et al.*, 2018b). Interestingly, it appears that preimplantation embryos inherit mtDNA methylation patterns from oocytes and that mtDNA methylation status can be altered by ovarian environment. Such findings emphasise the sensitivity of gametes and embryos to mtDNA methylation and epigenetic programming of development (Sirard, 2019). Still, the epigenetic role of mtDNA methylation during gametogenesis and embryogenesis is yet to be investigated.

1.5.3 Histone modifications

Covalent post-translational histone modifications, such as methylation, acetylation, phosphorylation, ubiquitylation, sumoylation (Bannister and Kouzarides, 2011), influence gene expression by remodelling chromatin architecture or by recruiting histone modifiers. Histone methylation is catalysed by histone lysine *N*-methyltransferases (HMT/KMT) and protein arginine *N*-methyltransferases (PRMT), respectively (Morera *et al.*, 2016). Methylation occurs primarily on the side chains of lysine and arginine residues of histone tails. Lysine may be mono-, di-, or trimethylated on its amine group, whereas arginine may be mono- or di-methylated on its guanidyl group (Lan and Shi, 2009; Ng *et al.*, 2009). These marks are both repressive and facilitative in gene transcription depending on the site and degree of methylation (Bannister *et al.*, 2002). For instance, monomethylation of lysine 9 on histone 3 (H3K9), H3K27, H4K20, H3K79 and H2BK5 is linked to transcriptional activation, whilst trimethylation of H3K27, H3K9 and H3K79 is linked to transcriptional repression (Barksi *et al.*, 2007).

1.5.4 RNA methylation

Gene expression can also be regulated via RNA methylation which occurs at cytosine residues in RNA. Amort *et al.* (2017) mapped 5mC modifications in the epitranscriptome of murine brain and ESCs, presenting the first comprehensive dataset of cytosine methylation in mRNA. To date, N⁶-methyladenosine (m⁶A) is the best-studied RNA modification occurring in various eukaryotic RNA species, such as mRNA and long noncoding RNAs (lncRNAs; Willyard, 2017). Methylation of m⁶A is catalysed by a multicomponent complex, including methyltransferase-like 3 (METTL3) and METTL14 enzymes, alongside ancilliary proteins, such as WT1 associated protein (WTAP) in mammals (Lee *et al.*, 2014). Diverse functions of m⁶A include regulation of cellular pluripotency, programming and differentiation; transcript stability, splicing and protein translation; and the cell stress response. Recent work uncovered a protective function of m⁶A in DNA damage repair indicating that RNA methylation offers more than epigenetic regulation (Yue *et al.*, 2015; Xiang *et al.*, 2017).

1.5.5 Demethylation machinery

Given that methylation can respond to environmental signals in differentiated tissues, it follows that the biochemical process should be reversible (Szyf *et al.*, 2016). Various epigenetic erasers have been identified, including histone deacetylases (HDACs) and demethylases (e.g. LSD1; Gillette and Hill, 2015). DNA methylation can be passively depleted through DNA replication or actively removed by ten-eleven translocation (TET) enzymes and m⁶A thymine DNA glycosylase-mediated (TDG) base excision repair (Kohli and Zhang, 2013). Two m⁶A demethylases have been identified; fat mass and obesity associated protein (FTO) and alkB homology 5 (ALKBH5; Batista, 2017). These mechanisms facilitate turnover of methyl groups, highlighting the dynamic and plastic nature of epigenetic gene regulation, particularly during mammalian development.

1.5.5.1 Cytosine hydroxymethylation (5hmC)

5-hydroxymethylcytosine (5hmC) is an intermediate product of the DNA demethylation process catalysed by ten-eleven translocation 1 enzyme (TET1; Tahiliani *et al.*, 2009; Xu *et al.*, 2011). The conversion of 5mC to 5hmC significantly reduces the binding of methyl-CpG binding proteins (MBPs) to DNA which, in turn, inhibits the recruitment of histone-modifying enzymes that promote chromatin condensation and inactivation (Valinluck *et al.*, 2004). Hence, 5hmC is an epigenetic signature characteristic of euchromatin and active gene transcription (Shi *et al.*, 2017).

The distribution of 5hmC is influenced by histone modification, binding proteins and chromatin configuration during cell differentiation and specification (Shi *et al.*, 2017). Typically, 5hmC accumulates within gene promoters decorated with dual histone marks required for transcriptional activation and repression. These bivalent domains poise the expression of developmental genes, rendering 5hmC part of the molecular machinery responsible for pluripotency switch in ESCs, neural and cancer cells (Kriaucionis and Heintz, 2009; Thomson and Meehan, 2017).

Whether 5hmC is merely a demethylation product or a functional epigenetic modification during gametogenesis and embryogenesis remains unclear. During the wave of global demethylation that occurs during early embryogenesis, there is a loss of 5mC and a concurrent accumulation of 5hmC

within both parental pronuclei (Wossidlo *et al.*, 2011; Inoue and Zhang, 2011). The distribution and abundance of these methylaton marks is, therefore, expected to change during stage-specific methylation reprogramming of the preimplantation embryo. If these two marks oppose one another, 5hmC may function as a transitional mark of poised chromatin that overcomes gene silencing by 5mC (Song *et al.*, 2011; Ficz *et al.*, 2011). Then, as *de novo* methylation ensues in morula stage embryos, the gradual accumulation of 5mC (and loss of 5hmC) drives cell differentiation and lineage specification (Cao *et al.*, 2014). In Day 12 bovine blastocysts, the enrichment of 5hmC at repeat sequences, such as long interspersed nuclear elements (LINEs) and long terminal repeats (LTRs), implicates a unique regulatory phase of demethylation during trophoctoderm elongation and placental development (de Montera *et al.*, 2013). It is thought that specific 5mCs are likely to be targeted for oxidative demethylation and carboxylation to 5-carboxylcytosine (5caC) for complete excision by thymine DNA glycosylase (TDG; He *et al.*, 2011).

1.6 DNA methylation analysis

In the burgeoning field of epigenetics, there are numerous assays available to analyse DNA methylation within cell samples, however, methods vary according to their robustness, high-throughput capabilities and cost (Kurdyukov and Bullock, 2016). In general, methods have been developed to profile genome-wide DNA methylation, or differential methylation at specific gene loci or regulatory regions of interest. An overview of common methods is presented in Table 1.3 and Table 1.4.

Table 1.3 Methods for profiling whole genome DNA methylation.

Method	DNA (ng)	Advantage(s)	Limitation(s)	Reference(s)
High performance liquid chromatography (HPLC, HPLC-UV)	300 – 10,000	Measures 5mC/Cytosine ratio	Requires specialised instrumentation	Kuo <i>et al.</i> (1980)
Liquid chromatography-mass spectrometry (LC-MS/MS)	100 – 1,000	Detects ~5% difference, Profiles poor quality DNA (FFPE samples)	Expensive, Requires specialised instrumentation	Song <i>et al.</i> (2005)
Enzyme-linked immunosorbent assay (ELISA)	100 – 1,000	Rapid, Easy-to-use	Variable results, Estimates DNA methylation	Manzardo and Butler (2016)
Amplification/Restriction fragment length polymorphism (AFLP, RFLP)	500	Inexpensive, Suitable for species with limited DNA sequence annotation	Profiles low % of genome, Relies on good PCR band resolution	Paun and Schönswetter (2012)
Luminometric methylation assay (LUMA)	250 – 500	High specificity, Detects low DNA methylation	Requires high quality DNA for enzyme digest	Karimi <i>et al.</i> (2006)
LINE-1 Pyrosequencing	50	High throughput, Detects ~5% difference	Profiles 17% of genome	Estécio <i>et al.</i> (2007)

Abbreviation(s): 5mC, 5-methylcytosine; FFPE, formalin-fixed paraffin-embedded.

Table 1.4 Methods for profiling differentially methylated regions (DMRs).

Method	DNA (ng)	Advantage(s)	Limitation(s)	Reference(s)
Methyl-sensitive cut counting (MSCC)	1,000 – 5,000	No BS required, Rapid, Easy-to-use	Requires high quality DNA for enzyme digest	Guo <i>et al.</i> (2011)
Array/Bead hybridisation (Illumina)	>500	Time and cost effective, Targets 5mC-enriched regions, i.e. promoters, UTR	Custom panels required for non-human species, Limited by DNA sequence information	Marabita <i>et al.</i> (2013)
Methylated DNA immunoprecipitation (MethylCap, MeDIP, MIRA)	>50	Profiles poor quality DNA, Provides high coverage – no restriction enzymes required	Requires further interrogation by NGS sequencing methods	Hsu <i>et al.</i> (2014)
Whole genome bisulphite sequencing (WGBS)	<30	Most comprehensive, Profiles 100% CpGs, Low amount of starting material required (125 pg)	Expensive, Requires complex NGS data analysis, Reduced genome complexity makes sequence alignment difficult	Miura and Ito (2015)
Reduced representation bisulphite sequencing (RRBS)	<30	Gold standard, Reduced cost, Reduced NGS data analysis, Profiles ~85% CGIs	Requires high quality DNA for enzyme digest, Reduced genome complexity makes sequence alignment difficult	Meissner <i>et al.</i> (2005); Guo <i>et al.</i> (2015)

Abbreviation(s): BS, bisulphite sequencing; CGIs, CpG islands; MBD, Methyl CpG-binding domain; NGS, next generation sequencing; UTRs, untranslated regions.

1.6.1 DNA methylation analysis of preimplantation embryos

Numerous studies assessing DNA methylation in mammalian embryos have used immunofluorescence to detect 5mC using specific antibodies (Dean *et al.*, 2001; Beaujean *et al.*, 2004; Park *et al.*, 2007; Bonilla *et al.*, 2010; Dobbs *et al.*, 2013; Acosta *et al.*, 2016). Although immunostaining techniques are descriptive and provide information about the overall methylation dynamics, they are semi-quantitative and do not provide sequence-specific information about differentially methylated regions (DMRs). Sequence-based approaches, such as the EmbryoGENE DNA Methylation Array, have been developed to study the epigenome of bovine embryos (Salilew-Wondim *et al.*, 2015; O'Doherty *et al.*, 2018; Laskowski *et al.*, 2018). Whilst probe hybridisation techniques are more specific than immunostaining methods, arrays are limited by species-specific DNA sequence information and a finite number of probes in their construction (Duan *et al.*, 2019).

More recently, studies have employed high throughput bisulphite sequencing (BS) techniques to profile the embryonic methylome. Considered the 'gold standard' method (Kurdyukov and Bullock, 2016), BS enables single-cell and single base resolution DNA methylation analysis (Guo *et al.*, 2015; Smallwood *et al.*, 2014). Bisulphite treatment deaminates unmethylated cytosine to uracil (U), and converted residues are read as thymine (T), as determined by PCR amplification and DNA sequencing. As 5mC residues are protected against this conversion, they are read as cytosine (C). Comparing BS reads to untreated DNA samples, or aligning reads to the species reference genome, enables identification of methylated cytosines (Kurdyukov and Bullock, 2016).

With next-generation sequencing (NGS) technologies, BS facilitates DNA methylation analysis across an entire genome. Whole-genome bisulphite sequencing (WGBS) is the most comprehensive of all existing methods (Table 1.4) that has been used to reveal the methylation status of all CpG sites in ESCs, spermatozoa, oocytes, or embryos (Smallwood *et al.*, 2014; Li *et al.*, 2018; Duan *et al.*, 2019; Chan *et al.*, 2019). However, WGBS is costly and requires complex NGS data analysis. Reduced representation bisulphite sequencing (RRBS) is a less expensive approach to profiling the methylome. By sequencing the 5mC-enriched fraction of the genome, RRBS permits increased sequencing coverage and, therefore, enhances precision in identifying DMRs (Kurdyukov and Bullock, 2016; Table 1.4). Base-resolution

methods for profiling DNA methylation facilitate comprehensive assessments of the extent to which the external environment, i.e. nutrition or *in vitro* culture conditions, might impair epigenetic reprogramming of the preimplantation embryo.

1.7 Assisted reproductive technology (ART) and epigenetics

Assisted reproductive technologies (ART) and *in vitro* embryo culture can lead to defective fetal programming in humans and animals (Menezo *et al.*, 2010; Menezo *et al.*, 2019; Young *et al.*, 2001; Anckaert and Fair, 2015; Lin *et al.*, 2008). Early studies in sheep and cattle revealed that embryos subjected to embryo manipulation, i.e. somatic cell nuclear transfer (SCNT), or non-physiological *in vitro* embryo culture environments resulted in the development of unusually large offspring that also exhibited congenital malformations (Young *et al.*, 1998; Sinclair *et al.*, 2000; Young *et al.*, 2001). Aside macrosomia (enlarged body), characteristic malformations included macroglossia (enlarged tongue), visceromegaly and abdominal wall defects (umbilical hernia). Increased incidence of dystocia, and fetal and neonatal losses in affected animals has limited large-scale use of *in vitro* embryo production (IVP) technologies.

This fetal overgrowth phenotype observed in ruminants, referred to as large offspring syndrome (LOS), shares phenotypic and epigenetic similarities with Beckwith-Wiedemann syndrome (BWS) in humans (Maher *et al.*, 2003; Chen *et al.*, 2013; Chen *et al.*, 2015). Both overgrowth syndromes share common features, such as alterations in organ and tissue development, placental anomalies, and loss of methylation at imprinted loci involved in embryonic growth and development. As discussed in Section 1.1.1.1, genomic imprints are vulnerable to epigenetic modifications during the periconceptual period wherein oocytes are matured and fertilised, and embryos are cultured *in vitro* (Young *et al.*, 1998; Sinclair *et al.*, 2000; Young *et al.*, 2001; Chen *et al.*, 2013; Chen *et al.*, 2015). Of relevance is the loss of methylation and expression of the *insulin like growth factor 2 receptor (IGF2R)* gene following ovine embryo culture (Young *et al.*, 2001; Discussed in Chapter 4, Section 4.3.2.6).

In support of the early studies in ruminants, recent evidence found a positive correlation between ART conception, and aberrant methylation of imprinted genes and increased fetal birthweight in humans (Mäkinen *et al.*, 2013; El Hajj

et al., 2017; Cortessis *et al.*, 2018; Berntsen and Pinborg, 2018; Zhang *et al.*, 2019; Hattori *et al.*, 2019). Whilst the environmental factors that programme such disorders have not yet been identified, possible effects may be attributed to suboptimal culture media used during IVP (Velker *et al.*, 2012). Ruminant studies have identified a link between the addition of serum to culture media and LOS (Thompson *et al.*, 1995; Young *et al.*, 2001; Rooke *et al.*, 2007). Nevertheless, as serum contains undefined growth factors and macromolecules the composition of media is unknown with batch-to-batch variation.

Many commercial human embryo culture media are formulated based on research using animal models which raises questions regarding the safety and efficacy of their use for human embryology (Harper *et al.*, 2012). The precise metabolic requirements of embryos, as well as the medium's influence over gene expression during development from the oocyte to blastocyst stage, must be defined in an effort to standardise optimal culture media formulations for different species (Simpoulou *et al.*, 2018). Although ART have proved beneficial for clinical, commercial and research purposes, resulting in more than 7 million births worldwide (Novakovic *et al.*, 2019), there is a plea for a more careful approach to IVP, and a strong case for demanding full transparency concerning the composition and scientific rationale behind the development of 'safe' embryo culture media (Sunde *et al.*, 2016).

1.7.1 1C metabolites in *in vitro* embryo production (IVP) media

The composition of 1C metabolites in culture media is essential to our understanding of epigenetic programming via DNA methylation within mammalian cells and embryos during IVP. The wide variation in media composition of 1C substrates and cofactors reflects the high degree of experimentation and little standardisation between embryo production protocols (Table 1.5). Over the past decade, IVP protocols have rapidly transitioned from culturing gametes and embryos in simple salt solutions, such as Earle's or Tyrode's buffers, to complex tissue culture media, such as Hams' F-10 and TCM199 (Sunde *et al.*, 2016).

Table 1.5 1C metabolites in commercial cell and embryo culture media.

Adapted from source(s): Sigma Aldrich (<https://www.sigmaaldrich.com>); Morbeck *et al.* (2014).

	One-carbon (1C) metabolites* (µmol/L)									
	Met	Chol	Gly	Ser	Cys	GSH	B9	B12	B6	B2
Cell culture										
Lebovitz L-15	502.6	7.2	2664.2	1903.1	990.4	-	2.3	-	4.9	0.2
Waymouth's 752/1 MB	335.1	1790.8	666.0	-	698.7	-	0.9	0.1	4.9	2.7
DMEM	201.1	28.6	399.6	399.7	199.9	-	9.1	-	19.5	1.1
IMDM	201.1	28.6	399.6	399.7	291.3	-	9.1	0.0	22.7	1.1
TCM199	100.5	3.6	66.0	237.9	83.0	0.2	0.0	-	0.2	0.0
MEM	100.5	7.2	99.9	99.9	99.9	-	2.3	-	5.7	0.3
RPMI-1460	100.5	21.5	133.2	285.5	208.2	-	2.3	0.0	4.9	0.5
Williams' E	100.5	10.7	666.0	95.2	413.3	0.2	2.3	1.5	5.7	0.3
McCoy's 5A	100.0	35.8	100.0	250.1	200.1	1.5	22.7	1.5	5.2	0.5
BME	50.3	7.2	-	-	50.0	1.5	2.3	-	5.7	0.3
MDCB	30.0	100.0	100.0	100.0	55.7	-	1.8	0.1	0.3	0.3
Ham's F-10	30.0	5.0	100.0	99.9	222.1	-	3.0	1.0	1.0	1.0
Ham's F-12	30.0	100.0	100.0	99.9	222.1	-	3.0	1.0	0.3	0.1
NCTC-109	29.8	9.0	180.0	102.3	1881.7	60.9	0.1	7.4	0.7	0.1
Embryo culture										
InVitroCare IVC1	0.0	-	0.0	0.0	0.0	-	-	-	-	-
InVitroCare IVC3	100.0	-	88.0	88.0	11.0	-	-	-	-	-
Origio ISM1	89.0	-	1312.0	82.0	34.0	-	-	-	-	-
Origio BA	54.0	-	462.0	80.0	24.0	-	-	-	-	-
Vitrolife G-1™	0.0	-	94.0	95.0	0.0	-	-	-	-	-
Vitrolife G-2™	63.0	-	97.0	98.0	47.0	-	-	-	-	-
Sage QACM	0.0	-	89.0	89.0	0.0	-	-	-	-	-
Sage QABM	56.0	-	92.0	89.0	41.0	-	-	-	-	-
Cook SICM	4.0	-	5147.0	81.0	1.0	-	-	-	-	-
Cook SIBM	43.0	-	5226.0	81.0	25.0	-	-	-	-	-
Irvine CSC	53.0	-	43.0	42.0	39.0	-	-	-	-	-
IVFOnline Global	51.0	-	42.0	44.0	43.0	-	-	-	-	-

(-), concentration data not disclosed. Abbreviation(s): BA, BlastAssist; BME, Basal Medium Eagle; CSC, Continuous Single Culture; DMEM, Dulbecco's Modified Eagle's Medium; IMDM, Iscove's Modified Dulbecco's Medium; ISM1, Innovative Sequential Media 1; MEM, Minimum Essential Medium; QABM, Quinn's Advantage Blastocyst Medium; QACM, Quinn's Advantage Cleavage Medium; RPMI, Roswell Park Memorial Institute Medium; SIBM, Sydney IVF Blastocyst Media; SICM, Sydney IVF Cleavage Media; TCM199, tissue culture medium 199. *1C Metabolites: B2, vitamin B₂/riboflavin/flavin mononucleotide•Na/flavin adenine dinucleotide•2Na; GSH, glutathione (reduced)/glutathione•Na; B6, vitamin B₆/pyridoxal•HCl/pyridoxine•HCl; B9, folic acid/folinic acid•Ca; B12, vitamin B₁₂/cobalamin; Chol, choline chloride/choline birtartrate; Cys, L-cysteine/cysteine•HCl/L-cystine/cystine•2HCl; Gly, L-glycine; Met, L-methionine; Ser, L-serine.

Evaluation of the potential impacts of culture media composition on embryo development is challenging as commercial media formulations contain an array of constituents, including salts, sugars, amino acids, lipids, vitamins, trace elements, hormones and other bioactive molecules (Chronopoulou and Harper, 2015). These constituents are present in different forms that vary in stability, bioavailability and bioactivity (Schnellbaecher *et al.*, 2019), and their concentration within media formulations are often not fully documented, disclosed or justified (Sunde *et al.*, 2016). Considering the earlier discussion

regarding supplementation of media with serum, the addition of human serum albumin to commercial media exposes the embryo to a more physiological, albeit undefined nutritional and hormonal milieu (Orsi *et al.*, 2005).

In addition, contemporary protocols often combine media from different manufacturers during sequential media systems that aim to meet embryonic requirements according to developmental stage (Biggers and Summers, 2008). For example, the InVitroCare two-step sequential media is devoid of methionine during early cleavage stages (IVC1) and increases to 100 $\mu\text{mol/L}$ during blastocyst development (IVC3; Table 1.5). The advantage of using a two-step culture system over a continuous single culture system (i.e. Irvine CSC) remains under investigation (Dieamant *et al.*, 2017). Of note is the discrepancy in methionine concentrations between cell and embryo culture media, which range from 0 to 500 $\mu\text{mol/L}$ between formulations (Table 1.5). As methionine is the direct precursor to universal methyl donor, SAM (Figure 1.1), it will be important to elucidate the developmental and epigenetic effects of altering its concentration during *in vitro* embryo production.

1.7.2 Methionine and epigenetic programming

There is an accumulating body of evidence that methionine directly influences the metabolism of SAM and SAH, with implications for DNA methylation in various mammalian tissues (reviewed by Zhang, 2018). Theoretically, the addition of methionine is expected to increase DNA methylation of genes and down-regulate gene expression. In practice, however, the epigenetic effects of methionine on DNA methylation are not always as predicted. Table 1.6 illustrates that tissue- and species-specific effects of methionine can manifest as global and/or locus-specific alterations to DNA methylation. The aforementioned point is further complicated by the finding that DNA methylation does not always repress but can enhance gene expression (Orsorio *et al.*, 2016).

Table 1.6 Epigenetic effects of methionine on mammalian cells and embryos.

Methionine treatment	Species	Intervention stage	Duration	Cell type	Metabolic/epigenetic/transcriptomic effects
Diet (0.3 - 3.0%) Finklestein and Martin (1986)	Rat	250 g	7 d	Liver	↓ SAM:SAH ratio ↓ MTHFR, ↑ MAT, ↑ BHMT, ↑ CBS expression
Diet (0.3 - 2.3%) Rowling <i>et al.</i> (2002)	Rat	54 - 74 g	10 d	Liver	↑ SAM:SAH ratio
Diet (0.3, 2.0%) Amaral <i>et al.</i> (2011)	Rat	35-40 d	6 wk	Kidney	↑ SAH - SAM:SAH ratio
Diet (0, 0.5%) Devlin <i>et al.</i> (2004)	Mouse	50 d	8 wk	Liver/ Brain	↓ SAM:SAH ratio
Injection (6.6 mmol/kg) Tremolizzo <i>et al.</i> (2002)	Mouse	60 d	15 d	Brain	↓ SAM:SAH ratio ↑ <i>Reln</i> promoter methylation ↓ <i>RELN</i> expression
Injection (5.2 mmol/kg) Dong <i>et al.</i> (2005)	Mouse	20 g	3 – 15 d	Brain	↓ <i>RELN</i> , ↓ <i>GAD67</i> expression ↑ MeCP2 binding <i>Reln/Gad67</i> promoter
Diet (0, 1.7%) Yang <i>et al.</i> (2015)	Mouse	42 d	20 wk	Serum	↑ SAM:SAH ratio
Diet (0.172, 0.39%) Tang <i>et al.</i> (2017)	Mouse	After mating (E0.5)	8-14 d (E8.5-14.5)	Embryonic stem cells (SIRT1-KO)	↓ H3K4me3 methylation Met restriction, ↑ <i>Mat2a</i> expression in wildtype mESCs
Diet (0.07, 0.19% DMI) Osorio <i>et al.</i> (2016)	Cow	21 d before parturition	51 d (to 30 d lactation)	Liver	↓ DNA methylation ↑ PPARA promoter methylation ↑ PPARA expression
Diet (0.9 kg/DMI) Batistel <i>et al.</i> (2019)	Cow	28 d before parturition	28 d (to term)	Placenta	↑ 1C metabolites ↑ <i>DNMT3A</i> expression ↓ DNA methylation (females)
Diet (0.08 % DMI) Acosta <i>et al.</i> (2016)	Cow	21 d before parturition	51 d (to 30 d lactation)	Day 7 embryo	↑ Lipid accumulation ↓ DNA methylation
Diet (1.89, 2.43% MP) Peñagaricano <i>et al.</i> (2013)	Cow	Calving until embryo flushing	70 d (post-partum)	Day 7 embryo	276 DEGs (embryo development and immune response)
Embryo culture (0 - 400 µmol/L) Bonilla <i>et al.</i> (2010)	Cow	Zygote (Day 0 IVC)	8 d	Day 8 embryo	DNA methylation unaffected ↑ GSH content without Met
Embryo culture (0 – 10 mmol/L ethionine) Met antagonist Ikeda <i>et al.</i> (2012)	Cow	5-cell (Day 3 IVC)	5 d	Day 8 embryo	↓ SAM with Met restriction ↓ DNA methylation ↑ <i>NANOG</i> , ↑ <i>TEAD4</i> expression
Cell culture (0 – 120 µmol/L) Shiraki <i>et al.</i> (2014)	Human	-	0-48 hr	Embryonic stem cells	↓ SAM, ↓ Hcy with Met restriction ↓ DNA/H3K4me3 methylation ↓ <i>NANOG</i> expression ↑ p53-p38 signaling
Cell culture (3, 100 µmol/L) Dai <i>et al.</i> (2018)	Human	-	25 hr	HCT116 colon cancer cell line	↓ H3K4me3 with Met restriction

Arrows: ↑ increase, ↓ decrease, - no change. (%) Methionine proportion of diet. Intervention stage classified by age, weight or stage of gestation. Abbreviation(s): BHMT, betaine homocysteine S-methyltransferase; CBS, cystathionine β-synthase; DEGs, differentially expressed genes; DMI, dry matter intake; DNMT3A, DNA methyltransferase 3A; GAD₆₇, glutamic acid decarboxylase; GSH, glutathione; IVC, *in vitro* culture; MAT, methionine adenosyltransferase; mESCs, murine embryonic stem cells; MTHFR, methylenetetrahydrofolate reductase; NANOG, NANOG homeobox protein; PPARA, Peroxisome proliferator-activator receptor alpha; RELN, reelin; SAH, S-adenosyl homocysteine; SAM, S-adenosylmethionine; SIRT1-KO, Sirtuin 1-knockout; TEAD4, Tea domain transcription factor 4.

Despite the evidence that methionine availability alters the transcriptome of bovine preimplantation embryos *in vivo* (Peñagaricano *et al.*, 2013), the effect of methionine on the methylome of the mammalian embryo remains inconclusive. Surprisingly, dietary supplementation of rumen-protected methionine at a rate of 0.08% of dry matter intake reduced global DNA methylation in bovine embryos (Acosta *et al.*, 2016). *In vitro* studies have shown that methionine inhibition by culturing bovine embryos with antimetabolite ethionine (1-10 mmol/L) reduced DNA methylation (Ikeda *et al.*, 2012). On the contrary, Bonilla and colleagues (2010) found no effect of methionine concentration (0 to 21 $\mu\text{mol/L}$) on DNA methylation in cultured blastocysts. Such findings, however, should be interpreted with caution since all experiments used immunofluorescent detection of 5mC which lacks sensitivity and base-resolution, as discussed previously (Section 1.6.1).

1.8 Working hypothesis

The foregoing discussion provides evidence that maternal nutrition during the periconceptional period programs offspring development to a large extent via 1C metabolism, and that dietary inadequacies of 1C substrates and cofactors during this vulnerable period can have long-lasting consequences for adult health and disease.

Most of the research investigating the function of 1C metabolism pertains to studies undertaken in the rodent liver, with limited research conducted in domestic livestock species. It is of agricultural and economic importance to understand the regulation of 1C metabolism in ruminants which have a low dietary intake of methyl nutrients due to their degradation by rumen microorganisms and, therefore, rely on methylneogenesis (transmethylation flux through 1C metabolic pathways) as a source of labile methyl groups (Snowell and Xue, 1987). Furthermore, little is known about how 1C metabolism functions in the mammalian ovary and preimplantation embryo. Previous research has uncovered important species-specific differences in 1C metabolism transcript expression (Section 1.4), however, our understanding of the regulatory aspects and the impact of nutritional perturbations on these pathways in reproductive cell types remains limited.

With this in mind, this thesis first addresses the hypothesis that dietary deficiencies in key 1C substrates and cofactors can perturb 1C metabolism,

potentially leading to an aberrant 1C metabolome within the ruminant liver. As the largest metabolic organ of the body that is responsible for almost 50% of methionine metabolism and 85% of methylation reactions (Lu and Mato, 2012), it is likely that relevant reductions in dietary methyl availability may lead to significant alterations in hepatic 1C metabolite levels. In order to test this hypothesis, novel analytical methods were developed for the simultaneous quantification of B vitamins, folates and 1C-related amines in ovine liver harvested from abattoir-derived (Ab) controls, and methyl-deficient (MD) animals following dietary restriction of 1C metabolites. Hepatic concentrations of individual 1C metabolites were compared between Ab and MD sheep to assess the metabolic burden of dietary methyl deficiency (Chapter 2).

Next, based on the premise that the bovine preimplantation embryo may metabolise methionine differently to hepatocytes (Section 1.4), the hypothesis is advanced that bovine embryonic cells are particularly sensitive to methyl-group availability and, therefore, highly sensitive to epigenetic programming during the preimplantation period. Given that methionine is the first limiting amino acid in dairy cattle nutrition (Wiltbank *et al.*, 2014), and that its variable concentration in the diet and culture media can influence reproductive performance in cows (Toledo *et al.*, 2017), Chapter 3 and Chapter 4 sought to elucidate the developmental and epigenetic implications of altering methionine concentration during *in vitro* production of bovine embryos.

Non-physiological embryo culture conditions and physical manipulation of embryos can lead to heritable alterations to the epigenome that are linked to adverse developmental outcomes (Young *et al.*, 1998; Young *et al.*, 2001; Young *et al.*, 2003). Chapter 5 sought to evaluate the effect of somatic donor cell type on epigenetic reprogramming via DNA methylation in hepatocytes isolated from cloned sheep.

Chapter 2

Quantification of folates, B vitamins and 1C-related metabolites in ovine liver by HILIC-MS/MS

2.1 Introduction

The impairment of 1C metabolism can cause disruption to DNA synthesis and repair, and epigenetic regulation of gene expression, all of which can have detrimental effects on the health of an organism (Xu and Sinclair, 2015). The function of 1C metabolic pathways can be monitored by the quantitative measurement of key 1C intermediates in blood or metabolically active tissue, such as liver (Xu *et al.*, 2020).

B vitamins, including folates (vitamin B₉), B₁₂, B₆ and B₂, are cofactors of cellular methylation reactions, including Hcy remethylation to methionine, that serve as a reserve storage pool or as direct precursors for the synthesis of 1C coenzymes (Selhub, 2002). Specific 1C-related amines also modulate Hcy status by facilitating its remethylation to methionine or its catabolism via the *transsulphuration* pathway (Finkelstein, 2000; Ueland *et al.*, 2005; Appendix Figure 2.1; Appendix Table 2.1).

Dietary restriction of these 1C metabolites is associated with several metabolic disease conditions in ruminants, such as ill-thrift, pine, white-liver disease and hepatic lipidosis. Such conditions are characterised by anorexia, cachexia, anaemia, compromised immune function and impaired fertility, and are associated with low plasma or liver vitamin B₁₂ concentrations (Suttle, 2010).

The interrelationship between B₁₂ and folate-mediated 1C metabolism is important in sheep, especially weaned lambs, due to their increased susceptibility to cobalt (Co) deficiency (Grace, 1994). Cobalt is a trace-element required for the microbial synthesis of B₁₂ in the rumen. Levels of Co are normally adequate to meet the metabolic demands of sheep. However, if dietary sources are limiting, Co deprivation can manifest as vitamin B₁₂ deficiency with adverse consequences for B₁₂-dependent metabolic pathways, including methionine synthesis (Somers and Gawthorne, 1969; McDowell, 2000; Suttle, 2010; Xu *et al.*, 2020).

Most research on 1C metabolism in sheep liver has focused on enzyme activity (Xue and Snoswell, 1985; Xue and Snoswell, 1986; Snoswell and Xue, 1987). Comparative studies of sheep and rat liver identified species-specific differences in methionine metabolism that may explain, at least in part, an adaptation of the ruminant to low dietary methyl group intake. The degradation of choline by rumen microbes leads to low betaine availability. It appears that sheep compensate for low betaine availability by expressing a lower hepatic

capacity of BHMT and a higher capacity of MTR (Neill *et al.*, 1979; Xue and Snoswell, 1985; Snoswell and Xue, 1987). Other enzymatic differences include a lower capacity of glycine *N*-methyltransferase (GNMT) and CBS in sheep liver (Xue and Snoswell, 1986). Collectively, these differences demonstrate an increased reliance on the B12-dependent remethylation of Hcy by MTR, and the preferential partitioning of methyl groups for transmethylation reactions in the ruminant liver.

The effects of feeding a methyl deficient (MD) diet have been investigated in sheep and have system-wide physiological and metabolic consequences. Restricting the supply of B vitamins (B12 and folate) and methionine from the diet of mature ewes caused a significant reduction in plasma B12, methionine and folate concentrations, and elevated plasma Hcy and methylmalonic (MMA) (Kanakparambil *et al.*, 2009). Feeding the same diet during the periconceptual period led to widespread epigenetic modifications to the genome associated with increased adiposity, insulin resistance, altered immune function and hypertension in adult offspring (Sinclair *et al.*, 2007). To our knowledge, however, no study has investigated the effect of dietary methyl deficiency on key 1C metabolite concentrations in sheep liver. Quantitative assessments of 1C intermediates and co-substrates would provide valuable insights into dietary-mediated 1C metabolic function in ruminant species.

Various analytical approaches have been developed for the quantification of 1C metabolites, including microbiological assay, radioimmunoassays, capillary electrophoresis, and HPLC methods coupled with coulometric electrochemical, UV or fluorescence detection (Ndaw *et al.*, 2001; Pfeiffer *et al.*, 2004; Patring *et al.*, 2005; Lebidzińska *et al.*, 2008; Zhou *et al.*, 2012; Forteschi *et al.*, 2016). Although LC-MS/MS methods have been used to quantify B vitamins or folates in plants, animal tissues and biofluids (Garratt *et al.*, 2005; Midttun *et al.*, 2005; Gentili *et al.*, 2008; Midttun *et al.*, 2013; Puts *et al.*, 2015; Oosterink *et al.*, 2015; Phillips, 2015), most methods involve complex and time-consuming sample preparation and are limited to quantifying individual or a subset of metabolites without the capacity to analyse a comprehensive set in one analytical run. In general, studies report the total content of vitamins without measuring the chemically distinct bioactive forms individually. Knowledge of the variation and tissue-specific distribution of individual coenzymes could aid our understanding of the metabolic burden of methyl deficiency and facilitate more accurate deficiency diagnosis in ruminants.

Active variants of B vitamins are present in free and phosphorylated forms at varying concentrations (Merril and Henderson, 1990), and folates are present as mono- and polyglutamates of varying glutamate chain length (Garratt *et al.*, 2005). All vitamers are susceptible to degradation by light, heat, oxygen and pH (Monajjemzadeh *et al.*, 2014). The diverse physicochemical properties and chemical instability of 1C metabolites presents a significant analytical challenge to develop methods for their simultaneous quantification in complex mammalian tissue. Hence, the objective of the present study was to develop analytical methods for the comprehensive and quantitative profiling of B vitamins, folates and 1C-related amines in sheep liver, and specifically, to investigate the effect of dietary methyl deficiency on key 1C metabolite concentrations in sheep liver.

2.2 Materials and methods

2.2.1 Animals, treatments and tissue collection

All procedures were conducted in accordance with the requirements of the UK Home Office Animals (Scientific Procedures) Act (1986) and were approved by the University of Nottingham Animal Welfare and Ethical Review Board.

A total of 356 purebred weaned and pubertal Texel lambs were recruited from 11 farms in the UK. Approximately half of these lambs were male. The control cohort ($n=266$) originated from five farms and were slaughtered at regional abattoirs between May and September. The treatment cohort ($n=90$) originated from six farms located in Derbyshire, Devon, Gloucestershire, Leicestershire, Northamptonshire and Worcestershire, and were transported to the University farm at 12 weeks of age to be fed a methyl deficient (MD) diet prior to slaughter. Power equations were used to calculate the sample size for study cohorts.

2.2.1.1 Methyl deficient (MD) cohort

At the start of the study, animals were penned in pairs according to farm origin, sex and body weight. A blood sample was taken by jugular venepuncture on arrival to assess trace-element status (primarily Co) by inductively coupled plasma mass spectrometry (ICP-MS) analysis using the method described in Appendix 2.1. As it can take several weeks to deplete sheep of endogenous B12 reserves (Kennedy *et al.*, 1994), animals were adjusted to a concentrate diet of Co deficient (<0.09 mg/kg dry matter; DM) and sulphur (S) deficient (<1

mg/kg DM) barley and hay for 4 weeks prior to the introduction of the experimental diet. A reduction in Co and S diminishes the capacity of the rumen microorganisms to synthesise B12 and sulphur-containing amino acids, respectively (Kanakaparambil *et al.*, 2009).

Seven MD animals were prematurely withdrawn from the study due to their incapacity to thrive under experimental conditions as newly weaned lambs. For the duration of the study (12 weeks), animals were fed a Co and S deficient concentrate diet *ad libitum* and Co deficient hay at a fixed rate of 200g/lamb/day. The concentrate diet, containing 42% barley, 30% oat feed, 25% maize and 3% urea, was based on that offered previously (Sinclair *et al.*, 2007; Kanakaparambil *et al.*, 2009) and was designed to meet the requirements for maintenance and growth of recently weaned lambs (ARC, 1980). The mineral composition of the MD diet is presented in Table 2.1.

Table 2.1 Macro and micro mineral composition of methyl deficient (MD) concentrate diet and cobalt (Co) deficient hay.

	Concentrate diet	Hay
Chemical analyses†		
Dry matter (g/kg)	888	860
Metabolisable energy (MJ/kg DM)	12.9	7.0
Crude protein (g/kg DM)	134	67
Macro mineral, g/kg DM		
Phosphorous (P)	2.2	1.6
Potassium (K)	4.9	12.3
Sodium (Na)	0.07	0.8
Magnesium (Mg)	0.8	1.2
Calcium (Ca)	0.5	3.7
Sulphur (S)	0.8	1.0
Macro mineral, mg/kg DM		
Boron (B)	4.9	9.6
Copper (Cu)	2.5	4.8
Manganese (Mn)	14.6	133.4
Zinc (Zn)	18.0	23.2
Selenium (Se)	0.06	0.03
Cobalt (Co)	0.02	0.2

† Proximate analyses undertaken by Scotland's Rural College (SRUC), Bush Estate, Edinburgh

Feed intakes of the MD diet were recorded for each pen at 3- and 4-day intervals, lamb liveweights were recorded fortnightly and blood samples taken weekly. Lambs remained on the experimental diet until serum B₁₂ concentrations remained below 200 pmol/L for ≥6 weeks and plasma Hcy had

been rising for ≥ 4 weeks to ≥ 9 $\mu\text{mol/L}$. At this experimental endpoint, lambs were slaughtered, and liver samples collected.

2.2.1.2 Tissue collection

Fresh liver samples were harvested immediately after the slaughter of control (abattoir, Ab) and MD animals. However, liver samples were collected from animals in each of the study cohorts at two independent time points and, therefore, were not analysed in parallel. Diced sections (5 mm^3) from the same region of the right lobe of the liver were collected on each occasion and snap frozen in liquid nitrogen within 15 min of exsanguination. Tissue samples were stored at -80°C until metabolomic analyses.

2.2.1.3 Blood analysis

Blood samples were collected from lambs weekly by jugular venepuncture into lithium heparin vacutainers, and vacutainers containing no additive. Samples were centrifuged for 15 min at 4,250 $\times g$. Plasma and serum fractions were stored at -20°C until analysed.

2.2.1.3.1 Vitamin B₁₂

Serum B12 was measured using the IMMULITE® 2000 system at SRUC, Edinburgh, UK. This solid-phase, competitive chemiluminescent enzyme immunoassay involves an automated alkaline denaturation procedure (catalogue no. L2KVB2). Serum is treated with dithiothreitol (DDT) and sodium hydroxide/potassium cyanide (NaOH/KCN) solution in a reaction tube. Following a 30 min incubation, the sample is transferred to a second tube containing B12-coated polystyrene beads and hog intrinsic factor (HIF). A second 30 min incubation facilitates the release of B12 from endogenous binding proteins by alkaline denaturation. The released B12 competes with immobilised B12 for binding with HIF. During a final 30 min incubation, alkaline phosphatase-labelled anti-hog intrinsic factor is added which binds HIF that is immobilised on the B12-coated bead. Unbound enzyme conjugate is removed by centrifugal wash. The bound conjugate is quantified using chemiluminescent substrate, dioxetane. Light emitted when dioxetane reacts with alkaline phosphatase is detected by a photomultiplier tube. The amount of light emitted is proportional to the concentration of B12 in the sample. A sample volume of

75 μL was required for this assay. The limit of detection (LOD) was 111 pmol/L and the upper limit was 738 pmol/L. The intra-assay coefficient of variation (CV%) was 13.0, 7.0 and 6.2 for low, medium and high-quality control (QC) samples, respectively. The inter-assay CV% was 15.0, 6.0 and 7.9, for low, medium and high QC samples, respectively.

2.2.1.3.2 Homocysteine (Hcy)

Plasma homocysteine (Hcy) was measured using an Imola Autoanalyser (RX Imola; Randox Laboratories Ltd., Antrim, UK) using the Hcy kit (Randox laboratories; catalogue no. HY4036). Bound or dimerised Hcy (oxidised form) is reduced to free Hcy which reacts with serine to form cystathionine, as catalysed by cystathionine β -synthase (CBS). Cystathionine is catabolised by cystathionine β -lyase (CBL) to produce Hcy, pyruvate and ammonia. Pyruvate is converted to lactate by lactate dehydrogenase (LDH), using nicotinamide adenine dinucleotide (NADH) coenzyme. The rate of NADH conversion to NAD^+ is proportional to the concentration of Hcy ($\Delta\text{A}340\text{ nm}$). The LOD was 1.74 $\mu\text{mol/L}$ and the upper limit was 47.9 $\mu\text{mol/L}$. The CV% was 9.32, 6.77 and 5.40 for low, medium and high QC samples, respectively.

2.2.1.3.3 Methylmalonic acid (MMA)

Plasma methylmalonic acid (MMA) was measured by gas chromatography-mass spectrometry (GC-MS) following derivatisation and extraction, based on the method of [Kanakkaparambil *et al.* \(2009\)](#). Briefly, 50 μL plasma and 5 μL internal standard, 4-chlorobutyric acid (CBA; 250 $\mu\text{mol/L}$), were added to 250 μL 12% boron trifluoride methanol ($\text{BF}_3\text{-MeOH}$) in a 2.5 mL screw-capped glass vial. The mixture was vortexed for 30 s and heated at 95°C for 15 min in a heating block. After cooling, 250 μL distilled water and 250 μL dichloromethane (CH_2Cl_2) was added to the vial. The mixture was vortexed for 30 s and centrifuged for 8 min at 2,500 xg and 4°C to separate the layers. The lower CH_2Cl_2 layer was transferred to a screw-capped autosampler glass vial with insert for GC-MS analysis.

The GC-MS method used a DB-WAX column (crosslinked polyethylene glycol; J&W Scientific Agilent technology; 30 mm x 0.25 mm; 0.15 μm film thickness). The injection volume was 1 μL for SCAN mode for qualification and selected ion monitoring (SIM) mode for quantification, both using splitless mode. The

injection port and MS selective detector interference temperatures were 260°C and 280°C, respectively. The carrier gas (He) was set at a constant flow rate of 0.1 mL/min. The chromatographic conditions were 50°C for 2 min, 8°C min⁻¹ until 150°C and a final increase of 100°C min⁻¹ until 220°C. The MS was tuned regularly and operated in electron impact ionisation mode with the ionisation energy of 70 eV. SCAN mode measured at 20-500 m/z. SIM ions were set at 115 m/z for MMA and 105 m/z for CBA. Plasma MMA concentrations were quantified by the method of standard addition using a calibration range from 0.156 to 20 µmol/L and plotting the ratio of peak area of analyte (MMA) to that of the internal standard (CBA). Results were reported as µmol/L plasma. The LOD was 0.15 µmol/L and the CV% was 0.44, 1.03 and 0.83 for low, medium and high QC samples, respectively.

2.2.2 Liver 1C metabolite quantification

A total of 37 one-carbon metabolites and related compounds were measured in 356 Texel sheep liver samples. Hydrophilic interaction liquid chromatography-mass spectrometry (HILIC-MS/MS) methods for the quantification of B vitamins and folates were undertaken in collaboration with postdoctoral researcher, Dr Juan Xu (Section 2.2.2.1). High-performance liquid chromatography (HPLC) and GC-MS methods for the quantification of related amino acids, polyamines and propionate metabolites were undertaken in collaboration with fellow PhD student, Dr Amey Brassington (Appendix 2.2 to Appendix 2.4).

2.2.2.1 HILIC-MS/MS

The 'B vitamin' method measured ten B vitamins and four 1C-related amines (Table 2.2). The 'folate' method measured seven folates and three key methionine cycle analytes (Table 2.3).

2.2.2.1.1 Analytical grade reagents

B vitamin method: Methanol (MeOH), acetic acid and acetonitrile (ACN) were purchased from Fisher Scientific (Loughborough, UK). Unless otherwise stated, the following reagents were purchased from Sigma-Aldrich (Poole, UK); ammonium formate, formic acid and 2-mecaptoethanol (MCE). B vitamin standards; thiamine hydrochloride (B1), (-)-riboflavin (B2), riboflavin 5'-monophosphate sodium salt hydrate (flavin mononucleotide; FMN), flavin

adenine dinucleotide disodium salt hydrate (FAD), pyridoxine hydrochloride (PN), pyridoxamine dihydrochloride (PM), pyridoxal hydrochloride (PL), pyridoxal 5'-phosphate (PLP), vitamin B₁₂ (CNCbl), coenzyme B₁₂ (AdoCbl) and methylcobalamin hydrate (MeCbl; Alfa Aesar, Lancashire, UK). One-carbon amine standards; L-cystathionine (Cth), betaine/trimethylglycine (TMG), N,N-dimethylglycine (DMG) and sarcosine (Sar). Internal standards (IS); vitamin B₁ hydrochloride (4,5,4-methyl-¹³C₃; B₁-¹³C₃) and deuterated pyridoxine hydrochloride (methyl-D₃; PN-d₃) were purchased from Cambridge Isotope laboratories (Massachusetts, USA), and 8-bromoadenosine 3',5'-cyclic monophosphate (8-Br-cAMP) was purchased from Sigma-Aldrich (Poole, UK). High purity water was produced by a Millipore water purification system (Millipore S.A.S., Molsheim, France).

Folate method: Potassium phosphate monobasic (KH₂PO₄), potassium phosphate dibasic (K₂HPO₄), L-ascorbic acid, citric acid, ammonium carbonate and acetonitrile were purchased from Fisher Scientific (Loughborough, UK). 2-mercaptoethanol (MCE) was purchased from Sigma-Aldrich (Poole, UK). Folate standards were purchased from Schircks Laboratories (Jona, Switzerland) including folic acid (FA), 7,8-dihydrofolic acid (DHF), (6R,S)-5,6,7,8-tetrahydrofolic acid trichloride (THF), (6R,S)-5-formyl-5,6,7,8-tetrahydrofolic acid, calcium salt (5-fTHF), (6R,S)-5,10-methenyl-5,6,7,8-tetrahydrofolic acid, chloride (CH=THF), (6R,S)-5,10-methylene-5,6,7,8-tetrahydrofolic acid, calcium (CH₂THF), (6R,S)-5-methyl-5,6,7,8-tetrahydrofolic acid, calcium salt (5-mTHF). S-adenosyl L-methionine (SAM), S-adenosylhomocysteine (SAH), and DL-Homocysteine (Hcy) were purchased from Sigma-Aldrich (Poole, UK). Internal standard (IS); methotrexate (MTX), was purchased from Schircks Laboratories and internal standard (IS), S-adenosylhomocysteine-d₄ (SAH-d₄), was purchased from Cambridge Bioscience (Cambridge, UK).

Table 2.2 B vitamin and 1C-related amine analytes measured by HILIC-MS/MS.

B vitamin method			
Thiamine (B1)	Riboflavin (RF)	Flavin mononucleotide (FMN)	Flavin adenine dinucleotide (FAD)
Pyridoxine (PN)	Pyridoxamine (PM)	Pyridoxal (PL)	Pyridoxal 5'-phosphate (PLP)
Cyanocobalamin (CNCbl)	Adenosylcobalamin (AdoCbl)	Methylcobalamin (MeCbl)	Cystathionine (Cth)
Vitamin B ₁ hydrochloride (B1- ¹³ C ₃)*	Pyridoxine-d ₃ (PN-d ₃)*	8-bromoadenosine 3',5'- cyclic monophosphate (8-Br-cAMP)*	Trimethylglycine (TMG)
			Sarcosine (Sar)

*Internal standard (IS)

Table 2.3 Folate and methionine cycle analytes measured by HILIC-MS/MS.

Folate method		
Folic acid (FA)	Dihydrofolate (DHF)	Tetrahydrofolate (THF)
5-Formyltetrahydrofolate (5-fTHF)	5,10-Methylenetetrahydrofolate (CH ₂ THF)	5,10-Methenyltetrahydrofolate (CH=THF)
5-Methyltetrahydrofolate (5-mTHF)	S-Adenosyl methionine (SAM)	S-Adenosyl homocysteine (SAH)
Homocysteine (Hcy)	Methotrexate (MTX)*	S-Adenosyl homocysteine-d ₄ (SAH-d ₄)*

*Internal standard (IS)

2.2.2.1.2 Standard preparation and calibration

B vitamin method: Stock solutions of B12, B6, B2, B1 and 1C amines were prepared in 0.01 M aqueous HCl at a final concentration of 10 $\mu\text{mol/L}$, except for FAD, Cth, Sar and TMG which were prepared at a final concentration of 1 mmol/L. Methylcobalamin and deuterated IS, PN-d₃, were prepared in pure MeOH. All stock solutions were stored at -80°C . Aqueous bovine serum albumin (10% BSA; Sigma Aldrich cat no. A6003) was used as a surrogate matrix for the preparation of eight extracted calibration standards. These were prepared by adding 150 μL ACN buffer (95% ACN, 1% acetic acid, 0.1% ascorbic acid and 0.1% MCE) containing a suitable range of standard concentrations into 50 μL 10% BSA containing the IS mix. The final concentration of each IS was 1 $\mu\text{mol/L}$.

Folate method: Stock solutions of folates, SAM, SAH and Hcy standard metabolites, plus IS (MTX and SAH-d₄), were prepared in potassium phosphate extraction buffer (KH_2PO_4 and K_2HPO_4 ; 40 mmol/L) containing 0.1% L-ascorbic acid, 0.15% citric acid and 0.1% MCE (adjusted to pH 7 with NaOH), each at a final concentration of 100 $\mu\text{mol/L}$. All stock solutions were stored at -80°C . As before, 10% BSA was used for the preparation of eight extracted calibration standards. These were prepared by adding 150 μL extraction buffer to 50 μL 10% BSA containing the IS mix. The final concentration of each IS was 100 nmol/L.

2.2.2.1.3 Sample extraction

B vitamin method: 50 mg frozen liver were extracted with 300 μL ACN buffer containing 1 $\mu\text{mol/L}$ of IS mix (B₁-¹³C₃, PN-d₃ and 8-Br-cAMP). Homogenisation was performed using a TissueLyser (RetschQiagene) with two disruption steps at 25 Hz for 2.5 min, freezing samples between steps. Liver homogenates were incubated at 50°C in a water bath for 15 min, rapidly cooled on ice and centrifuged for 15 min at 2,000 xg and 4°C. Further deproteination was undertaken by the addition of 100 μL cold ACN to 100 μL liver homogenate. After vortexing for 10 s and a final centrifugation step, the clear supernatant was transferred into an amber HPLC vial for LC-MS/MS analysis.

Folate method: 50 mg frozen liver were extracted with 250 μL cold potassium phosphate buffer containing 100 nmol/L of IS mix (MTX and SAH-d₄). Homogenisation was performed using a TissueLyser (RetschQiagene) with two

disruption steps at 25 Hz for 2.5 min, freezing samples between steps. Liver homogenates were incubated at 100°C in a water bath for 2 min to deactivate the conjugate enzyme responsible for polyglutamation and rapidly cooled in ice. Homogenates were vortexed for 10 s and centrifuged for 10 min at 9,000 xg and 4°C.

For the quantification of folate monoglutamates, 100 µL liver supernatant was transferred to a 0.5 mL Microcon-10kDa centrifugal filter unit with ultracel-10 membrane (Merck Millipore) and centrifuged for 30 min at 16,000 xg and 4°C. The filtrate was transferred to an amber HPLC vial for LC-MS/MS analysis. This extraction procedure was applied to liver and QC samples.

For the quantification of total folates (mono- and polyglutamates), 75 µL potassium phosphate buffer and 25 µL rat serum (Sigma-Aldrich) was added to 100 µL liver supernatant and mixed gently. The contents were incubated at 37°C in a water bath for 2 hours to allow enzymatic cleavage of glutamate residues from folates by γ -glutamyl hydrolase (GGH) in serum. Next, the contents were incubated at 100°C for 1 min to deactivate GGH, rapidly cooled on ice and centrifuged for 5 min at 10,000 xg. The supernatant (100 µL) was transferred to a 0.5 mL Microcon-10kDa centrifugal filter unit and further centrifuged for 30 min at 16,000 xg and 4°C. The filtrate was transferred to an amber HPLC vial for LC-MS/MS analysis.

2.2.2.1.4 LC-MS/MS analysis

LC-MS/MS analyses were performed on a LC-10AD systems (Shimadzu, Kyoto, Japan) equipped with a SIL-HTC autosampler coupled to an ABI 4000 QTRAP tandem mass spectrometer using an electrospray ion source (Turbo Ion Spray™; SCIEX, Foster City, CA) in positive ionisation mode. Chromatographic separation was performed on a Sequant ZIC-pHILIC column (150 × 4.6 mm, 5 µm particle size) with a guard column (Sequant ZIC-pHILIC, 20 × 2.1 mm, 5 µm particle size) maintained at 45°C. The autosampler was maintained at 4°C. Standards and samples were injected at a volume of 10 L with a flow rate of 0.4 mL/min.

Mobile phases for the B vitamin method were composed of aqueous ammonium formate buffer solution (20 mmol/L, adjusted to pH 3.5 with formic acid) for eluent A and 100% ACN for eluent B. Mobile phases for the folate method were composed of aqueous ammonium carbonate buffer solution (20 mmol/L, pH 9.1)

for eluent A and 100% ACN for eluent B. Gradient elution was carried out by the following program: isocratic hold on 80% B for 1 min, next a linear gradient from 80% B to 5% B for 5 min, followed by a linear gradient back to 80% in 2 min, then isocratic hold on 80% for another 5 min. The total run time was 13 min.

MS settings were as follows: ion source temperature (450°C), ion spray voltage (5000 V), curtain gas (25 psig), collision gas (8 psig), ion source gas 1 (20 psig), ion source gas 2 (20 psig) interface heater activated. Analyst software (Applied Biosystems/MDS SCIEX) was used for HPLC system control and data acquisition and processing. The MS/MS acquisition method (multiple reaction monitoring; MRM) was developed and the parameters are shown for the B vitamin method (Table 2.4) and folate method (Table 2.5). Two MRM transitions were monitored for each compound to use the ratio of quantifier and qualifier transition for compound identification. All compounds were quantified by the method of standard addition using an 8-point calibration constructed by plotting the ratio of the peak area of analyte to that of the relevant internal standard. For the B vitamin method, 8-Br-cAMP was used for B12, B2 and 1C amine analytes; PN-d₃ was used for B6 analytes; and, B1-¹³C₃ was used for B1. For the folate method, MTX was used for folate analytes and SAH-d₄ was used for methionine cycle metabolites.

For batch analysis, bulk QC samples were made from homogenised sheep liver spiked with a known concentration of analyte standards. These QC samples were used to monitor assay performance across batches.

Table 2.4 Mass spectrometer parameters for identification of B vitamins and 1C-related amines. Adapted from [Xu et al. \(2020\)](#).

Analyte	Retention time (min)	Q1 mass (amu)	Q3 mass (amu)	DP	CE	CXP
B vitamins						
CNCbl	5.82	678.54	147.30	81	63	12
AdoCbl	6.46	790.56	665.50	96	31	16
MeCbl	6.07	673.16	147.20	76	77	12
PN	7.85	169.21	134.10	56	31	10
PM	6.79	170.08	152.00	41	21	10
PL	6.59	168.23	94.20	31	37	6
PLP	7.17	248.06	122.00	31	41	12
RF						
FMN	6.13	457.10	359.10	96	33	12
FAD	6.38	786.27	348.00	111	33	10
B ₁	7.23	265.15	122.10	26	21	8
1C amines						
Cth	7.39	223.10	134.10	56	21	10
TMG	6.33	118.09	59.10	66	27	10
DMG	6.49	104.03	58.20	23	21	2
Sar	6.84	89.87	44.10	36	19	6
Internal standards						
B ₁ - ¹³ C ₃	7.20	267.80	123.00	35	19	10
PN-d ₃	6.80	173.00	136.00	35	25	10
8-Br-cAMP	6.00	407.80	214.00	35	35	10

Abbreviation(s): 8-Br-cAMP, 8-bromoadenosine 3',5'-cyclic monophosphate; AdoCbl, adenosylcobalamin; amu, atomic mass unit; B₁-¹³C₃, vitamin B₁ hydrochloride 4,5,4-methyl-¹³C₃; B₁, thiamine; CE, collision energy; CNCbl, cyanocobalamin; Cth, cystathionine; CXP, collision cell exit potential; DMG, dimethylglycine DP, declustering potential; FAD, flavin adenine dinucleotide; FMN, flavin mononucleotide; MeCbl, methylcobalamin; PL, pyridoxal; PLP, pyridoxal 5'-phosphate; PN-d₃, pyridoxine hydrochloride methyl-D₃; PN, pyridoxine; PM, pyridoxamine; Q1, quadrupole 1; Q2, quadrupole 2; RF, riboflavin; Sar, sarcosine; TMG, trimethylglycine.

Table 2.5 Mass spectrometer parameters for identification of folates and methionine cycle metabolites.

Analyte	Retention time (min)	Q1 mass (amu)	Q3 mass (amu)	DP	CE	CXP
Folates						
FA	7.42	442.23	295.10	71	25	18
DHF	7.36	444.19	178.10	66	19	12
THF	7.23	446.20	299.20	96	29	18
5-fTHF	7.11	474.10	327.20	86	31	10
CH=THF	7.07	456.11	412.20	151	43	12
CH ₂ THF	7.09	458.12	311.10	76	29	8
5-mTHF	6.93	460.10	313.20	76	29	18
Met cycle metabolites						
SAM	7.69	399.12	250.10	56	25	16
SAH	7.21	385.13	134.10	71	31	10
Hcy	7.34	136.03	56.10	31	29	8
Internal standards						
MTX	6.60	455.11	308.10	86	29	8
SAH-d ₄	7.23	389.19	138.10	71	29	10

Abbreviation(s): 5-fTHF, 5-formyltetrahydrofolate; 5-mTHF, 5-methyltetrahydrofolate; amu, atomic mass unit; CE, collision energy; CH=THF, 5,10-methenyltetrahydrofolate; CH₂THF, 5,10-methylenetetrahydrofolate; CXP, collision cell exit potential. DHF, dihydrofolate; DP, declustering potential; FA, folic acid; Hcy, homocysteine; Met, methionine; MTX, methotrexate; Q1, quadrupole 1; Q2, quadrupole 2; SAH-d₄, S-adenosyl homocysteine-d₄; SAH, S-adenosyl homocysteine; SAM, S-adenosylmethionine; THF, tetrahydrofolate.

2.2.2.1.5 Method validation

Method validation followed standard guidelines for bioanalytical method development (FDA, 2018), based on the method of Xu *et al.* (2020). Briefly, 10% BSA in water was used as a surrogate blank matrix for validation experiments since this gave an equivalent protein load compared with sheep liver. Selectivity was demonstrated by the ability of the assay to differentiate and quantify the specific analytes of interest in the presence of other components (Figure 2.1).

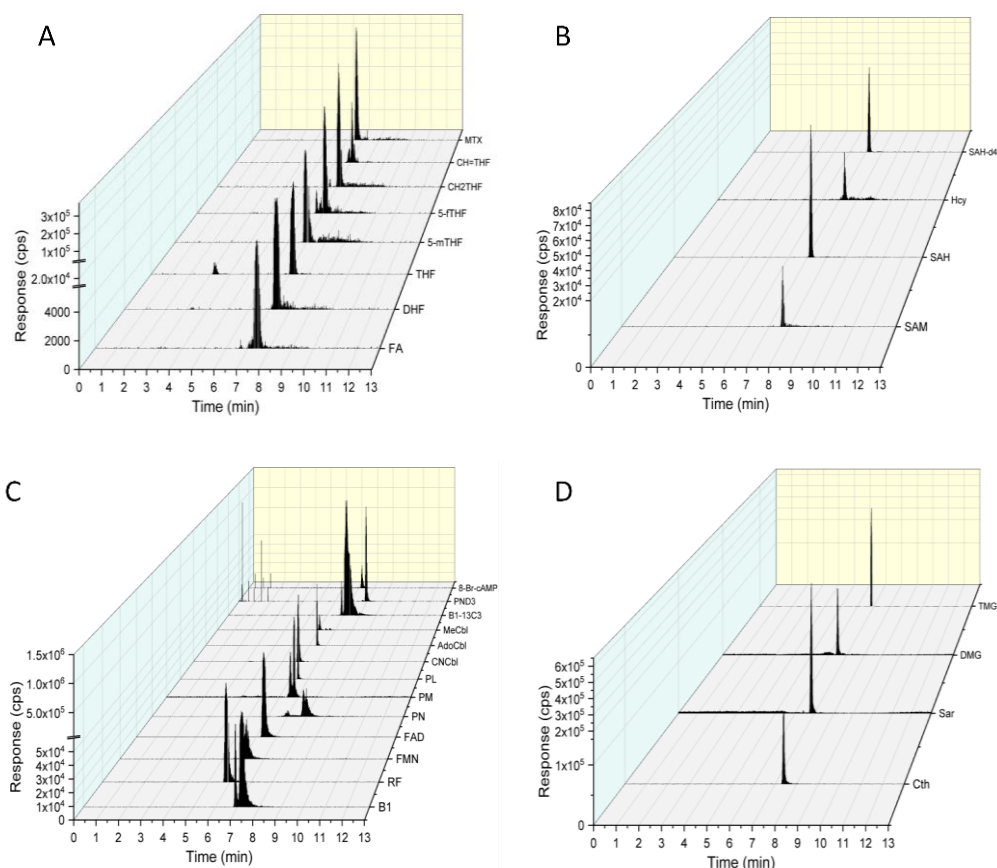


Figure 2.1 HILIC-MS/MS MRM chromatograms for 1C metabolites quantified in sheep liver.

Folic acid (FA), dihydrofolate (DHF), tetrahydrofolate (THF), 5-methyltetrahydrofolate (5-mTHF), 5-formyltetrahydrofolate (5-fTHF), 5,10-methylenetetrahydrofolate (CH₂THF), 5,10-methenyltetrahydrofolate (CH=THF), methotrexate (MTX) (A). S-adenosylmethionine (SAM), S-adenosylhomocysteine (SAH), homocysteine (Hcy), S-adenosylhomocysteine-d₄ (SAH-d₄) (B). Thiamine (B1), riboflavin (RF), flavin mononucleotide (FMN), flavin adenine dinucleotide (FAD), pyridoxine (PN), pyridoxamine (PM), pyridoxal (PL), cyanocobalamin (CNCbl), adenosylcobalamin (AdoCbl), methylcobalamin (MeCbl), thiamine hydrochloride (B1-13C₃), pyridoxine-d₃ (PN-d₃), 8-bromoadenosine 3',5'-cyclic monophosphate (8-Br-cAMP) (C). Cystathionine (Cth), sarcosine (Sar), dimethylglycine (DMG), trimethylglycine (TMG) (D).

Calibration curves were linear ($r \geq 0.97$) over reported concentration ranges for all analytes measured in both methods, except for PLP which did not calibrate accurately and was, therefore, excluded from the study (Table 2.6, Table 2.7). The limit of detection (LOD, $S/N=3$) and quantification (LOQ, $S/N=10$) were determined over three replicates.

Table 2.6 Validation data for quantification of B vitamins and 1C-related amines in sheep liver.

Analyte	Linear range (nmol/L)	LOD (pmol/g)	Precision (RSD%)	Slope	R ²
CNCbl	0.8-100	4.7	30.8	0.03736	0.99
AdoCbl	0.8-100	4.7	29.9	0.01070	0.99
MeCbl	0.8-100	4.7	14.9	0.00551	0.99
PN	0.8-100	4.7	8.8	0.00177	0.99
PM	0.8-100	4.7	9.8	0.00577	0.98
PL	0.8-100	4.7	9.9	0.00368	0.97
RF	3.9-500	23.5	7.8	0.03217	0.99
FMN	3.9-500	23.5	13.3	0.00570	0.99
B1	3.9-500	23.5	7.19	0.00193	0.99
DMG	3.9-500	23.5	8.13	0.02103	0.99
	(μmol/L)	(nmol/g)			
FAD	0.8-250	4.7	29.3	0.00010	0.99
Cth	0.05-7	0.3	26.9	0.00215	0.99
TMG	1.6-100	9.4	9.1	0.00663	0.99
Sar	1.7-150	7.0	11.2	0.00060	0.98

Abbreviation(s): AdoCbl, adenosylcobalamin; B1, thiamine; CNCbl, cyanocobalamin; Cth, cystathionine; DMG, dimethylglycine; FAD, flavin adenine dinucleotide; FMN, flavin mononucleotide; LOD, limit of detection; MeCbl, methylcobalamin; PL, pyridoxal; PM, pyridoxamine; PN, pyridoxine; R², correlation coefficient; RSD%, relative standard deviation; RF, riboflavin; Sar, sarcosine; TMG, trimethylglycine.

Table 2.7 Validation data for quantification of folates and methionine cycle metabolites in sheep liver.

Analyte	Linear range (nmol/L)	LOD (pmol/g)	Precision (RSD%)	Slope	R ²
FA	5-75	0.8	26.0	0.00021	0.99
DHF	20-300	1.5	15.27	0.00011	0.99
THF	10-600	0.8	18.96	0.00007	0.99
5-fTHF	5-150	1.5	19.89	0.00031	0.99
CH=THF	5-150	1.5	12.15	0.00002	0.98
CH ₂ THF	5-300	0.8	16.84	0.00042	0.99
5-mTHF	25-1200	0.4	18.34	0.00013	0.99
	(μmol/L)	LOD (nmol/g)			
SAM	0.08-2.4	0.4	16.70	0.00193	0.99
SAH	0.08-9.6	0.4	6.90	0.00897	0.99
Hcy	0.08-9.6	0.4	15.53	0.00001	0.98

Abbreviation(s): 5-fTHF, 5-formyltetrahydrofolate; 5-mTHF, 5-methyltetrahydrofolate; CH=THF, 5,10-methenyltetrahydrofolate; CH₂THF, 5,10-methylenetetrahydrofolate; DHF, dihydrofolate; FA, folic acid; Hcy, homocysteine; LOD, limit of detection; R², correlation coefficient; RSD%, relative standard deviation; SAH, S-adenosyl homocysteine; SAM, S-adenosylmethionine; THF, tetrahydrofolate.

Precision of the method (RSD%) was determined by analysis of inter-assay QC samples ($n=3$) under the same experimental conditions. For analytes measured using the B vitamin method, the RSD% values were <15%, except for AdoCbl (30.8%), MeCbl (29.9%), FAD (29.3%) and Cth (26.9; Table 2.6). For analytes measured using the folate method, RSD% values were 15-20%, except for FA (26.0%; Table 2.7).

2.2.2.1.6 Statistical data analysis

Data analysis was performed using Analyst software version 1.6.3 (Applied Biosystems/MDS, analytical Technologies, Concord, Ontario, Canada). Selectivity graphs were designed using Origin 2018b software (OriginLab Corporation, Massachusetts, (USA)). Statistical analyses were performed within the Genstat statistical package (19th Edition, VSN International, 2011). Data were log-transformed to address issues of homogeneity of variance, additivity and normality as required (following analysis of plotted residuals). Concentrations of individual metabolites were compared between Ab and MD sheep liver by analysis of variance (ANOVA) and a P -value ≤ 0.05 was deemed statistically significant. Concentration data are reported as means (\pm standard error of means; SEM), and are presented as box plots designed using GraphPad Prism 8 software. Boxplots depict the mean (as the data was analysed using a parametric test, i.e. ANOVA), median and inter-quartile ranges with whiskers set at 1st and 99th percentiles (for visual depiction).

2.3 Results and Discussion

2.3.1 Blood biomarkers

Weekly blood sample analysis showed that lambs maintained on the MD diet became B12-deficient during the 12-week trial period. As expected, low dietary Co intakes caused mean serum B12 concentrations to decrease from 397 pmol/L (week 2) to 115 pmol/L by week 10, and concentrations remained low thereafter (Figure 2.2A). These data indicate that lambs were B12-sufficient (>350 pmol/L) at the beginning of the study but became B12-deficient by week 4 when concentrations declined below 250 pmol/L (deficiency threshold; [Suttle, 2005](#)). As B12 decreased, mean plasma Hcy concentrations increased from 5.87 μ mol/L (week 1) to 9.90 μ mol/L (week 12), demonstrating marginal B12

deficiency (Figure 2.2A). Plasma methylmalonic acid (MMA) concentrations were unresponsive to B12 ($<7 \mu\text{mol/L}$) until week 6 (Gruner *et al.*, 2004) but increased from 4.5 to 21.6 $\mu\text{mol/L}$, thereby exceeding the normal plasma concentration of $<10 \mu\text{mol/L}$ for barley-fed lambs (Figure 2.2B; O'Harte *et al.*, 1989). The inverse relationship between blood vitamin B₁₂ and biomarkers of B12 deficiency denotes that the MD diet engendered a B12-deficient metabolic state in lambs that would be expected to perturb 1C metabolism, thereby leading to an aberrant metabolome in the liver.

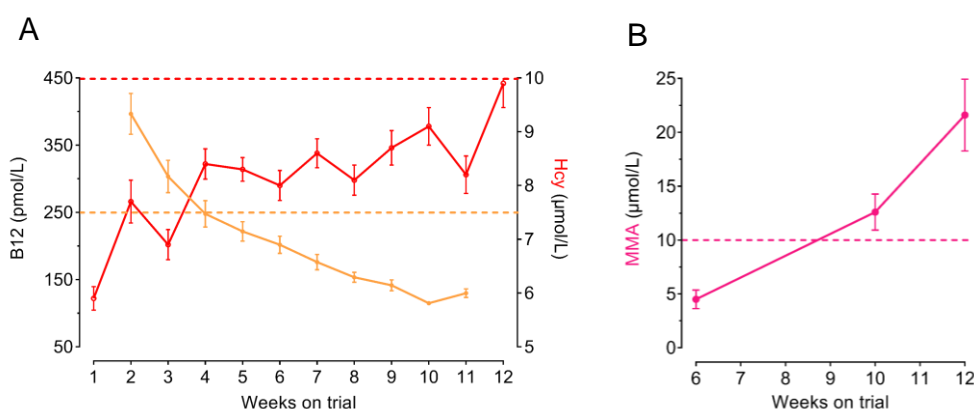


Figure 2.2 Plasma homocysteine (Hcy) and methylmalonic acid (MMA) concentrations increase as a result of Vitamin B₁₂ deficiency in Texel lambs.

Serum B12 concentrations (●) and plasma homocysteine (Hcy) concentrations (○) over time ($n=83$) (A). Mean plasma methylmalonic acid (MMA) concentrations (●) over time ($n=83$) (B). Data presented as mean \pm SEM. Reference concentration for B12 deficiency (---; Suttle, 2005). Reference concentration for normal Hcy (---; Kennedy *et al.*, 1992) and MMA concentration (---; O'Harte *et al.*, 1989).

2.3.2 Liver metabolites

In order to investigate the metabolic burden of dietary methyl deficiency, 1C metabolites and related compounds were quantified by HILIC-MS/MS, HPLC and GC-MS in sheep liver collected from UK abattoirs (Ab; $n=266$) and in methyl deficient sheep liver (MD; $n=83$).

2.3.2.1 Vitamin B₁₂

The term 'B12' generically refers to a group of Co-containing, organometallic compounds, known as cobalamins (Takahashi-Iñiguez *et al.*, 2012). The two bioactive forms of cobalamin (Cbl) are methylcobalamin (MeCbl) and adenosylcobalamin (AdoCbl). Cyanocobalamin (CNCbl), the synthetic form of B12 used in dietary supplements (Farquharson and Adams, 1976), is

biologically inert but can be converted to the bioactive forms for coenzyme activity (Martinelli *et al.*, 2011; Figure 2.3A). Vitamin B₁₂ is released into the cell cytosol in the form of hydroxocobalamin (OHCbl) and reduced to Cbl before binding methionine synthase (MTR; EC 2.1.1.13). Upon binding the enzyme, Cbl is methylated to form MeCbl (Shane, 2008), the cofactor required for re-methylation of homocysteine (Hcy) in the terminal step of methionine synthesis. Alternatively, Cbl can be transported to the mitochondria and converted to AdoCbl, the cofactor required for methylmalonyl-CoA mutase (MUT; EC 5.4.99.2; Figure 2.3A). This enzyme catalyses isomerisation of methylmalonyl-CoA to succinyl-CoA in propionate metabolism (Appendix Figure 2.1), an important step prior to gluconeogenesis in ruminants (Shane, 2008; Forny *et al.*, 2014).

Since Cbl contains one Co atom, it is assumed that the requirement of ruminants for B₁₂ equal the requirement of ruminal microbes for Co (McDowell, 2000). Continuing with the aforementioned discussion (Section 2.1), the Co content of the diet is the primary limiting factor for the synthesis of B₁₂ by rumen microbes. Under Co-deficient conditions, the decline in serum B₁₂ precedes the decline in liver stores (Booth and Spray, 1960). Thus, it is not surprising that the decrease in serum B₁₂ observed amongst Co-deficient animals in the present study (Figure 2.2A) led to a significant decline in all three species of vitamin B₁₂ in liver ($P < 0.001$; Figure 2.3B).

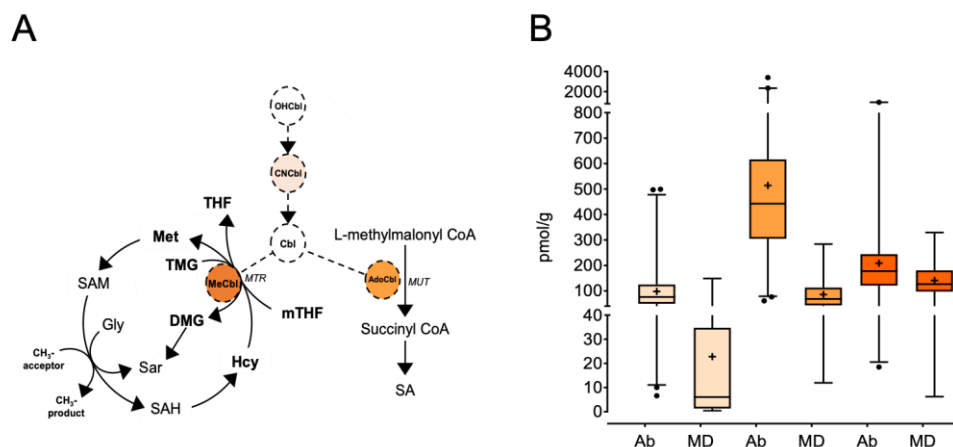


Figure 2.3 Vitamin B₁₂ species are decreased in methyl deficient sheep liver.

B₁₂ cofactors in one-carbon (1C) metabolism (A). Concentrations (pmol/g wet weight liver) of cyanocobalamin, CNCbl (□) ($P < 0.001$); adenosylcobalamin, AdoCbl (■) ($P < 0.001$); methylcobalamin, MeCbl (■) ($P < 0.001$) in abattoir-derived (Ab; $n = 266$) and methyl deficient (MD; $n = 83$) sheep liver (B). Individual vitamer concentrations (colour-coded) between Ab and MD sheep compared by ANOVA. Mean (+), median, interquartile ranges, and 1st and 99th percentiles. Dots in boxplots represent outliers.

The ~4-fold higher mean concentration of CNCbl measured in Ab sheep liver (Ab: 98.0 ± 5.14 vs MD: 22.8 ± 3.57 pmol/g) is likely to be an effect of dietary environment as sheep slaughtered in the abattoir were reared on different farms and fed different diets. In some cases, CNCbl may have been incorporated as a dietary supplement in Ab animals which may account for the large variation of CNCbl concentrations in Ab liver. The concentration range of CNCbl measured in MD liver (0.38 to 148.64 pmol/g) could be explained by the small amount of CNCbl that is synthesised by rumen microbes (Johnson *et al.*, 1956).

Although not statistically tested, adenosylcobalamin (AdoCbl) was the most abundant form of B12 present in Ab sheep liver (502.6 ± 19.74 pmol/g; Figure 2.3B), measuring 2-fold higher than MeCbl (Xu *et al.*, 2020). These findings are consistent with reports that B12 is stored as AdoCbl in animal tissues (Shane, 2008; Quadros, 2010; Kelly *et al.*, 2006), and that the metabolic demand of sheep for AdoCbl is normally higher than MeCbl due to its involvement in propionic acid (PPA) metabolism for gluconeogenesis in ruminants (McDowell, 2000; Kelly *et al.*, 2006). Indeed, the propionate-succinate pathway (Figure 1.2) appears to be the first rate-limiting pathway in B12 deficiency (Furlong *et al.*, 2010), as characterised by the ~6-fold decrease in AdoCbl (Figure 2.3B), and the marked increase in plasma MMA (Figure 2.2B) and liver MMA concentrations in MD sheep in the present study (discussed later, Section 2.3.2.9). Although not statistically tested, mean hepatic concentrations of MeCbl were higher than AdoCbl in MD sheep. If concentrations of MeCbl are associated with MTR enzyme activity and turnover (Quadros and Jacobsen, 1995), the altered profile of these two B12 coenzyme forms may directly reflect altered function of the hepatic 1C metabolism under methyl deficient conditions. Perhaps there was an increased demand for the MeCbl cofactor and Hcy remethylation to methionine in MD sheep. Although speculative, these observations identify subtle downstream metabolic effects associated with modest reductions in dietary Co.

2.3.2.2 Vitamin B₆

The extended family of vitamin B₆ comprises the alcohol, pyridoxine (PN); the amine, pyridoxamine (PM); the aldehyde, pyridoxal (PL); and, their respective phosphorylated derivatives (Merril and Henderson, 1990; Colinas and Fitzpatrick, 2016). Dietary B6 compounds are absorbed in the small intestine in their de-phosphorylated forms (Albersen *et al.*, 2013). Pyridoxine (PN), the most

commonly supplemented form of B6 (Albersen *et al.*, 2013), and PM are rapidly transformed to PL in the intestinal tissues and this is released into the portal blood (Sakurai *et al.*, 1992). Circulating PL is taken up by the liver, the principal site of B6 metabolism, and re-phosphorylated by pyridoxal kinase (PK; EC 2.7.1.35) before conversion to the bioactive coenzyme, pyridoxal 5'-phosphate (PLP; Albersen *et al.*, 2013), which functions as a cofactor in >140 catalytic reactions (Percudani and Peracchi, 2003). In the context of 1C metabolism, PLP is a cofactor for serine hydroxymethyltransferase (SHMT; EC 2.1.2.1), an enzyme that catalyses the simultaneous conversion of serine (Ser) to glycine (Gly) and tetrahydrofolate (THF) to 5,10-methylenetetrahydrofolate (CH₂THF) in the folate cycle (Appaji Rao *et al.*, 2003). In addition, PLP is a coenzyme for cystathionine β-synthase (CBS; EC 4.2.1.22) and cystathionine γ-lyase (CTH; EC 4.4.1.1) enzymes of the *trans*sulphuration pathway (Figure 2.4A). The former catalyses the conversion of Hcy to cystathionine (Cth) and the latter catalyses the conversion of Cth to cysteine (Cys; Perry *et al.*, 2007), thus demonstrating the role of B6 in lowering Hcy concentrations (Miodownik *et al.*, 2007).

All measured B6 species were lower ($P < 0.05$) in MD liver than Ab liver (Figure 2.4B). Pyridoxamine was the predominant form of B6 in Ab liver, followed by supplemental form, PN (Figure 2.4B). The large variation in PN and PM concentrations in Ab sheep liver is a likely consequence of the varied diet these sheep received prior to slaughter.

Due to its high instability and susceptibility to degradation (Mohammed-Ahmed *et al.*, 2017), PLP measured below the limit of detection (<LOD) in MD liver (Section 2.2.2.1.5) and only trace levels were detected in Ab liver (Xu *et al.*, 2020). Liver PL concentrations were, therefore, used as a proxy measurement of bioactive B6 in the present study. Mean PL concentrations were marginally decreased in the MD liver (Ab: 240.3 ± 6.41 vs MD: 219.7 ± 14.61 pmol/g; $P = 0.019$) which may reflect a marginal decrease its bioactive phosphorylated derivative. Since all forms of B6 are interconvertible, it is possible that PN and PM are readily converted to PL for phosphorylation to the bioactive form to maintain B6 coenzyme function (McCormick and Chen, 1999).

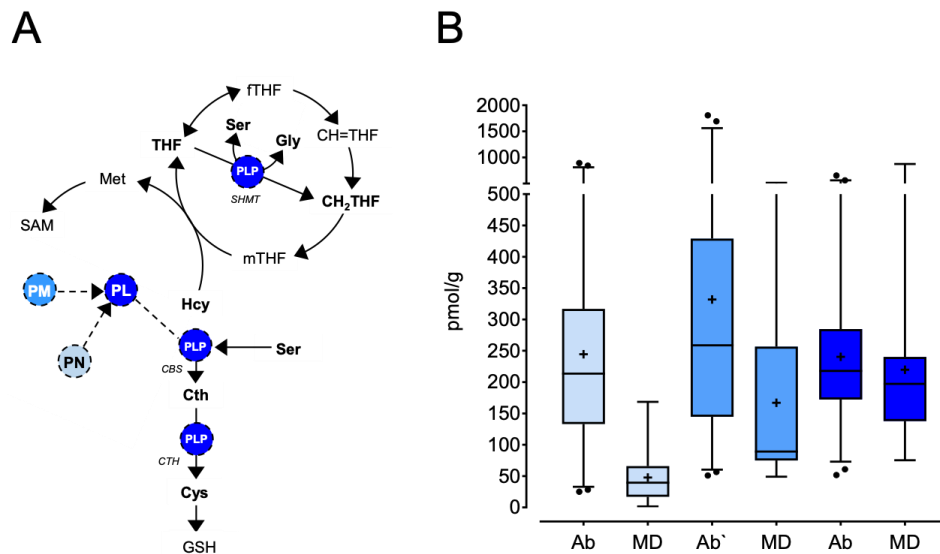


Figure 2.4 Vitamin B₆ species are decreased in methyl deficient sheep liver.

B6 cofactors in one-carbon (1C) metabolism (**A**). Concentrations (pmol/g wet weight liver) of pyridoxine, PN ($P < 0.001$); pyridoxamine, PM ($P < 0.001$); pyridoxal, PL ($P = 0.019$) in abattoir-derived (Ab; $n = 266$) and methyl deficient (MD; $n = 83$) sheep liver (**B**). Individual vitamer concentrations (colour-coded) between Ab and MD sheep compared by ANOVA. Mean (+), median, interquartile ranges, and 1st and 99th percentiles. Dots in boxplots represent outliers.

2.3.2.3 Vitamin B₂

Vitamin B₂ exists in nature as riboflavin (RF) and its coenzyme derivatives, flavin mononucleotide (FMN) and flavin adenine dinucleotide (FAD). Only a small amount of B₂ is present in dietary sources as RF whilst the majority (~90%) is present as FAD and, to a lesser degree, FMN (Powers, 2003). Flavin-dependent enzymes use FMN and FAD as cofactors in numerous oxidation-reduction reactions in primary metabolic pathways, including the tricarboxylic acid (TCA) cycle, fatty acid catabolism (β -oxidation) and amino acid degradation (Lienhart *et al.*, 2013). In 1C metabolism, MTHFR requires FAD as a cofactor to convert 5,10-methylenetetrahydrofolate (CH₂THF) to 5-methyltetrahydrofolate (5-mTHF) in the folate cycle (Figure 2.5A; Garca-Minguillan *et al.*, 2014). Methionine synthase reductase (MTRR; EC 1.16.1.8) utilises both FMN and FAD as cofactors to reactivate methionine synthase (MTR) via reductive re-methylation of cob(II)alamin to methylcob(III)alamin, thereby facilitating Hcy re-methylation to Met (Figure 2.5A; Leclerc *et al.*, 1998; Garca-Minguillan *et al.*, 2014). Additionally, two consecutive enzymes in choline metabolism; dimethylglycine dehydrogenase (DMDGH; EC 1.5.99.2) and sarcosine dehydrogenase (SARDH; EC 1.5.99.1), covalently bind the FAD cofactor to

catalyse the oxidative demethylation of dimethylglycine (DMG) to sarcosine (Sar) and Sar to glycine (Gly), respectively (Porter *et al.*, 1985; Figure 2.5B). Both enzymes use THF to capture 1C units released by oxidative demethylation of substrates, yielding CH₂THF in the process (Lienhart *et al.*, 2013).

Importantly, flavin-dependent enzymes are also involved in the biosynthesis of other B vitamin cofactors. For instance, vitamin B₆ metabolism requires pyridoxine 5'-phosphate oxidase (PNPO; EC 1.4.3.5), an FMN-dependent enzyme that converts Met phosphorylated PN to its bioactive form, PLP (Choi *et al.*, 1983; Figure 2.4A). It follows that 1C metabolism involves the concerted actions and interactions of various B vitamin cofactors (Sauberlich, 1980).

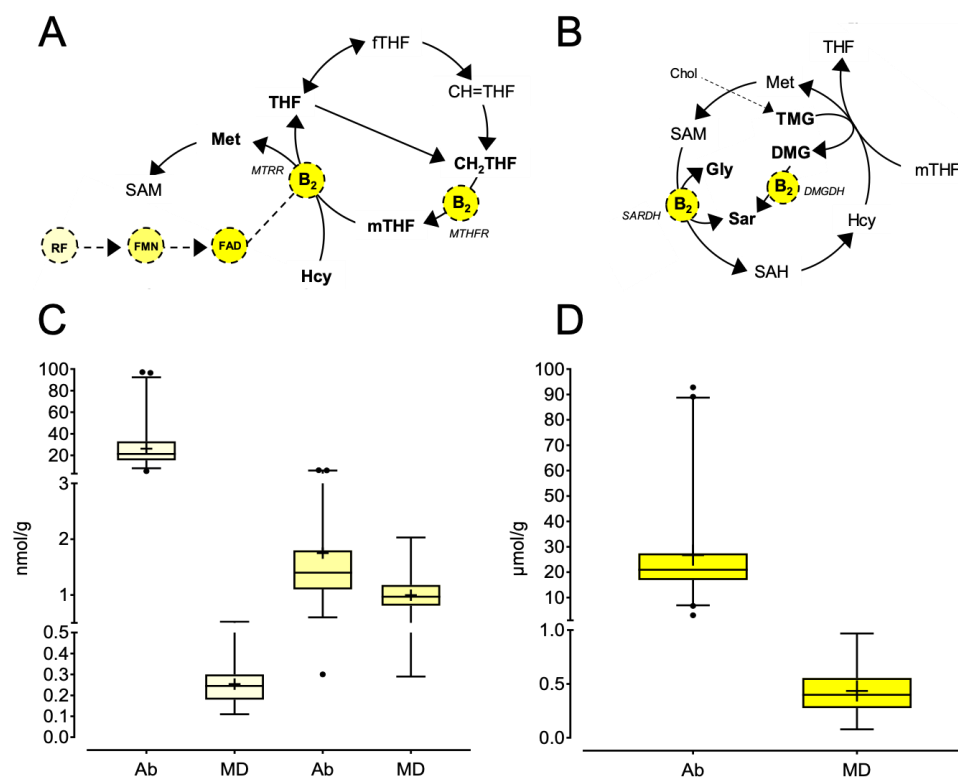


Figure 2.5 Vitamin B₂ species are decreased in methyl deficient sheep liver.

B₂ cofactors in one-carbon (1C) metabolism (A). B₂ cofactors in choline metabolism (B). Concentrations (nmol/g wet weight liver) of riboflavin, RF (□) ($P < 0.001$); flavin mononucleotide, FMN (■) ($P < 0.001$) (C) and concentrations (μmol/g wet weight liver) of flavin adenine dinucleotide, FAD (■) ($P < 0.001$) in abattoir-derived (Ab; $n = 266$) and methyl deficient (MD; $n = 83$) sheep liver (D). Individual vitamer concentrations (colour-coded) between Ab and MD sheep compared by ANOVA. Mean (+), median, interquartile ranges, and 1st and 99th percentiles. Dots in boxplots represent outliers.

Flavin adenine dinucleotide (FAD) was the major form of B₂ in Ab liver (Xu *et al.*, 2020), measuring ~60-fold higher than concentrations in MD liver (Ab: 26.7 ± 1.17 vs MD: 0.4 ± 0.02 μmol/g; Figure 2.5D). Precursors, RF and FMN, were

also significantly reduced in MD liver (Figure 2.5C). The low B2 concentrations observed in MD lambs may reflect their relatively immature age and stage of rumen development (Luecke *et al.*, 1950; Poe *et al.*, 1972). Adult ruminants do not have a specific dietary requirement for RF due to its microbial synthesis in the rumen, however, RF deficiency has been demonstrated in young ruminants whose rumen microflora is not yet fully established (McDowell, 2000). This may explain, at least in part, the significant decrease in hepatic RF concentrations observed in MD lambs (Ab: 26.2 ± 0.97 vs MD: 0.3 ± 0.01 nmol/g; Figure 2.5C). Moreover, feeding conditions, such as forage to concentrate ratios (Zhang *et al.*, 2017b; Seck *et al.*, 2017), and diet composition (Fonty *et al.*, 1987) can influence microbial synthesis of RF. Thus, the ruminal RF content of the recently weaned lamb during its transition to the MD concentrate diet may be quite different to that of abattoir-derived sheep, which may have been predominantly pasture-fed.

Free RF is absorbed by enterocytes of the small intestine and undergoes phosphorylation to FMN, catalysed by cytosolic flavokinase (EC 2.7.1.26). Flavin mononucleotide is readily converted to FAD by FAD-dependent enzyme, FAD synthetase (EC 2.7.7.2; Powers, 2003; Figure 2.5A). The efficient conversion of FMN to FAD may provide a plausible explanation for why the mean liver FMN concentration does not decrease to the same extent as RF and FAD concentrations in MD sheep liver (Figure 2.5C).

2.3.2.4 Vitamin B₁

Vitamin B₁ (thiamine) is not directly related to 1C metabolism but is fundamental for energy production (Lonsdale, 2006) and is, therefore, relevant to the present study. The phosphate ester of vitamin B₁, thiamine pyrophosphate (TPP), is the rate-limiting enzyme cofactor for regulatory enzymes involved in carbohydrate metabolism, including pyruvate dehydrogenase (PDH; EC 1.2.4.1) and α -ketoglutarate dehydrogenase (KGDH; EC 1.2.4.2; Lonsdale, 2015; Figure 2.6A). The former catalyses the decarboxylation of pyruvate to acetyl CoA (Lonsdale, 2006) whilst the latter converts α -ketoglutarate (α -KG) to succinyl-CoA in the TCA cycle (McLain *et al.*, 2011; Figure 2.6A). Thus, it follows that the energy generated from oxidation of glucose is highly dependent on TPP (Lonsdale, 2006).

Thiamine is primarily stored in the liver, however, it is one of the most poorly stored B vitamins and most mammals fed a thiamine-deficient diet will deplete their body reserves within 14-18 days (Oseizagha *et al.*, 2013; Ensminger *et al.*, 1990). In humans, thiamine deficiency can lead to serious neurological conditions, such as Beriberi (Lonsdale, 2015) and delirium (Osiezagha *et al.*, 2013). In ruminants, thiamine deficiency can cause polioencephalomalacia, also referred to as cerebrocortical necrosis (McGuirk, 1987). Considering the interrelationships between B vitamin cofactors mentioned earlier (Section 2.3.2.3), it may not seem surprising that thiamine deficiency is often accompanied by deficiencies of other B vitamins. This is demonstrated in the current study, as MD sheep present with significantly lower concentrations of hepatic B12, B6 and B2 (Figure 2.3 to Figure 2.5) in addition to lower hepatic thiamine (Ab: 3.0 ± 0.13 vs MD: 0.4 ± 0.04 nmol/g; $P < 0.001$; Figure 2.6B).

It is possible that subclinical thiamine deficiency can lead to a reduction in synthesis of other B vitamins since certain strains of bacteria require thiamine to grow and colonise the rumen (McDowell *et al.*, 2000). Thiamine deficiency is common in weaned lambs, particularly those fed high fermentable-starch (i.e. barley-based) diets (Karapinar *et al.*, 2008) such as that fed in the current study.

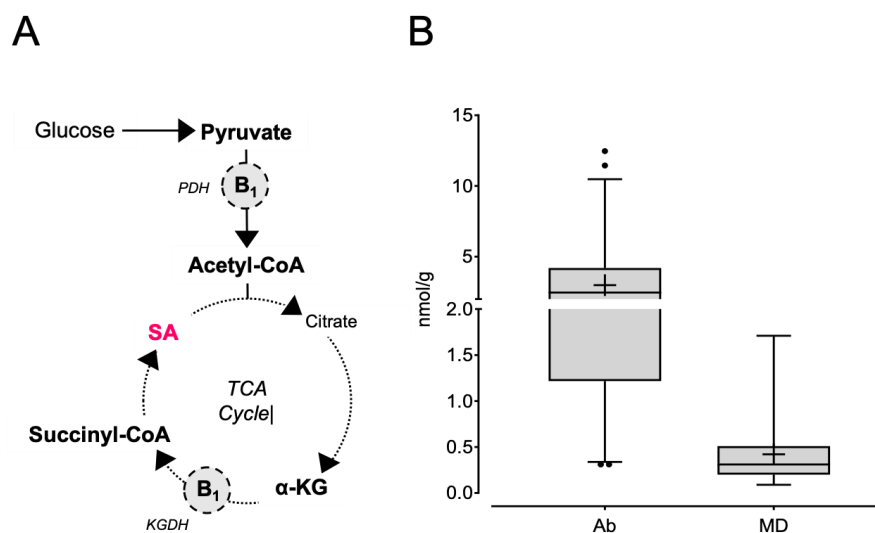


Figure 2.6 Vitamin B₁ (thiamine) is decreased in methyl deficient sheep liver.

B1 cofactor in energy metabolism (Tricarboxylic acid cycle) (**A**). Concentrations (nmol/g wet weight liver) of thiamine, B1 □ ($P < 0.001$) in abattoir-derived (Ab; $n=266$) and methyl deficient (MD; $n=83$) sheep liver (**B**). Individual vitamer concentrations between Ab and MD sheep compared by ANOVA. Mean (+), median, interquartile ranges, and 1st and 99th percentiles. Dots in boxplots represent outliers.

2.3.2.5 Vitamin B₉ (folates)

Natural folates are interconverted between different oxidation states (e.g. methylene, methyl, formyl; [Ducker and Rabinowitz, 2017](#)) and are most abundant in their polyglutamated form within cells (Figure 2.7). Their conjugation to glutamate residues, catalysed by folylpolyglutamate synthetase (FPGS; EC 6.3.2.17), enhances their co-enzyme affinity, cellular retention and stability ([Mehrshahi *et al.*, 2010](#)). The synthetic folate, folic acid (FA), exists in monoglutamate form only ([Melse-Boonstra *et al.*, 2002](#)). Although hepatic FA concentration ranges were similar in both cohorts, MD sheep exhibited higher mean FA concentrations than Ab sheep (Ab: 5.8 ± 0.40 vs MD: 21.0 ± 0.86 pmol/g; $P < 0.001$; Figure 2.7B). This observation is surprising given that MD sheep were not supplemented with FA during the study, however, this result could be explained by differences in hindgut absorption of FA between cohorts ([Milman, 2012](#)) or it may be an artefact of the assay since the relative standard deviation (RSD%) for FA was high (26%) indicating poor repeatability (Section 2.2.2.1.5).

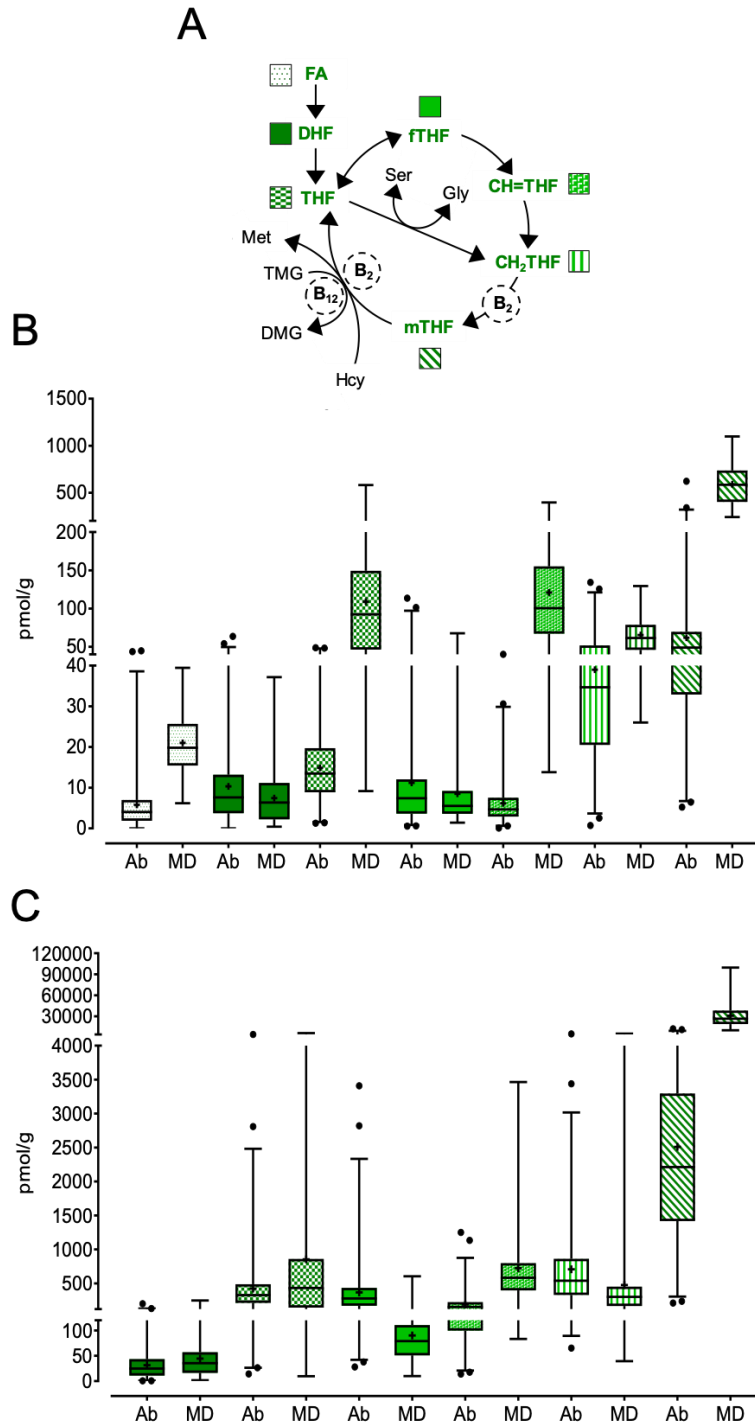
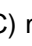






Figure 2.7 5-methyltetrahydrofolate accumulates in methyl deficient sheep liver.

Folate cofactors in one-carbon (1C) metabolism; folic acid, FA ; dihydrofolate, DHF ; tetrahydrofolate, THF ; 5-formyltetrahydrofolate, 5-fTHF ; 5,10-methenyltetrahydrofolate, CH=THF ; 5,10-methylenetetrahydrofolate, CH₂THF ; 5-methyltetrahydrofolate, 5-mTHF (A). Concentrations (pmol/g wet weight liver) of monoglutamated folates (B). Concentrations (pmol/g wet weight liver) of total folates (mono- and polyglutamated) folates in abattoir-derived (Ab; *n*=266) and methyl deficient (MD; *n*=83) sheep liver (C). Individual vitamer concentrations (colour-coded) between Ab and MD sheep compared by ANOVA. Mean (+), median, interquartile ranges, and 1st and 99th percentiles. Dots in boxplots represent outliers.

Early investigations in sheep reported that B12 deficiency caused depletion of intracellular folate concentrations in the liver (Dawbarn *et al.*, 1958). According to Smith and Osborne-White (1973), B12-deficient sheep liver were more severely depleted in THF and formyltetrahydrofolate (fTHF) than in 5-mTHF, and this depletion was most pronounced in folate polyglutamates than monoglutamates as deficiency advanced. In contrast, the present study found that dietary methyl deficiency caused an increase of specific folate species in the liver. Both monoglutamate and polyglutamated forms of tetrahydrofolate (THF) and 5,10-methenyltetrahydrofolate (CH=THF) were significantly increased in MD liver ($P < 0.001$; Figure 2.7B and Figure 2.7C).

Of particular interest is the >10-fold increase in hepatic 5-mTHF in MD sheep. A central hypothesis to account for this observation is the 'methyl-folate trap' whereby B12 deficiency leads to reduced MTR activity. Consequently, intracellular folate becomes 'trapped' as 5-mTHF because it cannot be converted to THF or revert back to CH₂THF (Shane and Stokstad, 1985; Miller *et al.*, 2009; Figure 2.7A).

Not only does folate accumulate in B12 deficiency, but it can also remain in its monoglutamated form due to an impairment of polyglutamation within the liver (Smith and Osborne-White, 1973). This impairment may arise due to a lack of suitable substrate for polyglutamate synthesis or a direct requirement for B12 for polyglutamation (Perry *et al.*, 1976). This may explain why concentrations of polyglutamated folates do not increase to the same extent as their monoglutamated counterparts, or why monoglutamate concentrations of CH₂THF increase whilst polyglutamate concentrations decrease in methyl deficient sheep (Figure 2.7). Another theory is that folylpolyglutamate synthetase (FPGS) activity is upregulated in B12-deficient sheep liver, thereby providing a compensatory mechanism to conserve bioactive folate coenzymes (Gawthorne and Smith, 1974).

Unlike previous studies in sheep, which examined the effect of B12 deficiency in isolation, the present study examines the effect of methyl deficiency more generally. It is likely that dietary restriction of Co, S and methionine contributes toward system-wide alterations to biochemistry, physiology and metabolism, causing aberrant flux through the folate cycle and the accumulation of several folate intermediates.

2.3.2.6 Methionine cycle metabolites

The methionine cycle regulates the balance between methionine and cysteine (Cys) for protein synthesis, provides the substrate for polyamine synthesis (discussed later, Section 2.3.2.8), and facilitates methyl group transfer from 5-mTHF to an array of substrates, thereby constituting the principal mechanism for cellular transmethylation reactions in mammals (Finkelstein, 1990). In the liver, two isoforms of methionine adenosyltransferase (MATI/III; EC 2.5.1.6) catalyse the conversion of methionine to the universal methyl donor, SAM (Martinov *et al.*, 2000). After transfer of a methyl group, SAM is converted to S-adenosylhomocysteine (SAH). Under normal physiological conditions, SAH is hydrolysed to Hcy which is removed via re-methylation to methionine to close the metabolic loop, or by degradation to Cys in the *transsulphuration* pathway (Caudill *et al.*, 2001; Figure 2.8A).

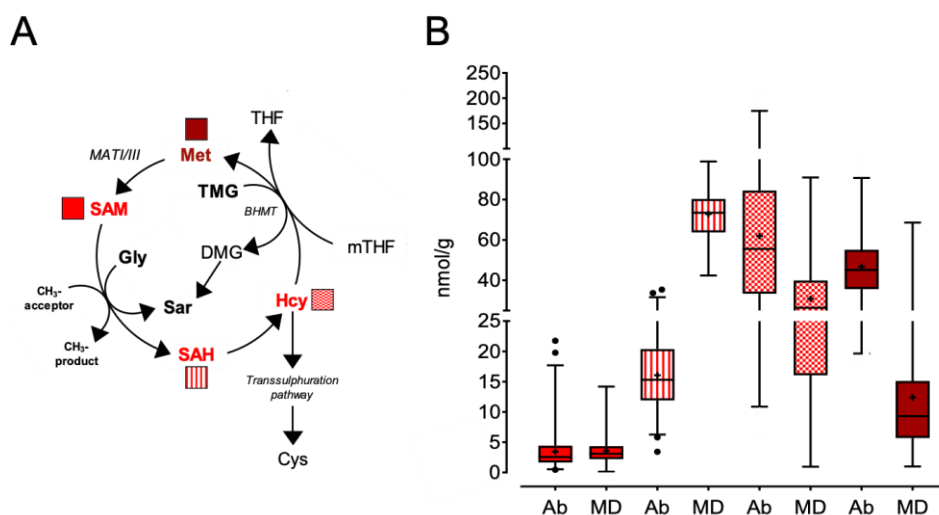


Figure 2.8 Concentrations of methionine cycle metabolites are altered in methyl deficient sheep liver.

Methionine metabolism (A). Concentrations (nmol/g wet weight liver) of S-adenosylmethionine, SAM (■) ($P=0.155$); S-adenosylhomocysteine, SAH (▨) ($P<0.001$); homocysteine, Hcy (▩) ($P<0.001$); Methionine, Met (■) ($P<0.001$) in abattoir-derived (Ab; $n=266$) and methyl deficient (MD; $n=83$) sheep liver (B). Individual metabolite concentrations (colour-coded) between Ab and MD sheep compared by ANOVA. Mean (+), median, interquartile ranges, and 1st and 99th percentiles. Dots in boxplots represent outliers.

As an expected consequence of feeding a sulphur-deficient diet, MD sheep exhibited significantly lower hepatic methionine concentrations than Ab sheep (Ab: 46.7 ± 0.91 vs MD: 12.4 ± 1.26 nmol/g; $P<0.001$; Figure 2.8B). The MD diet had no effect on hepatic SAM concentration (Ab: 3.5 ± 0.18 vs MD: 3.6 ± 0.25

nmol/g; $P=0.155$) but caused a significant increase in SAH concentration (Ab: 16.1 ± 0.34 vs MD: 72.9 ± 1.32 nmol/g; $P<0.001$), thereby potentially reducing the SAM:SAH ratio (Figure 2.8A). As discussed earlier (Section 1.3.1.1), the SAM:SAH ratio is commonly used as an indicator of cellular transmethylation potential; a decreased ratio is predictive of reduced methylation capacity (Caudill *et al.*, 2001). As SAH is a potent inhibitor of methyltransferase enzymes, its accumulation leads to cellular hypomethylation and the dysregulation of integral metabolic reactions. Thus, SAH needs to be eliminated from the cell (Finkelstein, 1990). A study in methyl deficient rodents showed that a rise in intracellular SAH was most consistently associated with global DNA hypomethylation, whilst reduced concentrations of SAM alone was not sufficient to affect DNA methylation (Caudill *et al.*, 2001). Therefore, it is possible that elevated SAH was sufficient to cause hypomethylation of DNA in MD sheep hepatocytes, however, this line of enquiry is beyond the scope of the present study.

Considering the increase in plasma Hcy (Figure 2.2A) and hepatic SAH, it seems paradoxical that Hcy concentrations should be 2-fold lower in MD than Ab sheep liver (Ab: 61.9 ± 2.32 vs MD: 30.9 ± 2.33 nmol/g; $P<0.001$; Figure 2.8B). There are, however, putative explanations for this decrease; i) animals fed the MD diet became low in S meaning that their capacity to synthesise sulphur-containing amino acids (i.e. Hcy) was reduced (Škovierová *et al.*, 2016); ii) unlike many other tissues, the liver possesses a secondary pathway for Hcy remethylation catalysed by BHMT and, therefore, has an additional level of regulation over Hcy concentrations (Feng *et al.*, 2011); and, iii) intracellular Hcy is readily egressed to maintain concentrations at a low level in order to prevent toxic accumulation of SAH (Finkelstein, 2000; Ulrich *et al.*, 2008). As SAH is not readily transported across the cell membrane, Hcy may serve as an exportable form of SAH to preserve cellular methylation status (Caudill *et al.*, 2001). In support of the hypothesis proposed by Yi *et al.* (2000), plasma Hcy concentrations provide a more reliable biomarker for intracellular SAH and cellular methylation capacity than intracellular Hcy concentrations.

2.3.2.7 1C-related amino acids and derivatives

One-carbon metabolism integrates 1C units from amino acids, including serine (Ser) and glycine (Gly), both of which are nutritionally non-essential amino acids that are biosynthetically linked (Fell and Snell, 1988; Locasale, 2013; Pérez-

Torres *et al.*, 2017; Figure 2.9A). A substantial amount of Ser can be synthesised *de novo* from glucose (Fell and Snell, 1988) and converted to Gly by donation of a 1C unit to THF forming CH₂THF, thereby driving the folate cycle. This reaction, catalysed by the bidirectional PLP-dependent enzyme, serine hydroxymethyltransferase (SHMT), is at near equilibrium and can be easily reversed (Shane, 2008; Ramos *et al.*, 2017; Figure 2.9A).

Mammals possess two distinct isoforms of SHMT; cytosolic and mitochondrial (Garrow *et al.*, 1993). The mitochondrial isoform is ubiquitously expressed and thought to be responsible for generating the majority of 1C units for cytosolic 1C metabolism (MacFarlane *et al.*, 2008). In contrast, expression of the cytosolic isoform is limited to the liver and kidney where its principal function may be to synthesise Ser from Gly for gluconeogenesis (Shane, 2008).

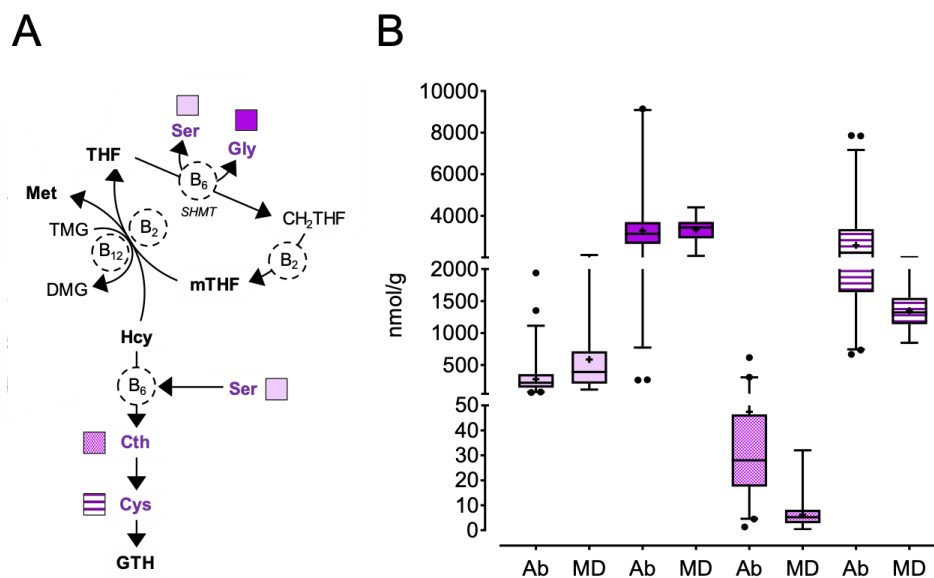


Figure 2.9 Amino acids drive folate metabolism and *transsulphuration* in sheep liver.

Amino acids in one-carbon (1C) metabolism (A). Concentrations (nmol/g wet weight liver) of serine, Ser (□) ($P < 0.001$); glycine, Gly (■) ($P = 0.233$); cystathionine, Cth (▣) ($P < 0.001$); cysteine, Cys (▤) ($P < 0.001$) (B) in abattoir-derived (Ab; $n = 266$) and methyl deficient (MD; $n = 83$) sheep liver. Individual metabolite concentrations (colour-coded) between Ab and MD sheep compared by ANOVA. Mean (+), median, interquartile ranges, and 1st and 99th percentiles. Dots in boxplots represent outliers.

Hepatic Ser concentrations were significantly increased in MD sheep (Ab: 279.0 ± 12.84 vs MD: 586.4 ± 54.36 nmol/g; $P < 0.001$) but Gly concentrations were unaffected by methyl deficiency (Ab: 3316.8 ± 74.06 vs MD: 3343.8 ± 63.47 nmol/g; $P = 0.233$; Figure 2.9B). It may be that tissue concentrations of Gly are regulated by the mitochondrial glycine cleavage system (GCS), the principal

pathway of Gly catabolism whereby glycine dehydrogenase (GLDC; EC 1.4.1.10) catalyses the degradation of glycine to yield 1C for the methylation of THF (Amelio *et al.*, 2014). It is postulated that the GCS protects cells from Gly toxicity (Kim *et al.*, 2015). Whilst there is no definitive explanation for the increased concentration of Ser in MD sheep liver, it is possible that decreased concentrations of vitamin B₆ observed in MD sheep liver (Section 2.3.2.2) caused a reduction in catalytic activity of SHMT, thereby reducing Ser conversion to Gly (Scheer *et al.*, 2005; Perry *et al.*, 2007). Low B₆ could also lead to reduced activity of B₆-dependent enzymes in the two-step transsulphuration pathway which may contribute to the accumulation of Ser (Figure 2.9A).

Reduced flux through the *transsulphuration* pathway is reflected by the reduction of intermediates, Cth and Cys, in MD sheep liver compared with Ab sheep liver ($P < 0.001$; Figure 2.9B). Of relevance is the 2-fold reduction of essential amino acid, Cys, in MD lambs that were actively growing a fleece during the study. Wool contains a high content of sulphur-containing amino acid, Cys, and, therefore, requires large amounts of Cys or methionine for the generation of Cys, for its growth (Nezamidoust *et al.*, 2014). The depletion of hepatic Cys and methionine, as limiting amino acids for wool production, was reflected in a subset of MD sheep that exhibited poor quality fleece growth towards the end of the study.

Aside the *transsulphuration* pathway, a parallel pathway for Hcy metabolism is trimethylglycine (TMG)-dependent. Trimethylglycine, otherwise known as betaine, is a methyl donor in the remethylation of Hcy to Met, catalysed by BHMT (Ueland *et al.*, 2005). A product of this remethylation reaction, dimethylglycine (DMG), can be converted to sarcosine (Sar) by dimethylglycine dehydrogenase (DMGDH; EC 1.5.99.2; Obeid, 2013; Figure 2.10A).

Hepatic TMG concentrations are reduced ~3-fold in MD than Ab lambs (Ab: 1116.3 ± 27.21 vs MD: 381.2 ± 32.76 nmol/g; $P < 0.001$). As might be expected, low substrate (TMG) availability lowers product (methionine and DMG) formation (Ab: 3.5 ± 0.31 vs MD: 1.0 ± 0.10 nmol/g; $P < 0.001$; Figure 2.8B, Figure 2.10B). Surprisingly, hepatic sarcosine (Sar) significantly increased in MD lambs (Ab: 157.8 ± 3.98 vs MD: 512.0 ± 24.80 nmol/g; $P < 0.001$). This may be a result of increased glycine-*N* methyltransferase (GNMT) activity, a hepatic enzyme that converts SAM to SAH whilst generating Sar from Gly (Luka *et al.*, 2009; Figure 2.10A). Based on the elevated concentrations of SAH in MD sheep

liver (Figure 2.8), it is possible that increased flux from SAM to SAH is responsible for the high Sar concentrations measured. It is also possible that lower concentrations of vitamin B₂ cofactor, FAD, measured in MD sheep liver (Figure 2.5D) could reduce the catalytic activity of SARDH enzyme, thereby leading to the reduced catabolism of Sar in MD sheep liver (Figure 2.5B).

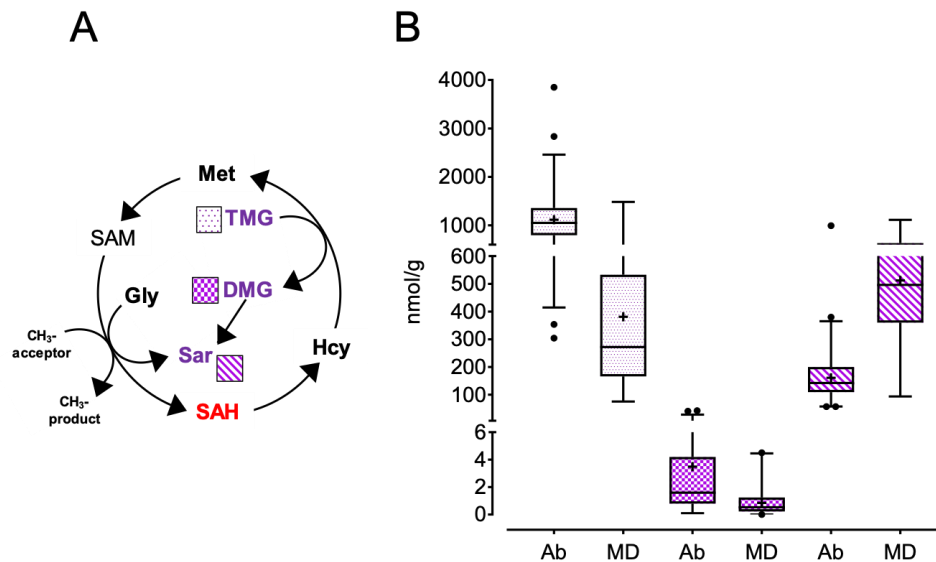
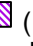
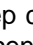



Figure 2.10 Amino acids facilitate the remethylation of homocysteine (Hcy) to methionine (Met) in sheep liver.

Amino acids in one-carbon (1C) metabolism (A). Concentrations (nmol/g wet weight liver) of trimethylglycine TMG,  ($P<0.001$); Dimethylglycine, DMG  ($P<0.001$); Sarcosine, Sar  ($P<0.001$); (B) in abattoir-derived (Ab; $n=266$) and methyl deficient (MD; $n=83$) sheep liver. Individual metabolite concentrations (colour-coded) between Ab and MD sheep compared by ANOVA. Mean (+), median, interquartile ranges, and 1st and 99th percentiles. Dots in boxplots represent outliers.

2.3.2.8 Polyamine metabolites

S-adenosylmethionine (SAM) is an essential substrate for polyamine biosynthesis (Bistulfi *et al.*, 2010). SAM becomes decarboxylated (dcSAM), as catalysed by S-adenosylmethionine decarboxylase (SAMDC; EC 4.1.1.50) and donates aminopropyl groups for the synthesis of higher polyamines, spermidine (Spd) and spermine (Spm) from precursor, putrescine (Put; Pegg *et al.*, 2006; Gamble *et al.*, 2012; Figure 2.11A). Polyamines are growth factors involved in the proliferation and differentiation of mammalian cells (Canellakis *et al.*, 1989). Whilst they are ubiquitous in all cells, their concentration is greatest in self-renewing and regenerative tissues, such as liver (Pegg *et al.*, 2016; Larqué *et al.*, 2007). Hepatic polyamines were significantly increased in MD sheep; Put (Ab: 14.5 ± 0.34 vs MD: 62.8 ± 4.52 nmol/g; $P<0.001$), Spd (Ab: 13.5 ± 0.99 vs

MD: 274.0 ± 20.67 ; $P < 0.001$) and Spm (Ab: 55.6 ± 5.63 vs MD: 475.5 ± 32.85 ; $P < 0.001$; Figure 2.11B). The present findings agree with those of [Sun et al. \(2002\)](#) who reported that hepatic Spd and Spm concentrations in methyl deficient rats were 58 and 67% higher, respectively, than in controls.

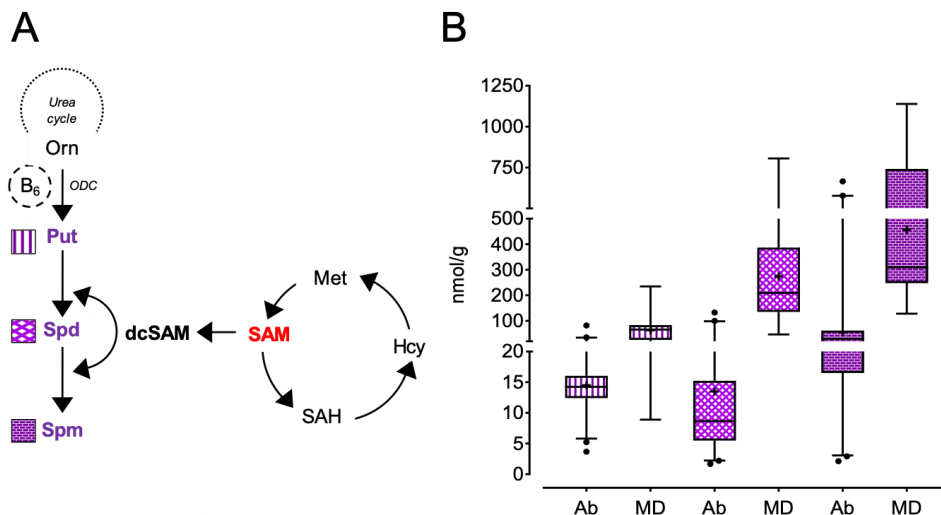


Figure 2.11 Polyamines increase in methyl deficient sheep liver.

Polyamine metabolism (**A**). Concentrations (nmol/g wet weight liver) of putrescine, Put (■) ($P < 0.001$); spermidine, Spd (■) ($P < 0.001$); spermine, Spm (■) ($P < 0.001$) (**B**) in abattoir-derived (Ab; $n=266$) and methyl deficient (MD; $n=83$) sheep liver. Individual metabolite concentrations (colour-coded) between Ab and MD sheep compared by ANOVA. Mean (+), median, interquartile ranges, and 1st and 99th percentiles. Dots in boxplots represent outliers.

The origin of this increase remains uncertain. It has been proposed that the catalytic activity of rate-limiting enzymes in polyamine biosynthesis, such as ODC and SAMDC, are regulated by the SAM:SAH ratio ([Kramer et al., 1987](#)). As SAH is a competitive inhibitor of most SAM-mediated reactions ([Finkelstein, 1990](#)), the metabolic partitioning of SAM as a methyl donor (transmethylation) or aminopropyl donor (polyamine biosynthesis) is determined by the relative affinity of SAH for the aforementioned decarboxylase and methyltransferase enzymes ([Kramer et al., 1987](#)). Perhaps a reduced SAM:SAH ratio leads to the upregulation of decarboxylase activity which serves to divert available SAM to polyamine biosynthesis at the expense of transmethylation reactions, at least in proliferating cells.

Similarly, methionine deprivation has been reported to induce SAMDC catalytic activity ([Tidsdale, 1981](#)). Together, regulatory controls over polyamine metabolism enzymes evoked by reduced methionine and a decreased

SAM:SAH ratio lends credence to the case for increased liver polyamine concentrations in MD sheep liver.

2.3.2.9 Propionate metabolites

Gluconeogenesis is of great importance in ruminants as almost all dietary carbohydrates are fermented to volatile fatty acids (VFA) in the rumen (Young *et al.*, 1977). Whilst propionic acid (PPA) is the only major VFA that contributes to gluconeogenesis (Black *et al.*, 1961; McDowell, 2000), a diverse pool of biomolecules can be catabolised to produce propionyl-CoA (Tretter *et al.*, 2016; Snyder *et al.*, 2015; Figure 2.12A). In the mitochondria, propionyl-CoA is carboxylated to D-methylmalonyl-CoA and epimerised to its L-stereoisomer (Tretter *et al.*, 2016; Ballhausen *et al.*, 2009). In turn, L-methylmalonyl-CoA is converted to succinyl-CoA by AdoCbl-dependent enzyme, methylmalonyl-CoA mutase (MUT). Finally, succinyl-CoA is incorporated into the tricarboxylic acid (TCA) cycle and converted to succinic acid (SA) for use in gluconeogenesis (De Vadder *et al.*, 2016; Figure 2.12A).

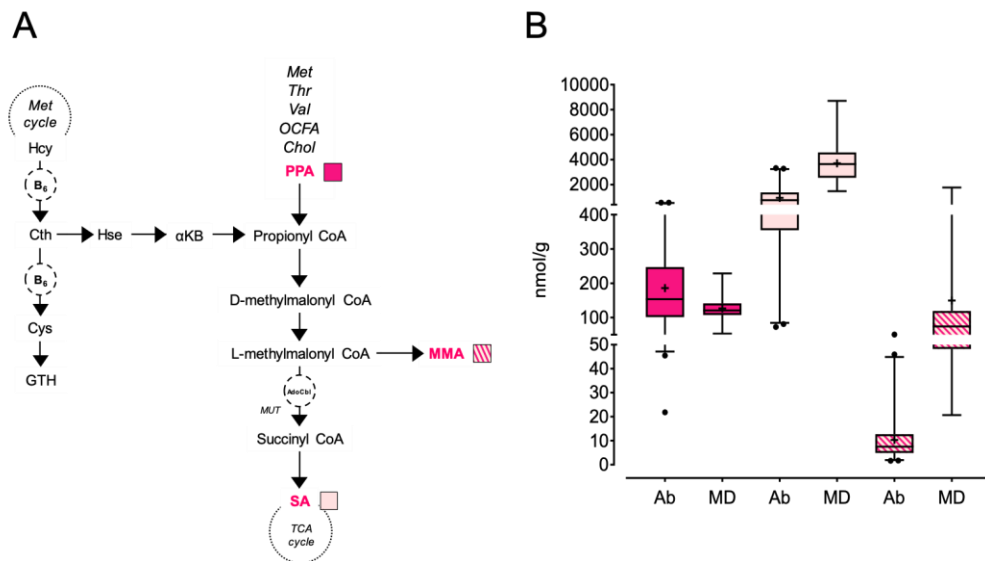


Figure 2.12 The propionate metabolome is altered in methyl deficient sheep liver.

Propionate metabolism (**A**). Concentrations (nmol/g wet weight liver) of propionic acid, PPA ■ ($P < 0.001$); succinic acid, SA □ ($P < 0.001$); methylmalonic acid, MMA ▨ ($P < 0.001$) (**B**) in abattoir-derived (Ab; $n = 266$) and methyl deficient (MD; $n = 83$) sheep liver. Individual metabolite concentrations (colour-coded) between Ab and MD sheep compared by ANOVA. Mean (+), median, interquartile ranges, and 1st and 99th percentiles. Dots in boxplots represent outliers.

Hepatic concentrations of PPA were decreased in MD sheep compared with Ab sheep (Ab: 186.1 ± 6.92 vs MD: 126.8 ± 3.59 nmol/g; $P < 0.001$) whilst SA and

MMA concentrations were increased ($P < 0.001$; Figure 2.12B). Such findings correspond with those reported by [Kennedy and others \(1991\)](#) where feeding lambs a Co-deficient concentrate diet caused a decrease in ruminal PPA but a 1000-fold increase in SA concentrations, highlighting an imbalance between PPA- and SA-producing microbes. Ruminal SA can be absorbed, leading to elevated plasma SA concentrations in Co-deficient animals ([Kennedy et al., 1991](#)). Thus, absorbed SA can partially overcome the detrimental effects of decreased MUT activity induced by AdoCbl deficiency on gluconeogenesis (Section 2.3.2.1; Figure 2.3B). The ~15-fold increase in hepatic MMA concentrations measured in MD sheep (Ab: 10.3 ± 0.51 vs MD: 149.6 ± 27.66 nmol/g; $P < 0.001$) highlights the metabolic effect of AdoCbl deficiency on MUT enzyme activity. With the aforementioned points considered (Section 2.3.1), plasma MMA is a robust biomarker of vitamin B₁₂ deficiency ([McMullin et al., 2001](#)) and its accumulation in liver has been attributed to AdoCbl deficiency in mammals ([Smith et al., 1969](#); [Toyoshima et al., 1996](#)).

2.4 Concluding remarks

The methods described herein are capable of the simultaneous quantification of 1C metabolites and related compounds in a complex tissue matrix, such as sheep liver. The HILIC/MS-MS methods used a simple extraction procedure, a short analytical run time and a simple mobile phase. Such metabolomic platforms will be useful for modelling 1C metabolism and linked biochemical pathways in order to facilitate dietary and genetic studies of metabolic health and epigenetic regulation of gene expression.

The large natural variation in hepatic levels of individual 1C metabolites in our sheep study populations reflects the dietary and genetic variation in our chosen outbred model species. Total 1C metabolite concentrations reported herein agree with those published elsewhere (Appendix Table 2.2), with the exception of vitamin B₆ where concentrations reported in the literature are >10-fold higher. This discrepancy is likely due to differences in analytical methodologies employed. Previous studies converted all B6 vitamers, including their phosphate esters, to free forms ([Williams et al., 2007](#); [Fukuwatari et al., 2008](#)) before measuring total B6 by microbiological assay ([Fukuwatari et al., 2008](#)) or reverse-phase HPLC coupled with electrochemical detection ([Wehling and Wetzel, 1984](#); [Williams et al., 2007](#); [Williams, 2007](#)). Such approaches are

quantitative but do not discriminate between individual free and phosphorylated vitamers (Zhang *et al.*, 2018).

The present study provides the first comparison of the relative abundance of bioactive 1C metabolites in MD sheep liver. A detailed description of specific coenzyme forms can facilitate a more accurate deficiency diagnosis and a more thorough understanding about the function of 1C metabolism in response to dietary methyl deficiency.

This study, however, was not without its limitations. Although a comprehensive set of metabolites were measured, it was not possible to measure every species present in liver. By way of example, vitamin B₁₂ comprises hydroxocobalamin (OH-Cbl) and additional analogues (i.e. cobamides and cobinamides). Collectively, these analogues constitute ~50% of sheep liver corrinoids (Kelly *et al.*, 2006). However, due to their lack of vitamin B₁₂ activity they were not included.

It is also important to acknowledge that measurements of metabolite pools do not accurately reflect flux through metabolic pathways, but rather provide a 'snapshot in time' of metabolic status. Metabolite pools are not static but are able to exchange with one another via numerous interconversion pathways. This is further complicated by the fact that enzymes within these pathways are activated and/or inhibited by intermediates elsewhere within the metabolic network (Reed *et al.*, 2004). A case in point refers to the allosteric regulation of methyltransferase and decarboxylase enzymes by SAH (Section 2.3.2.8). The present study did not determine hepatic 1C enzyme expression or catalytic activity (which may arise due to SNPs). Nor did it measure 1C metabolite concentrations in blood which may have provided valuable information about the systemic effects of dietary methyl deficiency.

The metabolomic analyses were conducted for Ab and MD study cohorts separately. Ideally, contemporaneous animals would have been allocated to the control or MD diet, maintained on-study for the same duration, and their liver samples collected, processed and analysed simultaneously, but this was not logistically feasible. Therefore, to avoid artefacts associated with conducting the metabolomic analyses for Ab and MD sheep at two independent time points (i.e. following slaughter at the abattoir for Ab sheep versus following dietary restriction for MD sheep), identical laboratory materials and methods were adopted for both analyses.

In summary, relevant reductions in dietary methyl availability can lead to significant alterations in hepatic 1C metabolite concentrations with downstream consequences for functional metabolism at the cell, tissue and whole organism level. These findings support the concept that 1C metabolism does not operate in isolation but is a central integrator of energy and nutrient status.

Based on the premise that reproductive and embryonic cells metabolise methyl groups differently to hepatocytes, it is possible that the relative concentration of 1C metabolites will differ from those found in liver. Now that these sensitive mass spectrometry-based metabolomic platforms have been developed, future experiments can explore the effects of dietary methyl deficiency and inborn errors of 1C metabolism in various cells, tissues and biofluids of sheep and related ruminant species. Such experiments will bring an unprecedented level of mechanistic insight into nutritional biochemistry-mediated epigenetic modifications that take place during the periconceptual period, particularly in cells of the ruminant ovary and preimplantation embryo.

Chapter 3

Methionine, 1C metabolism and bovine preimplantation embryo development

3.1 Introduction

The developmental potential of the mammalian preimplantation embryo is determined to a large extent by its nutritional environment (Bonilla *et al.*, 2010). Nutritional perturbations brought about by parental diet or embryo culture can affect key developmental and epigenetic programming events that occur during preimplantation development, thereby modifying adult health-related phenotypes in offspring (Xu and Sinclair, 2015). The importance of an optimal environment for early embryonic development is illustrated by the comparison of embryos produced under *in vivo* and *in vitro* conditions. *In vitro* produced cattle embryos can exhibit biochemical and molecular characteristics that compromise their ability to survive cryopreservation and their competency for establishing a pregnancy following embryo transfer (Hansen and Block, 2004). The nutrient composition of *in vitro* embryo production (IVP) media is responsible for at least some of these ultrastructural alterations (Dumoulin *et al.*, 2010; Nelissen *et al.*, 2012; Simpoulou *et al.*, 2018).

As demonstrated in Chapter 1 (Section 1.7.1), the lack of standardisation of IVP media has led to a wide variation in the composition of 1C metabolites (Anckaert *et al.*, 2010). Notably, methionine ranges from 0 to 500 $\mu\text{mol/L}$ between formulations (Table 1.5). Concentrations of methionine in commercially available culture media can be >10-fold higher than concentrations measured in the female reproductive tract (Hugentobler *et al.*, 2007) and >20-fold higher than the methionine requirement of bovine preimplantation embryos (Bonilla *et al.*, 2010; Table 3.1).

Table 3.1 Methionine concentrations in culture media can be >10-fold higher than those found in physiological fluids.

	Methionine ($\mu\text{mol/L}$)	
	Bovine	Human
Blood plasma/serum	16 – 35	27 – 30
Reproductive tract	31 – 49	7 – 49
Cell/embryo culture media	0 – 500	0 - 500
Embryo requirement	14 – 21	?

Source(s): Hugentobler *et al.* (2007); Bonilla *et al.* (2010); Kermack *et al.* (2015); Tarahomi *et al.* (2019)

It is unknown whether there are nutritional or physiological circumstances which could cause methionine concentrations to decline below $\sim 30 \mu\text{mol/L}$ in the

bovine reproductive tract. Even cows fed a diet low in crude protein (14%) had an average plasma concentration of ~21 $\mu\text{mol/L}$ (Piepenbrink *et al.*, 1996). However, due to its microbial degradation within the rumen, methionine is the first rate-limiting amino acid in the diet of dairy cows and is, therefore, often supplemented as a protected formulation (Wiltbank *et al.*, 2014). Feeding rumen-protected methionine to lactating dairy cows is reported to increase plasma concentrations of methionine (Koenig *et al.*, 2002; Ordway *et al.*, 2009; Preynat *et al.*, 2009) with potential benefits for reproductive performance, as characterised by increased embryonic size, embryonic survival and pregnancy maintenance (Acosta *et al.*, 2016; Toledo *et al.*, 2017).

Due to the challenges of studying human embryos, there are few data on methionine metabolism during human pregnancy (Kalhan, 2009; Drábková *et al.*, 2016). Methionine is not endogenously synthesised in sufficient quantities by humans and must be obtained from the diet. As animal proteins are a primary source of methionine in human diets (Shoob *et al.*, 2001), it follows that vegetarians and vegans are at risk of methionine deficiency (Krajcovicová-Kudlácková *et al.*, 2000; McCarty *et al.*, 2009) and, consequently, adverse reproductive outcomes (General Introduction, Table 1). Similarly, methionine-rich diets are associated with reduced risk of NTDs in pregnant women (Shoob *et al.*, 2001; Shaw *et al.*, 2004). Methionine has long been recognised as the most toxic amino acid (Benevenga and Steele, 1984; Garlick, 2006) where excess concentrations can have detrimental effects on embryo development (Rees *et al.*, 2006). Certain pathophysiological conditions lead to excess methionine in humans. A case in point concerns Mudd's disease, a condition caused by mutations in the *MAT1A* gene that is characterised by persistent hypermethioninemia (>2000 $\mu\text{mol/L}$), aberrant cellular methylation and central nervous system abnormalities (Chien *et al.*, 2015; Nashabat *et al.*, 2018; Figure 1.1, Appendix Table 1.1).

Based on the premise that the bovine preimplantation embryo metabolises methionine differently to hepatocytes (Section 1.4), the present study advances the hypothesis that bovine embryonic cells are particularly sensitive to methionine (i.e. methyl group) availability during the preimplantation period. As a domestic livestock species of commercial relevance, it is important to investigate the effects of altering methionine during *in vitro* production of bovine embryos. Furthermore, the bovine preimplantation embryo provides a suitable model for understanding the development and differentiation of the early human

embryo (Shojaei Saadi *et al.*, 2016; Sirard, 2019; Figure 3.1). The cow typically carries a single conceptus and has a similar gestation length to the human (Bebbere *et al.*, 2013). Furthermore, the timings of key developmental events that occur during early embryogenesis, including minor and major embryonic genome activation (4-cell and 8-cell stage, respectively) and cell lineage specification, are conserved in both species (Kurosaka *et al.*, 2004; Graf *et al.*, 2014). According to Ménéz and Hérubel (2002), biochemical, metabolic and intrinsic regulatory processes are similar in cattle and human embryo development. Analogous embryo culture systems are used for both species and ART procedures, including IVF and SCNT, are well established in cattle, thereby facilitating reverse genetic studies (Simmet *et al.*, 2018). As an annotated *Bos taurus* genome is available, cattle also offer a useful model to study methylome changes during early development in response to culture conditions (de Montera *et al.*, 2013; See Chapter 4).

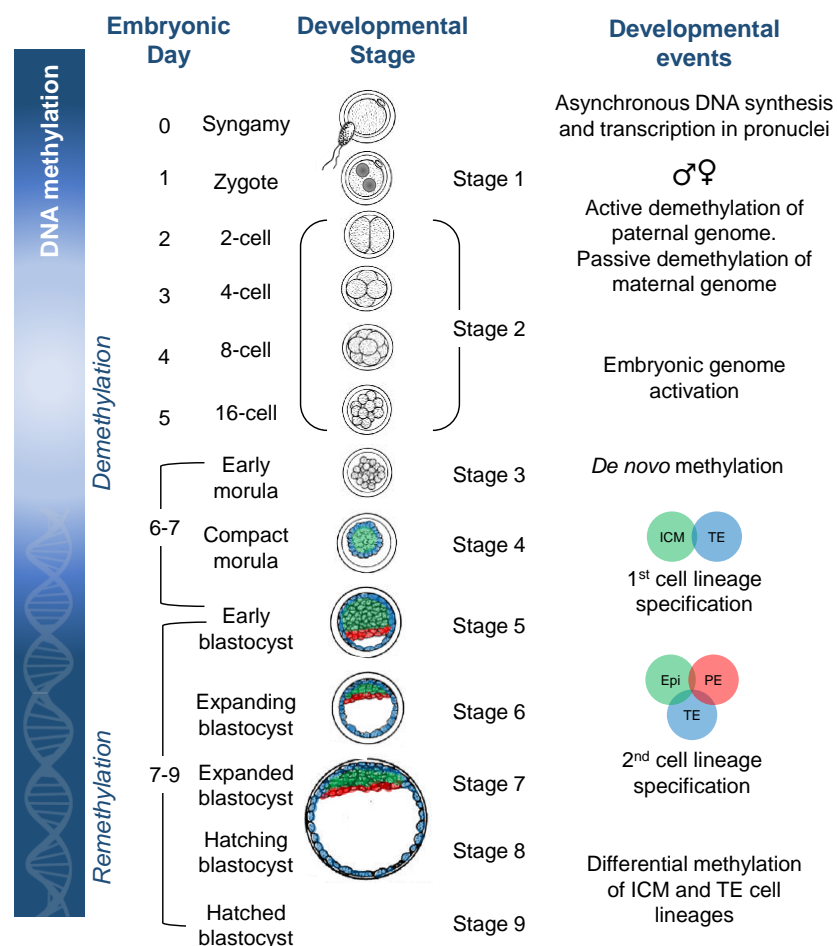


Figure 3.1 Developmental stages and epigenetic events in bovine preimplantation embryos.

Source: Clare *et al.* (unpublished). Abbreviation(s): DNA, deoxyribonucleic acid; Epi, epiblast; ICM, inner cell mass; PE, primitive endoderm; TE, trophectoderm.

The present study, therefore, comprised two experiments in order to enhance our understanding of methionine metabolism in bovine ovarian cells, oocytes and preimplantation embryos. Given that transcripts encoding methionine cycle enzymes (i.e. *MAT1A* and *BHMT*) were either absent or expressed at low levels in these cell types (Kwong *et al.*, 2010), the first experiment (Methionine cycle enzyme transcripts; Section 3.2.1) sought to confirm the expression of methionine cycle enzyme transcripts; *MAT2A* and *BHMT* isoforms, in somatic cells of the bovine ovary, oocytes and embryos. The *MAT1A* isoform is largely specific to the liver, whereas the low K_m *MAT2A* isoform is expressed in extrahepatic tissues, including reproductive cells (Finkelstein, 1999). An evolutionary gene duplication event took place at the root of the mammalian clade giving rise to *BHMT* and *BHMT2* paralogs. The BHMT enzyme uses trimethylglycine (TMG/betaine) as a methyl donor substrate for the remethylation of Hcy to methionine, whereas BHMT2 uses S-methylmethionine (SMM; Ganu *et al.*, 2015; Figure 3.2). Genetic variation and functional divergence between BHMT isoforms have been characterised in several mammalian species, including humans, pigs and mice (Appendix Table 3.2), however, little is known about the tissue distribution and function of BHMT2 (Li *et al.*, 2008), particularly in mammalian reproductive cells and embryos. The second experiment (Methionine and embryo development during culture; Section 3.2.2) sought to establish the developmental competence of embryos produced under *in vitro* culture conditions with 0 (non-physiological), 10 (low physiological), 50 (high physiological), and 500 (supraphysiological) $\mu\text{mol/L}$ added methionine (Figure 3.2). Experimental endpoints involved the assessment of gross morphological and developmental parameters, including blastocyst stage, grade, cell lineage allocation and sex ratio.

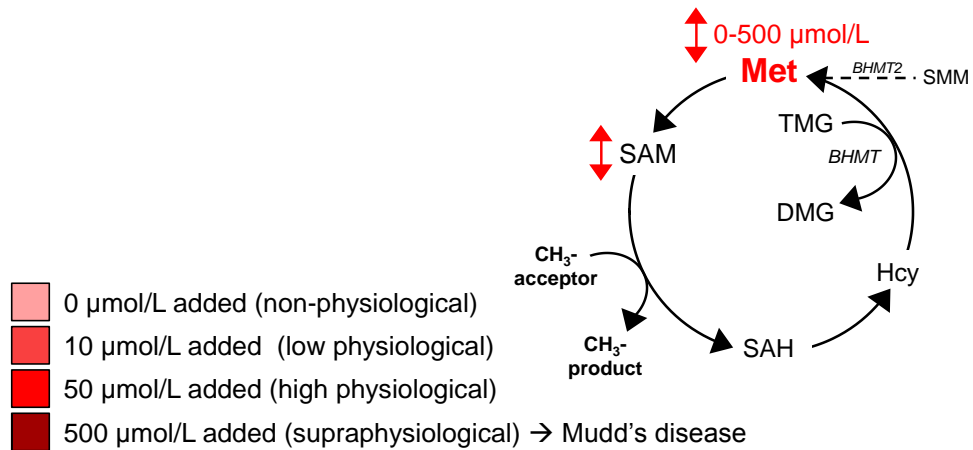


Figure 3.2. Methionine concentrations added during *in vitro* production of bovine blastocysts.

Enzymes in *italics*; *BHMT*, betaine homocysteine S-methyltransferase; *BHMT2*, betaine homocysteine S-methyltransferase 2. Substrates: DMG, dimethylglycine; Met, methionine; SAH, S-adenosylhomocysteine; SAM, S-adenosylmethionine; SMM, S-methylmethionine; TMG, trimethylglycine.

3.2 Materials and methods

3.2.1 Methionine cycle enzyme transcripts

The expression of methionine cycle enzyme transcripts; *MAT2A*, *BHMT* and *BHMT2*, were analysed in bovine ovarian granulosa cells (GC), cumulus cells (CC), germinal vesicle (GV) oocytes, metaphase II (MII) oocytes and preimplantation embryos at various developmental stages.

3.2.1.1 Sample collection

3.2.1.1.1 Liver (positive control)

Bovine liver samples were harvested immediately following slaughter. Diced sections (5 mm³) were submerged in 2 mL RNA*later*® tissue storage reagent (Sigma-Aldrich, Poole, UK). Samples were stored at 4°C overnight and transferred to -20°C for long-term storage.

3.2.1.1.2 Germinal vesicle (GV) oocytes

Ovaries were collected from the abattoir and kept in 39°C pre-warmed phosphate buffered saline (PBS) until arrival at the laboratory. Ovaries were

rinsed with 70% ethanol and washed with PBS (39°C). Non-haemorrhagic small to medium size follicles (3-9 mm) were aspirated using a 19-gauge needle and a 10 mL syringe. The contents of each follicle were deposited into a pre-warmed 50 mL falcon tube and kept at 39°C. Oocytes were graded using a four-point scale adapted from [Goodhand *et al.* \(1999\)](#) according to the number of layers of compact cumulus and amount of granulation in cytoplasm (Appendix 3.1).

Grade 1 and 2 cumulus-oocyte complexes (COCs) were transferred to a 35 mm petridish containing warm PBS with 0.1% PVP (w/v) and washed three times. Cumulus-oocyte complexes were incubated in PBS/PVP containing 1 mg/mL hyaluronidase at 39°C for 2 min to aid the removal of granulosa and cumulus cells from oocytes. Cumulus-oocyte complexes were transferred to a 15 ml falcon tube containing 3 mL PBS/PVP and denuded by vortexing for 3 min. The suspension was transferred to a 35 mm petridish to recover the denuded oocytes and the wall of the falcon tube was rinsed with 1 mL PBS/PVP to ensure complete recovery. Recovered oocytes were washed three times in PBS/PVP and groups of 10 oocytes were transferred to 1 mL Eppendorf tubes before centrifugation for 2 min at maximum speed. The supernatant was removed leaving oocytes in a minimal volume (~2 µL) for snap freezing in liquid nitrogen and storage at -80°C until RNA extraction.

3.2.1.1.3 Cumulus cells (CC)

The remaining PBS/PVP suspension used for vortexing and washing oocytes contained cumulus cells (CC) and was pooled into a 15 mL falcon tube. Tubes were centrifuged for 2 min at maximum speed and the supernatant discarded. The cell pellet was resuspended by vortexing in 1 mL fresh PBS/PVP and transferred to a 1 mL Eppendorf tube. The tube was centrifuged for 2 min at maximum speed, the supernatant was discarded, and the pellet was resuspended once again in 100 µL fresh PBS/PVP. Five microliters of cell suspension were added to 5 µL trypan blue (0.4% w/w) and 5 µL PBS and a live/dead cell count was achieved using a haemocytometer to ensure a sufficient number of cells were available for the mRNA extraction kit. Finally, the CC pellet was centrifuged for 2 min at maximum speed and the supernatant was removed before being snap frozen in liquid nitrogen. Cell samples were stored at -80°C until RNA extraction.

3.2.1.1.4 Granulosa cells (GC)

The remaining follicular fluid containing GC was split equally between 15 mL falcon tubes and centrifuged for 2.5 min at 2,000 xg. The supernatant was discarded and the cell pellet resuspended in 1 mL fresh PBS/PVP using a Pasteur pipette. The cell suspensions were centrifuged for 2.5 min at 2,000 xg and the supernatant discarded. Potential erythrocytes were lysed by the addition of 9 mL warm dH₂O. The cell pellet was quickly mixed before the addition of 1 mL 10X PBS to prevent granulosa cells lysing. The suspension was centrifuged for 2.5 min at 2,000 xg once again, the cell pellet was resuspended in 1 mL fresh PBS/PVP and the suspension passed through a cell strainer (70 µm; Fisher Scientific) to remove debris. The cell suspension was centrifuged for 2 min at 2,000 xg, the supernatant was discarded and the GC pellet was resuspended in 1 mL fresh PBS/PVP. Five microliters of cell suspension was added to 50 µL trypan blue (0.4% w/w) and 145 µL PBS and a live/dead cell count was achieved using a haemocytometer to ensure a sufficient number of cells were available for the mRNA extraction kit. Finally, the GC pellet was centrifuged for 2 min at maximum speed and the supernatant was removed before being snap frozen in liquid nitrogen. Cell samples were stored at -80°C until RNA extraction.

3.2.1.2 *In vitro* embryo production (IVP)

Unless otherwise stated, all reagents were obtained from Sigma-Aldrich (Poole, UK). For a description of all media used for standard bovine IVP, see Appendix 3.2). Morphological assessment of embryos was based on that of [Bó and Mapletoft \(2013\)](#) according to International Embryo Technology Society (IETS) criteria. Evaluation of bovine embryos was achieved with a stereomicroscope at 50 to 100X magnification with the embryo in a small holding dish. Staging and grading of embryos was according to IETS guidelines (Appendix 3.3).

3.2.1.2.1 Metaphase II (MII) oocytes, zygotes and embryos

Graded COCs were matured in groups of ~30 in 400 µL maturation media in 4-well plates under 5% CO₂ in air for 22-24 h. Cumulus-oocyte complexes were transferred to 50 µL drops containing oocyte wash medium under mineral oil. Careful pipetting of COCs allowed for oocyte isolation and a reduction in expanded cumulus cell layers to facilitate fertilisation. After washing, COCs

were transferred to 50 μL drops of pre-equilibrated fertilisation medium (39°C, 5% CO_2/air) under mineral oil. Motile spermatozoa from a single bull were added to each drop (1×10^6 spermatozoa per mL fertilisation medium) and fertilisation was performed for 18-20 h. For a detailed description of sperm preparation by swim-up method see Appendix 3.4.

The day of IVF was counted as Day 0 of embryo development. Following IVF, presumptive zygotes were transferred to an Eppendorf containing 0.4 mL pre-equilibrated synthetic oviductal fluid (SOF) HEPES holding medium (39°C, 5% $\text{CO}_2/5\% \text{O}_2$) and denuded from attached sperm and remaining cumulus cells by vortexing for 1 min. Presumptive zygotes were washed in pre-equilibrated SOF HEPES holding media (35 mm Petri dish) and transferred in groups to 4-well plates containing 400 μL pre-equilibrated SOF culture medium (39°C, 5% $\text{CO}_2/5\% \text{O}_2$). Embryo culture media was renewed on Day 2, 4 and 6 of culture.

Metaphase II (MII) oocytes were collected following 22-24 h of *in vitro* maturation based on the visual observation of extrusion of the first polar body (Ikeda *et al.*, 2010). Matured MII oocytes and CC were recovered using the protocols described in Sections 3.2.1.1.2 and 3.2.1.1.3, respectively. Embryos were classified according to their stage of development (Appendix 3.3). Zygotes were collected at Day 1 (~24 h post fertilisation), 2-cell embryos at Day 2 (~48 hpi), 4-cell and 8-cell embryos at Day 3 (~72 hpi), 8-16 cell embryos at Day 4 and Day 5 (96 and 120 hpi), morulae at Day 6 (~144 hpi), early expanding blastocysts, late expanded blastocysts, hatching and hatched blastocysts were collected on Day 7, Day 8 and Day 9 (~168, 192 and 216 hpi). At each sample collection, oocytes and embryos were pooled in groups of 10 in minimal volume (~2 μL) PBS/PVP, snap frozen in liquid nitrogen and stored at -80°C until RNA extraction.

3.2.1.3 RNA extraction

3.2.1.3.1 Liver and granulosa cells

Total RNA was extracted from bovine liver and granulosa cells using the RNeasy Mini Kit (Qiagen Ltd., West Sussex, UK) following the manufacturer's protocol. Briefly, 20 mg liver were homogenised using a Polytron 4000 on ice in Buffer RLT containing 1% (v/v) 2-mercaptoethanol (600 μL). Up to 1×10^7 granulosa cells were homogenised in the buffer by passing the lysate through a

20-gauge needle and syringe 10 times. Following homogenisation, samples were centrifuged at maximum speed for 3 min. The supernatant was withdrawn, transferred to a new microcentrifuge tube and mixed with 1 volume of 50% ethanol before being passed through a QIAshredder spin column (Qiagen Ltd.). The column containing RNA was successively washed, once with Buffer RW1 (700 μ L) and twice with Buffer RPE (500 μ L) before RNA elution using 40 μ L RNase free water. A 2 μ L aliquot was taken to determine the concentration of RNA by measuring the absorbance at 260 nm (A₂₆₀) using a Nanodrop Spectrophotometer (ND-1000; UK) For liver, the 260/280 ratio was 2.14. For granulosa cells, the 260/280 ratio was 1.98. Remaining RNA was stored at -80°C. Approximately 900 ng liver RNA was used for reverse transcription. RNA was diluted to 0.1 μ g/ μ L before complementary DNA (cDNA) synthesis.

3.2.1.3.2 Cumulus cells, oocytes and blastocysts

Due to the small amount of starting material, Poly A+ RNA was extracted from CC, oocytes (GV and MII) and blastocysts using Dynabeads® mRNA DIRECT™ purification kit (Invitrogen Ltd., Paisley, UK), following the manufacturer's protocol. Ten bovine blastocysts grouped by stage were used per extraction. This method uses short sequences of oligo(dT)₂₅ which are covalently bound to the surface of the Dynabeads. These oligo-dTs hybridize to the polyA tail of mRNA to allow its magnetic isolation. Samples were lysed in 150 μ L lysis/binding buffer at room temperature for 20 min. Following lysis, 40 μ L Dynabeads were added to each sample. The contents were mixed at room temperature for 10 min using a gyratory rocker. One sample was handled at a time while the others were kept on ice. Samples were placed in a magnetic field so that beads were caught by the magnet and the supernatant was discarded. The beads were washed three times in 100 μ L washing Buffer A and two times with 100 μ L washing Buffer B. For washing, beads were mixed by gentle vortexing and washing buffers were exchanged using the magnetic field. After the final wash, beads were resuspended in 10 μ L RNase free water and incubated at 65°C for 2 min. Tubes were immediately cooled on ice for 3 min before transfer to the magnetic field. The supernatant containing mRNA was transferred to a fresh tube and kept on ice. If reverse transcription was not conducted immediately, RNA was stored at -80°C.

3.2.1.4 Reverse transcription (RT)

Complementary DNA (cDNA) was synthesised using the QuantiTect® Reverse Transcription kit (Qiagen Ltd.) due to its ability to reverse transcribe very small amounts of RNA (~1 pg). Ten microliters of purified RNA were incubated with 2 µL gDNA Wipeout Buffer (7X) and 2 µL RNase free water at 42°C for 2 min to eliminate contaminating gDNA. Samples were immediately placed on ice and 1 µL the reaction was removed for a negative control (-RT) reaction and the equivalent volume of water added before reverse transcription (RT). The total volume of each PCR (+RT) reaction was 20 µL, containing 1 µL Quantiscript reverse transcriptase, 4 µL Quantiscript RT buffer (5X), 1 µL RT Primer mix (random primers and oligo dT), 1 µL diluted gDNA Wipeout Buffer (1:6) and 13 µL DNase treated RNA. The +RT reaction was mixed by flicking the tube and incubated at 42°C for 30 min followed by incubation at 95°C for 3 min to inactivate the enzyme. Resultant cDNA products were stored at -20°C until amplification by polymerase chain reaction (PCR).

3.2.1.5 Polymerase chain reaction (RT-PCR)

3.2.1.5.1 Primer design

Transcript expression of methionine cycle enzymes; *MAT2A*, *BHMT* and *BHMT2*, was determined by RT-PCR using the Eppendorf AG 22331 (Hamburg, Germany). All transcripts were visualised relative to the housekeeping gene, β -*actin* (*ACTB*). Despite the fact that the RT kit effectively eliminates gDNA, primers were designed to span exon-exon boundaries, thereby further minimising the detection of gDNA. Gene-specific primers were designed using Primer Express software version 3.0.1 (Applied Biosystems, Warrington, UK). Since *BHMT* and *BHMT2* gene paralogs have high protein sequence homology (~73%; Li *et al.*, 2008; Appendix Chapter 3), it was important to design primers that specifically amplify each isoform. The *Bos taurus* cDNA sequence for each gene paralog was downloaded using Ensembl genome browser 95 (<https://www.ensembl.org>) and their sequence homology was compared using the ClustalW2 Multiple Sequence Alignment tool (<https://www.ebi.ac.uk>; Appendix 3.5). Primer specificity was confirmed using Primer-BLAST software. Forward and reverse primers for *BHMT* and *BHMT2* were supplied by Sigma-Aldrich (Poole, UK). Primers for *MAT2A* and housekeeping gene, *ACTB*, were

supplied by Eurofins Genomics (GmbH, Anzinger Str. 7A, 85560, Ebersberg, Germany; Table 3.2). All primers were diluted with RNase free water to a final concentration of 10 pmol/ μ L.

Table 3.2 Primers used for methionine cycle enzyme transcript expression.

Gene		Primer sequence (5'-3')	NCBI accession no.
<i>MAT2A</i>	FP	AGTGCCCAAAAAGCTTAAATATTGA	NM_001101131
	RP	CTTTCCCGCAGAGCTTGAGG	
<i>BHMT</i>	FP	AGAGAAAATATCCGGGCAGAAAG	NM_001011679.1
	RP	TCACACCCCCTGCTACCAAA	
<i>BHMT2</i>	FP	AGCCTGTGGGAAGCTGTAAACA	XM_003586514.5
	RP	CCCCCTGCTACCAAAGCAT	
<i>ACTB</i>	FP	CGTCCGTGACATCAAGGAGAA	NM_173979.3
	RP	CGCGGTGGCCATCTCCTG	

3.2.1.5.2 Transcript expression

Polymerase chain reaction was performed in a total volume of 20 μ L containing 10 μ L LightCycler® 480 Probes Master 2X (Roche Diagnostic Ltd.), 0.6 μ L forward and reverse primers, 2 μ L cDNA template and RNase free water. A negative reagent control (RC) sample was run for each tested primer set using water instead of cDNA template. In order to check for DNA contamination in samples, the –RT reaction was run using *ACTB* primer pair since this does not span an exon-exon junction (Appendix 3.6). The amplification program consisted of denaturation at 95°C for 10 s, followed by 38 cycles as follows: 95°C for 10 s, 58°C for 15 s, 72°C for 15 s, and 72°C for 10 s; with a final hold at 10°C. PCR products (10 μ L plus 2 μ L 6X loading dye; promega cat no. G1881) were run on 2.5% agarose gel stained with ethidium bromide (EtBr; 0.5 μ g/mL) and resultant bands visualised under UV light. Images were captured using the UVP GelDoc-IT imaging system. PCR products were sequenced to confirm primer specificity using liver cDNA by Source Bioscience (Nottingham, UK; Appendix 3.7).

3.2.2 Methionine and embryo development during culture

In vitro maturation (IVM), fertilisation (IVF) and embryo culture (IVC) media were formulated to contain 0, 10, 50 and 500 μ mol/L added methionine. All reagents were obtained from Sigma-Aldrich (Poole, UK), except for methionine-free TCM199 41150 media which was formulated by Gibco™ (ThermoFisher Scientific). Methionine-free Basal Eagle's medium (BME) [50X] was formulated

in-house to contain essential amino acids excluding methionine. For full details of custom-made BME and methionine stocks solutions see Appendix 3.8.

3.2.2.1 High performance liquid chromatography (HPLC)

Concentrations of methionine and additional amino acids in custom-made IVP media formulations were confirmed by HPLC. Amino acid concentrations in ovarian follicular fluid were also compared to culture media. The method used an Agilent 1100 HPLC and the injection programme is described in Appendix 2.2.

3.2.2.1.1 Analytical grade reagents

Methanol (MeOH), acetonitrile (ACN) and sodium phosphate dibasic (Na_2HPO_4) were purchased from Fisher Scientific (Loughborough, UK). 5-Sulphosalicylic acid dehydrate (SSA) was purchased from Acros (Fisher Scientific). Amino acid standard powders; L-Asparagine (Asn), L-Glutamine (Gln), L-Citrulline (Cit) and L-Tryptophan (Trp); amino acid standard mix (AAS18) containing L-Alanine (Ala), L-Arginine (Arg), L-Aspartic acid (Asp), L-Cystine, L-Glutamic acid (Glu), L-Leucine (Leu), L-Lysine (Lys), L-Serine (Ser), L-Threonine (Thr), L-Tyrosine (Tyr), L-Valine (L), L-Histidine (His), L-Isoleucine (Ile), L-Methionine (Met), L-Phenylalanine (Phe), Glycine (Gly) and internal standard, Norvaline (NVA) was purchased from Sigma-Aldrich (Poole, UK). Derivatisation reagents, O-phthalaldehyde (OPA) and 3-mercaptopropionic acid (MPA), were also purchased from Sigma-Aldrich (Poole, UK).

3.2.2.1.2 Standard preparation and calibration

Stock solutions of individual amino acids (Asn, Gln, Cit and Trp) and internal standard (NVA) were prepared in water to a final concentration of 10 mmol/L. Amino acid standard mix (AAS18) was aliquoted at 2.5 mmol/L. All stock solutions were stored at -20°C to prevent degradation. As IVP media contains fetal calf serum (FCS, 10% v/v) or bovine serum albumin (BSA, <0.6% w/v), water containing 6 mg/mL BSA (Sigma Aldrich cat no. A6003) was used as a surrogate blank matrix for the preparation of extracted calibration standards over a suitable concentration range. The final IS concentration of NVA was 200 $\mu\text{mol/L}$.

3.2.2.1.3 Method validation

Calibration curves were linear over the range of 0-600 µmol/L for all compounds. L-Aspartic acid could not be accurately measured due to co-elution with an interfering peak. Selectivity was demonstrated by the ability of the assay to differentiate and quantify the specific analytes of interest in the presence of other components. The lowest concentration of the analytes with an accuracy of 80–120% was regarded as the lower limit of quantification (LLOQ). Intra-day precision (CV%) was assessed by conducting analyses of at least three replicate QC samples in the analytical batch. Recovery (%) was calculated as measured analyte concentration/standard analyte concentration*100. Method validation parameters for the determination of amino acids are reported in Table 3.3.

Table 3.3 Validation data for quantification of amino acids in IVP media and ovarian follicular fluid.

Amino acid analyte	R.T. (min)	LLOQ (µmol/L)	Intra-day precision (CV%)	Slope	R ²	Recovery (%)
Glu	3.20	5	4.20	0.0022	0.99	99.6
Asn	7.24	25	4.43	0.0020	0.99	93.7
Ser	7.29	25	5.52	0.0044	0.99	98.4
Gln	8.49	25	6.13	0.0035	0.99	100.8
His	8.96	1.25	11.63	0.0027	0.99	117.9
Gly	9.09	5	13.39	0.0087	0.99	100.1
Thr	9.40	25	4.98	0.0032	0.99	98.3
Cit	10.12	25	1.72	0.0040	0.99	103.5
Arg	11.01	25	3.66	0.0073	0.99	93.2
Ala	11.24	50	10.53	0.0023	0.99	85.4
Tyr	13.37	12.5	4.74	0.0032	0.99	84.6
Cys	15.74	2.5	11.28	0.0037	0.98	96.9
Val	15.98	12.5	10.79	0.0041	0.99	104.6
Met	16.36	25	3.25	0.0051	0.99	100.9
NVA*	16.87	-	-	-	-	-
Trp	17.79	12.5	10.61	0.0046	0.99	83.8
Phe	18.32	25	6.99	0.0038	1.00	101.3
Ile	15.57	25	5.45	0.0036	0.99	101.8
Leu	19.60	25	3.15	0.0041	0.99	104.9
Lys	20.86	25	4.26	0.0023	0.99	119.4

*Norvaline (NVA); internal standard

3.2.2.1.4 Follicular fluid collection

Abattoir derived ovaries were rinsed with 70% ethanol and washed with PBS. Upon assessment of ovarian luteal morphology, ten ovaries at oestrous cycle stage III (11-17 days) were selected for aspiration based on criteria defined by Ireland *et al.* (1980). Stage III ovaries were selected as the mid-range of all oestrus cycle stages (I-IV) and were characterised by absence of a red/brown

colouration leaving the corpus luteum orange/yellow with visible apical vasculature (Figure 3.3A; Orsi *et al.*, 2005; Putluru *et al.*, 2016). Individual follicles were graded on the basis of dominance using follicle size and follicular fluid volume as markers. Based on the method of Orsi *et al.* (2005), fluid from non-dominant (2 to 6 mm diameter) and dominant follicles (6 to >15 mm diameter) was collected in 2 mL syringes fitted with 19-gauge needles and the mean fluid volume recorded (Figure 3.3B).

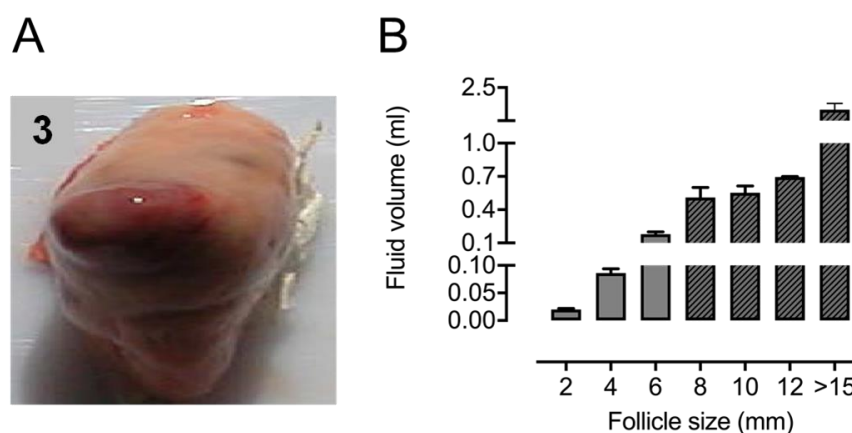


Figure 3.3 Ovarian follicular fluid volume increases with follicular dominance.

Bovine ovary at oestrus cycle stage III (11-17 days). Source: Putluru *et al.* (2016) (A). Fluid volume according to follicle size (2 mm, $n=60$; 4 mm, $n=12$; 6 mm, $n=5$; 8 mm, $n=2$; 10, $n=2$; 12, $n=2$; >15 mm, $n=3$). Non-dominant follicle (<8 mm); dominant follicle (>8 mm) (B). Data presented as mean \pm SEM.

3.2.2.1.5 IVP media and follicular fluid sample extraction

Due to the aspiration of small follicular fluid volumes from non-dominant follicles (<300 μ L), aspirant samples were pooled to contain a minimum volume of 500 μ L for amino acid analysis by HPLC (2 mm, $n=30$ follicles; 4 mm, $n=8$; 6 mm, $n=4$; 8 mm, $n=1$; 10 mm, $n=1$; 12 mm, $n=1$; >15 mm, $n=1$). Pooled samples were centrifuged for 5 min at 900 xg to remove cell debris and stored at -80°C until amino acid extraction. Pooled samples were analysed in duplicate or triplicate. For each follicular fluid and IVP media sample to be deproteinized, a microcentrifuge tube was prepared containing 30 mg 5-sulphosalicylic acid (SSA) powder and cooled to 4°C . Ten μ L NVA (10 mmol/L) and 490 μ L each sample was added to the tube containing SSA. The contents were vortexed and kept at 4°C for 1 h. Following protein precipitation, the mixture was centrifuged for 15 min at 14,500 xg . The supernatant was transferred to a 1 mL syringe and filtered using a Millex-GP syringe filter unit, 0.22 μm (Merck Millipore). The filtrate was transferred to an amber HPLC vial for HPLC analysis.

3.2.2.2 Methionine-adjusted *in vitro* embryo production (IVP)

Bovine embryo production was conducted as described previously (Section 3.2.1.2) but with the following modifications. Grade 1 and 2 COCs were matured in groups of ~30 in 400 µL modified maturation medium (0, 10, 50 and 500 µmol/L added methionine) for 22 h. Matured COCs were inseminated with frozen thawed bull sperm at a concentration of 1×10^6 sperm/mL in modified fertilisation medium (0, 10, 50 and 500 µmol/L added methionine). Semen from the same bull was used for all experiments. Presumptive zygotes were denuded, washed in pre-equilibrated methionine-free SOF HEPES holding media and cultured in 400 µL modified SOF culture medium supplemented with custom-made BME (0, 10, 50 and 500 µmol/L added methionine) until Day 8 post insemination. Media was renewed every 48 h. Cleavage was assessed on Day 2 (48 hpi) and embryo development was assessed on Day 7 and 8. Blastocysts were harvested on Day 8 ($n=135$) to assess gross morphological and developmental parameters (stage, grade, cell lineage allocation and primary sex ratio). Treatments were replicated on a minimum of three occasions.

3.2.2.2.1 Whole-mount immunofluorescence

To investigate the effect of methionine on cell lineage allocation, Day 8 blastocysts ($n=85$) cultured at 0, 10 and 50 µmol/L added methionine media were immunostained according to [Nichols *et al.* \(2009\)](#). Primary antibody rabbit anti-human NANOG (dilution factor 1:400, Peprotech cat no. 500-P236) and secondary antibody Alexa Fluor™ 488 (1:500; Invitrogen cat no. A32790) was used to stain the epiblast (Epi). Primary antibody goat anti-human SOX17 (1:750; R&D cat no. AF1924) and secondary antibody Alexa Fluor™ 647 (1:500; Invitrogen cat no. A21447) was used to stain the primitive endoderm (PE). Fluoroshield™ with DAPI was used to visualise the trophectoderm (TE).

The zona pellucida was removed from blastocysts using Pronase (0.5% w/v) for approximately 1 min. Zona-free blastocysts were washed twice with warm PBS/PVP (0.1% w/v) and fixed using 4% paraformaldehyde for 15 min. Fixed blastocysts were washed three times for 5 min each in PBS/BSA (1% w/v) before permeabilisation in Triton-X100 in PBS (0.1% v/v) at room temperature for 15 min. Blastocysts were washed again, transferred into blocking solution

(containing 82% of 5% PBS/BSA, 9% donkey serum and 9% 3 M glycine) and incubated at room temperature for 1 h. After blocking, blastocysts were transferred to a 96 mini-well plate loaded with primary antibody and incubated at 4°C overnight. To remove unbound primary antibody, blastocysts were washed four times for 10 min each in PBS/BSA (1% w/v) and transferred to a 96 mini-well plate loaded with secondary antibody, and incubated at room temperature for 1 h. Following incubation with secondary antibody, blastocysts were washed again in PBS/BSA (1% w/v) and mounted with minimal volume of medium on slides using Fluoroshield™ with DAPI (Sigma-Aldrich). Mounted blastocysts were covered with a coverslip, sealed with nail varnish and differential staining was visualised using an epifluorescent microscope (Leica, DM4000B; Germany). Images obtained under 40X magnification were used to count total, TE, ICM, Epi and PE cells using FIJI software (Image J with cell counter plug-in).

3.2.2.2.2 Embryo sexing by polymerase chain reaction (PCR)

Day 8 bovine blastocysts ($n=62$) underwent multiplex PCR to investigate the effect of methionine concentration during *in vitro* culture on the primary sex ratio. The zona pellucida was removed from blastocysts using Pronase (0.5% w/v). Zona-free blastocysts were washed three times in PBS/PVP (0.1% v/v) and transferred in minimal volume to PCR tubes. Samples were snap frozen in liquid nitrogen and stored at -80°C until PCR analysis.

Y-chromosome specific (*SRY*) and bovine specific (*BSP*) primers were supplied by Eurofins Genomics (Table 3.4). All primers were diluted with RNase free water to a final concentration of 10 pmol/μL. Polymerase chain reaction was conducted using the Eppendorf AG 22331 in a total volume of 25 μL, containing 12.5 μL Immomix red (Bioline), 0.125 μL forward and reverse *BSP* primers, 1.25 μL forward and reverse *SRY* primers, 7.75 μL RNase free water and 2 μL DNA from single embryos or positive control DNA (1 ng DNA extracted from bovine male liver and female granulosa cells).

The amplification program consisted of an initial step at 95°C for 10 min to lyse embryonic cells, followed by 38 cycles as follows: 95°C for 30 s, 55°C for 30 s, 72°C for 1 min, and 72°C for 7 min; with a final hold at 10°C. PCR products were run on 1.6% agarose gel stained with EtBr (0.5 μg/mL) and resultant

amplification products visualised under UV light. Images were captured using the UVP GelDoc-IT imaging system.

Table 3.4 Primers used for sex determination of Day 8 bovine blastocysts.

Gene		Primer sequence (5'-3')	Product (bp)	NCBI accession no.
SRY	FP	TGAAACAAGACCAAACCGGG	339	EU581861.1
	RP	TCCATGGACTTGCTCTACTGT		
BSP	FP	TTTACCTTAGAACAAACCGAGGCA	538	Rattanasuk <i>et al.</i> (2011)
	RP	TACGGAAAGGAAAGATGACCTGAC		

3.2.2.2.3 Statistical data analysis

Statistical analyses were performed within the Genstat statistical package (19th Edition, VSN International, 2011). Proportion data were analysed using generalised linear regression models assuming binomial errors and used logit-link functions. Count data were analysed using generalised linear regression models assuming poisson errors and used log-link functions. Data are presented as adjusted means with SEM.

3.3 Results and Discussion

3.3.1 Methionine cycle enzyme transcripts

RT-PCR experiments qualitatively revealed the temporal mRNA expression patterns of methionine cycle enzymes (*MAT2A* and *BHMT/2*) in bovine ovarian cells, oocytes and preimplantation embryos. All target enzymes plus the internal control (*ACTB*) were detected in bovine liver which is the principal site of 1C metabolism and a tissue characterised to express the complete set of 1C metabolism enzymes (Mato *et al.*, 2008; Lu and Mato, 2012). In line with previous studies (Kwong *et al.*, 2010; Ikeda *et al.*, 2010), *MAT2A* was detected in ovarian cells, oocytes and embryos throughout all stages of preimplantation development (Figure 3.4).

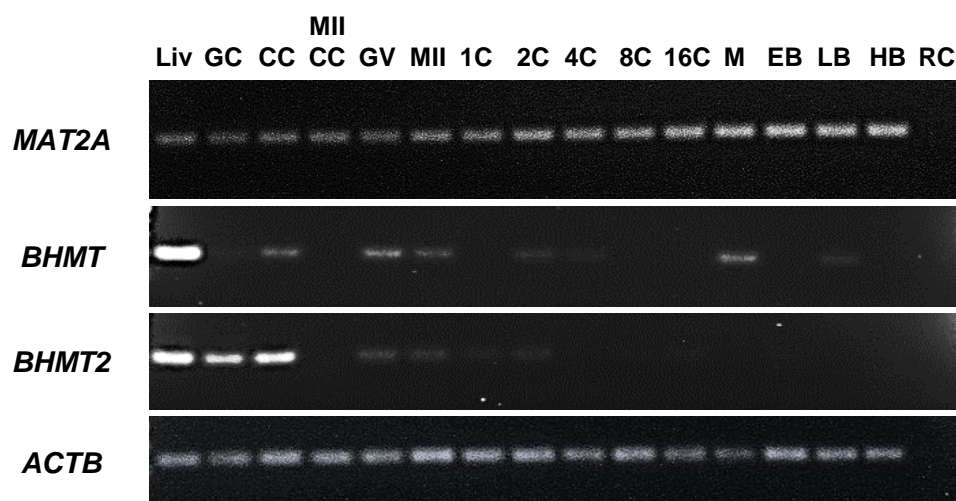


Figure 3.4 *MAT2A*, *BHMT* and *BHMT2* transcript expression in bovine ovarian cells, oocytes and preimplantation embryos.

Liver (Liv) positive control; granulosa cells (GC); cumulus cells (CC), matured cumulus cells (MII CC); germinal vesicle oocytes (GV); metaphase II matured oocytes (MII); zygotes (1C); embryos: 2 cell (2C); 4 cell (4C); 8 cell (8C); 8-16 cell (8-16C); morulae (M); Day 7 early blastocysts (EB); Day 8 late blastocysts (LB); Day 9 hatching blastocysts (HB); reagent control (RC).

Interestingly, visible amplification products for *BHMT2* were detected in bovine CC and GC but were not clearly detected in matured CC, oocytes or preimplantation embryos (Figure 3.4). The substrate for *BHMT2*, S-methylmethionine (SMM), is a natural sulfonium analogue of SAM that is unique to plants and present in high quantities in corn-based diets (Augsburger *et al.*, 2005; Appendix Chapter 3). A fraction of SMM escapes ruminal fermentation and can be used as a source of by-pass methionine and methyl groups in ruminants (Matsuo *et al.*, 1980; Hegedüs *et al.*, 1995; Augspurger *et al.*, 2005). In addition, SMM is a precursor of the osmolyte, dimethylsufoniopropionate (Rouillon *et al.*, 1999). The mechanism of uptake and the biological function of SMM within cells of the bovine ovary are unknown and warrant further investigation in order to elucidate the role of *BHMT2* within these cell types.

Weak but visible bands detected for both *BHMT* isoforms in GV and MII oocytes could be an experimental artefact due to overexposure of the gel (Figure 3.4). The presence of *BHMT* mRNA, however, supports findings of Ikeda and colleagues (2010) who detected *BHMT* transcript expression in bovine GV and MII oocytes, and Benkhalifa *et al.* (2008) who detected *BHMT* and *BHMT2* expression in human oocytes. The finding that oocytes express *BHMT* isoforms suggests that these germ cells harbour alternative pathways for methionine production and are, therefore, equipped with a unique methylation machinery

required for the establishment of the oocyte-specific methylome that takes place during the later stages of oogenesis (Ikeda *et al.*, 2010; Demond, 2020).

The present study detected transient *BHMT* mRNA expression at the morula stage of bovine embryos (Figure 3.4). This observation agrees with previous studies using bovine (Ikeda *et al.*, 2010) and murine embryos (Lee *et al.*, 2012; Section 1.4). In mice, *Bhmt* mRNA was first expressed in morulae before decreasing in blastocysts, whilst BHMT protein expression and activity was not detected until the blastocyst stage (Lee *et al.*, 2012). As for mice, it is possible that translation of the *BHMT* transcript does not begin until a later stage of development in bovine embryos. Measuring BHMT enzyme expression and activity was beyond the scope of the current study, however, an experiment of this nature could help to resolve contradictory findings regarding *BHMT* mRNA and enzyme expression, and its putative role in methionine metabolism in the bovine preimplantation embryo (Ikeda *et al.*, 2010; Kwong *et al.*, 2010).

3.3.2 Methionine and embryo development during culture

3.3.2.1 Methionine composition of custom-made IVP media

High performance liquid chromatography (HPLC) analyses confirmed concentrations of methionine in custom-made IVP media formulations (Figure 3.5). Although below the LLOQ, a basal level of methionine was present in all media formulations, including 0 $\mu\text{mol/L}$ added methionine (non-physiological concentration), due to the addition of macromolecules, fetal calf serum (FCS) and bovine serum albumin (BSA), to media (Leibfried-Rutledge *et al.*, 1986). Supplementation of IVM media with 10% FCS contributed $\sim 3\text{--}4 \mu\text{mol/L}$ of methionine (Figure 3.5A). Supplementation of IVF and IVC media with 0.6% and 0.3% BSA, respectively, contributed $<3 \mu\text{mol/L}$ (Figure 3.5B, Figure 3.5C).

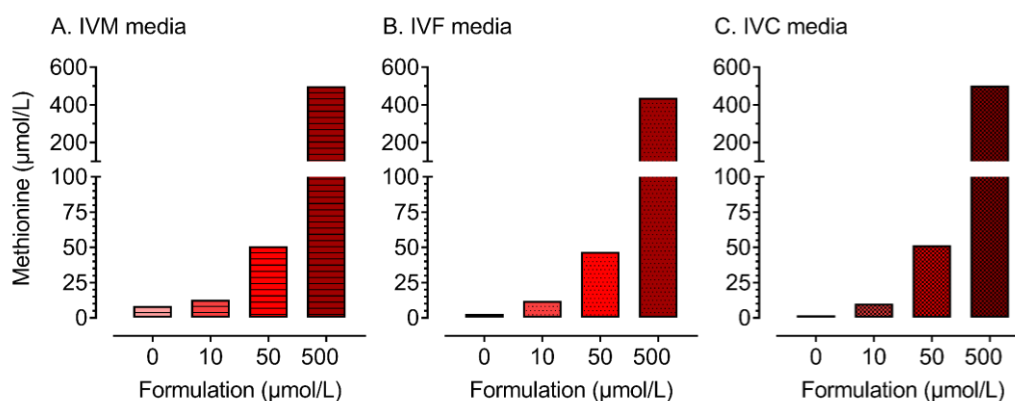


Figure 3.5 Concentrations of methionine in custom-made *in vitro* embryo production media formulations.

IVM, *in vitro* maturation media (A). IVF, *in vitro* fertilisation media (B). IVC, *in vitro* culture media (C). Data is based on one replicate to confirm added methionine concentration.

3.3.2.2 Amino acid composition of custom-made IVP media

The amino acid profile of custom-made IVM and IVC media are presented in Figure 3.6. Amino acids were undetected in IVF media as this formulation is not supplemented with amino acids other than through the addition of BSA. The overall profile of amino acids in custom-made methionine-free TCM199 IVM media (Gibco™) was similar to that of the commercial TCM199 GlutaMAX™ formulation routinely used in our laboratory. However, there was a large discrepancy between glutamine (Gln) concentrations disclosed in the commercial formulation and those measured in custom-made media (Figure 3.6A).

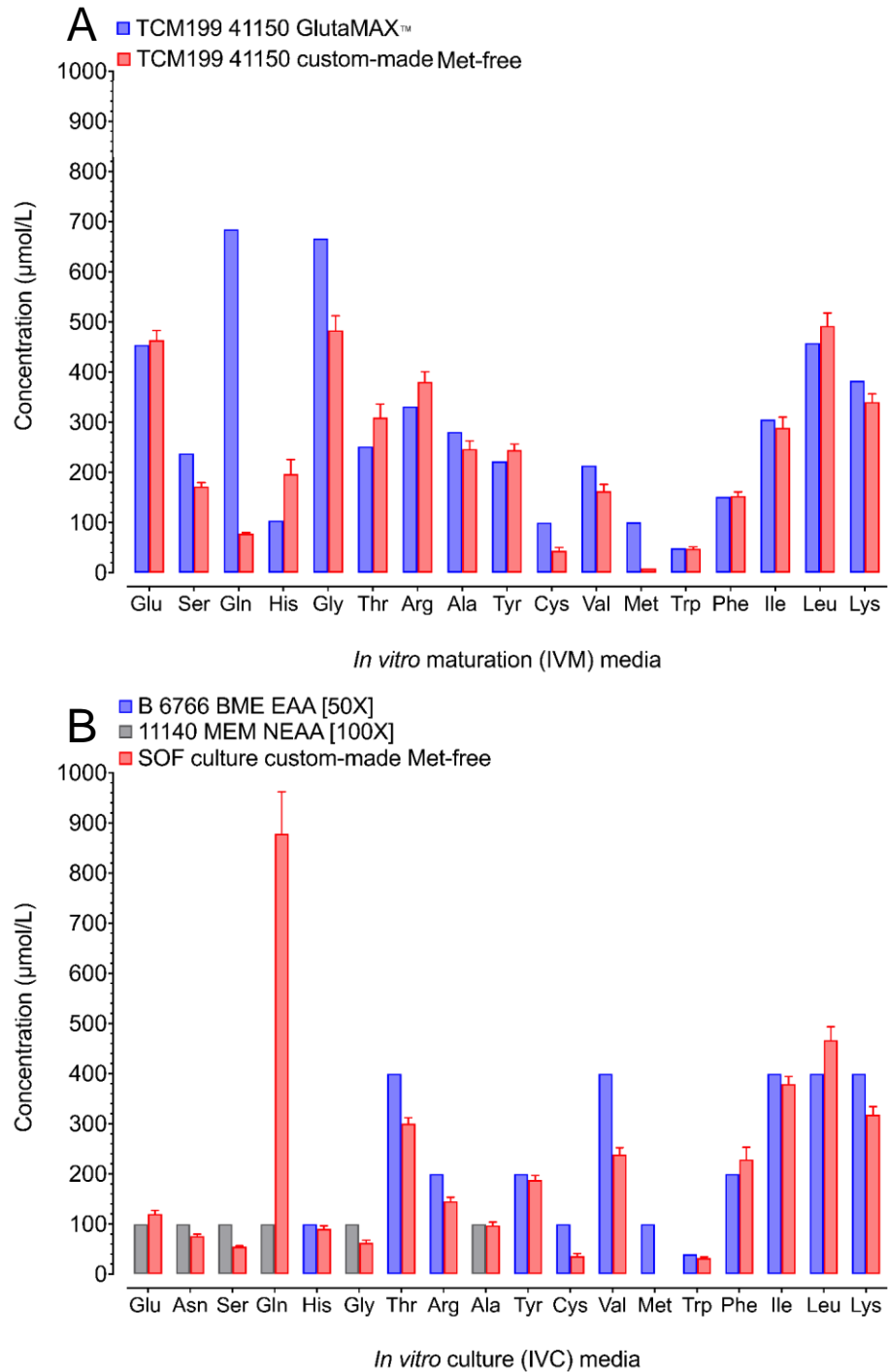


Figure 3.6 Amino acid profile of *in vitro* maturation (IVM) media (A) and *in vitro* culture (IVC) media (B).

Custom-made media samples analysed over four replicates. Data presented as mean \pm SEM. Abbreviation(s): Ala, alanine; Arg, arginine; Asn, asparagine; BME, Basal Medium Eagle; Cys, cystine; EAA, essential amino acids; Gln, glutamine; Glu, glutamate; Gly, glycine; His, histidine; Ile, isoleucine; Leu, leucine; Lys, lysine; MEM, Minimum Essential Medium; Met, methionine; NEAA, non-essential amino acids; Phe, phenylalanine; Ser, serine; Thr, threonine; Trp, tryptophan; Tyr, tyrosine; Val, valine.

Due to the high lability of Gln at physiological pH (Khan and Elia, 1991; Jagušić *et al.*, 2016), the GlutaMAX™ supplement is a dipeptide, L-alanine-L-glutamine, which is more soluble and more stable in aqueous solution and, therefore, does not spontaneously degrade. Since it was not possible to measure this dipetide molecule using the HPLC method, concentrations of Gln could not be accurately determined in IVM media (Figure 3.6A).

With respect to embryo culture, the classic subdivision of amino acids is into 'essential' and 'non-essential' groups. This subdivision is an over-simplification and misleading given that all amino acids are essential for protein synthesis and cellular function in the early embryo (Sturmey *et al.*, 2008). During culture, essential amino acids (EAA) are typically supplemented to IVC media through the addition of Basal Eagle's Medium (BME) [50X] vitamin solution (4% v/v). Formulations include amino acids that are classified as essential; histidine (His), arginine (Arg), valine (Val), methionine (Met), tryptophan (Trp), phenylalanine (Phe), isoleucine (Ile), leucine (Leu) and lysine (Lys), as well as non-essential amino acids (NEAA) that become conditionally essential under culture conditions; cystine (Cys), threonine (Thr) and tyrosine (Tyr; Morbeck *et al.*, 2014; Figure 3.6B). As discussed above (Section 3.3.2.1), basal levels of methionine present in custom-made methionine-free IVM and IVC media formulations were below the LLOQ (Table 3.3).

Non-essential amino acids; glutamate (Glu), asparagine (Asn), serine (Ser), glutamine (Gln), glycine (Gly) and alanine (Ala), are typically supplemented to IVC media through the addition of Minimum Essential Medium (MEM) [100X] solution (1% v/v). Glutamine is one of the most abundant amino acids in the female mammalian reproductive tract (Orsi *et al.*, 2005; Harris *et al.*, 2005) that has a stimulatory effect on preimplantation embryo growth and development (Lane and Gardner, 1997; Chen *et al.*, 2018). Because the concentration of Gln in MEM is low (~100 µmol/L) and unstable in solution, 1 mmol/L of Gln is routinely added to regular media used in IVF laboratories (Lane and Gardner, 1993; Lane and Gardner, 1997b). Following its addition to our custom-made IVC media, the final Gln concentration was 878.3 ± 84 µmol/L (Figure 3.6B). As with all amino acids, however, the spontaneous degradation of Gln leads to the accumulation of ammonium ions (urea) in culture media which can change pH and osmolarity with embryo-toxic consequences (Gardner and Lane, 1993; Orsi and Leese, 2004). Therefore, to avoid ammonium toxicity, it was critical to renew culture media every 48 h.

3.3.2.3 Amino acid composition of bovine follicular fluid

Ovarian follicular fluid has been used to support the *in vitro* maturation of bovine oocytes albeit with varying degrees of success (Sirard and First, 1988; Takagi *et al.*, 1998; Heidari *et al.*, 2019). Considering that nutrient concentrations are typically non-physiological in mammalian IVM systems (Nakawaza *et al.*, 1997), the addition of follicular fluid aims to expose COCs to a more physiological hormonal and nutritional milieu (Orsi *et al.*, 2005). Clearly, fluid within the developing antral follicle contains substances required for oocyte maturation and fertilisation (Gérard *et al.*, 2002). Efforts have, therefore, been made to model nutrient profiles of IVM media on that of preovulatory follicular fluid in order to improve oocyte and embryo developmental potential (Krishner and Bavister, 1998).

The profile of amino acids in follicular fluid has been characterised in several mammalian species (Leese and Lenton, 1990; Gérard *et al.*, 2002; Sinclair *et al.*, 2008). In cattle, the amino acid composition varies throughout the oestrous cycle and is influenced by follicular dominance. In line with reports by Orsi and others (2005), the present study found that the concentrations of certain amino acids were negatively correlated with follicular fluid volume. In particular, Glu, Gln, Arg and Ala, tend to decrease with follicular dominance (Figure 3.7).

Previous studies investigating the amino acid composition of bovine follicular fluid reported quantitatively similar profiles (Orsi *et al.*, 2005; Sinclair *et al.*, 2008) with Gln, Ala and Gly presenting as the most abundant amino acids (Orsi *et al.*, 2005; Hugentobler *et al.*, 2007; Sinclair *et al.*, 2008). Discrepancies between studies may be accounted for by differences in analytical technique, i.e. HPLC (present study) vs GC-MS (Sinclair *et al.*, 2008) and the absence of follicular segregation according to oestrus stage across studies. By way of example, the present study reports a ~3-fold lower concentration of Gly in follicular fluid than concentrations reported by Sinclair *et al.* (2008) (Figure 3.8). This is not surprising given that Gly concentrations can fluctuate markedly in follicular fluid according to stage of oestrus, starting at >800 µmol/L at Stage I and declining to <300 µmol/L at later stages (Orsi *et al.*, 2005).

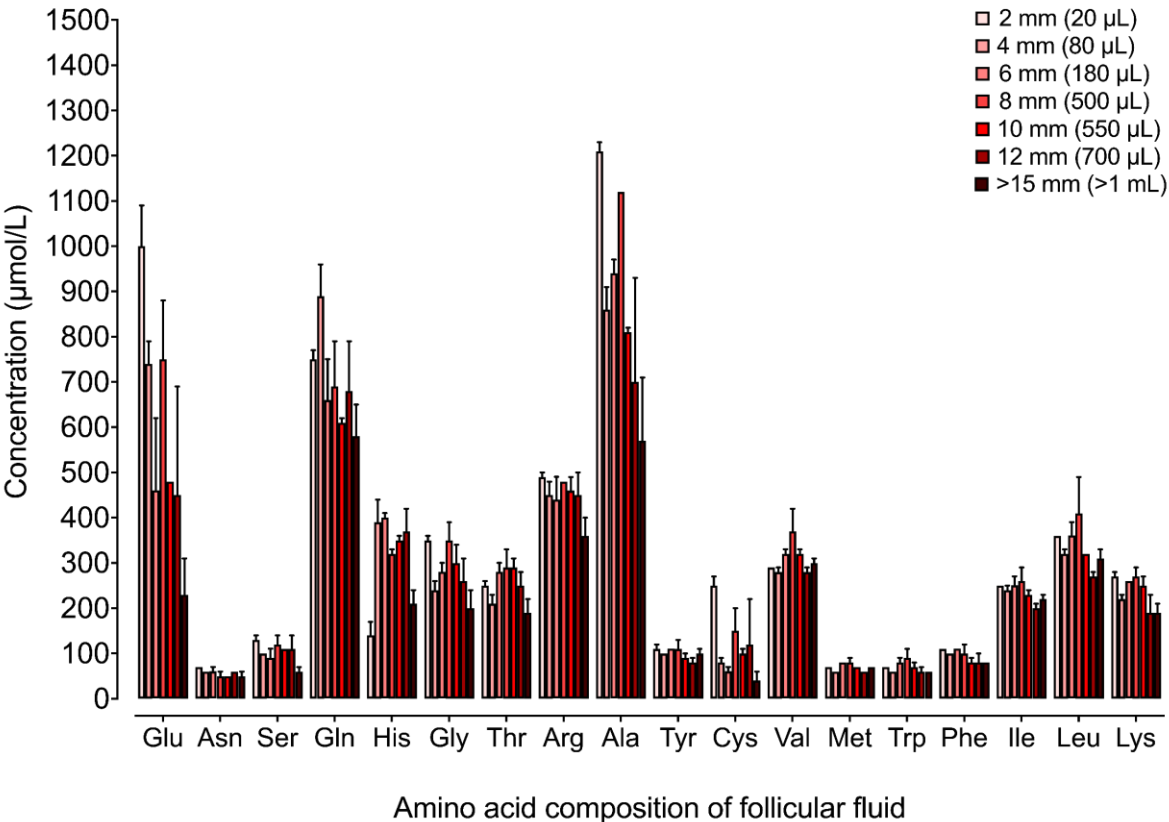


Figure 3.7 Amino acid composition of bovine follicular fluid by follicular size.

Pooled follicular fluid samples analysed in duplicate. Data presented as mean \pm SEM. Abbreviation(s): Ala, alanine; Arg, arginine; Asn, asparagine; Cys, cystine; Gln, glutamine; Glu, glutamate; Gly, glycine; His, histidine; Ile, isoleucine; Leu, leucine; Lys, lysine; Met, methionine; Phe, phenylalanine; Ser, serine; Thr, threonine; Trp, tryptophan; Tyr, tyrosine; Val, valine.

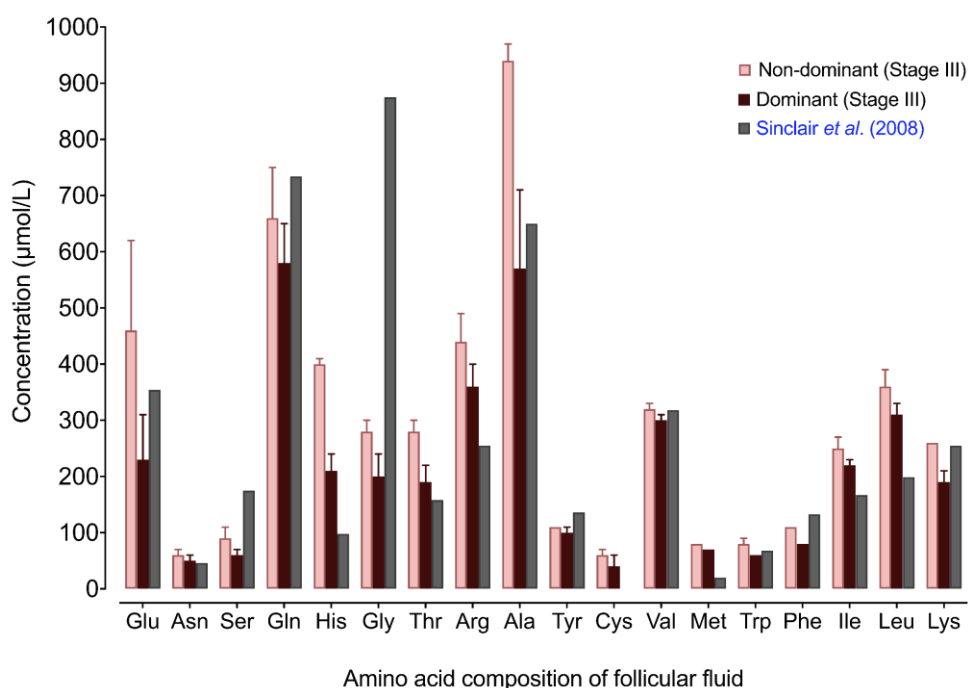


Figure 3.8 A study comparison of the amino acid profile in bovine follicular fluid aspirated from non-dominant (2 to 6 mm) and dominant (6 to >15 mm) ovarian follicles.

Pooled follicular fluid samples analysed in duplicate. Data presented as mean \pm SEM. Abbreviation(s): Ala, alanine; Arg, arginine; Asn, asparagine; Cys, cystine; Gln, glutamine; Glu, glutamate; Gly, glycine; His, histidine; Ile, isoleucine; Leu, leucine; Lys, lysine; Met, methionine; Phe, phenylalanine; Ser, serine; Thr, threonine; Trp, tryptophan; Tyr, tyrosine; Val, valine.

The amino acid profile of custom-made IVM media used for all methionine-adjusted IVP experiments in Chapter 3 was similar to that of Stage III bovine preovulatory follicular fluid (*in vivo*), with the exception of 1C metabolites Gly and Ser which were present at higher concentrations in IVM media than in follicular fluid, and Ala which was 3-fold higher in follicular fluid than in IVM media (Figure 3.9). Glycine is an organic osmolyte required for the regulation of cell volume homeostasis in oocytes and early cleavage stage embryos (Steeves *et al.*, 2003; Tartia *et al.*, 2009; Cao *et al.*, 2016). Both Gly and Ser are required for glutathione (GSH) synthesis and are required to protect oocytes against oxidative stress (Mattaini *et al.*, 2016; Udhe *et al.*, 2018). The interconversion of Ser and Gly catalysed by SHMT in the folate cycle facilitates methyl donation required for nucleotide synthesis (Figure 1.1), hence, both amino acids can be used interchangeably to support cell growth and development during *in vitro* maturation. The higher concentration of Ala in follicular fluid (Figure 3.9) supports observations of Elhassan *et al.* (2001), who found that Ala

concentrations were >3 mmol/L in bovine follicular, oviductal and uterine fluid, thereby exceeding concentrations in IVP media.

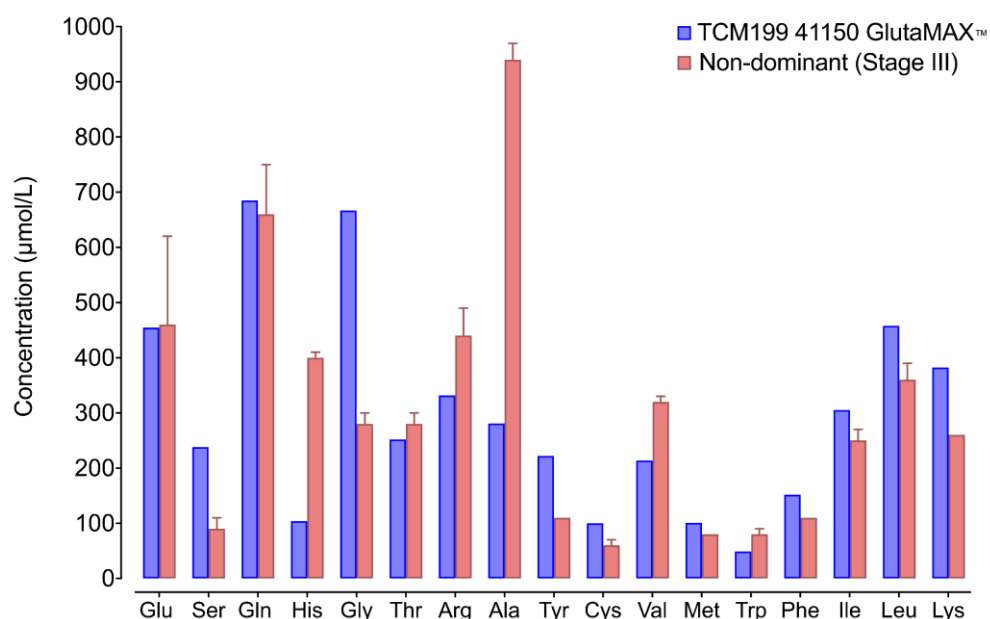


Figure 3.9 A comparison of amino acids in custom-made TCM199 IVM formulation and preovulatory ovarian follicular fluid.

Data presented as mean \pm SEM. Abbreviation(s): Ala, alanine; Arg, arginine; Asn, asparagine; Cys, cystine; Gln, glutamine; Glu, glutamate; Gly, glycine; His, histidine; Ile, isoleucine; Leu, leucine; Lys, lysine; Met, methionine; Phe, phenylalanine; Ser, serine; Thr, threonine; Trp, tryptophan; Tyr, tyrosine; Val, valine.

The media concentration of amino acids is one matter, but the ratio of amino acids is another. It is understood that mammalian oocytes and embryos possess an array of specialised amino acid transport systems that each transport a range of related compounds (Van Winkle, 2001; Pelland *et al.*, 2009; Guyader-Joly *et al.*, 1996). Thus, when amino acids are present at the same concentration, competition for transporter binding sites inhibits the entry of some amino acids, leading to disequilibrium within the endogenous pool (Ménézo and Hérubel, 2002). Of particular relevance to the following discussion is the interaction between methionine and Gly. Concentrations of Gly can exceed 1.2 mmol/L in the female bovine reproductive tract; such concentrations are >20-fold higher than those of methionine (Hugentobler *et al.*, 2007; Herrick *et al.*, 2016). The high Gly:Met ratio permits entry of Gly into the cells (Ménézo and Hérubel, 2002) and will be an important consideration for investigating the effects of adding methionine to media formulations during bovine IVP.

3.3.2.4 *In vitro* embryo production with added methionine

To our knowledge, this is the first investigation into the effect of altering methionine concentration during *in vitro* maturation, fertilisation and culture of bovine embryos. An earlier study by [Bonilla and colleagues \(2010\)](#) assessed the effects of altering methionine concentration (0-400 $\mu\text{mol/L}$) from the point of embryo culture. However, in the present study, methionine treatments were introduced from the point of oocyte maturation as this more suitably recapitulates the 'physiological' environment. *In vivo*, gametes and embryos encounter moderate fluctuations in methionine ([Hugentobler et al., 2007](#); [Bonilla et al., 2010](#)) rather than extreme concentration changes brought about by *in vitro* culture.

3.3.2.4.1 Gross morphology

Embryos and blastocysts cultured in modified media containing 0, 10, 50 and 500 $\mu\text{mol/L}$ of added methionine were morphologically assessed according to IETS criteria (Appendix 3.3). Whilst there was a tendency for the proportion of cleaved embryos to be lowest in those cultured in non-physiological medium (0 $\mu\text{mol/L}$ added), there was no significant effect of methionine concentration on the proportion of embryos cleaved on Day 2 (Figure 3.10).

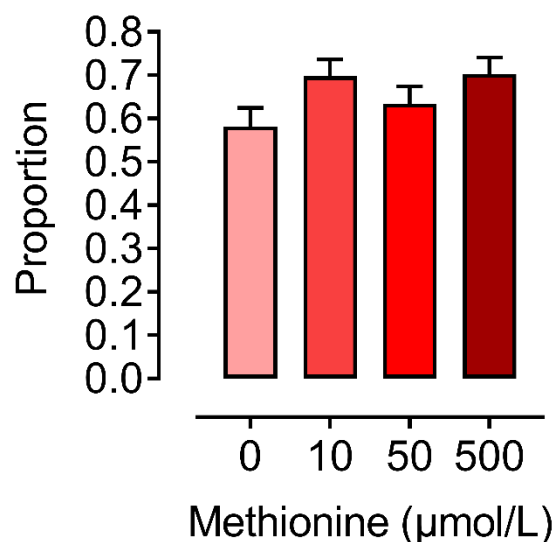


Figure 3.10 Methionine concentration during bovine IVP had no effect on the proportion of inseminated oocytes that cleaved by Day 2 ($P=0.147$).

Data obtained over eight experimental replicates and analysed by generalised linear regression assuming binomial errors. Total number of inseminated oocytes ($n=1,000$). Data presented as mean \pm SEM.

These findings were consistent with those of [Bonilla *et al.* \(2010\)](#) and suggest that the methionine requirements of the oocyte, zygote and early cleavage embryo are satisfied by oocyte stores and the increase in protein catabolism that occurs during oocyte maturation. Recent work by [Udhe *et al.* \(2018\)](#) reported a ~5-fold increase in media concentrations of methionine during bovine oocyte maturation. This egression of methionine from oocytes indicates that methionine is not limiting but is dispensible during oocyte maturation. Evidence suggests that methionine consumption and incorporation into proteins increases after the 8-cell stage and compaction ([Partridge and Leese, 1996](#)), coinciding with bovine embryonic genome activation (EGA; [Graf *et al.*, 2014](#); Figure 3.1). However, protein synthesis in the bovine blastocyst is reported to increase substantially at the blastocyst stage ([Edwards *et al.*, 1997](#)). Indeed, results from the present study found an effect ($P<0.001$) of methionine concentration on blastocyst development at Day 7 (Figure 3.11A, Figure 3.11B).

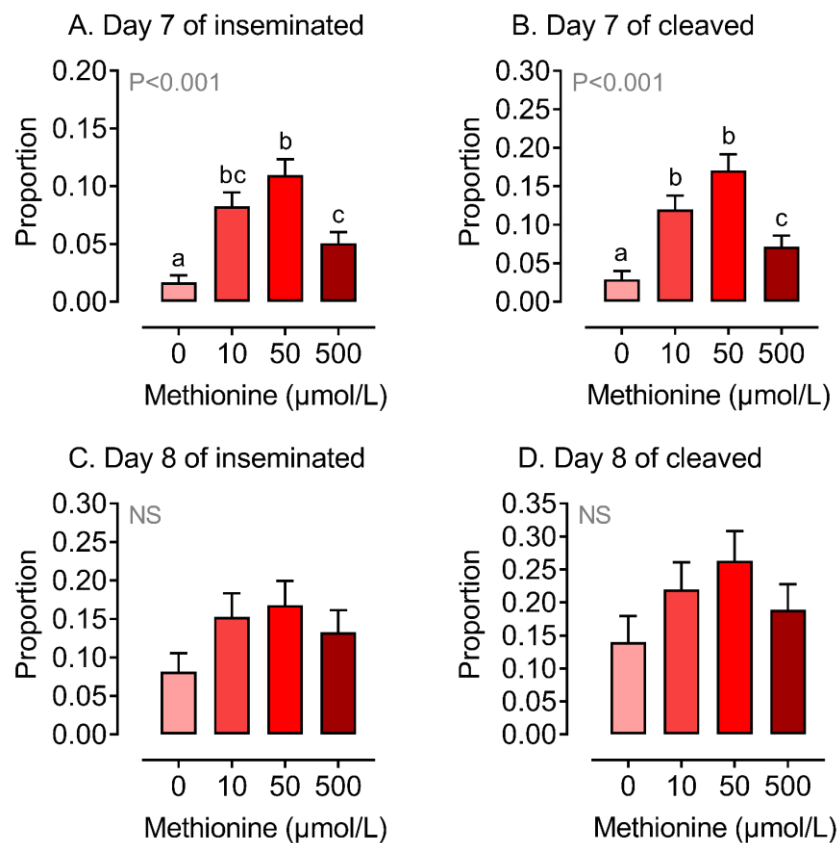


Figure 3.11 Added methionine increases ($P<0.001$) the proportion of blastocysts by Day 7.

Data obtained over eight experimental replicates and analysed by generalised linear regression assuming binomial errors. Total number of blastocysts assessed ($n=135$). Data presented as mean \pm SEM. Means labelled (a, b, c) differ ($P<0.05$).

Embryos cultured in non-physiological media (0 $\mu\text{mol/L}$ added methionine) were least likely to develop to blastocysts on Day 7 ($P < 0.001$). However, albeit small, a proportion of embryos did reach the blastocyst stage by Day 8 (0.14 ± 0.039 ; Figure 3.11D). There is likely to be some variation in the absolute requirements of individual bovine embryos for methionine (Bonilla *et al.*, 2010). Perhaps the requirements of certain embryos are satisfied by the remethylation of Hcy to methionine (Škovierová *et al.*, 2016) or an increased capacity for methionine uptake under deficient conditions (Guyader-Joly *et al.*, 1997). It follows that amino acid metabolism serves as a biomarker of developmental potential in bovine blastocysts (Sturmeay *et al.*, 2010). Similarly, embryos cultured in suprphysiological media (500 $\mu\text{mol/L}$ added methionine) exhibited reduced development to the blastocyst stage (Figure 3.11A, Figure 3.11C). Although not statistically significant, of the physiological methionine concentrations tested, 50 $\mu\text{mol/L}$ of added methionine appears best for blastocyst development (Figure 3.11C, Figure 3.11D).

A small proportion of embryos cultured in non-physiological and suprphysiological concentrations of methionine were advanced in development (i.e. Stage 7-9; late expanded, hatching or hatched from the zona pellucida) on Day 8 ($P < 0.05$; Figure 3.12A; Appendix 3.3). Methionine concentrations are thought to influence blastocyst expansion and hatching by regulating blastocoel cavity size (Bonilla *et al.*, 2010). This role is exerted through the conversion of methionine to methyl donor, SAM, which methylates cell membrane lipids and proteins to mediate their fluidity (Muriel *et al.*, 1993). A prime example is the regulation of the integral membrane protein, Na⁺/K⁺-ATPase. This enzyme is responsible for maintaining cell volume, and intra- and extra-cellular electrolyte balance by catalysing the export and import of sodium and potassium ions, respectively (Lees, 1991). In rodents, maternal hypermethioninemia decreased Na⁺/K⁺-ATPase activity, thereby impairing sodium-potassium exchange in the developing brain of pups (Schweinberger *et al.*, 2014). A similar effect of high methionine within cells of the bovine preimplantation embryo might explain, at least in part, the reduction in cavitation and blastocyst expansion observed at the suprphysiological concentration of methionine used in the present study (Figure 3.12A).

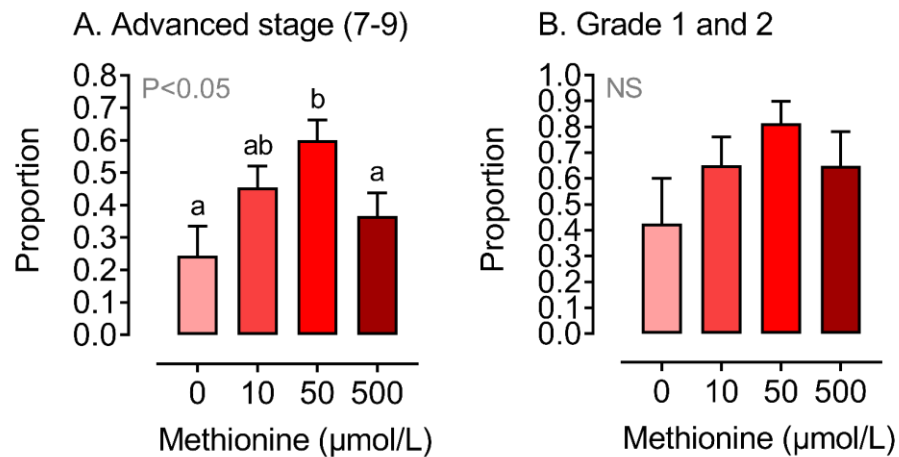


Figure 3.12 Physiological (10 and 50 µmol/L) methionine increases the proportion ($P<0.05$) of advanced transferable blastocysts.

Proportion of Day 8 blastocysts that were advanced stage; late expanded, hatching or hatched (**A**) and of grade 1 and 2 transferable quality (**B**). Data obtained over eight experimental replicates and analysed by generalised linear regression assuming binomial errors. Total number of blastocysts ($n=135$). Data presented as mean \pm SEM. Means labelled (a, b) differ ($P<0.05$).

Although not statistically significant, non-physiological (0 µmol/L added) and suprphysiological (500 µmol/L added) concentrations of methionine during IVP decreased the proportion of Grade 1 and 2 (transferable) blastocysts (Figure 3.12B). The greatest proportion of advanced stage and transferable grade blastocysts were derived during culture in the high physiological methionine concentration (i.e. 50 µmol/L added; Figure 3.12).

With all aforementioned points considered, methionine deficiency and excess appear to be detrimental to bovine preimplantation embryo development. Methionine is recognised as the most toxic amino acid (Benevenga and Steele, 1984; Garlick, 2006) since its catabolism can produce high levels of volatile sulphurous compounds (Komarnisky *et al.*, 2003). Thus, it is not surprising that continual culture at suprphysiological concentrations of methionine reduces embryo viability. As discussed above, the catabolism of amino acids, i.e. methionine, can lead to the production of ammonium ions which is detrimental to embryo development (Gardner and Lane, 1993; Orsi and Leese, 2004). Moreover, excess methionine is diverted towards catabolic pathways which requires other amino acids, such as Gly and Ser (Rees *et al.*, 2006). Methionine is converted to cysteine and further oxidised to sulphate via the *transsulphuration* pathway using CTH and CBS enzymes (Figure 1.1), or via cysteine dioxygenase (CDO; Ueki *et al.*, 2011). However, early studies in

human and rodent fetal liver reported absence of CTH and CDO enzymes, indicating that the developing fetus has a limited capacity to generate sulphate from sulphur-containing amino acids until later stages of gestation (Gaul *et al.*, 1972; Rakoczy *et al.*, 2015).

Continuing with the earlier discussion (Section 3.3.2.3), the balance of methionine relative to other amino acids is critical for normal embryo metabolism and development. At the same molar concentrations, methionine almost completely prevents Gly entry into the preimplantation embryo due to its high affinity for the same transporter (Gly-specific transport system; Khatchadourian *et al.*, 1994). As demonstrated in Figure 3.6B, the typical Gly concentration of IVC media is 100 $\mu\text{mol/L}$ based on the composition of Minimum Essential Medium (Partridge and Leese, 1996). As a high Gly:Met ratio permits entry of Gly into the cells (Khatchadourian *et al.*, 1994; Ménézo and Hérubel, 2002), culturing embryos in supraphysiological methionine concentrations would shift this ratio, thereby leading to Gly deficiency. Due to the diverse roles of Gly in antioxidant balance and osmoregulation, Gly deficiency is likely to have widespread effects on embryo growth and development (Steeves *et al.*, 2003; Tartia *et al.*, 2009; Cao *et al.*, 2016). Such adverse effects of methionine-induced Gly deficiency have been observed at the whole organism level. Rats fed low protein diets (10% casein) with methionine levels 3- to 4-fold greater than the estimated requirement (0.5-0.6% of the diet) exhibited suppression of voluntary food intake and near-cessation of growth (Harper *et al.*, 1970). However, dietary Gly supplementation can reverse this growth retarded phenotype in animals fed a high-methionine diet (Benevenga and Steele, 1984).

In relation to 1C metabolism, methionine deficiency or excess is likely to perturb intracellular SAM pools with downstream consequences for methyl metabolism in embryos. Shojaei Saadi *et al.* (2016) cultured bovine embryos in a high but non-lethal dose of SAM (2 $\mu\text{mol/L}$) from the 8-cell stage to blastocyst stage, and found that SAM treatment significantly increased blastocyst expansion and hatching on Day 8 (Hatching rate: 82% SAM-treated v 33% controls). Ikeda *et al.* (2012) found that culturing embryos with 10 mmol/L of ethionine, a structural analogue of methionine, inhibited the morula-to-blastocyst transition in bovine embryos but that supplementation of ethionine cultures with SAM (1-2 $\mu\text{mol/L}$) partially restored blastocyst development. Taken together, these findings suggest an important role of methionine in methyl donation during bovine

preimplantation embryo development and remains the focus of further investigation (Chapter 4).

3.3.2.4.2 Cell lineage specification

The proliferation of blastomeres is one of the main factors involved in blastocyst expansion and hatching (Shojai Saadi *et al.*, 2016). It was, therefore, hypothesised that cell number and allocation to the ICM and TE might differ according to methionine treatment. As the high physiological methionine concentration (50 $\mu\text{mol/L}$ added) yielded the greatest proportion of advanced blastocysts (Figure 3.12A), it was expected that blastocysts cultured in this concentration would have greater cell numbers and have differentiated earlier than those cultured in lower methionine concentrations.

The bovine embryo transits from the morula to blastocyst stage between days 5-8 post fertilisation (Figure 3.1). The final stage of blastocyst formation is characterised by the emergence of the pluripotent Epi and PE cell lineages (within the ICM), and the TE (Kuijk *et al.*, 2012). NANOG is first expressed in the 8-cell bovine embryo whilst SOX17 expression begins at the 16-32 cell stage. SOX17 is co-expressed with NANOG during early embryogenesis, but these markers become mutually exclusive by the late blastocyst stage; NANOG is expressed in the Epi and SOX17 is expressed in the PE. Thus, immunofluorescence analysis of NANOG and SOX17 were used as reliable readouts of Epi and PE, respectively (Canizo *et al.*, 2019; Figure 3.13).

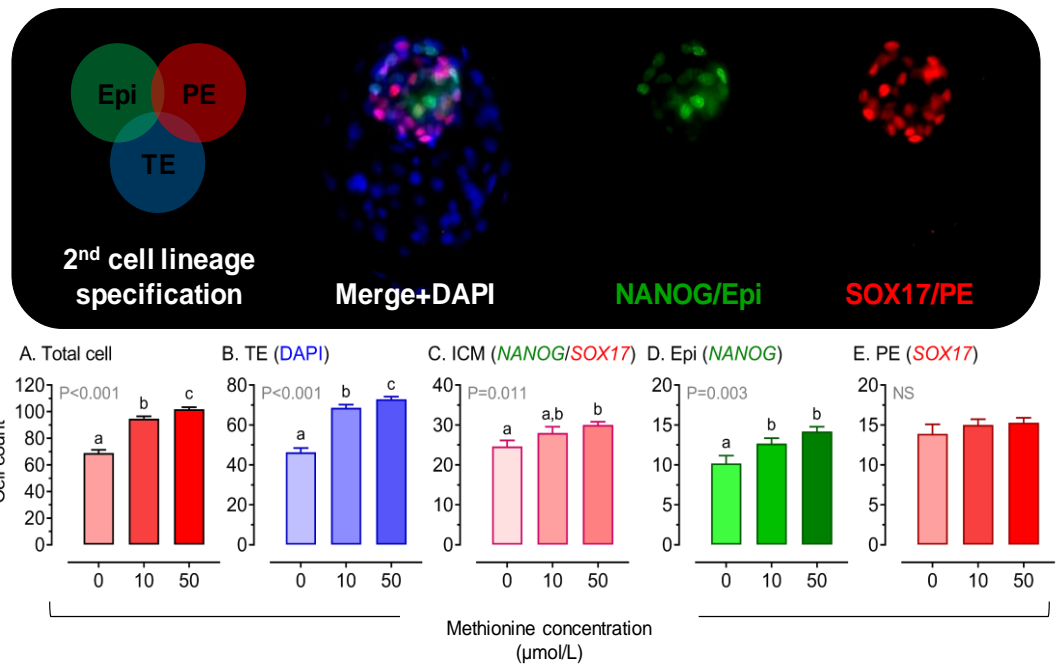


Figure 3.13 Blastocyst cell number increases ($P<0.001$) in a dose-dependent manner with methionine.

Total cell count (**A**); trophectoderm (TE) cell count (**B**); inner cell mass (ICM) cell count (**C**); epiblast (Epi) cell count (**D**); primitive endoderm (PE) cell count (**E**). Data obtained over four experimental replicates and analysed by generalised linear regression assuming poisson errors. Total number of blastocysts ($n=85$). Data presented as mean \pm SEM. Means labelled (a, b, c) differ ($P<0.05$).

Blastocyst total cell number increased ($P<0.001$) in a dose-dependent manner with increased methionine (Figure 3.13A). This observation was accompanied by significant ($P<0.001$) outgrowth of the TE, the first epithelium formed in development that forms extraembryonic lineages, including the placenta (Figure 3.13B). Non-physiological concentrations of methionine (0 $\mu\text{mol/L}$ added) significantly ($P=0.011$) reduced outgrowth of the ICM (Figure 3.13C). This observation was accompanied by a reduction ($P=0.003$) of cells in the epiblast (Epi); the lineage that will give rise to the embryo proper (Figure 3.13D). Primitive endoderm (PE) cells, which will give rise to the yolk sac, were unaffected by methionine concentration ($P=0.557$; Figure 3.13E).

Previous research has not evaluated the effect of methionine on the allocation of embryonic cells to Epi and PE lineages within the ICM, but methionine deficiency may reduce total cell numbers and skew the ratio of ICM to TE cells within Day 8 bovine blastocysts (Lane and Gardner, 1997). By way of example, culturing bovine embryos with methionine antagonist, ethionine, from the 5-cell stage reduced the total number of blastocyst cells (Ikeda *et al.*, 2012). Similarly, when early cleavage stage bovine embryos (1 to 8-cell) were cultured with the

MAT2A inhibitor, fluorinated N,N-dialkylaminostilbene-5 (FIDAS; 10 and 20 $\mu\text{mol/L}$), ICM and TE cell proliferation was impaired, and blastocoel formation reduced. This inhibitory effect was alleviated by concomitant supplementation with a high concentration of methionine (1 mmol/L; Ikeda *et al.*, 2017). In support of the finding that TE cell proliferation was significantly altered by methionine concentration (Figure 3.13B), Bonilla *et al.* (2010) also reported a numerically lower ratio of TE cells in blastocysts cultured without methionine. According to Houghton *et al.* (2006), the TE consumes more oxygen, produces more ATP, possesses a greater number of mitochondria and has a higher rate of methionine depletion than the ICM. The pluripotent ICM displays relatively quiescent metabolism in comparison to that of the TE. Thus, it is not surprising that these cell lineages proliferate differently in response to methionine concentration.

Collectively, these studies highlight the importance of methionine as the immediate precursor for SAM biosynthesis, and provide evidence of the role of methylation in cell lineage specification within the bovine preimplantation embryo.

3.3.2.4.3 Primary sex ratio

Sex-specific sensitivity to 1C metabolites in the maternal diet or IVP media can affect embryonic development in a sexually dimorphic manner, thereby skewing the ratio of male to female embryos (Sturmeiy *et al.*, 2010; Sadre-Marandi *et al.*, 2018). Culturing bovine embryos in SAM (2 $\mu\text{mol/L}$) caused a shift in sex ratio in favour of male blastocysts (Shojaei Saadi *et al.*, 2016). It was, therefore, hypothesised that increasing methionine during culture would increase the proportion of male blastocysts. Although not statistically significant, embryo sexing by PCR revealed that physiological methionine concentrations increased the proportion of male blastocysts on Day 8 in a dose-dependent manner up to 50 $\mu\text{mol/L}$. Interestingly, 0 $\mu\text{mol/L}$ added methionine significantly reduced the proportion ($P=0.022$; Figure 3.14). It appears that male embryos are less developmentally competent following culture in non-physiological methionine (0 $\mu\text{mol/L}$), whereas female embryos appear to be more tolerant under methionine-deficient conditions (Figure 3.14A). Previous research in cattle embryos showed sexually dimorphic differences in methionine metabolism between male and female embryos, and females showed increased depletion of methionine during *in vitro* culture compared to males (Sturmeiy *et al.*, 2010).

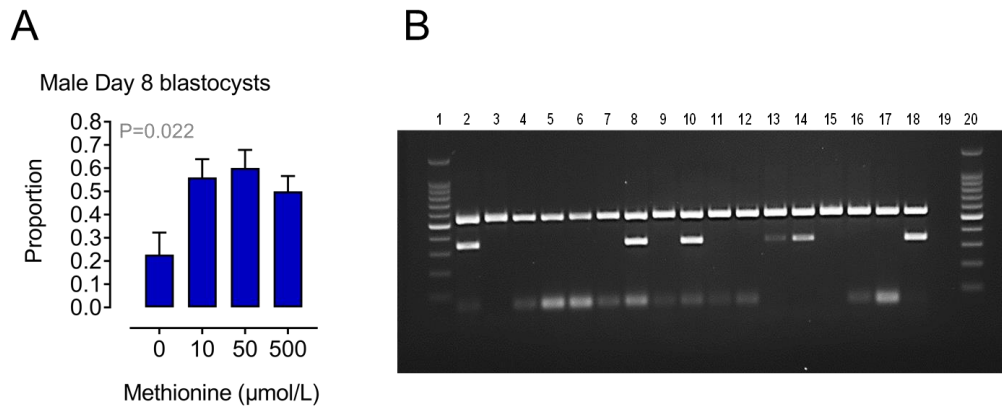


Figure 3.14 Non-physiological (0 $\mu\text{mol/L}$) methionine concentration reduces ($P=0.022$) the proportion of male blastocysts.

Data obtained over three experimental replicates and analysed by generalised linear regression assuming binomial errors. Total number of blastocysts ($n=62$). Data presented as mean \pm SEM (**A**). PCR gel electrophoresis to determine the effect of methionine on sex of bovine embryos. *BSP* amplicon (X chromosome; 538 bp) and *SRY* amplicon (Y chromosome; 339 bp) (**B**). Lanes 1 and 20: 100 bp marker. 2: Male liver +ve control; 3: Female liver +ve control. Lanes 4 to 19: cleaved embryos. Lane 19: reagent control (RC).

Research examining sexually dimorphic differences in embryonic growth and survival of human embryos demonstrated that female embryos can respond to sub-optimal culture environments by altering the expression of multiple genes and proteins to regulate their growth in an attempt to survive environmental insults. On the contrary, males appear to be less versatile and are, therefore, at higher risk of developmental arrest (Clifton, 2010; Rubessa *et al.*, 2011; Alur, 2019). This example of sexual dimorphism has been observed in natural populations of ruminant species wherein the sex ratio is biased towards female embryo development when nutritional resources are limited. This maternal adaptive strategy is thought to compensate for the high metabolic cost of rearing males during times of nutritional stress (Clutton-Brock *et al.*, 1986; Kruuk *et al.*, 1999).

A sex-specific response to methionine metabolism has been observed previously. In sheep and rats, methionine deficiency caused metabolic programming of obesity, insulin resistance and hypertension in male offspring (Sinclair *et al.*, 2007; Maloney *et al.*, 2011). As male and female embryos differ in their cellular metabolism, developmental rate, gene transcription and epigenetic processes (Mao *et al.*, 2010; Gallou-Kabani *et al.*, 2010; Rubessa *et al.*, 2011), the precise mechanisms underpinning this sex-specific sensitivity to methionine are unclear (Laguna-Barraza *et al.*, 2012). One possible mechanism

relates to the difference in sex chromosome dosage. Phenotypic differences in male and female embryos may be attributed to transcriptional differences resulting from unbalanced expression of X-linked genes and the differential expression of autosomal genes that are regulated by sex chromosomes (Bermejo-Alvarez *et al.*, 2011). Such genes are involved in protein translation, catabolism and transport; epigenetic regulation of gene expression via DNA methylation; and, mitochondrial activity with widespread effects on molecular and metabolic pathways that can influence embryonic survival rate or long-term effects for offspring health (Bermejo-Alvarez *et al.*, 2008; Bermejo-Alvarez *et al.*, 2010; Sturmeay *et al.*, 2010; Heras *et al.*, 2016).

3.4 Concluding remarks

HPLC analyses of custom-made IVP media accurately confirmed concentrations of methionine in treatments used for *in vitro* production of bovine embryos. In addition, the profile of other amino acids in custom-made IVM and IVC media was similar to that of commercial media routinely used in our laboratory. Altering the concentration of methionine within normal physiological ranges (10 and 50 $\mu\text{mol/L}$) during IVP affects bovine preimplantation embryo development. In support of conclusions drawn by Bonilla and others (2010), the methionine requirement of the bovine embryo resides within physiological limits. Of those concentrations tested, the high physiological concentration (50 $\mu\text{mol/L}$ added methionine) appeared to be best for development, yielding the greatest proportion of advanced blastocysts that were expanding, hatching or hatched. Blastocysts cultured at this concentration also had the highest total cell number which was accompanied by a significant increase in TE cells.

Culturing embryos in non-physiological methionine (0 $\mu\text{mol/L}$) reduced the proportion of male blastocysts compared to females. These findings suggest that sexually dimorphic sensitivity to aberrant culture conditions may originate at the earliest stages of periconceptual development. Based on the observation that SAM supplementation also favoured male blastocyst development during bovine embryo culture (Shojaei Saadi *et al.*, 2016), it is hypothesised that epigenetic modifications to DNA methylation are responsible for the sex-specific nutritionally programmed effects of methionine. Methylation is also involved in the regulation of cell proliferation, lineage specification and blastocyst expansion (Muriel *et al.*, 1993; Ikeda *et al.*, 2017), therefore, a

primary function of methionine during early embryogenesis is likely exerted through the production of methyl donor, SAM.

Given that culture media concentrations of methionine range from 0 to 500 $\mu\text{mol/L}$ (Table 1.5), it was important to investigate the developmental effects of culturing embryos in clinically relevant concentrations. As was expected, non-physiological (0 $\mu\text{mol/L}$) and supraphysiological (500 $\mu\text{mol/L}$) concentrations were detrimental to bovine blastocyst development. Even moderate changes to methionine, within physiological limits, affected the gross morphology of preimplantation blastocysts, thereby emphasising the importance of providing an optimal nutritional environment for healthy embryo development. The visual assessment of embryo morphology is an inadequate metric to evaluate the safety and efficacy of the culture media composition of methionine. Hence, an epigenetic assessment provides a valuable adjunct to elucidate the molecular mechanisms that may underpin the observed phenotypic effects of methionine observed during *in vitro* bovine embryo culture.

Chapter 4

Methionine and epigenetic programming of the bovine preimplantation embryo

4.1 Introduction

DNA methylation is an important epigenetic modification that underpins dynamic reprogramming during mammalian embryogenesis (Morgan *et al.*, 2005; Guo *et al.*, 2014). Primarily, 5-methylcytosine (5mC) is involved in transcriptional regulation of gene expression, retrotransposon silencing, X-chromosome inactivation and genomic imprinting (Hochberg *et al.*, 2011; Smith and Meissner, 2013; Messerschmidt *et al.*, 2014). The periconceptual nutritional environment, particularly the availability of 1C substrates and cofactors, can induce alterations to the embryonic methylome, which can lead to permanent changes in the phenotype of offspring (Sinclair *et al.*, 2007; Maloney *et al.*, 2011). Some of the most remarkable examples of modifying epigenetically sensitive genes via maternal diet were demonstrated with metastable epialleles in yellow agouti (A^{vy}) mice. Methyl donor supplementation during pregnancy increased DNA methylation and altered body composition, and metabolism of offspring of A^{vy} mice (Wolff *et al.*, 1998; Waterland and Jirtle, 2003; Dolinoy, 2008; discussed in Section 1.1.1.2).

Studies in ruminants have also shown that methyl donor availability during the periconceptual period can induce epigenetic changes in offspring. Relevant reductions of methionine and other 1C metabolites in the diet of pregnant ewes led to hypomethylation of 88% of loci in offspring fetal liver. As 53% of the affected loci were specific to males, the observed epigenetic response to low methyl group availability appeared to be sex-specific (Sinclair *et al.*, 2007). On the contrary, feeding methyl rich diets to pregnant ewes increased methylation and altered the expression of imprinted genes, *insulin like growth factor 2 receptor (IGF2R)* and *H19*, in fetal tissues (Lan *et al.*, 2013). Imprinted genes are differentially methylated to allow parent-of-origin-specific monoallelic expression during fetal development. It follows that this subset of genes are particularly sensitive to aberrant methylation during periconceptual development (Kappil *et al.*, 2015). It is, therefore, anticipated that exposure to nutritional insult (e.g. low methionine), non-physiological *in vitro* culture environments and embryo manipulations during ART may interfere with the establishment and/or maintenance of genomic imprinting in gametes and preimplantation embryos (Young *et al.*, 1998; Sinclair *et al.*, 2000; Young *et al.*, 2001; Anckaert *et al.*, 2010; Chen *et al.*, 2013; Chen *et al.*, 2015).

The effect of methionine concentration on the methylome of bovine embryos remains inconclusive. [Peñagaricano and others \(2013\)](#) reported that feeding dairy cattle a marginal difference in maternal dietary methionine (1.89 v 2.43% methionine of metabolisable protein) was sufficient to cause significant changes to the methylome and transcriptome of Day 7 embryos. The expression of 72% of genes that were critical for embryonic development and adult physiological function (i.e. immune response) were decreased at the higher methionine intake as a likely result of increased DNA methylation at CpG islands (CGIs) in the gene promoters ([Peñagaricano et al., 2013](#)). Conversely, [Acosta et al. \(2016\)](#) found that supplementation of the maternal diet with methionine (0.08% of dry matter intake) reduced cytosine methylation in flushed embryos at Day 6.5.

The addition of methionine (0, 7 and 21 $\mu\text{mol/L}$) during *in vitro* culture of bovine embryos was found to have no significant effect on cytosine methylation at Day 8 ([Bonilla et al., 2010](#)). However, the addition of the downstream product of methionine, SAM (2 $\mu\text{mol/L}$), during culture increased cytosine methylation in Day 8 bovine blastocysts ([Shojaei Saadi et al., 2016](#)). Similarly, the inhibition of methionine by the addition of methionine antagonist, ethionine (1-10 mmol/L), during culture reduced cytosine methylation in blastocysts ([Ikeda et al., 2012](#)). These inconsistent findings are likely to be due to different methodologies employed to measure 5mC methylation in embryos. A large number of studies have measured the intensity of fluorescence after labeling with anti-methylcytosine ([Dean et al., 2001](#); [Beaujean et al., 2004](#); [Park et al., 2007](#); [Bonilla et al., 2010](#); [Dobbs et al., 2013](#); [Acosta et al., 2016](#)). Whilst immunostaining techniques are descriptive and can provide information about overall methylation dynamics, they are only semi-quantitative and cannot provide sequence-specific information about differentially methylated regions (DMRs). Thus, determination of the effect of methionine supplementation on specific DNA methylation patterns in developmentally important genes is required in order to understand the functional ramifications for offspring health and physiology.

Based on the observation that altering methionine within physiological ranges during IVP affected the gross morphology of bovine blastocysts (Chapter 3), it was hypothesised that a subtle reduction in physiological methionine during IVP would cause epigenetic changes in preimplantation embryos with implications for altered gene expression. The present study, therefore, sought to compare the cytosine (CpG) methylation status in the ICM and TE of Day 8 bovine

embryos following culture in physiologically high (50 $\mu\text{mol/L}$) and low (10 $\mu\text{mol/L}$) concentrations of added methionine using reduced representation bisulphite sequencing (RRBS), a 'gold standard' method that provides genome-wide coverage of dense areas of CpGs methylation (e.g. CGIs) with single-base resolution (Chatterjee *et al.*, 2012; Guo *et al.*, 2015).

4.2 Materials and methods

4.2.1 *In vitro* embryo production

Full details of IVP procedures for bovine embryos were as described in Section 3.2.1.2 using custom-made media supplemented with high (50 $\mu\text{mol/L}$) and low (10 $\mu\text{mol/L}$) added methionine (Appendix 3.8). As DNA methylation can be influenced by stage of development, only Day 8 blastocysts that were \geq Stage 7 (i.e. late expanded, hatching or hatched) were selected for RRBS analysis from each treatment. DNA methylation can also be influenced by embryo sex. As reported in Chapter 3 (Section 3.3.2.4.3), a statistically similar proportion of male blastocysts developed in each physiological concentration (Figure 3.14A). As blastocysts produced for RRBS analysis were not sexed it was assumed that similar proportions of male and female blastocysts were used. It was also confirmed that stage of development on Day 8 was not influenced by embryo sex. Following culture in 50 $\mu\text{mol/L}$ of methionine, 90% of male and 83% of female blastocysts were \geq Stage 7. At 10 $\mu\text{mol/L}$, 67% of male and 67% of female blastocysts were \geq Stage 7.

4.2.2 Immunodissection of bovine blastocysts

Inner cell mass (ICM) and trophectoderm (TE) cells were isolated from Day 8 bovine blastocysts (Stage 7-9, Grade 1 and 2) by immunodissection based on the method of Bogliotti *et al.* (2018) with the following modifications. The zona pellucida was removed using Pronase (0.5% w/v) and embryos were washed twice in warm PVP/PBS (0.1% w/v) before incubation in SOF HEPES holding medium containing 50% anti-bovine serum (Jackson ImmunoResearch) at 38°C for 1 h. Following incubation, blastocysts were washed and incubated in SOF HEPES holding medium containing 50% guinea pig complement (Innovative Research) at 38°C for 3-5 min. Following an additional wash, the ICM was isolated from the TE using a small-bore glass pipette. Matched ICM and TE cell

samples were pooled by lineage ($n=5$; Table 4.1) and transferred to a PCR tube in 1 μL sterile PBS. Cell samples were kept on dry ice until storage at -80°C until DNA methylation analysis by reduced representation bisulphite sequencing (RRBS).

Table 4.1 Immunodissected inner cell mass (ICM) and trophectoderm (TE) cells isolated from Day 8 bovine blastocysts were pooled ($n=5$) by lineage for DNA methylation analysis.

Rep	Methionine ($\mu\text{mol/L}$)			
	50		10	
	ICM	TE	ICM	TE
1	5	5	5	5
2	5	5	5	5
3	5	5	5	5

Whole embryos ($n=5$) cultured in each physiological methionine concentration (50 and 10 $\mu\text{mol/L}$) immunodissected. Three experimental replicates. Matched ICM and TE samples were pooled. Total number of blastocysts ($n=30$).

4.2.3 Validation of cell lineage purity

To assess the purity of the immunodissected cell samples, the relative expression of trophectoderm-specific marker, *GATA3* (Ozawa *et al.*, 2012), was measured in pooled ICM and TE samples by qPCR. This validation experiment was conducted over 5 replicates (each replicate constituted pooled ICM ($n=15$) and pooled TE ($n=15$) samples). Whole blastocysts ($n=40$) were used for optimisation and validation of the qPCR method.

4.2.3.1 RNA extraction and cDNA synthesis

Poly A+ RNA was extracted from pooled whole blastocysts ($n=40$), pooled ICM ($n=15$) and pooled TE ($n=15$) using Dynabeads mRNA DIRECT kit (Invitrogen Ltd., Paisley, UK) and reverse transcription to cDNA was achieved using QuantiTect RT kit (Qiagen Ltd), as described previously (Section 3.2.1.3.2 and 3.2.1.4). Following DNase treatment using the kit, 1 μL was removed for -RT reaction and the equivalent volume of water was added before RT. Blastocyst, ICM and TE cDNA was diluted to a final concentration of 0.1 blastocyst/ μL , 0.25 ICM/ μL and 0.25 TE/ μL , respectively.

4.2.3.2 Primer design

Primers for *GATA3* and eight reference genes were designed using Primer Express software version 3.0.1 (Applied Biosystems) and were supplied by Eurofins Genomics (Ebersberg, Germany; Table 4.2). Primers were tested using bovine liver cDNA and PCR products were sequenced by Source Bioscience (Nottingham, UK). Calibration standard curves constituting a 5-fold dilution series of blastocyst cDNA were conducted to verify assay linearity and efficiency of amplification (Appendix 4.1). Data were normalised to the four most stable reference genes (*YWHAZ*, *TBP*, *H2AFZ*, *B2M*) using Reference Gene Selector tool in CFX Maestro™ Software based on GeNorm algorithm (Figure 4.1). Reference gene selection was confirmed using geNorm software based on geNorm M and V values (Appendix 4.2).

Table 4.2. Primers used for the detection of trophectoderm-specific marker, *GATA3*, and reference genes in bovine blastocysts and immunodissected embryonic cell samples.

Gene		Primer sequence (5'-3')	Product (bp)	NCBI accession no.
<i>GATA3</i>	FP	AACATCGACGGTCAAGGCAA	217	NM_001076804.1
	RP	GGTGGATGGACGTCTTGGAG		
<i>YWHAZ</i>	FP	GATATCTGCAATGATGTACTGTCTCTTTT	107	NM_174814.2
	RP	CGGTAGTAGTCTCCTTTTCATTTTCAA		
<i>TBP</i>	FP	GAATATAATCCCAAGCGTTTTGCT	103	NM_001075742.1
	RP	TGGCTCCTGTGCACACCAT		
<i>H2AFZ</i>	FP	GCAGGAAATGCATCGAAAGAC	126	NM_174809.2
	RP	AATGACACCACCACCAGCAATT		
<i>B2M</i>	FP	ATCCAGCGTCCTCCAAAGATTC	132	NM_173893
	RP	CTCCCCATTCTTCAGCAAATCG		

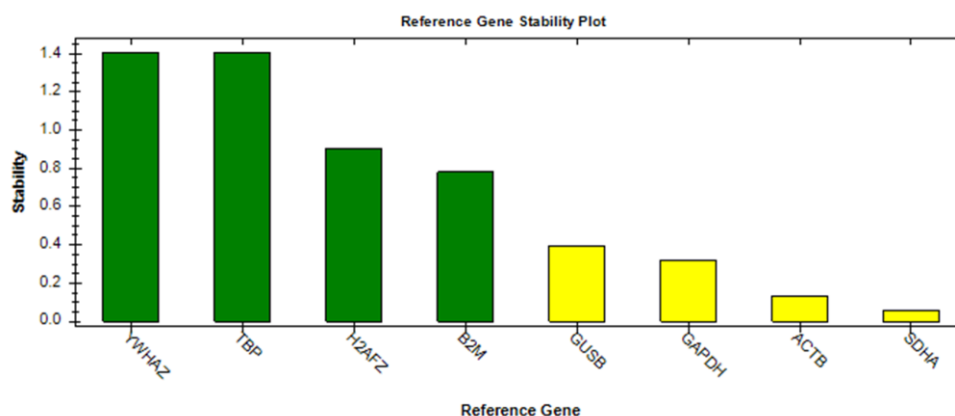


Figure 4.1 Reference gene stability plot using Reference Gene Selector Tool in CFX Maestro™ software.

Green: Reference genes are stable and represent minimal variation across samples tested. Any genes can be selected from this group for use as reference genes. **Yellow:** Reference genes are not ideally stable and represent moderate variation across samples tested. At least three of these reference genes can be used for study analysis.

4.2.3.3 Quantitative real-time PCR

The qPCR reaction contained 10 µL QuantiNova® SYBR® Green (Qiagen Ltd.), 1 µL each primer, 2 µL cDNA template and 6 µL RNase free water. A negative no template control sample was run for each tested primer set using water instead of cDNA template, and minus reverse transcription (–RT) controls were tested to confirm the absence of gDNA. Each 20 µL sample was analysed in duplicate using low profile, non-skirted, clear 96-well plates in the Bio-Rad thermal cycler CFX96 Real-Time System (Bio-Rad, Hercules, CA, USA). The amplification programme included enzyme activation at 95°C for 2 min, followed by 40 cycles of 2-step cycling: 95°C for 5 s (denaturation) and 60°C for 10 s (annealing and extension).

4.2.4 DNA methylation analysis

4.2.4.1 Reagents

Unless otherwise stated, the following reagents were purchased from Sigma-Aldrich. *Lysis buffer*: Tris-HCl (1 M), EDTA (50 mmol/L), Triton X-100, KCl (1M), Nuclease-free PCR water, and Protease (20 mg/mL; Qiagen). *Msp1 digest master mix*, *End-repair/dA tailing master mix* and *adapter ligation mix*: Msp1

restriction endonuclease (Thermo Fisher Scientific), Tango buffer (Thermo Fisher Scientific), unmethylated λ -DNA (Promega), Klenow fragment, exo- (NEB), dNTP set (NEB), Blunt-end/TA DNA ligase master mix (NEB), Methylated adaptors NEBNext® oligo for Illumina methylated adaptor index primer set 1 (NEB) and USER™ enzyme (NEB). *tRNA stock*: yeast tRNA, Binding buffer. *Purification*: Zymo DNA clean and concentrator kit (Zymo), Buffer EB (10 mmol/L Tris; Qiagen). *Bisulphite conversion*: EZ DNA Methylation-Gold™ kit (Cambridge Biosciences). *PCR Library Preparation*: KAPA KiFi HS Uracil+ master mix (Roche), absolute ethanol (Thermo Fisher Scientific), MinElute PCR kit (Qiagen), MinElute gel extraction kit (Qiagen), 50 bp marker (Thermo Fisher Scientific), 100 bp marker (Promega) and Qubit HS dsDNA high-sensitivity assay kit (Thermo Fisher Scientific).

4.2.4.2 Reduced Representation Bisulphite Sequencing (RRBS)

Library preparation for RRBS described by [Guo *et al.* \(2015\)](#) was optimised in our laboratory by Dr. WY Kwong. Stock and working solutions were prepared as described in Appendix 4.3. To improve the suitability of RRBS for a low number of embryonic cells and to minimise the loss of DNA, the following experimental steps were integrated into a single-tube reaction using 1.5 mL LoBind Eppendorf tubes:

4.2.4.2.1 gDNA purification

Pooled ICM and separately pooled TE cell samples were thawed and briefly centrifuged. Four μ L lysis buffer containing protease was added to cell samples to release gDNA. Tube contents were mixed and centrifuged before incubation at 50°C for 3 h and then 75°C for 30 min to inactivate the protease enzyme.

4.2.4.2.2 Restriction enzyme (Msp1) digestion

Each sample was centrifuged once again before the addition of 13 μ L Msp1 digestion mixture containing restriction endonuclease enzyme. Unmethylated λ -DNA (8 pg/ μ L) was spiked into all samples before Msp1 digestion to monitor the rate of bisulphite conversion. The digestion mixture was incubated at 37°C for 3 h and then 80°C for 20 min to inactivate Msp1 before another brief centrifugation and storage on ice.

4.2.4.2.3 End-repair and dA tailing

Two μL end-repair/dA tailing master mix containing Klenow fragment, end-repair dNTP mix and Tango buffer (1X) was added to the Msp1 digestion mixture and incubated at 37°C for 40 min. This was followed by an incubation at 75°C for 15 min to inactivate DNA Polymerase 1, Klenow fragment. Tubes were briefly centrifuged and kept on ice.

4.2.4.2.4 Adapter ligation

Samples were incubated at 20°C for 20 min with 5 μL adapter ligation mix containing 20-fold diluted methylated adapter. Next, 3 μL USERTM (Uracil-Specific Excision Reagent enzyme) was added to each sample. The contents were mixed and centrifuged before incubation at 37°C for 15 min. Samples were centrifuged again and kept on ice. Binding buffer containing 10 ng/ μL tRNA was added to DNA samples and purification was achieved using Zymo DNA clean and concentrator kit. Samples were eluted in 10 μL EB buffer in a 0.2 mL PCR tube and stored at -80°C until bisulphite conversion.

4.2.4.2.5 Bisulphite conversion

Bisulphite conversion of DNA was achieved using the EZ DNA-Methylation GoldTM kit according to the manufacturer's protocol. First, 10 μL water was added to the DNA sample (to achieve a final volume of 20 μL), followed by 130 μL CT Conversion Reagent. The DNA sample contents were mixed and centrifuged prior to bisulphite conversion. The double-stranded DNA was denatured during incubation at 98°C for 10 min, then at 64°C for 2.5 h to ensure full bisulphite conversion, with a final hold at 4°C . All steps were performed in a PCR thermocycler.

Bisulphite converted DNA was subjected to on-column desulphonation and purification using Zymo-SpinTM column technology using 10 ng tRNA as a protective carrier. Briefly, M-Binding Buffer (600 μL) plus the converted DNA sample were loaded into a Zymo-SpinTM IC column placed inside a collection tube. The contents were mixed by gentle inversion before centrifugation for 30 s at maximum speed. The flow-through was discarded. Next, 100 μL M-Wash Buffer was added to the column and the contents were centrifuged for 30 s at maximum speed. M-Desulphonation Buffer (200 μL) was added to the column

and left to incubate at room temperature for 15-20 min. Following incubation, the contents were centrifuged for 30 s, 200 μ L M-Wash Buffer was added to the column and the contents were centrifuged once more. This wash step was repeated. The column was placed in a 1.5 mL microcentrifuge tube and 10 μ L EB buffer was added directly to the column matrix before centrifugation for 30 s to elute the DNA. Bisulphite treated DNA samples were stored at -80°C until use.

i) RRBS Library Preparation

The purified DNA was subjected to amplification by PCR using the RRBS Library Preparation master mix containing KAPA HiFi uracil+ DNA polymerase. The amplification conditions were as follows: 95°C for 45 s, followed by 16 cycles of 15 s at 95°C , 60°C for 30 s, and 72°C for 1 min. PCR products were purified using the MiniElute PCR kit (Qiagen) and DNA was eluted in 12 μ L EB buffer. The speed-vac was used for 5 min to remove residual ethanol and 10 μ L water was added to each DNA sample.

4.2.4.3 Library quality control (QC)

Following PCR enrichment, 1 μ L purified PCR product was quantified using the Qubit HS dsDNA kit and stored at -80°C . The remaining sample volume was sent to Edinburgh genomics (University of Edinburgh, UK) for quality control, pooling and next-generation sequencing. DNA concentration, quality and integrity were confirmed using the Agilent TapeStation. Libraries were pooled and amplified DNA fragments of 200-600 bp were size-selected and primer adapters removed using the BluePippin system.

4.2.4.3.1 Multiplex sequencing

The final 12 quality-ensured libraries were multiplexed and sequenced on one lane of an Illumina NovaSeq™6000 (S1 flow cell) to achieve an average of ~78 million 150 bp paired-end reads. Data were de-multiplexed with bcl2fastq conversion software and quality control was conducted using Sequencing Analysis Viewer (SAV) and FASTQC (Babraham Bioinformatics) software. Sequences met the standard Illumina quality criteria of cluster density, pass filter and quality scores (Q) and were converted to FASTQ files using standard Illumina pipeline (Aspera software).

4.2.4.4 Bioinformatic Data Analysis

Raw paired-end FASTQ files were trimmed to remove adapter sequences and low quality bases using skewer with commands (-Q 20, -q 3) (<https://sourceforge.net/projects/skewer>; Table 4.3). Clean reads were aligned to the *Bos taurus* reference genome (Bta.ARS-UCD1.2, April 2018) using bisulphite read mapper with default settings (Bowtie2; Krueger and Andrews, 2011). Duplicate reads were marked using MarkDuplicates (Picard tools) and methylation values extracted using bismark_methylation_extractor module (commands --no_overlap --paired-end). Methylation values were extracted from output Sequence Alignment Map (SAM) files using methylKit v1.4.0 (nolap=TRUE, mincov=5, minqual=20; Akalin *et al.*, 2012). To avoid identification of methylation differences that are related to underlying breed differences, bases at known variant positions (SNPs) were removed.

Table 4.3 Summary of Bismark final alignment report.

Cell lineage	ICM		TE	
Methionine (µmol/L)	50	10	50	10
Replicate	64,582,554 ^a	70,125,142 ^a	83,302,871 ^a	102,310,417 ^a
1	18,826,935 ^b (29.2) ^c	20,930,071 ^b (29.8) ^c	23,538,817 ^b (28.3) ^c	31,671,654 ^b (31.0) ^c
2	63,884,223 ^a 18,968,032 ^b (29.7) ^c	82,902,050 ^a 25,559,151 ^b (30.8) ^c	77,140,135 ^a 21,008,778 ^b (27.2) ^c	83,057,058 ^a 24,657,595 ^b (29.7) ^c
3	89,320,723 ^a 26,120,363 ^b (29.2) ^c	78,350,625 ^a 22,750,802 ^b (29.0) ^c	59,062,149 ^a 17,074,286 ^b (28.9) ^c	81,772,406 ^a 23,879,134 ^b (29.2) ^c

Total sequence pairs read following quality trimming^a. Number of paired alignments with unique best hit^b. Mapping efficiency (%): measure of the sequence pairs that map uniquely to the reference genome^c.

Differentially methylated sites (DMS) between groups were identified using the Chi-squared test in methylKit and annotated using the genomation package (Akalin *et al.*, 2012; Akalin *et al.*, 2015). Due to the inherent level of variability of microarray-based hybridisation techniques that are associated with sample preparation, loading, microarray probes and detection, it is common to introduce a minimum difference threshold to select out DMS with minimal methylation difference between two biological conditions (Du *et al.*, 2010). Therefore, DMS results were filtered for 'in gene/promoter' to remove intergenic regions, and for a 'minimum difference threshold of 20% methylation' between experimental combinations.

4.2.4.4.1 Gene set enrichment analysis (GSEA)

Enrichment of gene ontologies (GO) and pathways using KEGG (Kyoto Encyclopedia of Genes and Genomes) was performed using hypergeometric tests in the (Not) Ingenuity Pathway Analysis (NIPA) tool (<https://github.com/ADAC-UoN/NIPA>). To narrow the number of genes, a sliding window approach was used to identify DMS within candidate genes identified within experimental combinations highlighted in Figure 4.2.

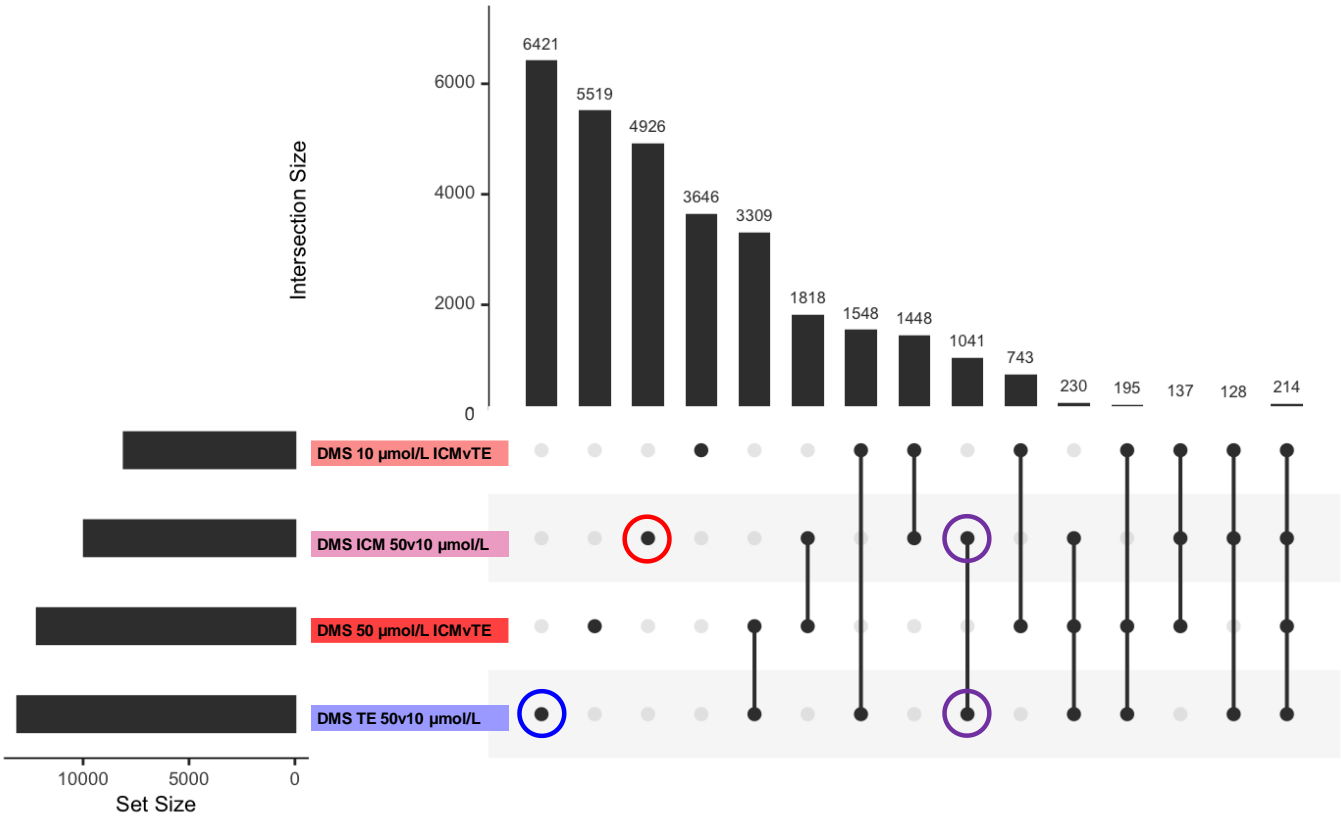


Figure 4.2 UpSet R plot demonstrates intersection size between the numbers of differentially methylated sites (DMS) across experimental combinations.

Blue circle: DMS affected by methionine concentration in trophoctoderm (TE) only ($n=6,421$). Red circle: DMS affected by methionine concentration in inner cell mass (ICM) only ($n=4,926$). Purple circle(s): DMS affected by methionine concentration in both embryonic cell lineages ($n=1,041$).

Based on the premise that regulatory regions of the genome that are important for gene transcription contain clusters of CpGs (Li and Zhang, 2014), genes that possessed ≥ 5 DMS within a sliding window size of 1 kb were selected for gene set enrichment analysis (GSEA). A total of 401 clusters of DMS in 179 genes were identified in the ICM, and 614 clusters of DMS in 267 genes within the TE (Appendix 4.4). Annotated pathways associated with GO terms, such as 'Biological Process', 'Cellular Component' and 'Molecular Function', and pathways within the KEGG database were identified as significant based on functional enrichment of genes with differentially methylated clusters of CpGs (differentially methylated sites; DMS). The Benjamini Hochberg procedure (Benjamini and Hochberg, 1995) was applied to account for multiple testing. Functional categories with FDR ≤ 0.05 were considered significant (Appendix 4.5).

4.2.5 *IGF2R* and *AIRN* transcript expression

Bioinformatic data analysis included the identification of DMS within imprinted genes documented within the Catalogue of Imprinted Genes (University of Otago, NZ; <http://igc.otago.ac.nz/home.html>). A differentially methylated imprinted gene of relevance to the present study was *insulin like growth factor 2 receptor*, *IGF2R* (discussed later; Section 4.3.2.6). Transcript expression analysis was undertaken over four experimental replicates to measure expression levels of *IGF2R* gene and its antisense lncRNA transcript, *AIRN*, in pooled bovine Day 8 blastocysts ($n=15$ minimum per replicate) that were cultured in physiologically high (50 $\mu\text{mol/L}$ added) and low (10 $\mu\text{mol/L}$ added) methionine concentrations.

4.2.5.1 RNA extraction and cDNA synthesis

RNA extraction and reverse transcription and quantitative real-time PCR was performed using the protocol described previously (Sections 3.2.1.3.2 and 3.2.1.4). Blastocyst cDNA was diluted to a final concentration of 0.75 blastocyst/ μL .

4.2.5.2 Quantitative real-time PCR

Primers for *IGF2R* and *AIRN* transcripts were designed using NCBI blast software and were supplied by Eurofins Genomics (Ebersberg, Germany; Table

4.4). Primers were tested using liver cDNA and DNA extracted from bovine ovaries (Appendix 4.6). PCR products were sequenced by Source Bioscience (Appendix 4.7). Calibration standard curves constituting a 5-fold dilution series of liver cDNA (Appendix 4.8) and a 3-fold dilution series of blastocyst cDNA (Appendix 4.9) were conducted to verify assay linearity and efficiency of amplification. Quantitative real-time PCR was conducted as described above (Section 4.2.3.3) and data were normalised to *TBP* and *B2M* reference genes using Reference Gene Selector tool in CFX Maestro™ Software based on GeNorm algorithm (Section 4.2.3.2).

Table 4.4 Primers used for the detection of *IGF2R* and *AIRN* in bovine blastocysts and immunodissected embryonic cell samples.

Gene		Primer sequence (5'-3')	Product (bp)	NCBI accession no.
<i>IGF2R</i>	FP	GCAGCCTGTATACCCATCCC	152	NM_174352.2
	RP	ATCAAACACGTACCCGCTGT		
<i>AIRN</i>	FP	GTGATCAACCTGGATTGCTGC	185	NR_104052.1
	RP	AAGCCTGGGATTCTGACTGG		

4.2.6 Statistical data analysis

Statistical analyses of gene transcript expression were conducted using ANOVA within the Genstat statistical package (20th Edition, VSN International, 2011). Transcript expression data are reported as means with SEM and presented as histograms using GraphPad Prism 8 software. Differentially methylated sites (DMS) between treatments and sliding windows were identified using the Chi-squared test. Gene ontology terms and pathways with an FDR adjusted *P*-value ≤ 0.05 were deemed statistically significant. Mean methylation (%) of genes was determined using linear mixed model (residual maximum likelihood; REML) analysis within Genstat. The fixed model included the terms 'Replicate', 'Lineage' and 'Methionine' (Rep+Lineage*Met) for comparisons of differential methylation between embryonic cell lineages at two physiological methionine concentrations. The random model included individual DMS. These data are presented as means with SEM.

4.3 Results and Discussion

4.3.1 Validation of cell lineage purity

The immunodissection technique offers the advantage of recovering ICM cells from blastocysts without mechanical damage. However, due to the nature of the technique there is a risk of TE contamination in ICM samples (Handyside and Barton, 1977). To validate cell lineage purity in ICM cell samples used for RRBS analysis, pooled ICM were examined for TE contamination by measuring the relative expression of TE-specific marker, *GATA binding protein 3* (*GATA3*), in immunodissected ICM and TE cell samples.

In the bovine embryo, lineage commitment towards TE cell fate is under the control of transcription factors; YAP1, TEAD4, CDX2 and *GATA3* (Ozawa *et al.*, 2012; Negrón-Pérez *et al.*, 2017). As a TE regulator that functions downstream of TEAD4 and in parallel with CDX2 (Wu *et al.*, 2016), *GATA3* is reported to be expressed to a greater extent (2.69-fold) in the bovine TE than in the ICM and, therefore, can be considered a reliable marker of TE lineage (Ozawa *et al.*, 2012). In the present study, qPCR results showed a 5.27-fold difference in *GATA3* expression between ICM and TE cell lineages, with relative expression values of 0.18 ± 0.015 and 0.95 ± 0.160 for ICM and TE, respectively ($P=0.004$; Figure 4.3B).

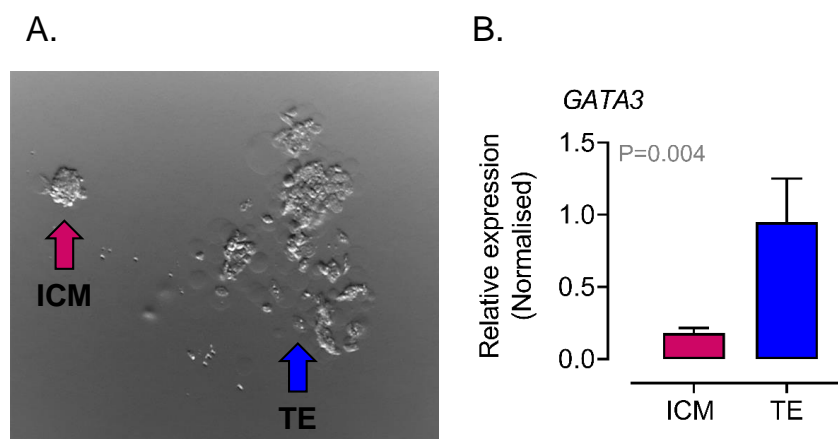


Figure 4.3 Enrichment of bovine embryonic cell populations following immunodissection.

Microscopy image of immunodissected inner cell mass (ICM) and trophectoderm (TE) cells from Day 8 blastocyst (A). Relative expression of TE marker, *GATA3*, in immunodissected ICM and TE ($n=15$ cell samples pooled over four experimental replicates; $P=0.004$). Relative expression data analysed by ANOVA and presented as mean \pm SEM (B).

A similar pattern of enrichment was observed following immunosurgery in murine blastocysts. Quantitative RT-PCR analysis showed that the ICM expressed significantly less *Gata3* mRNA levels relative to the whole blastocyst (Home *et al.*, 2009). Taken together, these findings confirm that *Gata3/GATA3* expression is selectively upregulated within the TE but not the ICM lineage in bovine and murine blastocysts.

Whilst the expression of *GATA3* was significantly higher for TE than ICM, there are explanations for a reduced enrichment of the primary embryonic cell populations following immunodissection: (i) *GATA3* is expressed at the morula stage of embryo development, thus, there may be residual transcript expression within the ICM on Day 8 (Home *et al.*, 2009); (ii) the small amount of *GATA3* transcript detected in the bovine ICM could be due to polar TE cells adhering to the ICM; and, (iii) the immunodissection technique involves complement-mediated lysis of antibody-coated TE cells, therefore, TE cells are lysed whilst ICM cells remain intact (Kurome *et al.*, 2018; Figure 4.3A). Lysed TE cells can be difficult to recover and the cytotoxic effect of immunodissection on TE cells could lead to mRNA degradation. However, because DNA is more stable than RNA (Wang and Kool, 1995), and because DNA methylation is stable at room temperature (Vilahur *et al.*, 2013), it was hypothesised that the recovery of DNA for methylation analysis was unaffected by the immunodissection technique.

4.3.2 DNA methylation analyses by RRBS

4.3.2.1 Mean methylation (%)

Reduced representation bisulphite sequencing (RRBS) analyses demonstrated a significant effect of methionine concentration, within physiological limits (50 v 10 $\mu\text{mol/L}$ added methionine), on the abundance of CpG methylation within the bovine ICM and TE ($P < 0.001$). However, there was no significant difference in CpG methylation between the two embryonic lineages ($P = 0.836$; Figure 4.4A). Cytosine methylation can also occur at CHG and CHH sites throughout the genome, where 'H' represents a cytosine (C), thymine (T) or adenine (A) nucleotide (de Montera *et al.*, 2013). As discussed earlier (Section 1.5.1.2), non-CpG methylation has been detected in mammalian oocytes (Guo *et al.*, 2014b; Tomizawa *et al.*, 2011), human embryonic stem cells (Lister *et al.*, 2009), and early bovine embryos, and follows a similar enrichment pattern to CpG methylation located within CGIs and gene bodies (Jiang *et al.*, 2018). The

present study detected a relatively low abundance of non-CpG methylation in bovine embryonic cells compared to that of CpG methylation. CHG and CHH methylation was 8-fold and 42-fold lower, respectively (Figure 4.4B, Figure 4.4C).

The abundance of non-CpG methylation was unaffected by methionine concentration and did not differ between the two primary cell lineages (Figure 4.4). As the primary site of DNA methylation that accounts for up to 80% of the total DNA methylation content in mammalian cells ([Lim and Maher, 2010](#); [Ziller *et al.*, 2011](#)), cytosine methylation in the CpG dinucleotide context is considered the most relevant methylation mark and is the focus of the forthcoming discussion.

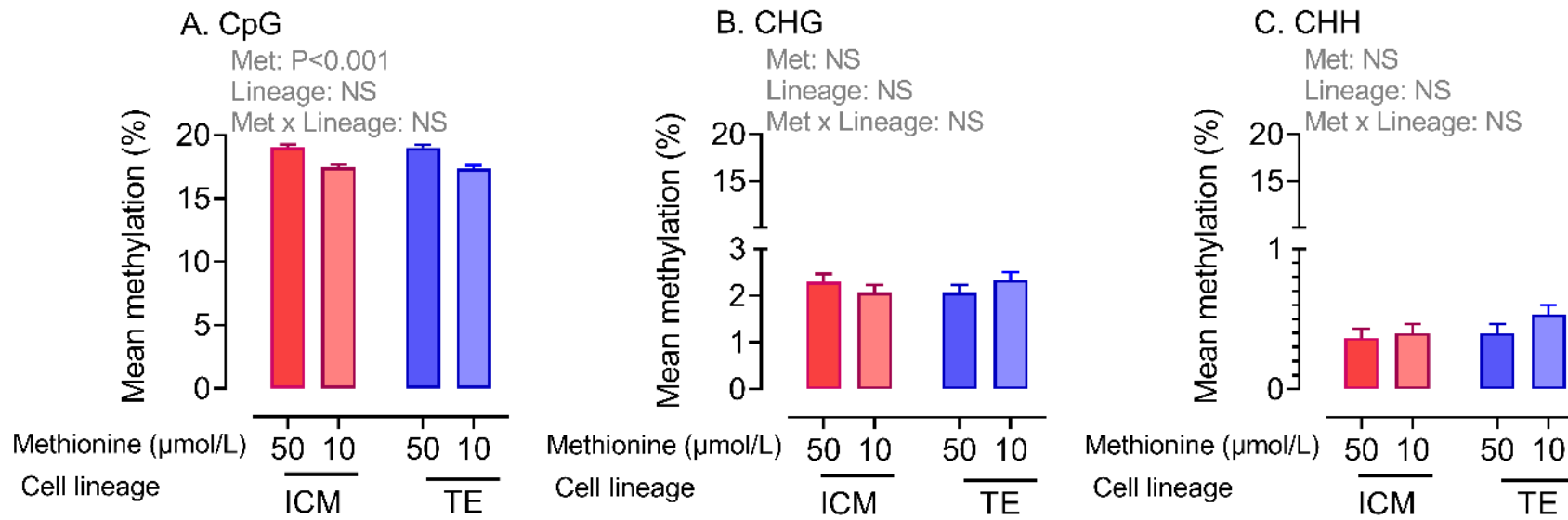


Figure 4.4 Low methionine significantly reduced mean cytosine methylation (%) in inner cell mass (ICM) and trophectoderm (TE).

Mean methylation (%) in CpG ($P < 0.001$) (A) CHG ($P = 0.924$) (B) and CHH ($P = 0.253$) context (C). CHG and CHH are cytosine methylation sites where 'H' represents a cytosine (C), thymine (T) or adenine (A) nucleotide. Data presented as mean \pm SEM.

4.3.2.2 Directional methylation

Table 4.5 shows the number of sites (CpGs), transcripts and genes that were differentially methylated between the ICM and TE following embryo culture in each physiological methionine concentration (50 v 10 $\mu\text{mol/L}$), and those that were differentially methylated within each cell lineage (ICM v TE) when the methionine concentration was altered within physiological ranges. There was a greater number of differentially methylated sites (DMS) between the ICM and TE following culture in the high methionine concentration than in the low concentration (12,213 v 8,088 for 50 $\mu\text{mol/L}$ and 10 $\mu\text{mol/L}$, respectively). It follows that the number of differentially methylated transcripts and genes was also increased in the high methionine concentration (Table 4.5). Considering the role of methionine as the direct precursor to the methyl donor, SAM, it was not surprising that culturing embryos at the higher methionine concentration yielded a greater percentage of DMS with increased methylation (54.6% hypermethylated v 45.4% hypomethylated); while culturing under low concentrations yielded a greater percentage of DMS that had decreased methylation (41.6% hypermethylated v 58.4% hypomethylated).

Table 4.5 A count of differentially methylated sites (DMS), genes and transcripts, and directional methylation for each experimental combination (%).

Variable	Methionine ($\mu\text{mol/L}$)		Cell lineage	
	50	10	ICM	TE
	ICMvTE	ICMvTE	50v10	50v10
DMS count	12,213	8,088	9,991	13,123
↑ Methylation	6,671 (54.6)	3,365 (41.6)	2,449 (24.5)	2,361 (18.0)
↓ Methylation	5,542 (45.4)	4,723 (58.4)	7,542 (75.5)	10,762 (82.0)
Transcripts	1,773	1,427	1,576	1,743
Genes	1,768	1,425	1,573	1,738

Arrows represent direction of methylation; hypermethylation (↑) and hypomethylation (↓). Abbreviation(s): Differentially methylated site, DMS; inner cell mass, ICM; trophectoderm, TE.

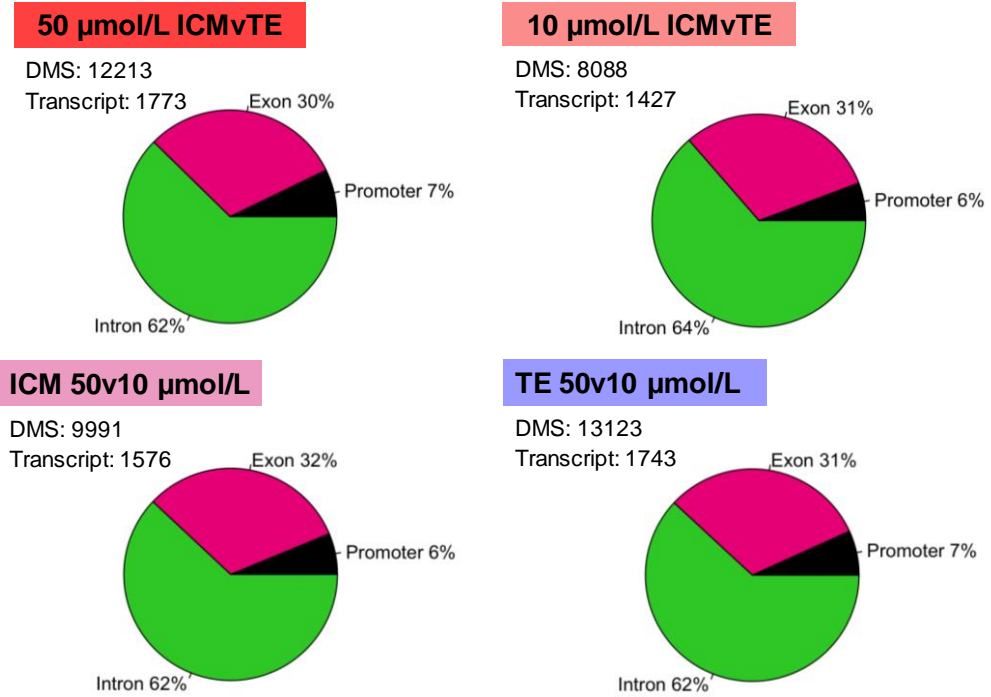
A greater number of DMS, transcripts and genes were identified in the TE than within the ICM lineage when methionine was reduced from 50 to 10 $\mu\text{mol/L}$ (Table 4.5). This epigenetic asymmetry may be explained by the cell lineage-specific DNA methylation profile that is established within the Day 8 bovine blastocyst. During the wave of *de novo* methylation that coincides with the first

cell lineage specification event (Figure 3.1), TE-specific methylation takes place within the bovine preimplantation embryo culminating in a higher degree of methylation within this extraembryonic cell lineage (Hou *et al.*, 2007; Nakanishi *et al.*, 2012; Dobbs *et al.*, 2013). More than 75% of DMS were hypomethylated in both cell lineages following culture in low methionine (Table 4.5). In support of gross phenotypic observations reported in Chapter 3, the molecular results presented herein demonstrate that subtle alterations to physiological methionine concentration during bovine IVP can epigenetically modify DNA methylation in both primary cell lineages of the Day 8 blastocyst.

4.3.2.3 Distribution of DMS

The distribution of DMS across genomic regions (promoter, exon, intron, CGI and shore) was similar for each experimental combination analysed. Of the DMS identified, 6-7% were located in gene promoters, 30-32% were located in exons and 62-64% were located in introns (Figure 4.5A). Approximately 54% of DMS were located in CGIs and ~46% were located in CGI shores (Figure 4.5B). Other studies report a similar distribution pattern of CpG methylation within genomic regions in mammalian cells. For example, Wang and Karmideen (2019) used RRBS to map the methylome within porcine testis and found that the lowest percentage of methylated CpGs were located in gene promoters (0.33%), followed by exons (1.71%), introns (5.95%) and intergenic regions (92.01%). The authors also measured more methylated CpGs in CGIs (36.86%) than in CGI shores (21.65%). This common distribution pattern is a consequence of basic gene anatomy and the restriction enzyme-based RRBS method. The utility of the Msp1-based approach is limited to a specific subset of CpG sites in the genome that are predominantly found in promoters and CGIs. These regions are, therefore, selectively enriched whilst others (i.e. CGI shores) are under-represented (Smith *et al.*, 2009; Doherty and Couldrey, 2014). Nevertheless, the RRBS method provides sufficient information to map the global effect of methionine during culture on CpG methylation within the primary cell lineages of the bovine preimplantation embryo.

A.



B.

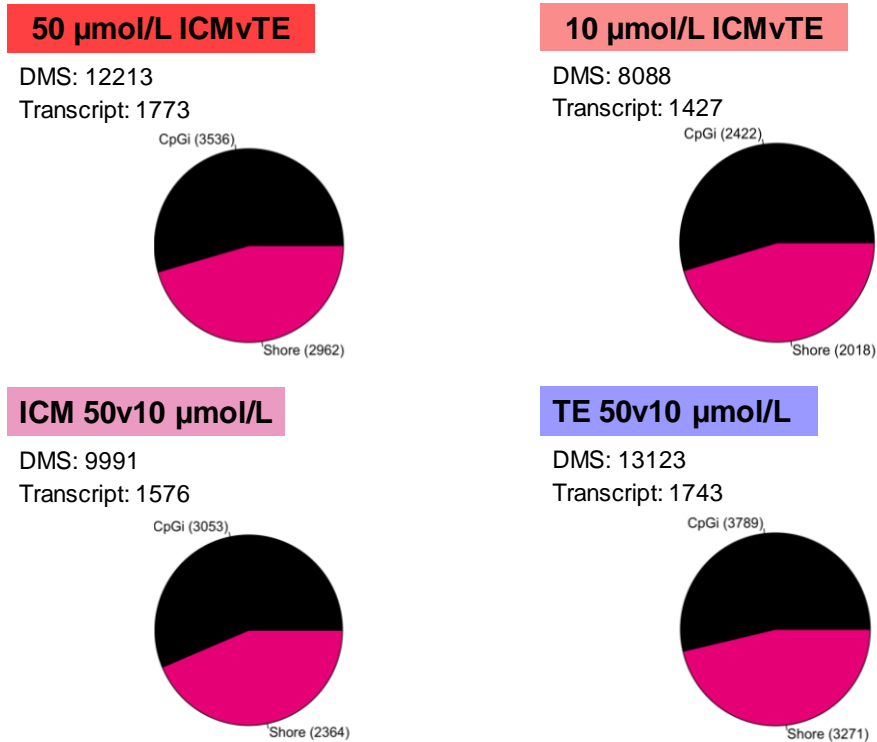


Figure 4.5 Distribution of differentially methylated sites (DMS) across genomic regions for each experimental combination.

Promoter, Intron, Exon (A). CpG island (CGI) and CpG island shore (B). Abbreviation(s): Differently methylated site, DMS; inner cell mass, ICM; trophectoderm, TE.

Culturing bovine embryos under low physiological concentrations of methionine caused hypomethylation of CpGs within all genomic regions (Table 4.6). The effect of CpG methylation on gene expression depends on the genomic context in which it occurs (Song *et al.*, 2005; Jones, 2012). In the traditional view, gene promoter methylation has been associated with transcriptional silencing (Niesen *et al.*, 2005). In recent years, other genomic regions have been recognised to play critical roles in the regulation of gene transcription. For instance, intragenic methylation can mark intron-exon boundaries, thereby influencing the regulation of alternative transcription start sites, exon usage and splicing (Yegnasubramanian *et al.*, 2011; Messerschmidt *et al.*, 2014). Differentially methylated regions (DMRs) are distributed in various functional gene elements, including CGIs, repetitive sequences, non-coding RNAs, exons and introns. Indeed, 50% of intronic DMRs appear to affect transcription elongation. As introns are regions rich in enhancers, intronic methylation can impact transcription factor binding and gene expression (Brenet *et al.*, 2011; Zhao *et al.*, 2015; Luo *et al.*, 2018; Anastasiadi *et al.*, 2018). It is, therefore, important to investigate the effect of methionine on CpG methylation within various functional regions, such as DMRs within genes of interest (discussed later; Section 4.3.2.6).

Table 4.6 Distribution and direction of differentially methylated sites (DMS) for each experimental combination (%)

Region	Methionine ($\mu\text{mol/L}$)		Cell lineage	
	50	10	ICM	TE
	ICMvTE	ICMvTE	50v10	50v10
Promoter	931	488	656	950
↑ Methylation	557 (59.8)	198 (40.6)	190 (29.0)	163 (17.2)
↓ Methylation	374 (40.2)	290 (59.4)	466 (71.0)	787 (82.8)
Exonic	3,951	2,592	3,322	4,372
↑ Methylation	2,177 (55.1)	1,120 (43.2)	703 (21.2)	723 (16.5)
↓ Methylation	1,774 (44.9)	1,472 (56.8)	2,619 (78.8)	3,649 (83.5)
Intronic	8,082	5,391	6,495	8,655
↑ Methylation	4,421 (54.7)	2,227 (41.3)	1,660 (25.6)	1,592 (18.4)
↓ Methylation	3,661 (45.3)	3,164 (58.7)	4,835 (74.4)	7,063 (81.6)
CGIs	3,536	2,422	3,053	1,709
↑ Methylation	1,719 (48.6)	907 (37.4)	697 (22.8)	354 (20.7)
↓ Methylation	1,817 (51.4)	1,515 (62.6)	2,356 (77.2)	1,355 (79.3)
CGI shores	2,962	2,018	2,364	2,394
↑ Methylation	1,732 (58.5)	906 (44.9)	562 (23.8)	421 (17.6)
↓ Methylation	1,230 (41.5)	1,112 (55.1)	1,802 (76.2)	1,973 (82.4)

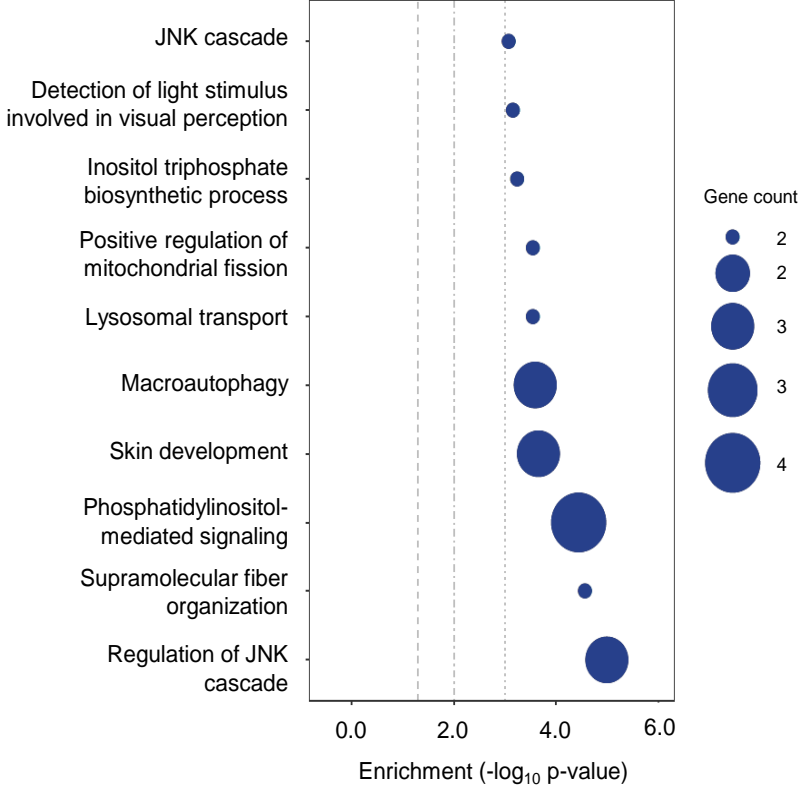
Arrows represent direction of methylation; hypermethylation (↑) and hypomethylation (↓). Abbreviation(s): CGI, CpG island; ICM, inner cell mass; TE, trophectoderm.

4.3.2.4 Enriched pathways and genes

Gene set enrichment analysis (GSEA) revealed Gene Ontology (GO) terms and KEGG pathways that were significantly enriched (FDR <0.05) with differentially methylated genes between the two physiological methionine concentrations (50 v 10 $\mu\text{mol/L}$) during bovine embryo culture. Genes harbouring clusters of ≥ 5 DMS (within 1 kb) were analysed (ICM = 179 genes, TE = 267 genes; Appendix 4.4). A total of 121 GO terms and 30 KEGG pathways containing genes with DMS clusters were significantly enriched in the ICM, and a total of 144 GO terms and 96 KEGG pathways containing DMS clusters were significantly enriched in the TE (Appendix 4.5). Due to the greater number of DMS, transcripts and genes identified in the TE cell lineage than in the ICM (Table 4.5), it is not surprising that a greater number of enriched terms and pathways were identified within the TE. The top 10 most statistically significant terms and pathways enriched within the ICM and TE are presented in Figure 4.6 to 4.9.

The most significant terms/pathways enriched within the ICM (FDR=0.0002) were 'Regulation of JNK cascade', 'MAP-kinase scaffold activity' and 'Phosphatidylinositol signalling system' (Figure 4.6, Figure 4.7). Collectively, these pathways are involved in cellular processes during embryo development, including cell growth, migration, invasion and apoptosis (Zhao *et al.*, 2016; Zeke *et al.*, 2016). In the TE, the most significant terms/pathways (FDR=0.0001) were associated with cellular transport, including 'Calcium ion transmembrane transport into cytosol', 'Secretory granule membrane' and 'Glutamate-gated calcium ion channel activity' (Figure 4.8, Figure 4.9).

A. Biological Process GO (ICM)



B. Cellular Component GO (ICM)

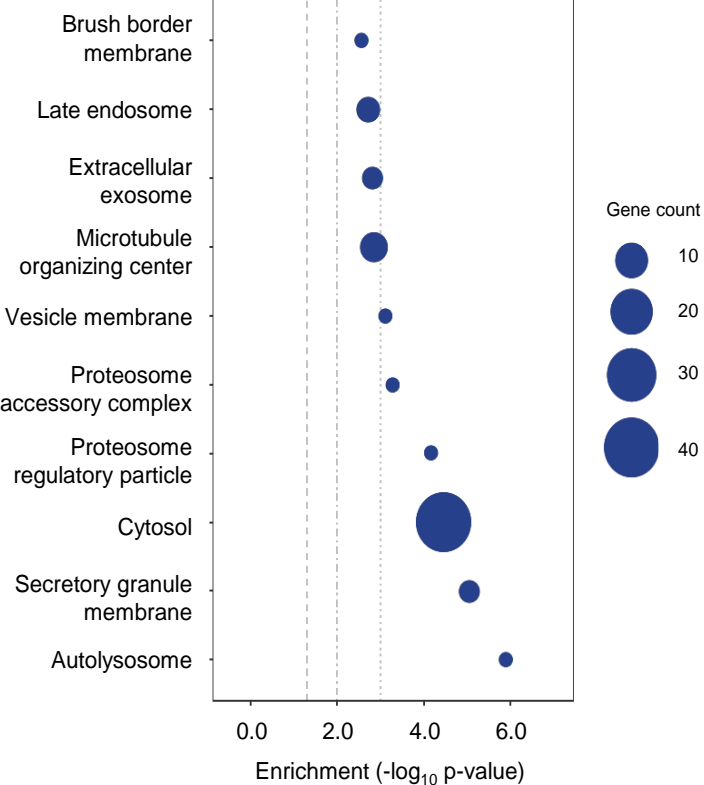
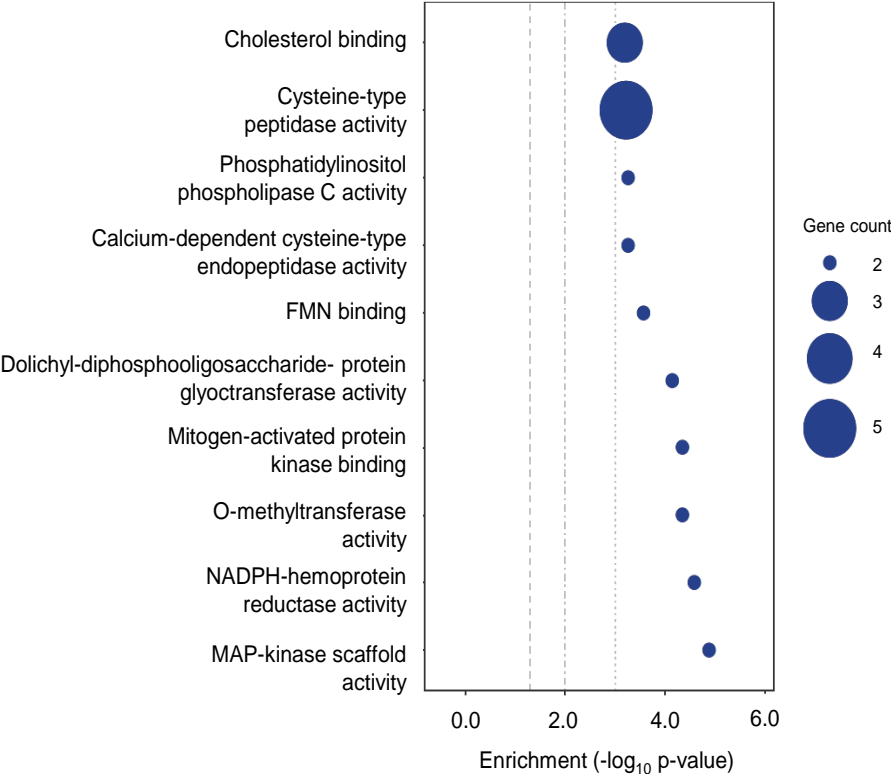


Figure 4.6 Top 10 significantly enriched Biological Process (A) and Cellular Component (B) Gene Ontology (GO) terms in the bovine inner cell mass (ICM) when methionine concentration is reduced within physiological range during IVP.

A. Molecular Function GO (ICM)



B. KEGG Pathways (ICM)

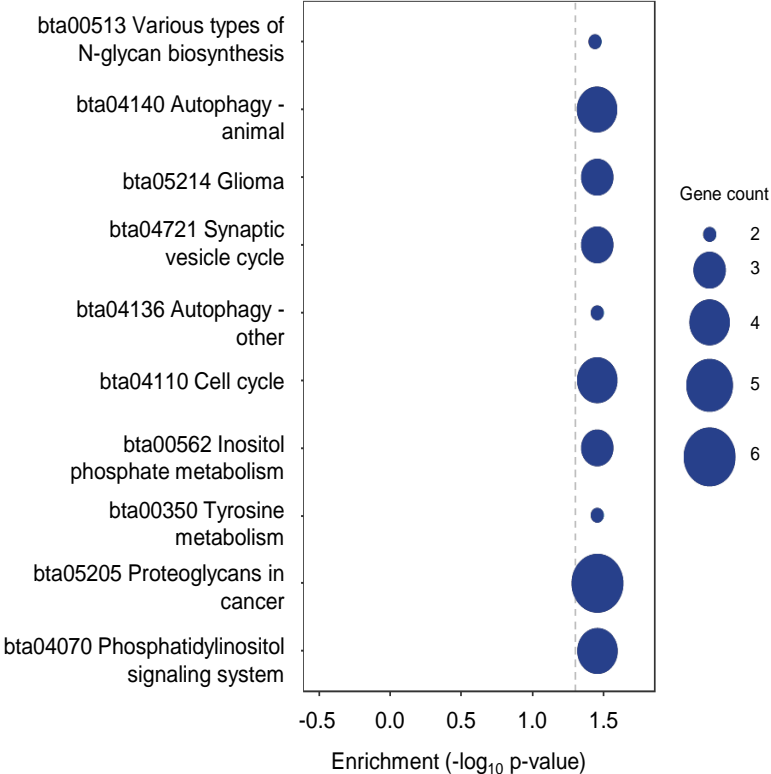
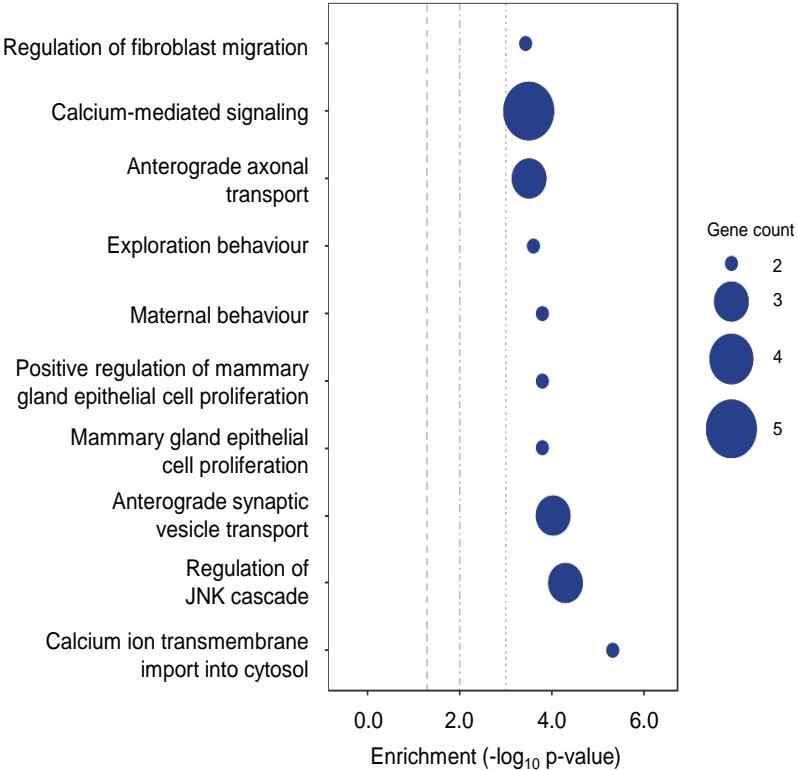


Figure 4.7 Top 10 significantly enriched Molecular Function Gene Ontology (GO) terms (A) and KEGG Pathways (B) in the bovine inner cell mass (ICM) when methionine concentration is reduced within physiological range during IVP.

A. Biological Process GO (TE)



B. Cellular Component GO (TE)

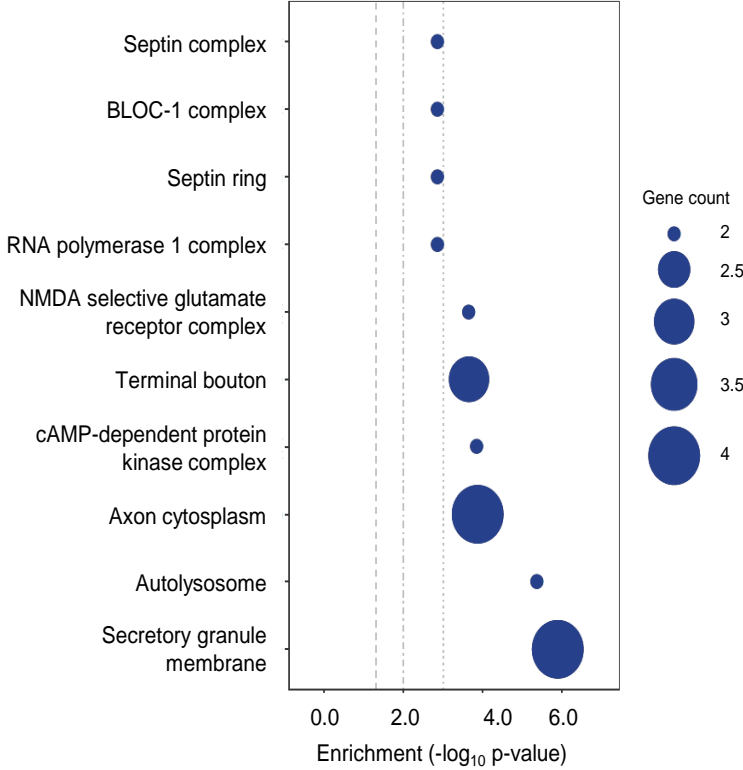
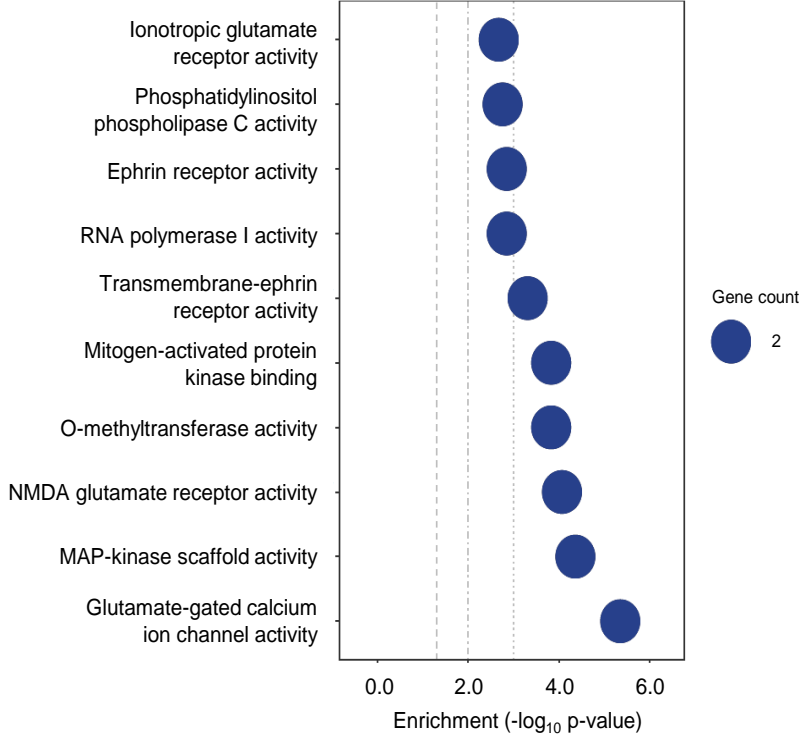


Figure 4.8 Top 10 significantly enriched Biological Process (A) and Cellular Component (B) Gene Ontology (GO) terms in the bovine trophectoderm (TE) when methionine concentration is reduced within physiological range during IVP.

A. Molecular Function GO (TE)



B. KEGG Pathways (TE)

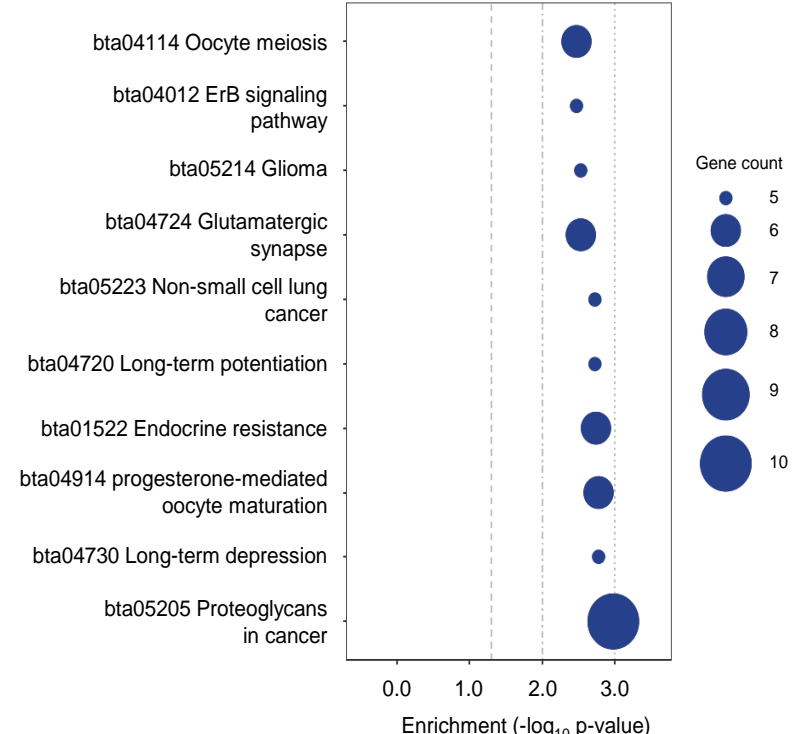


Figure 4.9 Top 10 significantly enriched Molecular Function Gene Ontology (GO) terms (A) and KEGG Pathways (B) in the bovine trophectoderm (TE) when methionine concentration is reduced within physiological range during IVP.

In GSEA, pathways are statistically tested for over-representation in the experimental gene list relative to what is expected by chance. Several common statistical tests consider the number of genes detected in the experiment, their relative ranking and the number of genes annotated to a pathway of interest. Whilst GSEA offers mechanistic insight into large gene lists generated from genomics experiments, it is important to acknowledge that they can be biased towards well-known pathways and can make unrealistic assumptions about statistical independence amongst genes, ignoring the fact that some genes are co-expressed and that some pathways share genes in common (Reimand *et al.*, 2019). It follows that statistically significant pathways often comprise a small number of differentially methylated genes of interest (GOI). Thus, in order to avoid testing overly narrow categories, the present study analysed the top five GO terms and KEGG pathways that comprised the highest number of differentially methylated GOI (Table 4.7, Table 4.8). Interestingly, pathways with the greatest number of differentially methylated GOI that were enriched in the ICM following altered methionine concentration during embryo culture were broadly associated with protein catabolism and autophagy. The term 'Cytosol' represents 40 GOI and is involved in protein complex formation (Table 4.7B). 'Hydrolase' (18 GOI) and 'Proteolysis' (11 GOI) terms relate to the hydrolysis of proteins into amino acids by the cleavage of peptide bonds (Table 4.8A, Table 4.7A).

In the TE, 'Protein kinase activity' (15 GOI) comprised the greatest number of differentially methylated GOI (Table 4.8A). Responsible for the transfer of phosphates between substrates (Cheng *et al.*, 2011), protein kinases are vital for cell cycle progression, apoptosis and differentiation, and are implicated in the control of TE development in the mammalian embryo (Kamei *et al.*, 1997; Yang *et al.*, 2016). Additional terms included 'Cytoskeleton' (13 GOI) and 'Pathways in cancer' (13 GOI; Table 4.7B, Table 4.8B). Similar to cancer cells, TE cells exhibit high rates of protein turnover and energy metabolism (Houghton *et al.*, 2006; Kelleher *et al.*, 2006). It is, therefore, plausible that differential methylation of genes involved in cell proliferation and differentiation provides an epigenetic mechanism responsible for the significant effect of methionine on TE-specific outgrowth (Chapter 3; Figure 3.13B). Terms and pathways enriched in both cell lineages that had the greatest number of differentially methylated GOI were 'Metabolic pathways' (Table 4.8B) 'Phosphorylation' (Table 4.7A) and 'Kinase activity' (Table 4.8A). These terms were related to others that were

exclusively enriched in the ICM or TE. This is because GSEA pathway boundaries are arbitrary and the identification of multifunctional genes can lead to the enrichment of several related pathways (Reimand *et al.*, 2019).

Genes of interest (GOI) with the highest number of DMS were selected from the first GO term and KEGG pathway in order to illustrate the effects of altering physiological methionine concentrations during bovine embryo culture on specific loci (Table 4.9). Of the pathways presented, *dopamine β -hydroxylase (DBH)* had the most differentially methylated CpGs (131 DMS and 146 DMS in the ICM and TE, respectively). The gene that encodes the DBH enzyme is responsible for the conversion of dopamine to noradrenaline, a catecholamine that participates in a number of physiological processes, including the stress response (LeBanc and Ducharme, 2007). In mice, disruption of the *Dbh* gene impaired cardiac development (Osuala *et al.*, 2012) and cellular immunity (Alaniz *et al.*, 1999). *Phospholipase C like 2 (PLCL2)*, a differentially methylated gene that features in multiple cellular pathways within the bovine embryo, is involved in the regulation of immune function by acting as a negative regulator of B cell activation (Takenaka *et al.*, 2003). Whilst Day 8 bovine embryos do not yet have an immune system, differential methylation of key genes could be viewed as an important preparatory step for subsequent embryonic differentiation.

Genes critical for early mammalian embryo development were differentially methylated following reduced methionine. By way of example, *negative elongation factor A (NEFLA)*, a member of the NEFL complex that regulates RNA polymerase II pausing in gene transcription (Adelman and Lis, 2012), was differentially methylated within the bovine ICM (Table 4.9). Recently, *Nefla* has been identified as a maternal factor that can modulate gene regulatory and metabolic networks within murine ESCs to reprogramme totipotency (Hu *et al.*, 2020), perhaps illuminating a potential role of *NEFLA* in the molecular control of developmental potency within the bovine ICM. *Wnt family member 7A (WNT7A)* was another developmentally important gene that was differentially methylated within the bovine TE (Table 4.9). *WNT7A* is an embryokine that mediates cell proliferation, cell fate and patterning, thereby increasing the competence of bovine embryos to develop to the blastocyst stage (Tríbulo *et al.*, 2018) via its involvement in the β -catenin-dependent pathway, and β -catenin independent pathways such as PI3K/Akt, RAC/JNK, and extracellular signal-regulated kinase 5/PPAR- γ (Lan *et al.*, 2019).

Table 4.7 Top five enriched Biological Process (A) and Cellular Component (B) Gene Ontology (GO) terms ranked by number of differentially methylated genes of interest.

A. Biological Process GO

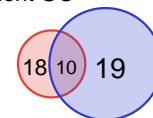


Inner-cell mass ICM (<i>n</i> =38)	GOI	FDR (q-value)
GO:0006508 Proteolysis	11	0.0456
GO:0050821 Protein stabilisation	5	0.0060
GO:0006914 Autophagy	4	0.0060
GO:0010468 Gene expression	4	0.0433
GO:0046854 Phosphatidylinositol phosphorylation	3	0.0060

Trophectoderm TE (<i>n</i> =58)	GOI	FDR (q-value)
GO:0035556 Intracellular signal transduction	11	0.0326
GO:0010628 Regulation of gene expression	9	0.0207
GO:0018108 Peptidyl-tyrosine phosphorylation	5	0.0148
GO:0048490 Anterograde synaptic transport	3	0.0013
GO:0008089 Anterograde axonal transport	3	0.0024

ICM and TE (<i>n</i> =29)	GOI		FDR (q-value)	
	ICM	TE	ICM	TE
GO:0016310 Phosphorylation	10	13	0.0168	0.0256
GO:0048015 Phosphatidylinositol signalling	4	3	0.0006	0.0096
GO:0043410 Regulation of MAPK cascade	3	4	0.0154	0.0149
GO:0045766 Regulation of angiogenesis	3	4	0.0221	0.0233
GO:0019722 Calcium signalling	2	5	0.0367	0.0025

B. Cellular Component GO



Inner-cell mass ICM (<i>n</i> =18)	GOI	FDR (q-value)
GO:0005829 Cytosol	40	0.0009
GO:0005815 Microtubule organisation	6	0.0069
GO:0030424 Axon	5	0.0359
GO:0062023 Collagen containing ECM	3	0.0179
GO:0005930 Axoneme	3	0.0150

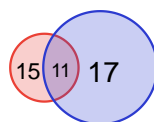
Trophectoderm TE (<i>n</i> =19)	GOI	FDR (q-value)
GO:0005856 Cytoskeleton	13	0.0393
GO:0005623 Cell	8	0.0397
GO:0030496 Midbody	6	0.0127
GO:0098978 Glutamatergic synapse	6	0.0391
GO:0031514 Motile cilium	4	0.0165

ICM and TE (<i>n</i> =10)	GOI		FDR (q-value)	
	ICM	TE	ICM	TE
GO:0005770 Late endosome	4	4	0.0089	0.0338
GO:0030667 Secretory granule	3	4	0.0003	0.0001
GO:0070062 Extracellular endosome	3	3	0.0075	0.0268
GO:0030659 Cytoplasmic vesicle	3	3	0.0138	0.0435
GO:1904115 Axon cytoplasm	2	4	0.0149	0.0040

Abbreviation(s): GOI, genes of interest; FDR, false discovery rate; ICM, inner cell mass; TE, trophoctoderm. Venn diagram: pathways enriched in ICM (red circle); pathways enriched in TE (blue circle); pathways enriched in ICM and TE (purple intersection).

Table 4.8 Top five enriched Molecular Function Gene Ontology (GO) terms (A) and KEGG Pathways (B) ranked by number of differentially methylated genes of interest.

A. Molecular Function GO



Inner-cell mass ICM (n=15)	GOI	FDR (q-value)
GO:0016787 Hydrolase activity	18	0.0417
GO:0008233 Peptidase activity	9	0.0186
GO:0008234 Cysteine-type peptidase activity	5	0.0033
GO:0004175 Endopeptidase activity	4	0.0052
GO:0008201 Heparin binding	4	0.0110

Trophectoderm TE (n=17)	GOI	FDR (q-value)
GO:0004672 Protein kinase activity	15	0.0392
GO:0004713 Protein tyrosine kinase activity	4	0.0447
GO:0004402 Histone acetyltransferase activity	3	0.0106
GO:0004714 Receptor protein tyrosine kinase	3	0.0279
GO:0022849 Glutamate-gated ion channel activity	2	0.0001

ICM and TE (n=11)	GOI		FDR (q-value)	
	ICM	TE	ICM	TE
GO:0016301 Kinase activity	9	12	0.0291	0.0412
GO:0030165 PDZ domain binding	2	3	0.0225	0.0171
GO:0008081 Phosphoric diester hydrolase	2	3	0.0432	0.0351
GO:0015485 Cholesterol binding	3	2	0.0033	0.0478
GO:0005078 MAP-kinase scaffold	2	2	0.0002	0.0007

B. KEGG Pathways



Inner-cell mass ICM (n=15)	GOI	FDR (q-value)
bta00562 Inositol phosphate metabolism	3	0.0349
bta04152 AMPK signalling pathway	3	0.0457
bta04136 Autophagy – other	2	0.0349
bta00513 N-Glycan biosynthesis	2	0.0361
bta03050 Proteasome	2	0.0361

Trophectoderm TE (n=17)	GOI	FDR (q-value)
bta05200 Pathways in cancer	13	0.0072
bta04151 PI3K-Akt signalling	10	0.0078
bta04010 MAPK signalling	9	0.0065
bta04014 Ras signalling	8	0.0065
bta05166 HTLV-I infection	8	0.0065

ICM and TE (n=22)	GOI		FDR (q-value)	
	ICM	TE	ICM	TE
bta01100 Metabolic pathways	17	25	0.0457	0.0157
bta05205 Proteoglycans in cancer	6	10	0.0348	0.0010
bta04360 Axon guidance	4	6	0.0449	0.0112
bta04140 Autophagy – animal	4	5	0.0351	0.0133
bta04390 Hippo signalling pathway	4	5	0.0361	0.0161

Abbreviation(s): GOI, genes of interest; FDR, false discovery rate; ICM, inner cell mass; TE, trophectoderm. Venn diagram: pathways enriched in ICM (red circle); pathways enriched in TE (blue circle); pathways enriched in ICM and TE (purple intersection).

Table 4.9 Genes of interest (GOI) with the highest number of differentially methylated sites (DMS) selected from the first Gene Ontology (GO) term and KEGG Pathway.

Pathways enriched in ICM		Differentially methylated GOI		CpGs		Promoter		Exon		Intron		CGI		Shore	
BP	GO:0006508 Proteolysis	<i>PMPCA</i>	Peptidase, mitochondrial processing alpha subunit	48		1		22		27		24		20	
CC	GO:0005829 Cytosol	<i>NELFA</i>	Negative elongation factor complex member A	50		1		15		35		31		10	
MF	GO:0016787 Hydrolase	<i>PLCL2</i>	Phospholipase C like 2	92		0		9		85		38		19	
KEGG	bta00562 Inositol phosphate metabolism	<i>PLCG1</i>	Phospholipase C gamma 1	24		0		6		18		10		5	

Pathways enriched in TE		Differentially methylated GOI		CpGs		Promoter		Exon		Intron		CGI		Shore	
BP	GO:0035556 Signal transduction	<i>PLCL2</i>	Phospholipase C like 2	118		0		6		112		51		16	
CC	GO:0005856 Cytoskeleton	<i>FARP1</i>	FERM, ARH/RhoGEF and pleckstrin domain protein 1	49		1		3		46		5		17	
MF	GO:0004672 Protein kinase	<i>IGF1R</i>	Insulin like growth factor 1 receptor	61		1		19		57		29		11	
KEGG	bta05200 Pathways in cancer	<i>WNT7A</i>	Wnt family member 7A	69		0		3		57		16		31	

Pathways enriched in ICM and TE		Differentially methylated GOI		CpGs		Promoter		Exon		Intron		CGI		Shore	
				ICM	TE	ICM	TE	ICM	TE	ICM	TE	ICM	TE	ICM	TE
BP	GO:0016310 Phosphorylation	<i>TOLLIP</i>	Toll interacting protein	70	83	4	4	32	31	38	47	23	39	34	34
CC	GO:0005770 Late endosome	<i>IGF2R</i>	Insulin like growth factor 2 receptor	25	51	0	11	7	5	18	46	8	32	10	12
MF	GO:0016301 Kinase activity	<i>PRKAR1B</i>	Protein kinase cAMP-dependent type 1 subunit β	56	81	0	1	6	15	53	75	35	45	16	32
KEGG	bta01100 Metabolic pathways	<i>DBH</i>	Dopamine β -hydroxylase	131	146	5	9	22	24	103	115	38	55	50	61

Abbreviation(s): BP, Biological Process; CC, Cellular Component; CGI, CpG island; ICM, inner cell mass; KEGG, Kyoto Encyclopedia of Genes and Genomes; MF, Molecular Function; TE, trophectoderm. DMS distribution across genomic regions show an excess of annotation due to overlapping genes and inaccurate annotation of promoter regions in *Bos taurus* genome (Bta.ARS-UCD1.2, April 2018).

Insulin-like growth factors, IGF1 and IGF2, are potent mitogens that play a predominant part in embryonic growth and morphogenesis (Kowalick *et al.*, 1999). It follows that aberrant methylation and expression of their respective receptors can have detrimental consequences for embryo development (Agrogiannis *et al.*, 2014). Both *IGF1R* and *IGF2R* genes were differentially methylated in the bovine embryo following altered methionine during culture (Table 4.9). Of particular interest is the methylation status of the imprinted locus, *IGF2R*, due to its association with LOS in ruminants (discussed later).

4.3.2.5 Imprinted genes

Genomic imprinting is an epigenetic mechanism that leads to parental allele-specific gene expression (Barlow and Bartolomei, 2014). Around 150 imprinted genes have been identified in humans and mice, and ~30 have been identified in cattle (Chen *et al.*, 2016; Table 4.10). Imprinted genes play a pivotal role in fetoplacental growth and development, metabolism and postnatal behaviour (Fowden *et al.*, 2006; Smith *et al.*, 2006; Glenn *et al.*, 1997). Their monoallelic expression is governed by asymmetrical epigenetic marks on either the maternal or paternal allele. Typically, imprinted genes are organised in clusters that are regulated by CpG-rich domains known as imprint control regions and/or DMRs (Barlow and Bartolomei, 2014). It follows that aberrant CpG methylation within these regulatory domains has been implicated in imprinting disorders. In humans, loss of imprinting (LOI) of *CDKN1C*, *H19* and *IGF2* is associated with Beckwith-Wiedemann syndrome (BWS; Sinclair *et al.*, 2000; Chen *et al.*, 2013); LOI of *MEST* is associated with Silver-Russell syndrome (Riesewijk *et al.*, 1998); and, LOI of *UBE3A* and *SNRPN* is associated with Prader-Willi syndrome and Angelman syndrome (Glenn *et al.*, 1997).

In the present study, six imprinted genes (*PEG10*, *NAP1L5*, *IGF2R*, *NNAT*, *SNRPN* and *PHLDA2*) were differentially methylated in Day 8 bovine embryos as a consequence of reduced methionine (50 v 10 $\mu\text{mol/L}$) during IVP (Table 4.10). In both embryonic cell lineages, DMS were generally hypomethylated following culture in the low physiological methionine concentration (10 $\mu\text{mol/L}$) relative to the high concentration (50 $\mu\text{mol/L}$; Figure 4.10).

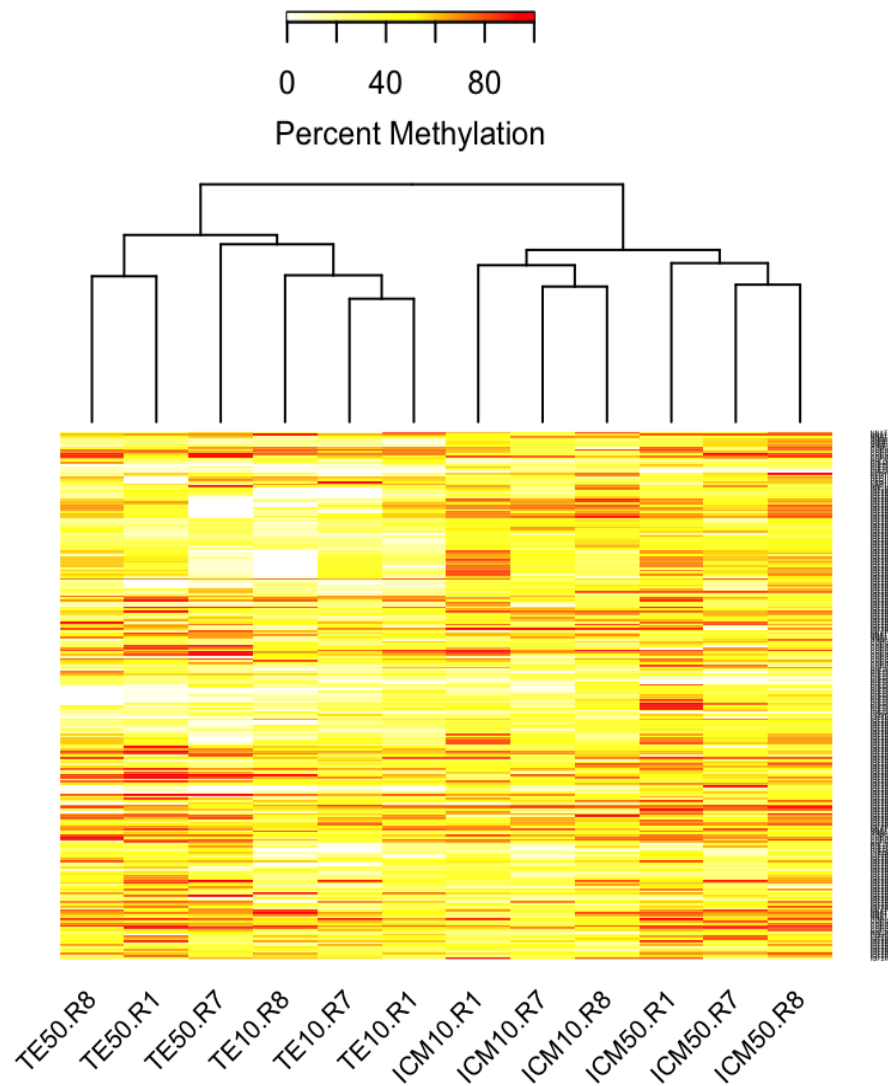


Figure 4.10 Low physiological methionine concentration during culture decreases CpG methylation of six imprinted genes within the primary cell lineages of the Day 8 bovine preimplantation embryo.

Colours indicate methylation level (%) from low (white) to high (red) of differentially methylated sites (DMS) within imprinted genes enriched within the trophectoderm (TE) and inner cell mass (ICM) at physiologically high (50 $\mu\text{mol/L}$) and low (10 $\mu\text{mol/L}$) methionine concentration during *in vitro* embryo culture.

The *insulin-like growth factor 2 receptor (IGF2R)* had the greatest number of CpGs (156 DMS) that were significantly ($P < 0.001$) hypomethylated in the ICM and TE as a consequence of reduced physiological methionine (50 v 10 $\mu\text{mol/L}$) during IVP (Figure 4.11A). Since reduced methylation of *IGF2R* appears to be causative of the fetal overgrowth phenotype, known as large offspring syndrome (LOS) in ruminants exposed to ART procedures (Young *et al.*, 2001; Young *et al.*, 2003; Section 1.7), this gene was selected for further investigation into the effect of low methionine during bovine embryo culture on the methylation status of CpGs within a specific regulatory region of the *IGF2R* gene (Section 4.3.2.6).

Small nuclear ribonucleoprotein polypeptide (SNRPN) is another imprinted gene implicated in LOS in cattle (Smith *et al.*, 2015) that was hypomethylated in both embryonic cell lineages due to low methionine ($P < 0.001$; Figure 4.11E). Demethylation of the maternal *SNRPN* DMR in embryonic and extraembryonic tissues of *in vitro* and SCNT derived bovine embryos indicates that embryo manipulations can induce epigenetic alterations in imprinted genes that persist beyond implantation (>Day 19; Lucifero *et al.*, 2006; Suzuki *et al.*, 2009).

Imprinted genes that are specifically important for the regulation of placental growth were differentially methylated in the present study. Cytosine methylation of the paternally imprinted *pleckstrin homology-like domain family A member 2 (PHLDA2)* gene was significantly reduced in both cell lineages following culture in 10 $\mu\text{mol/L}$ methionine ($P < 0.001$; Figure 4.11B). Reduced expression of *PHLDA2* in the bovine placenta is associated with placentomegaly following SCNT (Guillomot *et al.*, 2010). Similar observations have been reported in *Phlda2*-null mice that exhibited placental overgrowth (Frank *et al.*, 2002). In contrast, LOI of *PHLDA2* in human placenta is linked to intrauterine growth restriction (Salas *et al.*, 2004; Diplas *et al.*, 2009). These findings support the conclusion that *PHLDA2* serves as a regulator of placental growth in mammals. There was a significant interaction between methionine concentration and cell lineage on the methylation status of *paternally expressed 10 (PEG10)*; $P = 0.03$; Figure 4.11D). A functional study of *Peg10* using a knockout mouse model caused early embryonic lethality owing to placental defects (Ono *et al.*, 2006). Similarly, silencing of *PEG10* in human placental extracts inhibited trophoblast proliferation and invasion (Chen *et al.*, 2015), thereby supporting its critical role in normal placental formation.

Although not statistically significant, *neuronatin (NNAT)* had 12 DMS that were generally hypomethylated in both cell lineages following culture in low

physiological methionine ($P=0.075$; Figure 4.11C) and *nucleosome assembly protein 1-like 5* (*NAP1L5*) had 2 DMS that were hypermethylated in low physiological methionine ($P=0.204$; Figure 4.11F). Both of these genes are maternally imprinted and paternally expressed in multiple fetal tissues in cattle, including the brain, lung, liver, kidney, intestine, muscle, ovary and eye (Zhaitoun and Khatib, 2006), suggesting broad roles of these imprinted genes in fetal development.

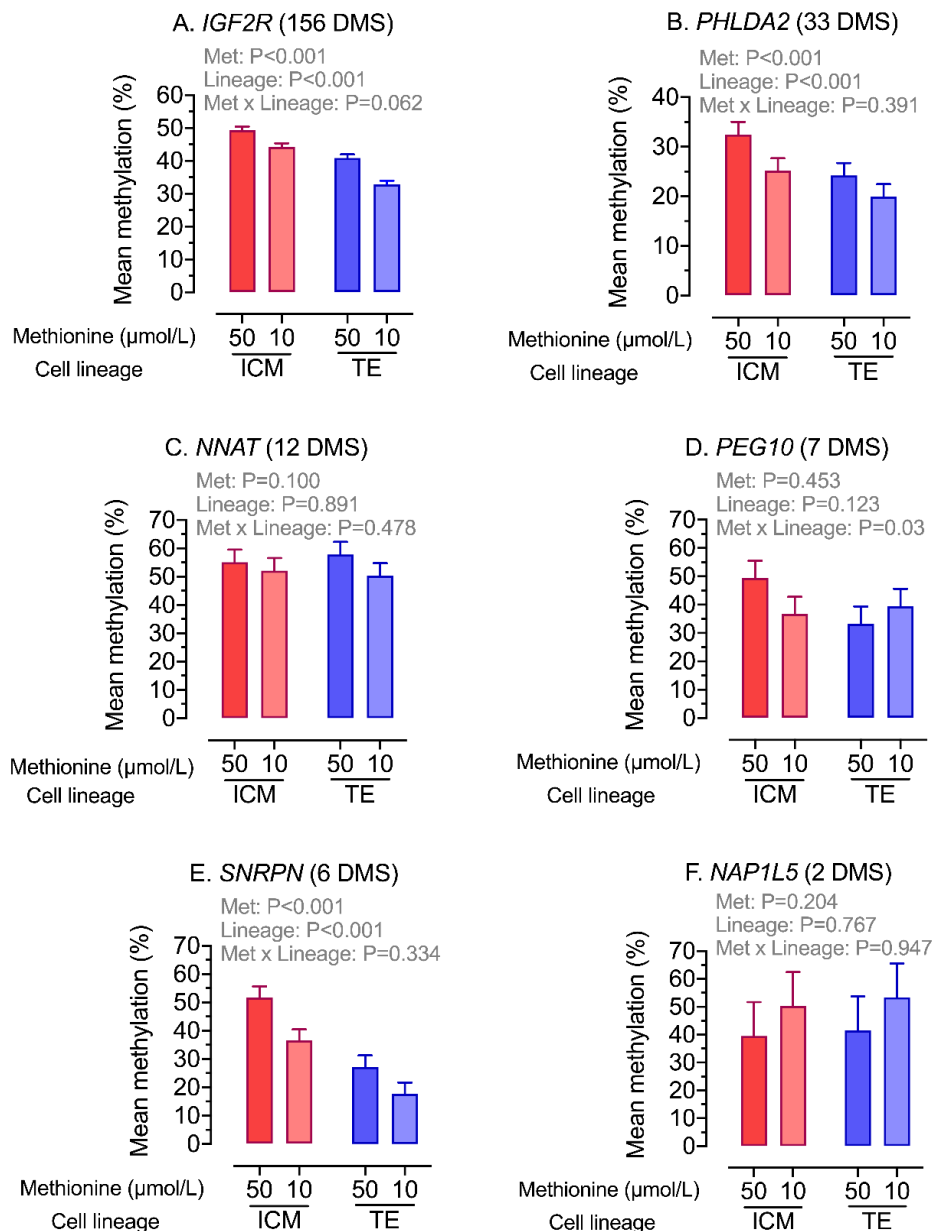


Figure 4.11 Mean methylation (%) of six differentially methylated imprinted genes in bovine inner cell mass (ICM) and trophectoderm (TE) following culture in physiologically high (50 $\mu\text{mol/L}$) and low (10 $\mu\text{mol/L}$) methionine.

4.3.2.6 *Insulin-like growth factor 2 receptor (IGF2R)*

The *IGF2R* gene, otherwise known as the cation-dependent mannose-6-phosphate receptor, encodes a multifunctional protein that is involved in lysosomal trafficking, tumour suppression, T-cell mediated immunity and fetal growth (Wang *et al.*, 1994; Lau *et al.*, 1994; Motyka *et al.*, 2000; Killian *et al.*, 2001). Its involvement in regulating fetal growth is facilitated through binding IGF2 for degradation and removing the potent mitogen from the circulation (Barker *et al.*, 1993; Wang *et al.*, 1994). The imprinted expression of *IGF2R* is conserved across diverse mammalian species, including cattle (Long and Cai, 2007), sheep (Young *et al.*, 2001), pigs (McElroy *et al.*, 2007), mice (Barlow *et al.*, 1991), rats (Vu *et al.*, 2006), dogs (O'Sullivan *et al.*, 2007), kangaroos (Yandell *et al.*, 1999) and opossums (Weidman *et al.*, 2006). *IGF2R* does not appear to be imprinted in monotremes or primates (Kalscheuer *et al.*, 1993; Killian *et al.*, 2001) and its imprinted expression in humans remains ambiguous. Adult human tissues lack imprinted expression (Kalscheuer *et al.*, 1993; Ogawa *et al.*, 1993) whereas fetal tissues and Wilm's tumours are imprinted in some cases, however, the trait is highly polymorphic (Yotova *et al.*, 2008). This broad conservation across eutherian mammals reinforces the proposed link between genomic imprinting and parental-specific control of fetoplacental growth and development (Haig, 2004; Killian *et al.*, 2000). It follows that the fetal overgrowth phenotype exhibited by cattle and sheep that is caused by aberrant *IGF2R* imprinting is also conserved. In mice, disrupted *Igf2r* expression also leads to excessive fetal and placental growth, cardiac abnormalities, cleft palate and increased perinatal mortality. It is assumed that reduced *Igf2r* stimulates fetal growth because of impaired IGF2 clearance from the circulation (Baker *et al.*, 1993; Lau *et al.*, 1994; Wang *et al.*, 1994; Melnick *et al.*, 1998). However, plasma levels of IGF2 in sheep fetuses with LOS were not significantly higher than controls (Young *et al.*, 2001), thus, the physiological and epigenetic mechanisms of *IGF2R* imprinting are postulated to differ across species.

Most of the research investigating the regulation of *IGF2R* imprinting pertains to studies with mice, with relatively little research conducted in cattle. In both species, the *Igf2r/IGF2R* gene is paternally imprinted and transcribed exclusively from the maternal allele in all fetal and adult tissues examined (heart, liver, kidney, lung, skeletal muscle and placenta), with the exception of the brain (Yotova *et al.*, 2008; Bebbere *et al.*, 2013). In both species, *Igf2r/IGF2R* imprinting is developmental stage- and tissue-specific. Initially,

Igf2r/IGF2R expression levels are biallelic and switch to maternal expression after implantation (Lerchner and Barlow, 1997; Long and Cai, 2007). In cattle, the degree to which paternal *IGF2R* is repressed differs between tissues of endodermal (liver and lung), mesodermal (heart, skeletal muscle) and ectodermal origin (brain). Moreover, the expression of *IGF2R* was reported to be 3- to 4-fold higher in bovine placenta than in fetal tissues. This is reflective of 'partial imprinting' in extraembryonic tissues (Bebbere *et al.*, 2013), a mechanism whereby both parental alleles are differently expressed instead of the complete silencing of one parental allele and full expression of the other (Baran *et al.*, 2015). Expression of both parental *IGF2R* alleles in the TE may provide a plausible explanation for the significantly lower CpG methylation measured in this lineage relative to the ICM in both methionine treatments ($P < 0.001$; Figure 4.11A).

4.3.2.6.1 Regulation of *IGF2R* imprinting

The *IGF2R* gene comprises 48 exons and is part of an imprinted cluster that contains maternally expressed *SLC22A2* and *SLC22A3*, and paternally expressed long non-coding ncRNA (lncRNA), *Airn/AIRN* (Antisense to Igf2r RNA Noncoding), in addition to non-imprinted genes; *SLC22A1*, *MAS1*, and *PLG* (Stöger *et al.*, 1993; Wutz *et al.*, 1997; Latos *et al.*, 2012). In mice, this imprinted cluster spans 500 kb on chromosome 17 (Yotova *et al.*, 2008). In cattle, the analogous cluster is located on chromosome 9 (Farmer *et al.*, 2016). In both species, the *Igf2r/IGF2R* gene encodes two reciprocally imprinted transcripts, each of which is associated with a DMR (Wutz *et al.*, 1997; Long and Cai, 2007). DMR1 encompasses the *Igf2r/IGF2R* promoter CGI that is methylated on the paternally inherited allele. DMR2 is located within intron 2 of the *Igf2r/IGF2R* gene and encompasses the *Airn/AIRN* promoter CGI that is methylated on the maternally inherited allele (Wutz *et al.*, 1997; Long and Cai, 2007; Figure 4.12A).

In cattle, DMR2 is 2,620 bp in length. Bovine *AIRN* is an unspliced, polyadenylated lncRNA that is 117 kb long and transcribed from the paternal allele in the antisense orientation from the transcription start site located 623 bp upstream of DMR2. *AIRN* transcription extends into intron 1 of the neighbouring gene, *MAS1*, thereby overlapping *IGF2R* and silencing its expression by transcriptional interference (Farmer *et al.*, 2016; Latos *et al.*, 2012; Figure 4.12A). How *AIRN* silences non-overlapped imprinted genes *SLC22A2* and

SLC22A3, remains disputed. Recently, it was proposed that *AIRN* targets distant promoters and recruits repressive chromatin complexes. Whilst such interactions are lost once silencing is established, silenced genes are covered with H3K27me3 modifications on the repressed paternal allele (Andergassen *et al.*, 2019; Figure 4.12A).

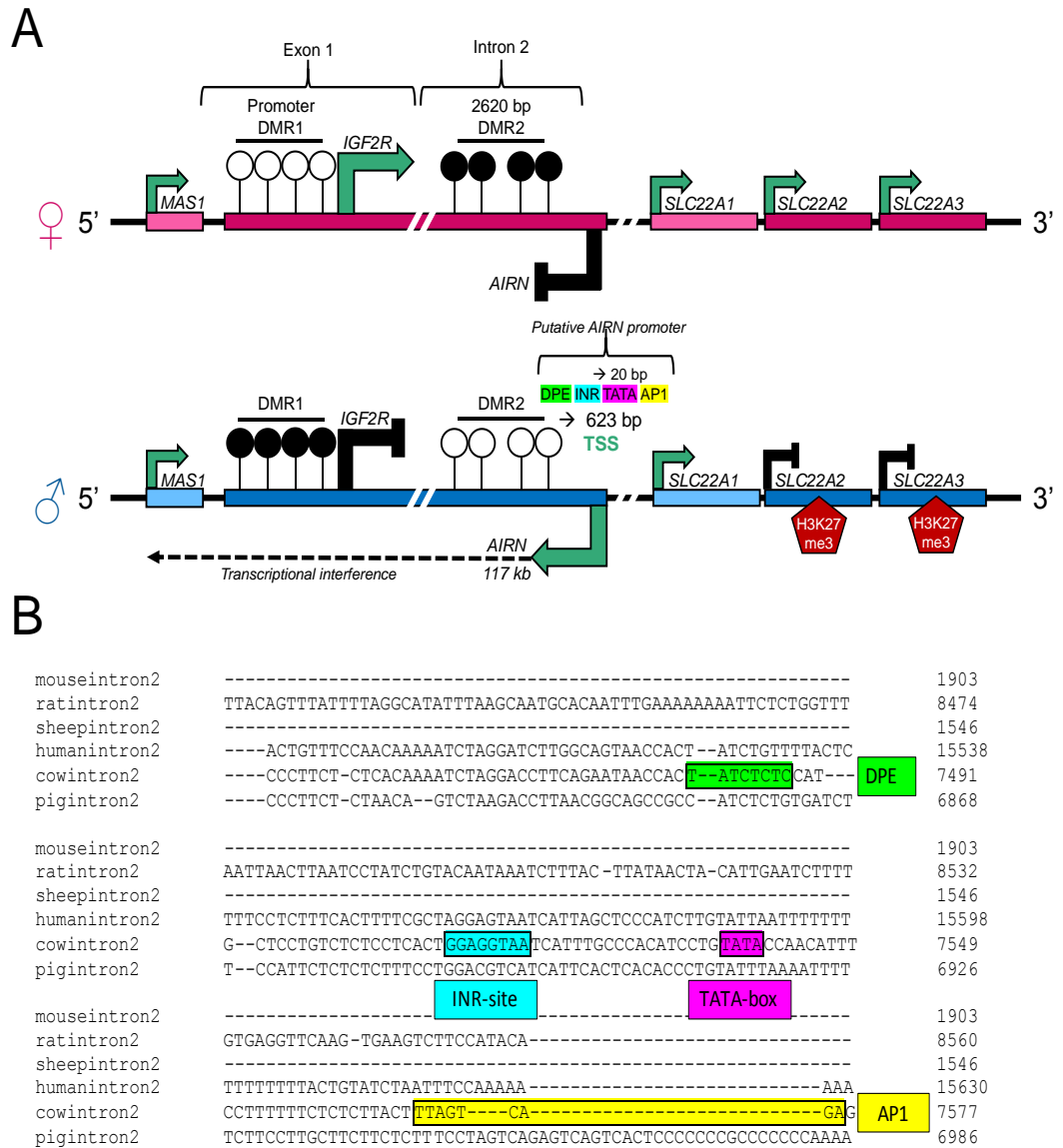


Figure 4.12 Bovine *IGF2R* gene is imprinted by antisense transcript, *AIRN*.

Source: Clare *et al.* (unpublished). Bovine genomic region on Chromosome 9 specific to *Igf2r/IGF2R* and *AIRN* (A). Multiple sequence alignment for *Igf2r/IGF2R* intron 2 with putative transcription initiation site and consensus binding site of core promoter elements in the bovine genomic region. Nucleotide numbers refer to location on chromosomes (B). Abbreviation(s): AP1, activator protein 1; DPE, downstream promoter element; INR, initiation response element.

The *AIRN* promoter region was identified by analysing the bovine *IGF2R* sequence (<https://www.ensembl.org/>; ENSBTAG00000002402) in an antisense direction upstream of DMR2 for possible core promoter elements (Figure 4.12B). In accordance with consensus sequences reported by Farmer and colleagues (2016), a TATA-box was identified 20 bp upstream of the transcription start site; an activator protein-1 (AP1) binding site was identified upstream of the TATA-box (Suslov *et al.*, 2010); and, an initiation response element (INR-site) and down-stream promoter element (DPE) was identified downstream of the TATA-box (Burke and Kadonaga, 1997). This clustering of four initiation sequences within 200 bp of the bovine *AIRN* promoter has also been observed in the murine *Airn* promoter sequence (Lyle *et al.*, 2000), suggesting that DMR2 encompasses the promoter in both species. Putative DMR2 regions have also been identified in sheep (Young *et al.*, 2003), pigs (Shen *et al.*, 2012), rats (Killian *et al.*, 2000), and humans (Reisewijk *et al.*, 1995), however, the nucleotide sequence homology and core promoter elements differ between species (Figure 4.12B; discussed later).

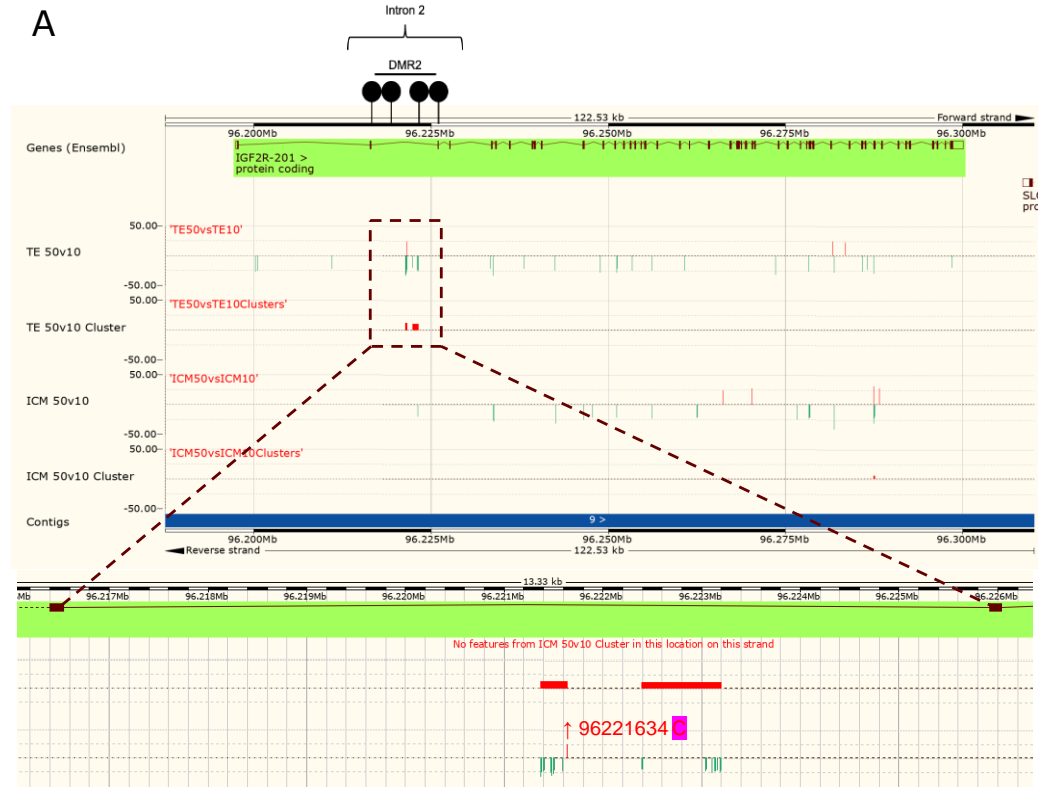
4.3.2.6.2 Loss of methylation in DMR2

The present study identified two clusters of DMS that were hypomethylated within DMR2 in the TE of bovine embryos following culture in low physiological methionine (50 v 10 $\mu\text{mol/L}$; Figure 4.13). Only one DMS was hypermethylated at nucleotide position 96221634 (Figure 4.13B). The methylation status of each DMS located within the second intron of *IGF2R* in the TE lineage can be found in Appendix 4.10. In the ICM, DMR2 methylation was relatively unaffected by the reduction in methionine as demonstrated by the hypomethylation of only one DMS (Figure 4.13A).

Little is understood about the loss of DMR2 methylation in bovine placenta since previous studies have focused on DMR2 methylation in fetal tissues following ART procedures. Long and Cai (2007) reported that tissue-specific variation in DMR2 methylation levels in the liver, brain, heart and lung of normal bovine fetuses ranged from 54 to 99%. These levels were disrupted in tissues from cloned fetuses, and methylation levels decreased to 25% in the heart. In addition, loss of DMR2 methylation on the maternal allele in LOS bovine fetuses following SCNT was associated with decreased *IGF2R* transcript abundance (Chen *et al.*, 2017). Similar observations have been reported in sheep. Ovine *IGF2R* DMR2 had strongly reduced levels of DNA methylation in tongue tissue

following SCNT (Young *et al.*, 2003) and hypomethylation of this regulatory region was correlated with reduced expression of *IGF2R* by 30-60% in LOS fetuses relative to controls (Young *et al.*, 2001). Collectively, these results show that *IGF2R* was not fully reprogrammed during early development after nuclear transfer and that this locus may be similarly dysregulated in ruminant species.

Multiple sequence alignment revealed high *IGF2R* gene sequence homology between cattle and sheep (91.9%). However, intron 2 was less conserved (45.8%) and the two cluster regions within DMR2 did not align despite the phylogenetic similarity between the two species (Appendix 4.11). Intriguingly, intron 2 was more conserved between cattle and pigs (74%), and the first and second DMS clusters were 87.1 and 88.0% homologous between the two species, respectively. Cytosine residues that were differentially methylated in cattle embryos within the second cluster were highly conserved between cattle and pigs (90.9%). A high percentage of cytosines in the second cluster were conserved in humans (81.8%; Appendix 4.11). Whilst DMR2 harbours a maternal-specific methylation imprint in pigs and humans (Shen *et al.*, 2012; Reisewijk *et al.*, 1995), there is no evidence for paternal *AIRN* transcription in either species (Braunschweig, 2012; Oudejans *et al.*, 2001), highlighting evolutionary differences in nucleotide sequence and imprinting status of *IGF2R* between species (Killian *et al.*, 2000).



B

```

AAGGTGCTGAGAAGGCTCGGCGCCCGCAGGCTGGGCCCCGTGGCCCGCCGGGAGGCG
GTCGCCAGGCCGAGCAGCCTCAGGAGGTCGGGTTGGAGCTCGGCCGGGCTCGGCCGCG
AGCGCCGAGGGCGGCAGGCGAGGCCCGGCCGCTGGCACGGGCCTGGTGGGCGACT
CTGGTGAGCGGGCGAGCGCGCAGGGTCTGCAGGACCCGGGCTGGCCTGGCCGGCGGGCG
CGTGGCTGGGGCTGGCGGGCGCGGGCGAGCGCTGCGGACGGCGCCCTGGCGCGCAGGG
TCGAGAGGACCCGGCGCGCCGGGCTGCAGAGCCTGGCTGGTCTGACGGGCTCGGGCG
AGCGTGGCCTGGCGGGAGCCCTGGCGTGCAGGGTCTGGGAGGACCTCGCGGGGCTGGCCG
GTAGCGTGTGGCCGGTCTGGTGGGTCCGGGTGAACGTGGCCTGGTCTGGCGGGCCGG
CGAGCGCGCCTGGAGAGCCCGCCTGGAGAGCGCTGTCTGGAGGGCCAGCGCGTGGT
TGGCGGACCCGGCGGGTCTGGCGGCCCGGCGCTGGAGACCCGGATCGGGTGGACCGCC
ACTGCCTGGCGGGCTCGGCAAGTGCGGTTGGTCTGGCGGGCCAGGCGAGCGCGCTCG
GTCTGGGGGCTCTGCCTGGAGGCTGCGGTTCGGACAGGTCTGGCAGGCCCTGGACGCGG
GCCTGGTCTGGAGGACCCGGCCTGGAGAGCGCGGCTGGAGGACCCGGCGGGTCTAGTC
TGGTGGGGTCTCGCCAGTGTCTGGTCTGGTGGGCCCGGGTGGAGCTCGGCCTGGTCTG
CGGACCTGGCCTGGAGAGCGCGCTCTGGAGGACCCGGCGCGGCTGGCGGGCCCTGGCG
AGCGCGGCTGGCGGGCCCGGGCGCAGGGTCTGAAGGACCCGGCGTGGCCTGGCTTGG
GAGCTCGGCTGGTCTGGCGGACCCGGCCTGGAGAGCGCCGTCTGGTGGGCTGGCGCG
GTGGCCTCGTTGGAGGACCCGGCCTGGAGACCGTATCTGGAGGGCTGGAGGCGCACCG
TCTGGCGGGTCCGAGGACCCGGCGCATCTGGTGGGCCCGGTGAGCGCGAGCTGGTCT
GGTGGGCCAGCGCGCGCGGCTGGTCTGGTGGACCCGGCCTGGAGAGCGGTGGTAG
GACCCGGCGCGCGGTCTGGCGGGCTGGCGGGTCCGGTGGCCGAGCGCGCGGTCTG
GAGGACCCAGCGCGGTCTGGCGGACCCGGCCTGGAGAGCGCGGTCTGGAGGACCCGGCG
GGCCTGGCGGGCCTGGGCGGACCGGCTGGTCTGGCGGGCCTGGCGGAGACCCGGGT
CTGGCCGGCACGGCGCGCGCAGCCGGTCTGGAGGACCCGGCCTGGAGAGCGCGGCTGG
AGGACCCGGCGCGGTCTGGTCTGGTGGGGCCCGCCAGTGTGGTCTGGTCTGGCGCGCC
GGCTGGAGAGCGTGGTCTGGCGGGCCCGCGCGCGGTCTGGAGGACCCGGCGCGATCTG
GCGGGCCCGGCGAGCGCGGCCAGCCATTTGGCGCGTCTCGGGAGCTGGCCGTGGGC
CTGGCGTCTGGCCCGCCCGCCCGCAGTCTCGCCCGGCTTCTCGCCGGGAGGACGGCCA
GGCTGGCCGGGGTGGCGGGAGTCCGCGCGGGGGCGCTGCCGGGTGCACCGGGCCT
CTTGGCGAGTGGCGGGTGGGCAATCGGTCTGGCCAGTAGGCGGAGGAGGGGCTGCAG
GCAGGCTGGACGGGCGAGGGGCGGGTCCGATGGGGCCTGAGCTGAGGGACCGCGCT
GTCCCAGCGCGCGCGCGGAGCTGGCCGGTCCGTCTCGGCTCAAGGCCAGGGCCCG
    
```

Figure 4.13 Two clusters of DMS were hypomethylated within DMR2 of the *IGF2R* gene in the trophectoderm (TE) lineage following bovine embryo culture in low physiological methionine (50 v 10 μmol/L).

Bedgraphs demonstrate loss (↓, hypomethylation) and gain (↑, hypermethylation) of methylation at individual cytosine residues, and location of DMS clusters (A). Nucleotide sequence showing the two clusters in red. Hypomethylated cytosines in blue and hypermethylated cytosine (position 96221634) in pink (B).

4.3.2.6.3 *IGF2R* and *AIRN* transcript expression

It was hypothesised that culturing bovine embryos in low physiological methionine (10 $\mu\text{mol/L}$) would cause loss of methylation within DMR2 of *IGF2R* (on the maternal allele) which, in turn, would cause biallelic expression of antisense transcript, *AIRN*, thereby causing repression of *IGF2R* gene expression from both parental alleles. Whilst there was a significant difference between *IGF2R* and *AIRN* transcript expression ($P < 0.001$), there was no significant effect of methionine during embryo culture ($P = 0.405$; Figure 4.14). There are several explanations for why the loss of methylation observed had no effect on *IGF2R/AIRN* imprinted expression in the present study.

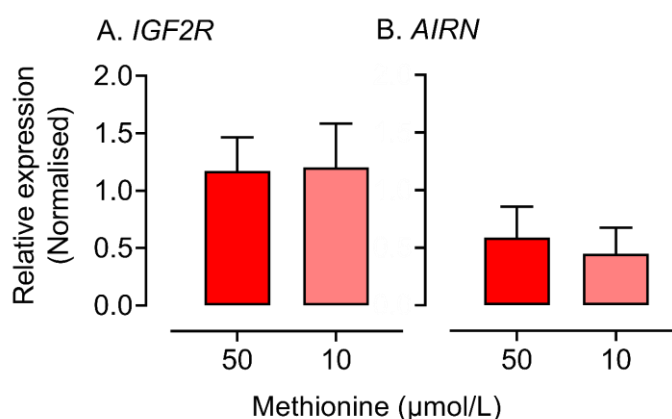


Figure 4.14 Relative transcript expression of *IGF2R* (A) and antisense transcript, *AIRN* (B) in Day 8 bovine blastocysts cultured at physiologically high and low methionine concentrations.

Relative expression data analysed by ANOVA and presented as mean \pm SEM. Significant difference between *IGF2R* and *AIRN* transcript expression ($P < 0.001$); no effect of physiological methionine concentration ($P = 0.405$). Abbreviation(s): *AIRN*, Antisense to *IGF2R* RNA noncoding; *IGF2R*, insulin like growth factor 2 receptor.

Studies have reported that *IGF2R* expression levels in preimplantation cattle embryos are biallelic and switch to maternal expression after implantation (Lerchner and Barlow, 1997; Long and Cai, 2007) at which stage the gene is only partially imprinted in the placenta (Bebbere *et al.*, 2013). Indeed, Farmer *et al.* (2013) reported absence of *AIRN* in pools (2 to 11) of bovine embryos until Day 18, a stage of development that coincides with implantation and maternal recognition of pregnancy (Thatcher *et al.*, 1984). Albeit 2- to 3-fold lower than *IGF2R* expression, the present study measured detectable levels of *AIRN* in pools (15 to 28) of Day 8 preimplantation blastocysts. It is important to acknowledge that developmental stage, cell lineage and inter-individual genetic

variation may lead to variability in the degree of imprinting between embryos that cannot be identified by measuring transcript abundance in pools of embryos. A solution would be to measure transcript expression in individual embryos, or in immunodissected ICM and TE cells, however, the qPCR methods used in this study were not adequately sensitive to measure these low abundance transcripts with accuracy and reliability. Another factor to consider is that it was not possible to determine the parental origin of methylation using pools of embryos.

Whilst hypomethylation of DMR2 has been associated with decreased *IGF2R* expression in cattle fetuses, it is not necessarily downregulated by *AIRN*. As discussed earlier (Section 4.3.2.6.2), [Chen et al. \(2017\)](#) correlated loss of DMR2 methylation with loss of *IGF2R* expression in skeletal muscle of LOS fetuses, however, *AIRN* was biallelically expressed in LOS and control fetuses. The precise function of DMR2 in regulating imprinted expression of *IGF2R* by *AIRN* remains unclear. It has been proposed that the CGI within DMR2, located at the 5'-end of the *AIRN* transcription start site (Figure 4.12), is required for RNA polymerase II transcript initiation, elongation and processivity. However, it is the CGI sequence (i.e. tandem direct repeats) rather than its methylation status that correlates with efficiency of *AIRN* transcription ([Koerner et al., 2012](#)). Furthermore, additional regulatory elements, such as DMR1 methylation and histone modifications, are likely to operate in synergy with *AIRN* to repress paternal *IGF2R* ([Sleutels et al., 2002](#); [Long and Cai, 2007](#)).

It is uncertain whether the TE-specific loss of DMR2 methylation in Day 8 bovine preimplantation embryos as a consequence of reduced methionine during embryo culture is sufficient to affect *IGF2R* gene dosage at later stages of development. These results illustrate that subtle reductions in physiological methionine levels alone can influence the methylation status of *IGF2R*, thereby raising questions about the safety and efficacy of current *in vitro* embryo production protocols, particularly those involving invasive embryo manipulation techniques (e.g. SCNT), extended culture periods or non-physiological methionine concentrations.

4.4 Concluding remarks

The findings presented herein support the conclusion that altering the concentration of methionine, within physiological limits (50 v 10 $\mu\text{mol/L}$), during

the periconceptual period can lead to epigenetic alterations to DNA methylation of genes that regulate developmental processes in the bovine preimplantation embryo. Specifically, culturing gametes and embryos in low physiological methionine (10 $\mu\text{mol/L}$) reduced CpG methylation within key genomic regions of the ICM and TE, demonstrating that both primary cell lineages of the Day 8 blastocyst are sensitive to subtle reductions in methionine during the first week of preimplantation development. Given that methionine is a rate-limiting amino acid in maternal diets (Laurichesse *et al.*, 1998; Schwab and Broderick, 2017) and that concentrations in commercial embryo culture media range from 0 to 500 $\mu\text{mol/L}$ in ART procedures (Table 1.5) these findings are of concern regarding the safety and efficacy of dietary and culture media supplementation of methionine during early embryonic development.

Methionine supplementation during *in vitro* embryo culture was previously reported to have no effect on DNA methylation in whole blastocysts (Bonilla *et al.*, 2010). This conclusion, however, was drawn using an insensitive and non-specific immunocytochemistry approach to quantification. To date, no study has examined the effect of methionine on the methylome within the ICM and TE independently. Reduced representation bisulphite sequencing (RRBS) analyses of CpG methylation within immunodissected embryonic cell samples provides a high level of refinement in this regard. The methodology was sufficiently sensitive to reveal lineage- and sequence-specific methylation differences in response to a moderate decrease in methionine. The observation that the TE had a greater number of hypomethylated DMS than the ICM following culture in low physiological methionine reaffirmed that the primary cell lineages acquire distinct methylation marks during preimplantation development (Morgan *et al.*, 2005) and that the contribution made by these two embryonic cell types to methionine metabolism in the blastocyst is different. It has been postulated that the TE has a higher metabolic rate and methionine turnover relative to the ICM (Houghton *et al.*, 2006). Moreover, GSEA identified that statistically significant GO terms and pathways enriched within the ICM were associated with protein catabolism and autophagy, whereas significant terms and pathways enriched within the TE were associated with cellular transport. The differential methylation of imprinted genes, principally *IGF2R*, between the ICM and TE also highlights epigenetic, transcriptomic and functional metabolic differences between the embryonic and extraembryonic lineages that could not have been identified by analysing methylation in intact blastocysts.

Despite the fact that RRBS enriches functional regions of the genome by selectively targeting CpG-rich regions (i.e. CGIs/DMRs) for sequencing at single-nucleotide resolution ([Chatterjee *et al.*, 2012](#)), the approach is limited by restriction enzymes that cleave DNA at specific sites. This biased sequence selection means that CpG-poor regions are under-represented in the library ([Doherty and Couldrey, 2014](#)). Moreover, the method cannot distinguish between 5mC and 5hmC methylation. Although 5hmC has been detected in bovine embryos and is enriched at repeat sequences, such as LINEs and LTRs ([de Montera *et al.*, 2013](#)), its precise role in regulating gene transcription during embryo development is unknown. Future experiments assessing the effect of methionine on the embryonic methylome could employ oxidative bisulphite sequencing ([Booth *et al.*, 2013](#)) to elucidate the function and interplay between 5mC and 5hmC modifications during early development.

Chapter 5

Donor cell type and epigenetic reprogramming of cloned sheep hepatocytes

5.1 Introduction

July 2021 will mark the 25th anniversary of the birth of 'Dolly', the first mammal to be cloned from an adult cell by somatic cell nuclear transfer (SCNT; [Wilmut *et al.*, 1997](#)). The potential of SCNT to induce pluripotency in terminally differentiated cells has since been demonstrated in more than 20 mammalian species ([Matoba and Zhang, 2018](#)), including human cells ([Tachibana *et al.*, 2013](#); [Yamada *et al.*, 2014](#)). Aside basic research, SCNT has many applications that promise to benefit livestock production and regenerative medicine, such as reproductive and therapeutic cloning (i.e. transgenic animal and autologous stem cell production) ([Niemann and Lucas-Hahn, 2012](#); Figure 5.1).

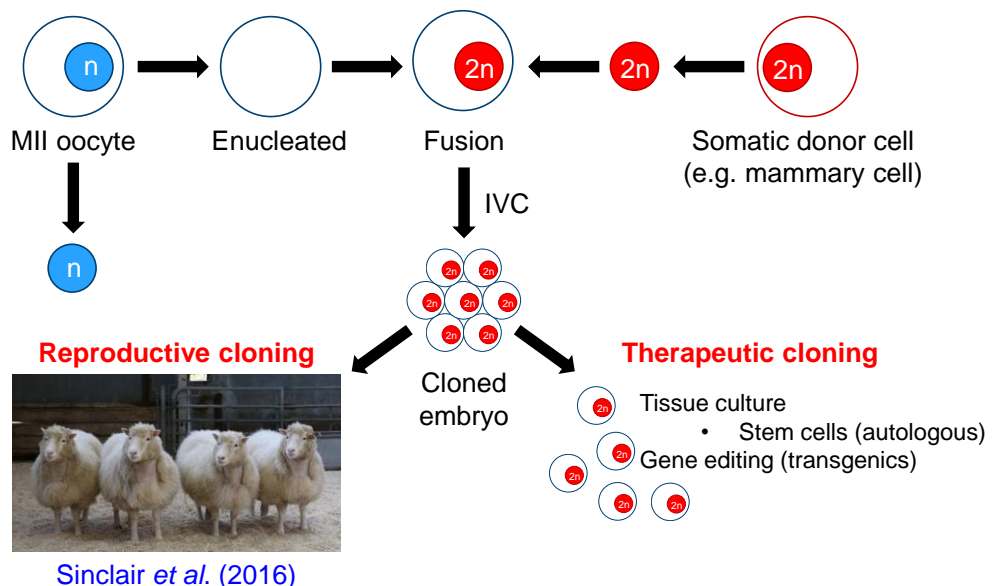


Figure 5.1 Procedure and potential applications of somatic cell nuclear transfer (SCNT).

Abbreviation(s): 2n, diploid; IVC, *in vitro* culture; MII, metaphase II; n, haploid.

Despite recent technological advances in SCNT ([Ogura *et al.*, 2013](#)), its practical use is limited by low efficiency (1-5%; [Gouveia *et al.*, 2020](#); [Wang *et al.*, 2020](#)) which is exemplified by early pregnancy and/or perinatal losses of reconstructed cloned embryos ([Hill *et al.*, 1999](#); [Rhind *et al.*, 2003](#)). Incomplete epigenetic reprogramming of somatic cell nuclei leads to aberrant DNA methylation ([Wang *et al.*, 2020](#)). Studies have reported that cloned embryos only partially demethylate their genomes and begin the *de novo* methylation process earlier than their *in vivo*-derived counterparts, which means that donor cell methylation is maintained ([Dean *et al.*, 2001](#); [Kang *et al.*, 2003](#)). This can

result in the continuous expression of tissue-specific genes and inefficient activation of genes critical for embryonic development, thereby reducing the developmental competence of cloned embryos (Peat and Reik, 2012; Niemann, 2016). Epigenetic perturbations associated with SCNT may contribute to embryonic mortality and congenital abnormalities in offspring. Such abnormalities include organ defects (e.g. kidney and heart), enlarged placentomes and enlarged umbilical cords, high-birth weight and LOS (Kang *et al.*, 2003; Rhind *et al.*, 2003; Smith *et al.*, 2012). As discussed in Chapter 4 (Section 4.3.2.5), there is an association between SCNT, aberrant methylation of imprinted genes and LOS in ruminant fetuses. By way of illustration, loss of methylation at *IGF2R* DMR2 is correlated with aberrant *IGF2R* expression in tissues derived from cloned sheep and cattle (Young *et al.*, 2001; Chen *et al.*, 2017).

Several factors are believed to affect the efficiency of epigenetic reprogramming following SCNT. Such factors include oocyte source and quality; cell cycle synchronisation between donor cells and recipient oocytes; timing of fusion and activation; *in vitro* embryo culture conditions of the reconstructed cloned embryo; and, donor cell type (Campbell and Alberio, 2003; Kato and Tsunoda, 2010; Akagi *et al.*, 2014). Various different somatic cell types have been used for nuclear transfer, including mammary epithelial cells (Wilmut *et al.*, 1997), fetal fibroblasts (Rathbone *et al.*, 2010), sertoli cells (Ogura *et al.*, 2000), ovarian cumulus cells, macrophages (Wakayama and Yanagimachi, 2001) and leukocytes (Galli *et al.*, 1999). However, there is limited information available with regard to the effect of donor cell type on cloning efficiency.

The epigenetic status of the donor cell genome, which encompasses a tissue-specific DNA methylome and chromatin structure, varies according to cell phenotype and genotype (Inoue *et al.*, 2003). In support of comparative mouse cloning experiments that used early blastomeres, ESCs and terminally differentiated cells (Oback and Wells, 2007), it has been postulated that nuclear reprogramming and cloning efficiency can be increased by selecting less terminally differentiated cell types as nuclear donors. For example, the reprogrammability of early blastocysts appears to be higher than that of somatic cells (Oback and Wells, 2007). It has not been determined conclusively whether differentiation status of the donor cell affects efficiency of epigenetic reprogramming after SCNT. The present study, therefore, sought to investigate the effect of donor cell type on cloning efficiency by measuring DNA methylation

in hepatocytes isolated from cloned Finn Dorset (D) and Lleyn (L) sheep derived from mammary epithelial (OP5) and fetal fibroblast (LFF4) donor cells, respectively. Finn Dorset and L sheep breeds were selected as they have both been used for SCNT experimentation and were used to investigate the healthy ageing of cloned sheep (Sinclair *et al.*, 2016). Three experimental comparisons assessed cytosine methylation reprogramming between: i) hepatocytes derived from cloned sheep (DvL); ii) Finn Dorset hepatocytes and their mammary epithelial donor cell line (DvOP5); and, iii) Lleyn hepatocytes and their fetal fibroblast donor cell line (LvLFF4).

5.2 Materials and methods

5.2.1 Animals, treatments and tissue collection

All procedures were conducted in accordance with the requirements of the UK Home Office Animals (Scientific Procedures) Act (1986) and were approved by the University of Nottingham Animal Welfare and Ethical Review Board.

Animals used for this study were the same as those used to assess the healthy ageing of cloned sheep by Sinclair *et al.* (2016). Four Finn-Dorset clones (D1 to D4) born in July 2007 were derived from the same mammary epithelial cell line (OP5) used as the somatic cell nuclear donor for the cloning of 'Dolly', as reported by Wilmut *et al.* (1997). Five Lleyn clones (L1 to L5) born in June 2008 were derived from the primary fetal fibroblast cell line (LFF4), as reported by Rathbone *et al.* (2010).

5.2.1.1 Donor cell culture

Ovine mammary epithelial cells were isolated from a 6-year-old Finn Dorset ewe in the last trimester of pregnancy and cultured for three to six passages in TCM199 and F12 (supplemented with mammogenic hormones) before use as OP5 somatic cell nuclear donors (Finch *et al.*, 1996; Wilmut *et al.*, 1997). Ovine primary fetal fibroblasts were isolated from a Day 30 fetus obtained from a purebred Lleyn ewe and cultured for two passages in Dulbecco's modified eagle's medium (DMEM) supplemented with FCS before use as LFF4 somatic cell nuclear donors (Rathbone *et al.*, 2010).

5.2.1.2 Somatic cell nuclear transfer (SCNT)

All procedures were based on those of [Campbell *et al.* \(1996\)](#). Briefly, MII arrested oocytes were stripped of cumulus cells by vortexing, washed in SOF HEPES holding medium and enucleated using a glass micropipette. Enucleated oocytes were cultured in maturation medium supplemented with 10 mmol/L caffeine for 6 h (18-24 h post-onset of maturation). At 24 h post-onset of maturation, somatic donor cell nuclei (OP5 or LFF4) were fused with an enucleated oocyte using two DC pulses. Fused couplets were activated by a 5 min exposure to 5 mmol/L calcium ionophore and a 5 h incubation in modified SOF medium. After activation, reconstructed embryos were cultured under mineral oil in pre-equilibrated SOF culture medium (39°C, 5% CO₂/5% O₂). Cleavage was assessed on Day 2 and blastocyst development on Day 7. Up to three blastocysts were surgically transferred into the uterus of synchronised surrogate ewes. The genetic identity of cloned offspring was confirmed using 21 microsatellite markers, including those recommended by the International Society of Animal Genetics ([Sinclair *et al.*, 2016](#)).

5.2.1.3 Isolation of hepatocytes

Fresh liver samples were harvested immediately following the slaughter of cloned Finn Dorset (D; $n=4$) and Lleyn (L; $n=5$) ewes. Primary ovine hepatocytes were isolated using a two-step collagenase perfusion method based on the method of [Shibany *et al.* \(2016\)](#). For D clones, the average cell yield was $15.3 \pm 2.05 \times 10^7$ cells/g perfused liver tissue, and the viability and purity of cell samples were $94.6 \pm 1.47\%$ and $97.4 \pm 0.41\%$, respectively. For L clones, the average cell yield was $99.2 \pm 9.14 \times 10^6$ cells/g perfused liver tissue, and the viability and purity of cell samples were $96.6 \pm 0.44\%$ and $97.1 \pm 0.78\%$, respectively.

5.2.2 DNA methylation analysis

Reduced representation bisulphite sequencing (RRBS) was conducted to measure cytosine (CpG) methylation in hepatocytes isolated from cloned Finn Dorset (D) and Lleyn (L) sheep, and their respective somatic donor cell lines (OP5 and LFF4). The RRBS method employed was similar to that described in Chapter 4 (Section 4.2.4) but with the following modifications. DNA was extracted from homogenised hepatocyte cell samples and somatic donor cell lines using the Qiagen DNeasy kit. For each sample, DNA was eluted in 150 μ L EB buffer and concentrated by ethanol precipitation. Briefly, 405 μ L ice cold ethanol (100% v/v) and 13.5 μ L sodium acetate (3M) was added to each DNA sample and the contents were incubated at -80°C for 1 hour. Samples were centrifuged for 20 min at 13,000 $\times g$ in the cold room. The supernatant was removed, washed with 500 μ L ethanol (75% v/v) twice. The samples were centrifuged for 20 min at 13,000 $\times g$ after each wash. The supernatant was removed and the DNA pellet was air-dried until clear for 10-15 min at room temperature. The pellet was resuspended in 25 μ L RNase free water and stored 20°C until bisulphite conversion. Full details of working and stock solutions and methods used for Msp1 restriction enzyme digestion, end-repair and dA tailing, adapter ligation, bisulphite conversion and RRBS library preparation are listed in Appendix 5.1.

5.2.2.1 Library quality control (QC)

Quality control, pooling and next-generation sequencing of bisulphite converted DNA samples was conducted by Deep Seq (The University of Nottingham, UK). DNA concentration, quality and integrity were confirmed using the Agilent TapeStation. Libraries were pooled and amplified DNA fragments of 200-400 bp were size-selected and primer adapters removed using the BluePippin system.

5.2.2.2 Multiplex sequencing

The final 11 quality-ensured libraries were multiplexed and sequenced on an Illumina NextSeq 500 to achieve an average of ~33 million 75 bp paired-end reads. Data were de-multiplexed with bcl2fastq conversion software and quality control was conducted using Sequencing Analysis Viewer (SAV) and FASTQC

(Babraham Bioinformatics) software. Sequences met the standard Illumina quality criteria of cluster density, pass filter and quality scores (Q), and were converted to FASTQ files using standard Illumina pipeline (Aspera software).

5.2.2.3 Bioinformatic Data Analysis

Analysis was conducted as described in Chapter 4 (Section 4.2.4.4) but with the following modifications. Briefly, raw paired-end FASTQ files were trimmed to remove adapter sequences and low quality bases (-Q 20, -q 3) and reads were aligned to the *Ovis aries* reference genome (Oar v3.1, April 2012) using bisulphite read mapper with default settings (Bowtie2; [Krueger and Andrews, 2011](#); Table 5.1). Duplicate reads were marked and methylation values extracted as described above (Section 4.2.4.4). To avoid identification of methylation differences that are related to Finn Dorset and Lleyn breed differences, bases at known variant positions (SNPs) were removed. Differentially methylated sites (DMS) between groups were identified and results were filtered for a 'minimum difference threshold of 10% methylation' between experimental combinations.

Table 5.1 Summary of Bismark final alignment report.

Replicate	Hepatocytes		Donor cell	
	Finn Dorset (D)	Lleyn (L)	Mammary (OP5)	Fibroblast (LFF4)
1	26,934,703 ^a	23,161,065 ^a	11,447,143 ^a	104,679,515 ^a
	11,918,193 ^b	9,841,851 ^b	10,088,425 ^b	48,790,696 ^b
	(44.2) ^c	(42.5) ^c	(44.9) ^c	(46.6) ^c
2	24,237,849 ^a	31,918,792 ^a	-	-
	11,534,956 ^b	14,447,491 ^b	-	-
	(47.6) ^c	(45.3) ^c	-	-
3	30,487,827 ^a	26,430,474 ^a	-	-
	14,787,691 ^b	10,552,266 ^b	-	-
	(48.5) ^c	(39.9) ^c	-	-
4	30,408,350 ^a	26,693,119 ^a	-	-
	13,827,199 ^b	11,803,131 ^b	-	-
	(45.5) ^c	(44.2) ^c	-	-
5	-	27,433,294 ^a	-	-
	-	12,286,345 ^b	-	-
	-	(44.8) ^c	-	-

Total sequence pairs read following quality trimming^a. Number of paired alignments with unique best hit^b. Mapping efficiency (%): measure of the sequence pairs that map uniquely to the reference genome^c.

5.2.2.3.1 Gene set enrichment analysis (GSEA)

Enrichment of gene ontologies (GO) was performed using hypergeometric tests in the (Not) Ingenuity Pathway Analysis (NIPA) tool (<https://github.com/ADAC-UoN/NIPA>). As before, genes that possessed clusters of DMS (≥ 5 DMS within a sliding window size of 1 kb) were selected for gene set enrichment analysis (GSEA). A total of 545 clusters of DMS in 409 genes were identified between Finn Dorset and Lleyn hepatocytes (DvL); 7,846 clusters of DMS in 3,569 genes were identified between Finn Dorset hepatocytes and their mammary epithelial donor cell line (DvOP5); and, 10,581 clusters of DMS in 4,486 genes were identified between Lleyn hepatocytes and their fetal fibroblast donor cell line (LvLFF4). Annotated pathways associated with 'Biological Process', 'Cellular Component' and 'Molecular Function' GO terms were identified as significant based on functional enrichment of genes with clusters of differentially methylated sites (DMS).

5.2.3 Statistical data analysis

Differentially methylated sites (DMS) between experimental comparisons and sliding windows were identified using the Chi-squared test. Gene ontology terms with an FDR adjusted P -value ≤ 0.05 were deemed statistically significant. Differences in mean methylation (%) of genes between isolated hepatocytes and founder somatic cells for each clonal group were determined using linear mixed model (REML) analysis within Genstat. The fixed model included the terms 'Dolly' (Finn Dorset) and 'Lleyn' for comparisons of differential methylation between each founder cell line and their respective clonal population of isolated hepatocytes, and the random model included individual DMS. These data are presented as means with SEM.

5.3 Results and Discussion

5.3.1 Overall CpG methylation

RRBS analyses identified a total of 609,854 CpGs in all samples (D, L, OP5 and LFF4), of which 547,719 CpGs were identified as methylated (Figure 5.2). The majority of CpGs ($n=336,128$) were methylated to some degree in all four cell types, however, a subset of methylated CpGs were unique to each cell type, thereby highlighting the presence of cell type-specific DNA methylation signatures (Varley *et al.*, 2013). The fetal skin fibroblast (LFF4) cell line had the greatest number of methylated CpGs ($n=472,897$), whereas the mammary epithelial cell line (OP5) had the lowest number ($n=377,669$). The number of methylated CpGs was greater in Lleyn than Finn Dorset hepatocytes (463,410 v 459,795, respectively). This modest difference in global methylation between hepatocytes derived from D and L clones could be due to genotype (DvL) or the donor cell line (OP5vLFF4) from which they were derived.

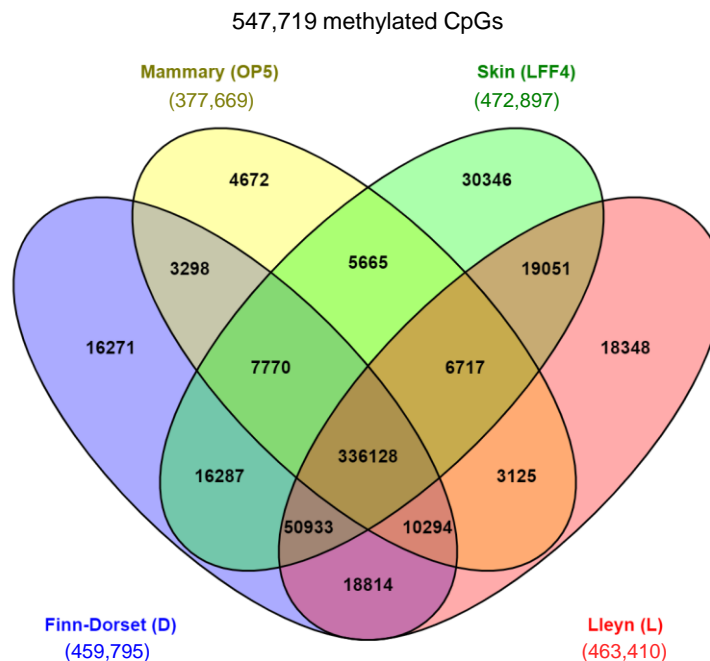


Figure 5.2 Distribution of methylated CpGs across hepatocyte cell samples derived from cloned Finn Dorset (D) and Lleyn (L) sheep, and their respective somatic donor cell lines.

Source: Venny 2.1.0, bioinfogp (<https://bioinfogp.cnb.csic.es/tools/venny/index.html>). Number of methylated CpGs in parentheses.

Pearson correlation coefficients were established for comparisons between samples using percent methylation values (Figure 5.3). Methylation was most strongly correlated (0.951) between hepatocytes isolated from D clones, closely followed by L clones (0.942; Figure 5.3A). Finn Dorset and L clone hepatocytes were more highly correlated (0.936) with one another than they were with their respective donor cell lines (D v OP5: 0.793; L v LLF4: 0.826). Taken together, these findings suggest that global CpG methylation is largely influenced by cell phenotype and function rather than epigenetic reprogramming following nuclear transfer.

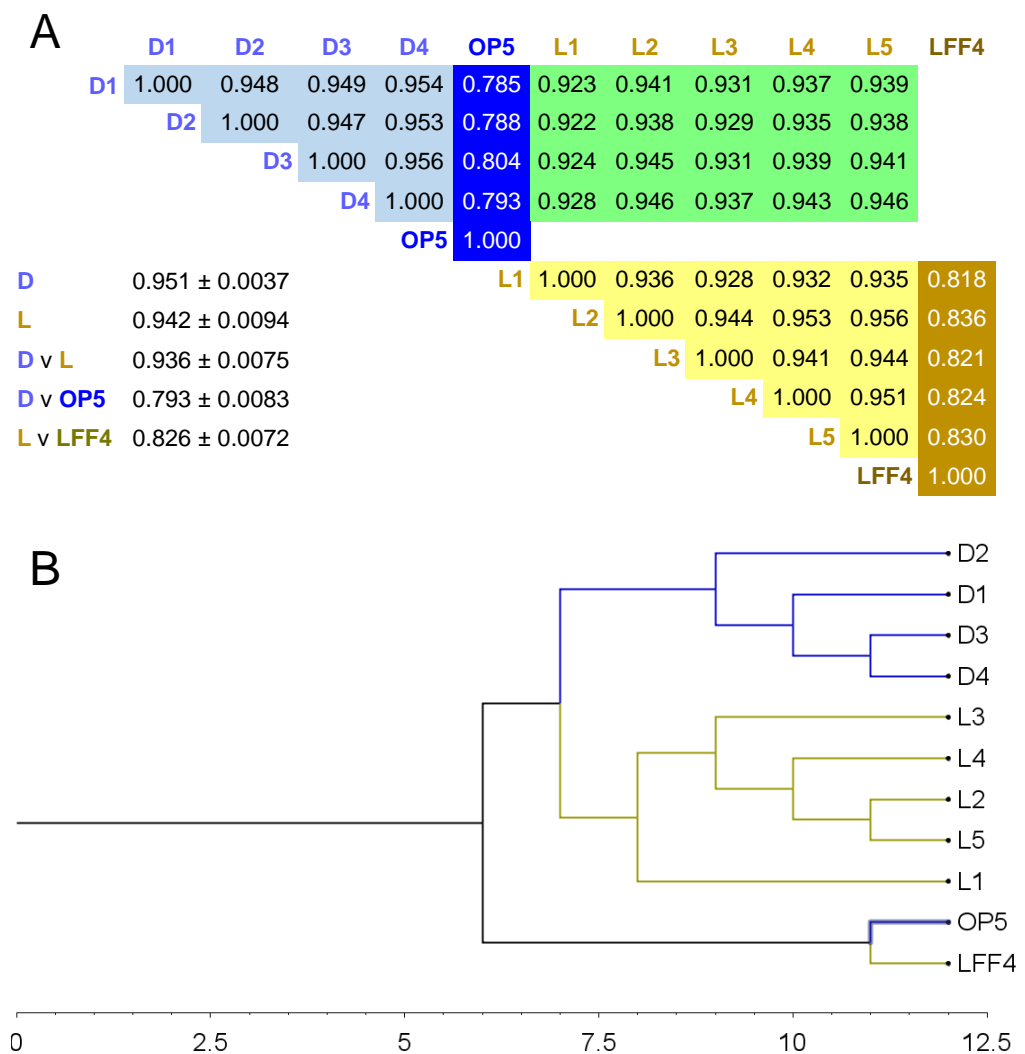


Figure 5.3 Correlation of CpG methylation (%) between cell samples ($n=11$).

Correlation matrix shows conservation of methylated CpGs between hepatocytes isolated from cloned sheep and their derivative cell lines (**A**). Cladogram plot shows clustering of cell types based on methylation similarity (**B**). Abbreviation(s): D1 to D4, Finn-Dorset clone hepatocyte samples; L1 to L5, Lley clone hepatocyte cell samples; LFF4, Lley fetal fibroblast; OP5, mammary donor cell line.

5.3.2 Directional methylation

Table 5.2 shows the number of CpGs and genes that were differentially methylated between D and L clone hepatocytes, and their respective donor cell lines at the 10% minimum difference threshold. It was not surprising that the hepatocytes shared the lowest count of DMS ($n=22,984$) and differentially methylated genes ($n=8,047$) given that they are the same cell type. As stated earlier, differential methylation of CpGs between D and L clone hepatocytes is confounded by difference in genotype (DvL) and donor cell line (OP5vLFF4).

There was a greater number of DMS and differentially methylated genes between L hepatocytes and their LFF4 donor cell line, than between D hepatocytes and their OP5 donor cell line (Table 5.2). Such findings suggest that the level of CpG methylation within the mammary epithelial cells is more similar to those of clone hepatocytes than is the case for the fetal fibroblasts. In both comparisons, a higher percentage of DMS are hypomethylated in clone hepatocytes relative to the donor cell line (DvOP5: 54.9% and LvLFF4: 62.1%, respectively) demonstrating that, in general, these somatic donor cells lose methylation during epigenetic reprogramming to become hepatocytes.

Table 5.2 A count of differentially methylated sites (DMS) and genes, and directional methylation for each experimental combination (%).

Variable	<u>D</u> v L	<u>D</u> v OP5	<u>L</u> v LFF4
DMS count	22,984	112,937	152,869
↑ Methylation	10,134 (44.1)	50,934 (45.1)	57,935 (37.9)
↓ Methylation	12,850 (55.9)	62,003 (54.9)	94,934 (62.1)
Genes	8,047	13,966	15,807

Arrows represent direction of methylation (hypermethylation, ↑; hypomethylation, ↓) in cell sample as represented by underlined abbreviation (D relative to L/OP5, and L relative to LFF4). Abbreviation(s): Differentially methylated site, DMS; Finn Dorset (D); Lley (L); LFF4, Lley fetal fibroblast; OP5, mammary donor cell line.

5.3.3 Distribution of DMS

A similar genomic distribution pattern of CpG methylation was observed across experimental comparisons. Around 8-9% of DMS were located in gene promoters, 13-15% were located in exons and 34-39% were located in introns. Around ~17% of DMS were located in CGIs and ~23% were located in CGI shores (Table 5.3). As discussed in Chapter 4 (Section 4.3.2.3), this pattern of methylation is commonly observed in studies using RRBS due to basic gene anatomy and the method of DNA methylation analysis which enriches a representative sample of the genome. The percentages of hyper- and hypomethylated CpGs were similar for each genomic region studied (Table 5.3).

Table 5.3 Distribution of differentially methylated sites (DMS) for each experimental combination (%).

Region	<u>D</u> v L	<u>D</u> v OP5	<u>L</u> v LFF4
Promoter	1,874 (8.2)	9,800 (8.7)	13,486 (8.8)
↑ Methylation	833 (44.5)	3,621 (36.9)	3,600 (26.7)
↓ Methylation	1,041 (55.5)	6,179 (63.1)	9,886 (73.3)
Exonic	3,366 (14.6)	15,182 (13.4)	21,021 (13.8)
↑ Methylation	1,378 (40.9)	5,533 (36.4)	6,327 (30.1)
↓ Methylation	1,988 (59.1)	9,649 (63.6)	14,694 (69.9)
Intronic	8,874 (38.6)	42,337 (37.5)	58,329 (38.2)
↑ Methylation	3,646 (41.1)	18,467 (43.6)	22,896 (39.3)
↓ Methylation	5,228 (58.9)	23,870 (56.4)	35,433 (60.7)
CGIs	4,005 (17.4)	20,103 (17.8)	24,728 (16.2)
↑ Methylation	1,903 (47.5)	7,008 (34.9)	6,303 (25.5)
↓ Methylation	2,102 (52.5)	13,095 (65.1)	18,425 (74.5)
CGI shores	5,123 (22.3)	26,151 (23.1)	34,946 (22.9)
↑ Methylation	2,014 (39.3)	11,274 (43.1)	12,393 (35.5)
↓ Methylation	3,109 (60.7)	14,877 (56.9)	22,553 (64.5)

Arrows represent direction of methylation (hypermethylation, ↑; hypomethylation, ↓) in cell sample as represented by underlined abbreviation (D relative to L/OP5, and L relative to LFF4). Abbreviation(s): Differentially methylated site, DMS; Finn Dorset (D); Lleyn (L); LFF4, Lleyn fetal fibroblast; OP5, mammary donor cell line.

5.3.4 Enriched pathways and genes

The flowchart summarises the systematic methodology of GSEA and the selection of GOI for comparative methylation analysis (Figure 5.4). As clusters of methylated CpGs appear to be important for the regulation of gene transcription (Li and Zhang, 2014), genes that possessed ≥ 5 DMS within 1 kb were selected for GSEA (DvOP5: 3,569 genes; LvLFF4: 4,486 genes).

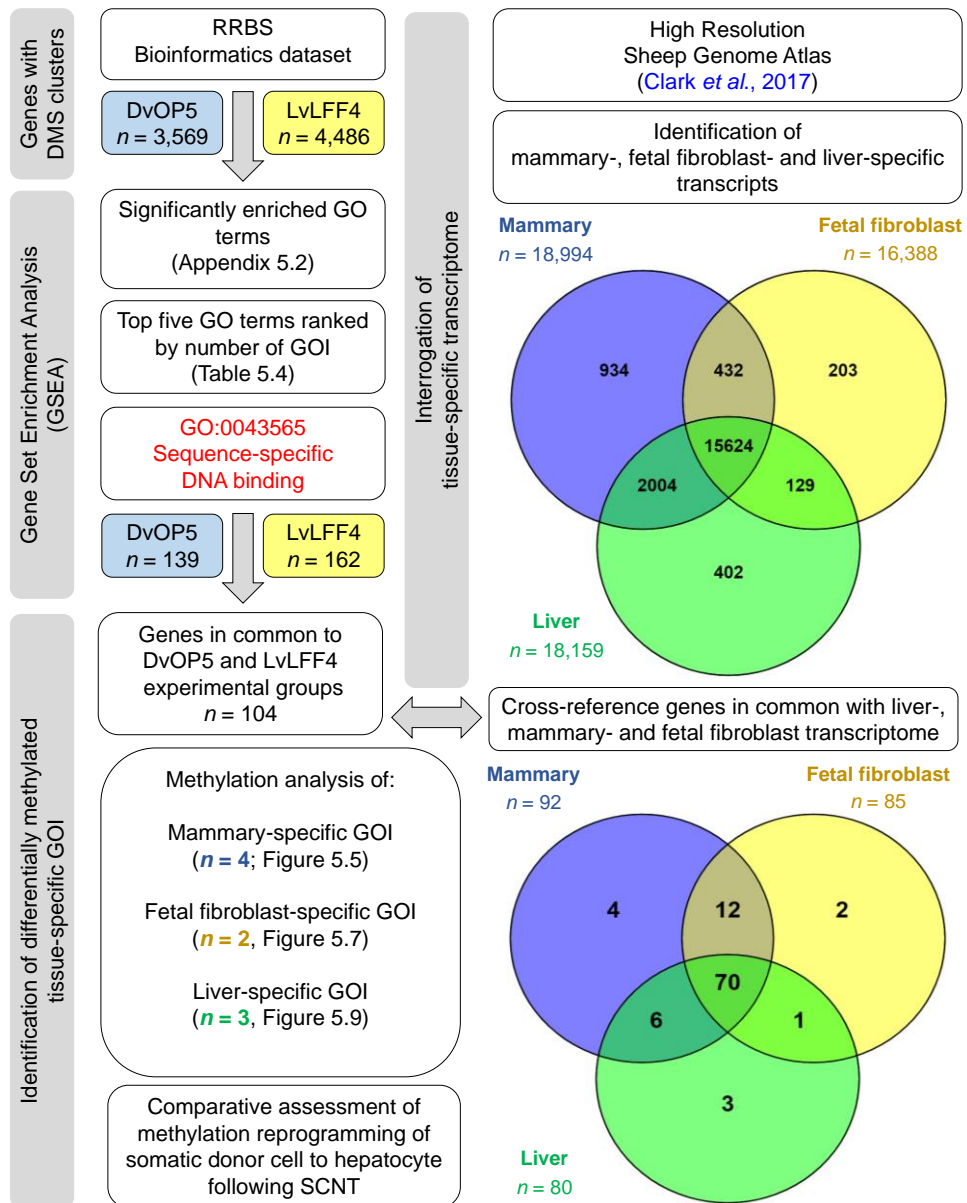


Figure 5.4 Flowchart of the methodology used to select differentially methylated tissue-specific genes ($n=9$) between donor cell lines and clone hepatocytes.

Mammary-specific genes ($n=4$); fetal fibroblast-specific genes ($n=2$); liver-specific genes ($n=3$) were selected for detailed methylation analysis. Abbreviation(s): D, Finn Dorset; DMS, differentially methylated site; GO, gene ontology; GOI, genes of interest; L, Lley; LFF4, Lley fetal fibroblast; OP5, mammary donor cell line; RRBS, reduced representation bisulphite sequencing; SCNT, somatic cell nuclear transfer.

All GO terms associated with 'Biological Process', 'Cellular Component' and 'Molecular Function' significantly enriched within DvOP5 and LvLFF4 experimental comparisons are presented in Appendix 5.2. The top five terms were ranked by number of GOI (Table 5.4). Biological Process GO terms with the greatest number of differentially methylated GOI were involved in 'anterior/posterior pattern specification' (33 GOI) and 'Negative regulation of fat cell differentiation' (15 GOI) for DvOP5 and LvLFF4 experimental comparisons, respectively (Table 5.4A).

The 'Sequence-specific DNA binding' Molecular Function GO term was selected for further investigation as it was significantly enriched in both experimental comparisons and comprised a high number of differentially methylated GOI (DvOP5: 139 genes, LvLFF4: 162 genes; Table 5.4C). Of those GOI, 104 genes were common to both DvOP5 and LvLFF4 comparisons (Appendix 5.3). Due to the high number of common genes, a reductionist approach was taken to minimise the number of genes to a manageable list for comparative methylation analysis. In order to do so, common genes ($n=104$) were cross-referenced with the 'high resolution atlas of gene expression in the domestic sheep (*Ovis aries*)' published by the Roslin Institute, Edinburgh, UK (Clark *et al.*, 2017; Dataset S2: <https://doi.org/10.1371/journal.pgen.1006997.s005>).

Interrogation of the atlas revealed 18,994 genes expressed in the mammary gland of an adult Texel ewe; 16,388 genes expressed in the 35 Day Texel x Scottish Blackface (TxBF) sheep fetal fibroblast; and 18,159 genes expressed in the adult Texel liver. Of those, 934 genes were specific to the mammary gland; 203 genes were specific to the fetal fibroblast; and, 402 genes were specific to the liver (Figure 5.4). Although transcriptomic differences between sheep genotypes (e.g. Finn Dorset v Texel and Lleyn v TxBF) were expected, the tissue-specific transcriptome data published by Clark *et al.* (2017) provided suitable gene candidates for comparative DNA methylation analysis in the present study.

Of those 104 common genes enriched within the 'Sequence-specific DNA binding' GO term, 92 are expressed in the mammary gland; 85 in the fetal fibroblast; and, 80 in the liver (Figure 5.4). Tissue-specific genes were selected to compare methylation reprogramming between clone hepatocytes and their respective donor cell lines (mammary, $n=4$; fetal fibroblast, $n=2$; liver, $n=3$) based on the hypothesis that expressed genes would exhibit a different degree and pattern of methylation than genes repressed in specific-tissues.

Table 5.4 Top five enriched Gene Ontology (GO) terms ranked by number of differentially methylated genes of interest (GOI).

A. Biological Process GO

Finn-Dorset (D) v OP5 cell line (n=186)			Lleyln (L) v LFF4 cell line (n=193)				
	GOI	FDR (q-value)		GOI	FDR (q-value)		
GO:0009952	Anterior/posterior patterning	33	0.0019	GO:0045599	Regulation of fat cell differentiation	15	0.0471
GO:0060021	Roof of mouth development	21	0.0275	GO:0035115	Embryonic forelimb morphogenesis	13	0.0435
GO:0042472	Inner ear morphogenesis	19	0.0060	GO:0010596	Endothelial cell differentiation	11	0.0050
GO:0006909	Phagocytosis	15	0.0403	GO:0030878	Thyroid gland development	10	0.0426
GO:0001656	Metanephros development	14	0.0001	GO:0032331	Chondrocyte differentiation	9	0.0255

B. Cellular Component

Finn-Dorset (D) v OP5 cell line (n=7)			Lleyln (L) v LFF4 cell line (n=12)				
	GOI	FDR (q-value)		GOI	FDR (q-value)		
GO:0044309	Neurone spine	3	0.04782	GO:0033093	Weibel-Palade body	3	0.0000
GO:0098839	Postsynaptic density membrane	3	0.04782	GO:0035976	TF AP-1 complex	3	0.0000
GO:0005610	Laminin-5 complex	2	0.0000	GO:0005608	Laminin-3 complex	2	0.0000
GO:0005899	Insulin receptor complex	2	0.0000	GO:0005899	Insulin receptor complex	2	0.0000
GO:0031095	Platelet dense tubular network	2	0.0000	GO:0017109	Glutamate-cysteine ligase complex	2	0.0000

C. Molecular Function

Finn-Dorset (D) v OP5 cell line (n=30)			Lleyln (L) v LFF4 cell line (n=43)				
	GOI	FDR (q-value)		GOI	FDR (q-value)		
GO:0003700	DNA binding TF activity	160	0.0227	GO:0043565	Sequence-specific DNA binding	162	0.0040
GO:0043565	Sequence-specific DNA binding	139	0.0004	GO:0005089	Rho guanyl-NT exchange factor	14	0.0023
GO:0000981	DNA binding TF activity, RNAPII	37	0.0169	GO:0071889	14-3-3 protein binding	8	0.0380
GO:0005089	Rho guanyl-nucleotide exchange	13	0.0008	GO:0001972	Retanoic acid binding	7	0.0074
GO:0001972	Retanoic acid binding	8	0.0001	GO:0004668	Protein-arginine deaminase activity	5	0.0000

Abbreviation(s): FDR, false discovery rate; GOI, genes of interest; LFF4, Lleyln fetal fibroblast; OP5, mammary donor cell line.

5.3.4.1 Mammary-specific genes

Figure 5.5 shows mammary-specific genes (*POU5F1*, *BARHL2*, *SOX30*, *LMX1A*) enriched within the 'Sequence-specific DNA binding' GO term ranked according to their total number of DMS clusters. In general, DMS within these mammary specific genes were hypermethylated in the OP5 and LFF4 somatic donor cell lines relative to the clone hepatocytes. Furthermore, their degree of hypermethylation was significantly greater in the OP5 mammary cell line relative to the D clone hepatocyte, than in the LFF4 cell line relative to the L clone hepatocyte ($P < 0.001$; Figure 5.5B, Figure 5.5D). The exception to this rule was *LIM Homeobox Transcription Factor 1 Alpha (LMX1A)* which was generally hypermethylated in the D clone hepatocyte relative to the OP5 mammary cell line. Out of 14 DMS identified in the *LMX1A* gene sequence, six DMS located at the 5'-end were hypomethylated in the D clone hepatocyte, whereas eight located towards the 3'-end of were hypermethylated in the D clone hepatocyte relative to the OP5 mammary cell line (Figure 5.5E).

The *POU class 5 homeobox 1 (POU5F1)* gene had the greatest number of DMS clusters ($n=3$) in both DvOP5 and LvLFF4 experimental combinations (Figure 5.5A). The *POU5F1* gene encodes octamer-binding transcription factor-4 (OCT4), a protein that establishes and maintains pluripotency during embryonic development and serves as a core molecular marker of stem cells (Shi and Jin, 2010). Although silenced in the vast majority of terminally differentiated somatic cell types, expression of *POU5F1* is upregulated in the lactating mammary gland, thereby highlighting a potential role of the pluripotency gene network in mammary stem cell self-renewal that drives the remodelling of the gland into a fully mature milk-secretory organ (Hassiotou *et al.*, 2013).

The five-exon structure of *POU5F1* is conserved across mammalian orthologs (Medvedev *et al.*, 2008). However, little is known about epigenetic regulation of *POU5F1* gene expression in sheep, thus, its regulatory regions have not been fully deciphered. The present study found clusters of DMS within the *POU5F1* gene that were located around the exon-intron 1 junction in both DvOP5 and LvLFF4 experimental comparisons (Figure 5.6). A study in rabbit blastocysts reported progressive methylation within the 5' regulatory region and the first exon that accompanied cellular differentiation and the gradual repression of *POU5F1* (Canon *et al.*, 2018). Whilst the biological relevance of this pattern of differential methylation is uncertain in the absence of complementary

transcriptomic data, it follows that methylation within this region may be responsible for the transcriptional regulation of *POU5F1*.

In humans, the *POU5F1* gene comprises three main isoforms (*OCT4A*, *OCT4B* and *OCT4B1*) that are generated by alternative splicing. These variants are different at the 5'-end and identical at the 3'-end as exon 1 is present in *OCT4A* but is spliced in *OCT4B* and *OCT4B1* (Wang and Dai, 2010). If similar *POU5F1* transcript variants exist in sheep, perhaps the sharp transition in methylation that surrounds the exon-intron 1 boundary (Figure 5.6) marks the regulatory region for alternative splicing of the ovine *POU5F1* gene.

5.3.4.2 Fetal fibroblast-specific genes

Figure 5.7 presents the differential methylation of fetal fibroblast-specific genes enriched within the 'Sequence-specific DNA binding' GO term between somatic donor cell lines and clone hepatocytes. *Paired like homeodomain 1 (PITX1)* and *Paired box protein Pax-7 (PAX7)* are transcription factors involved in the reprogramming of fetal fibroblasts into skeletal muscle progenitor cells (Ito et al., 2017). Differentially methylated sites identified within both genes were hypermethylated in the LFF4 donor cell line relative to the L clone hepatocytes (Figure 5.7B, Figure 5.7C). However, DMS within the *PAX7* gene were hypomethylated in the OP5 mammary cell line relative to the D clone hepatocyte (Figure 5.7C).

Methylation analysis of individual DMS across the *PITX1* gene shows that DMS at the 5'-end of the sequence tend to be hypermethylated in the somatic donor cell lines relative to the clone hepatocytes, whilst those at the 3'-end of the sequence tend to be hypomethylated in the donor cells relative to clone hepatocytes (Figure 5.7B, Figure 5.8). This pattern of differential methylation along the gene sequence was similar for both DvOP5 and LvLFF4 experimental comparisons. However, the degree of differential methylation was greater between D and OP5, than between L and LFF4 (Figure 5.7B, Figure 5.8). The observation that CpG methylation was altered in the same direction at common sites for both experimental comparisons suggests that their specific methylation status may be, at least in part, important for cell fate reprogramming to produce hepatocytes irrespective of the somatic donor cell type.

A recent assessment of the DNA methylation profile of the *PITX1* gene in the goat mammary gland revealed that methylation of a CGI located within the 3'-

flanking region of the gene was correlated with lactation performance. A reduction in methylation was observed within this region during lactation, however, the gene was not expressed in the mammary gland during the dry or lactational period (Zhao *et al.*, 2019). Since differential methylation was observed within the 3' region of *PITX1* between the OP5 mammary cell line and D clone hepatocytes in the present study, it is plausible that methylation within this genomic region could provide an epigenetic marker of cell phenotype and function (e.g. indicator of lactational performance) independent of mRNA transcript expression.

Genetic markers in the form of SNPs and copy-number variations have been identified and associated with complex production traits in livestock (König *et al.*, 2009). It is, however, accepted that genomic information alone does not account for all of the heritable variation in traits of interest. A review by Ibeagha-Awemu and Zhao (2015) discusses the potential of epigenetic marker-assisted selection (eMAS) in livestock production programmes. Essentially, this entails the use of stable and transgenerationally inherited epigenetic marks (e.g. DNA methylation) that can be used as prognostic tools for certain phenotypic traits and disease aetiology (Flintoft, 2010). The characterisation of stable and functional epigenetic modifications could not only prove useful for eMAS in selective breeding at the DNA level (Zhao *et al.*, 2019), but may also prove useful targets to further investigate and evaluate the economic, health and wellbeing traits of cloned animals.

5.3.4.3 Liver-specific genes

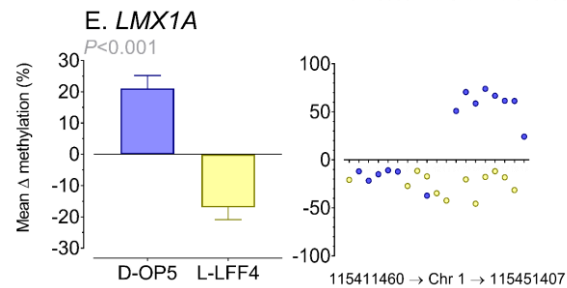
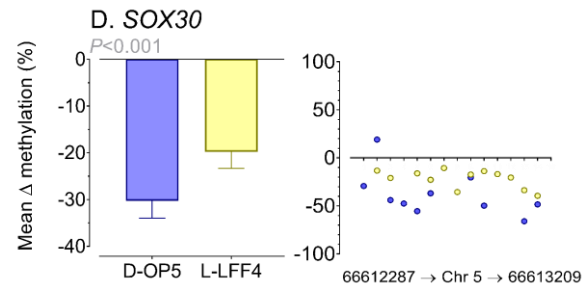
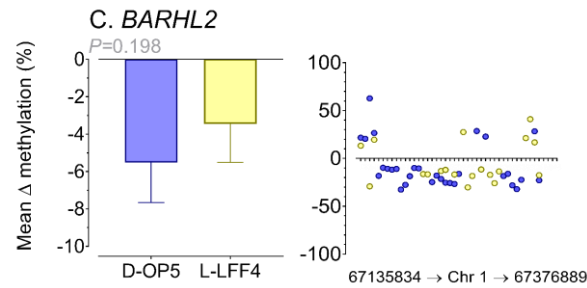
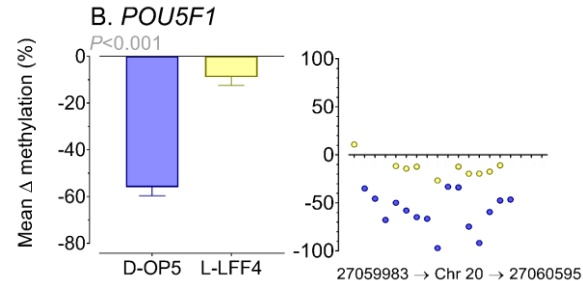
The differential methylation of liver-specific genes between the somatic donor cell lines and clone hepatocytes is presented in Figure 5.9. *Lim homeobox 5* (*LHX5*) is involved in patterning and differentiation of diverse cell types during embryonic development, primarily cells within the central nervous system (Zhao *et al.*, 2000; Figure 5.9D). Forkhead box transcription factors (*FOXA2* and *FOXN4*) are critical for the development of numerous endodermal tissues, including the liver (Lee *et al.*, 2005; Gosalia *et al.*, 2015; Figure 5.9B, Figure 5.9C). In particular, the *Forkhead box A2* (*FOXA2*) is a 'pioneer' transcription factor meaning that it recognises binding sites on nucleosomal DNA and alters chromatin structure to permit the recruitment of downstream transcription factors during endoderm differentiation (Cernilogar *et al.*, 2019).

Differentially methylated sites identified within the *FOXA2* gene were generally hypomethylated in OP5 and LFF4 donor cell lines relative to D and L clone hepatocytes (Figure 5.9B, Figure 5.10). It may seem paradoxical that tissue-specific genes, such as *FOXA2*, that are expressed exclusively in the liver (and not in the mammary cell or fetal fibroblast) have DMS that were hypermethylated in clone hepatocytes but hypomethylated in the OP5 and LFF4 cell lines. An unexpected methylation pattern was also described by [Halpern and others \(2014\)](#), who found a CGI within the promoter region of the human *FOXA2* gene that displayed high levels of methylation in expressing tissues, but low levels in non-expressing tissues. The authors postulated that the lack of CpG methylation permitted the binding of repressive proteins, such as Polycomb complexes, which in turn inhibited *FOXA2* gene expression ([Halpern et al., 2014](#)).

Figure 5.10 shows that the majority of DMS that were hypermethylated in the liver (and hypomethylated in the donor cell line) were common to both experimental comparisons (DvOP5 and LvLFF4) and were located within the exon 2 of the *FOXA2* gene. Whilst it is well-accepted that the enrichment of DNA methylation within gene bodies is positively correlated with gene expression ([Yang et al., 2014](#)), the functional significance of CpG hypermethylation within the final exon of *FOXA2* with respect to gene transcription is unknown.

A. Mammary-specific genes

GOI with DMS clusters (n=4)	DvOP5		LvLFF4	
	Cluster count	DMS count	Cluster count	DMS count
<i>POU5F1</i>	3	15	3	10
<i>BARHL2</i>	3	30	2	19
<i>SOX30</i>	2	10	2	12
<i>LMX1A</i>	1	14	1	12



Data analysed using REML analysis. Bars represent mean \pm SEM. Scatter plots represent mean difference (Δ) in methylation between clone hepatocyte and donor cell line (D-OP5, L-LFF4) at individual DMS in 5' \rightarrow 3' orientation along gene sequence.

Abbreviation(s): BARHL2, BarH Like Homeobox 2 ; Chr, chromosome; D, Finn Dorset; DMS, differentially methylated site; GOI, gene of interest; L, Lley; LFF4, Lley fetal fibroblast; LMX1A, LIM Homeobox Transcription Factor 1 Alpha; OP5, mammary donor cell line; POU5F1, POU class 5 homeobox 1; SOX30, SRY-Box Transcription Factor 30.

Figure 5.5 Differential methylation of mammary-specific genes (n=4) between clone sheep hepatocytes and their somatic donor cell lines.

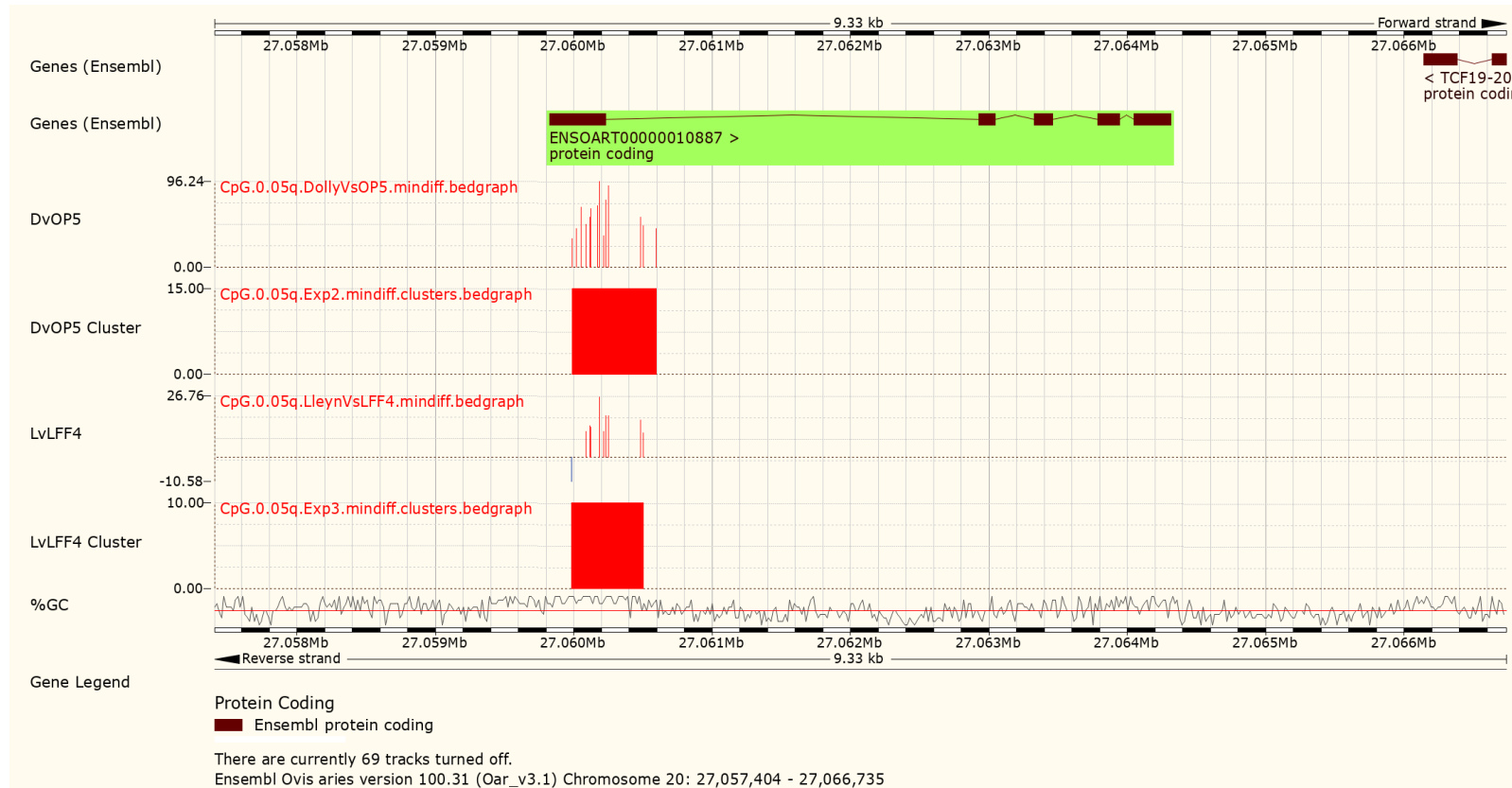
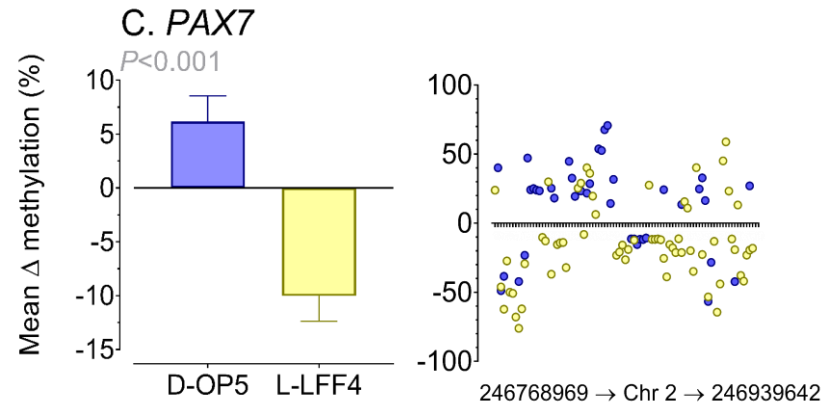
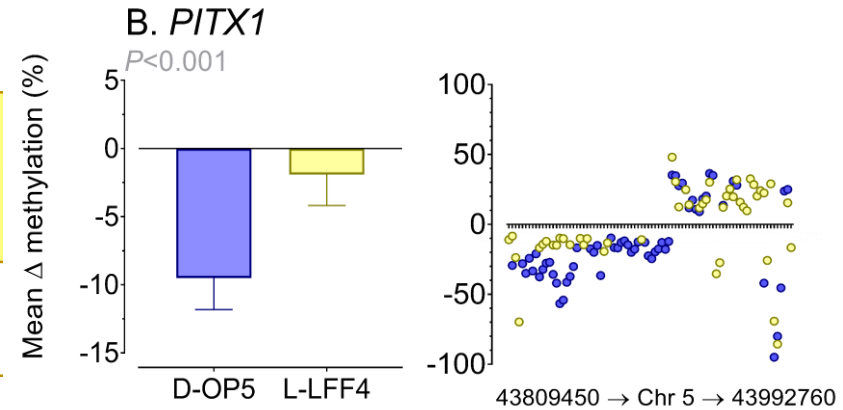


Figure 5.6 Clusters of differentially methylated sites (DMS) in the *POU5F1* gene are hypermethylated in somatic donor cell line (OP5 and LFF4) relative to clone hepatocyte (D and L).

Bedgraphs demonstrate loss (↓, hypomethylation) and gain (↑, hypermethylation) of methylation at individual cytosine residues, and location of DMS clusters (red boxes). Abbreviation(s): D, Finn Dorset; L, Lley; LFF4, Lley fetal fibroblast; OP5, mammary donor cell line; *POU5F1*, *POU* class 5 homeobox 1.

A. Fetal fibroblast-specific genes

GOI with DMS clusters (n=2)	DvOP5		LvLFF4	
	Cluster count	DMS count	Cluster count	DMS count
<i>PITX1</i>	7	61	5	48
<i>PAX7</i>	1	40	6	64



Data analysed using REML analysis. Bars represent mean \pm SEM. Scatter plots represent mean difference (Δ) in methylation between clone hepatocyte and donor cell line (D-OP5, L-LFF4) at individual DMS in 5' \rightarrow 3' orientation along gene sequence.

Abbreviation(s): Chr, chromosome; D, Finn Dorset; DMS, differentially methylated site; GOI, gene of interest; L, Lley; LFF4, Lley fetal fibroblast; OP5, mammary donor cell line; PAX7, Paired Box 7; PITX1, Paired Like Homeodomain 1.

Figure 5.7 Differential methylation of fetal fibroblast-specific genes (n=2) between clone sheep hepatocytes and their somatic donor cell lines.

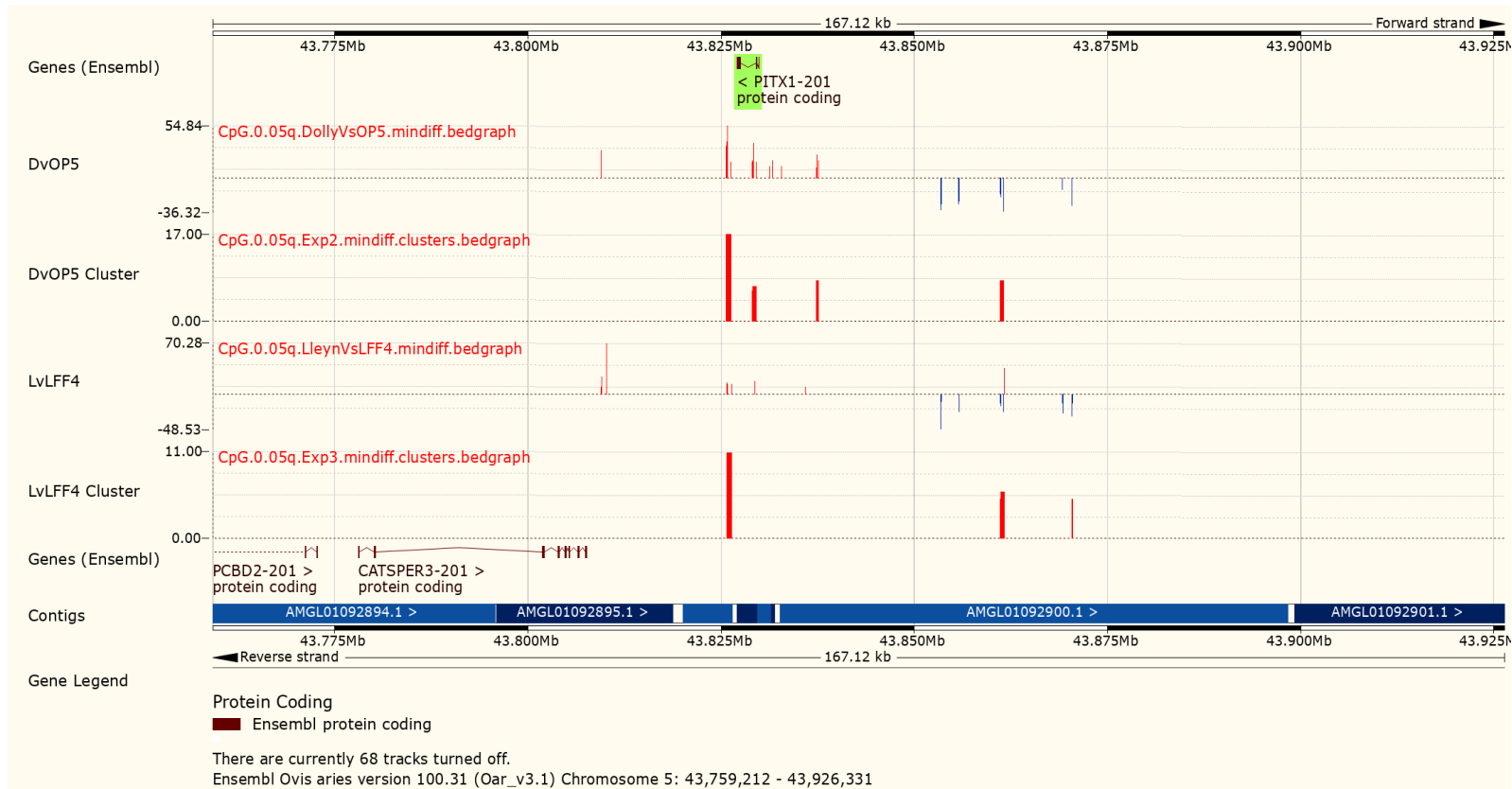


Figure 5.8 Clusters of differentially methylated sites (DMS) in the *PITX1* gene are hypermethylated in somatic donor cell line (OP5 and LFF4) relative to clone hepatocyte (D and L).

Bedgraphs demonstrate loss (↓, hypomethylation) and gain (↑, hypermethylation) of methylation at individual cytosine residues, and location of DMS clusters (red bars). Abbreviation(s): D, Finn Dorset; L, Lley; LFF4, Lley fetal fibroblast; OP5, mammary donor cell line; *PITX1*, Paired like Homeodomain 1.

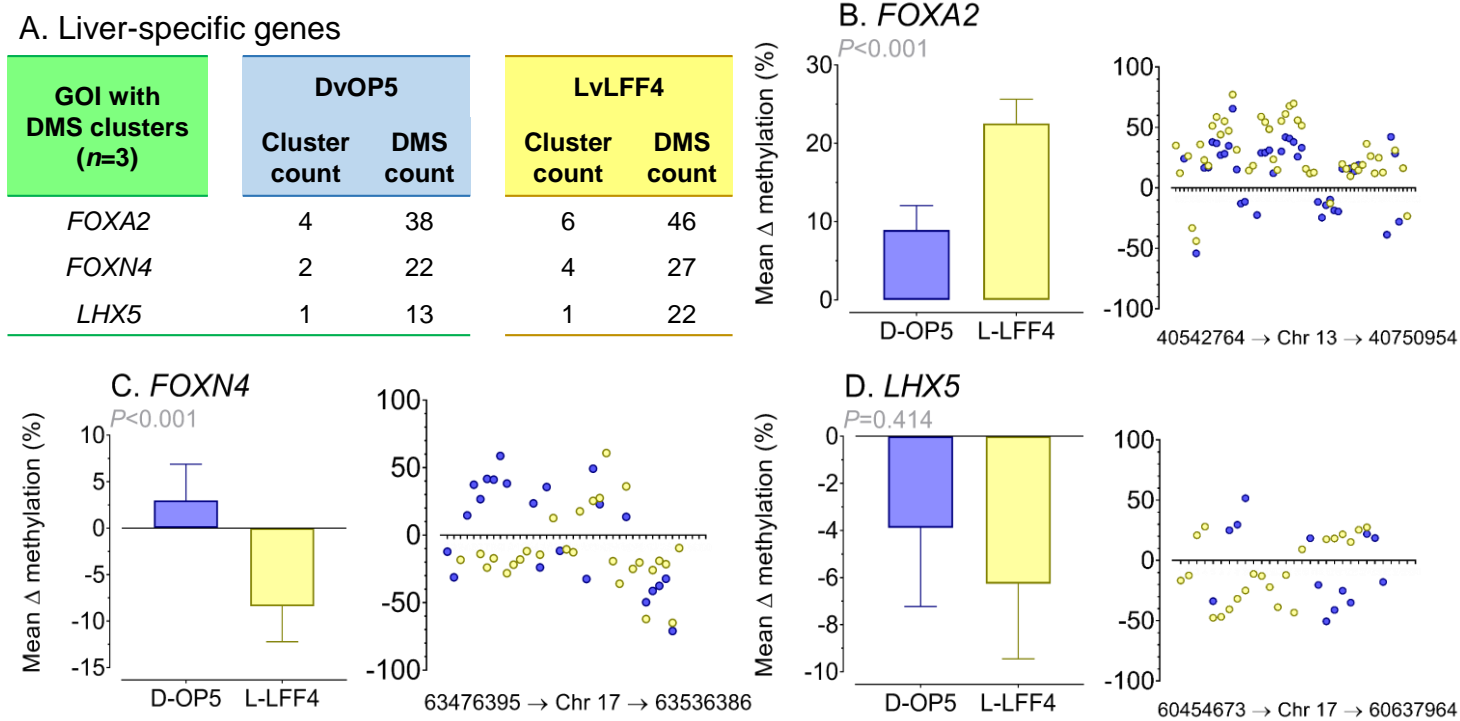


Figure 5.9 Differential methylation of liver-specific genes (n=3) between clone sheep hepatocytes and their somatic donor cell lines.

Data analysed using REML analysis. Bars represent mean \pm SEM. Scatter plots represent mean difference (Δ) in methylation between clone hepatocyte and donor cell line (D-OP5, L-LFF4) at individual DMS in 5' \rightarrow 3' orientation along gene sequence. Abbreviation(s): Chr, chromosome; D, Finn Dorset; DMS, differentially methylated site; FOXA2, Forkhead box protein A2; FOXN4, Forkhead Box N4; GOI, gene of interest; L, Lley; LFF4, Lley fetal fibroblast; LHX5, LIM homeobox 5; OP5, mammary donor cell line.



Figure 5.10 Clusters of differentially methylated sites (DMS) in the FOXA2 gene are hypomethylated in somatic donor cell line (OP5 and LFF4) relative to clone hepatocyte (D and L).

Bedgraphs demonstrate loss (↓, hypomethylation) and gain (↑, hypermethylation) of methylation at individual cytosine residues, and location of DMS clusters ■. Abbreviation(s): D, Finn Dorset; FOXA2, Forkhead Box A2; L, Lley; LFF4, Lley fetal fibroblast; OP5, mammary donor cell line.

5.3.5 Imprinted genes

As referred to earlier (Section 5.1), SCNT has been linked to aberrant methylation of imprinted genes and developmental anomalies in mammalian offspring (Young *et al.*, 2001; Chen *et al.*, 2017). The present study identified 16 genes that are recognised as imprinted in sheep or cattle (Catalogue of Imprinted Genes; <http://igc.otago.ac.nz/home.html>) that were differentially methylated between DvOP5 and/or LvLFF4 experimental comparisons (Table 5.5).

Table 5.5 Imprinted genes in sheep and/or cattle that were differentially methylated between clone hepatocytes and donor cell lines.

Gene	DvOP5		LvLFF4	
	Cluster count	DMS count	Cluster count	DMS count
<i>DLK1</i>	7	65	6	64
<i>GRB10</i>	4	39	9	69
<i>IGF2R</i>	3	41	5	61
<i>SLC6A3</i>	3	28	1	26
<i>IGF2</i>	2	18	5	29
<i>GNAS</i>	1	7	7	39
<i>USP29</i>	1	8	1	8
<i>UBE3A</i>	1	5	1	5
<i>PLAGL1</i>	1	6	-	5
<i>PEG10</i>	-	2	3	23
<i>MKRN3</i>	-	17	2	28
<i>MAGEL2</i>	-	2	1	5
<i>NAP1L5</i>	-	1	-	-
<i>PON3</i>	-	1	-	4
<i>MAGI2</i>	-	1	-	3
<i>NNAT</i>	-	1	-	3

Adapted from the Catalogue of Imprinted Genes (<http://igc.otago.ac.nz/home.html>). Abbreviation(s): D, Finn Dorset; DMS, differentially methylated site; L, Lleyn; LFF4, Lleyn fetal fibroblast; OP5, mammary donor cell line. Imprinted genes with differentially methylated sites (DMS). Paternally imprinted gene (♂), maternally imprinted gene (♀). Genes in white represent 6 of 20 records in ovine catalogue. Genes shaded in grey: 10 of 45 records in bovine catalogue.

Clear differences in CpG methylation of imprinted genes between D clone hepatocytes and their founder OP5 mammary cell line were observed (Figure 5.11A). Likewise, patterns of methylation in imprinted genes were distinct between L clone hepatocytes and the LFF4 cell line (Figure 5.11B). Differences in methylation of imprinted genes between D and L hepatocytes are likely due to differences in genotype (Figure 5.11). As genomic imprinting is species-, tissue- and stage-specific, with some genes partially imprinted in certain tissues (Bebbere *et al.*, 2013; O'Doherty *et al.*, 2015), it is uncertain whether the differential methylation measured between clone hepatocytes and their donor

cell lines had any effect on the imprinted status of these genes in the cell types studied. Moreover, without methylation assessment of positive control hepatocytes isolated from an uncloned (i.e. naturally conceived) Finn Dorset and Lleyen sheep, it was not possible to determine the effect of the SCNT procedure on the methylation status of imprinted genes in the liver of cloned sheep.

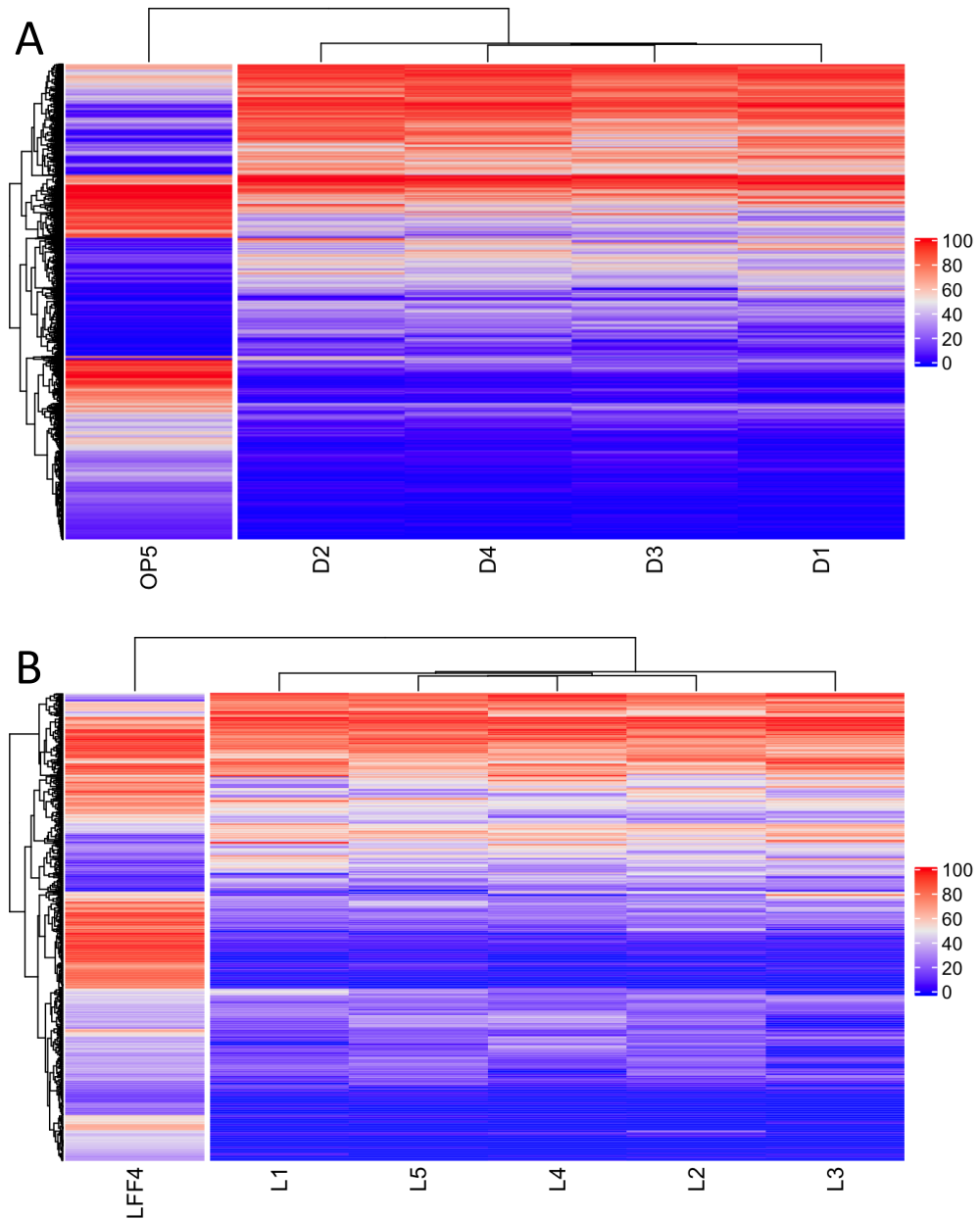


Figure 5.11 CpG methylation levels of imprinted genes ($n=16$) differ between the OP5 donor cell line and D clone hepatocytes (A), and between the LFF4 donor cell line and L clone hepatocytes (B).

Colours indicate methylation level (%) from low (blue) to high (red) of differentially methylated sites (DMS) within imprinted genes enriched within mammary cell (OP5), Lleyen fetal fibroblast (LFF4), Finn Dorset hepatocyte (D) and Lleyen hepatocyte (L).

5.3.5.1 *Delta-like 1 (DLK1)* and *Growth factor receptor bound protein 10 (GRB10)*

Imprinted genes that harboured the greatest number of DMS between DvOP5 and LvLFF4 experimental comparisons were *Delta-like 1 (DLK1)* and *Growth factor receptor bound protein 10 (GRB10)*, respectively (Table 5.5; Figure 5.12). The *DLK1* gene encodes a ligand that promotes fetal growth and restricts adipose deposition, whereas *GRB10* encodes a signalling protein that restricts fetal growth and promotes adipose deposition (Madon-Simon *et al.*, 2014). Both genes are reciprocally imprinted and antagonistically expressed to define a mammalian growth axis independent of the *insulin-like growth factor (IGF)* pathway (Madon-Simon *et al.*, 2014). It follows that genetic and epigenetic dysregulation of these genes can lead to disproportionate fetal growth, and impaired energy metabolism (Charalambous *et al.*, 2003; Madon-Simon *et al.*, 2014). In sheep, a SNP (A-to-G substitution) located within the *DLK1-DIO3* imprinted gene cluster on ovine chromosome 18 imposes a distinct hypomethylation mark in *cis* orientation that leads to long-range intergenic transcription and ectopic expression of *DLK1* in skeletal muscle which, in turn, results in the ‘callipyge’ muscular hypertrophy phenotype (Takeda *et al.*, 2006; O’Doherty *et al.*, 2015). In mice, mutant studies have associated LOI of *DLK1* with adult-onset obesity and metabolic syndrome (Peters, 2014).

Like many imprinted genes, *DLK1* and *GRB10* share complex tissue-specific expression patterns, however, most of the research pertains to studies in mice where both genes are imprinted in the liver (Gagne *et al.*, 2014), embryonic fibroblasts (Tran *et al.*, 2014) and mammary epithelial cells (Cowley *et al.*, 2014; Hanin and Ferguson-Smith, 2020). The present study found that DMS located within the *DLK1* gene were generally hypermethylated in clone hepatocytes relative to their respective donor cell lines. In particular, the methylation difference between the D clone hepatocyte and the OP5 cell line was significantly greater than the difference between the L clone hepatocyte and the LFF4 cell line ($P < 0.001$; Figure 5.12A). Conversely, Figure 5.12B shows that DMS located within *GRB10* were typically hypomethylated in clone hepatocytes compared to their donor cell lines. Because monoallelic bivalent chromatin domains (i.e. parent allele-specific histone modifications) have been implicated in the regulation of expression of *GRB10* and other imprinted genes (Sanz *et al.*, 2008), CpG methylation alone cannot explain tissue-specific differences in

genomic imprinting nor can it explain the full effect of SCNT on the epigenetic reprogramming of imprinted genes.

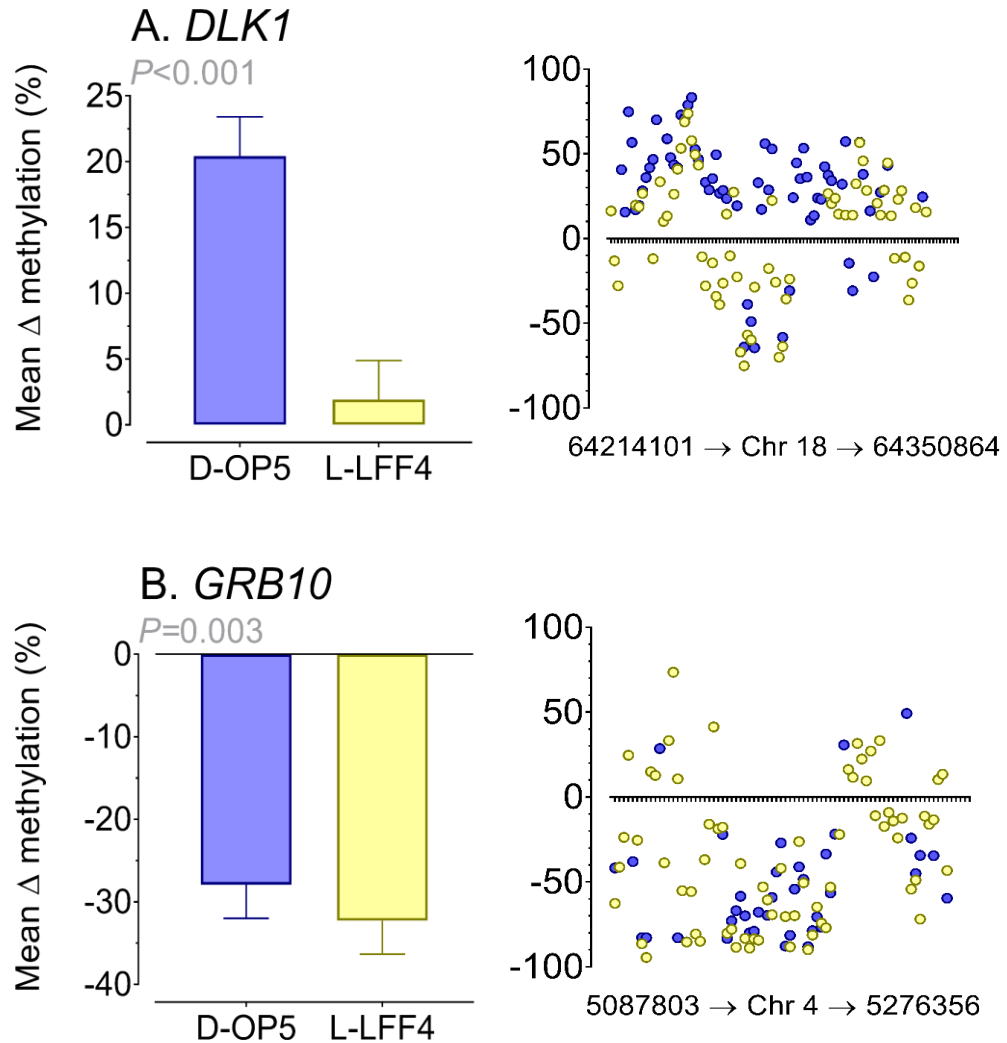


Figure 5.12 Differential methylation of imprinted genes, *DLK1* and *GRB10*, between clone sheep hepatocytes and their somatic donor cell lines.

Data analysed using REML analysis. Bars represent mean \pm SEM. Scatter plots represent mean difference (Δ) in methylation between clone hepatocyte and donor cell line (D-OP5, L-LFF4) at individual DMS in 5' \rightarrow 3' orientation along gene sequence.

Abbreviation(s): Chr, chromosome; D, Finn Dorset; *DLK1*, Delta-like 1; DMS, differentially methylated site; *GRB10*, Growth factor receptor bound protein 10; L, Lleyn; LFF4, Lleyn fetal fibroblast; OP5, mammary donor cell line.

5.3.5.2 *Insulin-like growth factor 2 receptor (IGF2R)*

In keeping with the previous discussion concerning nuclear transfer and aberrant imprinted expression of *IGF2R*, the present study identified clusters of CpGs located within the *IGF2R* gene that were differentially methylated between DvOP5 and LvLFF4 experimental comparisons (Table 5.5; Figure 5.13). The majority of the DMS were hypomethylated in clone hepatocytes relative to their donor cell lines. However, methylation differences were significantly greater between D clone hepatocytes and the OP5 cell line, than between L clone hepatocytes and the LFF4 cell line ($P < 0.05$; Figure 5.13). Differentially methylated sites were located in several exonic and intronic regions of the gene. Only one CpG (nucleotide position 82885570) was differentially methylated within intron 2 which is the genomic region comprising the putative regulatory region, DMR2 (Figure 5.14).

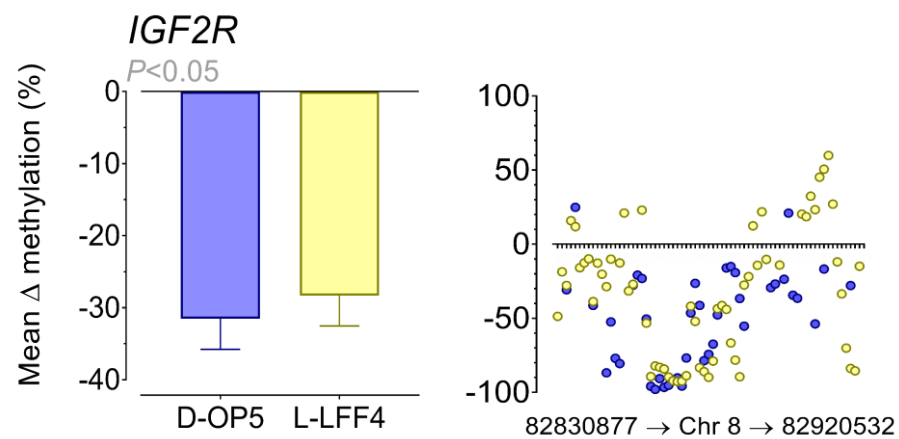


Figure 5.13 Differential methylation of *IGF2R* gene between clone sheep hepatocytes and their somatic donor cell lines.

Data analysed using REML analysis. Bars represent mean \pm SEM. Scatter plots represent mean difference (Δ) in methylation between clone hepatocyte and donor cell line (D-OP5, L-LFF4) at individual DMS in 5' \rightarrow 3' orientation along gene sequence.

Abbreviation(s): Chr, chromosome; D, Finn Dorset; IGF2R, insulin-like growth factor 2 receptor; L, Lley; LFF4, Lley fetal fibroblast; OP5, mammary donor cell line.

In sheep, *IGF2R* is thought to be paternally imprinted and maternally expressed in adult somatic tissues (Table 5.5; Killian *et al.*, 2001). As mentioned previously, it is uncertain whether the differential methylation detected between clone hepatocytes and their donor cell lines affects the imprinted status of *IGF2R* in these cell types. As discussed in Section 4.3.2.6.3, a plethora of chromatin structural features, such as histone modifications, operate in

conjunction with differential methylation to distinguish the parental alleles at the imprint control region (Sleutels *et al.*, 2002; Long and Cai, 2007). Thus, with respect to genomic imprinting, development and long-term health, DNA methylation is only a small part of the complex story.

Hypomethylation within *IGF2R* DMR2 has been associated with SCNT and LOS in sheep (Young *et al.*, 2001; Young *et al.*, 2003). However, *IGF2R* methylation levels appeared normal in adult somatic tissues derived from cloned calves that died within 24 h of birth relative to healthy clones and animals born by artificial insemination (Smith *et al.*, 2015). Furthermore, maternal *IGF2R* DMRs in tissues isolated from *in vivo*-derived or cloned individuals were consistently hypermethylated, irrespective of whether the clones were born in good health. Yet, the finding that biallelic *IGF2R* expression was higher in *in vivo*-derived animals than in clones implies that an alternative epigenetic mechanism may be responsible for altering its expression following nuclear transfer (Smith *et al.*, 2015).

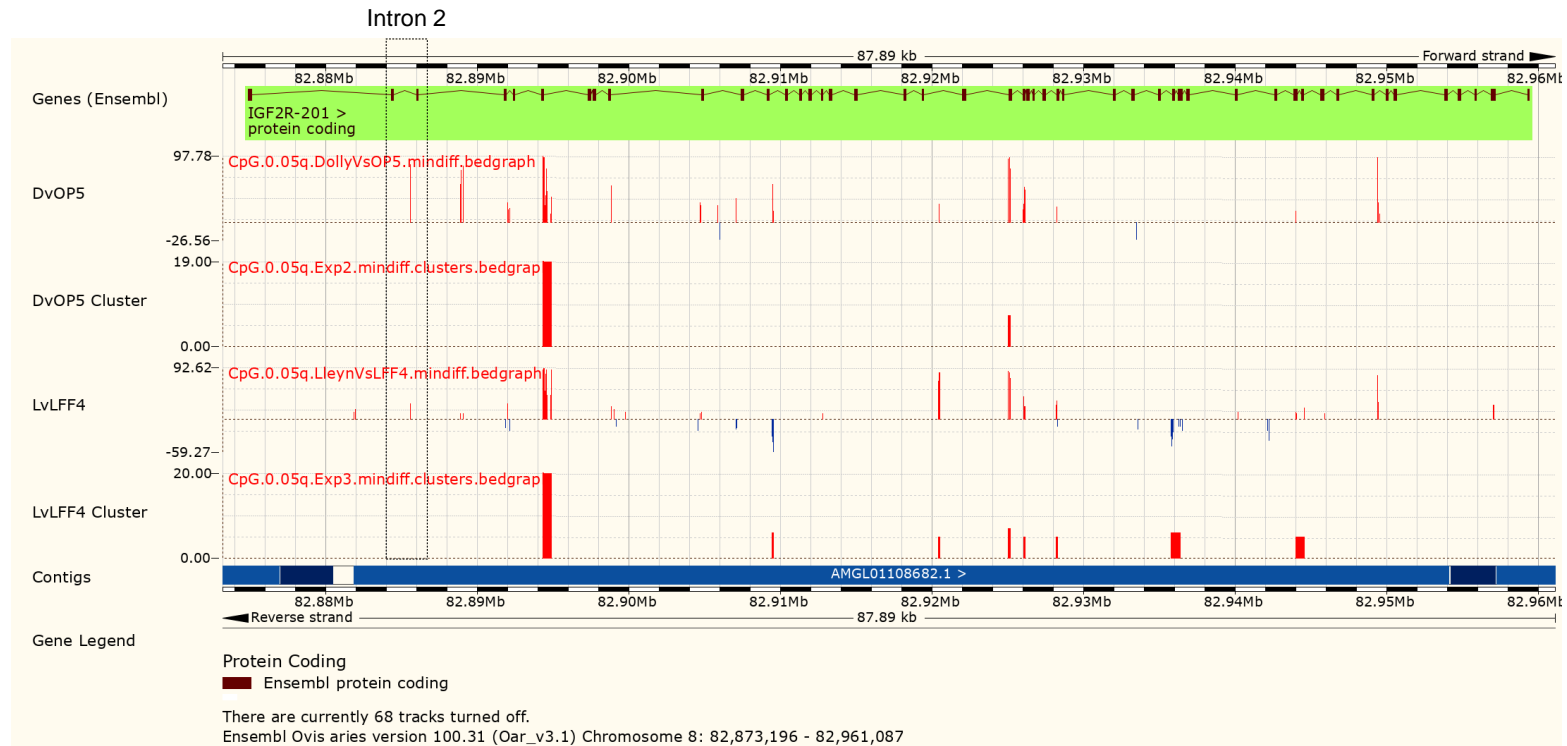


Figure 5.14 Clusters of differentially methylated sites (DMS) in the *IGF2R* gene between somatic donor cell line (OP5 and LFF4) and clone hepatocyte (D and L).

Bedgraphs demonstrate loss (↓, hypomethylation) and gain (↑, hypermethylation) of methylation at individual cytosine residues, and location of DMS clusters ■
 Abbreviation(s): D, Finn Dorset; IGF2R, insulin-like growth factor 2 receptor; L, Lleyn; LFF4, Lleyn fetal fibroblast; OP5, mammary donor cell line.

5.4 Concluding remarks

Reduced representation bisulphite sequencing (RRBS) analyses revealed cell type-specific DNA methylation signatures between clone hepatocytes and their respective somatic donor cell lines. The finding that methylation was more closely correlated between D and L clone hepatocytes than between clones and their founder cells indicated that the hepatic methylome was driven primarily by cell phenotype and function, rather than by methylation reprogramming errors following SCNT. Given that the cloned animals used in the present study developed to term and aged healthily according to measured musculoskeletal, metabolic and blood pressure parameters (Sinclair *et al.*, 2016), it may be assumed that epigenetic reprogramming was successfully achieved to facilitate their normal development to an advanced age.

The present study measured a higher degree of differential methylation between L clone hepatocytes and their LFF4 donor cell line, than between D clone hepatocytes and their OP5 donor cell line. The LFF4 cell line was more hypermethylated relative to the L clone hepatocyte (Table 5.2). Whether or not this greater difference in somatic donor cell type methylation had any bearing on the efficiency of epigenetic reprogramming remains inconclusive. Measuring the effect of donor cell type on methylation reprogramming of isolated hepatocytes following SCNT was confounded by the fact that donor cells were derived from two different sheep breeds. Although nucleotide bases at known SNP positions were removed during bioinformatic analyses in order to avoid methylation differences that were related to genotype, it is plausible that there was a minor effect of genotype on epigenetic regulation of gene expression via DNA methylation. Hepatocytes isolated from a contemporaneous group of naturally conceived sheep that were of the same age, genotype (D and L) and environment would, therefore, have served as ideal positive control samples to accurately assess whether the methylation status of clone hepatocytes was due to aberrant epigenetic reprogramming or cell type.

Gene set enrichment analysis identified a subset of genes that encoded transcription factor proteins involved in 'Sequence-specific DNA binding' as differentially methylated between clone hepatocytes and their donor cell lines. This was not surprising given that transcription factors govern the complex system of gene expression control that permits cellular differentiation and development in multicellular organisms (Davidson, 2010). In addition to

investigating the differential methylation between clone hepatocytes and their respective donor cell lines (DvOP5, LvLFF4), it may be interesting to explore differential methylation of these transcription factor genes between the two donor cell lines (OP5vLFF4) to determine the methylation difference between them. Replicate samples of somatic donor cell lines would be required for DNA methylation analysis in order to do this accurately and reliably.

As the present study did not measure the transcriptome of the clone hepatocytes and their respective donor cell lines, it was useful to select tissue-specific GOI for detailed methylation analyses using the Sheep Genome Atlas (Clark *et al.*, 2017). As the largest open access resource of any livestock species, the atlas provides RNA-seq libraries from cells and tissues that represent the major organ systems from prenatal, neonatal, juvenile and adult developmental time points. Whilst reuse of the atlas spared time, duplication of effort and financial expense, there are a number of caveats which concern the validity of its use to assess cell type-specific methylation in the current study. Firstly, transcriptomic data published in the atlas is restricted to Texel and TxBF sheep with no available data for D or L genotypes. Secondly, the data is representative of isolated cell populations (e.g. mammary gland, embryonic fibroblast) rather than cell lines (e.g. OP5, LFF4) which could be epigenetically different if methylation differences are induced by cell culture. Thirdly, it is important to acknowledge that methylation differences between cell types do not necessarily correlate with transcriptional (or translational) differences. Future work could, therefore, measure mRNA transcript abundance of the nine mammary-, fetal fibroblast- and liver-specific transcription factor genes that were differentially methylated between clone hepatocytes and donor cells.

Several imprinted genes were differentially methylated between clone hepatocytes and donor cells. Since imprinted genes affect various livestock production traits, including milk yield, carcass quality, fat and muscle deposition, and embryonic development (Smith *et al.*, 2015), an improved understanding of their functional sequences, methylation status, and transcriptional/translational control in different ruminant tissues is warranted to assess the merit of cloning as a safe and efficacious reproductive technology of the future. Studies investigating the involvement of imprinted genes in the aetiology of fetal overgrowth following SCNT could compare the methylome of donor cells with cell types (cardiovascular, neural) commonly affected in LOS in cloned animals.

Chapter 6

Discussion and Conclusion

6.1 General discussion

One-carbon metabolism serves as a biochemical conduit between external environment and epigenetic regulation of early development (Clare *et al.*, 2019). The periconceptual period is highly sensitive to the availability of methionine and other key 1C metabolites for the provision of methyl donors for methylation reactions (Sinclair *et al.*, 2007; Louis *et al.*, 2008; Maloney *et al.*, 2011; Steegers-Theunissen *et al.*, 2013; Padhee *et al.*, 2015). It is well-documented that reproductive failures and problems associated with epigenetic programming of offspring health are due to disturbances in 1C pathways during periconceptual development. It follows that altering the levels of 1C substrates and cofactors (e.g. methionine) in the maternal diet (*in vivo*) or in embryo culture media (*in vitro*) can affect epigenetic programming of mammalian development via changes to DNA methylation (Chapter 1; Table 1.6). In addition, embryo manipulation procedures during ART (e.g. IVP and SCNT) can lead to heritable alterations to the epigenome that are linked to subsequent development and late-onset chronic disease (Young *et al.*, 1998; Young *et al.*, 2001; Young *et al.*, 2003; Kohda and Ishino, 2013).

Whilst 1C metabolite status during periconceptual development has an important impact on pregnancy outcome (Chapter 1; Section 1.1.1.2), most of the research investigating the function of 1C metabolic pathways pertains to studies undertaken in the liver where the full complement of 1C metabolism enzymes are expressed (Balaghi *et al.*, 1993). Comparatively little research has been conducted in reproductive cells and embryos, however, the literature suggests that 1C metabolism is functional in these cell types (Steele *et al.*, 2005; Bhenkhalifa *et al.*, 2010; Ikeda *et al.*, 2010; Lee *et al.*, 2012). Due to the absence or low expression of specific methionine cycle enzyme transcripts (*MAT1A* and *BHMT*) in bovine ovarian and embryonic cells (Kwong *et al.*, 2010), it has been proposed that 1C metabolism functions differently in these cell types compared to the liver. Species- and tissue-specific differences in 1C metabolism mean that mathematical models based on the rodent liver are not entirely suitable to model 1C metabolic function in all mammalian species and tissue types. In addition, the complexity and multitude of allosteric interactions involved in 1C metabolism makes it a considerable challenge to evaluate the impact of nutritional or environmental perturbation to 1C pathways within different cell types.

Understanding the function of 1C metabolism in ruminants is of considerable economic importance to the livestock production industry. Cattle and sheep have low dietary intake of methyl donors in the post-ruminant state and are, therefore, sensitive to perturbations to 1C metabolic pathways (Snoswell and Xue, 1987). Moreover, ART procedures that involve the *in vitro* handling of gametes and embryos have been employed to achieve genetic improvement in domestic ruminant species (Chakravarthi and Sri Balaji, 2010). Since embryonic manipulation and non-physiological *in vitro* culture environments can lead to defective epigenetic reprogramming and fetal overgrowth in livestock species (Young *et al.*, 2001), the widespread application of these technologies remains limited. This thesis, therefore, sought to improve current understanding of the regulation of 1C metabolism in the ruminant liver, ovary and preimplantation embryo through *in vivo* and *in vitro* nutritional supplementation experiments coupled with metabolomic, transcriptomic and epigenetic analyses.

6.2 Summary of key findings

Most of the research investigating 1C metabolism in ruminants have used enzyme activity assays in sheep liver (Xue and Snoswell, 1985; Xue and Snoswell, 1986; Snoswell and Xue, 1987). However, the function of 1C metabolism can also be monitored by the quantitative measurement of hepatic 1C metabolic intermediates (Xu *et al.*, 2020). As the liver is the largest metabolic organ of the body responsible for 50% of methionine metabolism and 85% of methylation reactions (Lu and Mato, 2012), it was hypothesised that relevant reductions in dietary methyl group availability would lead to significant alterations to hepatic 1C metabolite concentrations. The study reported in Chapter 2 addressed this hypothesis in sheep, and provided an unprecedented insight into the metabolic burden of methyl deficiency in an outbred population of domestic ruminant species. Not only are sheep a species of clinical interest with respect to methyl group (i.e. vitamin B₁₂) deficiency, but they are a suitable model for humans.

There was a considerable heterogeneity in hepatic levels of individual 1C metabolites measured in Ab and MD sheep study populations which reflected the dietary and genetic variation in the chosen model species. Importantly, there was a significant difference in hepatic levels of B vitamins, folates and 1C-related amines between Ab and MD sheep. Diminished methionine and B vitamins (primarily B₁₂), caused an accumulation of 5-mTHF in liver during a

physiological response to impending methyl deficiency known as the 'methyl-
folate trap'. In particular, the marked reduction in B vitamins, which serve as
bioactive coenzymes or as a reserve pool for coenzyme synthesis, had a
cumulative 'knock-on' effect throughout linked 1C metabolism pathways in MD
liver. This 'knock-on' effect was illustrated by a decrease in amino acid
intermediates, and concurrent increase in polyamines and propionate
metabolites in MD liver. This study confirmed that moderate reductions to
dietary inputs can have a global impact on 1C metabolism and related pathways
in sheep liver, ultimately leading to system-wide alterations to biochemistry and
physiology.

Extending from ruminant hepatocytes to reproductive cells, Chapter 3
investigated the effect of altering methyl group (i.e. methionine) availability on
bovine preimplantation embryo development. The first experiment confirmed
that cells of the bovine follicle-enclosed oocyte and preimplantation embryo lack
specific methionine cycle enzymes and may, therefore, be particularly sensitive
to methionine supply. In accordance with previous studies, *MAT2A* was
detected in the somatic cells of the ovary, oocyte and preimplantation embryo
(Ikeda *et al.*, 2010; Kwong *et al.*, 2010), and *BHMT* was detected in oocytes and
morulae (Benkhalifa *et al.*, 2008; Ikeda *et al.*, 2010; Lee *et al.*, 2012). It is
possible that transient expression of *BHMT* at the morula stage precedes
protein translation at the blastocyst stage in bovine embryos, however, further
research is required for clarity. This study was the first to detect *BHMT2* in
somatic cells of the bovine ovary and the oocyte, suggesting that reproductive
cells are equipped to use S-methylmethionine (SMM) to generate methionine
(Chapter 3; Section 3.3.1). However, the levels of this substrate in follicular fluid,
ovarian cells and oocytes have not been measured and the mechanisms of
uptake in reproductive cells are unknown.

The second experiment of Chapter 3 sought to establish the developmental
competence of bovine embryos produced under *in vitro* culture conditions
containing 0, 10, 50 and 500 $\mu\text{mol/L}$ of added methionine. Although previous
studies introduced variable methionine concentrations from the point of embryo
culture (Bonilla *et al.*, 2010), no such study had investigated the effect of altering
methionine from the point of oocyte maturation. This study reported that altering
methionine throughout all stages of IVP had a significant effect on embryo
development. Embryos cultured in non-physiological (0 $\mu\text{mol/L}$ added) or
supraphysiological (500 $\mu\text{mol/L}$ added) methionine concentrations exhibited

reduced development to blastocyst stage, and a low proportion of these embryos were developmentally advanced relative to embryos cultured at physiological concentrations. Of those tested, the high physiological concentration of methionine (50 $\mu\text{mol/L}$ added) appeared to be optimal for development, as reflected by the increased proportion of advanced, grade 1 (transferable quality) blastocysts that possessed the greatest total cell number and TE outgrowth.

In addition to the observed phenotypic effects, Chapter 4 found that reducing methionine within physiological limits (from 50 to 10 $\mu\text{mol/L}$ added) during IVP significantly reduced DNA methylation within the primary cell lineages of Day 8 bovine blastocysts. Although both cell lineages were hypomethylated following culture in low methionine, the TE had a greater number of DMS compared to the ICM. Moreover, different GO terms and KEGG pathways were significantly enriched between the cell lineages following culture in low methionine. Terms enriched within the ICM were involved in protein catabolism and autophagy, whereas terms enriched within the TE were involved in cellular transport and cell cycle progression. Taken together, these findings imply that the contribution of the two primary cell lineages to methionine metabolism within the whole blastocyst is different and warrants further investigation.

Six imprinted genes, including *IGF2R*, were differentially methylated in bovine blastocysts in response to low physiological methionine. Loss of methylation within DMR2 of *IGF2R* appears to be causative of LOS in ruminants exposed to ART procedures (Young *et al.*, 2001; Young *et al.*, 2003). Detailed methylation analysis of this regulatory region identified two clusters of DMS within DMR2 that were hypomethylated in the TE of Day 8 bovine blastocysts following culture in low physiological methionine. Considering that *IGF2R* expression is not imprinted by the paternal *AIRN* transcript until the postimplantation stage (Day 18), it was not surprising that methionine concentration had no effect on *IGF2R* and *AIRN* transcript expression in Day 8 bovine blastocysts. Repeating these methylation and transcriptomic analyses in cell lineages isolated from postimplantation stage embryos would help to illuminate the putative role of DMR2 methylation on imprinted expression of *IGF2R* by *AIRN*.

In addition to the nutrient composition of culture media, accumulating evidence suggests that embryonic manipulation during ART procedures, such as SCNT, can alter the epigenome of embryos with adverse effects for offspring health

and development (Kang *et al.*, 2003; Rhind *et al.*, 2003; Smith *et al.*, 2012). One-carbon metabolic pathways provide a biochemical conduit between environment and epigenetic regulation of mammalian development by supplying methyl groups for methylation reactions. It follows that perturbations to 1C pathways, brought about by embryo manipulation or nonphysiological culture environments used in SCNT, can disrupt the dynamic methylation reprogramming events that take place during early embryo development (Figure 3.1). In some cases, this can lead to the developmental failure of cloned embryos. As discussed earlier (Section 5.1), it has been reported that cloned embryos only partially demethylate their genomes and begin the *de novo* methylation process earlier than their *in vivo*-derived counterparts (Dean *et al.*, 2001; Kang *et al.*, 2001). If donor cell methylation patterns are maintained this can result in the continuous expression of tissue-specific genes and inefficient activation of genes critical for embryonic development, thereby reducing the competence of reconstructed embryos (Peat and Reik, 2012; Niemann *et al.*, 2016).

With this in mind, Chapter 5 investigated the effect of somatic donor cell type (e.g. OP5, mammary; LFF4, fetal fibroblast) on reprogramming efficiency by measuring CpG methylation in hepatocytes isolated from Finn Dorset (D) and Lleyn (L) cloned sheep. In general, somatic cell nuclei were hypermethylated relative to clone hepatocytes, and the difference in methylation was greatest between LFF4 donor cells and L clone hepatocytes. A subset of imprinted genes, and genes encoding transcription factors in mammary, fetal fibroblast and liver cells, were differentially methylated between donor cells and clone hepatocytes. However, in the absence of a positive control (i.e. hepatocytes isolated from naturally conceived D and L sheep), it was not possible to determine whether the differential methylation between donor cells and clone hepatocytes was a consequence of SCNT. Likewise, without measuring transcript abundance to corroborate methylation data, it was not possible to determine whether differential methylation had any effect on gene expression in the cell types analysed.

6.3 Clinical impact

The outcomes of this thesis provide evidence that relevant reductions in the dietary provision of methyl groups can perturb epigenetic programming of mammalian development. As a central integrator of nutrient status, insults to 1C

metabolism, particularly during the periconceptional period, can exert a global impact on cellular biochemistry and epigenetics, with implications for long-term health and disease. Whilst the primary objective of this research was to investigate the function of 1C metabolism within cells of the ruminant liver, ovary and preimplantation embryo, the experimental findings can be translated to humans. Cattle and sheep are valuable models for biomedical research due to their physiological parallels with humans, especially during preimplantation embryo development ([Ménézo and Hérubel, 2002](#); [Sirard, 2019](#)).

It follows that dietary restriction of 1C metabolites is associated with several serious health conditions in humans and ruminants which, if left untreated, can result in death ([Suttle, 2010](#); [Hannibal *et al.*, 2016](#)). It follows that accurate deficiency diagnosis is critical. It has been established that measuring standalone biomarkers of methyl deficiency, such as total serum B12 or MMA, has limited diagnostic value ([Hannibal *et al.*, 2016](#)). Therefore, the commercialisation of simple analytical platforms that can quantify a comprehensive suite of chemically distinct, bioactive 1C metabolites in complex mammalian biofluids and tissues are required. Metabolomic platforms, such as those developed in Chapter 2, could be used in corroboration with epigenomic and transcriptomic studies to facilitate dietary and genetic studies of metabolic health in humans and animals. Such platforms may also prove useful for the quantitative profiling of 1C metabolites in commercial cell and embryo culture media, or in spent culture media as a non-invasive method of evaluating the function of 1C metabolism.

The implications emerging from the studies presented herein emphasise the importance of methionine for the mammalian preimplantation embryo. In support of findings reported by [Bonilla *et al.* \(2010\)](#), a lower proportion of bovine embryos that were cultured in nonphysiological or supraphysiological concentrations of methionine developed to blastocyst stage, and fewer blastocysts were developmentally advanced (i.e. late expanded, hatching or hatched) at these concentrations. Taken together, these findings indicate that bovine preimplantation embryo development is sensitive to methionine during the first week of development. The MAT2A enzyme, which is responsible for SAM biosynthesis from methionine, has been detected in bovine embryos of various developmental stages up to Day 8 (Chapter 3; [Ikeda *et al.*, 2010](#); [Kwong *et al.*, 2010](#)). The low K_m range of MAT2A (4-10 $\mu\text{mol/L}$) means that the maximal rate (V_{max}) of reaction is reached at physiological methionine concentrations (i.e.

<50 $\mu\text{mol/L}$; Frau *et al.*, 2013). Thus, it appears that bovine embryonic cells are not well-equipped to metabolise concentrations outside of this range. In addition, subtle reductions in methionine during IVP caused global hypomethylation within the primary cell lineages of bovine blastocysts. The epigenetic effect of methionine in mammalian cells and embryos has been well-documented (Section 1.7.2; Table 1.6). More specifically, Ikeda *et al.* (2012) reported that culturing bovine embryos in the presence of methionine antagonist, ethionine, reduced DNA methylation, and, *in vivo* dietary supplementation of methionine altered the transcriptome of bovine embryos (Peñagaricano *et al.*, 2013).

The sensitivity of the mammalian preimplantation embryo to small fluctuations in methionine is relevant for several reasons. Firstly, methionine deficiency and excess have been implicated in adverse reproductive health outcomes in humans (General Introduction, Table 1) and animals (Rees *et al.*, 2006).

Secondly, methionine is not endogenously synthesised by mammals and, therefore, must be obtained in the diet (Shoob *et al.*, 2001). As a rate-limiting amino acid in both human and animal diets (Laurichesse *et al.*, 1998; Wiltbank *et al.*, 2014; Schwab and Broderick, 2017), more attention must be paid to the dietary inclusion of methionine, particularly during the periconceptual period. As discussed above (General Introduction), most of the research concerning periconceptual nutrition has focused on the preventative effect of folic acid supplementation against NTDs (De-Regil *et al.*, 2010). Yet, as animal proteins are a primary source of methionine in human diets, vegetarian and vegans may be at increased the risk of methionine (and B12) deficiency (Krajcovicová-Kudláčková *et al.*, 2000; McCarty *et al.*, 2009) and, consequently, adverse reproductive outcomes during periconceptual development. As increasing concerns over health, environment and economic consequences of a diet rich in animal produce focuses the attention on those who exclude these foods from their diet (Appelby and Key, 2015), it is important to investigate the health effects of methionine (and methyl group) deficiency in this subpopulation. In dairy cattle diets, the supplementation of rumen-protected methionine results in higher milk production, better metabolic health, and improved reproductive performance (Toledo *et al.*, 2017). Thus, determining the optimal level of methionine in metabolisable protein for maximising milk protein production, fertility and reproduction is required to maximise profitability within the industry (Cho *et al.*, 2007; Morton *et al.*, 2017).

Thirdly, the concentration of methionine in cell and embryo culture media varies dramatically between formulations, ranging from 0 to 500 $\mu\text{mol/L}$ (Section 1.7.1; Table 1.5). This wide variation in concentration reflects the lack of standardisation between embryo production protocols with respect to IVP media formulations, thereby raising questions for the safety and efficacy of their commercial use. As media concentrations of key 1C substrates and cofactors, including folate (B9) and vitamin B₁₂, are not routinely measured or disclosed (Sunde *et al.*, 2016; Table 1.5), knowledge of their interaction with methionine and other 1C metabolites during the consecutive stages of IVP is unknown. In keeping with the earlier discussion concerning the comprehensive profiling of 1C metabolites, robust analytical platforms to enable their simultaneous quantification could form part of a robust quality control and efficacy evaluation of commercial cell and embryo culture media.

This thesis also confirmed that *in vitro* embryo culture conditions and manipulation procedures used during ART can disturb 1C metabolism in gametes and preimplantation embryos, causing epigenetic alterations to DNA methylation affecting developmentally important genes. A case in point refers to the differential methylation of imprinted genes, such as *IGF2R*, following *in vitro* culture at low physiological methionine (Section 4.3.2.6) and following SCNT (Section 5.3.5.2). Several factors are thought to affect the epigenetic reprogramming of cloned embryos, including donor cell type, oocyte quality, timing of fusion and activation, and *in vitro* culture conditions of the reconstructed cloned embryo (Campbell and Alberio, 2003; Kato and Tsunoda, 2010; Akagi *et al.*, 2014). With this in mind, the potential adverse impact of exposure to nonphysiological concentrations of 1C metabolites during embryo culture is confounded by the invasive nuclear transfer technique, and extensive handling of gametes and embryos thereafter.

The processes underlying the epigenetic reprogramming of cloned embryos and IVP embryos are different, thus, it is likely that cloned embryos have different physiology and nutritional requirements as they undergo reconstruction (Mastromonaco *et al.*, 2004; Cordova *et al.*, 2017). It follows that media must be developed according to the special physiology and metabolic requirements of cloned embryos. However, studies evaluating suitable culture conditions for the successful reprogramming of cloned embryos are limited.

Investigation into the effect of adding protein macromolecules during the culture of cloned bovine embryos found that supplementation of SOF media with BSA

and FCS promoted development of cloned embryos to blastocyst stage (Choi *et al.*, 2002). Yet, as discussed in Chapter 1 (Section 1.7), the addition of serum to media has been implicated in fetal overgrowth in ruminants (Thompson *et al.*, 1995; Young *et al.*, 2001; Rooke *et al.*, 2007). The development of BSA- and serum-free culture media for cloned embryos is, therefore, important to avoid postnatal complications associated with exposure to these macromolecules *in vitro*.

Similarly, supplementation of culture media with antioxidants, such as vitamin C and flavones, improved the developmental competence of cloned embryos as evidenced by enhanced morulae compaction, blastocyst production and the expression of developmentally important genes (Li *et al.*, 2014; Su *et al.*, 2014). In addition, co-culture with buffalo rat liver, and bovine oviduct, cumulus and granulosa cells have been shown to improve the development of cloned embryos (Saikhun *et al.*, 2002; Lu *et al.*, 2005; Li *et al.*, 2007). Despite the efforts taken to develop suitable culture media, successful *in vitro* preimplantation development does not necessarily contribute to improving pregnancy outcomes following embryo transfer (Cordova *et al.*, 2017).

To our knowledge, no study has specifically investigated the effect of supplementing embryo culture media with 1C metabolites on the development of cloned embryos. There is, however, evidence to suggest that the addition of epigenetic modifying agents, such as DNMT1 and HDAC inhibitors (i.e. 5-aza-2'-deoxycytidine, trichostatin A, scriptaid and valproic acid), can improve genomic methylation reprogramming and transcript expression in embryos following SCNT (Zhao *et al.*, 2010; Costa-Borges *et al.*, 2010; Xu *et al.*, 2013). In accordance with the findings presented in Chapter 4, it is hypothesised that adding methionine to media may alter the methylation reprogramming of reconstructed embryos. This would be a promising 'non-chemical' (nutrient-based) alternative to using chemical epigenetic modifiers for improving SCNT efficiency.

Although the effect of 1C metabolite concentrations on the epigenetic reprogramming of cloned embryos remains to be elucidated, the effect is likely to vary according to species as oocytes from different species have different developmental competencies. For example, results by Lu *et al.* (2005) reported that bovine oocytes directed cloned embryo development more effectively than buffalo oocytes when buffalo adult fibroblasts were used as donor cells. Likewise, the effect of 1C metabolites on cloned embryo development is likely

to vary according to donor cell type as donor cells have different metabolic demands (Rakha, 2015). Studies in mice demonstrated that where cumulus cells were used as nuclear donors, a higher yield of blastocysts were produced in Whitten's medium (or Whitten's medium followed by potassium simplex optimisation medium; KSOM) owing to its high glucose concentration relative to other media (Chung *et al.*, 2002). Because normal embryos do not require glucose during the early cleavage stages, these results reveal unusual medium requirements that are indicative of altered kinetics, metabolism and physiology of cloned embryos. Sequential media that is tailored to respond to the changing requirements of reconstructed embryos may improve efficiency of epigenetic reprogramming following SCNT.

Aside optimising culture media for reconstructed embryos, another approach is to optimise donor cell culture. A recent study showed that folic acid deprivation of bovine fetal fibroblast donor cells for 6 days prior to SCNT improved epigenetic reprogramming of cloned embryos by inducing DNA hypomethylation (Jozi *et al.*, 2020). It follows that altering levels of 1C metabolites during donor cell culture can modulate epigenetic signatures in terminally differentiated somatic cell nuclei, thereby improving the efficiency of SCNT for agricultural and biomedical purposes.

6.4 General conclusions and future research

Tissue- and species-specific differences in the function of 1C metabolism render some cell types more sensitive to dietary and environmental perturbations of 1C metabolism. This thesis demonstrates that 1C metabolic pathways are tightly regulated within physiological methionine concentration ranges within the mammalian preimplantation embryo. Subtle alterations to methionine concentration were sufficient to trigger nutrient-mediated phenotypic and molecular epigenetic changes to DNA methylation in Day 8 bovine embryos with potential implications for long-term offspring health. Collectively, the findings presented herein emphasise the importance of optimal methionine status during the periconceptual period and ART procedures. Whilst future research priorities have been mentioned throughout this thesis, an elaborative summary is provided here.

The detection of genes encoding *BHMT* isoforms in ovarian cells, oocytes and morulae (Chapter 3) suggests that mammalian reproductive and embryonic

cells harbour alternative pathways for methionine metabolism and are, therefore, equipped with a unique methylation machinery required for the establishment of a cell type-specific methylome. To elucidate the relationship between *BHMT/2* mRNA transcription, protein translation and enzyme activity, a combination of assays could be employed using somatic, germ and embryonic cells of various stages of mammalian development.

Protein expression could be determined by Western blot analysis. However, due to the high amino acid sequence homology between BHMT and BHMT2 proteins (Li *et al.*, 2008; Ganu *et al.*, 2011; Appendix Table 3.1), it would be vital that the primary antibody recognises an epitope comprising an amino acid sequence unique to each BHMT isoform in order to ensure their specific binding and detection. Radiochemical enzyme activity assays could be used to assess the catalytic activity of BHMT isoforms. BHMT enzyme activity could be measured using the method of Garrow *et al.* (1996) which uses [methyl-¹⁴C]betaine as a radiolabelled substrate. The method is based on detecting the transfer of [³H]methyl groups from [¹⁴C]betaine (TMG) to Hcy, thereby producing [³H]dimethylglycine (DMG) and [³H]methionine reaction products. As described by Szegedi and others (2008), BHMT2 enzyme activity could be measured using the same method but with [methyl-¹⁴C]-S-methylmethionine as the radiolabelled substrate. Using the sensitive mass spectrometry-based platforms developed in Chapter 2, the quantification of BHMT/2 enzyme substrates, betaine (TMG) and SMM, would provide a useful adjunct to corroborate the aforementioned transcriptomic and proteomic assays. Extending these analyses to non-ruminant species, such as rodents and pigs, could help to illuminate tissue- and species-specific differences in methionine metabolism.

Future experiments could use these mass spectrometry-based platforms to investigate the effects of dietary methyl deficiency and inborn errors of 1C metabolism by measuring a comprehensive suite of 1C metabolites in reproductive cells, tissues and biofluids of various mammalian species. Such integrated metabolomic analyses would bring an unprecedented level of mechanistic insight into the nutritional biochemistry-mediated epigenetic modifications that take place during the periconceptional period, particularly in cells of the mammalian ovary and preimplantation embryo. Furthermore, as the suppliers of culture media do not typically disclose concentrations of 1C metabolites, such as FA and vitamin B₁₂, it would be of merit to measure their abundance, if present, in commercial formulations. It would then be possible to

compare media concentrations with physiological concentrations measured in bovine follicular and uterine fluid.

Once culture medium-specific concentration ranges have been established, it would be of value to extend the observations reported in Chapters 3 and 4 by investigating the effect of altering methionine in the presence of altered FA and B12 concentrations during bovine embryo culture. As B12 is the cofactor for methionine synthase (MTR); the enzyme responsible for the generation of methionine from Hcy, it would be interesting to ascertain whether media supplementation of B12 can rescue the gross phenotypic and epigenetic effects of methionine deficiency observed in the present study. Similarly, as B12 deficiency reduces MTR activity, thereby causing the 'methyl-folate trap' (Chapter 2; Section 2.3.2.5), it would be interesting to investigate whether FA supplementation rescues the effect of a methionine and/or B12 deficiency in mammalian embryos. A possible experimental design is detailed in Table 6.1.

Table 6.1 Experimental design for methyl supplementation study.

Treatment groups (<i>n</i> =3)			Control group
Methionine (0 µmol/L added)	Vitamin B ₁₂ (pmol/L)	Folic acid (nmol/L)	Methionine (50 µmol/L added)
-	+	-	+
-	-	+	+
-	+	+	+

Concentration units based on normal blood reference ranges. Culture media composition deplete in 1C metabolite (-); culture media composition replete in 1C metabolite (+).

Based on the observation that the high physiological concentration of methionine (50 µmol/L) appeared to be the best for bovine embryo development (Chapter 3), this concentration could be used to culture control embryos (Table 6.1). Preliminary research would be required in order to make a judicious decision regarding the concentrations of B12 and FA to be added to methionine-deficient culture media based on: i) levels measured in culture media formulations; ii) physiological levels measured in bovine reproductive fluids; and, iii) supraphysiological levels reached following dietary supplementation in humans (e.g. 400 µg/d FA). Gross morphological embryo assessments coupled with epigenomic and transcriptomic data would provide an unprecedented insight into the importance of methyl donor supplementation during the periconceptual period and ART.

Although strictly beyond the scope of the present study, which focused on the impact of maternal diet and embryo culture media composition on epigenetic programming of embryo development, there is compelling evidence that paternal diet programmes offspring health via sperm and seminal plasma-specific pathways. *In vivo* dietary trials have found that feeding male mice a low protein diet (LPD) or a methyl-deficient diet is associated with negative pregnancy outcomes (e.g. congenital defects), and cardiovascular and metabolic dysfunction in offspring (Lambrot *et al.*, 2013; Watkins and Sinclair, 2014; Watkins *et al.*, 2018). Recently, Morgan *et al.* (2020) reported that feeding a LPD supplemented with methyl donors had a significant impact on testicular morphology by increasing seminiferous tubule luminal area in male mice. The underlying mechanisms for how sub-optimal paternal diet elicits poor offspring development is an emerging field of research. Specifically, the effects of methyl supplementation on semen parameters during IVF have not been explored. Whilst the exposure of male gametes to the *in vitro* environment is short (<24h) relative to oocytes and embryos, the effect of altering methionine and additional 1C metabolites on sperm physiology and epigenomics during IVF cannot be disregarded and warrants further investigation.

The developmental, epigenomic and transcriptomic analyses presented in this thesis used pools of bovine embryos. However, considering the human-like genetic heterogeneity of outbred ruminant species, inter-individual and inter-breed (i.e. ethnic) variation in 1C metabolism and tolerance to methyl deficiency is expected. It will be important to extend future research to include multiomics analyses using individual embryos in order to evaluate how SNPs within key 1C enzymes (Appendix Table 1.1) interact with diet to confer risk to NTDs and other developmental anomalies in embryos and adults. Single-cell and parental allele-specific multiomics sequencing techniques, such as those detailed by Guo *et al.* (2017), would facilitate a thorough investigation into the effect of gene-nutrient interactions on the epigenomic reprogramming of mammalian embryonic development and offspring health. In particular, single-cell techniques would be suitable for the analyses of genome-scale chromatin state and DNA methylation dynamics in ICM and TE cells immunodissected from individual embryos. Moreover, a parental allele-specific assessment of DNA methylation would enhance current understanding of the epigenetic regulation of imprinted genes, such as *IGF2R*, in distinct embryonic cell lineages.

This thesis demonstrated that culturing bovine preimplantation embryos to Day 8 in low physiological methionine caused significant hypomethylation of CpGs located within DMR2 of the *IGF2R* gene. Since loss of methylation within this imprint control region has been associated with LOS in ruminants following ART procedures (Young *et al.*, 2001; Young *et al.*, 2003; Section 1.7), the imprinting status of *IGF2R* remains an important line of enquiry. The *IGF2R* gene is not paternally imprinted by antisense transcript, *AIRN*, until ~Day 18 in bovine embryos. Hence, a temporal and tissue-specific multiomic analysis using individual postimplantation stage embryos would be useful to: i) illuminate the role of DMR2 methylation in *IGF2R* imprinting by *AIRN* in embryonic and extraembryonic lineages; and, ii) evaluate the persistent effect, if any, of methionine on *IGF2R* imprinting during protracted periods of embryo culture.

Chapter 5 assessed the effect of donor cell type on the efficiency of reprogramming following SCNT by measuring DNA methylation in hepatocytes isolated from cloned sheep. Without positive control hepatocyte samples isolated from a contemporaneous group of naturally conceived sheep, it was not possible to ascertain whether the methylation status of clone hepatocytes was due to aberrant epigenetic reprogramming following SCNT or a mere consequence of cell type. Therefore, further investigation including control hepatocyte samples would help to confirm the findings of this study. Given that hepatocytes were isolated from healthy, aged cloned sheep, it can be assumed that epigenetic reprogramming was successfully achieved to permit their normal development into old age. In order to understand the effect of donor cell type used during SCNT on epigenetic reprogramming specifically during embryo development, future experiments could analyse the methylome of preimplantation embryos cloned from mammary epithelial (OP5) and fetal fibroblast (LFF4) donor cells, using the methylome of embryos produced by IVP and/or natural conception as a comparison. Future assessments of the embryonic methylome could use oxidative bisulphite sequencing (Booth *et al.*, 2013) to elucidate the complex interplay between 5mC and 5hmC modifications during early development.

Advancing the hypothesis that cloned embryos have unique metabolic and nutritional demands and, therefore, require specialist media formulations to support their reconstruction and epigenetic reprogramming (discussed earlier), particular focus should be given to the development and optimisation of safe and efficacious culture media for cloned embryos. Such experiments would also

present an opportunity to improve culture media for downstream applications, such as regenerative medicine. Immunodissection of the ICM is effective in the derivation of ESC lines for cell replacement therapy, disease modelling and basic research (Bogliotti *et al.*, 2018). Since embryo culture media composition affects ESC derivation efficiency (Chen *et al.*, 2009), it would be beneficial to evaluate the epigenetic and transcriptomic effect of *in vitro* blastocyst culture conditions on isolated ICM cells used for stem cell culture.

In summary, the findings of this thesis promote and support the importance of 1C metabolism and the provision of an optimal methyl balance for reproductive biology in mammals. The variety of experimental approaches (biochemical, molecular and genetic) to study the regulation of 1C metabolism in the ruminant liver, ovary and preimplantation embryo highlight important species- and tissue-specific differences in methionine metabolism. Such differences must be considered in order to provide an optimal nutritional environment to support healthy *in vivo* and *in vitro* growth and development of mammalian cells and embryos.

References

- Acosta DAV, Denicol AC, Tribulo P, Rivelli MI, Skenandore C, *et al.* (2016) Effects of rumen-protected methionine and choline supplementation on the preimplantation embryo in Holstein cows. *Theriogenology*. 85(9): 1669-1679
- Adelman K and Lis JT (2012) Promoter-proximal pausing of RNA polymerase II: emerging roles in metazoans. *Nat. Rev. Genet.* 13: 720–731
- Agricultural Research Council (ARC, 1980) The Nutrient Requirements of Ruminant Livestock. Slough UK: Commonwealth Agricultural Bureaux
- Agrogiannis GD, Sifakis S, Patsouris ES and Konstantinidou AE (2014) Insulin-like Growth Factors in Embryonic and Fetal Growth and Skeletal Development (Review). *Mol Med Rep.* 10(2): 579-84
- Akagi S, Matsukawa K and Takahashi S (2014) Factors Affecting the Development of Somatic Cell Nuclear Transfer Embryos in Cattle. *J Reprod Dev.* 60(5): 329–335
- Akalin A, Franke V, Vlahoviček K, Mason CE and Schübeler D (2015) Genomation: A Toolkit to Summarize, Annotate and Visualize Genomic Intervals. *Bioinformatics.* 31(7): 1127-9
- Akalin A, Kormaksson M, Li S, Garrett-Bakelman FE, Figueroa ME, *et al.* (2012) methylKit: a comprehensive R package for the analysis of genome-wide DNA methylation profiles. *Genome Biology.* 13: R87
- Alaniz RC, Thomas SA, Perez-Melgosa M, Mueller K, Farr AG, *et al.* (1999) Dopamine Beta-Hydroxylase Deficiency Impairs Cellular Immunity. *Proc Natl Acad Sci U S A.* 96(5): 2274-8
- Albers E (2009) Metabolic characteristics and importance of the universal methionine salvage pathway recycling methionine from 5'-methylthioadenosine. *IUBMB Life.* 61(12): 1132-42
- Albersen M, Bosma M, Knoers NV, de Ruiter BH, Diekman EF, *et al.* (2013) The intestine plays a substantial role in human vitamin B6 metabolism: a Caco-2 cell model. *PLoS One.* 8(1): e54113
- Alur P (2019) Sex Differences in Nutrition, Growth, and Metabolism in Preterm Infants. *Front Pediatr.* 7: 22
- Amaral CL, Bueno Rde B, Burim RV, Queiroz RH, Bianchi Mde L, *et al.* (2011) The effects of dietary supplementation of methionine on genomic stability and p53 gene promoter methylation in rats. *Mutat Res.* 722(1): 78-83
- Amarasekera M, Martino D, Ashley S, Harb H, Kesper D, *et al.* (2014) Genome-wide DNA methylation profiling identifies a folate-sensitive region of differential methylation upstream of ZFP57-imprinting regulator in humans. *FASEB J.* 28(9): 4068-76
- Amelio I, Cutruzzolá F, Antonov A, Agostini M and Melino G (2014) Serine and glycine metabolism in cancer. *Trends Biochem Sci.* 39(4): 191-8
- Amort T, Rieder D, Wille A, Khokhlova-Cubberley D, Riml C, *et al.* (2017) Distinct 5-methylcytosine profiles in poly(A) RNA from mouse embryonic stem cells and brain. *Genome Biol.* 18(1): 1
- Anastasiadi D, Esteve-Codina A and Piferrer F (2018) Consistent inverse correlation between DNA methylation of the first intron and gene expression across tissues and species. *Epigenetics Chromatin.* 11(1): 37
- Anckaert E and Fair T (2015) DNA methylation reprogramming during oogenesis and interference by reproductive technologies: Studies in mouse and bovine models. *Reprod Fertil Dev.* 27(5): 739-54
- Anckaert E, Romero S, Adriaenssens T and Smits J (2010) Effects of low methyl donor levels in culture medium during mouse follicle culture on oocyte imprinting establishment. *Biol Reprod.* 83(3): 377-86

- Andergassen D, Muckenhuber M, Bammer PC, Kulinski TM, Theussl HC, *et al.* (2019) The Airn lncRNA does not require any DNA elements within its locus to silence distant imprinted genes. *PLoS Genet.* 15(7): e1008268
- Anderson OS, Sant KE and Dolinoy DC (2012) Nutrition and epigenetics: an interplay of dietary methyl donors, one-carbon metabolism and DNA methylation. *J Nutr Biochem.* 23(8): 853-9
- Appaji Rao N, Ambili M, Jala VR, Subramanya HS and Savithri HS (2003) Structure-function relationship in serine hydroxymethyltransferase. *Biochim Biophys Acta.* 1647(1-2): 24-29
- Appleby PN and Key TJ (2016) The long-term health of vegetarians and vegans. *Proc Nutr Soc.* 75(3): 287-93
- Aquilano K, Baldelli S and Ciriolo MR (2014) Glutathione: new roles in redox signaling for an old antioxidant. *Front Pharmacol.* 5: 196
- Araújo JR, Correia-Branco A, Ramalho C, Gonçalves P, Pinho MJ, *et al.* (2013) L-methionine placental uptake: characterization and modulation in gestational diabetes mellitus. *Reprod Sci.* 20(12): 1492-507
- Augsburger NR, Scherer CS, Garrow TA and Baker DH (2005) Dietary S-methylmethionine, a component of foods, has choline-sparing activity in chickens. *J Nutr.* 135(7): 1712-7
- Baker J, Liu JP, Robertson EJ and Efstratiadis A (1993) Role of Insulin-Like Growth Factors in Embryonic and Postnatal Growth. *Cell.* 75(1): 73-82
- Balaghi M, Horne DW and Wagner C (1993) Hepatic one-carbon metabolism in early folate deficiency in rats. *Biochem J.* 291(Pt 1): 145-9
- Ballhausen D, Mittaz L, Boulat O, Bonafé L and Braissant O (2009) Evidence for catabolic pathway of propionate metabolism in CNS: expression pattern of methylmalonyl-CoA mutase and propionyl-CoA carboxylase alpha-subunit in developing and adult rat brain. *Neuroscience.* 164(2): 578-87
- Bannister AJ and Kouzarides T (2011) Regulation of chromatin by histone modifications. *Review Cell Res.* 21(3): 381-95
- Bannister AJ, Schneider R and Kouzarides T (2002) Histone methylation: dynamic or static? *Cell.* 109(7): 801-6
- Barakat TS and Gribnau J (2012) X chromosome inactivation in the cycle of life. *Development.* 139(12): 2085-9
- Baran Y, Subramaniam M, Biton A, Tukiainen T, Tsang EK, *et al.* (2015) The Landscape of Genomic Imprinting Across Diverse Adult Human Tissues. *Genome Res.* 25(7): 927-36
- Barker DJ (1995) The fetal and infant origins of disease. *Eur J Clin Invest.* 25: 457-63
- Barker DJ and Osmond C (1986) Infant mortality, childhood nutrition, and ischaemic heart disease in England and Wales. *Lancet.* 1(8489): 1077-81
- Barker DJ and Osmond C (1988) Low birth weight and hypertension. *BMJ.* 297(6641): 134-5
- Barker DJ, Winter PD, Osmond C, Margetts B and Simmonds SJ (1989) Weight in infancy and death from ischaemic heart disease. *Lancet.* 2(8663): 577-80
- Barlow DP and Bartolomei MS (2014) Genomic imprinting in mammals. *Cold Spring Harb Perspect Biol.* 6(2). pii: a018382
- Barlow DP, Stöger R, Herrman BG, Saito K and Schweifer N (1991) The mouse insulin-like growth factor type-2 receptor is imprinted and closely linked to the Tme locus. *Nature.* 349: 84-87

- Barrès R, Osler ME, Yan J, Rune A, Fritz T, *et al.* (2009) Non-CpG methylation of the PGC-1 α promoter through DNMT3B controls mitochondrial density. *Cell Metab.* 10(3): 189-98
- Barski A, Cuddapah S, Cui K, Roh TY, Schones DE, *et al.* (2007) High-resolution profiling of histone methylations in the human genome. *Cell.* 129(4): 823-37
- Batista PJ (2017) The RNA Modification N6-methyladenosine and Its Implications in Human Disease. *Genomics Proteomics Bioinformatics.* 15(3): 154-163
- Batistel F, Alharthi AS, Yambao RRC, Elolimy AA, Pan YX, *et al.* (2019) Methionine Supply During Late-Gestation Triggers Offspring Sex-Specific Divergent Changes in Metabolic and Epigenetic Signatures in Bovine Placenta. *J Nutr.* 149(1): 6-17
- Bearak J, Popinchalk A, Alkema L and Sedgh G (2018) Global, regional, and subregional trends in unintended pregnancy and its outcomes from 1990 to 2014: estimates from a Bayesian hierarchical model. *Lancet Glob Health.* 6(4): e380-e389
- Beaudin AE and Stover PJ (2009) Insights into metabolic mechanisms underlying folate-responsive neural tube defects: a minireview. *Birth Defects Res A Clin Mol Teratol.* 85(4): 274-84
- Beaujean N, Hartshorne G, Cavilla J, Taylor J, Gardner J, *et al.* (2004) Non-conservation of mammalian preimplantation methylation dynamics. *Curr Biol.* 14(7): R266-7
- Bebbere D, Bauersachs S, Fürst RW, Reichenbach HD, Reichenbach M, *et al.* (2013) Tissue-specific and minor inter-individual variation in imprinting of IGF2R is a common feature of *Bos taurus* Concepti and not correlated with fetal weight. *PLoS One.* 8(4): e59564
- Bellizzi D, D'Aquila P, Scafone T, Giordano M, Riso V, *et al.* (2013) The control region of mitochondrial DNA shows an unusual CpG and non-CpG methylation pattern. *DNA Res.* 20(6): 537-47
- Benevenga NJ and Steele RD (1984) Adverse effects of excessive consumption of amino acids. *Annu Rev Nutr.* 4: 157-81
- Benjamini Y and Hochberg Y (1995) Controlling the false discovery rate - a practical and powerful approach to multiple testing. *J R Stat Soc Series B.* 57: 289-300
- Benkhalifa M, Bacrie PC, Dumont M, Junca AM, Belloc S, *et al.* (2008) Imprinting in the human oocyte: homocysteine recycling to methionine through methyltetrahydrofolate homocysteine methyl transferase (MTR) and betaine homocysteine methyl transferase (BHMT 2). *Fertility and Sterility - Abstract.* 90(1): S328
- Benkhalifa M, Montjean D, Cohen-Bacrie P and Ménéz Y (2010) Imprinting: RNA expression for homocysteine recycling in the human oocyte. *Fertil Steril.* 93(5): 1585-90
- Bergen NE, Jaddoe VW, Timmermans S, Hofman A, Lindemans J, *et al.* (2012) Homocysteine and folate concentrations in early pregnancy and the risk of adverse pregnancy outcomes: the Generation R Study. *BJOG.* 119(6): 739-51
- Berker B, Kaya C, Aytac R and Satioglu H (2009) Homocysteine concentrations in follicular fluid are associated with poor oocyte and embryo qualities in polycystic ovary syndrome patients undergoing assisted reproduction. *Hum Reprod.* 24(9): 2293-302
- Bermejo-Alvarez P, Rizos D, Lonergan P and Gutierrez-Adan A (2011) Transcriptional sexual dimorphism during preimplantation embryo development and its consequences for developmental competence and adult health and disease. *Reproduction.* 141(5): 563-70
- Bermejo-Alvarez P, Rizos D, Rath D, Lonergan P and Gutierrez-Adan A (2008) Epigenetic differences between male and female bovine blastocysts produced in vitro. *Physiol Genomics.* 32(2): 264-72

- Bermejo-Alvarez P, Rizos D, Rath D, Lonergan P and Gutierrez-Adan A (2010) Sex determines the expression level of one third of the actively expressed genes in bovine blastocysts. *Proc Natl Acad Sci U S A*. 107(8): 3394-9
- Berntsen S and Pinborg A (2018) Large for gestational age and macrosomia in singletons born after frozen/thawed embryo transfer (FET) in assisted reproductive technology (ART). *Birth Defects Res*. 110(8): 630-643
- Biggers JD and Summers MC (2008) Choosing a culture medium: making informed choices. *Fertil Steril*. 90(3): 473-83
- Bistulfi G, Vandette E, Matsui S and Smiraglia DJ (2010) Mild folate deficiency induces genetic and epigenetic instability and phenotype changes in prostate cancer cells. *BMC Biol*. 8: 6
- Black L, Kleiber M and Brown AM (1961) Butyrate Metabolism in the Lactating Cow. *J Biol Chem*. 236(9): 2399-2403
- Blom HJ and Smulders Y (2011) Overview of homocysteine and folate metabolism. With special references to cardiovascular disease and neural tube defects. *J Inherit Metab Dis*. 34(1): 75-81
- Bó G and Mapletoft RJ (2013) Evaluation and classification of bovine embryos. *Animal Reproduction*. 10(3): 344-348
- Bogliotti YS, Wu J, Vilarino M, Okamura D, Soto DA, *et al.* (2018) Efficient derivation of stable primed pluripotent embryonic stem cells from bovine blastocysts. *Proc Natl Acad Sci U S A*. 115(9): 2090-2095
- Bonilla L, Luchini D, Devillard E and Hansen PJ (2010) Methionine requirements for the preimplantation bovine embryo. *J Reprod Dev*. 56(5): 527-32
- Booth MA and Spray GH (1960) Vitamin B12 activity in serum and liver of rats after total gastrectomy. *Br J Haematol*. 6: 288-295
- Booth MJ, Ost TWB, Beraldi D, Bell NM, Branco MR, *et al.* (2013) Oxidative Bisulfite Sequencing of 5-methylcytosine and 5-hydroxymethylcytosine. *Nat Protoc*. 8(10): 1841-51
- Boxmeer JC, Brouns RM, Lindemans J, Steegers EA, Martini E, *et al.* (2008) Preconception folic acid treatment affects the microenvironment of the maturing oocyte in humans. *Fertil Steril*. 89(6): 1766-70
- Boxmeer JC, Macklon NS, Lindemans J, Beckers NG, Eijkemans MJ, *et al.* (2009) IVF outcomes are associated with biomarkers of the homocysteine pathway in monofollicular fluid. *Hum Reprod*. 24(5): 1059-66
- Boyama BA, Cepni I, Imamoglu M, Oncul M, Tuten A, *et al.* (2016) Homocysteine in embryo culture media as a predictor of pregnancy outcome in assisted reproductive technology. *Gynecol Endocrinol*. 32(3): 193-5
- Braunschweig MH (2001) Biallelic transcription of the porcine IGF2R gene. *Gene*. 500(2): 181-5
- Brenet F, Moh M, Funk P, Feierstein E, Viale AJ, *et al.* (2011) DNA methylation of the first exon is tightly linked to transcriptional silencing. *PLoS One*. 6(1): e14524
- Brustolin S, Giugliani R and Félix TM (2010) Genetics of homocysteine metabolism and associated disorders. *Braz J Med Biol Res*. 43(1): 1-7
- Burke TW and Kadonaga JT (1997) The Downstream Core Promoter Element, DPE, Is Conserved From *Drosophila* to Humans and Is Recognized by TAFII60 of *Drosophila*. *Genes Dev*. 11(22): 3020-31
- Campbell KH, McWhir J, Ritchie WA and Wilmut I (1996) Sheep Cloned by Nuclear Transfer From a Cultured Cell Line. *Nature*. 380(6569): 64-6
- Campbell KHS and Alberio (2003) Reprogramming the Genome: Role of the Cell Cycle. *Reprod Suppl*. 61: 477-94

- Canellakis ZN, Marsh LL and Bondy PK (1989) Polyamines and their derivatives as modulators in growth and differentiation. *Yale J Biol Med.* 62(5): 481-91
- Canizo JR, Ynsaurralde Rivolta AE, Vazquez Echeagaray C, Suvá M, Alberio V, *et al.* (2019) A dose-dependent response to MEK inhibition determines hypoblast fate in bovine embryos. *BMC Dev Biol.* 19(1): 13
- Canon E, Jouneau L, Blachère T, Peynot N, Daniel N, *et al.* (2018) Progressive methylation of POU5F1 regulatory regions during blastocyst development. *Reproduction.* 156(2): 145-161
- Canovas S and Ross PJ (2016) Epigenetics in preimplantation mammalian development. *Theriogenology.* 86(1): 69-79
- Cao XY, Rose J, Wang SY, Liu Y, Zhao M, *et al.* (2016) Glycine increases preimplantation development of mouse oocytes following vitrification at the germinal vesicle stage. *Sci Rep.* 6: 37262
- Cao Z, Zhou N, Zhang Y, Zhang Y, Wu R, *et al.* (2014) Dynamic reprogramming of 5-hydroxymethylcytosine during early porcine embryogenesis. *Theriogenology.* 81(3): 496-508
- Castegna A, Iacobazzi V and Infantino V (2015) The mitochondrial side of epigenetics. *Physiol Genomics.* 47(8): 299-307
- Castro R, Rivera I, Struys EA, Jansen EE, Ravasco P, *et al.* (2003) Increased homocysteine and S-adenosylhomocysteine concentrations and DNA hypomethylation in vascular disease. *Clin Chem.* 49(8): 1292-6
- Caudill MA, Wang JC, Melnyk S, Pogribny IP, Jernigan S, *et al.* (2001) Intracellular S-adenosylhomocysteine concentrations predict global DNA hypomethylation in tissues of methyl-deficient cystathionine beta-synthase heterozygous mice. *J Nutr.* 131(11): 2811-8
- Cavallé-Busquets P, Inglés-Puig M, Fernandez-Ballart J, Haro-Barceló J, Rojas-Gómez A, *et al.* (2020) Moderately elevated first trimester fasting plasma total homocysteine is associated with increased probability of miscarriage. The Reus-Tarragona Birth Cohort Study. *Biochimie.* 173: 62-67
- Cernilogar FM, Hasenöder S, Wang Z, Scheibner K, Burtscher I, *et al.* (2019) Pre-marked chromatin and transcription factor co-binding shape the pioneering activity of Foxa2. *Nucleic Acids Res.* 47(17): 9069-9086
- Chadwick LH, McCandless SE, Silverman GL, Schwartz S, Westaway D, *et al.* (2000) Betaine-homocysteine methyltransferase-2: cDNA cloning, gene sequence, physical mapping, and expression of the human and mouse genes. *Genomics.* 70(1): 66-73
- Chakravarthi PV and Sri Balaji N (2010) Use of Assisted Reproductive Technologies for Livestock Development. *Veterinary World.* 3(5): 238-240
- Chan D, Shao X, Dumargne MC, Aarabi M, Simon MM, *et al.* (2019) Customized MethylC-Capture Sequencing to Evaluate Variation in the Human Sperm DNA Methylome Representative of Altered Folate Metabolism. *Environ Health Perspect.* 127(8): 87002
- Chan J, Deng L, Mikael LG, Yan J, Pickell L, *et al.* (2010) Low dietary choline and low dietary riboflavin during pregnancy influence reproductive outcomes and heart development in mice. *Am J Clin Nutr.* 91(4): 1035-43
- Charalambous M, Smith FM, Bennett WR, Crew TE, Mackenzie F, *et al.* (2003) Disruption of the imprinted Grb10 gene leads to disproportionate overgrowth by an Igf2-independent mechanism. *Proc Natl Acad Sci U S A.* 100(14): 8292-7
- Chatterjee A, Rodger EJ, Stockwell PA, Weeks RJ and Morison IM (2012) Technical considerations for reduced representation bisulfite sequencing with multiplexed libraries. *J Biomed Biotechnol.* 2012: 741542

- Chédin F, Lieber MR and Hsieh CL (2002) The DNA methyltransferase-like protein DNMT3L stimulates de novo methylation by Dnmt3a. *Proc Natl Acad Sci U S A*. 99(26): 16916-21
- Chen AE, Egli D, Niakan K, Deng J, Akutsu H, *et al.* (2009) Optimal timing of inner cell mass isolation increases the efficiency of human embryonic stem cell derivation and allows generation of sibling cell lines. *Cell Stem Cell*. 4(2): 103-6
- Chen NC, Yang F, Capecchi LM, Gu Z, Schafer AI, *et al.* (2010) Regulation of homocysteine metabolism and methylation in human and mouse tissues. *FASEB J*. 24(8): 2804-17
- Chen PR, Redel BK, Spate LD, Ji T, Rojas Salazar S, *et al.* (2018) Glutamine supplementation enhances development of in vitro-produced porcine embryos and increases leucine consumption from the medium. *Biol Reprod*. 99(5): 938–948
- Chen Z, Hagen DE, Elsik CG, Ji T, Morris CJ, *et al.* (2015) Characterization of global loss of imprinting in fetal overgrowth syndrome induced by assisted reproduction. *Proc Natl Acad Sci U S A*. 112(15): 4618-23
- Chen Z, Hagen DE, Tieming J, Elsik CG and Rivera RM (2017) Global misregulation of genes largely uncoupled to DNA methylome epimutations characterizes a congenital overgrowth syndrome. *Sci Rep*. 7: 12667
- Chen Z, Hagen DE, Wang J, Elsik CG, Ji T, *et al.* (2016) Global assessment of imprinted gene expression in the bovine conceptus by next generation sequencing. *Epigenetics*. 11(7): 501-16
- Chen Z, Robbins KM, Wells KD and Rivera RM (2013) Large offspring syndrome: a bovine model for the human loss-of-imprinting overgrowth syndrome Beckwith-Wiedemann. *Epigenetics*. 8(6): 591-601
- Cheng HC, Qi RZ, Paudel H and Zhu HJ (2011) Regulation and function of protein kinases and phosphatases. *Enzyme Res*. 2011: 794089
- Chien YH, Abdenur JE, Baronio F, Bannick AA, Corrales F, *et al.* (2015) Mudd's disease (MAT I/III deficiency): a survey of data for MAT1A homozygotes and compound heterozygotes. *Orphanet J Rare Dis*. 10: 99
- Cho J, Overton TR, Schwab CG and Tauer LW (2007) Determining the amount of rumen-protected methionine supplement that corresponds to the optimal levels of methionine in metabolizable protein for maximizing milk protein production and profit on dairy farms. *J Dairy Sci*. 90(10): 4908-16
- Choi JD, Bowers-Komro M, Davis MD, Edmondson DE and McCormick DB (1983) Kinetic properties of pyridoxamine (pyridoxine)-5'-phosphate oxidase from rabbit liver. *J Biol Chem*. 258(2): 840-5
- Choi YH, Lee BC, Lim JM, Kang SK and Hwang WS (2002) Optimization of culture medium for cloned bovine embryos and its influence on pregnancy and delivery outcome. *Theriogenology*. 58(6): 1187–1197
- Chou HY, Lin YH, Shiu GL, Tang HY, Cheng ML, *et al.* (2014) ADI1, a methionine salvage pathway enzyme. *iBiochem Cell Biol*. 82(1): 18-26
- Chronopoulou E and Harper JC (2015) IVF culture media: past, present and future. *Hum Reprod Update*. 21(1): 39-55
- Chung YG, Mann MRW, Bartolomei MS and Latham KE (2002) Nuclear-Cytoplasmic “Tug of War” During Cloning: Effects of Somatic Cell Nuclei on Culture Medium Preferences of Preimplantation Cloned Mouse Embryos. *Biol. Reprod*. 66(4): 1178-1184
- Clare CE, Brassington AH, Kwong WY and Sinclair K (2019) One-Carbon Metabolism: Linking Nutritional Biochemistry to Epigenetic Programming of Long-Term Development. *Annu Rev Anim Biosci*. 7: 263-87

- Clarke EL, Bush SJ, McCulloch MEB, Farquhar L, Young R, *et al.* (2017) A high resolution atlas of gene expression in the domestic sheep (*Ovis aries*). *PLoS Genet.* 13(9): e1006997
- Clifton VL (2010) Review: Sex and the human placenta: mediating differential strategies of fetal growth and survival. *Placenta.* 31: S33-9
- Clutton-Brock H, Albon SD and Guinness FE (1986) Great expectations: dominance, breeding success and offspring sex ratios in red deer. *Anim. Behav.* 34(20): 460-471
- Cole LK, Vance JE and Vance DE (2012) Phosphatidylcholine biosynthesis and lipoprotein metabolism. *Biochim Biophys Acta.* 1821(5): 754-61
- Colinas M and Fitzpatrick TB (2016) Interaction between vitamin B6 metabolism, nitrogen metabolism and autoimmunity. *Plant Signal Behav.* 11(4): e1161876
- Cooney CA, Dave AA and Wolff GL (2002) Maternal methyl supplements in mice affect epigenetic variation and DNA methylation of offspring. *J Nutr.* 132(8): 2393S-2400S
- Cooper BA and Lowenstein L (1966) Vitamin B-12-folate interrelationships in megaloblastic anaemia. *Br J Haematol.* 12(3): 283-96
- Cordaux R and Batzer MA (2009) The impact of retrotransposons on human genome evolution. *Nat Rev Genet.* 10(10): 691-703
- Cordova A, King WA and Mastro Monaco GF (2017) Choosing a culture medium for SCNT and iSCNT reconstructed embryos: from domestic to wildlife species. *J Anim Sci Technol.* 59: 24
- Cortessis VK, Azadian M, Buxbaum J, Sanogo F, Song AY, *et al.* (2018) Comprehensive meta-analysis reveals association between multiple imprinting disorders and conception by assisted reproductive technology. *J Assist Reprod Genet.* 35(6): 943-952
- Costa-Borges N, Santaló J and Ibáñez E (2010) Comparison between the effects of valproic acid and trichostatin A on the in vitro development, blastocyst quality, and full-term development of mouse somatic cell nuclear transfer embryos. *Cell Reprogram.* 12(4): 437-46
- Cowley M, Garfield AS, Madon-Simon M, Charalambous M, Clarkson RW, *et al.* (2014) Developmental Programming Mediated by Complementary Roles of Imprinted *Grb10* in Mother and Pup. *PLoS Biol.* 12(2): e1001799
- Crider KS, Bailey LB and Berry RJ (2011) Folic acid food fortification-its history, effect, concerns, and future directions. *Nutrients.* 3(3): 370-84
- da Silva RP, Eudy BJ and Deminice R (2020) One-Carbon Metabolism in Fatty Liver Disease and Fibrosis: One-Carbon to Rule Them All. *J Nutr.* 150(5): 994-1003
- Dai Z, Mentch SJ, Gao X, Nichenametla SN and Locasale JW (2018) Methionine metabolism influences genomic architecture and gene expression through H3K4me3 peak width. *Nat Commun.* 9(1): 1955
- Dasarathy J, Gruca LL, Bennett C, Parimi PS, Duenas C, *et al.* (2010) Methionine metabolism in human pregnancy. *Am J Clin Nutr.* 91(2): 357-65
- Davidson EH (2010) Emerging properties of animal gene regulatory networks. *Nature.* 468(7326): 911–920
- Davison JM, Mellott TJ, Kovacheva VP and Blusztajn JK (2009) Gestational choline supply regulates methylation of histone H3, expression of histone methyltransferases G9a (*Kmt1c*) and Suv39h1 (*Kmt1a*), and DNA methylation of their genes in rat fetal liver and brain. *J Biol Chem.* 284(4): 1982-9
- Dawbarn MC, Hine DC and Smith J (1958) Folic acid activity in the liver of sheep. III. The effect of vitamin B12 deficiency on the concentration of folic acid and citrovorum factor. *Aust J Exp Biol Med Sci.* 36(6): 541-545

- de Montera B, Fournier E, Shojaei Saadi HA, Gagné D, Laflamme I, *et al.* (2013) Combined methylation mapping of 5mC and 5hmC during early embryonic stages in bovine. *BMC Genomics*. 14: 406
- De Vadder F, Kovatcheva-Datchary P, Zitoun C, Duchamp A, Bäckhed F and Mithieux G (2016) Microbiota-Produced Succinate Improves Glucose Homeostasis via Intestinal Gluconeogenesis. *Cell Metab*. 24(1): 151-157.
- De Wals P, Tairou F, Van Allen MI, Uh SH, Lowry RB, *et al.* (2007) Reduction in neural-tube defects after folic acid fortification in Canada. *N Engl J Med*. 357(2): 135-42
- Dean W, Santos F, Stojkovic M, Zakhartchenko V, Walter J, *et al.* (2001) Conservation of methylation reprogramming in mammalian development: aberrant reprogramming in cloned embryos. *Proc Natl Acad Sci U S A*. 98(24): 13734-8
- Deaton AM and Bird A (2011) CpG islands and the regulation of transcription. *Genes Dev*. 25(10): 1010-22
- Demond H and Kelsey G (2020) The enigma of DNA methylation in the mammalian oocyte. *F1000 Res*. 9: 146
- De-Regil LM, Fernández-Gaxiola AC, Dowswell T and Peña-Rosas JP (2010) Effects and safety of periconceptional folate supplementation for preventing birth defects. *Cochrane Database Syst Rev*. 6(10): CD007950
- Devlin AM, Arning E, Bottiglieri T, Faraci FM, Rozen R, *et al.* (2004) Effect of Mthfr genotype on diet-induced hyperhomocysteinemia and vascular function in mice. *Blood*. 103(7): 2624-9
- Dhillon VS, Shahid M and Husain SA (2007) Associations of MTHFR DNMT3b 4977 bp deletion in mtDNA and GSTM1 deletion, and aberrant CpG island hypermethylation of GSTM1 in non-obstructive infertility in Indian men. *Mol Hum Reprod*. 13(4): 213-22
- Dieamant F, Petersen CG, Mauri AL, Comar V, Mattila M, *et al.* (2017) Single versus sequential culture medium: which is better at improving ongoing pregnancy rates? A systematic review and meta-analysis. *JBRA Assist Reprod*. 21(3): 240-246
- Diplas AI, Lambertini L, Lee MJ, Sperling R, Lee YL, *et al.* (2009) Differential expression of imprinted genes in normal and IUGR human placentas. *Epigenetics*. 4(4): 235-40
- Ditscheid B, Fünfstück R, Busch M, Schubert R, Gerth J, *et al.* (2005) Effect of L-methionine supplementation on plasma homocysteine and other free amino acids: a placebo-controlled double-blind cross-over study. *Eur J Clin Nutr*. 59(6): 768-75
- Dobbs KB, Rodriguez M, Sudano MJ, Ortega MS and Hansen PJ (2013) Dynamics of DNA methylation during early development of the preimplantation bovine embryo. *PLoS One*. 8(6): e66230
- Doherty R and Couldrey C (2014) Exploring genome wide bisulfite sequencing for DNA methylation analysis in livestock: a technical assessment. *Front Genet*. 5: 126
- Dolinoy DC (2008) The agouti mouse model: an epigenetic biosensor for nutritional and environmental alterations on the fetal epigenome. *Nutr Rev*. 66(1): S7-11
- Dominguez-Salas P, Moore SE, Baker MS, Bergen AW, Cox SE, *et al.* (2014) Maternal nutrition at conception modulates DNA methylation of human metastable epialleles. *Nat Commun*. 5: 3746
- Dong E, Agis-Balboa RC, Simonini MV, Grayson DR, Costa E, *et al.* (2005) Reelin and glutamic acid decarboxylase67 promoter remodeling in an epigenetic methionine-induced mouse model of schizophrenia. *Proc Natl Acad Sci U S A*. 102(35): 12578-83
- Drábková P, Andrllová L, Hampl R and Kandár R (2016) Amino acid metabolism in human embryos. *Physiol Res*. 65(5): 823-832

- Du P, Zhang X, Huang C-C, Jafari N, Kibbe WA, *et al.* (2010) Comparison of Beta-value and M-value Methods for Quantifying Methylation Levels by Microarray Analysis. *BMC Bioinformatics*. 11: 587
- Duan JE, Jiang ZC, Alqahtani F, Mandoiu I, Dong H, *et al.* (2019) Methylome Dynamics of Bovine Gametes and in vivo Early Embryos. *Front Genet*. 10: 512
- Ducker GS and Rabinowitz JD (2017) One-carbon metabolism in health and disease. *Cell Metab*. 25: 27–42
- Dumoulin JC, Land JA, Van Montfoort AP, Nelissen EC, Coonen E, *et al.* (2010) Effect of in vitro culture of human embryos on birthweight of newborns. *Hum Reprod*. 25(3): 605-12
- Dunford LJ, Sinclair KD, Kwong WY, Sturrock C, Clifford BL, *et al.* (2014) Maternal protein-energy malnutrition during early pregnancy in sheep impacts the fetal ornithine cycle to reduce fetal kidney microvascular development. *FASEB J*. 28(11): 4880-92
- Dunlop AL, Jack B and Frey K (2007) National recommendations for preconception care: the essential role of the family physician. *J Am Board Fam Med*. 20(1): 81-4
- Ebisch IM, Peters WH, Thomas CM, Wetzels AM, Peer PG, *et al.* (2006) Homocysteine, glutathione and related thiols affect fertility parameters in the (sub)fertile couple. *Hum Reprod*. 21(7): 1725-33
- Edwards JL, Ealy AD, Monterroso VH and Hansen PJ (1997) Ontogeny of temperature-regulated heat shock protein 70 synthesis in preimplantation bovine embryos. *Mol Reprod Dev*. 48(1): 25-33
- Edwards LJ and McMillen IC (2002) Periconceptional nutrition programs development of the cardiovascular system in the fetal sheep. *Am J Physiol Regul Integr Comp Physiol*. 283(3): R669-79
- El Hajj N, Haertle L, Dittrich M, Denk S, Lehnen H, *et al.* (2017) DNA methylation signatures in cord blood of ICSI children. *Hum Reprod*. 32(8): 1761-1769
- Elhassan YM, Wu G, Leanez AC, Tasca RJ, Watson AJ, *et al.* (2001) Amino acid concentrations in fluids from the bovine oviduct and uterus and in KSOM-based culture media. *Theriogenology*. 55(9): 1907-18
- Ensminger, M. E., J. E. Oldfield, and W. W. Heinemann eds. (1990) Feeds and Nutrition. 2nd ed. Ensminger Publishing Co. Clovis, California
- Estécio MR, Gharibyan V, Shen L, Ibrahim AE, Doshi K, *et al.* (2007) LINE-1 hypomethylation in cancer is highly variable and inversely correlated with microsatellite instability. *PLoS One*. 2(5): e399
- Farmer WT, Farin PW, Piedrahita JA, Bischoff SR and Farin CE (2013) Expression of antisense of insulin-like growth factor-2 receptor RNA non-coding (AIRN) during early gestation in cattle. *Anim Reprod*. 138(1-2): 64-73
- Farmer WT, Sommer JR and Farin CE (2016) Sequence Characterization of Bovine Antisense to Insulin-Like Growth Factor Type 2 Receptor Non-Coding RNA (AIRN). *J Genet Genome Res*. 3: 026
- Farquharson J and Adams JF (1976) The forms of vitamin B12 in foods. *Br J Nutr*. 36(1): 127-136
- Fell DA and Snell K (1988) Control analysis of mammalian serine biosynthesis. Feedback inhibition on the final step. *Biochem J*. 256(1): 97-101
- Feng Q, Kalari K, Fridley BL, Jenkins G, Ji Y, *et al.* (2011) Betaine-homocysteine methyltransferase: human liver genotype-phenotype correlation. *Mol Genet Metab*. 102(2): 126-33
- Feng S, Jacobsen SE and Reik W (2010) Epigenetic reprogramming in plant and animal development. *Science*. 330(6004): 622-7

- Ferraro S, Panzeri A and Panteghini M (2017) Tackling serum folate test in European countries within the health technology assessment paradigm: request appropriateness, assays and health outcomes. *Clin Chem Lab Med.* 55(9): 1262-1275
- Ficz G, Branco MR, Seisenberger S, Santos F, Krueger F, *et al.* (2011) Dynamic regulation of 5-hydroxymethylcytosine in mouse ES cells and during differentiation. *Nature.* 473(7347): 398-402
- Field MS and Stover PJ (2018) Safety of folic acid. *Ann N Y Acad Sci.* 1414(1): 59-71
- Finch LM, Craig VA, Kind AJ, Schnieke A, Scott A, *et al.* (1996) Primary Culture of Ovine Mammary Epithelial Cells. *Biochem Soc Trans.* 24(3): 369S
- Finkelstein JD (1990) Methionine metabolism in mammals. *J Nutr Biochem.* 1(5): 228-37
- Finkelstein JD (2000) Pathways and regulation of homocysteine metabolism in mammals. *Semin Thromb Hemost.* 26(3): 219-25
- Finkelstein JD and Martin JJ (1984) Methionine metabolism in mammals: distribution of homocysteine between competing pathways. *J. Biol. Chem.* 259(15): 9508–13
- Finkelstein JD and Martin JJ (1986) Methionine metabolism in mammals. Adaptation to methionine excess. *J Biol Chem.* 261(4): 1582-7
- Fleming TP, Watkins AJ, Velazquez MA, Mathers JC, Prentice AM, *et al.* (2018) Origins of lifetime health around the time of conception: causes and consequences. *Lancet.* 391(10132): 1842-52
- Flintoft L (2010) Adding epigenetics to the mix. *Nature Reviews Genetics.* 11: 95
- Fonty G, Gouet P, Jouany J-P and Senaud J (1987) Establishment of the Microflora and Anaerobic Fungi in the Rumen of Lambs. *J Gen Microbiol.* 133: 1835-1
- Forny P, Froese DS, Suormala T, Yue WW and Baumgartner MR (2014) Functional characterization and categorization of missense mutations that cause methylmalonyl-CoA mutase (MUT) deficiency. *Hum Mutat.* 35(12): 1449-58
- Forteschi M, Zinellu A, Assaretti S, Mangoni AA, Pintus G, *et al.* (2016) An isotope dilution capillary electrophoresis/tandem mass spectrometry (CE-MS/MS) method for the simultaneous measurement of choline, betaine, and dimethylglycine concentrations in human plasma. *Anal Bioanal Chem.* 408(26): 7505-12
- Fowden AL, Sibley C, Reik W and Constancia M (2006) Imprinted Genes, Placental Development and Fetal Growth. *Horm Res.* 65(3): 50-8
- Frank D, Fortino W, Clark L, Musalo R, Wang W, *et al.* (2002) Placental overgrowth in mice lacking the imprinted gene *Ipl*. *Proc. Natl Acad. Sci. USA.* 99: 7490-95
- Frau M, Feo F and Pascale RM (2013) Pleiotropic effects of methionine adenosyltransferases deregulation as determinants of liver cancer progression and prognosis. *J Hepatol.* 59(4): 830-41
- Fukuwatari T, Wada H and Shibata K (2008) Age-related alterations of B-group vitamin contents in urine, blood and liver from rats. *J. Nutr. Sci. Vitaminol. (Tokyo).* 54(5): 357-362
- Furlong JM, Sedcole JR and Sykes AR (2010) An evaluation of plasma homocysteine in the assessment of vitamin B12 status of pasture-fed sheep. *N Z Vet J.* 58(1): 11-6
- Gagne A, Hochman A, Qureshi M, Tong C, Arbon J, *et al.* (2014) Analysis of DNA methylation acquisition at the imprinted *Dlk1* locus reveals asymmetry at CpG dyads. *Epigenetics Chromatin.* 7: 9
- Galli C, Duchi R, Moor RM and Lazzari G (1999) Mammalian leukocytes contain all the genetic information necessary for the development of a new individual. *Cloning.* 1(3): 161-70

- Gallou-Kabani C, Gabory A, Tost J, Karimi M, Mayeur S, *et al.* (2010) Sex- and diet-specific changes of imprinted gene expression and DNA methylation in mouse placenta under a high-fat diet. *PLoS One*. 5(12): e14398
- Gamble LD, Hogarty MD, Liu X, Ziegler DS, Marshall G, *et al.* (2012) Polyamine pathway inhibition as a novel therapeutic approach to treating neuroblastoma. *Front Oncol*. 2: 162
- Ganu R, Garrow T, Koutmos M, Rund L and Schook LB (2013) Splicing variants of the porcine betaine-homocysteine S-methyltransferase gene: implications for mammalian metabolism. *Gene*. 529(2): 228-37
- Ganu RS, Ishida Y, Koutmos M, Kolokotronis SO, Roca AL, *et al.* (2015) Evolutionary Analyses and Natural Selection of Betaine-Homocysteine S-Methyltransferase (BHMT) and BHMT2 Genes. *PLoS One*. 10(7): e0134084
- García-Minguillán CJ, Fernandez-Ballart JD, Ceruelo S, Ríos L, Bueno O, Berrocal-Zaragoza MI, Molloy AM, *et al.* (2014) Riboflavin status modifies the effects of methylenetetrahydrofolate reductase (MTHFR) and methionine synthase reductase (MTRR) polymorphisms on homocysteine. *Genes Nutr*. 9(6): 435
- Gardner DK and Lane M (1993) Amino acids and ammonium regulate mouse embryo development in culture. *Biol Reprod*. 48(2): 377-85
- Garlick PJ (2006) Toxicity of methionine in humans. *Nutr*. 136(6 Suppl): 1722S-1725S
- Garratt LC, Ortori CA, Tucker GA, Sablitzky F, Bennett MJ and Barrett DA (2005) Comprehensive metabolic profiling of mono- and polyglutamated folates and their precursors in plant and animal tissue using liquid chromatography/negative ion electrospray ionisation tandem mass spectrometry. *Rapid Commun Mass Spectrom*. 19(17): 2390-2398
- Garrow TA (1996) Purification, kinetic properties, and cDNA cloning of mammalian betaine-homocysteine methyltransferase. *J Biol Chem*. 271(37): 22831-8
- Garrow TA, Brenner AA, Whitehead VM, Chen XN, Duncan RG, *et al.* (1993) Cloning of human cDNAs encoding mitochondrial and cytosolic serine hydroxymethyltransferases and chromosomal localization. *J Biol Chem*. 268(16): 11910-6
- Gaughan DJ, Kluijtmans LA, Barbaux S, McMaster D, Young IS, *et al.* (2001) The methionine synthase reductase (MTRR) A66G polymorphism is a novel genetic determinant of plasma homocysteine concentrations. *Atherosclerosis*. 157(2): 451-6
- Gaull G, Sturman JA and Räihä NC (1972) Development of Mammalian Sulfur Metabolism: Absence of Cystathionase in Human Fetal Tissues. *Pediatr Res*. 6(6): 538-47
- Gawthorne JM and Smith RM (1974) Folic acid metabolism in vitamin B12-deficient sheep. Effects of injected methionine on methotrexate transport and the activity of enzymes associated with folate metabolism in liver. *Biochem J*. 142(1): 119-26
- Gentili A, Caretti F, D'Ascenzo G, Marchese S, Perret D, *et al.* (2008) Simultaneous determination of water-soluble vitamins in selected food matrices by liquid chromatography/electrospray ionization tandem mass spectrometry. *Rapid Commun Mass Spectrom*. 22(13): 2029-43
- Gérard N, Loiseau S, Duchamp G and Seguin F (2002) Analysis of the variations of follicular fluid composition during follicular growth and maturation in the mare using proton nuclear magnetic resonance (1H NMR). *Reproduction*. 124(2): 241-8
- Gernand AD, Schulze KJ, Stewart CP, West KP Jr and Christian P (2016) Micronutrient deficiencies in pregnancy worldwide: health effects and prevention. *Nat Rev Endocrinol*. 12(5): 274-89
- Gillette TG and Hill JA (2015) Readers, writers, and erasers: chromatin as the whiteboard of heart disease. *Circ Res*. 116(7): 1245-53

- Gilsing AM, Crowe FL, Lloyd-Wright Z, Sanders TA, Appleby PN, *et al.* (2010) Serum concentrations of vitamin B12 and folate in British male omnivores, vegetarians and vegans: results from a cross-sectional analysis of the EPIC-Oxford cohort study. *Eur J Clin Nutr.* 64(9): 933-9
- Glenn CC, Driscoll DJ, Yang TP and Nicholls RD (1997) Genomic Imprinting: Potential Function and Mechanisms Revealed by the Prader-Willi and Angelman Syndromes. *Mol Hum Reprod.* 3(4): 321-32
- Goll MG, Kirpekar F, Maggert KA, Yoder JA, Hsieh CL, *et al.* (2006) Methylation of tRNA^{Asp} by the DNA methyltransferase homolog Dnmt2. *Science.* 311(5759): 395-8
- Goodhand KL, Watt RG, Staines ME, Hutchinson JS, and Broadbent PJ (1999) In vivo oocyte recovery and in vitro embryo production from bovine donors aspirated at different frequencies or following FSH treatment. *Theriogenology.* 51(5): 951-61
- Gosalia N, Yang R, Kerschner JL and Harris A (2015) FOXA2 regulates a network of genes involved in critical functions of human intestinal epithelial cells. *Physiol Genomics.* 47(7): 290-7
- Gouveia C, Huyser C, Egli D and Pepper MS (2020) Lessons Learned from Somatic Cell Nuclear Transfer. *Int J Mol Sci.* 21(7): 2314
- Grace N (1994) *Managing trace element deficiencies : the diagnosis and prevention of selenium, cobalt, copper and iodine deficiencies in New Zealand grazing livestock.* AgResearch. Available at: <https://trove.nla.gov.au/work/23931838?q&versionId=28942302> (Accessed: 18 June 2018)
- Graf A, Krebs S, Zakhartchenko V, Schwalb B, Blum H, *et al.* (2014) Fine mapping of genome activation in bovine embryos by RNA sequencing. *Proc Natl Acad Sci U S A.* 111(11): 4139-44
- Groot GS and Kroon AM (1979) Mitochondrial DNA from various organisms does not contain internally methylated cytosine in -CCGG- sequences. *Biochim Biophys Acta.* 564(2): 355-7
- Gruner TM, Sedcole JR, Furlong JM and Sykes AR (2004) A critical evaluation of serum methylmalonic acid and vitamin B12 for the assessment of cobalt deficiency of growing lambs in New Zealand. *Z Vet J.* 52(3): 137-44
- Guillomot M, Taghouti G, Constant F, Constant S, Hue I, *et al.* (2010) Abnormal Expression of the Imprinted Gene Phlda2 in Cloned Bovine Placenta. *Placenta.* 31(6): 482-90
- Guo F, Li L, Jingyun L, Xinglong W, Hu B, *et al.* (2017) Single-cell multi-omics sequencing of mouse early embryos and embryonic stem cells. *Cell Res.* 27(8): 967-988
- Guo F, Li X, Liang D, Li T, Zhu P, *et al.* (2014) Active and passive demethylation of male and female pronuclear DNA in the mammalian zygote. *Cell Stem Cell.* 15(4): 447-459
- Guo H, Zhu P, Guo F, Li X, Wu X, *et al.* (2015) Profiling DNA methylome landscapes of mammalian cells with single-cell reduced-representation bisulfite sequencing. *Nat Protoc.* 10(5): 645-59
- Guo H, Zhu P, Yan L, Li R, Hu B, *et al.* (2014b) The DNA methylation landscape of human early embryos. *Nature.* 511(7511): 606-10
- Guo JU, Ma DK, Mo H, Ball MP, Jang MH, *et al.* (2011) Neuronal activity modifies the DNA methylation landscape in the adult brain. *Nat Neurosci.* 14(10): 1345-51
- Guyader-Joly C, Khatchadourian C and Ménézo Y (1997) Glycine and methionine transport by bovine embryos. *Zygote.* 5(3): 273-6

- Haggarty P, Hoad G, Campbell DM, Horgan GW, Piyathilake C, *et al.* (2013) Folate in pregnancy and imprinted gene and repeat element methylation in the offspring. *Am J Clin Nutr.* 97(1): 94-9
- Hague WM (2003) Homocysteine and pregnancy. *Best Pract Res Clin Obstet Gynaecol.* 17(3): 459-69
- Haig D (2004) Genomic imprinting and kinship: how good is the evidence? *Annu Rev Genet.* 38: 553-85
- Halpern KB, Vana T and Walker MD (2014) Paradoxical Role of DNA Methylation in Activation of FoxA2 Gene Expression during Endoderm Development. *J Biol Chem.* 289(34): 23882–23892
- Hambidge KM, Krebs NF, Westcott JE, Garces A, Goudar SS, *et al.* (2014) Preconception maternal nutrition: a multi-site randomized controlled trial. *BMC Pregnancy Childbirth.* 14: 111
- Hammiche F, Laven JS, van Mil N, de Cock M, de Vries JH, *et al.* (2011) Tailored preconceptional dietary and lifestyle counselling in a tertiary outpatient clinic in The Netherlands. *Hum Reprod.* 26(9): 2432-41
- Handyside AH and Barton SC (1977) Evaluation of the technique of immunosurgery for the isolation of inner cell masses from mouse blastocysts. *J Embryol Exp Morphol.* 37(1): 217-26
- Hanin G and Ferguson-Smith AC (2020) The evolution of genomic imprinting: Epigenetic control of mammary gland development and postnatal resource control. *Wiley Interdiscip Rev Syst Biol Med.* 12(3): e1476
- Hannibal L, Lysne V, Bjørke-Monsen A-L, Behringer S, Grünert SC, *et al.* (2016) Biomarkers and Algorithms for the Diagnosis of Vitamin B12 Deficiency. *Front Mol Biosci.* 3: 27
- Hansen PJ and Block J (2004) Towards an embryocentric world: the current and potential uses of embryo technologies in dairy production. *Reprod Fertil Dev.* 16(1-2): 1-14
- Hao M, Zhao W, Zhang L, Wang H and Yang X (2016) Low folate levels are associated with methylation-mediated transcriptional repression of miR-203 and miR-375 during cervical carcinogenesis. *Oncol Lett.* 11(6): 3863-3869
- Harper AE, Benevenga NJ and Wohlhueter RM (1970) Effects of ingestion of disproportionate amounts of amino acids. *Physiol Rev.* 50(3): 428-558
- Harper J, Magli MC, Lundin K, Barratt CL and Brison D (2012) When and how should new technology be introduced into the IVF laboratory? *Hum Reprod.* 27(2): 303-13
- Harris SE, Gopichandran N, Picton HM, Leese HJ and Orsi NM (2005) Nutrient Concentrations in Murine Follicular Fluid and the Female Reproductive Tract. *Theriogenology.* 64(4): 992-1006
- Hassiotou F, Hepworth AR, Beltran AS, Mathews MM, Stuebe AM, *et al.* (2013) Expression of the Pluripotency Transcription Factor OCT4 in the Normal and Aberrant Mammary Gland. *Front Oncol.* 3: 79
- Hata K, Okano M, Lei H and Li E (2002) Dnmt3L cooperates with the Dnmt3 family of de novo DNA methyltransferases to establish maternal imprints in mice. *Development.* 129(8): 1983-93
- Hattori H, Hiura H, Kitamura A, Miyauchi N, Kobayashi N, *et al.* (2019) Association of four imprinting disorders and ART. *Clin Epigenetics.* 11(1): 21
- He YF, Li BZ, Li Z, Liu P, Wang Y, *et al.* (2011) Tet-mediated formation of 5-carboxylcytosine and its excision by TDG in mammalian DNA. *Science.* 333(6047): 1303-7

- Hegedüs M, Fekete S, Veresegyházy T, Andrásosfzky E and Brydl E (1995) Effect of methionine and its related compounds on rumen bacterial activity. *Arch Tierernahr.* 47(3): 287-94
- Heidari M, Kafi M, Mirzaei A, Asaadi A and Mokhtari A (2019) Effects of follicular fluid of preovulatory follicles of repeat breeder dairy cows with subclinical endometritis on oocyte developmental competence. *Anim Reprod Sci.* 205: 62-69
- Hemberger M, Dean W and Reik W (2009) Epigenetic dynamics of stem cells and cell lineage commitment: digging Waddington's canal. *Nat Rev Mol Cell Biol.* 10(8): 526-37
- Heras S, De Coninck DIM, Van Poucke M, Goossens K, Bogado Pascottini O, *et al.* (2016) Suboptimal culture conditions induce more deviations in gene expression in male than female bovine blastocysts. *BMC Genomics.* 17: 72
- Herrick JR, Lyons SM, Greene AF, Broeckling CD, Schoolcraft WB, *et al.* (2016) Direct and Osmolarity-Dependent Effects of Glycine on Preimplantation Bovine Embryos. *PLoS One.* 11(7): e0159581
- Hertrampf E and Cortés F (2008) National food-fortification program with folic acid in Chile. *Food Nutr Bull.* 29(2): S231-7
- Hill JR, Rousset AJ, Cibelli JB, Edwards JF, Hooper NL, *et al.* (1999) Clinical and Pathologic Features of Cloned Transgenic Calves and Fetuses (13 Case Studies). *Theriogenology.* 51(8): 1451-65
- Ho V, Ashbury JE, Taylor S, Vanner S and King WD (2015) Gene-specific DNA methylation of DNMT3B and MTHFR and colorectal adenoma risk. *Mutat Res.* 782: 1-6
- Ho V, Massey TE and King WD (2013) Effects of methionine synthase and methylenetetrahydrofolate reductase gene polymorphisms on markers of one-carbon metabolism. *Genes Nutr.* 8(6): 571-80
- Hochberg Z, Feil R, Constancia M, Fraga M, Junien C, *et al.* (2011) Child health, developmental plasticity, and epigenetic programming. *Endocr Rev.* 32(2): 159-22
- Home P, Ray S, Dutta D, Bronshteyn I, Larson M, *et al.* (2009) GATA3 is selectively expressed in the trophectoderm of peri-implantation embryo and directly regulates Cdx2 gene expression. *J Biol Chem.* 284(42): 28729-37
- Honein MA, Paulozzi LJ, Mathews TJ, Erickson JD and Wong LY (2001) Impact of folic acid fortification of the US food supply on the occurrence of neural tube defects. *JAMA.* 285(23): 2981-6
- Hou J, Liu L, Lei T, Cui X, An X, *et al.* (2007) Genomic DNA methylation patterns in bovine preimplantation embryos derived from in vitro fertilization. *Sci China C Life Sci.* 50(1): 56-61
- Houghton FD (2006) Energy Metabolism of the Inner Cell Mass and Trophectoderm of the Mouse Blastocyst. *Differentiation.* 74(1): 11-8
- Hoyo C, Murtha AP, Schildkraut JM, Jirtle RL, Demark-Wahnefried W, *et al.* (2011) Methylation variation at IGF2 differentially methylated regions and maternal folic acid use before and during pregnancy. *Epigenetics.* 6(7): 928-36
- Hsu HK, Weng YI, Hsu PY, Huang TH and Huang YW (2014) Detection of DNA methylation by MeDIP and MBDCap assays: an overview of techniques. *Methods Mol Biol.* 1105: 61-70
- Hu Z, Tan DEK, Chia G, Tan H, Leong HF, *et al.* (2020) Maternal factor NELFA drives a 2C-like state in mouse embryonic stem cells. *Nat Cell Biol.* 22(2): 175-186
- Hugentobler SA, Diskin MG, Leese HJ, Humpherson PG, Watson T, *et al.* (2007) Amino acids in oviduct and uterine fluid and blood plasma during the estrous cycle in the bovine. *Mol Reprod Dev.* 74(4): 445-54

- Huidobro C, Toraño EG, Fernández AF, Urduñigo RG, Rodríguez RM, *et al.* (2013) A DNA methylation signature associated with the epigenetic repression of glycine N-methyltransferase in human hepatocellular carcinoma. *J Mol Med (Berl)*. 91(8): 939-50
- Ibeagha-Awemu E and Zhao X (2015) Epigenetic marks: regulators of livestock phenotypes and conceivable sources of missing variation in livestock improvement programs. *Front Genet*. 6: 302
- Ideraabdullah FY and Zeisel SH (2018) Dietary Modulation of the Epigenome. *Physiol Rev*. 98(2): 667-695
- Ikeda S, Kawahara-Miki R, Iwata H, Sugimoto M and Kume S (2017) Role of methionine adenosyltransferase 2A in bovine preimplantation development and its associated genomic regions. *Sci Rep*. 7: 3800
- Ikeda S, Namekawa T, Sugimoto M and Kume S (2010) Expression of methylation pathway enzymes in bovine oocytes and preimplantation embryos. *J Exp Zool A Ecol Genet Physiol*. 313(3): 129-36
- Ikeda S, Sugimoto M and Kume S (2012) Importance of methionine metabolism in morula-to-blastocyst transition in bovine preimplantation embryos. *J Reprod Dev*. 58(1): 91-7
- Ikeda S, Sugimoto M and Kume S (2018) The RPMI-1640 vitamin mixture promotes bovine blastocyst development in vitro and downregulates gene expression of TXNIP with epigenetic modification of associated histones. *J Dev Orig Health Dis*. 9(1): 87-94
- Inoue A and Zhang Y (2011) Replication-dependent loss of 5-hydroxymethylcytosine in mouse preimplantation embryos. *Science*. 334(6053): 194
- Inoue K, Ogonuki N, Mochida K, Yamamoto Y, Takano K, Kohda, *et al.* (2003) Effects of donor cell type and genotype on the efficiency of mouse somatic cell cloning. *Biol Reprod*. 69(4): 1394-400
- Ireland JJ, Murphee RL and Coulson PB (1980) Accuracy of predicting stages of bovine estrous cycle by gross appearance of the corpus luteum. *J Dairy Sci*. 63(1): 155-60
- Ito N, Kii I, Shimizu N, Tanaka H and Takeda S (2017) Direct reprogramming of fibroblasts into skeletal muscle progenitor cells by transcription factors enriched in undifferentiated subpopulation of satellite cells. *Sci Rep*. 7: 8097
- Jacobsen DW (1998) Homocysteine and vitamins in cardiovascular disease. *Clin Chem*. 44(8 Pt 2): 1833-43
- Jagušić M, Forčić D, Brgles M, Kutle L, Šantak M, *et al.* (2016) Stability of Minimum Essential Medium functionality despite L-glutamine decomposition. *Cytotechnology*. 68(4): 1171-83
- Jang HS, Shin WJ, Lee JE and Do JT (2017) CpG and Non-CpG Methylation in Epigenetic Gene Regulation and Brain Function. *Genes (Basel)*. 8(6): E148
- Jeziorska DM, Murray RJS, De Gobbi M, Gaentzsch R, Garrick D, *et al.* (2017) DNA methylation of intragenic CpG islands depends on their transcriptional activity during differentiation and disease. *Proc Natl Acad Sci U S A*. 114(36): E7526-E7535
- Jiang X, Yan J, West AA, Perry CA, Malysheva OV, *et al.* (2012) Maternal choline intake alters the epigenetic state of fetal cortisol-regulating genes in humans. *FASEB J*. 26(8): 3563-74
- Jiang Z, Lin J, Dong H, Zheng X, Marjani SL, *et al.* (2018) DNA methylomes of bovine gametes and in vivo produced preimplantation embryos. *Biol Reprod*. 99(5): 949-95
- Jin B and Robertson KD (2013) DNA methyltransferases, DNA damage repair, and cancer. *Adv Exp Med Biol*. 754: 3-29
- Johnson RR, Bentley OG and Moxon AL (1956) Synthesis in vitro and in vivo of Co60 containing vitamin B12-active substances by rumen microorganisms. *J Biol Chem*. 218(1): 379-90

- Jones PA (2012) Functions of DNA Methylation: Islands, Start Sites, Gene Bodies and Beyond. *Nat Rev Genet.* 13(7): 484-92
- Jozi M, Jafarpour F, Moradi R, Ghazvini Zadegan F, Karbalaie K, *et al.* (2020) Induced DNA hypomethylation by Folic Acid Deprivation in Bovine Fibroblast Donor Cells Improves Reprogramming of Somatic Cell Nuclear Transfer Embryos. *Sci. Rep.* 10: 5076
- Jurkowska RZ, Jurkowski TP and Jeltsch A (2011) Structure and function of mammalian DNA methyltransferases. *Chembiochem.* 12(2): 206-22
- Kaiser S, Jurkowski TP, Kellner S, Schneider D, Jeltsch A, *et al.* (2017) The RNA methyltransferase Dnmt2 methylates DNA in the structural context of a tRNA. *RNA Biol.* 14(9): 1241-1251
- Kalhan SC (2009) Metabolism of methionine in vivo: impact of pregnancy, protein restriction, and fatty liver disease. *Nestle Nutr Workshop Ser Pediatr Program.* 63: 121-31
- Kalhan SC (2016) One Carbon Metabolism in Pregnancy: Impact on Maternal, Fetal and Neonatal Health. *Mol Cell Endocrinol.* 435: 48–60
- Kalscheuer VM, Mariman EC, Schepens MT, Rehder H and Ropers HH (1993) The insulin-like growth factor type-2 receptor gene is imprinted in the mouse but not in humans. *Nat Genet.* 5(1): 74-8
- Kamei T, Hamlin GP, Chapman BM, Burkhardt AL, Bolen JB, *et al.* (1997) Signaling pathways controlling trophoblast cell differentiation: Src family protein tyrosine kinases in the rat. *Biol Reprod.* 57(6): 1302-11
- Kanakkaparambil R, Singh R, Li D, Webb R and Sinclair KD (2009) B-vitamin and homocysteine status determines ovarian response to gonadotropin treatment in sheep. *Biol Reprod.* 80(4): 43-52
- Kang YK, Lee KK and Han YM (2003) Reprogramming DNA Methylation in the Preimplantation Stage: Peeping With Dolly's Eyes. *Curr Opin Cell Biol.* 15(3): 290-5
- Kanno K, Wu MK, Scapa EF, Roderick SL and Cohen DE (2007) Structure and function of phosphatidylcholine transfer protein (PC-TP)/StarD2. *Biochim Biophys Acta.* 1771(6): 654-62
- Kappil MA, Green BB, Armstrong DA, Sharp AJ, Lambertini L, *et al.* (2015) Placental expression profile of imprinted genes impacts birth weight. *Epigenetics.* 10(9): 842-9
- Karapinar T, Dabak M, Kizil O and Balikci E (2008) Severe thiamine deficiency in sheep with acute ruminal lactic acidosis. *J Vet Intern Med.* 22(3): 662-5
- Karimi M, Johansson S, Stach D, Corcoran M, Grandér D, *et al.* (2006) LUMA (LUMinometric Methylation Assay) --a high throughput method to the analysis of genomic DNA methylation. *Exp Cell Res.* 312(11): 1989-95
- Kato Y and Tsunoda Y (2010) Role of the Donor Nuclei in Cloning Efficiency: Can the Ooplasm Reprogram Any Nucleus? *Int J Dev Biol.* 54(11-12): 1623-9
- Kelleher FC, Fennelly D and Mairin R (2006) Common Critical Pathways in Embryogenesis and Cancer. *Acta Oncol.* 45(4): 375-88
- Kelly RJ, Gruner TM, Furlong JM and Sykes AR (2006) Analysis of corrinoids in ovine tissues. *Biomed Chromatogr.* 20(8): 806-14
- Kennedy DG, Blanchflower WJ, Scott JM, Weir DG, Molloy AM, *et al.* (1992) Cobalt-vitamin B-12 deficiency decreases methionine synthase activity and phospholipid methylation in sheep. *J Nutr.* 122(7): 1384-1390
- Kennedy DG, Kennedy S, Blanchflower WJ, Scott JM, Weir DG, *et al.* (1994) Cobalt-vitamin B12 deficiency causes accumulation of odd-numbered, branched-chain fatty acids in the tissues of sheep. *Br J Nutr.* 71(1): 67-76

- Kennedy DG, Young PB, McCaughey WJ, Kennedy S and Blanchflower WJ (1991) Rumen succinate production may ameliorate the effects of cobalt-vitamin B-12 deficiency on methylmalonyl CoA mutase in sheep. *J Nutr.* 121(8): 1236-42
- Kermack AJ, Finn-Sell S, Cheong YC, Brook N, Eckert JJ, *et al.* (2015) Amino acid composition of human uterine fluid: association with age, lifestyle and gynaecological pathology. *Hum Reprod.* 30(4): 917-24
- Khan K and Elia M (1991) Factors affecting the stability of L-glutamine in solution. *Clin Nutr.* 10(4): 186-92
- Khatchadourian C, Guillaud J and Menezo Y (1994) Interactions in glycine and methionine uptake, conversion and incorporation into proteins in the preimplantation mouse embryo. *Zygote.* 2(4): 301-6
- Killian JK, Byrd JC, Jirtle JV, Munday BL, Stoskopf MK, *et al.* (2000) M6P/IGF2R Imprinting Evolution in Mammals. *Mol Cell.* 5(4): 707-16
- Killian JK, Nolan CM, Wylie AA, Li T, Vu TH, *et al.* (2001) Divergent evolution in M6P/IGF2R imprinting from the Jurassic to the Quaternary. *Hum Mol Genet.* 10(17): 1721-8
- Kim D, Fiske BP, Birsoy K, Freinkman E, Kami K, *et al.* (2015) SHMT2 drives glioma cell survival in ischaemia but imposes a dependence on glycine clearance. *Nature.* 520(7547): 363-7
- Kim S, Fenech MF and Kim PJ (2018) Nutritionally recommended food for semi- to strict vegetarian diets based on large-scale nutrient composition data. *Sci Rep.* 8(1): 4344
- Koenig KM, Rode LM, Knight CD and Vázquez-Añón M (2002) Rumen degradation and availability of various amounts of liquid methionine hydroxy analog in lactating dairy cows. *J Dairy Sci.* 85(4): 930-8
- Koerner MV, Pauler FM, Hudson QJ, Santoro F, Sawicka A, *et al.* (2012) A Downstream CpG Island Controls Transcript Initiation and Elongation and the Methylation State of the Imprinted Airn Macro ncRNA Promoter. *PLoS Genet.* 8(3): e1002540
- Kohda T and Ishino F (2013) Embryo manipulation via assisted reproductive technology and epigenetic asymmetry in mammalian early development. *Philos Trans R Soc Lond B Biol Sci.* 368(1609): 20120353
- Kohli RM and Zhang Y (2013) TET enzymes, TDG and the dynamics of DNA demethylation. *Nature.* 502(7472): 472-9
- Komarnisky LA, Christopherson RJ and Basu TK (2003) Sulfur: its clinical and toxicologic aspects. *Nutrition.* 19(1): 54-61
- König S, Simianer H and Willam A (2009) Economic evaluation of genomic breeding programs. *J Dairy Sci.* 92(1): 382-91
- Korendyaseva TK, Kuvatov DN, Volkov VA, Martinov MV, Vitvitsky VM, *et al.* (2008) An allosteric mechanism for switching between parallel tracks in mammalian sulfur metabolism. *PLoS Comput Biol.* 4(5): e1000076
- Kost K, Landry DJ and Darroch JE (1998) The effects of pregnancy planning status on birth outcomes and infant care. *Fam Plann Perspect.* 30(5): 223-30
- Kovacheva VP, Mellott TJ, Davisosn JM, Wagner N, Lopez-Coviella I, *et al.* (2007) Gestational choline deficiency causes global and Igf2 gene DNA hypermethylation by up-regulation of Dnmt1 expression. *J Biol Chem.* 282(43): 31777-88
- Kowalik A, Liu HC, He ZY, Mele C, Barmat L, *et al.* (1999) Expression of the insulin-like growth factor-1 gene and its receptor in preimplantation mouse embryos; is it a marker of embryo viability? *Mol Hum Reprod.* 5(9): 861-5

- Krajcovicová-Kudláčková M, Blazíček P, Kopcová J, Béderová A and Babinská K (2000) Homocysteine levels in vegetarians versus omnivores. *Ann Nutr Metab.* 44(3): 135-8
- Kramer DL, Sufrin JR and Porter CW (1987) Relative effects of S-adenosylmethionine depletion on nucleic acid methylation and polyamine biosynthesis. *Biochem J.* 247(2): 259-65
- Kriaucionis S and Heintz N (2009) The nuclear DNA base 5-hydroxymethylcytosine is present in Purkinje neurons and the brain. *Science.* 324(5929): 929-30
- Krisher RL and Bavister BD (1998) Responses of oocytes and embryos to the culture environment. *Theriogenology.* 49(1): 103-14
- Krueger F and Andrews SR (2011) Bismark: a flexible aligner and methylation caller for Bisulfite-Seq applications. *Bioinformatics.* 27(11): 1571-2
- Kruuk LE, Clutton-Brock TH, Albon SD, Pemberton JM and Guinness FE (1999) Population Density Affects Sex Ratio Variation in Red Deer. *Nature.* 399(6735): 459-61
- Kuijk EW, van Tol LT, Van de Velde H, Wubbolts R, Welling M, *et al.* (2012) The roles of FGF and MAP kinase signaling in the segregation of the epiblast and hypoblast cell lineages in bovine and human embryos. *Development.* 139(5): 871-82
- Kuo KC, McCune RA, Gehrke CW, Midgett R and Ehrlich M (1980) Quantitative reversed-phase high performance liquid chromatographic determination of major and modified deoxyribonucleosides in DNA. *Nucleic Acids Res.* 8(20): 4763-76
- Kurdyukov S and Bullock M (2016) DNA Methylation Analysis: Choosing the Right Method. *Biology (Basel).* 5(1): 3
- Kuroki LM, Allsworth JE, Redding CA, Blume JD and Peipert JF (2008) Is a previous unplanned pregnancy a risk factor for a subsequent unplanned pregnancy? *Am J Obstet Gynecol.* 199(5): 517.e1-7
- Kurome M, Baehr A, Simmet K, Jemiller E-M, Egerer S, *et al.* (2019) Targeting α Gal Epitopes for Multi-Species Embryo Immunotherapy. *Reprod Fertil Dev.* 31(4): 820-826
- Kurosaka S, Eckardt S and McLaughlin KJ (2004) Pluripotent lineage definition in bovine embryos by Oct4 transcript localization. *Biol Reprod.* 71(5): 1578-82
- Kurpad AV, Anand P, Dwarkanath P, Hsu JW, Thomas T, *et al.* (2014) Whole body methionine kinetics, transmethylation, transsulfuration and remethylation during pregnancy. *Clin Nutr.* 33(1): 122-9
- Kwong WY, Adamiak SJ, Gwynn A, Singh R and Sinclair KD (2010) Endogenous folates and single-carbon metabolism in the ovarian follicle, oocyte and pre-implantation embryo. *Reproduction.* 139(4): 705-15
- Kwong WY, Miller DJ, Ursell E, Wild AE, Wilkins AP, *et al.* (2006) Imprinted gene expression in the rat embryo-fetal axis is altered in response to periconceptual maternal low protein diet. *Reproduction.* 132(2): 265-277
- Kwong WY, Miller DJ, Wilkins AP, Dear MS, Wright JN, *et al.* (2007) Maternal low protein diet restricted to the preimplantation period induces a gender-specific change on hepatic gene expression in rat fetuses. *Mol Reprod Dev.* 74(1): 48-56
- Kwong WY, Wild AE, Roberts P, Willis AC and Fleming TP (2000) Maternal undernutrition during the preimplantation period of rat development causes blastocyst abnormalities and programming of postnatal hypertension. *Development.* 127(19): 4195-4202
- Laguna-Barraza R, Bermejo-Alvarez P, Ramos-Ibeas P, de Frutos C, López-Cardona AP, *et al.* (2012) Sex-specific embryonic origin of postnatal phenotypic variability. *Reprod Fertil Dev.* 25(1): 38-47

- Lambert BD, Titgemeyer EC, Stokka GL, DeBey BM and Löest CA (2002) Methionine supply to growing steers affects hepatic activities of methionine synthase and betaine-homocysteine methyltransferase, but not cystathionine synthase. *J Nutr.* 132(7): 2004-9
- Lambrot R, Xu C, Saint-Phar S, Chountalos G, Cohen T, *et al.* (2013) Low paternal dietary folate alters the mouse sperm epigenome and is associated with negative pregnancy outcomes. *Nat Commun.* 4: 2889
- Lan F and Shi Y (2009) Epigenetic regulation: methylation of histone and non-histone proteins. *Sci China C Life Sci.* 52(4): 311-22
- Lan L, Wang W, Huang Y, Zhao C and Bu X (2019) WNT7A Overexpression Inhibits Growth and Migration of Hepatocellular Carcinoma via the β -Catenin Independent Pathway. *BioMed Research International.* 2019: Article ID 3605950
- Lan X, Cretney EC, Kropp J, Khateeb K, Berg MA, *et al.* (2013) Maternal Diet during Pregnancy Induces Gene Expression and DNA Methylation Changes in Fetal Tissues in Sheep. *Front Genet.* 5(4): 49
- Lande-Diner L, Zhang J, Ben-Porath I, Amariglio N, Keshet I, *et al.* (2007) Role of DNA methylation in stable gene repression. *J Biol Chem.* 282(16): 12194-200
- Lane M and Gardner DK (1997) Differential regulation of mouse embryo development and viability by amino acids. *J Reprod Fertil.* 109(1): 153-64
- Lane M and Gardner DK (1997b) Nonessential Amino Acids and Glutamine Decrease the Time of the First Three Cleavage Divisions and Increase Compaction of Mouse Zygotes in Vitro. *J Assist Reprod Genet.* 14(7): 398-403
- Langley-Evans SC (2006) Developmental programming of health and disease. *Proc Nutr Soc.* 65(1): 97-105
- Larqué E, Sabater-Molina M and Zamora S (2007) Biological significance of dietary polyamines. *Nutrition.* 23(1): 87-95
- Laskowski D, Humblot P, Sirard MA, Sjunnesson Y, Jhamat N, *et al.* (2018) DNA methylation pattern of bovine blastocysts associated with hyperinsulinemia in vitro. *Mol Reprod Dev.* 85(7): 599-611
- Latos PA, Pauler FM, Koerner MV, Şenergin HB, Hudson QJ, *et al.* (2012) Airn transcriptional overlap, but not its lncRNA products, induces imprinted Igf2r silencing. *Science.* 338(6113): 1469-72
- Lau MM, Stewart CE, Liu Z, Bhatt H, Rotwein P, *et al.* (1994) Loss of the imprinted IGF2/cation-independent mannose 6-phosphate receptor results in fetal overgrowth and perinatal lethality. *Genes Dev.* 8(24): 2953-63
- Laurichesse H, Tauveron I, Gourdon F, Cormerais L, Champredon C, *et al.* (1998) Threonine and methionine are limiting amino acids for protein synthesis in patients with AIDS. *J Nutr.* 128(8): 1342-8
- Lebiedzińska A, Dąbrowska M, Szefer P and Marszał M (2008) High-Performance Liquid Chromatography Method for the Determination of Folic Acid in Fortified Food Products. *Toxicol Mech Methods.* 18(6): 463-467
- LeBlanc J and Ducharme MB (2007) Plasma Dopamine and Noradrenaline Variations in Response to Stress. *Physiol Behav.* 91(2-3): 208-11
- Leclerc D, Wilson A, Dumas R, Gafuik C, Song D, *et al.* (1998) Cloning and mapping of a cDNA for methionine synthase reductase, a flavoprotein defective in patients with homocystinuria. *Proc Natl Acad Sci USA.* 95(6): 3059-64
- Lee C, Friedman JR, Fulmer JT and Kaestner KH (2005) The initiation of liver development is dependent on Foxa transcription factors. *Nature.* 435(7044): 944-7
- Lee JH, Park SJ and Nakai K (2017) Differential landscape of non-CpG methylation in embryonic stem cells and neurons caused by DNMT3s. *Sci Rep.* 7(1): 11295

- Lee M, Kim B and Kim VN (2014) Emerging roles of RNA modification: m(6)A and U-tail. *Cell*. 158(5): 980-987
- Lee MB, Kooistra M, Zhang B, Slow S, Fortier AL, *et al.* (2012) Betaine homocysteine methyltransferase is active in the mouse blastocyst and promotes inner cell mass development. *J Biol Chem*. 287(39): 33094-103
- Lees GJ (1991) Inhibition of sodium-potassium-ATPase: A Potentially Ubiquitous Mechanism Contributing to Central Nervous System Neuropathology. *Brain Res Brain Res Rev*. 16(3): 283-300
- Leese HJ and Lenton EA (1990) Glucose and lactate in human follicular fluid: concentrations and interrelationships. *Hum Reprod*. 5(8): 915-9
- Leibfried-Rutledge ML, Critser ES and First NL (1986) Effects of fetal calf serum and bovine serum albumin on in vitro maturation and fertilization of bovine and hamster cumulus-oocyte complexes. *Biol Reprod*. 35(4): 850-7
- Leonhardt H, Page AW, Weier HU and Bestor TH (1992) A targeting sequence directs DNA methyltransferase to sites of DNA replication in mammalian nuclei. *Cell*. 71(5): 865-73
- Lerchner W and Barlow DP (1997) Paternal repression of the imprinted mouse Igf2r locus occurs during implantation and is stable in all tissues of the post-implantation mouse embryo. *Mech Dev*. 61(1-2): 141-9
- Lévesque N, Leclerc D, Gayden T, Lazaris A, De Jay N, *et al.* (2016) Murine diet/tissue and human brain tumorigenesis alter Mthfr/MTHFR 5'-end methylation. *Mamm Genome*. 27(3-4): 122-34
- Li E (2002) Chromatin modification and epigenetic reprogramming in mammalian development. *Nat Rev Genet*. 3(9): 662-73
- Li E and Zhang Y (2014) DNA Methylation in Mammals. *Cold Spring Harb Perspect Biol*. 6(5): a019133
- Li F, Feng Q, Lee C, Wang S, Pelleycounter LL, *et al.* (2008) Human betaine-homocysteine methyltransferase (BHMT) and BHMT2: common gene sequence variation and functional characterization. *Mol Genet Metab*. 94(3): 326-35
- Li Q, Wang YS, Wang LJ, Zhang H, Li RZ, *et al.* (2014) Vitamin C supplementation enhances compact morulae formation but reduces the hatching blastocyst rate of bovine somatic cell nuclear transfer embryos. *Cell Reprogram*. 16(4): 290-7
- Li QN, Guo L, Hou Y, Ou XH, Liu Z, *et al.* (2018) The DNA methylation profile of oocytes in mice with hyperinsulinaemia and hyperandrogenism as detected by single-cell level whole genome bisulphite sequencing (SC-WGBS) technology. *Reprod Fertil Dev*. 30(12): 1713-1719
- Li Y, Li S, Dai Y, Du W, Zhao C, *et al.* (2007) Nuclear reprogramming in embryos generated by the transfer of yak (*Bos grunniens*) nuclei into bovine oocytes and comparison with bovine-bovine SCNT and bovine IVF embryos. *Theriogenology*. 67(8): 1331-8
- Lienhart WD, Gudipati V and Macheroux P (2013) The human flavoproteome. *Arch Biochem Biophys*. 535(2): 150-62
- Lim DH and Maher ER (2010) Genomic imprinting syndromes and cancer. *Adv Genet*. 70: 145-75
- Lin L, Li Q, Zhang L, Zhao D, Dai Y, *et al.* (2008) Aberrant epigenetic changes and gene expression in cloned cattle dying around birth. *BMC Dev Biol*. 8: 14
- Lister R and Ecker JR (2009) Finding the fifth base: genome-wide sequencing of cytosine methylation. *Genome Res*. 19(6): 959-66
- Locasale JW (2013) Serine, glycine and the one-carbon cycle: cancer metabolism in full circle. *Nat Rev Cancer*. 13(8): 572-58

- Long J-E and Cai X (2007) Igf-2r Expression Regulated by Epigenetic Modification and the Locus of Gene Imprinting Disrupted in Cloned Cattle. *Gene*. 388(1-2): 125-34
- Lonsdale D (2006) A review of the biochemistry, metabolism and clinical benefits of thiamin(e) and its derivatives. *Evid Based Complement Alternat Med*. 3(1): 49-59
- Lonsdale D (2015) Thiamine and magnesium deficiencies: keys to disease. *Med Hypotheses*. 84(2): 129-34
- Louis GM, Cooney MA, Lynch CD and Handal A (2008) Periconception window: advising the pregnancy-planning couple. *Fertil Steril*. 89(2): e119-21
- Lu F, Shi D, Wei J, Yang S and Wei Y (2005) Development of embryos reconstructed by interspecies nuclear transfer of adult fibroblasts between buffalo (*Bubalus bubalis*) and cattle (*Bos indicus*). *Theriogenology*. 64(6): 1309-19
- Lu SC and Mato JM (2012) S-adenosylmethionine in liver health, injury, and cancer. *Physiol Rev*. 92(4): 1515-42
- Lucifero D, Suzuki J, Bordignon V, Martel J, Vigneault C, *et al.* (2006) Bovine SNRPN methylation imprint in oocytes and day 17 in vitro produced and somatic cell nuclear transfer embryos. *Biol Reprod*. 75(4): 531-8
- Lucock M (2000) Folic acid: nutritional biochemistry, molecular biology, and role in disease processes. *Mol Genet Metab*. 1(1-2): 121-38
- Luecke RW, Culik R, Thorp F Jr, Blakeslee LH and Nelson RH (1950) Riboflavin deficiency in the lamb. *J Anim Sci*. 9(3): 420-5
- Luka Z, Mudd SH and Wagner C (2009) Glycine N-methyltransferase and regulation of S-adenosylmethionine levels. *J Biol Chem*. 284(34): 22507-11
- Luo R, Bai C, Yang L, Zheng Z, Su G, *et al.* (2018) DNA methylation subpatterns at distinct regulatory regions in human early embryos. *Open Biol*. 8(10): 180131
- Luo S, Valencia CA, Zhang J, Lee NC, Slone J, *et al.* (2018b) Biparental Inheritance of Mitochondrial DNA in Humans. *Proc Natl Acad Sci U S A*. 115(51): 13039-13044
- Lyle R, Watanabe D, te Vruchte D, Lerchner W, Smrzka OW, *et al.* (2000) The imprinted antisense RNA at the Igf2r locus overlaps but does not imprint Mas1. *Nat Genet*. 25(1): 19-21
- MacFarlane AJ, Liu X, Perry CA, Flodby P, Allen RH, *et al.* (2008) Cytoplasmic serine hydroxymethyltransferase regulates the metabolic partitioning of methylenetetrahydrofolate but is not essential in mice. *J Biol Chem*. 283(38): 25846-53
- Madon-Simon M, Cowley M, Garfield AS, Moorwood K, Bauer SR, *et al.* (2014) Antagonistic roles in fetal development and adult physiology for the oppositely imprinted Grb10 and Dlk1 genes. *BMC Biol*. 12: 771
- Maekawa M, Taniguchi T, Higashi H, Sugimura H, Sugano K, *et al.* (2004) Methylation of mitochondrial DNA is not a useful marker for cancer detection. *Clin Chem*. 50(8): 1480-1
- Maher ER, Brueton LA, Bowdin SC, Luharia A, Cooper W, *et al.* (2003) Beckwith-Wiedemann syndrome and assisted reproduction technology (ART). *J Med Genet*. 40(1): 62-4
- Mäkinen S, Söderström-Anttila V, Vainio J, Suikkari AM and Tuuri T (2013) Does long in vitro culture promote large for gestational age babies? *Hum Reprod*. 28(3): 828-34
- Maldonado MBC, de Rezende Neto NB, Nagamatsu ST, Carazzolle MF, Hoff JL, *et al.* (2019) Identification of bovine CpG SNPs as potential targets for epigenetic regulation via DNA methylation. *PLoS One*. 14(9): e0222329
- Malinow MR, Bostom AG and Krauss RM (1999) Homocyst(e)ine, diet, and cardiovascular diseases: a statement for healthcare professionals from the Nutrition Committee, American Heart Association. *Circulation*. 99(1): 178-82

- Maloney CA, Hay SM and Rees WD (2007) Folate deficiency during pregnancy impacts on methyl metabolism without affecting global DNA methylation in the rat fetus. *Br J Nutr.* 97(6): 1090
- Maloney CA, Hay SM, Young LE, Sinclair KD and Rees WD (2011) A methyl-deficient diet fed to rat dams during the peri-conception period programs glucose homeostasis in adult male but not female offspring. *J Nutr.* 141(1): 95-100
- Manzardo AM and Butler MG (2016) Examination of Global Methylation and Targeted Imprinted Genes in Prader-Willi Syndrome. *J Clin Epigenet.* 2(3): 26
- Mao J, Zhang X, Sieli PT, Falduto MT, Torres KE, *et al.* (2010) Contrasting effects of different maternal diets on sexually dimorphic gene expression in the murine placenta. *Proc Natl Acad Sci U S A.* 107(12): 5557-62
- Marabita F, Almgren M, Lindholm ME, Ruhrmann S, Fagerström-Billai F, *et al.* (2013) An evaluation of analysis pipelines for DNA methylation profiling using the Illumina HumanMethylation450 BeadChip platform. *Epigenetics.* 8(3): 333-46
- Martinelli D, Deodato F, Dionisi-Vici C (2011) Cobalamin C defect: natural history, pathophysiology, and treatment. *J Inherit Metab Dis.* 34(1): 127-135
- Martinov MV, Vitvitsky VM, Mosharov EV, Banerjee R and Ataullakhanov FI (2000) A substrate switch: a new mode of regulation in the methionine metabolic pathway. *J Theor Biol.* 204(4): 521-32
- Mason JB (2003) Biomarkers of nutrient exposure and status in one-carbon (methyl) metabolism. *J. Nutr.* 3: 941S–47S
- Mastromonaco GF, Semple E, Robert C, Rho GJ, Betts DH, *et al.* (2004) Different culture media requirements of IVF and nuclear transfer bovine embryos. *Reprod Domest Anim.* 39(6): 462-7
- Mato JM, Martínez-Chantar ML and Lu SC (2008) Methionine metabolism and liver disease. *Annu Rev Nutr.* 28: 273-93
- Matoba S and Zhang Y (2018) Somatic Cell Nuclear Transfer Reprogramming: Mechanisms and Applications. *Cell Stem Cell.* 23(4): 471-485
- Matsuo T, Seri K and Kato T (1980) Comparative effects of S-methylmethionine (vitamin U) and methionine on choline-deficient fatty liver in rats. *Arzneimittelforschung.* 30(1): 68-9
- Mattaini KR, Sullivan MR and Vander Heiden MG (2016) The importance of serine metabolism in cancer. *J Cell Biol.* 214(3): 249-57
- McCarty MF, Barroso-Aranda J and Contreras F (2009) The low-methionine content of vegan diets may make methionine restriction feasible as a life extension strategy. *Med Hypotheses.* 72(2): 125-8
- McCormick DB and Chen H (1999) Update on interconversions of vitamin B-6 with its coenzyme. *J Nutr.* 129(2): 325-327
- McCullough LE, Miller EE, Mendez MA, Murtha AP and Murphy SK (2016) Maternal B vitamins: effects on offspring weight and DNA methylation at genomically imprinted domains. *Clin Epigenetics.* 8: 8
- McDowell LR (2000) *Vitamins in Animal and Human Nutrition.* 2nd ed. Iowa State University Press, Ames
- McElroy SL, Kim JH, Kim S, Jeong YW, Lee EG, *et al.* (2008) Effects of Culture Conditions and Nuclear Transfer Protocols on Blastocyst Formation and mRNA Expression in Pre-Implantation Porcine Embryos. *Theriogenology.* 69(4): 416-25
- McGuirk SM (1987) Polioencephalomalacia. *Vet Clin North Am Food Anim Pract.* 3(1): 107-17

- McKay JA, Wong YK, Relton CL, Ford D and Mathers JC (2011) Maternal folate supply and sex influence gene-specific DNA methylation in the fetal gut. *Mol Nutr Food Res*. 55: 1717-23
- McKay JA, Xie L, Manus C, Langie SA, Maxwell RJ, *et al.* (2014) Metabolic effects of a high-fat diet post-weaning after low maternal dietary folate during pregnancy and lactation. *Mol Nutr Food Res*. 58: 1087-97
- McKeever MP, Weir DG, Molloy A and Scott JM (1991) Betaine-homocysteine methyltransferase: organ distribution in man, pig and rat and subcellular distribution in the rat. *Clin Sci (Lond)*. 81(4): 551-6
- McLain AL, Szweda PA and Szweda LI (2011) α -Ketoglutarate dehydrogenase: a mitochondrial redox sensor. *Free Radic Res*. 45(1): 29-36
- McMillen IC and Robinson JS (2005) Developmental origins of the metabolic syndrome: prediction, plasticity, and programming. *Physiol Rev*. 85(2): 571-633
- McMullin MF, Young PB, Bailie KE, Savage GA, Lappin TR and White R (2001) Homocysteine and methylmalonic acid as indicators of folate and vitamin B12 deficiency in pregnancy. *Clin Lab Haematol*. 23(3): 161-165
- McNeil CJ, Hay SM, Rucklidge GJ, Reid M, Duncan G, *et al.* (2008) Disruption of lipid metabolism in the liver of the pregnant rat fed folate-deficient and methyl donor-deficient diets. *Br J Nutr*. 99(2): 262-71
- McNulty H, Cuskelly G and Ward M (2000) Response of red blood cell folate to intervention: implications for folate recommendations for the prevention of neural tube defects. *Am J Clin Nutr*. 71(5): 1308S-11S
- Medvedev SP, Shevchenko AI, Elisaphenko EA, Nesterova TB, Brockdorff N, *et al.* (2008) Structure and expression pattern of Oct4 gene are conserved in vole *Microtus rossiaemeridionalis*. *BMC Genomics*. 9: 162
- Mehedint MG, Niculescu MD, Craciunescu CN and Zeisel SH (2010) Choline deficiency alters global histone methylation and epigenetic marking at the Re1 site of the calbindin 1 gene. *FASEB J*. 24(1): 184-95
- Mehrshahi P, Gonzalez-Jorge S, Akhtar TA, Ward JL, Santoyo-Castelazo A, *et al.* (2010) Functional analysis of folate polyglutamylation and its essential role in plant metabolism and development. *Plant J*. 64(2): 267-279
- Meissner A, Gnirke A, Bell GW, Ramsahoye B, Lander ES, *et al.* (2005) Reduced representation bisulfite sequencing for comparative high-resolution DNA methylation analysis. *Nucleic Acids Res*. 33(18): 5868-77
- Melnick M, Chen H, Buckley S, Warburton D and Jaskoll T (1998) Insulin-like growth factor II receptor, transforming growth factor-beta, and Cdk4 expression and the developmental epigenetics of mouse palate morphogenesis and dysmorphogenesis. *Dev Dyn*. 211(1): 11-25
- Melse-Boonstra A, de Bree A, Verhoef P, Bjørke-Monsen AL and Verschuren WM (2002) Dietary monoglutamate and polyglutamate folate are associated with plasma folate concentrations in Dutch men and women aged 20-65 years. *J Nutr*. 132(6): 1307-12
- Mendonça N, Granic A, Mathers JC, Martin-Ruiz C, Wesnes KA, *et al.* (2017) One-Carbon Metabolism Biomarkers and Cognitive Decline in the Very Old: The Newcastle 85+ Study. *J Am Med Dir Assoc*. 18(9): 806.e19-806.e27
- Menezo Y, Clément P and Dale B (2019) DNA Methylation Patterns in the Early Human Embryo and the Epigenetic/Imprinting Problems: A Plea for a More Careful Approach to Human Assisted Reproductive Technology (ART). *Int J Mol Sci*. 20(6): E1342
- Menezo Y, Elder K, Benkhalifa M and Dale B (2010) DNA methylation and gene expression in IVF. *Reprod Biomed Online*. 20(6): 709-10

- Ménézo YJ and Hérubel F (2002) Mouse and bovine models for human IVF. *Reprod Biomed Online*. 4(2): 170-5
- Mentch SJ and Locasale JW (2016) One-carbon metabolism and epigenetics: understanding the specificity. *Ann N Y Acad Sci*. 1363: 91-8
- Mentch SJ, Mehrmohamadi M, Huang L, Liu X, Gupta D, *et al.* (2015) Histone Methylation Dynamics and Gene Regulation Occur through the Sensing of One-Carbon Metabolism. *Cell Metab*. 22(5): 861-73
- Merrill AH Jr and Henderson JM (1990) Vitamin B6 metabolism by human liver. *Ann N Y Acad Sci*. 585: 110-117
- Messerschmidt DM, Knowles BB and Solter D (2014) DNA methylation dynamics during epigenetic reprogramming in the germline and preimplantation embryos. *Genes Dev*. 28(8): 812-28
- Midttun Ø, Hustad S, Schneede J, Vollset SE and Ueland PM (2007) Plasma vitamin B-6 forms and their relation to transsulfuration metabolites in a large, population-based study. *Am J Clin Nutr*. 86(1): 131-8
- Midttun Ø, Hustad S, Solheim E, Schneede J and Ueland PM (2005) Multianalyte quantification of vitamin B6 and B2 species in the nanomolar range in human plasma by liquid chromatography-tandem mass spectrometry. *Clin Chem*. 51(7): 1206-16
- Midttun Ø, Kvalheim G and Ueland PM (2013) High-throughput, low-volume, multianalyte quantification of plasma metabolites related to one-carbon metabolism using HPLC-MS/MS. *Anal Bioanal Chem*. 405(6): 2009-17
- Miller JW, Garrod MG, Allen LH, Haan MN and Green R (2009) Metabolic evidence of vitamin B-12 deficiency, including high homocysteine and methylmalonic acid and low holotranscobalamin, is more pronounced in older adults with elevated plasma folate. *Am J Clin Nutr*. 90(6): 1586-92
- Milman N (2012) Intestinal absorption of folic acid - new physiologic & molecular aspects. *Indian J Med Res*. 136(5): 725-8
- Miodownik C, Lerner V, Vishne T, Sela BA and Levine J (2007) High-dose vitamin B6 decreases homocysteine serum levels in patients with schizophrenia and schizoaffective disorders: a preliminary study. *Clin Neuropharmacol*. 30(1): 13-7
- Miura F and Ito T (2015) Highly sensitive targeted methylome sequencing by post-bisulfite adaptor tagging. *DNA Res*. 22(1): 13-8
- Mohamed-Ahmed AH, Wilson MP, Albuera M, Chen T, Mills PB, *et al.* (2017) Quality and stability of extemporaneous pyridoxal phosphate preparations used in the treatment of paediatric epilepsy. *J Pharm Pharmacol*. 69(4): 480-488
- Monajjemzadeh F, Ebrahimi F, Zakeri-Milani P and Valizadeh H (2014) Effects of formulation variables and storage conditions on light protected vitamin B12 mixed parenteral formulations. *Adv Pharm Bull*. 4(4): 329-38
- Morbeck DE, Krisher RL, Herrick JR, Baumann NA, Matern D, *et al.* (2014) Composition of commercial media used for human embryo culture. *Fertil Steril*. 102(3): 759-766.e9
- Morera L, Lübbert M and Jung M (2016) Targeting histone methyltransferases and demethylases in clinical trials for cancer therapy. *Clin Epigenetics*. 8: 57
- Morgan HD, Santos F, Green K, Dean W and Reik W (2005) Epigenetic reprogramming in mammals. *Hum Mol Genet*. 14(1): R47-58
- Morgan HD, Sutherland HG, Martin DI and Whitelaw E (1999) Epigenetic inheritance at the agouti locus in the mouse. *Nat Genet*. 23(3): 314-8
- Morgan HL, Ampong I, Eid N, Rouillon C, Griffiths HR, *et al.* (2020) Low protein diet and methyl-donor supplements modify testicular physiology in mice. *Reproduction*. 159(5): 627-641

- Morton JM, Auldist MJ, Douglas ML and Macmillan KL (2017) Milk protein concentration, estimated breeding value for fertility, and reproductive performance in lactating dairy cows. *J Dairy Sci.* 100(7): 5850-5862
- Motyka B, Korbitt G, Pinkoski MJ, Heibein JA, Caputo JA, *et al.* (2000) Mannose 6-phosphate/insulin-like growth factor II receptor is a death receptor for granzyme B during cytotoxic T cell-induced apoptosis. *Cell.* 103: 491–500
- Muriel P (1993) S-adenosyl-L-methionine Prevents and Reverses Erythrocyte Membrane Alterations in Cirrhosis. *J Appl Toxicol.* 13(3): 179-82
- Murín R, Vidomanová E, Kowtharapu BS, Hatok J and Dobrota D (2017) Role of S-adenosylmethionine cycle in carcinogenesis. *Gen Physiol Biophys.* 36(5): 513-520
- Nakanishi MO, Hayakawa K, Nakabayashi K, Hata K, Shiota K, *et al.* (2012) Trophoblast-specific DNA methylation occurs after the segregation of the trophectoderm and inner cell mass in the mouse periimplantation embryo. *Epigenetics.* 7(2): 173-82
- Nakazawa T, Ohashi K, Yamada M, Shinoda S, Saji F, *et al.* (1997) Effect of different concentrations of amino acids in human serum and follicular fluid on the development of one-cell mouse embryos in vitro. *J Reprod Fertil.* 111(2): 327-32
- Nashabat M, Al-Khenaizan S and Alfadhel M (2018) Methionine adenosyltransferase I/III deficiency: beyond the central nervous system manifestations. *Ther Clin Risk Manag.* 14: 225-229
- Ndaw S, Bergaentzlé M, Aoudé-Werner D, Lahély S and Hasselmann C (2001) Determination of folates in foods by high-performance liquid chromatography with fluorescence detection after precolumn conversion to 5-methyltetrahydrofolates. *J Chromatogr A.* 928(1): 77-90
- Negrón-Pérez VM, Zhang Y and Hansen PJ (2017) Single-cell gene expression of the bovine blastocyst. *Reproduction.* 154(5): 627-644
- Neill AR, Grime DW, Snoswell AM, Northrop AJ, Lindsay DB, *et al.* (1979) The low availability of dietary choline for the nutrition of the sheep. *Biochem J.* 180(3): 59-65
- Nelissen EC, Van Montfoort AP, Coonen E, Derhaag JG, Geraedts JP, *et al.* (2012) Further evidence that culture media affect perinatal outcome: findings after transfer of fresh and cryopreserved embryos. *Hum Reprod.* 27(7): 1966-76
- Nezamidoust M, Alikhani M, Ghorbani GR and Edriss MA (2014) Responses to betaine and inorganic sulphur of sheep in growth performance and fibre growth. *J Anim Physiol Anim Nutr (Berl).* 98(6): 1031-8
- Ng SS, Yue WW, Oppermann U and Kloise RJ (2009) Dynamic protein methylation in chromatin biology. *Cell Mol Life Sci.* 66(3): 407-22
- Nichols J, Silva J, Roode M and Smith A (2009) Suppression of Erk signalling promotes ground state pluripotency in the mouse embryo. *Development.* 136: 3215-3222
- Niculescu MD, Craciunescu CN and Zeisel SH (2006) Dietary choline deficiency alters global and gene-specific DNA methylation in the developing hippocampus of mouse fetal brains. *FASEB J.* 20(1): 43-9
- Niemann H (2016) Epigenetic Reprogramming in Mammalian Species After SCNT-based Cloning. *Theriogenology.* 86(1): 80-90
- Niemann H and Lucas-Hahn A (2012) Somatic Cell Nuclear Transfer Cloning: Practical Applications and Current Legislation. *Reprod Domest Anim.* 5: 2-10
- Niesen MI, Osborne AR, Yang H, Rastogi S, Challeppan S, *et al.* (2005) Activation of a Methylated Promoter Mediated by a Sequence-Specific DNA-binding Protein, RFX. *Biol Chem.* 280(47): 38914-22

- Novakovic B, Lewis S, Halliday J, Kennedy J, Burgner DP, *et al.* (2019) Assisted reproductive technologies are associated with limited epigenetic variation at birth that largely resolves by adulthood. *Nat Commun.* 10(1): 3922
- O'Sullivan FM, Murphy SK, Simel LR, McCann A, Callanan JJ, *et al.* (2007) Imprinted expression of the canine IGF2R, in the absence of an anti-sense transcript or promoter methylation. *Evol. Dev.* 9: 579–589
- Oback B and Wells DN (2007) Donor cell differentiation, reprogramming, and cloning efficiency: elusive or illusive correlation? *Mol Reprod Dev.* 74(5): 646-54
- Obeid R (2013) The metabolic burden of methyl donor deficiency with focus on the betaine homocysteine methyltransferase pathway. *Nutrients.* 5(9): 3481-95
- Obeid R, Murphy M, Solé-Navais P and Yajnik C (2017) Cobalamin Status from Pregnancy to Early Childhood: Lessons from Global Experience. *Adv Nutr.* 8(6): 971-979
- Obeid R, Oexle K, Reißmann A, Pietrzik K and Koletzko B (2016) Folate status and health: challenges and opportunities. *J Perinat Med.* 44(3): 261-8
- O'Doherty AM, McGettigan P, Irwin RE, Magee DA, Gagne D, *et al.* (2018) Intragenic sequences in the trophectoderm harbour the greatest proportion of methylation errors in day 17 bovine conceptuses generated using assisted reproductive technologies. *BMC Genomics.* 19(1): 438
- Ogawa O, McNoe LA, Eccles MR, Morison IM and Reeve AE (1993) Human insulin-like growth factor type I and type II receptors are not imprinted. *Hum. Mol. Genet.* 2(12): 2163-2165
- Ogura A, Inoue K and Wakayama T (2013) Recent Advancements in Cloning by Somatic Cell Nuclear Transfer. *Philos Trans R Soc Lond B Biol Sci.* 368(1609): 20110329
- Ogura A, Inoue K, Ogonuki N, Noguchi A, Takanko K, *et al.* (2000) Production of male cloned mice from fresh, cultured, and cryopreserved immature Sertoli cells. *Biol Reprod.* 62(6): 1579-84
- O'Harte FP, Kennedy DG, Blanchflower WJ and Rice DA (1989) Methylmalonic acid in the diagnosis of cobalt deficiency in barley-fed lambs. *Br J Nutr.* 62(3): 729-38
- Okuyama S, Ito S and Nishino Y (1976) Vitamin B2 metabolism in the isolated perfused rat liver. *Gastroenterol Jpn.* 11(1): 5-10
- Oliveros, J.C. (2007-2015) Venny. An interactive tool for comparing lists with Venn's diagrams. <https://bioinfogp.cnb.csic.es/tools/venny/index.html>
- Ono R, Nakamura K, Inoue K, Naruse M, Usami T, *et al.* (2006) Deletion of Peg10, an imprinted gene acquired from a retrotransposon, causes early embryonic lethality. *Nat Genet.* 38(1): 101-6
- Oosterink JE, Naninck EF, Korosi A, Lucassen PJ, van Goudoever JB, *et al.* (2015) Accurate measurement of the essential micronutrients methionine, homocysteine, vitamins B6, B12, B9 and their metabolites in plasma, brain and maternal milk of mice using LC/MS ion trap analysis. *J Chromatogr B Analyt Technol Biomed Life Sci.* 998-999: 106-13
- Ordway RS, Boucher SE, Whitehouse NL, Schwab CG and Sloan BK (2009) Effects of providing two forms of supplemental methionine to periparturient Holstein dairy cows on feed intake and lactational performance. *J Dairy Sci.* 92(10): 5154-66
- Orsi NM and Leese HJ (2004) Amino Acid Metabolism of Preimplantation Bovine Embryos Cultured With Bovine Serum Albumin or Polyvinyl Alcohol. *Theriogenology.* 61(2-3): 561-72
- Orsi NM, Gopichandran N, Leese HJ, Picton HM and Harris SE (2005) Fluctuations in bovine ovarian follicular fluid composition throughout the oestrous cycle. *Reproduction.* 129(2): 219-28

- Osiezagha K, Ali S, Freeman C, Barker NC, Jabeen S, *et al.* (2013) Thiamine deficiency and delirium. *Innov Clin Neurosci.* 10(4): 26-32
- Osorio JS, Jacometo CB, Zhou Z, Luchini D, Cardoso FC, *et al.* (2016) Hepatic global DNA and peroxisome proliferator-activated receptor alpha promoter methylation are altered in peripartal dairy cows fed rumen-protected methionine. *J Dairy Sci.* 99(1):234-44
- Osuala K, Baker CN, Nguyen HL, Martinez C, Weinshenker D, *et al.* (2012) Physiological and genomic consequences of adrenergic deficiency during embryonic/fetal development in mice: impact on retinoic acid metabolism. *Physiol Genomics.* 44(19): 934-47
- Oudejans CB, Westerman B, Wouters D, Gooyer S, Leegwater PA, *et al.* (2001) Allelic IGF2R Repression Does Not Correlate With Expression of Antisense RNA in Human Extraembryonic Tissues. *Genomics.* 73(3): 331-7
- Ozawa M, Sakatani M, Yao J, Shanker S, Yu F, *et al.* (2012) Global gene expression of the inner cell mass and trophectoderm of the bovine blastocyst. *BMC Dev Biol.* 12: 33
- Pacchiarotti A, Mohamed MA, Micara G, Linari A, Tranquilli D, *et al.* (2007) The possible role of hyperhomocysteinemia on IVF outcome. *J Assist Reprod Genet.* 24(10): 459-62
- Padhee M, Zhang S, Lie S, Wang KC, Botting KJ, *et al.* (2015) The periconceptual environment and cardiovascular disease: does in vitro embryo culture and transfer influence cardiovascular development and health? *Nutrients.* 7(3): 1378-425
- Park JS, Jeong YS, Shin ST, Lee KK and Kang YK (2007) Dynamic DNA methylation reprogramming: active demethylation and immediate remethylation in the male pronucleus of bovine zygotes. *Dev Dyn.* 236(9): 2523-33
- Partridge RJ and Leese HJ (1996) Consumption of amino acids by bovine preimplantation embryos. *Reprod Fertil Dev.* 8(6): 945-50
- Patil V, Ward RL and Hesson LB (2014) The evidence for functional non-CpG methylation in mammalian cells. *Epigenetics.* 9(6): 823-8
- Patring JD, Jastrebova JA, Hjortmo SB, Andlid TA and Jägerstad IM (2005) Development of a simplified method for the determination of folates in baker's yeast by HPLC with ultraviolet and fluorescence detection. *J Agric Food Chem.* 53(7): 2406-11
- Paun O and Schönswetter P (2012) Amplified fragment length polymorphism: an invaluable fingerprinting technique for genomic, transcriptomic, and epigenetic studies. *Methods Mol Biol.* 862: 75-87
- Peat JR and Reik W (2012) Incomplete Methylation Reprogramming in SCNT Embryos. *Nat Genet.* 44(9): 965-6
- Pedley AM and Benkovic SJ (2017) A New View into the Regulation of Purine Metabolism: The Purinosome. *Trends Biochem Sci.* 42(2): 141-154
- Pegg AE (2006) Regulation of ornithine decarboxylase. *J Biol Chem.* 281: 14529-32
- Pegg AE (2016) Functions of Polyamines in Mammals. *J Biol Chem.* 291: 14904-12
- Pelland AMD, Corbett HE and Baltz JM (2009) Amino Acid Transport Mechanisms in Mouse Oocytes During Growth and Meiotic Maturation. *Biol Reprod.* 81(6): 1041-54
- Peñagaricano F, Souza AH, Carvalho PD, Driver AM, Gamba R, *et al.* (2013) Effect of maternal methionine supplementation on the transcriptome of bovine preimplantation embryos. *PLoS One.* 8(8): e72302
- Percudani R and Peracchi A (2003) A genomic overview of pyridoxal-phosphate-dependent enzymes. *EMBO Rep.* 4(9): 850-854
- Pérez-Torres I, Zuniga-Munoz AM and Guarner-Lans V (2017) Beneficial Effects of the Amino Acid Glycine. *Mini Rev Med Chem.* 17(1): 15-32

- Perry C, Yu S, Chen J, Matharu KS and Stover PJ (2007) Effect of vitamin B6 availability on serine hydroxymethyltransferase in MCF-7 cells. *Arch Biochem Biophys.* 462(1): 21-27
- Perry J, Lumb M, Laundry M, Reynolds EH and Chanarin I (1976) Role of vitamin B12 in folate coenzyme synthesis. *Br J Haematol.* 32(2): 243-8
- Peters J (2014) The role of genomic imprinting in biology and disease: an expanding view. *Nat Rev Genet.* 15(8): 517-30
- Pfeiffer CM, Fazili Z, McCoy L, Zhang M and Gunter EW (2004) Determination of folate vitamers in human serum by stable-isotope-dilution tandem mass spectrometry and comparison with radioassay and microbiologic assay. *Clin Chem.* 50(2): 423-32
- Phillips MM (2015) Liquid chromatography with isotope-dilution mass spectrometry for determination of water-soluble vitamins in foods. *Anal Bioanal Chem.* 407(11): 2965-74
- Piepenbrink MS, Overton TR and Clark JH (1996) Response of cows fed a low crude protein diet to ruminally protected methionine and lysine. *J Dairy Sci.* 79(9): 1638-46
- Poe SE, Mitchell GE Jr and Ely DG (1972) Rumen development in lambs. 3. Microbial B-vitamin synthesis. *J Anim Sci.* 34(5): 826-9
- Porter DH, Cook RJ and Wagner C (1985) Enzymatic properties of dimethylglycine dehydrogenase and sarcosine dehydrogenase from rat liver. *Arch Biochem Biophys.* 243(2): 396-407
- Powers HJ (2003) Riboflavin (vitamin B-2) and health. *Am J Clin Nutr.* 77(6): 1352-1360
- Preynat A, Lapierre H, Thivierge MC, Palin MF, Matte JJ, *et al.* (2009) Influence of methionine supply on the response of lactational performance of dairy cows to supplementary folic acid and vitamin B12. *J Dairy Sci.* 92(4): 1685-95
- Pront R, Margalioth EJ, Green R, Eldar-Geva T, Maimoni Z, *et al.* (2009) Prevalence of low serum cobalamin in infertile couples. *Andrologia.* 41(1): 46-50
- Putluru RK, Kin YS and Lee CN (2016) Differential Expression of Superoxide Dismutases (SODs) in Bovine Corpus Luteum During Estrous Cycle and Pregnancy. *Pac. Agric. Nat. Resour..* 6: 11-20
- Puts J, de Groot M, Haex M and Jakobs B (2015) Simultaneous Determination of Underivatized Vitamin B1 and B6 in Whole Blood by Reversed Phase Ultra High Performance Liquid Chromatography Tandem Mass Spectrometry. *PLoS One.*10(7): e0132018
- Quadros EV (2010) Advances in the understanding of cobalamin assimilation and metabolism. *Br J Haematol.* 148(2): 195-204
- Quadros EV and Jacobsen DW (1995) The dynamics of cobalamin utilization in L-1210 mouse leukemia cells: a model of cellular cobalamin metabolism. *Biochim Biophys Acta.* 1244(2-3): 395-403
- Rakha A (2015) Cloning Efficiency and a Comparison between Donor Cell Types. *Clon Transgen.* 4: 3
- Rakoczy J, Lee S, Weerasekera SJ, Simmons DG and Dawson PA (2015) Placental and Fetal Cysteine Dioxygenase Gene Expression in Mouse Gestation. *Placenta.* 36(8): 956-9
- Ramos RJ, Pras-Raves ML, Gerrits J, van der Ham M, Willemsen M, *et al.* (2017) Vitamin B6 is essential for serine de novo biosynthesis. *J Inherit Metab Dis.* 40(6): 883-891
- Rathbone AJ, Fisher PA, Lee J-H, Craigon J and Campbell KHS (2010) Reprogramming of Ovine Somatic Cells With *Xenopus Laevis* Oocyte Extract Prior to SCNT Improves Live Birth Rate. *Cell Reprogram.* 12(5): 609-16

- Rattanasuk S, Parnpai R and Ketudat-Cairns M (2011) Multiplex polymerase chain reaction used for bovine embryo sex determination. *J Reprod Dev.* 57(4): 539-42
- Ravelli GP, Stein ZA and Susser MW (1976) Obesity in young men after famine exposure in utero and early infancy. *N Engl J Med.* 295(7): 349-53
- Razin A and Cedar H (1991) DNA methylation and gene expression. *Microbiol Rev.* 55(3): 451-8
- Reed MC, Nijhout HF, Sparks R and Ulrich CM (2004) A mathematical model of the methionine cycle. *J. Theor. Biol.* 226: 33-43
- Rees WD, Wilson FA and Maloney CA (2006) Sulfur amino acid metabolism in pregnancy: the impact of methionine in the maternal diet. *J Nutr.* 136(6): 1701S-1705S
- Reimand J, Isserlin R, Voisin V, Kucera M, Tannus-Lopes C, Rostamianfar A, *et al.* (2019) Pathway enrichment analysis and visualization of omics data using g:Profiler, GSEA, Cytoscape and EnrichmentMap. *Nat Protoc.* 14(2): 482-51
- Reznikoff-Etiévant MF, Zittoun J, Vaylet C, Pernet P and Milliez J (2002) Low Vitamin B(12) level as a risk factor for very early recurrent abortion *Eur J Obstet Gynecol Reprod Biol.* 104(2): 156-9
- Rhind SM, King TJ, Harkness LM, Bellamy C, Wallace W, *et al.* (2003) Cloned Lambs--Lessons From Pathology. *Nat Biotechnol.* 21(7): 744-5
- Riesewijk AM, Blagitko N, Schinzel AA, Hu L, Schulz U, *et al.* (1998) Evidence against a major role of PEG1/MEST in Silver-Russell syndrome. *Eur J Hum Genet.* 6(2): 114-20
- Riesewijk AM, Schepens MT, Welch EM, van den Berg-Loonen EM, Mariman EM, *et al.* (1996) Maternal-specific methylation of the human IGF2R gene is not accompanied by allele-specific transcription. *Genomics.* 31(1996): 158-166
- Rippin HL, Hutchinson J, Jewell J, Breda JJ and Cade JE (2017) Adult Nutrient Intakes from Current National Dietary Surveys of European Populations. *Nutrients.* 9(12): E1288
- Roje S (2006) S-Adenosyl-L-methionine: beyond the universal methyl group donor. *Phytochemistry.* 67(15): 1686-98
- Ronnenberg AG, Venners SA, Xu X, Chen C, Wang L, *et al.* (2007) Preconception B-vitamin and homocysteine status, conception, and early pregnancy loss. *Am J Epidemiol.* 166(3): 304-12
- Rooke JA, McEvoy TG, Ashworth CJ, Robinson JJ, Wilmut I, *et al.* (2007) Ovine fetal development is more sensitive to perturbation by the presence of serum in embryo culture before rather than after compaction. *Theriogenology.* 67(3): 639-47
- Rouillon A, Surdin-Kerjan Y and Thomas D (1999) Transport of sulfonium compounds. Characterization of the s-adenosylmethionine and s-methylmethionine permeases from the yeast *Saccharomyces cerevisiae*. *J Biol Chem.* 274(40): 28096-105
- Rowling MJ, McMullen MH, Chipman DC and Schalinske KL (2002) Hepatic glycine N-methyltransferase is up-regulated by excess dietary methionine in rats. *J Nutr.* 132(9): 2545-50
- Rubessa M, Boccia L, Campanile G, Longobardi V, Albarella S, *et al.* (2011) Effect of energy source during culture on in vitro embryo development, resistance to cryopreservation and sex ratio. *Theriogenology.* 76(7): 1347-55
- Sadre-Marandi F, Dahdoul T, Reed MC and Nijhout HF (2018) Sex Differences in Hepatic One-Carbon Metabolism. *BMC Syst Biol.* 12(1): 89
- Saikhun J, Pavasuthipaisit K, Jaruansuwan M and Kitiyanant Y (2002) Xenonuclear transplantation of buffalo (*Bubalus bubalis*) fetal and adult somatic cell nuclei into bovine (*Bos indicus*) oocyte cytoplasm and their subsequent development. *Theriogenology.* 57(7): 1829-37

- Sakurai T, Asakura T, Mizuno A, Matsuda M (1992) Absorption and metabolism of pyridoxamine in mice. II. Transformation of pyridoxamine to pyridoxal in intestinal tissues. *J Nutr Sci Vitaminol (Tokyo)*. 38(3): 227-233
- Salas M, John R, Saxena A, Barton S, Frank D, *et al.* (2004) Placental growth retardation due to loss of imprinting of Phlda2. *Mech Dev*. 121(10): 1199-210
- Salilew-Wondim D, Fournier E, Hoelker M, Saeed-Zidane M, Tholen E, *et al.* (2015) Genome-Wide DNA Methylation Patterns of Bovine Blastocysts Developed In Vivo from Embryos Completed Different Stages of Development In Vitro. *PLoS One*. 10(11): e0140467
- Santos F, Hendrich B, Reik W and Dean W (2002) Dynamic reprogramming of DNA methylation in the early mouse embryo. *Dev Biol*. 241(1): 172-82
- Sanz LA, Chamberlain S, Sabourin J-C, Henckel A, Magnuson T, *et al.* (2008) A mono-allelic bivalent chromatin domain controls tissue-specific imprinting at Grb10. *EMBO J*. 27(19): 2523-32
- Sauberlich HE (1980) Interactions of thiamin, riboflavin, and other B-vitamins. *Ann N Y Acad Sci*. 355: 80-97
- Scheer JB, Mackey AD and Gregory JF (2005) Activities of hepatic cytosolic and mitochondrial forms of serine hydroxymethyltransferase and hepatic glycine concentration are affected by vitamin B-6 intake in rats. *J Nutr*. 135(2): 233-8
- Schnellbaecher A, Binder D, Bellmaine S and Zimmer A (2019) Vitamins in cell culture media: Stability and stabilization strategies. *Biotechnol Bioeng*. 116(6): 1537-1555
- Schulz LC (2010) The Dutch Hunger Winter and the developmental origins of health and disease. *Proc Natl Acad Sci U S A*. 107(39): 16757-8
- Schwab CG and Broderick GA (2017) A 100-Year Review: Protein and amino acid nutrition in dairy cows. *J Dairy Sci*. 100(12): 10094-10112
- Schweinberger BM, Schwieder L, Scherer E, Sitta A, Vargas CR, *et al.* (2014) Development of an animal model for gestational hypermethioninemia in rat and its effect on brain Na⁺, K⁺-ATPase/Mg²⁺-ATPase activity and oxidative status of the offspring. *Metab Brain Dis*. 29(1): 153-60
- Seck M, Linton JAV, Allen MS, Castagnino DS, Chouinard PY, *et al.* (2017) Apparent ruminal synthesis of B vitamins in lactating dairy cows fed diets with different forage-to-concentrate ratios. *J Dairy Sci*. 100(3): 1914-1922
- Selhub J (1999) Homocysteine metabolism. *Annu Rev Nutr*. 19: 217-46
- Selhub J (2002) Folate, vitamin B12 and vitamin B6 and one carbon metabolism. *J Nutr Health Aging*. 6(1): 39-42
- Shane B (2008) Folate and vitamin B12 metabolism: overview and interaction with riboflavin, vitamin B6, and polymorphisms. *Food Nutr Bull*. 29(2): S5-16
- Shane B and Stokstad EL (1985) Vitamin B12-folate interrelationships. *Annu Rev Nutr*. 5: 115-41
- Shaw GM, Carmichael SL, Yang W, Selvin S and Schaffer DM (2004) Periconceptional dietary intake of choline and betaine and neural tube defects in offspring. *Am J Epidemiol*. 160(2): 102-9
- Shen C-J, Cheng WTK, Wu S-C, Chen H-L, Tsai T-C, *et al.* (2012) Differential Differences in Methylation Status of Putative Imprinted Genes Among Cloned Swine Genomes. *PLoS One*. 7(2): e32812
- Shi DQ, Ali I, Tang J and Yang WC (2017) New Insights into 5hmC DNA Modification: Generation, Distribution and Function. *Front Genet*. 8: 100
- Shi G and Jin Y (2010) Role of Oct4 in maintaining and regaining stem cell pluripotency. *Stem Cell Res Ther*. 1(5): 39

- Shibany KA, Töttemeyer S, Pratt SL and Paine SW (2016) Equine hepatocytes: isolation, cryopreservation, and applications to in vitro drug metabolism studies. *Pharmacol Res Perspect.* 4(5): e00268
- Shibata K, Shimizu A and Fukuwatari T (2013) Vitamin B1 Deficiency Does not Affect the Liver Concentrations of the Other Seven Kinds of B-Group Vitamins in Rats. *Nutr Metab Insights.* 6: 1-10
- Shiraki N, Shiraki Y, Tsuyama T, Obata F, Miura M, *et al.* (2014) Methionine metabolism regulates maintenance and differentiation of human pluripotent stem cells. *Cell Metab.* 19(5): 780-94
- Shock LS, Thakkar PV, Peterson EJ, Moran RG and Taylor SM (2011) DNA methyltransferase 1, cytosine methylation, and cytosine hydroxymethylation in mammalian mitochondria. *Proc Natl Acad Sci U S A.* 108(9): 3630-5
- Shojaei Saadi HA, Gagné D, Fournier É, Baldoceda Baldeon LM, Sirard MA, *et al.* (2016) Responses of bovine early embryos to S-adenosyl methionine supplementation in culture. *Epigenomics.* 8(8): 1039-60
- Shoob HD, Sargent RG, Thompson SJ, Best RG, Drane JW, *et al.* (2001) Dietary methionine is involved in the etiology of neural tube defect-affected pregnancies in humans. *J Nutr.* 131(10): 2653-8
- Shuvalov O, Petukhov A, Daks A, Fedorova O, Vasileva E, *et al.* (2017) One-carbon metabolism and nucleotide biosynthesis as attractive targets for anticancer therapy. *Oncotarget.* 8(14): 23955-23977
- Simmet K, Zakhartchenko V, Philippou-Massier J, Blum H, Klymiuk N, *et al.* (2018) OCT4/POU5F1 is required for NANOG expression in bovine blastocysts. *Proc Natl Acad Sci U S A.* 115(11): 2770-2775
- Simopoulou M, Sfakianoudis K, Rapani A, Giannelou P, Anifandis G, *et al.* (2018) Considerations Regarding Embryo Culture Conditions: From Media to Epigenetics. *In Vivo.* 32(3): 451-460
- Sinclair KD and Singh R (2007) Modelling the developmental origins of health and disease in the early embryo. *Theriogenology.* 67(1): 43-53
- Sinclair KD, Allegrucci C, Singh R, Gardner DS, Sebastian S, *et al.* (2007) DNA methylation, insulin resistance, and blood pressure in offspring determined by maternal periconceptional B vitamin and methionine status. *Proc Natl Acad Sci U S A.* 104(49): 19351-19356
- Sinclair KD, Corr SA, Gutierrez G, Fisher PA, Lee J-H, *et al.* (2016) Healthy ageing of cloned sheep. *Nature Communications.* 7: 12359
- Sinclair KD, Lunn LA, Kwong WY, Wonnacott K, Linforth RS, *et al.* (2008) Amino acid and fatty acid composition of follicular fluid as predictors of in-vitro embryo development. *Reprod Biomed Online.* 16(6): 859-68
- Sinclair KD, Rutherford KM, Wallace JM, Brameld JM, Stöger R, *et al.* (2016b) Epigenetics and developmental programming of welfare and production traits in farm animals. *Reprod Fertil Dev.* 28: 1443-78
- Sinclair KD, Young LE, Wilmut I and McEvoy TG (2000) In-utero overgrowth in ruminants following embryo culture: lessons from mice and a warning to men. *Hum Reprod.* 15(5): 68-86
- Sirard MA (2019) Distribution and dynamics of mitochondrial DNA methylation in oocytes, embryos and granulosa cells. *Sci Rep.* 9(1): 11937
- Sirard MA and First NL (1988) In vitro inhibition of oocyte nuclear maturation in the bovine. *Biol Reprod.* 39(2): 229-34
- Škovierová H, Vidomanová E, Mahmood S, Sopková J, Drgová A, *et al.* (2016) The Molecular and Cellular Effect of Homocysteine Metabolism Imbalance on Human Health. *Int J Mol Sci.* 17(10). pii: E1733

- Sleutels F, Zwart R and Barlow DP (2002) The non-coding Air RNA is required for silencing autosomal imprinted genes. *Nature*. 415(6873): 810-3
- Smallwood SA, Lee HJ, Angermueller C, Krueger F, Saadeh H, *et al.* (2014) Single-cell genome-wide bisulfite sequencing for assessing epigenetic heterogeneity. *Nat Methods*. 11(8): 817-820
- Smith AD and Refsum H (2016) Homocysteine, B Vitamins, and Cognitive Impairment. *Annu Rev Nutr*. 36: 211-39
- Smith FM, Garfield AS and Ward A (2006) Regulation of Growth and Metabolism by Imprinted Genes. *Cytogenet Genome Res*. 113(1-4): 279-91
- Smith LC, Suzuki J, Goff AK, Filion F, Murphy BD, *et al.* (2012) Developmental and Epigenetic Anomalies in Cloned Cattle. *Reprod Domest Anim*. 47(4): 107-14
- Smith LC, Therrien J, Filion F, Bressan F and Meirelles FV (2015) Epigenetic Consequences of Artificial Reproductive Technologies to the Bovine Imprinted Genes SNRPN, H19/IGF2, and IGF2R. *Front Genet*. 6: 58
- Smith RM and Osborne-White WS (1973) Folic acid metabolism in vitamin B12-deficient sheep. Depletion of liver folates. *Biochem J*. 136(2): 279-293
- Smith RM, Osborne-White WS and Russell GR (1969) Methylmalonic acid and coenzyme A concentrations in the livers of pair-fed vitamin B 12-deficient and vitamin B 12-treated sheep. *Biochem J*. 112(5): 703-7
- Smith ZD and Meissner A (2013) DNA methylation: roles in mammalian development. *Nat Rev Genet*. 14(3): 204-20
- Smith ZD, Gu H, Bock C, Gnirke A and Meissner A (2009) High-throughput Bisulfite Sequencing in Mammalian Genomes. *Methods*. 48(3): 226-32
- Snoswell AM and Xue GP (1987) Methyl group metabolism in sheep. *Comp Biochem Physiol B*. 88(2): 383-394
- Snyder NW, Basy SS, Worth AJ, Mesaros C and Blair IA (2015) Metabolism of propionic acid to a novel acyl-coenzyme A thioester by mammalian cell lines and platelets. *J Lipid Res*. 56(1): 142-50
- Somers M and Gawthorne JM (1969) The effect of dietary cobalt intake on the plasma vitamin B 12 concentration of sheep. *Aust J Exp Biol Med Sci*. 47(2): 227-233
- Song CX, Szulwach KE, Fu Y, Dai Q, Yi C, *et al.* (2011) Selective chemical labeling reveals the genome-wide distribution of 5-hydroxymethylcytosine. *Nat Biotechnol*. 29(1): 68-72
- Song L, James SR, Kazim L and Karpf AR (2005) Specific method for the determination of genomic DNA methylation by liquid chromatography-electrospray ionization tandem mass spectrometry. *Anal Chem*. 77(2): 504-10
- Spencer TE, Johnson GA, Bazer FW and Burghardt RC (2004) Implantation mechanisms: insights from the sheep. *Reproduction*. 128(6): 657-68
- Steegers-Theunissen RP, Obermann-Borst SA, Kremer D, Lindemans J, Siebel C, *et al.* (2009) Periconceptional maternal folic acid use of 400 microg per day is related to increased methylation of the IGF2 gene in the very young child. *PLoS One*. 4(11): e7845
- Steegers-Theunissen RP, Twigt J, Pestinger V and Sinclair KD (2013) The periconceptional period, reproduction and long-term health of offspring: the importance of one-carbon metabolism. *Hum Reprod Update*. 19(6): 640-55
- Steele W, Allegrucci C, Singh R, Lucas E, Priddle H, *et al.* (2005) Human embryonic stem cell methyl cycle enzyme expression: modelling epigenetic programming in assisted reproduction? *Reprod Biomed Online*. 10(6): 755-66

- Steeves CL, Hammer MA, Walker GB, Rae D, Stewart NA, *et al.* (2003) The glycine neurotransmitter transporter GLYT1 is an organic osmolyte transporter regulating cell volume in cleavage-stage embryos. *Proc Natl Acad Sci U S A.* 100(24): 13982-7
- Stein AD, Kahn HS, Rundle A, Zybert PA, van der Pal-de Bruin K, *et al.* (2007) Anthropometric measures in middle age after exposure to famine during gestation: evidence from the Dutch famine. *Am J Clin Nutr.* 85(3): 869-76
- Stephenson J, Heslehurst N, Hall J, Schoenaker DAJM, Hutchinson J, *et al.* (2018) Before the beginning: nutrition and lifestyle in the preconception period and its importance for future health. *Lancet.* 391(10132): 1830-41
- Stöger R, Kubicka P, Liu CG, Kafri T, Razin A, *et al.* (1993) Maternal-specific methylation of the imprinted mouse *Igf2r* locus identifies the expressed locus as carrying the imprinting signal. *Cell.* 73(1): 61-71
- Stover PJ (2009) One-carbon metabolism – genome interactions in folate-associated pathologies. *J. Nutr.* 139: 2402-5
- Stover PJ and Field MS (2011) Trafficking of intracellular folates. *Adv. Nutr.* 2: 325-31
- Sturmey RG, Bermejo-Alvarez P, Gutierrez-Adan A, Rizos D, Leese HJ, *et al.* (2010) Amino acid metabolism of bovine blastocysts: a biomarker of sex and viability. *Mol Reprod Dev.* 77(3): 285-96
- Sturmey RG, Brison DR and Leese HJ (2008) Symposium: innovative techniques in human embryo viability assessment. Assessing embryo viability by measurement of amino acid turnover. *Reprod Biomed Online.* 17(4): 486-96
- Su J, Wang Y, Li W, Gao M, Ma Y, *et al.* (2014) Effects of 3-hydroxyflavone on the cellular and molecular characteristics of bovine embryos produced by somatic-cell nuclear transfer. *Mol Reprod Dev.* 81(3): 257–269
- Sun D, Wollin A and Stephen AM (2002) Moderate folate deficiency influences polyamine synthesis in rats. *J Nutr.* 132(9): 2632-7
- Sun Q, Li X, Jia Y, Pan S, Li R, *et al.* (2016) Maternal betaine supplementation during gestation modifies hippocampal expression of GR and its regulatory miRNAs in neonatal piglets. *J Vet Med Sci.* 78(6): 921-8
- Sunde A, Brison D, Dumoulin J, Harper J, Lundin K, *et al.* (2016) Time to take human embryo culture seriously. *Hum Reprod.* 31(10): 2174-82
- Suslov S, Ponomarenko PM, Ponomarenko M, Drachkova IA, Arshinova TV, *et al.* (2010) TATA Box Polymorphisms in Genes of Commercial and Laboratory Animals and Plants Associated With Selectively Valuable Traits. *Genetika.* 46(4): 448-57
- Suttle NF (2005) Assessing the needs of sheep for trace elements. In practice. *British Medical Journal Publishing Group.* 27: 474-483
- Suttle NF (2010) Mineral nutrition of livestock (fourth ed.), CABI, Cambridge
- Suzuki J, Therrien J, Fillion F, Lefebvre R, Goff AK, *et al.* (2009) In Vitro Culture and Somatic Cell Nuclear Transfer Affect Imprinting of SNRPN Gene in Pre- And Post-Implantation Stages of Development in Cattle. *BMC Dev Biol.* 9: 9
- Szegedi SS, Castro CC, Koutmos M and Garrow TA (2008) Betaine-homocysteine S-methyltransferase-2 is an S-methylmethionine-homocysteine methyltransferase. *J Biol Chem.* 283(14): 8939-45
- Szyf M, Tang YY, Hill KG and Musci R (2016) The dynamic epigenome and its implications for behavioral interventions: a role for epigenetics to inform disorder prevention and health promotion. *Transl Behav Med.* 6(1): 55-62
- Tachibana M, Amato P, Sparman M, Marti Gutierrez N, Tippner-Hedges R, *et al.* (2013) Human Embryonic Stem Cells Derived by Somatic Cell Nuclear Transfer. *Cell.* 153(6): 1228-38

- Tahiliani M, Koh KP, Shen Y, Pastor WA, Bandukwala H, *et al.* (2009) Conversion of 5-methylcytosine to 5-hydroxymethylcytosine in mammalian DNA by MLL partner TET1. *Science*. 324(5929): 930-5
- Takagi M, Choi YH, Kamishita H, Ohtani M, Acosta TJ, *et al.* (1998) Evaluation of fluids from cystic follicles for in vitro maturation and fertilization of bovine oocytes. *Theriogenology*. 50(2): 307-20
- Takahashi-Iñiguez T, García-Hernandez E, Arreguín-Espinosa R, Flores ME (2012) Role of vitamin B12 on methylmalonyl-CoA mutase activity. *J Zhejiang Univ Sci B*. 13(6): 423-437
- Takeda H, Caiment F, Smit M, Hiard S, Tordoir X, *et al.* (2006) The callipyge mutation enhances bidirectional long-range DLK1-GTL2 intergenic transcription in cis. *Proc Natl Acad Sci U S A*. 103(21): 8119-24
- Takenaka K, Fukami K, Otsuki M, Nakamura Y, Kataoka Y, *et al.* (2003) Role of phospholipase C-L2, a novel phospholipase C-like protein that lacks lipase activity, in B-cell receptor signaling. *Mol Cell Biol*. 23(20): 7329-38
- Tang S, Fang Y, Huang G, Xu X, Padilla-Banks E, *et al.* (2017) Methionine metabolism is essential for SIRT1-regulated mouse embryonic stem cell maintenance and embryonic development. *EMBO J*. 36(21): 3175-3193
- Tarahomi M, Vaz FM, van Straalen JP, Schrauwen FAP, van Wely M, *et al.* (2019) The composition of human preimplantation embryo culture media and their stability during storage and culture. *Hum Reprod*. 34(8): 1450-1461
- Tartia AP, Rudraraju N, Richards T, Hammer MA, Talbot P, *et al.* (2009) Cell volume regulation is initiated in mouse oocytes after ovulation. *Development*. 136(13): 2247-54
- Temel S, van Voorst SF, Jack BW, Denktaş S and Steegers EA (2014) Evidence-based preconceptional lifestyle interventions. *Epidemiol Rev*. 36: 19-30
- Thatcher WW, Bartol FF and Knickerbocker JJ (1984) Maternal Recognition of Pregnancy in Cattle. *J Dairy Sci*. 67: 2797-2811
- Thompson JG, Gardner DK, Pugh PA, McMillan WH and Tervit HR (1995) Lamb birth weight is affected by culture system utilized during in vitro pre-elongation development of ovine embryos. *Biol Reprod*. 53(6): 1385-91
- Thomson JP and Meehan RR (2017) The application of genome-wide 5-hydroxymethylcytosine studies in cancer research. *Epigenomics*. 9(1): 77-91
- Tisdale MJ (1981) Effect of methionine deprivation on S-adenosylmethionine decarboxylase of tumour cells. *Biochim Biophys Acta*. 675(3-4): 366-372
- Toledo MZ, Baez GM, Garcia-Guerra A, Lobos NE, Guenther JN, *et al.* (2017) Effect of feeding rumen-protected methionine on productive and reproductive performance of dairy cows. *PLoS One*. 12(12): e0189117
- Tomizawa S, Kobayashi H, Watanabe T, Andrews S, Hata K, *et al.* (2011) Dynamic stage-specific changes in imprinted differentially methylated regions during early mammalian development and prevalence of non-CpG methylation in oocytes. *Development*. 138(5): 811-20
- Toyoshima S, Watanabe F, Saido H, Pezacka EH, Jacobsen DW, *et al.* (1996) Accumulation of methylmalonic acid caused by vitamin B12-deficiency disrupts normal cellular metabolism in rat liver. *Br J Nutr*. 75(6): 929-38
- Tran DA, Bai AY, Singh P, Wu X and Szabó PE (2014) Characterization of the imprinting signature of mouse embryo fibroblasts by RNA deep sequencing. *Nucleic Acids Res*. 42(3): 1772–1783
- Tremolizzo L, Carboni G, Ruzicka WB, Mitchell CP, Sugaya I, *et al.* (2002) An epigenetic mouse model for molecular and behavioral neuropathologies related to schizophrenia vulnerability. *Proc Natl Acad Sci U S A*. 99(26): 17095-100

- Tretter L, Patocs A and Chinopoulos C (2016) Succinate, an intermediate in metabolism, signal transduction, ROS, hypoxia, and tumorigenesis. *Biochim Biophys Acta*. 1857(8): 1086-1101
- Tríbulo P, Jumatayeva G, Lehloenya K, Moss JI, Negrón-Pérez VM, *et al.* (2018) Effects of Sex on Response of the Bovine Preimplantation Embryo to Insulin-Like Growth Factor 1, Activin A, and WNT7A. *MC Dev Biol*. 18(1): 16
- Tsitsiou E, Sibley CP, D'Souza SW, Catanescu O, Jacobsen DW, *et al.* (2009) Homocysteine transport by systems L, A and y+L across the microvillous plasma membrane of human placenta. *J Physiol*. 587(16): 4001-13
- U.S Department of Health and Human Services Food and Drug Administration, Center for Drug Evaluation and Research (CDER), Bioanalytical Method Validation, Guidance for Industry, May 2018, Available at:
<https://www.fda.gov/downloads/drugs/guidances/ucm070107.Pdf>
- Uekawa A, Katsushima K, Ogata A, Kawata T, Maeda N, *et al.* (2009) Change of epigenetic control of cystathionine beta-synthase gene expression through dietary vitamin B12 is not recovered by methionine supplementation. *J Nutrigenet Nutrigenomics*. 2(1): 29-36
- Ueki I, Roman HB, Valli A, Fieselmann K, Lam J, *et al.* (2011) Knockout of the Murine Cysteine Dioxygenase Gene Results in Severe Impairment in Ability to Synthesize Taurine and an Increased Catabolism of Cysteine to Hydrogen Sulfide. *Am J Physiol Endocrinol Metab*. 301(4): E668-84
- Ueland PM, Holm PI and Hustad S (2005) Betaine: a key modulator of one-carbon metabolism and homocysteine status. *Clin Chem Lab Med*. 43(10): 1069-75
- Uhde K, van Tol HTA, Stout TAE and Roelen BAJ (2018) Metabolomic profiles of bovine cumulus cells and cumulus-oocyte-complex-conditioned medium during maturation in vitro. *Sci Rep*. 8(1): 9477
- Ulrey CL, Liu L, Andrews LG and Tollefsbol TO (2005) The impact of metabolism on DNA methylation. *Hum Mol Genet*. 14: R139-47
- Ulrich CM, Neuhouser M, Liu AY, Boynton A, Gregory JF 3rd, *et al.* (2008) Mathematical modeling of folate metabolism: predicted effects of genetic polymorphisms on mechanisms and biomarkers relevant to carcinogenesis. *Cancer Epidemiol Biomarkers Prev*. 17(7): 1822-31
- Valinluck V, Tsai HH, Rogstad DK, Burdzy A, Bird A, *et al.* (2004) Oxidative damage to methyl-CpG sequences inhibits the binding of the methyl-CpG binding domain (MBD) of methyl-CpG binding protein 2 (MeCP2). *Nucleic Acids Res*. 32(14): 4100-8
- van der Wijst MG, van Tilburg AY, Ruiters MH and Rots MG (2017) Experimental mitochondria-targeted DNA methylation identifies GpC methylation, not CpG methylation, as potential regulator of mitochondrial gene expression. *Sci Rep*. 7(1): 177
- Van Winkle LJ (2001) Amino Acid Transport Regulation and Early Embryo Development. *Biol Reprod*. 64(1): 1-12
- Vance DE (2013) Physiological roles of phosphatidylethanolamine N-methyltransferase. *Biochim Biophys Acta*. 1831(3): 626-32
- Varley KE, Gertz J, Bowling KM, Parker SL, Reddy TE, *et al.* (2013) Dynamic DNA methylation across diverse human cell lines and tissues. *Genome Res*. 23(3): 555–5677
- Velker BA, Denomme MM and Mann MR (2012) Embryo culture and epigenetics. *Methods Mol Biol*. 912: 399-421
- Vilahir N, Baccarelli AA, Bustamante M, Agramunt S, Byun HM, *et al.* (2013) Storage conditions and stability of global DNA methylation in placental tissue. *Epigenomics*. 5(3): 341-8

- Visentin M, Diop-Bove N, Zhao R and Goldman ID (2014) The intestinal absorption of folates. *Annu Rev Physiol.* 76: 251-74
- Vu TH, Jirtle RL and Hoffman AR (2006) Cross-species clues of an epi- genetic imprinting regulatory code for the IGF2R gene. *Cytogenet. Genome Res.* 113: 202–208
- Wacker J, Frühauf J, Schulz M, Chiwora FM, Volz J, *et al.* (2000) Riboflavin deficiency and preeclampsia. *Obstet Gynecol.* 96(1): 38-44
- Wadhwa PD, Buss C, Entringer S and Swanson JM (2009) Developmental origins of health and disease: brief history of the approach and current focus on epigenetic mechanisms. *Semin Reprod Med.* 27(5): 358-68
- Wakayama T and Yanagimachi R (2001) Mouse cloning with nucleus donor cells of different age and type. *Mol Reprod Dev.* 58(4): 376-83
- Wald NJ, Morris JK and Blakemore C (2018) Public health failure in the prevention of neural tube defects: time to abandon the tolerable upper intake level of folate. *Public Health Rev.* 39: 2
- Wang S and Kool ET (1995) Origins of the large differences in stability of DNA and RNA helices: C-5 methyl and 2'-hydroxyl effects. *Biochemistry.* 34(12): 4125-32
- Wang X and Dai J (2010) Concise Review: Isoforms of OCT4 Contribute to the Confusing Diversity in Stem Cell Biology. *Stem Cells.* 28(5): 885–893
- Wang X and Kadarmideen HN (2019) An Epigenome-Wide DNA Methylation Map of Testis in Pigs for Study of Complex Traits. *Front. Genet.* 10: 405
- Wang X, Qu J, Li J, He H, Liu Z, *et al.* (2020) Epigenetic Reprogramming During Somatic Cell Nuclear Transfer: Recent Progress and Future Directions. *Front Genet.* 11: 205
- Wang ZQ, Fung MR, Barlow DP and Wagner EF (1994) Regulation of embryonic growth and lysosomal targeting by the imprinted Igf2/Mpr gene. *Nature.* 372(6505): 464-7
- Waterland RA and Jirtle RL (2003) Transposable elements: targets for early nutritional effects on epigenetic gene regulation. *Mol Cell Biol.* 23(15): 5293-300
- Waterland RA, Dolinoy DC, Lin JR, Smith CA, Shi X and Tahiliani KG (2006) Maternal methyl supplements increase offspring DNA methylation at Axin Fused. *Genesis.* 44(9): 401-6
- Waterland RA, Kellermayer R, Laritsky E, Rayco-Solon P, Harris RA, *et al.* (2010) Season of conception in rural Gambia affects DNA methylation at putative human metastable epialleles. *PLoS Genet.* 6(12): e1001252
- Waterland RA, Lin JR, Smith CA and Jirtle RL (2006b) Post-weaning diet affects genomic imprinting at the insulin-like growth factor 2 (Igf2) locus. *Hum Mol Genet.* 15(5): 705-16
- Watkins AJ and Sinclair KD (2014) Paternal low protein diet affects adult offspring cardiovascular and metabolic function in mice. *Am J Physiol Heart Circ Physiol.* 306(10): H1444-52
- Watkins AJ, Dias I, Tsuru H, Allen D, Emes RD, *et al.* (2018) Paternal diet programs offspring health through sperm- and seminal plasma-specific pathways in mice. *Proc Natl Acad Sci U S A.* 115(40): 10064-10069
- Watkins AJ, Ursell E, Panton R, Papenbrock T, Hollis L, *et al.* (2008) Adaptive responses by mouse early embryos to maternal diet protect fetal growth but predispose to adult onset disease. *Biol Reprod.* 78(2): 299-306
- Wehling RL and Wetzel DL (1984) Simultaneous determination of pyridoxine, riboflavin, and thiamin in fortified cereal products by high-performance liquid chromatography. *J. Agric. Food Chem.* 32(6): 1326-1331

- Weidman JR, Dolinoy DC, Maloney KA, Cheng JF and Jirtle RL (2006) Imprinting of opossum Igf2r in the absence of differential methylation and air. *Epigenetics*. 1: 49–54
- Williams DV, G. Levy G and Stobaus T (2007) Composition of Australian red meat 2002. 3. *Nutrient profile Food Aust.* 59(7): 331-341
- Williams PG (2007) Nutritional composition of red meat. *Nutr. Dietetics*. 64(4): S113-S119
- Willyard C (2017) An epigenetics gold rush: new controls for gene expression. *Nature*. 542(7642): 406-408
- Wilmot I, Schnieke AE, McWhir J, Kind AJ and Campbell KH (1997) Viable Offspring Derived From Fetal and Adult Mammalian Cells. *Nature*. 385(6619): 810-3
- Wilson MJ, Shivapurkar N and Poirier LA (1984) Hypomethylation of hepatic nuclear DNA in rats fed with a carcinogenic methyl-deficient diet. *Biochem J*. 218(3): 987-90
- Wiltbank MC, Shaver RD, Toledo MZ, Carvalho PD, Baez GM, *et al.* (2014) Potential benefits of feeding methionine on reproductive efficiency of lactating dairy cows. *Conference paper: Four-State Dairy Nutrition and Management*.
- Wolff GL, Kodell RL, Moore SR and Cooney CA (1998) Maternal epigenetics and methyl supplements affect agouti gene expression in Avy/a mice. *FASEB J*. 12(11): 949-57
- Wossidlo M, Nakamura T, Lepikhov K, Marques CJ, Zakhartchenko V, *et al.* (2011) 5-Hydroxymethylcytosine in the mammalian zygote is linked with epigenetic reprogramming. *Nat Commun*. 2: 241
- Wright MM, Howe AG and Zarembek V (2004) Cell membranes and apoptosis: role of cardiolipin, phosphatidylcholine, and anticancer lipid analogues. *Biochem Cell Biol*. 82(1): 18-26
- Wu X, Song M, Yang X, Liu X, Liu K, *et al.* (2016) Establishment of Bovine Embryonic Stem Cells After Knockdown of CDX2. *Sci Rep*. 6: 28343
- Wutz A, Smrzka OW, Schweifer N, Schellander K, Wagner EF, *et al.* (1997) Imprinted Expression of the Igf2r Gene Depends on an Intronic CpG Island. *Nature*. 389(6652): 745-9
- Xiang Y, Laurent B, Hsu CH, Nachtergaele S, Lu Z, *et al.* (2017) RNA m6A methylation regulates the ultraviolet-induced DNA damage response. *Nature*. 543(7646): 573-576
- Xu J and Sinclair KD (2015) One-carbon metabolism and epigenetic regulation of embryo development. *Reprod Fertil Dev*. 27(4): 667-76
- Xu J, Clare CE, Brassington AH, Sinclair KD and Barrett DA (2020) Comprehensive and quantitative profiling of B vitamins and related compounds in the mammalian liver. *J Chromatogr B Analyt Technol Biomed Life Sci*. 1136: 121884
- Xu W, Li Z, Yu B, He X, Shi J, *et al.* (2013) Effects of DNMT1 and HDAC Inhibitors on Gene-Specific Methylation Reprogramming during Porcine Somatic Cell Nuclear Transfer. *PLoS One*. 8(5): e64705.
- Xu Y, Wu F, Tan L, Kong L, Xiong L, *et al.* (2011) Genome-wide regulation of 5hmC, 5mC, and gene expression by Tet1 hydroxylase in mouse embryonic stem cells. *Mol Cell*. 42(4): 451-64
- Xue GP and Snoswell AM (1985) Comparative studies on the methionine synthesis in sheep and rat tissues. *Comp Biochem Physiol B*. 80(3): 489-94
- Xue GP and Snoswell AM (1986) Developmental changes in the activities of enzymes related to methyl group metabolism in sheep tissues. *Comp Biochem Physiol B*. 83(1): 115-20

- Yajnik CS, Deshpande SS, Jackson AA, Refsum H, Rao S, *et al.* (2008) Vitamin B12 and folate concentrations during pregnancy and insulin resistance in the offspring: the Pune Maternal Nutrition Study. *Diabetologia*. 51(1): 29-38
- Yamada M, Johannesson B, Sago I, Cole Burnett L, Kort DH, *et al.* (2014) Human oocytes reprogram adult somatic nuclei of a type 1 diabetic to diploid pluripotent stem cells. *Nature*. 510(7506): 533-6
- Yamashita T, Hashimoto S, Kaneko S, Nagai S, Toyoda N, *et al.* (2000) Comprehensive gene expression profile of a normal human liver. *Biochem Biophys Res Commun*. 269(1): 110-6
- Yandell CA, Dunbar AJ, Wheldrake JF and Upton Z (1999) The kangaroo cation-independent mannose 6-phosphate receptor binds insulin-like growth factor II with low affinity. *J. Biol. Chem*. 274: 27076–27082
- Yang AN, Zhang HP, Sun Y, Yang XL, Wang N, *et al.* (2015) High-methionine diets accelerate atherosclerosis by HHcy-mediated FABP4 gene demethylation pathway via DNMT1 in ApoE(-/-) mice. *FEBS Lett*. 589(24 Pt B): 3998-4009
- Yang X, Han H, De Carvalho DD, Lay FD, Jones PA, *et al.* (2014) Gene Body Methylation can alter Gene Expression and is a Therapeutic Target in Cancer. *Cancer Cell*. 26(4): 577–590
- Yegnasubramanian S, Wu Z, Haffner MC, Esopi D, Aryee MJ, *et al.* (2011) Chromosome-wide mapping of DNA methylation patterns in normal and malignant prostate cells reveals pervasive methylation of gene-associated and conserved intergenic sequences. *BMC Genomics*. 12: 313
- Yi P, Melnyk S, Pogribna M, Pogribny IP, Hine RJ, *et al.* (2000) Increase in plasma homocysteine associated with parallel increases in plasma S-adenosylhomocysteine and lymphocyte DNA hypomethylation. *J Biol Chem*. 275(38): 29318-23
- Yotova IY, Vlatkovic IM, Pauler FM, Warczok KE, Ambros PF, *et al.* (2008) Identification of the human homolog of the imprinted mouse Air non-coding RNA. *Genomics*. 92(6): 464-73
- Young JW (1977) Gluconeogenesis in cattle: significance and methodology. *J Dairy Sci*. 60(1): 1-15
- Young LE, Fernandes K, McEvoy TG, Butterwith SC, Gutierrez CG, *et al.* (2001) Epigenetic change in IGF2R is associated with fetal overgrowth after sheep embryo culture. *Nat Genet*. 27(2): 153-4
- Young LE, Schnieke AE, McCreath KJ, Wieckowski S, Konfortova G, *et al.* (2003) Conservation of IGF2-H19 and IGF2R Imprinting in Sheep: Effects of Somatic Cell Nuclear Transfer. *Mech Dev*. 120(12): 1433-42
- Young LE, Sinclair KD and Wilmut I (1998) Large offspring syndrome in cattle and sheep. *Rev Reprod*. 3(3): 155-63
- Young MF, Nguyen PH, Gonzalez Casanova I, Addo OY, Tran LM, *et al.* (2018) Role of maternal preconception nutrition on offspring growth and risk of stunting across the first 1000 days in Vietnam: A prospective cohort study. *PLoS One*. 13(8): e0203201
- Yue Y, Liu J and He C (2015) RNA N6-methyladenosine methylation in post-transcriptional gene expression regulation. *Genes Dev*. 29(13): 1343-55
- Zaitoun I and Khatib H (2006) Assessment of genomic imprinting of SLC38A4, NNAT, NAP1L5, and H19 in cattle. *BMC Genet*. (2006)7: 49
- Zeke A, Misheva M, Reményi A and Bogoyevitch MA (2016) JNK Signaling: Regulation and Functions Based on Complex Protein-Protein Partnerships. *Microbiol Mol Biol Rev*. 80(3): 793-83
- Zeng Y and Chen T (2019) DNA Methylation Reprogramming during Mammalian Development. *Genes (Basel)*. 10(4): E257

- Zhang B, Denomme MM, White CR, Leung KY, Lee MB, *et al.* (2015) Both the folate cycle and betaine-homocysteine methyltransferase contribute methyl groups for DNA methylation in mouse blastocysts. *FASEB J.* 29(3): 1069-794
- Zhang D, Wu B, Wang P, Wang Y, Lu P, *et al.* (2017) Non-CpG methylation by DNMT3B facilitates REST binding and gene silencing in developing mouse hearts. *Nucleic Acids Res.* 45(6): 3102-3115
- Zhang J, Shi H, Wang Y, Li S, Cao Z, *et al.* (2017b) Effect of Dietary Forage to Concentrate Ratios on Dynamic Profile Changes and Interactions of Ruminant Microbiota and Metabolites in Holstein Heifers. *Front Microbiol.* 8: 2206
- Zhang J, Wang Y, Liu H, Mao X, Chen Q, *et al.* (2019) Effect of in vitro culture period on birth weight after vitrified-warmed transfer cycles: analysis of 4,201 singleton newborns. *Fertil Steril.* 111(1): 97-104
- Zhang N (2018) Role of methionine on epigenetic modification of DNA methylation and gene expression in animals. *Anim Nutr.* 4(1): 11-16
- Zhang Y, Zhou WE, Yan JQ, Liu M, Zhou Y, *et al.* (2018) A Review of the Extraction and Determination Methods of Thirteen Essential Vitamins to the Human Body: An Update from 2010. *Molecules.* 23(6): E1484
- Zhao H, Xu J, Pang L, Zhang Y, Fan H, *et al.* (2015) Genome-wide DNA methylome reveals the dysfunction of intronic microRNAs in major psychosis. *BMC Med Genomics.* 8: 62
- Zhao H, Zhang S, Wu X, Pan C, Li X, *et al.* (2019) DNA methylation pattern of the goat PITX1 gene and its effects on milk performance. *Arch Anim Breed.* 62(1): 59–68
- Zhao J, Hao Y, Ross JW, Spate LD, Walters EM, *et al.* (2010) Histone Deacetylase Inhibitors Improve In Vitro and In Vivo Developmental Competence of Somatic Cell Nuclear Transfer Porcine Embryos. *Cell Reprogram.* 12(1): 75–83
- Zhao R, Matherly LH and Goldman ID (2009) Membrane transporters and folate homeostasis: intestinal absorption and transport into systemic compartments and tissues. *Expert Rev Mol Med.* 11: e4
- Zhao X-M, Cui L-S, Hao H-S, Wang H-Y, Zhao S-J, *et al.* (2016) Transcriptome analyses of inner cell mass and trophectoderm cells isolated by magnetic-activated cell sorting from bovine blastocysts using single cell RNA-seq. *Reprod Domest Anim.* 51(5): 726-35
- Zhao Y, Hermesz E, Yarolin MC and Westphal H (2000) Genomic structure, chromosomal localization and expression of the human LIM-homeobox gene LHX5. *Gene.* 260(1-2): 95-101
- Zhou Z, Yang Y, Li M, Kou C, Xiao P, *et al.* (2012) New Tween-80 microbiological assay of serum folate levels in humans and animals. *J AOAC Int.* 95(5): 1505-10
- Ziller MJ, Müller F, Liao J, Zhang Y, Gu H, *et al.* (2011) Genomic distribution and inter-sample variation of non-CpG methylation across human cell types. *PLoS Genet.* 7(12): e1002389

Appendices

Appendix Chapter 1

Appendix Table 1.1 One-carbon (1C) metabolism, epigenetic regulator gene variants and developmental outcomes in humans. Adapted from [Clare et al. \(2019\)](#).

1C metabolism gene	Variant	Risk association (↑ increase, ↓ decrease)	Effect of diet (↑ supplementation, ↓ restriction)	Ethnic population (<i>n</i>)	Reference(s)
<i>Methionine synthase</i> MTR	A2756G	↑ Orofacial clefts (OR=2.195)	-	Polish (122 cases, 82 controls)	Mostowska et al. (2006)
		↑ NTDs (OR=1.664), CCGA haplotype ↓ risk	-	Chinese Han (152 cases, 169 controls)	Cao et al. (2018)
<i>Methionine synthase reductase</i> MTRR	A66G	↑ Congenital heart disease (OR=1.35)	-	Mixed ethnicity (914 cases, 964 controls)	Cai et al. (2014)
		↓ Multiple birth defects	-	Chinese North (250 cases, 420 controls)	Zhang et al. (2014)
<i>Methionine adenosyltransferase 1A</i> MAT1A	G791A	↑ Mudd's disease (CNS abnormalities) ↑ Hcy (hyperhomocysteinemia) ↑ Met (hypermethioninemia)	↑ B6 adverse ↓ Met and ↑ SAM inconclusive	American (32 cases, 32 controls)	Chien et al. (2015); Pérez-Mato et al. (2001)
<i>Methionine adenosyltransferase 2A</i> MAT2A	A1031C, G1067A	↑ FTAAD, congenital bicuspid aortic valve defects	-	Family with autosomal dominance of FTAAD (<i>n</i> = 18)	Guo et al. (2015)
<i>Glycine N-methyltransferase</i> GNMT	C1298T	↑ Hcy	↓ Folate ↑ plasma Hcy in <i>TT</i>	Mixed/American (<i>n</i> = 114)	Beagle et al. (2005)
		↑ Prostate cancer (OR=1.62)	-	Mixed ethnicity (661 cases, 656 controls)	Chen et al. (2014)

Appendix Table 1.1 continued

1C metabolism gene	Variant	Risk association (↑ increase, ↓ decrease)	Effect of diet (↑ supplementation, ↓ restriction)	Ethnic population (n)	Reference(s)
<i>S-adenosylhomocysteine hydrolase</i> AHCY	G336A, A428G	↑ Congenital myopathy, delayed development	↓ Met, ↑ creatine, ↑ PC improves condition	AHCY-deficient (n = 1)	Barić et al. (2005)
	C145T, A257G	↑ Infant mortality, congenital myopathy, delayed development, ↑ Hcy, SAM, Met and creatine kinase	-	AHCY-deficient (n = 1)	Vugrek et al. (2009)
<i>Betaine homocysteine S- methyltransferase</i> BHMT	G742A	↑ NTDs	-	Caucasian American families (n = 304)	Boyles et al. (2006)
		↑ Down's syndrome (OR=4.96)	Pre-conceptional folate ↑ risk	Indian (228 cases, 200 controls)	Jaiswal et al. (2017)
<i>Choline dehydrogenase</i> CHDH	G432T	↑ Impaired spermatogenesis	-	Greek (200 oligospermic, 250 controls)	Lazaros et al. (2012)
<i>Methylene-tetrahydrofolate reductase</i> MTHFR	C677T	↓ DNA methylation in TT individuals	-	TT (105 cases), CC (187 controls)	Friso et al. (2002)
		↑ Male infertility (OR=1.39)	-	Mixed ethnicity (5575 cases, 5447 controls)	Gong et al. (2015)
<i>Dihydrofolate reductase</i> DHFR	19-bp del	↓ NTDs (RR=0.59)	-	Irish (283 cases, 256 controls)	Parle-McDermott et al. (2007)
		↑ Pre-term delivery (OR=3.0)	↓ Folate ↑ risk (OR=5.5)	Mixed ethnicity (n=324)	Johnson et al. (2005)

Appendix Table 1.1 continued

1C metabolism gene	Variant	Risk association (↑ increase, ↓ decrease)	Effect of diet (↑ supplementation, ↓ restriction)	Ethnic population (n)	Reference(s)
<i>Serine hydroxymethyltransferase</i> SHMT1	C1420T	↑ NTDs	-	Indian (372 cases, 552 controls)	Prasoona et al. (2017)
<i>Methylene-tetrahydrofolate dehydrogenase</i> MTHFD	G1958A	↑ NTDs ↑ Second trimester pregnancy loss (OR=1.64)	-	Indian (360 cases, 540 controls) Irish (125 cases, 625 controls)	Prasoona et al. (2016) Parle-McDermott et al. (2005)
<i>Thymidylate synthase</i> TYMS	6bp(del/del)	↑ Pre-term delivery, ↓ birth weight, fetal death, ↑ Hcy	-	Indian (209 cases, 194 controls)	Tiwari et al. (2017)
<i>Cystathionine-β-synthase</i> CBS	C699T	↑ Ischemia, late-onset preeclampsia (OR=2.1)	-	Norwegian (99 cases, 99 controls)	Koning et al. (2013)
	T833C	↑ Non-syndromic cleft lip and palate (OR=18.7)	-	Italian (n=134)	Rubini et al. (2005)
	C4673G	↓ Congenital heart disease (OR=0.85)	-	Chinese (2340 cases, 2270 controls)	Zhao et al. (2013)
<i>Cystathionine-γ-lyase</i> CTH	A426G	↑ Preeclampsia (OR=18.03)	-	Caucasian Polish (60 cases, 120 controls)	Mrozikiewicz et al. (2015)
<i>Phosphatidylethanolamine N-methyltransferase</i> PEMT	G774C	↑ Impaired spermatogenesis	-	Greek (200 oligospermic, 250 controls)	Lazaros et al. (2012)

Appendix Table 1.1 continued

1C metabolism gene	Variant	Risk association (↑ increase, ↓ decrease)	Effect of diet (↑ supplementation, ↓ restriction)	Ethnic population (n)	Reference(s)
<i>Phosphatidylethanolamine N-methyltransferase</i> PEMT	G523A	↑ Idiopathic male infertility (OR=7.91)	-	Swedish (153 cases, 184 controls)	Murphy et al. (2011)
		↑ NAFLD	-	Mixed ethnicity (28 cases, 59 controls)	Song et al. (2005)
<i>DNA methyltransferase 1 DNMT1</i>	rs4804490	↑ Male infertility	-	Chinese (833 cases, 410 controls)	Tang et al. (2017)
<i>DNA methyltransferase 3B DNMT3B</i>	G579T	↑ Recurrent spontaneous abortion	-	Slovenian (146 cases, 149 controls)	Barišić et al. (2017)
	<u>R832Q, S828P</u>	↑ ICF syndrome	-	Japanese (n=3)	Shirohzu et al. (2002)
<i>Histone methyltransferase EHMT1</i>	C2426T	↑ Kleefstra syndrome (hypotonia, developmental delay, brachycephaly, CHD, macroglossia and prognathism)	-	Patients (n=2)	Blackburn et al. (2017)
<i>Reduced folate carrier RFC1/SLC19A1</i>	A80G	↑ Autism, DNA hypomethylation in mothers	-	Mixed ethnicity (529 cases, 566 controls)	James et al. (2010)

Appendix Table 1.1 continued

1C metabolism gene	Variant	Risk association (↑ increase, ↓ decrease)	Effect of diet (↑ supplementation, ↓ restriction)	Ethnic population (<i>n</i>)	Reference(s)
<i>Folate receptor alpha</i> <i>FOLRα</i>	1816C/delC, G1841A	↑ Pregnancy loss in heterozygotes	-	Estonian (439 cases, 225 controls)	Laanpere et al. (2011)
<i>Transcobalamin receptor</i> <i>TCbIR/CD320</i>	rs2336573, rs9426	↑ NTDs (RR=6.59, 6.71)	-	Irish (551 cases, 999 controls)	Pangilinan et al. (2010)

Gene variants reported as nucleotide base substitutions; deletions (del), amino acid variant or RefSNP (rs) ID. Abbreviations: CHD, congenital heart defects; CNS, central nervous system; FTAAD, familial thoracic aortic aneurysms and dissections; ICF, immunodeficiency, centromeric instability and facial anomalies; NAFLD, non-alcoholic fatty liver disease; NTDs, neural tube defects; OR, odds ratio; RR, relative risk dissections. One-carbon (1C) substrates: Hcy, homocysteine, SAM, S-adenosylmethionine; Met, methionine; PC, phosphatidylcholine.

Appendix Table 1.2 Epigenetic and developmental consequences of targeted 1C metabolism gene deletions (or inhibition) in animal models.Adapted from [Clare et al. \(2019\)](#).

1C metabolism gene	Function	KO effect	Epigenetic/Developmental consequences	Supplementation effect	Reference(s)
<i>Methionine synthase</i> (<i>Mtr</i>) MTR	B ₁₂ -dependent Hcy re- methylation Demethylation of 5-mTHF to THF	-/+ mice exhibit ~50-60% ↓ enzyme activity and ↑ plasma Hcy -/- embryos die <i>in utero</i> before E9.5	↑ Hcy, ↓ Met and ↑ 5-mTHF, folate trapping perturbs 1C- metabolism and DNA synthesis during early embryogenesis	Folate, methionine, choline, betaine, hypoxanthine, inositol, threonine during pregnancy does not rescue MTR-deficient phenotype	Swanson et al. (2001)
<i>Methionine synthase reductase</i> (<i>Mtrr</i>) MTRR	Reductive reactivation of MTR by methylation of cob(I)alamin cofactor	KO results in embryonic lethality MTRR deficiency adversely impacts reproductive outcomes and cardiac development in mice	↑ Hcy, ↓ Met, ↑ 5-mTHF, folate trapping impairs growth in males, -/- dams have ↑ fetal resorptions, smaller placentae and embryos with myocardial hypoplasia and ventricular septal defects	Periconceptional supplementation with folic acid may reduce risk	Elmore et al. (2007) Deng et al. (2008)
<i>Methionine adenosyltransferase</i> 1A/2A (<i>Mat1a/Mat2a</i>) MAT1A MAT2A	SAM biosynthesis from Met	<i>Mat2a</i> inhibition reduces bovine blastocyst development <i>Mat2a</i> KO causes developmental defects in zebrafish embryos <i>Mat1a</i> KO mice are susceptible to acute liver injury	↓ Cell proliferation and blastocoel formation ↑ Pericardial oedema, malformed eyes, and short tail or no tail development ↑ Met, ↓ SAM, metabolic switch to <i>Mat2a</i> expression associated with rapid liver growth and differentiation	Met substrate alleviated reduction in blastocyst development Choline-deficient diet induced macrovesicular steatosis in mutant mice	Ikeda et al. (2017) Guo et al. (2015) Lu et al. (2001)

Appendix Table 1.2 continued

1C metabolism gene	Function	KO effect	Epigenetic/Developmental consequences	Supplementation effect	Reference(s)
<i>Glycine N-methyltransferase (Gnmt)</i> GNMT	Synthesis of Sar from Gly (using SAM as methyl donor) Regulates methylation via maintenance of SAM:SAH ratio	-/- mice have exhibit aberrant methylation pattern in liver, chronic hepatitis, glycogen storage disease and risk of hepatocellular carcinoma	↑ Met, ↑ SAM, ↑ SAM:SAH ratio causes global DNA hypermethylation , ↓ gluconeogenesis, hypoglycaemia, ↑ serum cholesterol	- - -	Luka et al. (2006) Liu et al. (2007) Liao et al. (2009)
<i>S-adenosylhomocysteine hydrolase (AHCY)</i> AHCY	Reversible hydrolysis of SAH to adenosine and Hcy	<i>Ahcy</i> KO causes embryonic lethality in mice	↑ SAH inhibits DNA methylation reactions, ↓ ICM proliferation and differentiation	-	Miller et al. (1994)
Betaine-homocysteine S-methyltransferase (<i>Bhmt</i>) BHMT	Re-methylation Hcy to Met and DMG using TMG (betaine)	<i>Bhmt</i> KO decreases blastocyst development -/+ mice have reduced body weight and ↑ susceptibility to fatty liver and hepatic carcinoma	↓ 40% in ICM cell number, ↓ OCT4 and NANOG expression ↑ HHcy, ↓ SAM:SAH ratio, ↓ 75% in cellular methylation, ↑ hepatic TMG and DMG, ↓ Chol and PC in several tissues, ↑ hepatic CHDH and GNMT	Blastocyst development and ICM number rescued by Met supplementation	Lee et al. (2012) Teng et al. (2011)


Appendix Table 1.2 continued

1C metabolism gene	Function	KO effect	Epigenetic/Developmental consequences	Supplementation effect	Reference(s)
Choline dehydrogenase (<i>Chdh</i>) CHDH	Oxidation of chol to TMG (betaine)	<i>Chdh</i> KO male mice are infertile	↑ HHcy, ↑ Chol and PC, ↓ testicular TMG, ↓ sperm motility, abnormal mitochondria in liver, heart, kidney and testes	Sperm motility doubled in -/- mice with TMG supplementation	Johnson et al. (2010)
Methylene-tetrahydrofolate reductase (<i>Mthfr</i>) MTHFR	Conversion of 5,10-CH ₂ THF to 5-mTHF (methyl donor for Hcy re-methylation to Met)	-/- mice have severe birth defects and die within 2 weeks post-partum -/- BALB/c mice have abnormal spermatogenesis and infertility	↑ HHcy, ↓ SAM in tissues (except liver), ↑ SAH, DNA hypomethylation in brain and ovaries, developmental retardation, ↓ body weight, short or kinked tail with kyphosis, facial abnormalities	- Post-weaning TMG supplementation improved fertility parameters	Chen et al. (2001) Kelly et al. (2005)
Dihydrofolate reductase (<i>Dhfr</i>) DHFR	Reduction of DHF to THF Reduction of FA to DHF	<i>Dhfr</i> KO impairs embryonic development in zebrafish	↑ Congenital cardiovascular defects ↓ Transcription factors in cardiac development	-	Sun et al. (2011)
Serine hydroxymethyltransferase (<i>Shmt1</i>) SHMT1	Conversion of SER to GLY and THF to 5,10-CH ₂ THF (substrate for thymidylate synthesis)	SHMT-deficiency causes NTDs in mice	Impairs <i>de novo</i> thymidylate biosynthesis by reducing TYMS enzyme concentrations (via <i>Pax3</i> interaction)	Mutant mice exhibit exencephaly in response to maternal folate- and choline-deficient diet	Beaudin et al. (2011)

Appendix Table 1.2 continued

1C metabolism gene	Function	KO effect	Epigenetic/Developmental consequences	Supplementation effect	Reference(s)
Methylene-tetrahydrofolate dehydrogenase (<i>Mthfd1/1L</i>) MTHFD	Production of 10-fTHF and THF used for synthesis of purines (<i>Mthfd1</i> ; mitochondrial formate production)	Loss of <i>MTHFD1 synthetase</i> causes embryo loss by E10.5 in mice, MTHFD1L-deficient mice are growth restricted with NTDs	Abnormal embryo development, ↓ <i>de novo</i> purine synthesis, ↓ cellular proliferation, craniorachischisis, exencephaly and/or a wavy neural tube.	Maternal supplementation with sodium formate partially rescues growth defect phenotype	Momb et al. (2013) Christensen et al. (2013)
Cystathionine-β-synthase (<i>Cbs</i>) CBS	B ₆ -dependent condensation of Hcy and Ser to Cth	CBS-deficient female mice have impaired fertility, homocysteinuria with mild hepatopathy, hypercoagulation, IUGR and die within 5 weeks post-partum	Irregular oestrus cycle, ↓ embryo growth, ↓ placental mass with morphological abnormalities, ↓ viable embryos, ↑ Hcy, ↑ Met, ↑ SAH, ↑ Cth and ↓ Cys, enlarged and multinucleated hepatocytes with microvesicular lipid droplets	Transplantation of CBS-deficient ovaries into normal ovariectomised recipient restores fertility, TMG treatment lowers Hcy and SAH levels, ameliorates hypercoagulation and reduces CTH	Guzmán et al. (2006) Maclean et al. (2010) Watanabe et al. (1995)
Cystathionine-γ-Lyase (<i>Cth</i>) CTH	Catabolism of Cth to Cys, α-KB and NH ₃	CTH-deficient mice have ↓ hydrogen sulphide (H ₂ S) production	↓ vasodilation leading to hypertension Dysregulation of H ₂ S metabolism impairs oviductal transport of embryos, ↑ risk of ectopic pregnancy	- -	Yang et al. (2008) Ning et al. (2014)

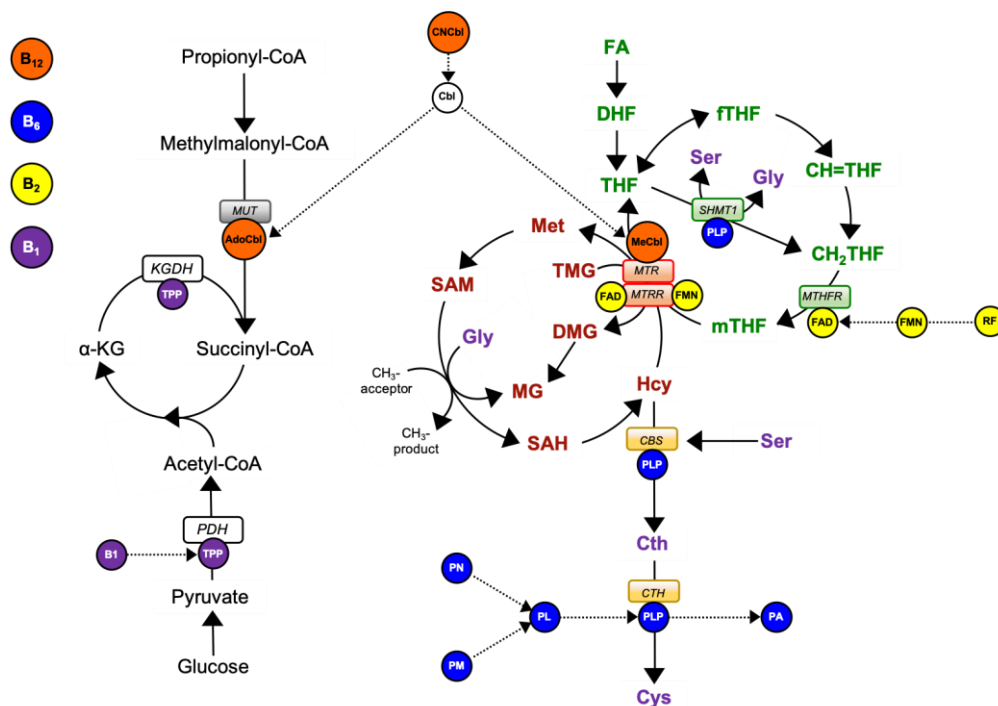
Appendix Table 1.2 continued

1C metabolism gene	Function	KO effect	Epigenetic/Developmental consequences	Supplementation effect	Reference(s)
Phosphatidylethanolamine <i>N</i> -methyltransferase (<i>Pemt</i>) 	<i>De novo</i> synthesis of chol Conversion of PE to PC in liver	-/- mice die when deprived of chol, ↑ progenitor cell mitosis in brain of -/- mice at E17	↑ SAM, ↑ Hypermethylation of proteins and DNA , ↓ DHA (C22:6; n-6) and AA (C24:4; n-3) PUFAs in membrane phospholipids, ↑ hepatic steatosis, ↑ Histone H3 phosphorylation	Chol supplementation rescues some but not all KO phenotypes	Walkey et al. (1997) Watkins et al. (2003) Zhu et al. (2003) Zhu et al. (2004)
DNA methyltransferase 1 (<i>Dnmt1</i>)	Maintenance of DNA methylation in mammalian cells	<i>Dnmt1</i> KO causes embryonic lethality in mice	↓ Reduction in 5mC, ↓ cell proliferation, ↓ embryo growth and delayed development	-	Li et al. (1992)
DNA methyltransferase 3 (<i>Dnmt3a/Dnmt3b/Dnmt3L</i>)	<i>De novo</i> methylation of DNA during mammalian development	<i>Dnmt3a/3b</i> deletion causes embryonic lethality in mice <i>Dnmt3L</i> -/- male mice infertile, +/- females die mid-gestation	<i>De novo</i> methylation blocked, DNMT3B KO causes hypomethylation of pericentromeric repeats . <i>Dnmt3L</i> -/- males lack germ cells, +/- females have abnormal imprinted genes	- -	Okano et al. (1999) Bourc'his et al. (2001)
Arginine N-methyltransferase (<i>Prmt</i>)	Methylation of arginine residues in proteins, e.g. histones	<i>Prmt</i> KO causes post-natal lethality in mice due to impaired CNS development, -/- mutant embryos fail to develop beyond E6.5	Post-natal growth retardation, reduced nuclei in white matter tracts, hypomyelination and hypomethylation of histone proteins	- -	Hashimoto et al. (2016) Pawlak et al. (2000)

Appendix Table 1.2 continued

1C metabolism gene	Function	KO effect	Epigenetic/Developmental consequences	Supplementation effect	Reference(s)
Reduced folate carrier (<i>Rfc1/Slc19a1</i>)	Carrier-mediated internalisation of major blood folates (e.g. 5-mTHF) into mammalian cells	RFC null embryos <i>in utero</i> before E9.5; 10% of <i>-/-</i> dams supplemented with FA gave birth to live pups but pups died within 12 days	Impaired development of hematopoietic organs; absent erythropoiesis in bone marrow and spleen; ↓ liver lymphoid in splenic white pulp and thymus; impaired renal and seminiferous tubule development	Near normal development sustained in <i>-/-</i> embryos at E18.5 when dams are supplemented with 1 mg FA daily	Zhao et al. (2001)
Folate binding protein 1/2, Folate receptor alpha (<i>Folbp1/2, Folr1</i>)	High affinity internalisation and delivery of folate into cell cytoplasm by <i>Folbp1</i> ; <i>Folbp2</i> binds folate poorly	<i>Folbp1 -/-</i> embryos die <i>in utero</i> by E10; <i>Folbp2 -/-</i> embryos develop normally	↓ Plasma folate, delayed embryonic development, ↓ number of somites, failed neural tube closure at E9.5, ↑ risk of NTDs, craniofacial anomalies, abdominal wall defects and congenital heart defects	Supplementation of <i>Folbp1</i> -deficient dams with folinic acid (5-fTHF) and 5-mTHF rescues most embryos from premature death in dose-dependent manner, irrespective of folate form	Piedrahita et al. (1999) Spiegelstein et al. (2004) Zhu et al. (2007)
Transcobalamin receptor (<i>TCblR, CD320</i>)	Cellular uptake of transcobalamin-bound Cbl (B12)	<i>-/-</i> mice develop normally but exhibit depleted Cbl in CNS and neuropathologic changes	↑ Hcy, ↑ MMA, ↓ SAM:SAH ratio, global DNA hypomethylation in brain, normal accumulation of Cbl in liver and kidney suggests separate Cbl uptake mechanisms exist in these tissues (i.e. Megalin)	- -	Lai et al. (2013) Arora et al. (2017)













Appendix Chapter 2



Appendix Figure 2.1 B vitamins, folates and 1C-related amines in one-carbon (1C) metabolism and propionate metabolism. Adapted from [Xu et al. \(2020\)](#).

Abbreviation(s): Folate cycle enzymes (green boxes): MTHFR, 5,10-methylenetetrahydrofolate reductase; SHMT1, serine hydroxymethyltransferase. Methionine cycle enzymes (red boxes): MTR, methionine synthase; MTRR, methionine synthase reductase. Transsulfuration pathway enzymes (yellow boxes): CBS, cystathionine β-synthase; CTH, cystathionine γ-lyase. Propionate pathway enzyme (grey box): MUT, methylmalonyl-CoA mutase. Tricarboxylic acid cycle enzymes (white boxes): KGDH, α-ketoglutarate dehydrogenase; PDH, pyruvate dehydrogenase. Vitamin B1 cofactors (purple circles): B1, thiamine; TPP, thiamine pyrophosphate. Vitamin B2 cofactors (yellow circles): RF, riboflavin; FMN, flavin mononucleotide; FAD, flavin adenine dinucleotide. Vitamin B6 cofactors (blue circles): PN, pyridoxine; PM, pyridoxamine; PL, pyridoxal; PLP, pyridoxal 5'-phosphate; PA, 4-pyridoxic acid. Vitamin B12 cofactors (orange circles): CNCbl, cyanocobalamin; MeCbl, methylcobalamin; AdoCbl, adenosylcobalamin. White circle: Cbl, cobalamin. Substrates: Cys, cysteine; CH=THF, 5,10-methenyltetrahydrofolate; CH₂THF, 5,10-methylenetetrahydrofolate; Cth, cystathionine; DHF, dihydrofolate; DMG, dimethylglycine; FA, folic acid; fTHF, 10-formyltetrahydrofolate; Gly, glycine; Hcy, homocysteine; Met, methionine; MG, methylglycine; mTHF, 5-methyltetrahydrofolate; SAH, S-adenosylhomocysteine; SAM, S-adenosylmethionine; Ser, serine; THF, tetrahydrofolate; TMG, trimethylglycine; α-KG, α-ketoglutarate. Solid arrows demonstrate flux through metabolic pathways. Dotted arrows demonstrate interconversion and interaction of B vitamin species with metabolic pathways.

Appendix Table 2.1 Function of B vitamin cofactors involved in 1C metabolism and related pathways.

	Cyanocobalamin (B12) Synthetic form of vitamin B ₁₂ that is biologically inert but converted to bioactive cofactors; AdoCbl and MeCbl (Farquharson and Adams, 1976; Martinelli <i>et al.</i> , 2011)		Pyridoxine (B6) Alcohol form of vitamin B ₆ that is commonly found in food and dietary that is readily converted to bioactive forms (Albersen <i>et al.</i> , 2013)
	Adenosylcobalamin (B12) Cofactor for mitochondrial MUT enzyme that catalyses isomerisation of methylmalonyl-CoA to succinyl-CoA in propionate metabolism (Shane, 2008)		Pyridoxamine (B6) Amine form of vitamin B ₆ that is readily transformed to PL (Sakurai <i>et al.</i> , 1992)
	Methylcobalamin (B12) Cofactor for MTR enzyme that catalyses remethylation of Hcy to Met in methionine cycle (Shane, 2008)		Pyridoxal (B6) Aldehyde form of vitamin B ₆ that is phosphorylated to form the bioactive cofactor, PLP (Albersen <i>et al.</i> , 2013)
	Riboflavin (B2) Dietary form of vitamin B ₂ that serves as a precursor for formation of bioactive forms. RF is phosphorylated to FMN (Powers, 2003)		Pyridoxal 5'-phosphate (B6) Cofactor for SHMT enzyme that catalyses simultaneous conversion of Ser to Gly, and THF to CH ₂ THF in the folate cycle (Appaji Rao <i>et al.</i> , 2003) Cofactor for CBS and CTH enzymes that catalyse the conversion of Hcy first to Cth and then to Cys in the transsulphuration pathway (Perry <i>et al.</i> , 2007)
	Flavin mononucleotide (B2) Cofactor for MTRR enzyme that restores MTR activity for remethylation of Hcy to Met in methionine cycle (García-Minguillán <i>et al.</i> , 2014)		Thiamine (B1) Form of vitamin B ₁ that is rapidly phosphorylated to bioactive form, TPP (de Jong <i>et al.</i> , 2004)
	Flavin adenine dinucleotide (B2) Cofactor for MTHFR enzyme that catalyses conversion of CH ₂ THF to 5-methyltetrahydrofolate 5-mTHF in the folate cycle Cofactor for MTRR enzyme that restores MTR activity for remethylation of Hcy to Met in methionine cycle (García-Minguillán <i>et al.</i> , 2014)		Thiamine pyrophosphate (B1) Cofactor for enzymes involved in oxidative phosphorylation; PDH catalyses the decarboxylation of pyruvate to acetyl-CoA and KGDH catalyses the conversion of α-KG to succinyl-CoA in the TCA cycle (Lonsdale, 2015; McLain <i>et al.</i> , 2011)

Appendix 2.1 Sheep blood plasma trace-element analysis by ICP-MS

Inductively coupled plasma mass spectrometry (ICP-MS) was used to measure trace-elements, primarily cobalt (Co), in sheep blood samples. No sample preparation step was required. Multi-element analysis was undertaken (Thermo-Fisher iCAP-Q) with a 'Flatpole collision cell' charged with 7% H₂ in He gas) upstream of the analytical quadrupole to reduce polyatomic interferences. Samples and calibration standards were diluted (0.5 mL into 20 mL) in a diluent containing 0.1% ionic surfactant containing Triton X-100 and anti-foam-B (Sigma Aldrich), plus 2% methanol (MeOH) and 1% nitric acid (HNO₃; Trace analysis grade, Fisher Scientific, 1 mL/min). Internal standards were scandium (Sc; 50 µg/L), germanium (Ge; 20 µg/L), rhodium (Rh; 10 µg/L) and iridium (Ir; 5 µg/L). Samples were introduced via a covered autosampler (Cetac ASX-520) through a concentric glass venturi nebuliser (Thermo-Fisher Scientific; 1 mL/min). Calibration standards ranged from 0 to 100 µg/L. Sample processing was conducted using Qtegra software (Thermo-Fisher Scientific).

Appendix 2.2 Sheep liver amino acid analysis by HPLC

Primary amino acids were quantified in sheep liver by high performance liquid chromatography (HPLC) with online derivitisation, based on the method of [Henderson *et al.* \(2000\)](#) with the following modifications. Briefly, 150 mg frozen liver were extracted with 150 µL 80% MeOH by homogenisation for 2 min. After centrifugation for 15 min at 14,500 xg, 120 µL supernatant and 3 µL internal standard, norvaline (NVA, 40 mmol/L), was transferred to a 2.5 mL screw-capped glass autosampler vial for HPLC analysis.

The method used an Agilent 1100 HPLC equipped with a binary solvent delivery system and gradient controller. Chromatographic separation was performed on a ZORBAX Eclipse-AAA column (4.6 x 150 mm, 3.5 µm) protected by a guard column and maintained at 40°C. The flow rate was set at 1.75 mL/min. The injection program was as follows:

1. Draw 2.5 µL from vial 1 (borate buffer, 0.5 M, pH 8.0)
2. Draw 0.5 µL from sample
3. Mix 3 µL "in air", max speed, 2x
4. Wait 0.5 min

5. Draw 0 μL from vial 2 (needle wash using water in uncapped vial)
6. Draw 0.5 μL from vial 3 (10 mg/mL OPA + 20 mg/mL MPA, in ACN)
7. Mix 3.5 μL "in air", max speed, 6x
8. Draw 0 μL from vial 2 (needle wash using water in uncapped vial)
9. Draw 0.5 μL from vial 4 (ACN)
10. Mix 4 μL "in air", max speed, 6x
11. Draw 0 μL from vial 6 (needle wash using ACN in uncapped vial)
12. Draw 16 μL from vial 5 (water)
13. Mix 10 μL "in air", max speed, 2x
14. Inject 10 μL of sample

Mobile phases were composed of Na_2HPO_4 (40 mmol/L, pH 7.8) for eluent A and ACN: MeOH: water (45:45:10, w/w/w) for eluent B. The total run time was 30 min. Gradient elution was carried out by the following program:

Mobile phase gradients for analysis of liver amino acids.

Time (min)	Eluent A (%)	Eluent B (%)
0	100	0
2	100	0
24	56	44
25	0	100
26	0	100
27	100	0
30	100	0

A fluorometer was used to monitor the elution of amino acids from the column (excitation wavelength=340 nm, emission wavelength=450 nm). Limits of quantification (LOQ) and inter-assay CV% was determined for all amino acids measured.

Limits of quantification and inter-assay CV% for amino acids.

Amino Acid	LOQ (nmol/g)	CV (%)
Aspartate (Asp)	31.3	14.7
Glutamate (Glu)	1250	3.9
Asparagine (Asn)	31.3	2.5
Serine (Ser)	31.3	5.5
Glutamine (Gln)	15.6	5.1
Histidine (His)	15.6	5.1
Glycine (Gly)	1250	6.1
Threonine (Thr)	15.6	5.7
Citrulline (Cit)	31.25	1.9
Tyrosine (Tyr)	15.6	4.8
Cystine (Cys)	62.5	18.8
Valine (Val)	15.6	6.6
Methionine (Met)	15.6	7.2
Tryptophan (Trp)	15.6	6.7
Phenylalanine (Phe)	15.6	4.7
Isoleucine (Ile)	31.3	2.7
Leucine (Leu)	31.3	2.1
Lysine (Lys)	31.3	3.2

Methionine coloured in red and relevant 1C-related amino acids coloured in purple.

Appendix 2.3 Sheep liver polyamine analysis by HPLC

Primary polyamines; putrescine (Put), spermidine (Spd) and spermidine (Spm), were quantified in sheep liver by HPLC based on the methods of [Sabri *et al.* \(1989\)](#) and [Magnes *et al.* \(2014\)](#). Briefly, 50 mg frozen liver were extracted with 500 μ L cold distilled water and 40 μ L perchloric acid (4M) by homogenisation for 2 min. After cooling on ice for 10 min, the homogenate was centrifuged for 15 min at 14,500 xg and 400 μ L supernatant was transferred to an Eppendorf tube. The pH of the supernatant was adjusted to 9.0 by the addition of 28 μ L potassium hydroxide (KOH, 4M). The sample was vortexed for 30 s and centrifuged for 10 min at 14,500 xg before 20 μ L were transferred to a new Eppendorf tube for derivatisation.

Twelve microliters of borate buffer (0.2 M) and 4 μ L 1,6-diaminohexane (DAH, 100 μ mol/L) were added to the 20 μ L sample. After brief vortexing, 40 μ L 9-fluorenylmethyl chloroformate (FMOC, 0.01 M in acetone) was added. The sample was vortexed for 1 min and left for 10 min at room temperature to allow derivitisation to proceed. After the addition of 48 μ L glycine reagent (0.04 M glycine in 0.2 M sodium borate, pH 9.0), the sample was vortexed for 30 s and left at room temperature for a further 2 min. Finally, 40 μ L dilution buffer (0.015 M NaOAc in ACN) was added, vortexed for 10 s and 100 μ L were transferred to a glass autosampler vial containing 400 μ L dilution buffer for HPLC analysis.

Using the Agilent 1100 HPLC (Appendix 2.2), 10 μ L sample was injected onto the Zorbax C18 HPLC column (250 x 4.6 mm, 5 μ m) protected by a guard column and maintained at 40°C. The flow rate was set at 1.2 mL/min. Mobile phases were composed of Na₂HPO₄ (40 mmol/L, pH 7.8) for eluent A and ACN: MeOH: water (45:45:10, w/w/w) for eluent B. The total run time was 30 min. Gradient elution was carried out by the following program:

Mobile phase gradients for analysis of liver polyamines.

Time (min)	Eluent A (%)	Eluent B (%)
0	50	50
5	50	50
28	0	100
28.5	0	100
29	50	50
30	50	50

A fluorometer was used to monitor the elution of polyamines from the column (excitation wavelength = 264, emission wavelength = 310). The LOD was 0.625

nmol/g for all three polyamines and the CV% was 2.08, 3.09 and 3.24 for Put, Spd and Spm QC samples, respectively.

Appendix 2.4 Liver propionate metabolites by GC-MS

Methylmalonic acid (MMA) and succinic acid (SA) concentrations were quantified in sheep liver by gas chromatography-mass spectrometry (GC-MS) based on the method of [Kanakkaparambail *et al.* \(2009\)](#) with the following modifications. Briefly, 50 mg frozen liver were extracted with 250 μ L 80% MeOH by homogenisation for 2 min. Samples were cooled on ice for 10 min. After centrifugation for 15 min at 14,500 xg, 200 μ L supernatant and 4 μ L internal standard (1 mmol/L 4-chlorobutyric acid in 1 mmol/L HCl) were transferred to a 2.5 mL screw-capped glass autosampler vial. To this, 250 μ L 12% boron trifluoride-methanol (BF₃-MeOH) were added and the sample was vortexed for 1 min and heated for 15 min at 95°C in a heating block. After cooling, 250 μ L distilled water and 250 μ L dichloromethane (CH₂Cl₂) were added to the vial, vortexed for 30 s and centrifuged for 10 min at 14,500 xg to separate the layers. The lower CH₂Cl₂ layer was transferred to a screw capped glass auto-sampler vial with insert for GC-MS analysis. The GC-MS method used was identical to the method described in Section 2.2.1.3.3. The LOD was 0.75 nmol/g for both MMA and SA and CV% was 8.37 and 10.98 for MMA and SA, respectively.

Propionic acid (PPA) concentrations were quantified by GC-MS based on the method of [Pouteau *et al.* \(2001\)](#). Briefly, 150 mg frozen liver were extracted with 750 μ L 5-sulfosalicylic acid (SSA, 0.04 mg/mL) by homogenisation for 2 min. Samples were cooled on ice for 2 min. After centrifugation for 15 min at 14,500 xg, 200 μ L supernatant was added to 20 μ L internal standard, 2-methylbutyric acid (MBA, 400 μ mol/L), 3.5 μ L HCl (37%) and 1 mL diethylether. The sample mixture was vortexed for 2 min and centrifuged for 10 min at 14,500 xg to separate the layers. From the upper layer, 600 μ L were transferred to a screw capped glass vial containing 3.5 μ L 1-(tert-butyldimethylsilyl)imidazole (TBDMS, 97%). The sample was vortexed for 2 min and heated for 30 min at 60°C. After cooling, the sample was analysed by GC-MS.

The GC-MS method used a DB-5MS column (J&W Scientific Agilent technology, 30 m x 0.25 mm; 0.25 μ m film thickness). The injection volume was 5 μ L for SCAN and SIM mode, both using splitless mode. The injection port and MS selective detector interference temperatures were 260°C and 250°C,

respectively. The carrier gas (He) was set at a constant flow rate of 1.3 mL/min. The chromatographic conditions were 40°C for 1 min, 70°C min⁻¹ until 60°C, 15°C min⁻¹ until 110°C, and a final increase of 70°C min⁻¹ until 250°C. The MS operated in electron impact ionisation mode with the ionisation energy of 70 eV. SCAN mode measured at m/z: 30-300. SIM ions were set at 131 for PPA and 159 for MBA. Liver PPA concentrations were quantified by the method of standard addition using a calibration range from 19.5 nmol/g to 5 µmol/g and plotting the ratio of peak area of analyte (PPA) to that of the internal standard (MBA). The LOD was 19.5 nmol/g and the CV% was 10.4, 6.3 and 6.5 for low, medium and high QCs, respectively. The inter-assay CV% was 4.7%.

Appendix Table 2.2 Total concentration ranges of 1C metabolites and related compounds in animal tissues.

	Concentration			Reference(s)
	Liver (pmol/g)	Muscle (pmol/g)	Blood (pmol/L)	
Vitamin B₁₂				
Sheep (total)	569-766 *79-3027 **64-734	0.6-7.0	164-2,757	Indyk <i>et al.</i> (2002); Ortigues-Marty <i>et al.</i> (2005); Sinclair <i>et al.</i> (2007); Mitchell <i>et al.</i> (2007); Williams <i>et al.</i> (2007); Hassan <i>et al.</i> (2012)
Cow	342-1,266	3-8	70-102	Ortigues-Marty <i>et al.</i> (2005); Williams <i>et al.</i> (2007); Hassan <i>et al.</i> (2012)
Deer	428-1,024	20-21	-	Tremain-Boon <i>et al.</i> (2002); Hassan <i>et al.</i> (2012)
Pig	149-183	3-4	50-127	Matte <i>et al.</i> (2010); Hassan <i>et al.</i> (2012); Guay <i>et al.</i> (2002)
Rat	50-100	-	3,000-7,180	Fukuwatari <i>et al.</i> (2008); Shibata <i>et al.</i> (2013)
Chicken	132-133	2-3	-	Hassan <i>et al.</i> (2012)
Vitamin B₉ (Folates)				
Sheep (total)	5,000-28,076 *10,355-211,847 **186,25-118,290	44	4,300-6,900	Smith and Osborne-White (1973); Kleppa and Stuen (2003); Williams (2007)
Cow	6312	22-261	24,000-6,1000	Williams (2007); Graulet <i>et al.</i> (2007); Müller (1993)
Deer	-	-	-	-
Pig	2,300,000	22-261	30,000-52,000	Müller (1993); Stangl <i>et al.</i> (2000); Halsted <i>et al.</i> (2002)
Rat	243,000-277,000	79,000-86,000	71,000-136,000	Crivello <i>et al.</i> (2010)
Chicken	10,720,000	101,000	54,300,000	Müller (1993); McCann <i>et al.</i> (1994)
Vitamin B₆				
Sheep (free forms)	28,937 *181-5,228 **175-1,250	5,371-43,678	-	Williams <i>et al.</i> (2007); Hassan <i>et al.</i> (2012)
Cow	40,402	8,190-28,390	-	Williams <i>et al.</i> (2007); Hassan <i>et al.</i> (2012)
Deer	28,937	10,374	-	Hassan <i>et al.</i> (2012)
Pig	34,942	12,558	-	Hassan <i>et al.</i> (2012)
Rat	20,000-48,900	-	1.0-2.1	Fukuwatari <i>et al.</i> (2008); Shibata <i>et al.</i> (2013)
Chicken	43,668	20,747	-	Hassan <i>et al.</i> (2012)
Vitamin B₂	(nmol/g)	(nmol/g)	(pmol/L)	
Sheep (Riboflavin)	74-93 *5-97 **0.1-1.1	4-7	-	Fukuwatari <i>et al.</i> (2008); Shibata <i>et al.</i> (2013); Williams <i>et al.</i> (2007); Hassan <i>et al.</i> (2012)
Cow	74-128	3-6	-	Williams <i>et al.</i> (2007); Hassan <i>et al.</i> (2012)
Deer	69-70	6-7	-	Hassan <i>et al.</i> (2012)
Pig	75-76	3-4	-	Hassan <i>et al.</i> (2012)
Rat	70-100	-	0.169	Fukuwatari <i>et al.</i> (2008); Shibata <i>et al.</i> (2013)
Chicken	90-91	4-5	-	Hassan <i>et al.</i> (2012)
Vitamin B₁				
Sheep (Thiamine)	9-15 *0.3-12.5 **0.09-1.71	3-6	-	Williams <i>et al.</i> (2007); Hassan <i>et al.</i> (2012)
Cow	8-12	1-4	-	Williams <i>et al.</i> (2007); Hassan <i>et al.</i> (2012)
Deer	12-13	3-4	-	Hassan <i>et al.</i> (2012)
Pig	16-17	15-16	-	Hassan <i>et al.</i> (2012)
Rat	30-40	-	0.3-0.4	Hassan <i>et al.</i> (2012)
Chicken	23-24	5-6	-	Hassan <i>et al.</i> (2012)

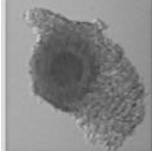
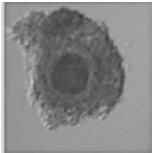
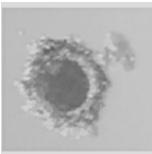
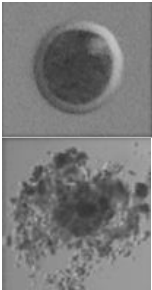
Total concentration range (per g of tissue wet weight) reported in present study in red.
*Abattoir derived (Ab) sheep liver; ** methyl deficient (MD) sheep liver.

Appendix Chapter 3

Appendix Table 3.2 A summary of betaine homocysteine S-methyltransferase (BHMT) enzyme isoforms and their methyl donor substrates.

Isoform	Betaine-homocysteine S-methyltransferase (BHMT; EC 2.1.1.5)	Betaine-homocysteine S-methyltransferase 2 (BHMT2; EC 2.1.1.10)
Reaction	Uses betaine/trimethylglycine (TMG) as methyl donor substrate to remethylate Hcy to methionine, generating dimethylglycine (DMG) by-product (Ganu <i>et al.</i> , 2015).	Uses S-methylmethionine (SMM) as a methyl donor substrate to remethylate Hcy to generate two molecules of methionine (Mládková <i>et al.</i> , 2012).
Inhibition	Dimethylglycine (DMG) is a strong inhibitor (Szegedi <i>et al.</i> , 2008).	SAM is a weak inhibitor; methionine is a stronger inhibitor of BHMT2 than BHMT (Szegedi <i>et al.</i> , 2008).
Species	Sea urchins, amphibians, reptiles, birds and mammals (Ganu <i>et al.</i> , 2015).	Mammals (all monotreme, marsupial and placental species examined; Ganu <i>et al.</i> , 2015).
Gene	Human <i>BHMT</i> gene maps to chromosome 5q13.1-5q15, spans ~20 kb, consists of 8 exons and 7 introns (Li <i>et al.</i> , 2008).	<i>BHMT2</i> gene is adjacently located on chromosome 5 ~22.3 kb upstream of <i>BHMT</i> due to tandem gene duplication event (Li <i>et al.</i> , 2008)
Homology	73-78% amino acid sequence homology (Li <i>et al.</i> , 2008; Ganu <i>et al.</i> , 2011). Crystal structures reveal mammalian BHMT proteins are highly conserved, e.g. Human and porcine BHMT are 84% identical at nucleotide level and 94% identical at amino acid level (Pajares and Pérez-Sala, 2006).	Monomeric protein comprising 373 amino acids (40 kDa; Li <i>et al.</i> , 2008; Szegedi <i>et al.</i> , 2008). Lacks 34 amino acids that encode the <i>oligomerisation domain</i> , therefore, BHMT2 does not oligomerise. Both isoforms may oligomerise into a tetramer of BHMT-BHMT2 dimers (Ganu <i>et al.</i> , 2015). Heterodimerisation may partially stabilise BHMT2, thereby preserving its activity and preventing its rapid degradation following expression (Mládková <i>et al.</i> , 2012; Szegedi <i>et al.</i> , 2008).
Protein Structure	406-7 amino acids (45 kDa; Chadwick <i>et al.</i> , 2000; Szegedi <i>et al.</i> , 2008). Forms a dimer of dimers (tetramer of monomer units; Ganu <i>et al.</i> , 2015). Zn ²⁺ atom linked to 3 essential Cys residues (217, 299, 300). First 318 residues of ORF encode a (β/α) ₈ barrel that contains Cys residues of catalytic site and Gln159 invariant residue for Hcy binding (Ganu <i>et al.</i> , 2013). Residues 319-406/7 encode <i>oligomerisation domain</i> of C-terminus including dimerization arm, hook, flexible linker and C terminal α-helix (Ganu <i>et al.</i> , 2015).	<i>BHMT2</i> mRNA tissue distribution patterns thought to reflect those of BHMT (Ganu <i>et al.</i> , 2015; Chadwick <i>et al.</i> , 2000). Less information on tissue specific BHMT2 activity. Determining whether BHMT2 is expressed in compensation for lack of BHMT, particularly in reproductive tissues, is critical to enhance current understanding of how 1C/Met metabolism behaves in these cell types. <i>BHMT2</i> expression has been reported in human oocyte (Benkhalifa <i>et al.</i> , 2008; Benkhalifa <i>et al.</i> , 2010). Low expression of <i>BHMT</i> isoforms in tissues other than liver and kidney could be due to CpG island methylation of their promoter region (Ganu <i>et al.</i> , 2011).
Tissue distribution	High abundance in liver and kidney, pancreas (Ganu <i>et al.</i> , 2015; Pajares and Pérez-Sala, 2006), eye lens, cochlea, brain, skeletal and cardiac muscle (Pérez-Miguelsanz <i>et al.</i> , 2017). <i>BHMT</i> expression in mouse oocyte promotes ICM development and DNA methylation (Anas <i>et al.</i> , 2008; Lee <i>et al.</i> , 2012; Zhang <i>et al.</i> , 2015). <i>BHMT</i> expressed in human ESCs (Steele <i>et al.</i> , 2005). Contradictory findings report detection of <i>BHMT</i> mRNA in bovine embryos of all developmental stages, except for 8-cell stage (Ikeda <i>et al.</i> , 2010), and complete absence of transcript in bovine ovary, oocyte and embryo (Kwong <i>et al.</i> , 2010). Conventionally understood to be cytoplasmic but nuclear subcellular distribution of BHMT has been recently discovered (Pérez-Miguelsanz <i>et al.</i> , 2017).	<i>BHMT2</i> mRNA tissue distribution patterns thought to reflect those of BHMT (Ganu <i>et al.</i> , 2015; Chadwick <i>et al.</i> , 2000). Less information on tissue specific BHMT2 activity. Determining whether BHMT2 is expressed in compensation for lack of BHMT, particularly in reproductive tissues, is critical to enhance current understanding of how 1C/Met metabolism behaves in these cell types. <i>BHMT2</i> expression has been reported in human oocyte (Benkhalifa <i>et al.</i> , 2008; Benkhalifa <i>et al.</i> , 2010). Low expression of <i>BHMT</i> isoforms in tissues other than liver and kidney could be due to CpG island methylation of their promoter region (Ganu <i>et al.</i> , 2011).
Other function(s)	BHMT as a 'moonlighting protein': 1) osmotic support/maintains tonicity via betaine concentrations (Ganu <i>et al.</i> , 2013); 2) structural protein; 3) Scaffold for enzyme function (Pérez-Miguelsanz <i>et al.</i> , 2017); 4) Eye lens as ψ-crystallin (Vansantha <i>et al.</i> , 1998).	BHMT2 as a 'moonlighting protein': 1) osmotic support/maintains tonicity via betaine concentrations (Ganu <i>et al.</i> , 2013); 2) structural protein; 3) Scaffold for enzyme function (Pérez-Miguelsanz <i>et al.</i> , 2017); 4) Eye lens as ψ-crystallin (Vansantha <i>et al.</i> , 1998).
Substrate	Betaine (N,N,N-trimethylglycine/TMG)	S-methylmethionine (SMM), S-methylmethionine Sulphonium Chloride, 'Vitamin U'
Source	Wheat, germ/bran, spinach, shellfish, sugarbeet. Mitochondrial oxidation of choline (Hogeveen <i>et al.</i> , 2013).	Yeast and criciferous plants (Ganu <i>et al.</i> , 2015). Cannot be synthesised by mammals as they lack methyltransferase (MMT) enzyme (Bourgis <i>et al.</i> , 1999; Kovatscheva and Popova, 1977) but is bioavailable in the animal diets (Augspurger <i>et al.</i> , 2005).
Specificity	BHMT can use SMM in vitro at low affinity Km/Kcat 5-fold lower than that for betaine (Szegedi <i>et al.</i> , 2008).	BHMT2 cannot use TMG/betaine (lacks 9 amino acids within N-terminus that confer specificity to BHMT; Ganu <i>et al.</i> , 2015).
Kinetics	Porcine liver BHMT Km for betaine = 0.023 mmol/L (Garrow, 2006).	Km for SMM = 0.94 mmol/L and similar turnover (K _{cat}) value to BHMT (Szegedi <i>et al.</i> , 2008).
Function	Osmolyte (Burg and Ferraris, 2008)	SMM is a precursor of the osmolyte, dimethylsulfoniopropionate (Rouillon <i>et al.</i> , 1999).

Appendix 3.1 Bovine COC grade and morphological description

Cumulus oocyte complex (COC) grade		Morphological description Adapted from source: Goodhand <i>et al.</i> (1999)	
1	Excellent/Good		>4 layers of compact, light or transparent cumulus with a clear, even cytoplasm.
2	Fair		Less compact, <4 layers cumulus and/or cytoplasm generally homogenous but with coarser appearance.
3	Poor		<4 layers cumulus and/or cytoplasm of irregular appearance with dark areas.
4	Denuded/ Degenerate		Completely denuded or strongly expanded degenerate cumulus with dark spots.

Appendix 3.2 *In vitro* embryo production (IVP) mediaStock components for *in vitro* bovine embryo production media

All stock components dissolved in tissue grade culture (TCG) water, sterile filtered and stored at 4°C or -20°C.

Component	MWt.	Mass (g)	Volume (mL)	Conc.	Storage
CaCl ₂	147.02	0.58808	20	200 mM	4°C
KCl	74.55	0.5964	50	160 mM	4°C
MgCl ₂ .6H ₂ O	203.30	1.10165	50	100 mM	4°C
NaCl	58.44	6.72	50	2.3 M	4°C
NaHCO ₃	84.01	2.1	100	250 mM	4°C
NaH ₂ PO ₄ .H ₂ O	137.98	0.2346	50	34 mM	4°C
Na lactate	-	-	-	60% syrup	4°C
HEPES	249.30	12.465	50	1 M	4°C
Na pyruvate	110.00	0.044	20	20 mM	-20°C
L-Glutamine	146.15	0.14615	10	100 mM	-20°C
KH ₂ PO ₄	136.09	1.3609	50	200 mM	4°C
MgSO ₄ .7H ₂ O	246.47	2.4647	50	200 mM	4°C
D(+)-Glucose	180.20	0.3604	10	200 mM	4°C
Na ₂ EDTA.2H ₂ O	372.24	0.372	10	100 mM	4°C
Trisodium citrate	294.10	2.95	50	200 mM	4°C
Myoinositol	180.16	2.5	50	278 mM	4°C
Heparin	-	0.05	5	10 mg/mL	-20°C
Hypotaurine+ Epinephrine	-	0.005	10	0.5 mg/mL	-20°C
Caffeine	194.19	0.485	50	50 mM	4°C

Search and collection medium (50 mL working solution)

47.5 mL TCM199 (HEPES), 2.5 mL FCS (5% v/v), 200 µL glutamine (100 mM), 500 µL penicillin/streptomycin. pH 7.3-7.4. Osmolarity: 290-300 mOsm. Filtered and stored at 4°C for up to 1 week. Warmed to 37°C 1 h before use.

Maturation medium (10 mL working solution)

9 mL TCM199, 1 mL FCS (10% v/v), 100 µL glutamine (100 mM), 100 µL Na Pyruvate (20 mM), 100 µL penicillin/streptomycin, 40 µL Pluset (LH/FSH stock, 5 IU/mL). pH 7.3-7.4, Osmolarity: 290-300 mOsm. Prepared day before use. Filtered and equilibrated in 5% CO₂ in air overnight.

Tyrode albumin lactate pyruvate (TALP) base medium (50 mL stock solution)

40 mL TCG water, 5 mL NaHCO₃ (250 mM), 2.17 mL NaCl (2.3 M), 550 µL MgCl₂ (100 mM), 500 µL CaCl₂ (200 mM), 500 µL NaH₂PO₄ (34 mM), 160 µL KCl (1 M), 152 µL Na lactate (60% syrup). Store in fridge for up to 1 week.

TALP oocyte wash medium (10 mL working solution)

10 mL TALP base, 30 mg BSA fatty acid free (FAF), 100 µL Na pyruvate (20 mM), 250 µL HEPES (1M), 100 µL penicillin/streptomycin. pH 7.3. Osmolarity: 275-285 mOsm. Filtered and stored at 4°C for up to 1 week. Warmed to 37°C 1 h before use.

TALP capacitation medium (10 mL working solution)

10 mL TALP base, 60 mg BSA FAF, 52 µL Na pyruvate (20 mM), 100 µL HEPES (1M), 100 µL penicillin/streptomycin. pH 7.4. Osmolarity: 295-305 mOsm. Filtered and stored at 4°C for up to 1 week. Warmed to 37°C 1 h before use.

TALP fertilisation medium (10 mL working solution)

10 mL TALP base, 60 mg BSA FAF, 100 µL Na pyruvate (20 mM), 100 µL penicillin/streptomycin, 400 µL caffeine (50 mM), 10 µL heparin (10 mg/mL), 10 µL hypotaurine+epinephrine (0.5 mg/mL). pH 7.4. Osmolarity: 290-300 mOsm. Filtered and stored at 4°C for up to 1 week. Pre-equilibrated in 5% CO₂ in air overnight.

Synthetic oviductal fluid (SOF) base medium (50 mL stock solution)

46 mL TCG water, 2.38 mL NaCl (2.3 M), 600 µL CaCl₂ (200 mM), 360 µL KCl (1M), 175 µL MgSO₄ (200 mM), 100 µL trisodium citrate (200 mM), 100 µL

phenol red (0.5% v/v), 50 μ L glucose (200 mM), 38 μ L Na lactate (60% syrup). Store in fridge for up to 1 week.

SOF HEPES holding medium (10 mL working solution)

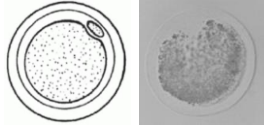
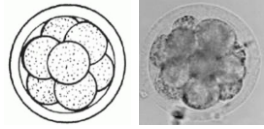
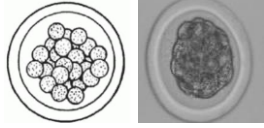
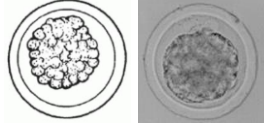
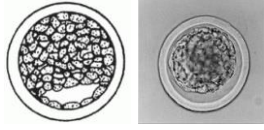
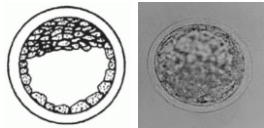
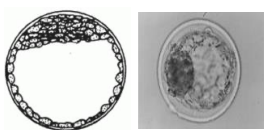
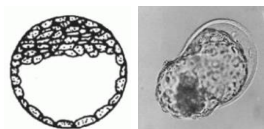
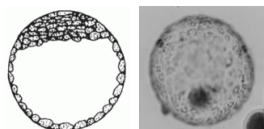
10 mL SOF base, 30 mg BSA FAF, 150 μ L NaHCO₃ (250 mM), 100 μ L BME amino acids [50X], 50 μ L MEM amino acids [100X], 100 μ L Na pyruvate (20 mM), 100 μ L glutamine (100 mM), 250 μ L HEPES (1M), 100 μ L penicillin/streptomycin. pH 7.4. Osmolarity: 270-290 mOsm. Filtered and stored at 4°C for up to 1 week. Warmed to 37°C 1 h before use.

SOF culture medium (10 mL working solution)

10 mL SOF base, 30 mg BSA FAF, 1 mL NaHCO₃ (250 mM), 400 μ L BME amino acids [50X], 100 μ L MEM amino acids [100X], 100 μ L Na pyruvate (20 mM), 100 μ L glutamine (100 mM), 100 μ L penicillin/streptomycin. pH 7.4. Osmolarity: 270-290 mOsm. Filtered and stored at 4°C for up to 1 week. Pre-equilibrated in 39°C, 5% CO₂/5% O₂ overnight.

Appendix 3.3 Bovine embryo stage and morphological description

Adapted from [Bó and Mapletoft \(2013\)](#)

Embryo	Stage code	Morphological description
	1	1-cell unfertilized ovum. Dead or degenerate.
	2	2- to 12-cell embryo. Dead or degenerate.
	3	Early morula containing at least 16 cells. Individual blastomeres difficult to discern from one another. Cellular mass of the embryo occupies most of the perivitelline space.
	4	Compact morula. Individual blastomeres have coalesced forming a compact mass. The embryo mass occupies 60-70% of the perivitelline space.
	5	Early blastocyst. Embryo has formed a blastocoele and gives the appearance of a signet ring. The embryo mass occupies 70-80% of perivitelline space. Quality assessment may prove challenging as it is difficult to differentiate between inner cell mass from trophectoderm cells.
	6	Mid blastocyst. Pronounced differentiation of the trophoblast layer and of the darker and compact inner cell mass. The blastocoele is well-defined and the embryo occupies most of the perivitelline space. Visual differentiation of inner cell mass and trophectoderm is possible.
	7	Late expanded blastocyst. Overall diameter of the embryo dramatically increases. Zona pellucida thins to ~one-third of its original thickness.
	8	Hatched blastocyst. Embryos are hatching or have completely shed zona pellucida. Hatched blastocysts may be spherical with a prominent blastocoele (signet ring appearance) or may be collapsed.
	9	Expanded hatched blastocyst. Identical in appearance to hatched stage 8 blastocyst but is significantly larger in diameter.

Appendix 3.4 Sperm preparation by swim-up method

For each IVF cycle, one straw containing 250 μ L frozen bull semen was rapidly thawed at 37°C in a water bath. Straw contents were released into a pre-warmed, sterile 1.5 mL Eppendorf tube and immediately layered under 1 mL of pre-warmed capacitation media in a 7 mL universal container. The container was transferred to a CO₂ incubator for 1 h to allow spermatozoa to swim up to the top of the capacitation media. Following incubation, the supernatant layer containing motile sperm was carefully transferred to a sterile pre-warmed 1.5 mL Eppendorf tube, leaving dead sperm within the diluent layer at the bottom. The motile sperm fraction was centrifuged for 20 min at 300 xg. Following centrifugation, the supernatant was carefully removed and the sperm pellet was resuspended in ~70 μ L capacitation medium. To count sperm using a haemocytometer, 10 μ L sperm suspension was added to 90 μ L water (1:10 dilution). A final concentration of 1×10^6 spermatozoa/mL was added to each 50 μ L fertilisation drop containing matured COCs.

Appendix 3.5 BHMT and BHMT2 multiple sequence alignment

BHMT and BHMT2 multiple sequence alignment (Clustal W2)

CLUSTAL O(1.2.4) multiple sequence alignment (bovine BHMT isoforms)

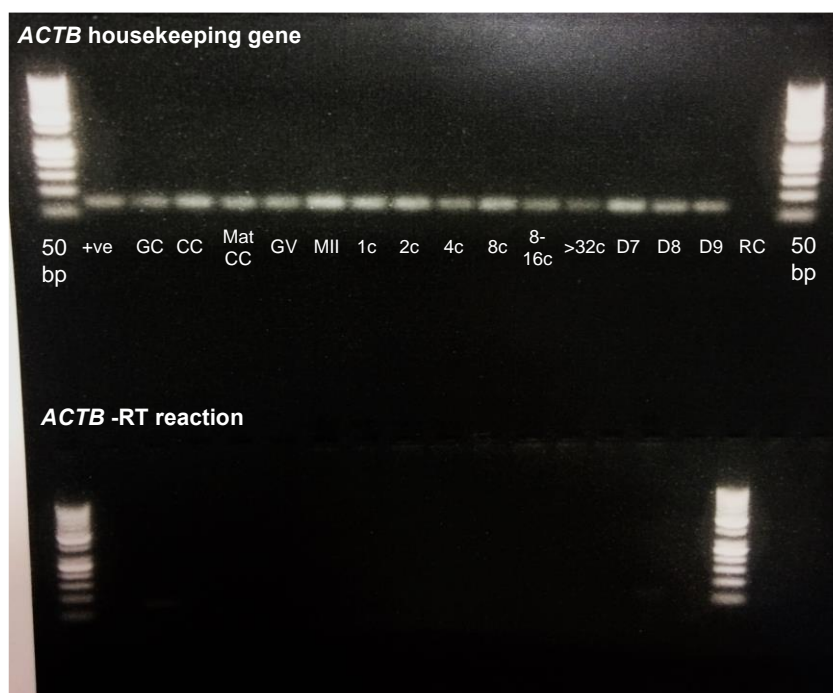
```

BHMT2      CTGGAACCTGCTTTTAGGAAAAATAAAAAGAAAGCGCCTTTTAGAACATCTGGATAGTGGG
BHMT       ATGGCACCGGCTGGGGCAAAAATGTCAAGAAAGCGCATCCTAGAACGGCTAAACTCTGGA
          * * * * * * * * * * * * * * * * * * * * * * * * * * * * * * * * * *
BHMT2      GAGGTTGTGGTTGGAGATGGCAGCTTCCCTCCTAACTCTGGAGAAGAGGGGCTACGTGAAG
BHMT       GAGGTCATCATCGGAGACGGAGGGTTTGTCTTTGCGCTGGAGAAGAGGGGCTACGTGAAG
          * * * * * * * * * * * * * * * * * * * * * * * * * * * * * * * * * *
BHMT2      GCCGGGCTCTGGACTCCAGAAGCCGTAGTAGAGCATCCAAACGCAAGGATGATTAATGCG
BHMT       GCAGGGCCCTGGACCCAGAAGCTGCTGTGGAACACCCAGAAGCAATTCGC-----CAA
          * * * * * * * * * * * * * * * * * * * * * * * * * * * * * * * * * *
BHMT2      TCTCACATGGAATCTTGGAGGTGGGATCAGATGTCATGCAGACTTTCACTTTTTCTGCC
BHMT       CTTCATCGAGATTCTCAGAGCTGGCTCGAATGTCATGCAGACCTTCACCTTCTATGCC
          * * * * * * * * * * * * * * * * * * * * * * * * * * * * * * * * * *
BHMT2      AGTGAGAACAATATGGAAAGCCTTGGGAAG-----CT
BHMT       AGTGAAGACAAGCTGGAGAACAGGGGGAAGTATGTTGCAGAGAAAATATCTGGCAGAAA
          * * * * * * * * * * * * * * * * * * * * * * * * * * * * * * * * * *
BHMT2      GTAAACAACCACTGCCTGTGACCTCGCCAGAGAAGTAGCCAACAAGGGGATGCTTTGGTA
BHMT       GTC AATGAAGCCGCTTGTGACATTGCCCGCAAGTGGCTGATGAAGGAGATGCCTGGT
          * * * * * * * * * * * * * * * * * * * * * * * * * * * * * * * * * *
BHMT2      GCAGGGGGGATCTGCCGGACATCGTTGTACGCACACCACAAGGATGAAGTTAGAATTA
BHMT       GCAGGGGGGATCTGCCGGACATCGTTGTACGCACACCACAAGGATGAAGTTAGAATTA
          * * * * * * * * * * * * * * * * * * * * * * * * * * * * * * * * * *
BHMT2      AAGCTTTTTCGACTACAGCTAGAGATTTTTGCCAGGAAAATGTAGATTTCTTGATTGCA
BHMT       AAAGTCTTTCAGCAACAGTTAGAGGCTTCGTAAGAAGAAGCTGGACTTCTTGATCGCA
          * * * * * * * * * * * * * * * * * * * * * * * * * * * * * * * * * *
BHMT2      GAGTATTTTGAACACGCTG-----TAGAAGCTTTAAAGAATCTGGA
BHMT       GAGTATTTTGAACATGTTGAAGAGGCTGTATGGGCAGTTGAAGCCTTGAAGCATCAGGG
          * * * * * * * * * * * * * * * * * * * * * * * * * * * * * * * * * *
BHMT2      GAGCCTGTGGCAGCCACTATGTGTATCGGCCAGAGGGAGACATGCATGGTGTAAACCT
BHMT       AAACCAGTGGCGCAACTATGTGCATCGGCCAGAGGGAGACTTGCACAGCGTGACCCT
          * * * * * * * * * * * * * * * * * * * * * * * * * * * * * * * * * *
BHMT2      GGGAATGTGCTGTGAAGCTGGTGAAGCAAGGGCCTCAGTTGTTGGTGTGAAGTCCGCA
BHMT       GGCGAGTGTGCAGTGCAGCTGGTTAAAGCAAGCTTCCATCGTGGGGTAAACTGCCAT
          * * * * * * * * * * * * * * * * * * * * * * * * * * * * * * * * * *
BHMT2      TTTGGGCCCTGGACCAGCCTGAAGCAATGAGCCTCATGAAGGAAGCCGACAGGCTGCA
BHMT       TTTGACCCCAATTAGCTTACAGACAGTGAAGCTCATGAAGAAGGCTGGAGGCTGGCC
          * * * * * * * * * * * * * * * * * * * * * * * * * * * * * * * * * *
BHMT2      GAGCTGAAAGCGCCCTGATGGTGTGGTCCCTGGGGTTCCACATGCCCGACTGTGGCA
BHMT       GGACTGAAAGCCACCTCATGAGCCAGCCCTTGGCCTACCACACTCTGACTGCGGCAAG
          * * * * * * * * * * * * * * * * * * * * * * * * * * * * * * * * * *
BHMT2      GGAGGGTTTCTGGATCTCCCTGAATATCCCTTGGCTGGAGCCAGAGTTGCAACCAGA
BHMT       CAGGGGTTTATGACCTGCCAGAATCCCTTTGACTGGAACCCAGAGTTGCAACCAGA
          * * * * * * * * * * * * * * * * * * * * * * * * * * * * * * * * * *
BHMT2      TGGGATATTCAAAAGATGCCAGAGAGGCTTACAACCTGGGGTTCAGGTACATAGGTGG
BHMT       TGGGATATTCAAAAGTATGCCAGAGAGGCTTACAACCTGGGGTTCAGGTACATAGGTGG
          * * * * * * * * * * * * * * * * * * * * * * * * * * * * * * * * * *
BHMT2      TGCTGTGGCTTTGAGCCCTATCACATCAGAGCGATTGCAGAGGAGCTGGCCCGAGAGA
BHMT       TGCTGTGGATTTGAACCTACCACATCAGGGCAATTGCAGAGGAGCTGGCTCCGGAGAGG
          * * * * * * * * * * * * * * * * * * * * * * * * * * * * * * * * * *
BHMT2      GGATTTTGTACCAGCTTTCAGAAAACATGGCAGCTGGGGAAGTGGTCTCAATATGCAC
BHMT       GGATTTTGTCCACTGGCTTTCAGAAAACATGGCAGCTGGGGAAGTGGTCTCAATATGCAC
          * * * * * * * * * * * * * * * * * * * * * * * * * * * * * * * * * *
BHMT2      ACCAAACCCTGGATTAGAGCCAACACAGGGCTAGAAGGGAGTATTGGGAGAATCTGCGG
BHMT       ACCAAACCCTGGATTAGAGCCAACACAGGGCTAGAAGGGAGTATTGGGAGAATCTGCGG
          * * * * * * * * * * * * * * * * * * * * * * * * * * * * * * * * * *
BHMT2      CTGGCTTCTGGCAGACCTGT---CCTTCATGTCAAAGCCAGATGCTTAA-----
BHMT       ATCGCCTCGGGCAGGCGGTACAACCTTCCATGTCAAAGCCGACGCTGGGGAGTGACC
          * * * * * * * * * * * * * * * * * * * * * * * * * * * * * * * * * *
BHMT2      -----
BHMT       AAAGGAACAGCCGAGCTTATGCAGCAGAAGGAAGCCACACGGAGCAGCAGCTGAGAGAG
          -----
BHMT2      -----

```

Red: Exon-Exon junction; Yellow: Forward Primers; Green; Reverse Primers.

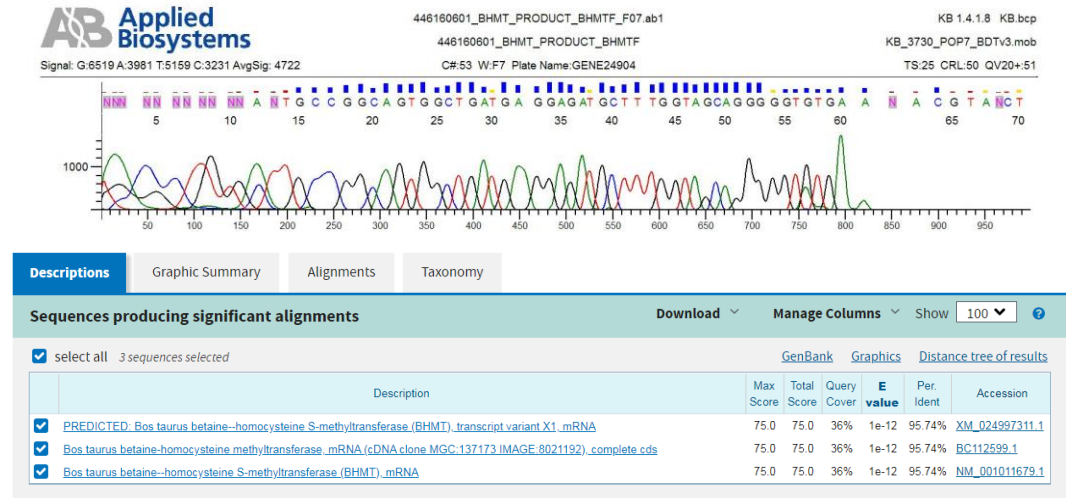
Appendix 3.6 Minus reverse transcription (-RT) for β -Actin (*ACTB*)



Appendix 3.7 Amplicon purification for sequencing

Pre-sequencing DNA purification was achieved using Zymo-Spin™ DNA purification kit. Briefly, cDNA fragments were excised from agarose gel using a razor blade and transferred to a 1.5 mL microcentrifuge tube. Gel samples were weighed and 3 volumes of Agarose Dissolving Buffer (ADB) were added to each gel slice. Samples were incubated at 55°C for 10 min until gel slices were completely dissolved. The melted agarose solution was transferred to a Zymo-Spin™ column in a collection tube and after centrifugation for 75 s at 10-16,000 xg, the flow-through was discarded. The column was washed twice by addition of 200 μ L DNA Wash Buffer and centrifugation for 45 s, discarding the flow-through each time. The column was placed into a 1.5 mL tube, 13 μ L DNA elution buffer (Buffer EB, Tris-Cl, pH 8.5; Qiagen Ltd.) was added directly to the column matrix and centrifuged for 75 s to elute the cDNA. The concentration of excised cDNA was measured using Nanodrop spectrophotometry and cDNA was diluted to 10 ng/ μ L. Primers were diluted to 3.2 pmol/ μ L. PCR products were sequenced by Source Bioscience (Nottingham, UK).

BHMT12 Amplicon sequencing (Source Biosciences, Nottingham, UK)



Bovine *BHMT* forward primer sequence and NCBI Blast output.



Bovine *BHMT2* forward primer sequence and NCBI Blast output.

Appendix 3.8 Custom-made IVP formulations and methionine stock solutions

Methionine-free maturation medium (10 mL working solution)

9 mL Methionine-free TCM199, 1 mL FCS (10% v/v), 100 µL Na Pyruvate (20 mM), 100 µL Penicillin/Streptomycin (P/S), 40 µL Pluset (LH/FSH stock, 5 IU/mL). pH 7.3-7.4, Osmolarity: 290-300 mOsm. Prepared day before use. Filtered and equilibrated in 5% CO₂ in air overnight.

Methionine-free Basal Eagle's Medium (BME) [50X]

In-house formulation based on commercial BME. To be added to modified Hepes-buffered synthetic oviductal fluid (SOF) holding media and SOF culture media.

Amino Acid Component B 6766 BME [50X]	MWt.	Mass (g)	BME [50X] conc. (mmol/L)	IVC media conc. (µmol/L)
L-Arginine monochloride	210.66	1.05	5	200
L-Cystine	240.30	0.6	2.5	100
L-Histidine	155.15	0.4	2.6	100
L-Isoleucine	131.18	1.3	9.9	400
L-Leucine	131.17	1.3	9.9	400
L-Lysine monohydrochloride	182.65	1.849	10.1	405
L-Phenylalanine	165.19	0.825	5.0	200
L-Threonine	119.12	1.2	10.1	400
L-Tryptophan	204.23	0.2	1.0	40
L-Tyrosine	181.19	0.9	5.0	200
L-Valine	117.15	1.175	10.0	400
L-Methionine*	149.21	0.375	2.5	100

*Typical methionine concentration in B 6766 BME [50X] formulation. Custom-made BME was formulated to exclude **methionine**.

Methionine stock solutions

Stock A (50 mmol/L): add 26.81 mL water to 0.2 g methionine

Stock B (5 mmol/L): add 2 mL Stock A to 18 mL water

Stock C (1 mmol/L): add 0.4 mL of Stock A to 19.6 mL water

Custom-made IVP media with added methionine (2.5 mL)

To make 500 $\mu\text{mol/L}$ IVP formulation: add 25 μL Stock A to 2.475 mL methionine-free media

To make 50 $\mu\text{mol/L}$ IVP formulation: add 25 μL Stock B to 2.475 mL methionine-free media

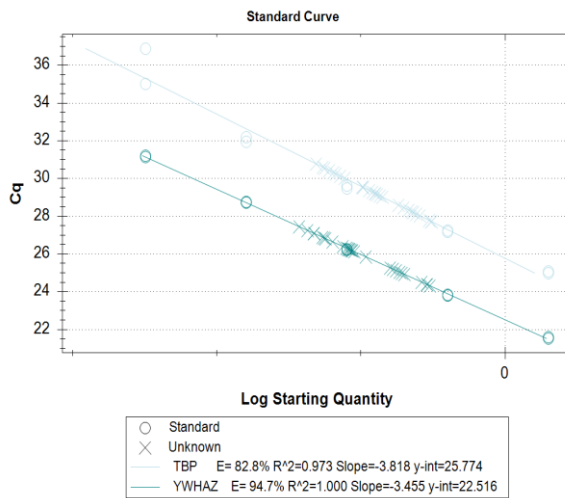
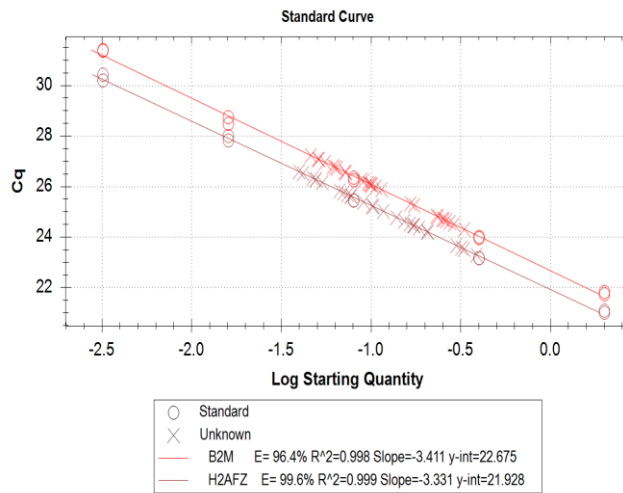
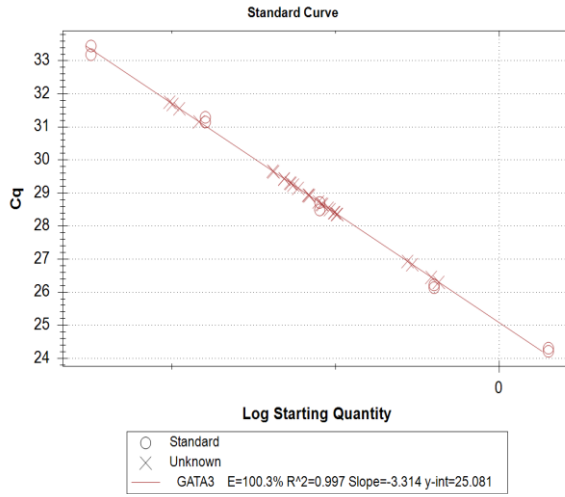
To make 10 $\mu\text{mol/L}$ IVP formulation: add 25 μL Stock C to 2.475 mL methionine-free media

To make 0 $\mu\text{mol/L}$ IVP formulation: 2.5 mL methionine-free media only

Appendix Chapter 4

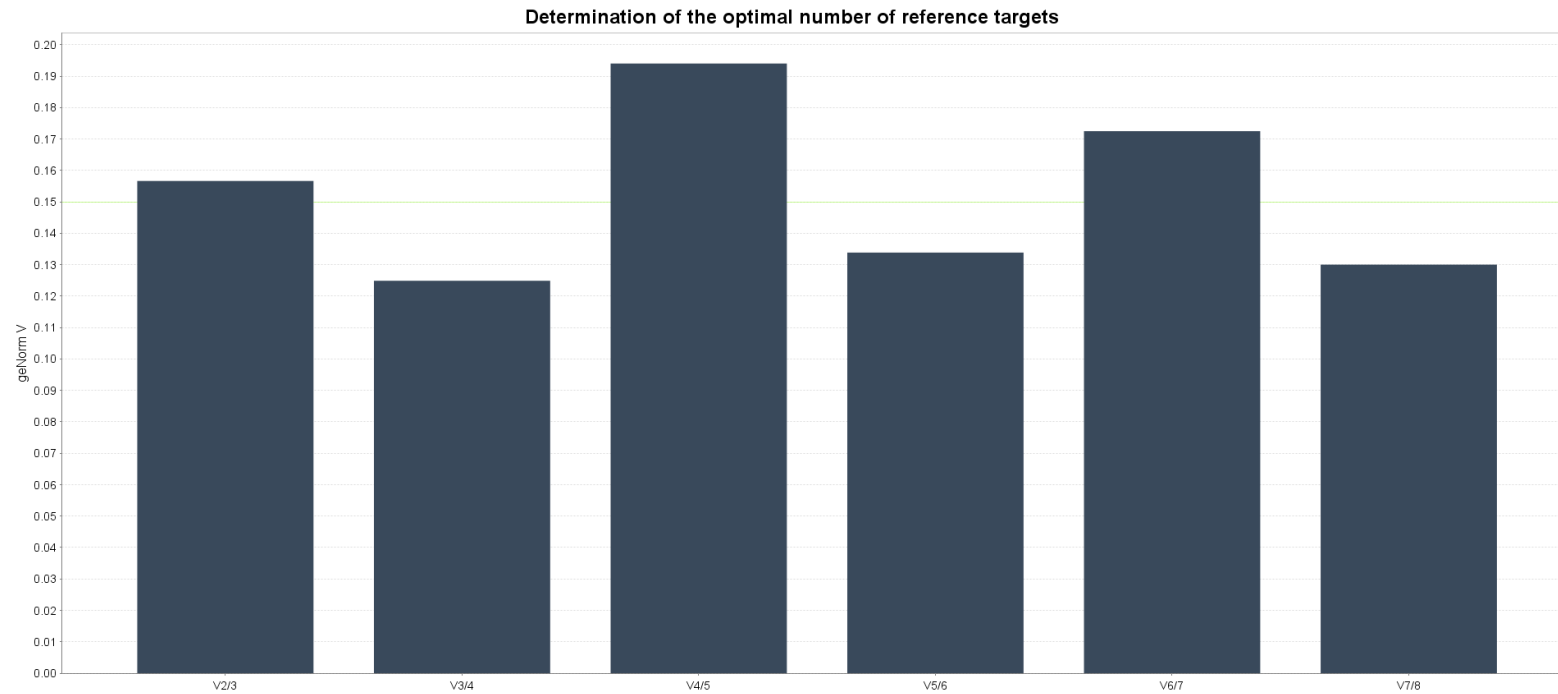
Appendix 4.1 Calibration standard curves for qPCR

GATA3 validation experiment



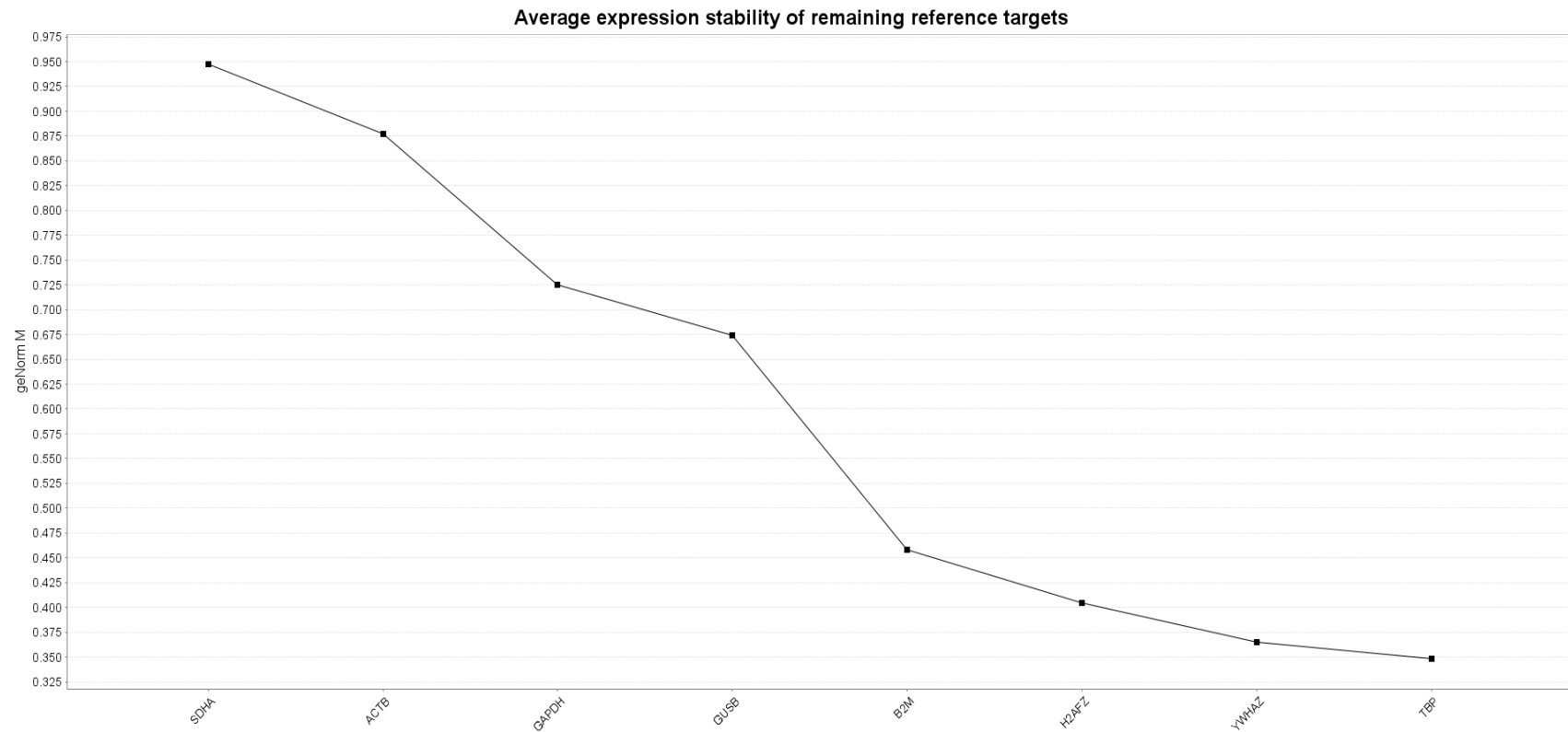
Appendix 4.2 Reference gene selection using geNorm

Reference gene selection using geNorm: Determination of the optimal number of reference genes



geNorm analysis was initiated on 3 samples (inner cell mass, trophoctoderm and blastocysts) using 8 candidate reference genes. *Optimal reference target selection:* The optimal reference target in this experimental situation is 3 (geNorm $V < 0.15$) when comparing a normalisation factor based on 3 or 4 most stable targets.

Reference gene selection using geNorm: Average expression stability of reference genes



geNorm analysis was initiated on 3 samples (inner cell mass, trophectoderm and blastocysts) using 8 candidate reference genes. *Reference target stability:* High reference target stability (average geNorm M ≤ 0.5)

Appendix 4.3 Stock and working solutions for RRBS analysis

gDNA Purification:

Protease (20 mg/mL) stock solution

Soak 20 mg lyophilised protease in 1 mL glycerol (50% v/v). Dissolve at 4°C for 30 min with occasional mixing. Aliquots of 200 µL stored at -20°C for 6 months.

EDTA (50 mmol/L) stock solution

Add 10 µL EDTA (0.5 M) to 90 µL nuclease-free PCR water.

Triton X-100 (10% v/v) stock solution

Add 10 µL Triton X-100 to 90 µL nuclease-free PCR water.

Lysis buffer working solution

Lysis buffer component	Volume (1 reaction, µL)	Final concentration
Tris-HCl (1 M)	0.1	20 mmol/L
EDTA (50 mmol/L)	0.1	2 mmol/L
KCl (1 M)	0.1	20 mmol/L
Triton X-100 (10% v/v)	0.15	0.3%
Protease (20 mg/mL)	0.25	1 mg/mL
Nuclease-free PCR water	3.2	-

Msp1 digest:

Unmethylated λ-DNA (8 pg/µL) stock solution

Add 5 µL λ-DNA (551 ng/µL) to 495 µL nuclease-free PCR water to make 5.51 ng/µL (Stock A). Add 5 µL Stock A to 29.4 µL of nuclease-free PCR water (Stock B).

Msp1 digest working solution

Msp1 digest component	Volume (1 reaction, µL)	Final concentration
10 U/µL Msp1	0.9	9 U
Tango buffer (10X)	1.8	1X
Unmethylated λ-DNA (8 pg/µL, Stock B)	1	8 pg
Nuclease-free PCR water	9.3	-

End-repair/dA tailing:End-repair dNTP stock solution

Add 100 μL 10 mmol/L dATP, 10 μL 10 mmol/L dGTP and 10 μL dCTP to 880 μL PCR water. Aliquots of 200 μL stored at -20°C for 6 months.

End-repair/dA tailing master mix (working solution)

End-repair/dA tailing mix component	Volume (1 reaction, μL)	Final concentration
5U/ μL Klenow fragment exo-	1	5 U
Tango buffer (10X)	0.2	1X
End-repair dNTP mix	0.8	dATP 40 $\mu\text{mol/L}$ dGTP 4 $\mu\text{mol/L}$ dCTP 4 $\mu\text{mol/L}$

Adaptor ligation:Ligation mix working solution

Ligation mix component	Volume (1 reaction, μL)
Diluted methylated adapter (20-fold, NEB)	1
Blund end/TA ligase mastermix (NEB)	2
Tango buffer (10X)	0.5
Nuclease-free PCR water	1.5

tRNA (10 ng/ μL) stock solution

Add 10 mg tRNA to 1 mL nuclease-free PCR and leave at room temperature for 10 min to dissolve. Aliquots of 200 μL stored at -80°C for 6 months.

Zymo DNA clean and concentrator working solution

Zymo DNA clean and concentrator mix component	Volume (1 reaction, μL)
Binding buffer	139
tRNA (10 ng/ μL)	1
DNA (sample)	28

Library Preparation (PCR):KAPA HiFi uracil + mix working solution

KAPA HiFi uracil + mix component	Volume (1 reaction, μL)
KAPA HiFi uracil + mix	25
Universal primer stock	2
Index primer stock	2
Bisulphite converted DNA	10
Nuclease-free PCR water	11

Appendix 4.4 Differentially methylated genes in bovine ICM and TE

Genes with clusters of differentially methylated sites (DMS) in bovine ICM following *in vitro* culture in altered methionine concentration

Genes with clusters of DMS (ICM, n=179)		Cluster count	DMS count
<i>MAD1L1</i>	Mitotic Arrest Deficient 1 Like 1	19	222
<i>RCC2</i>	Regulator of Chromosome Condensation 2	15	182
<i>TBC1D22A</i>	Tbc1 Domain Family Member 22A	12	77
<i>DBH</i>	Dopamine Beta-Hydroxylase	9	131
<i>MRPS25</i>	Mitochondrial Ribosomal Protein S25	7	37
<i>MST1</i>	Macrophage Stimulating 1	6	36
<i>TAFA5</i>	Tafa Chemokine Like Family Member 5	6	127
<i>PAXX</i>	Paxx Non-Homologous End Joining Factor	6	34
<i>NUP210</i>	Nucleoporin 210	5	85
<i>MICALL2</i>	Mical Like 2	5	38
<i>PRKAR1B</i>	Protein Kinase Camp-Dependent Type I Regulatory Subunit Beta	5	56
<i>PPP2R5B</i>	Protein Phosphatase 2 Regulatory Subunit B/Beta	5	38
<i>COMT</i>	Catechol-O-Methyltransferase	5	39
<i>ZADH2</i>	Zinc Binding Alcohol Dehydrogenase Domain Containing 2	5	26
<i>TSPO</i>	Translocator Protein	5	82
<i>MOB2</i>	Mob Kinase Activator 2	4	58
<i>MAMDC4</i>	Mam Domain Containing 4	4	26
<i>SPATA7</i>	Spermatogenesis Associated 7	4	25
<i>SELENOO</i>	Selenoprotein O	4	44
<i>PIPOX</i>	Pipecolic Acid and Sarcosine Oxidase	4	32
<i>LYRM4</i>	Lyr Motif Containing 4	4	73
<i>TOLLIP</i>	Toll Interacting Protein	4	70
<i>LPCAT1</i>	Lysophosphatidylcholine Acyltransferase 1	4	58
<i>DPYSL4</i>	Dihydropyrimidinase Like 4	4	31
<i>PLCL2</i>	Phospholipase C Like 2	4	92
<i>CFD</i>	Complement Factor D	4	17
<i>TSSK1B</i>	Testis Specific Serine Kinase 1B	4	28
<i>PANK4</i>	Pantothenate Kinase 4	4	44
<i>BAP1</i>	Brca1 Associated Protein 1	3	11
<i>SORCS3</i>	Sortilin Related Vps10 Domain Containing Receptor 3	3	98
<i>MAPK8IP3</i>	Mitogen-Activated Protein Kinase 8 Interacting Protein 3	3	32
<i>OSBP2</i>	Oxysterol Binding Protein 2	3	39
<i>PPP6R1</i>	Protein Phosphatase 6 Regulatory Subunit 1	3	21
<i>SIVA1</i>	Siva1 Apoptosis Inducing Factor	3	21
<i>NUBP2</i>	Nucleotide Binding Protein 2	3	16
<i>SLC25A47</i>	Solute Carrier Family 25 Member 47	3	15
<i>TPRA1</i>	Transmembrane Protein Adipocyte Associated 1	3	39
<i>NELFA</i>	Negative Elongation Factor Complex Member A	3	50
<i>COMP</i>	Cartilage Oligomeric Matrix Protein	3	38
<i>AMH</i>	Anti-Mullerian Hormone	3	12
<i>ATG4B</i>	Autophagy Related 4B Cysteine Peptidase	3	34
<i>IGF1R</i>	Insulin Like Growth Factor 1 Receptor	3	52
<i>C21H14orf180</i>	Chromosome 21 C14Orf180 Homolog	3	24
<i>ERF</i>	Ets2 Repressor Factor	3	11
<i>GTF3C4</i>	General Transcription Factor Iiic Subunit 4	3	21
<i>MUL1</i>	Mitochondrial E3 Ubiquitin Protein Ligase 1	3	10
<i>TMEM206</i>	Transmembrane Protein 206	3	22
<i>FKRP</i>	Fukutin Related Protein	3	28
<i>TRIM11</i>	Tripartite Motif Containing 11	3	42
<i>BMP2K</i>	Bmp2 Inducible Kinase	2	13
<i>ASPG</i>	Asparaginase	2	29
<i>EVPL</i>	Envoplakin	2	20
<i>CTU2</i>	Cytosolic Thiouridylase Subunit 2	2	28
<i>PI4KB</i>	Phosphatidylinositol 4-Kinase Beta	2	8
<i>COA8</i>	Cytochrome C Oxidase Assembly Factor 8	2	11
<i>C17H4orf45</i>	Chromosome 17 C4Orf45 Homolog	2	9
<i>DTNBP1</i>	Dystrobrevin Binding Protein 1	2	23
<i>IL21R</i>	Interleukin 21 Receptor	2	15
<i>GATA2</i>	Gata Binding Protein 2	2	14
<i>ACTN3</i>	Actinin Alpha 3	2	10
<i>PAFAH1B3</i>	Platelet Activating Factor Acetylhydrolase 1B Catalytic Subunit 3	2	22
<i>MED10</i>	Mediator Complex Subunit 10	2	24
<i>DNAJC30</i>	Dnaj Heat Shock Protein Family (Hsp40) Member C30	2	6
<i>VASN</i>	Vasorin	2	23
<i>VPS26B</i>	Vps26, Retromer Complex Component B	2	13

	Genes with clusters of DMS continued (ICM, n=179)	Cluster count	DMS count
<i>CRELD2</i>	Cysteine Rich with Egf Like Domains 2	2	17
<i>MFAP4</i>	Microfibril Associated Protein 4	2	13
<i>NNAT</i>	Neuronatin	2	8
<i>PACSIN1</i>	Protein Kinase C and Casein Kinase Substrate In Neurons 1	2	18
<i>REEP6</i>	Receptor Accessory Protein 6	2	10
<i>RABL6</i>	Rab, Member Ras Oncogene Family Like 6	2	20
<i>SULT2B1</i>	Sulfotransferase Family 2B Member 1	2	6
<i>PLCG1</i>	Phospholipase C Gamma 1	2	24
<i>LENG1</i>	Leukocyte Receptor Cluster Member 1	2	16
<i>CLBA1</i>	Clathrin Binding Box of Aftiphilin Containing 1	2	26
<i>DGCR8</i>	Dgcr8 Microprocessor Complex Subunit	2	18
<i>WNT7A</i>	Wnt Family Member 7A	2	64
<i>GPX4</i>	Glutathione Peroxidase 4	2	10
<i>WWOX</i>	Ww Domain Containing Oxidoreductase	2	57
<i>TWIST2</i>	Twist Family Bhlh Transcription Factor 2	2	31
<i>SLC1A7</i>	Solute Carrier Family 1 Member 7	2	19
<i>CELSR3</i>	Cadherin Egf Lag Seven-Pass G-Type Receptor 3	2	20
<i>CAPN7</i>	Calpain 7	2	28
<i>CCND1</i>	Cyclin D1	2	32
<i>IMPA1</i>	Inositol Monophosphatase 1	2	15
<i>C14H8orf33</i>	Chromosome 14 C8Orf33 Homolog	2	12
<i>NXN</i>	Nucleoredoxin	2	9
<i>PWWP2B</i>	Pwwp Domain Containing 2B	2	17
<i>SRSF4</i>	Serine and Arginine Rich Splicing Factor 4	2	16
<i>CHTF18</i>	Chromosome Transmission Fidelity Factor 18	2	25
<i>ARHGEF12</i>	Rho Guanine Nucleotide Exchange Factor 12	1	5
<i>TCIRG1</i>	T Cell Immune Regulator 1, Atpase H+ Transporting V0 Subunit A3	1	16
<i>CAPN2</i>	Calpain 2	1	13
<i>MARK4</i>	Microtubule Affinity Regulating Kinase 4	1	9
<i>SLC36A4</i>	Solute Carrier Family 36 Member 4	1	8
<i>VPS51</i>	Vps51 Subunit of Garp Complex	1	9
<i>CNGA3</i>	Cyclic Nucleotide Gated Channel Subunit Alpha 3	1	6
<i>UNC5D</i>	Unc-5 Netrin Receptor D	1	12
<i>ZSWIM7</i>	Zinc Finger Swim-Type Containing 7	1	18
<i>CRB1</i>	Crumbs Cell Polarity Complex Component 1	1	17
<i>ASMTL</i>	Acetylserotonin O-Methyltransferase Like	1	13
<i>GTF2A1L</i>	General Transcription Factor Iia Subunit 1 Like	1	8
<i>DUSP7</i>	Dual Specificity Phosphatase 7	1	8
<i>PSMD6</i>	Proteasome 26S Subunit, Non-Atpase 6	1	12
<i>TMCO3</i>	Transmembrane and Coiled-Coil Domains 3	1	21
<i>SLC27A4</i>	Solute Carrier Family 27 Member 4	1	10
<i>GRIN2B</i>	Glutamate Ionotropic Receptor Nmda Type Subunit 2B	1	13
<i>PIN1</i>	Peptidylprolyl Cis/Trans Isomerase, Nima-Interacting 1	1	10
<i>AGO2</i>	Argonaute Risc Catalytic Component 2	1	25
<i>POR</i>	Cytochrome P450 Oxidoreductase	1	18
<i>NOS3</i>	Nitric Oxide Synthase 3	1	20
<i>SNRNP25</i>	Small Nuclear Ribonucleoprotein U11/U12 Subunit 25	1	18
<i>TBL3</i>	Transducin Beta Like 3	1	11
<i>PIK3R4</i>	Phosphoinositide-3-Kinase Regulatory Subunit 4	1	11
<i>KIF17</i>	Kinesin Family Member 17	1	22
<i>URB1</i>	Urb1 Ribosome Biogenesis 1 Homolog (S. Cerevisiae)	1	21
<i>DDHD2</i>	Ddhd Domain Containing 2	1	8
<i>LNX2</i>	Ligand of Numb-Protein X 2	1	15
<i>CPLX1</i>	Complexin 1	1	11
<i>ADAMTS2</i>	Adam Metallopeptidase with Thrombospondin Type 1 Motif 2	1	27
<i>MAPK8IP2</i>	Mitogen-Activated Protein Kinase 8 Interacting Protein 2	1	19
<i>LRPAP1</i>	Ldl Receptor Related Protein Associated Protein 1	1	20
<i>STIP1</i>	Stress Induced Phosphoprotein 1	1	8
<i>IL17A</i>	Interleukin 17A	1	10
<i>SLC9A3</i>	Solute Carrier Family 9 Member A3	1	17
<i>TUBG2</i>	Tubulin Gamma 2	1	5
<i>NCAPH2</i>	Non-Smc Condensin Ii Complex Subunit H2	1	15
<i>NBAS</i>	Neuroblastoma Amplified Sequence	1	20
<i>IGF2R</i>	Insulin Like Growth Factor 2 Receptor	1	25
<i>PMPCA</i>	Peptidase, Mitochondrial Processing Alpha Subunit	1	48
<i>RADIL</i>	Rap Associating ith Dil Domain	1	25
<i>EFHC1</i>	Ef-Hand Domain Containing 1	1	9
<i>ACADSB</i>	Acyl-Coa Dehydrogenase Short/Branched Chain	1	5
<i>USP12</i>	Ubiquitin Specific Peptidase 12	1	11
<i>ADARB2</i>	Adenosine Deaminase Rna Specific B2 (Inactive)	1	21
<i>MBP</i>	Myelin Basic Protein	1	18
<i>ITGBL1</i>	Integrin Subunit Beta Like 1	1	5
<i>IPO4</i>	Importin 4	1	9
<i>STT3B</i>	Stt3 Oligosaccharyltransferase Complex Catalytic Subunit B	1	24

	Genes with clusters of DMS continued (ICM, n=179)	Cluster count	DMS count
<i>TTC7A</i>	Tetratricopeptide Repeat Domain 7A	1	13
<i>KDM8</i>	Lysine Demethylase 8	1	6
<i>GNAT2</i>	G Protein Subunit Alpha Transducin 2	1	7
<i>LONP1</i>	Lon Peptidase 1, Mitochondrial	1	8
<i>YDJC</i>	Ydj C Chitooligosaccharide Deacetylase Homolog	1	14
<i>ACTL7A</i>	Actin Like 7A	1	7
<i>LAMP1</i>	Lysosomal Associated Membrane Protein 1	1	19
<i>SPACA7</i>	Sperm Acrosome Associated 7	1	38
<i>MAP1LC3B</i>	Microtubule Associated Protein 1 Light Chain 3 Beta	1	11
<i>ANXA4</i>	Annexin A4	1	6
<i>TEX29</i>	Testis Expressed 29	1	26
<i>MCM7</i>	Minichromosome Maintenance Complex Component 7	1	5
<i>NLRP5</i>	Nlr Family Pyrin Domain Containing 5	1	14
<i>ERRF1</i>	ErbB Receptor Feedback Inhibitor 1	1	6
<i>ATPAF2</i>	Atp Synthase Mitochondrial F1 Complex Assembly Factor 2	1	20
<i>LRRC61</i>	Leucine Rich Repeat Containing 61	1	5
<i>EFCC1</i>	Ef-Hand and Coiled-Coil Domain Containing 1	1	11
<i>ASB1</i>	Ankyrin Repeat and Socs Box Containing 1	1	10
<i>CLCN1</i>	Chloride Voltage-Gated Channel 1	1	5
<i>ARHGDIG</i>	Rho Gdp Dissociation Inhibitor Gamma	1	15
<i>ANKRD13B</i>	Ankyrin Repeat Domain 13B	1	16
<i>TMEM184A</i>	Transmembrane Protein 184A	1	10
<i>PSMC5</i>	Proteasome 26S Subunit, Atpase 5	1	5
<i>CLPTM1</i>	Clptm1 Regulator of Gaba Type A Receptor Forward Trafficking	1	10
<i>TRMT61A</i>	Trna Methyltransferase 61A	1	6
<i>TADA2B</i>	Transcriptional Adaptor 2B	1	12
<i>CASKIN2</i>	Cask Interacting Protein 2	1	38
<i>OVOL3</i>	Ovo Like Zinc Finger 3	1	15
<i>RPN1</i>	Ribophorin I	1	16
<i>JAZF1</i>	Jazf Zinc Finger 1	1	15
<i>DFFA</i>	Dna Fragmentation Factor Subunit Alpha	1	16
<i>AMN</i>	Amnion Associated Transmembrane Protein	1	33
<i>ASAP3</i>	Arfgap With Sh3 Domain, Ankyrin Repeat and Ph Domain 3	1	10
<i>PSKH1</i>	Protein Serine Kinase H1	1	18
<i>ABL1</i>	Abl Proto-Oncogene 1, Non-Receptor Tyrosine Kinase	1	19
<i>GPATCH3</i>	G-Patch Domain Containing 3	1	7
<i>IGLON5</i>	Iglon Family Member 5	1	18
<i>SAMM50</i>	Samm50 Sorting and Assembly Machinery Component	1	10
<i>CHGA</i>	Chromogranin A	1	18
<i>DGKD</i>	Diacylglycerol Kinase Delta	1	41

Genes with clusters of differentially methylated sites (DMS) in bovine TE following *in vitro* culture in altered methionine concentration

Genes with clusters of DMS (TE, n=267)		Cluster count	DMS count
<i>MAD1L1</i>	Mitotic Arrest Deficient 1 Like 1	18	217
<i>RCC2</i>	Regulator of Chromosome Condensation 2	15	222
<i>COMT</i>	Catechol-O-Methyltransferase	14	73
<i>TBC1D22A</i>	Tbc1 Domain Family Member 22A	13	82
<i>SORCS3</i>	Sortilin Related Vps10 Domain Containing Receptor 3	12	154
<i>DBH</i>	Dopamine Beta-Hydroxylase	11	146
<i>TSPO</i>	Translocator Protein	10	130
<i>VAC14</i>	Vac14 Component of Pikfyve Complex	9	79
<i>NUP210</i>	Nucleoporin 210	9	113
<i>PANK4</i>	Pantothenate Kinase 4	8	54
<i>LPCAT1</i>	Lysophosphatidylcholine Acyltransferase 1	8	76
<i>TAF4</i>	Tafa Chemokine Like Family Member 5	7	124
<i>PMPCA</i>	Peptidase, Mitochondrial Processing Alpha Subunit	7	73
<i>AGXT</i>	Alanine--Glyoxylate And Serine--Pyruvate Aminotransferase	7	54
<i>DGKD</i>	Diacylglycerol Kinase Delta	7	65
<i>TOLLIP</i>	Toll Interacting Protein	7	83
<i>MST1</i>	Macrophage Stimulating 1	6	41
<i>PLCL2</i>	Phospholipase C Like 2	5	118
<i>LYRM4</i>	Lyr Motif Containing 4	5	77
<i>PRKAR1B</i>	Protein Kinase Camp-Dependent Type I Regulatory Subunit Beta	5	81
<i>NPAS1</i>	Neuronal Pas Domain Protein 1	5	21
<i>OSBP2</i>	Oxysterol Binding Protein 2	5	50
<i>MOB2</i>	Mob Kinase Activator 2	5	71
<i>CRELD2</i>	Cysteine Rich with Egf Like Domains 2	5	27
<i>MAPK8IP2</i>	Mitogen-Activated Protein Kinase 8 Interacting Protein 2	5	43
<i>PIPOX</i>	Pipecolic Acid and Sarcosine Oxidase	5	45
<i>RADIL</i>	Rap Associating with Dil Domain	4	44
<i>WWOX</i>	Ww Domain Containing Oxidoreductase	4	84
<i>NELFA</i>	Negative Elongation Factor Complex Member A	4	54
<i>TPRA1</i>	Transmembrane Protein Adipocyte Associated 1	4	49
<i>DTNBP1</i>	Dystrobrevin Binding Protein 1	4	44
<i>TMEM204</i>	Transmembrane Protein 204	4	38
<i>RPP40</i>	Ribonuclease P/Mrp Subunit P40	4	52
<i>PLCXD1</i>	Phosphatidylinositol-Specific Phospholipase C, X Domain Containing 1	4	76
<i>PAXX</i>	Paxx Non-Homologous End Joining Factor	4	35
<i>TWIST2</i>	Twist Family Bhlh Transcription Factor 2	4	54
<i>SELENOO</i>	Selenoprotein O	4	51
<i>TMEM129</i>	Transmembrane Protein 129	4	37
<i>ZNF784</i>	Zinc Finger Protein 784	4	28
<i>LRPAP1</i>	Ldl Receptor Related Protein Associated Protein 1	3	38
<i>MED10</i>	Mediator Complex Subunit 10	3	30
<i>YDJC</i>	Ydjc Chitooligosaccharide Deacetylase Homolog	3	21
<i>ADCK1</i>	Aarf Domain Containing Kinase 1	3	26
<i>IGF1R</i>	Insulin Like Growth Factor 1 Receptor	3	61
<i>ING5</i>	Inhibitor of Growth Family Member 5	3	25
<i>RNASEH1</i>	Ribonuclease H1	3	19
<i>RABL6</i>	Rab, Member Ras Oncogene Family Like 6	3	25
<i>VPS26B</i>	Vps26, Retromer Complex Component B	3	24
<i>LAMP1</i>	Lysosomal Associated Membrane Protein 1	3	26
<i>RECQL4</i>	Recq Like Helicase 4	3	15
<i>FERMT3</i>	Fermitin Family Member 3	3	17
<i>AMH</i>	Anti-Mullerian Hormone	3	11
<i>ANKRD13B</i>	Ankyrin Repeat Domain 13B	3	22
<i>SPACA7</i>	Sperm Acrosome Associated 7	3	41
<i>SEPTIN2</i>	Septin 2	3	25
<i>PKP1</i>	Plakophilin 1	3	37
<i>CCND1</i>	Cyclin D1	3	30
<i>C9H6orf120</i>	Chromosome 9 C6Orf120 Homolog	3	34
<i>FKRP</i>	Fukutin Related Protein	3	20
<i>IFT43</i>	Intraflagellar Transport 43	3	19
<i>DPYSL4</i>	Dihydropyrimidinase Like 4	3	46
<i>SLC25A47</i>	Solute Carrier Family 25 Member 47	3	25
<i>PWWP2B</i>	Pwpp Domain Containing 2B	3	7
<i>ANKH</i>	Ankh Inorganic Pyrophosphate Transport Regulator	3	59
<i>IRX4</i>	Iroquois Homeobox 4	3	16
<i>TCIRG1</i>	T Cell Immune Regulator 1, Atpase H+ Transporting V0 Subunit A3	3	28
<i>IGF2R</i>	Insulin Like Growth Factor 2 Receptor	3	51
<i>MAPK1</i>	Mitogen-Activated Protein Kinase 1	3	41
<i>TSSK1B</i>	Testis Specific Serine Kinase 1B	3	27

Genes with clusters of DMS continued (TE, n=267)		Cluster count	DMS count
<i>ABRAXAS2</i>	Abraxas 2, Brisc Complex Subunit	2	15
<i>ULK3</i>	Unc-51 Like Kinase 3	2	12
<i>MYADML2</i>	Myeloid Associated Differentiation Marker Like 2	2	11
<i>NSUN5</i>	Nop2/Sun Rna Methyltransferase 5	2	13
<i>GTF3C4</i>	General Transcription Factor Iiic Subunit 4	2	19
<i>PSMC4</i>	Proteasome 26S Subunit, Atpase 4	2	19
<i>ACTL7A</i>	Actin Like 7A	2	9
<i>P2RY11</i>	Purinergic Receptor P2Y11	2	19
<i>TEX29</i>	Testis Expressed 29	2	27
<i>SUSD2</i>	Sushi Domain Containing 2	2	19
<i>AP3D1</i>	Adaptor Related Protein Complex 3 Subunit Delta 1	2	9
<i>CAPN7</i>	Calpain 7	2	24
<i>LRRC47</i>	Leucine Rich Repeat Containing 47	2	10
<i>DHRS11</i>	Dehydrogenase/Reductase 11	2	7
<i>CPLX1</i>	Complexin 1	2	27
<i>LENG1</i>	Leukocyte Receptor Cluster Member 1	2	20
<i>ERF</i>	Ets2 Repressor Factor	2	10
<i>MMAB</i>	Metabolism of Cobalamin Associated B	2	17
<i>ERMARD</i>	Er Membrane Associated Rna Degradation	2	31
<i>SNRNP25</i>	Small Nuclear Ribonucleoprotein U11/U12 Subunit 25	2	26
<i>MARK4</i>	Microtubule Affinity Regulating Kinase 4	2	10
<i>TAF6L</i>	Tata-Box Binding Protein Associated Factor 6 Like	2	11
<i>EVPL</i>	Envoplakin	2	21
<i>WNT7A</i>	Wnt Family Member 7A	2	69
<i>PTBP1</i>	Polypyrimidine Tract Binding Protein 1	2	10
<i>COL13A1</i>	Collagen Type Xiii Alpha 1 Chain	2	20
<i>MRPL41</i>	Mitochondrial Ribosomal Protein L41	2	18
<i>PTK7</i>	Protein Tyrosine Kinase 7 (Inactive)	2	19
<i>CCNF</i>	Cyclin F	2	10
<i>SARM1</i>	Sterile Alpha and Tir Motif Containing 1	2	11
<i>SART1</i>	Spliceosome Associated Factor 1, Recruiter Of U4/U6.U5 Tri-Snmp	2	17
<i>VASN</i>	Vasorin	2	28
<i>AGO2</i>	Argonaute Risc Catalytic Component 2	2	32
<i>IFITM3</i>	Interferon Induced Transmembrane Protein 3	2	14
<i>PPP2R5B</i>	Protein Phosphatase 2 Regulatory Subunit B/Beta	2	33
<i>TOMM6</i>	Translocase of Outer Mitochondrial Membrane 6	2	13
<i>TUBB6</i>	Tubulin Beta 6 Class V	2	14
<i>MAP1LC3B</i>	Microtubule Associated Protein 1 Light Chain 3 Beta	2	12
<i>CASKIN2</i>	Cask Interacting Protein 2	2	53
<i>ORM1</i>	Orosomuroid 1	2	18
<i>TXNDC5</i>	Thioredoxin Domain Containing 5	2	35
<i>ATP5F1E</i>	Atp Synthase F1 Subunit Epsilon	2	9
<i>WDR45B</i>	Wd Repeat Domain 45B	2	11
<i>DGCR8</i>	Dgcr8 Microprocessor Complex Subunit	2	26
<i>RPN1</i>	Ribophorin I	2	19
<i>COMP</i>	Cartilage Oligomeric Matrix Protein	2	37
<i>PPP6R1</i>	Protein Phosphatase 6 Regulatory Subunit 1	2	18
<i>MICALL2</i>	Mical Like 2	2	31
<i>TRIM67</i>	Tripartite Motif Containing 67	2	14
<i>MYDGF</i>	Myeloid Derived Growth Factor	2	11
<i>HEBP2</i>	Heme Binding Protein 2	2	19
<i>CCDC70</i>	Coiled-Coil Domain Containing 70	2	18
<i>EPHA2</i>	Eph Receptor A2	2	21
<i>SLC1A7</i>	Solute Carrier Family 1 Member 7	2	16
<i>TRIM11</i>	Tripartite Motif Containing 11	2	37
<i>ERRF1</i>	ErbB Receptor Feedback Inhibitor 1	2	12
<i>MYO10</i>	Myosin X	2	24
<i>PLCG1</i>	Phospholipase C Gamma 1	2	39
<i>TMEM184A</i>	Transmembrane Protein 184A	2	21
<i>YARS</i>	Tyrosyl-Trna Synthetase	2	10
<i>ZADH2</i>	Zinc Binding Alcohol Dehydrogenase Domain Containing 2	2	21
<i>CITED4</i>	Cbp/P300 Interacting Transactivator With Glu/Asp Rich Carboxy-Terminal Domain 4	1	15
<i>ALKBH4</i>	Alkb Homolog 4, Lysine Demethylase	1	11
<i>LRRC61</i>	Leucine Rich Repeat Containing 61	1	8
<i>ASPG</i>	Asparaginase	1	21
<i>LNX2</i>	Ligand of Numb-Protein X 2	1	16
<i>DFFA</i>	Dna Fragmentation Factor Subunit Alpha	1	19
<i>ANTXR1</i>	Antxr Cell Adhesion Molecule 1	1	10
<i>GUCY2D</i>	Guanylate Cyclase 2D, Retinal	1	6
<i>DISP2</i>	Dispatched Rnd Transporter Family Member 2	1	10
<i>EFCC1</i>	Ef-Hand and Coiled-Coil Domain Containing 1	1	17
<i>GGA3</i>	Golgi Associated, Gamma Adaptin Ear Containing, Arf Binding Protein 3	1	9
<i>SELENOV</i>	Selenoprotein V	1	6
<i>PTK2</i>	Protein Tyrosine Kinase 2	1	32

Genes with clusters of DMS continued (TE, n=267)		Cluster count	DMS count
<i>POLR2L</i>	Rna Polymerase II Subunit L	1	17
<i>C17H4orf45</i>	Chromosome 17 C4orf45 Homolog	1	16
<i>PKIG</i>	Camp-Dependent Protein Kinase Inhibitor Gamma	1	7
<i>UNC13B</i>	Unc-13 Homolog B	1	10
<i>COG4</i>	Component of Oligomeric Golgi Complex 4	1	26
<i>WNT6</i>	Wnt Family Member 6	1	6
<i>ASMTL</i>	Acetylserotonin O-Methyltransferase Like	1	13
<i>ABL1</i>	Abl Proto-Oncogene 1, Non-Receptor Tyrosine Kinase	1	16
<i>GNA12</i>	G Protein Subunit Alpha 12	1	35
<i>SLC30A3</i>	Solute Carrier Family 30 Member 3	1	15
<i>JPH3</i>	Junctophilin 3	1	22
<i>MAPK8IP3</i>	Mitogen-Activated Protein Kinase 8 Interacting Protein 3	1	37
<i>ZNF703</i>	Zinc Finger Protein 703	1	10
<i>RMI2</i>	Recq Mediated Genome Instability 2	1	23
<i>BOK</i>	Bcl2 Family Apoptosis Regulator Bok	1	11
<i>TADA2B</i>	Transcriptional Adaptor 2B	1	20
<i>IMPA1</i>	Inositol Monophosphatase 1	1	10
<i>KLF10</i>	Kruppel Like Factor 10	1	6
<i>PNMT</i>	Phenylethanolamine N-Methyltransferase	1	7
<i>CDC16</i>	Cell Division Cycle 16	1	5
<i>RXRA</i>	Retinoid X Receptor Alpha	1	14
<i>NAT10</i>	N-Acetyltransferase 10	1	20
<i>SNX30</i>	Sorting Nexin Family Member 30	1	7
<i>OLFM1</i>	Olfactomedin 1	1	26
<i>RBPJL</i>	Recombination Signal Binding Protein for Immunoglobulin Kappa J Region Like	1	5
<i>FOXN4</i>	Forkhead Box N4	1	21
<i>SLX4IP</i>	Slx4 Interacting Protein	1	21
<i>SYCE1</i>	Synaptonemal Complex Central Element Protein 1	1	14
<i>GNG3</i>	G Protein Subunit Gamma 3	1	6
<i>HABP2</i>	Hyaluronan Binding Protein 2	1	10
<i>SERP2</i>	Stress Associated Endoplasmic Reticulum Protein Family Member 2	1	12
<i>BTBD17</i>	Btb Domain Containing 17	1	24
<i>SLC39A13</i>	Solute Carrier Family 39 Member 13	1	16
<i>KLHL36</i>	Kelch Like Family Member 36	1	6
<i>ACTN3</i>	Actin Alpha 3	1	14
<i>CES2</i>	Carboxylesterase 2	1	5
<i>NFKBIB</i>	Nfkb Inhibitor Beta	1	14
<i>CRHR1</i>	Corticotropin Releasing Hormone Receptor 1	1	5
<i>PPP1R37</i>	Protein Phosphatase 1 Regulatory Subunit 37	1	20
<i>C14H8orf33</i>	Chromosome 14 C8orf33 Homolog	1	7
<i>SEPTIN5</i>	Septin 5	1	14
<i>CRIP2</i>	Cysteine Rich Protein 2	1	7
<i>ASB1</i>	Ankyrin Repeat and Socs Box Containing 1	1	12
<i>BMP2K</i>	Bmp2 Inducible Kinase	1	7
<i>C11H2orf49</i>	Chromosome 11 C2orf49 Homolog	1	7
<i>ASIP</i>	Agouti Signaling Protein	1	6
<i>EXT2</i>	Exostosin Glycosyltransferase 2	1	15
<i>TMEM248</i>	Transmembrane Protein 248	1	6
<i>CUX2</i>	Cut Like Homeobox 2	1	15
<i>TIMM13</i>	Translocase of Inner Mitochondrial Membrane 13	1	6
<i>CLPTM1L</i>	Clptm1 Like	1	18
<i>DMP1</i>	Dentin Matrix Acidic Phosphoprotein 1	1	5
<i>MGC137055</i>	Uncharacterized Protein Mgc137055	1	6
<i>ATXN10</i>	Ataxin 10	1	18
<i>PMEPA1</i>	Prostate Transmembrane Protein, Androgen Induced 1	1	11
<i>IGSF3</i>	Immunoglobulin Superfamily Member 3	1	9
<i>SYT10</i>	Synaptotagmin 10	1	5
<i>TAGLN</i>	Transgelin	1	6
<i>AKAP2</i>	Paralemmin 2	1	8
<i>MFAP4</i>	Microfibril Associated Protein 4	1	11
<i>ARAF</i>	A-Raf Proto-Oncogene, Serine/Threonine Kinase	1	9
<i>IPO4</i>	Importin 4	1	9
<i>GPX4</i>	Glutathione Peroxidase 4	1	11
<i>AMFR</i>	Autocrine Motility Factor Receptor	1	14
<i>DHRS7B</i>	Dehydrogenase/Reductase 7B	1	10
<i>PACSL1</i>	Protein Kinase C and Casein Kinase Substrate in Neurons 1	1	37
<i>TBC1D17</i>	Tbc1 Domain Family Member 17	1	11
<i>PRKACA</i>	Protein Kinase Camp-Activated Catalytic Subunit Alpha	1	8
<i>EXOSC6</i>	Exosome Component 6	1	12
<i>CEBPD</i>	Ccaat Enhancer Binding Protein Delta	1	7
<i>RUFY4</i>	Run and Fyve Domain Containing 4	1	24
<i>CXCR5</i>	C-X-C Motif Chemokine Receptor 5	1	11
<i>COA8</i>	Cytochrome C Oxidase Assembly Factor 8	1	11
<i>GATA2</i>	Gata Binding Protein 2	1	17

Genes with clusters of DMS continued (TE, n=267)		Cluster count	DMS count
<i>NKD1</i>	Nkd Inhibitor of Wnt Signaling Pathway 1	1	15
<i>CD3EAP</i>	Cd3E Molecule Associated Protein	1	10
<i>EAF1</i>	E1f Associated Factor 1	1	12
<i>CCZ1</i>	Ccz1 Homolog, Vacuolar Protein Trafficking and Biogenesis Associated	1	8
<i>CHRNA4</i>	Cholinergic Receptor Nicotinic Alpha 4 Subunit	1	14
<i>NOS3</i>	Nitric Oxide Synthase 3	1	21
<i>PABPC4</i>	Poly(A) Binding Protein Cytoplasmic 4	1	11
<i>MRPS25</i>	Mitochondrial Ribosomal Protein S25	1	25
<i>DCAF7</i>	Ddb1 And Cul4 Associated Factor 7	1	7
<i>INTS9</i>	Integrator Complex Subunit 9	1	21
<i>KAT5</i>	Lysine Acetyltransferase 5	1	1
<i>OVOL1</i>	Ovo Like Transcriptional Repressor 1	1	10
<i>CTU2</i>	Cytosolic Thiouridylase Subunit 2	1	30
<i>PPP5C</i>	Protein Phosphatase 5 Catalytic Subunit	1	19
<i>PIN1</i>	Peptidylprolyl Cis/Trans Isomerase, Nima-Interacting 1	1	8
<i>PAFAH1B3</i>	Platelet Activating Factor Acetylhydrolase 1B Catalytic Subunit 3	1	20
<i>HS1BP3</i>	Hcls1 Binding Protein 3	1	16
<i>CCDC3</i>	Coiled-Coil Domain Containing 3	1	7
<i>PYGB</i>	Glycogen Phosphorylase B	1	14
<i>TMEM151A</i>	Transmembrane Protein 151A	1	14
<i>SAMM50</i>	Samm50 Sorting and Assembly Machinery Component	1	13
<i>GRIN2C</i>	Glutamate Ionotropic Receptor Nmda Type Subunit 2C	1	19
<i>RPRD1B</i>	Regulation of Nuclear Pre-Mrna Domain Containing 1B	1	8
<i>RPA2</i>	Replication Protein A2	1	5
<i>ATG4B</i>	Autophagy Related 4B Cysteine Peptidase	1	29
<i>TMEM206</i>	Transmembrane Protein 206	1	13
<i>CELSR3</i>	Cadherin Egf Lag Seven-Pass G-Type Receptor 3	1	15
<i>ARHGDI3</i>	Rho Gdp Dissociation Inhibitor Gamma	1	1
<i>CABP4</i>	Calcium Binding Protein 4	1	8
<i>PARD6B</i>	Par-6 Family Cell Polarity Regulator Beta	1	22
<i>FARP1</i>	Ferm, Arh/Rhogef And Pleckstrin Domain Protein 1	1	49
<i>MAMDC4</i>	Mam Domain Containing 4	1	22
<i>TBL3</i>	Transducin Beta Like 3	1	12
<i>EPHA10</i>	Eph Receptor A10	1	9
<i>SLC9A3</i>	Solute Carrier Family 9 Member A3	1	25
<i>NDUFS8</i>	Nadh: Ubiquinone Oxidoreductase Core Subunit S8	1	6
<i>PRLH</i>	Prolactin Releasing Hormone	1	12
<i>RAB26</i>	Rab26, Member Ras Oncogene Family	1	19
<i>GRIN2B</i>	Glutamate Ionotropic Receptor Nmda Type Subunit 2B	1	13
<i>CHPF2</i>	Chondroitin Polymerizing Factor 2	1	9
<i>AMN</i>	Amnion Associated Transmembrane Protein	1	43
<i>GALNTL5</i>	Polypeptide N-Acetylgalactosaminyltransferase Like 5	1	46
<i>ARHGEF17</i>	Rho Guanine Nucleotide Exchange Factor 17	1	9
<i>SERPIND1</i>	Serpin Family D Member 1	1	18
<i>TENM3</i>	Teneurin Transmembrane Protein 3	1	18
<i>RHOF</i>	Ras Homolog Family Member F, Filopodia Associated	1	7
<i>NLRP5</i>	Nlr Family Pyrin Domain Containing 5	1	19
<i>NDUFA4L2</i>	Ndufa4 Mitochondrial Complex Associated Like 2	1	27
<i>BLOC1S3</i>	Biogenesis of Lysosomal Organelles Complex 1 Subunit 3	1	6
<i>TPPP</i>	Tubulin Polymerization Promoting Protein	1	21

Appendix 4.5 GO terms enriched in bovine ICM and TE

Biological Process GO terms enriched in bovine ICM

	Biological Process GO (ICM, n=67)	FDR (q-value)
GO:0046328	Regulation of Jnk Cascade	0.00017
GO:0097435	Supramolecular Fiber Organization	0.00043
GO:0048015	Phosphatidylinositol-Mediated Signaling	0.00056
GO:0043588	Skin Development	0.00204
GO:0016236	Macroautophagy	0.00233
GO:0007041	Lysosomal Transport	0.00252
GO:0090141	Positive Regulation of Mitochondrial Fission	0.00252
GO:0032959	Inositol Trisphosphate Biosynthetic Process	0.00377
GO:0050908	Detection of Light Stimulus Involved in Visual Perception	0.00377
GO:0007254	Jnk Cascade	0.00426
GO:0007257	Activation of Jun Kinase Activity	0.00500
GO:0018279	Protein N-Linked Glycosylation Via Asparagine	0.00500
GO:0001932	Regulation of Protein Phosphorylation	0.00500
GO:0010634	Positive Regulation of Epithelial Cell Migration	0.00500
GO:0006914	Autophagy	0.00601
GO:0048286	Lung Alveolus Development	0.00601
GO:0046854	Phosphatidylinositol Phosphorylation	0.00601
GO:0050821	Protein Stabilization	0.00601
GO:0120163	Negative Regulation of Cold-Induced Thermogenesis	0.00791
GO:0006986	Response to Unfolded Protein	0.00885
GO:0008542	Visual Learning	0.00885
GO:0032456	Endocytic Recycling	0.00885
GO:0050804	Modulation of Chemical Synaptic Transmission	0.00944
GO:0006936	Muscle Contraction	0.00972
GO:0007052	Mitotic Spindle Organization	0.01036
GO:0032465	Regulation of Cytokinesis	0.01036
GO:0060173	Limb Development	0.01036
GO:0060349	Bone Morphogenesis	0.01036
GO:0031648	Protein Destabilization	0.01394
GO:0043410	Positive Regulation Of Mapk Cascade	0.01545
GO:0006898	Receptor-Mediated Endocytosis	0.01590
GO:0030199	Collagen Fibril Organization	0.01590
GO:0016310	Phosphorylation	0.01679
GO:0007613	Memory	0.01679
GO:0043666	Regulation of Phosphoprotein Phosphatase Activity	0.01679
GO:0030097	Hemopoiesis	0.01776
GO:0030512	Negative Regulation of Transforming Growth Factor Beta Receptor Signaling Pathway	0.01776
GO:0060041	Retina Development in Camera-Type Eye	0.01995
GO:0030855	Epithelial Cell Differentiation	0.02077
GO:0016485	Protein Processing	0.02196
GO:0048812	Neuron Projection Morphogenesis	0.02196
GO:0051209	Release of Sequestered Calcium Ion into Cytosol	0.02196
GO:0045766	Positive Regulation of Angiogenesis	0.02206
GO:0030030	Cell Projection Organization	0.02261
GO:0051216	Cartilage Development	0.02493
GO:0060079	Excitatory Postsynaptic Potential	0.02892
GO:0007266	Rho Protein Signal Transduction	0.02989
GO:0031647	Regulation of Protein Stability	0.02989
GO:0001503	Ossification	0.03200
GO:0007626	Locomotory Behavior	0.03302
GO:0090502	Rna Phosphodiester Bond Hydrolysis, Endonucleolytic	0.03302
GO:0016042	Lipid Catabolic Process	0.03302
GO:0009791	Post-Embryonic Development	0.03422
GO:0050790	Regulation of Catalytic Activity	0.03536
GO:0019722	Calcium-Mediated Signaling	0.03671
GO:0042147	Retrograde Transport, Endosome to Golgi	0.03671
GO:0008033	Trna Processing	0.03959
GO:0030163	Protein Catabolic Process	0.03959
GO:0032508	Dna Duplex Unwinding	0.04089
GO:0090630	Activation of Gtpase Activity	0.04264
GO:0010468	Regulation of Gene Expression	0.04327
GO:0008104	Protein Localization	0.04387
GO:0007420	Brain Development	0.04492
GO:0006508	Proteolysis	0.04564
GO:0001666	Response to Hypoxia	0.04654
GO:0006821	Chloride Transport	0.04654
GO:0006812	Cation Transport	0.04984

Cellular Component GO terms enriched in bovine ICM

	Cellular Component GO (ICM, n=28)	FDR (q-value)
GO:0044754	Autolysosome	0.000041
GO:0030667	Secretory Granule Membrane	0.000257
GO:0005829	Cytosol	0.000891
GO:0005838	Proteasome Regulatory Particle	0.001495
GO:0022624	Proteasome Accessory Complex	0.004420
GO:0012506	Vesicle Membrane	0.004759
GO:0005815	Microtubule Organizing Center	0.006897
GO:0070062	Extracellular Exosome	0.007543
GO:0005770	Late Endosome	0.008864
GO:0031526	Brush Border Membrane	0.010992
GO:0045171	Intercellular Bridge	0.012532
GO:0030659	Cytoplasmic Vesicle Membrane	0.013846
GO:0030139	Endocytic Vesicle	0.014871
GO:1904115	Axon Cytoplasm	0.014871
GO:0005930	Axoneme	0.015040
GO:0001917	Photoreceptor Inner Segment	0.016150
GO:0062023	Collagen-Containing Extracellular Matrix	0.017891
GO:0005902	Microvillus	0.020115
GO:0045335	Phagocytic Vesicle	0.025913
GO:0098685	Schaffer Collateral - Ca1 Synapse	0.025913
GO:0001726	Ruffle	0.030742
GO:0031901	Early Endosome Membrane	0.031968
GO:0030424	Axon	0.035881
GO:0005777	Peroxisome	0.039584
GO:0005635	Nuclear Envelope	0.043227
GO:0045177	Apical Part Of Cell	0.045588
GO:0000502	Proteasome Complex	0.046953
GO:0072686	Mitotic Spindle	0.046953

Molecular Function GO terms enriched in bovine ICM

	Molecular Function GO (ICM, n=26)	FDR (q-value)
GO:0005078	Map-Kinase Scaffold Activity	0.00024
GO:0003958	Nadph-Hemoprotein Reductase Activity	0.00046
GO:0008171	O-Methyltransferase Activity	0.00071
GO:0031434	Mitogen-Activated Protein Kinase Kinase Binding	0.00071
GO:0004579	Dolichyl-Diphosphooligosaccharide-Protein Glycotransferase Activity	0.00096
GO:0010181	Fmn Binding	0.00208
GO:0004198	Calcium-Dependent Cysteine-Type Endopeptidase Activity	0.00303
GO:0004435	Phosphatidylinositol Phospholipase C Activity	0.00303
GO:0008234	Cysteine-Type Peptidase Activity	0.00326
GO:0015485	Cholesterol Binding	0.00326
GO:0015299	Solute: Proton Antiporter Activity	0.00463
GO:0004175	Endopeptidase Activity	0.00517
GO:0005520	Insulin-Like Growth Factor Binding	0.00577
GO:0003725	Double-Stranded Rna Binding	0.00768
GO:0019894	Kinesin Binding	0.00882
GO:0050661	Nadp Binding	0.00948
GO:0048365	Rac Gtpase Binding	0.01020
GO:0008201	Heparin Binding	0.01098
GO:0003727	Single-Stranded Rna Binding	0.01103
GO:0050660	Flavin Adenine Dinucleotide Binding	0.01206
GO:0008233	Peptidase Activity	0.01864
GO:0030165	Pdz Domain Binding	0.02254
GO:0016301	Kinase Activity	0.02915
GO:0001664	G Protein-Coupled Receptor Binding	0.03597
GO:0016787	Hydrolase Activity	0.04172
GO:0008081	Phosphoric Diester Hydrolase Activity	0.04324

KEGG GO terms enriched in bovine ICM

	KEGG Pathway (ICM, n=30)	GOI	FDR (q-value)
bta04070	Phosphatidylinositol signalling	4	0.0348
bta05205	Proteoglycans in cancer	6	0.0348
bta00350	Tyrosine metabolism	2	0.0349
bta00562	Inositol phosphate metabolism	3	0.0349
bta04110	Cell cycle	4	0.0349
bta04136	Autophagy - other	2	0.0349
bta04721	Synaptic vesicle cycle	3	0.0349
bta05214	Glioma	3	0.0349
bta04140	Autophagy - animal	4	0.0351
bta00513	Various types of N-glycan bios	2	0.0361
bta03050	Proteasome	2	0.0361
bta04216	Ferroptosis	2	0.0361
bta04390	Hippo signaling pathway	4	0.0361
bta00510	N-Glycan biosynthesis	2	0.0421
bta00565	Ether lipid metabolism	2	0.0421
bta04933	AGE-RAGE signaling pathway in	3	0.0421
bta04066	HIF-1 signaling pathway	3	0.0449
bta04360	Axon guidance	4	0.0449
bta04370	VEGF signaling pathway	2	0.0449
bta04659	Th17 cell differentiation	3	0.0449
bta00140	Steroid hormone biosynthesis	2	0.0457
bta01100	Metabolic pathways	17	0.0457
bta04114	Oocyte meiosis	3	0.0457
bta04142	Lysosome	3	0.0457
bta04152	AMPK signaling pathway	3	0.0457
bta04510	Focal adhesion	4	0.0457
bta04722	Neurotrophin signaling pathway	3	0.0457
bta05223	Non-small cell lung cancer	2	0.0457
bta04728	Dopaminergic synapse	3	0.0467
bta05321	Inflammatory bowel disease (IB	2	0.0467

Biological Process GO terms enriched in bovine TE

Biological Process GO (TE, n=87)		FDR (q-value)
GO:0097553	Calcium Ion Transmembrane Import into Cytosol	0.000069
GO:0046328	Regulation of Jnk Cascade	0.000714
GO:0048490	Anterograde Synaptic Vesicle Transport	0.001308
GO:0033598	Mammary Gland Epithelial Cell Proliferation	0.002119
GO:0033601	Positive Regulation of Mammary Gland Epithelial Cell Proliferation	0.002119
GO:0042711	Maternal Behavior	0.002119
GO:0035640	Exploration Behavior	0.002255
GO:0008089	Anterograde Axonal Transport	0.002446
GO:0019722	Calcium-Mediated Signaling	0.002472
GO:0010762	Regulation of Fibroblast Migration	0.002869
GO:0014059	Regulation of Dopamine Secretion	0.005088
GO:0032434	Regulation of Proteasomal Ubiquitin-Dependent Protein Catabolic Process	0.005306
GO:2000463	Positive Regulation of Excitatory Postsynaptic Potential	0.005306
GO:0060079	Excitatory Postsynaptic Potential	0.007047
GO:0042113	B Cell Activation	0.007193
GO:0060291	Long-Term Synaptic Potentiation	0.007193
GO:0035249	Synaptic Transmission, Glutamatergic	0.007495
GO:0090502	Rna Phosphodiester Bond Hydrolysis, Endonucleolytic	0.007676
GO:0030500	Regulation of Bone Mineralization	0.007857
GO:0032959	Inositol Trisphosphate Biosynthetic Process	0.007857
GO:0071333	Cellular Response to Glucose Stimulus	0.007857
GO:0061640	Cytoskeleton-Dependent Cytokinesis	0.009465
GO:0070527	Platelet Aggregation	0.009465
GO:0048015	Phosphatidylinositol-Mediated Signaling	0.009634
GO:0006360	Transcription by Rna Polymerase I	0.009634
GO:0007254	Jnk Cascade	0.009634
GO:0007566	Embryo Implantation	0.009634
GO:0035094	Response to Nicotine	0.009634
GO:0060425	Lung Morphogenesis	0.009634
GO:0090630	Activation of Gtpase Activity	0.010983
GO:0007585	Respiratory Gaseous Exchange by Respiratory System	0.011160
GO:0043627	Response to Estrogen	0.011160
GO:0007613	Memory	0.011693
GO:0016573	Histone Acetylation	0.011813
GO:0030512	Negative Regulation of Transforming Growth Factor Beta Receptor Signaling Pathway	0.011813
GO:0030316	Osteoclast Differentiation	0.011813
GO:0035019	Somatic Stem Cell Population Maintenance	0.011813
GO:0035235	Ionotropic Glutamate Receptor Signaling Pathway	0.012635
GO:0043001	Golgi To Plasma Membrane Protein Transport	0.012635
GO:0001932	Regulation of Protein Phosphorylation	0.014141
GO:0048286	Lung Alveolus Development	0.014426
GO:0071310	Cellular Response to Organic Substance	0.014426
GO:0051209	Release of Sequestered Calcium Ion into Cytosol	0.014633
GO:0018108	Peptidyl-Tyrosine Phosphorylation	0.014778
GO:0043410	Positive Regulation of Mapk Cascade	0.014940
GO:0009749	Response to Glucose	0.016839
GO:0017157	Regulation of Exocytosis	0.016839
GO:0050890	Cognition	0.017679
GO:0000045	Autophagosome Assembly	0.019002
GO:0030282	Bone Mineralization	0.019614
GO:0120163	Negative Regulation of Cold-Induced Thermogenesis	0.019614
GO:0010628	Positive Regulation of Gene Expression	0.020741
GO:0007266	Rho Protein Signal Transduction	0.020741
GO:0007612	Learning	0.020741
GO:0000422	Autophagy of Mitochondrion	0.022415
GO:0006986	Response to Unfolded Protein	0.022415
GO:0042177	Negative Regulation of Protein Catabolic Process	0.022415
GO:0043588	Skin Development	0.022415
GO:0001503	Ossification	0.023104
GO:0045766	Positive Regulation of Angiogenesis	0.023335
GO:0016236	Macroautophagy	0.024114
GO:0048013	Ephrin Receptor Signaling Pathway	0.024114
GO:0016310	Phosphorylation	0.025626
GO:0007173	Epidermal Growth Factor Receptor Signaling Pathway	0.025709
GO:0060173	Limb Development	0.025709
GO:0060349	Bone Morphogenesis	0.025709
GO:0050804	Modulation of Chemical Synaptic Transmission	0.028875
GO:0007043	Cell-Cell Junction Assembly	0.029565
GO:0034446	Substrate Adhesion-Dependent Cell Spreading	0.029565
GO:2000300	Regulation of Synaptic Vesicle Exocytosis	0.031472
GO:0035556	Intracellular Signal Transduction	0.032589
GO:0008544	Epidermis Development	0.033407
GO:0048856	Anatomical Structure Development	0.035231
GO:0050885	Neuromuscular Process Controlling Balance	0.035231
GO:0030968	Endoplasmic Reticulum Unfolded Protein Response	0.037458

Biological Process GO continued (TE, n=87)		FDR (q-value)
GO:0042060	Wound Healing	0.037458
GO:0006898	Receptor-Mediated Endocytosis	0.038790
GO:0008630	Intrinsic Apoptotic Signaling Pathway in Response to Dna Damage	0.038790
GO:0031532	Actin Cytoskeleton Reorganization	0.038790
GO:0043666	Regulation of Phosphoprotein Phosphatase Activity	0.041338
GO:0048666	Neuron Development	0.041338
GO:0090501	Rna Phosphodiester Bond Hydrolysis	0.041338
GO:0009267	Cellular Response to Starvation	0.043233
GO:0006979	Response to Oxidative Stress	0.044099
GO:0010976	Positive Regulation of Neuron Projection Development	0.048129
GO:0060041	Retina Development in Camera-Type Eye	0.048129

Cellular Component GO terms enriched in bovine TE

Cellular Component GO (TE, n=29)		FDR (q-value)
GO:0030667	Secretory Granule Membrane	0.000052
GO:0044754	Autolysosome	0.000151
GO:1904115	Axon Cytoplasm	0.004027
GO:0005952	Camp-Dependent Protein Kinase Complex	0.004027
GO:0043195	Terminal Bouton	0.004138
GO:0017146	Nmda Selective Glutamate Receptor Complex	0.004138
GO:0005736	Rna Polymerase I Complex	0.011818
GO:0005940	Septin Ring	0.011818
GO:0031083	Bloc-1 Complex	0.011818
GO:0031105	Septin Complex	0.011818
GO:0000159	Protein Phosphatase Type 2A Complex	0.012503
GO:0030496	Midbody	0.012720
GO:0031514	Motile Cilium	0.016495
GO:0080008	Cul4-Ring E3 Ubiquitin Ligase Complex	0.018130
GO:0010008	Endosome Membrane	0.018130
GO:0031901	Early Endosome Membrane	0.026043
GO:0070062	Extracellular Exosome	0.026768
GO:0005938	Cell Cortex	0.027347
GO:0098839	Postsynaptic Density Membrane	0.028391
GO:0031526	Brush Border Membrane	0.029588
GO:0030672	Synaptic Vesicle Membrane	0.033627
GO:0045171	Intercellular Bridge	0.033757
GO:0005770	Late Endosome	0.033757
GO:0098978	Glutamatergic Synapse	0.039119
GO:0005856	Cytoskeleton	0.039261
GO:0030139	Endocytic Vesicle	0.039722
GO:0005623	Cell	0.039722
GO:0005834	Heterotrimeric G-Protein Complex	0.043310
GO:0030659	Cytoplasmic Vesicle Membrane	0.043501

Molecular Function GO terms enriched in bovine TE

Molecular Function (TE, n=28)		FDR (q-value)
GO:0022849	Glutamate-Gated Calcium Ion Channel Activity	0.000075
GO:0005078	Map-Kinase Scaffold Activity	0.000696
GO:0004972	Nmda Glutamate Receptor Activity	0.001317
GO:0008171	O-Methyltransferase Activity	0.002084
GO:0031434	Mitogen-Activated Protein Kinase Kinase Binding	0.002084
GO:0005005	Transmembrane-Ephrin Receptor Activity	0.003686
GO:0001054	Rna Polymerase I Activity	0.007726
GO:0005003	Ephrin Receptor Activity	0.007726
GO:0004435	Phosphatidylinositol Phospholipase C Activity	0.008366
GO:0004970	Ionotropic Glutamate Receptor Activity	0.010041
GO:0004402	Histone Acetyltransferase Activity	0.010637
GO:0030165	Pdz Domain Binding	0.017129
GO:0005520	Insulin-Like Growth Factor Binding	0.017501
GO:0008066	Glutamate Receptor Activity	0.017501
GO:0015276	Ligand-Gated Ion Channel Activity	0.018367
GO:0032266	Phosphatidylinositol-3-Phosphate Binding	0.023008
GO:0019894	Kinesin Binding	0.027568
GO:0004714	Transmembrane Receptor Protein Tyrosine Kinase Activity	0.027881
GO:0000993	Rna Polymerase Ii Complex Binding	0.029888
GO:0048365	Rac Gtpase Binding	0.029888
GO:0017048	Rho Gtpase Binding	0.034467
GO:0008081	Phosphoric Diester Hydrolase Activity	0.035140
GO:0005109	Frizzled Binding	0.039200
GO:0004672	Protein Kinase Activity	0.039200
GO:1904315	Transmitter-Gated Ion Channel Activity	0.040853
GO:0016301	Kinase Activity	0.041234
GO:0004713	Protein Tyrosine Kinase Activity	0.044652
GO:0015485	Cholesterol Binding	0.047796

KEGG GO terms enriched in bovine TE

KEGG Pathway continued (TE, n=96)		GOI	FDR (q-value)
bta05205	Proteoglycans in cancer	10	0.001044
bta04914	Progesterone-mediated oocyte maturation	6	0.00167
bta04730	Long-term depression	5	0.00167
bta01522	Endocrine resistance	6	0.001811
bta04720	Long-term potentiation	5	0.001862
bta05223	Non-small cell lung cancer	5	0.001862
bta04724	Glutamatergic synapse	6	0.002932
bta05214	Glioma	5	0.002932
bta04114	Oocyte meiosis	6	0.003363
bta04012	ErbB signaling pathway	5	0.003363
bta04370	VEGF signaling pathway	4	0.004547
bta04010	MAPK signaling pathway	9	0.006456
bta04014	Ras signaling pathway	8	0.006456
bta05166	HTLV-I infection	8	0.006456
bta04713	Circadian entrainment	5	0.006456
bta04916	Melanogenesis	5	0.006456
bta00350	Tyrosine metabolism	3	0.006456
bta05033	Nicotine addiction	3	0.006456
bta05216	Thyroid cancer	3	0.006456
bta05224	Breast cancer	6	0.006634
bta05218	Melanoma	4	0.006727
bta05219	Bladder cancer	3	0.006727
bta05200	Pathways in cancer	13	0.007228
bta05220	Chronic myeloid leukemia	4	0.007761
bta04151	PI3K-Akt signaling pathway	10	0.007835
bta04919	Thyroid hormone signaling pathway	5	0.007835
bta04721	Synaptic vesicle cycle	4	0.007835
bta01521	EGFR tyrosine kinase inhibitor resistance	4	0.007909
bta04722	Neurotrophin signaling pathway	5	0.008258
bta05030	Cocaine addiction	3	0.008258
bta04142	Lysosome	5	0.008336
bta04360	Axon guidance	6	0.011247
bta04728	Dopaminergic synapse	5	0.011247
bta05010	Alzheimer's disease	6	0.011267
bta04910	Insulin signaling pathway	5	0.012792

	KEGG Pathway continued (TE, n=96)	GOI	FDR (q-value)
bta04062	Chemokine signaling pathway	6	0.013289
bta04140	Autophagy - animal	5	0.013289
bta04371	Apelin signaling pathway	5	0.013289
bta04658	Th1 and Th2 cell differentiation	4	0.013289
bta05215	Prostate cancer	4	0.013289
bta05213	Endometrial cancer	3	0.013289
bta01100	Metabolic pathways	25	0.01572
bta04933	AGE-RAGE signaling pathway in diabetic complications	4	0.01572
bta05012	Parkinson's disease	5	0.015987
bta04390	Hippo signaling pathway	5	0.016067
bta04723	Retrograde endocannabinoid signaling	5	0.016067
bta05020	Prion diseases	2	0.016067
bta04066	HIF-1 signaling pathway	4	0.017916
bta05221	Acute myeloid leukemia	3	0.017916
bta05031	Amphetamine addiction	3	0.018347
bta04015	Rap1 signaling pathway	6	0.018877
bta04310	Wnt signaling pathway	5	0.018877
bta04659	Th17 cell differentiation	4	0.018877
bta04725	Cholinergic synapse	4	0.018877
bta03030	DNA replication	2	0.018877
bta04726	Serotonergic synapse	4	0.019673
bta04071	Sphingolipid signaling pathway	4	0.022283
bta04611	Platelet activation	4	0.022298
bta05212	Pancreatic cancer	3	0.022298
bta05034	Alcoholism	6	0.023158
bta04110	Cell cycle	4	0.023158
bta03008	Ribosome biogenesis in eukaryotes	3	0.027602
bta04976	Bile secretion	3	0.027602
bta00260	Glycine, serine and threonine metabolism	2	0.027602
bta05203	Viral carcinogenesis	6	0.027993
bta04068	FoxO signaling pathway	4	0.027993
bta04270	Vascular smooth muscle contraction	4	0.028613
bta04216	Ferroptosis	2	0.028613
bta05210	Colorectal cancer	3	0.032587
bta04550	Signaling pathways regulating pluripotency of stem cells	4	0.032913
bta04540	Gap junction	3	0.032913
bta00190	Oxidative phosphorylation	4	0.033271
bta04962	Vasopressin-regulated water reabsorption	2	0.033674
bta04510	Focal adhesion	5	0.034402
bta05016	Huntington's disease	5	0.034402
bta04666	Fc gamma R-mediated phagocytosis	3	0.034402
bta05222	Small cell lung cancer	3	0.034723
bta04340	Hedgehog signaling pathway	2	0.034723
bta05014	Amyotrophic lateral sclerosis (ALS)	2	0.034723
bta03015	mRNA surveillance pathway	3	0.03514
bta00565	Ether lipid metabolism	2	0.035272
bta03460	Fanconi anemia pathway	2	0.035272
bta04072	Phospholipase D signaling pathway	4	0.036981
bta04921	Oxytocin signaling pathway	4	0.036981
bta04070	Phosphatidylinositol signaling system	3	0.036981
bta05231	Choline metabolism in cancer	3	0.036981
bta04913	Ovarian steroidogenesis	2	0.036981
bta04150	mTOR signaling pathway	4	0.038497
bta04660	T cell receptor signaling pathway	3	0.044967
bta03013	RNA transport	4	0.046089
bta05160	Hepatitis C	4	0.046089
bta04213	Longevity regulating pathway - multiple species	2	0.047228
bta05217	Basal cell carcinoma	2	0.048274
bta04024	cAMP signaling pathway	5	0.048962
bta04080	Neuroactive ligand-receptor interaction	7	0.049791
bta04145	Phagosome	4	0.049791

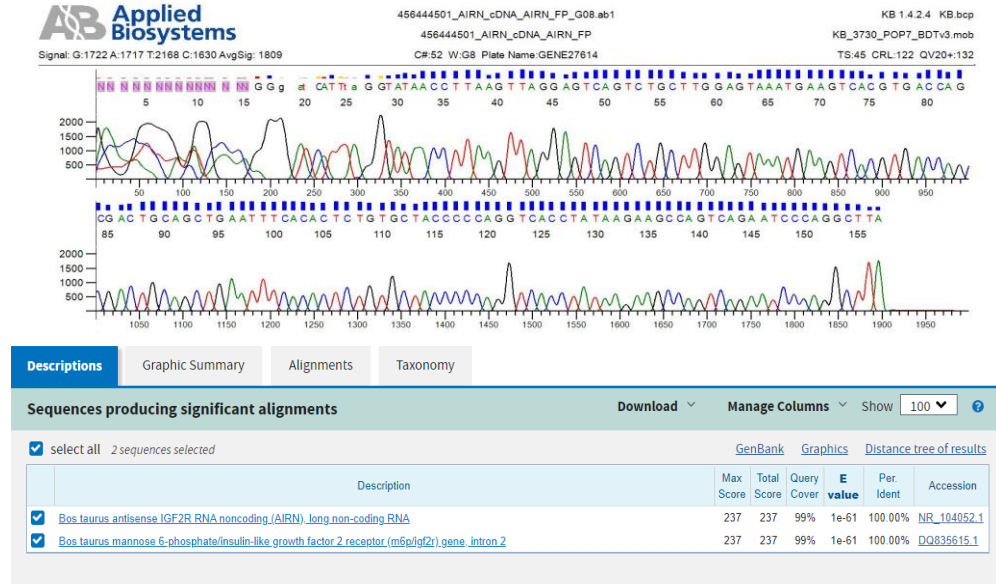
Appendix 4.6 *IGF2R* and *AIRN* primer test by RT-PCR

Lanes 1 and 12: 50 bp marker. 2: no product. 3: *IGF2R* bovine ovary DNA. 4: *IGF2R* bovine ovary DNA RC. 5: *IGF2R* bovine liver cDNA. 6: *IGF2R* bovine liver cDNA RC. 7: *AIRN* bovine ovary DNA. 8: *AIRN* bovine ovary DNA RC. 9: *AIRN* bovine liver cDNA. 10: *AIRN* bovine liver cDNA RC. 11: no product.

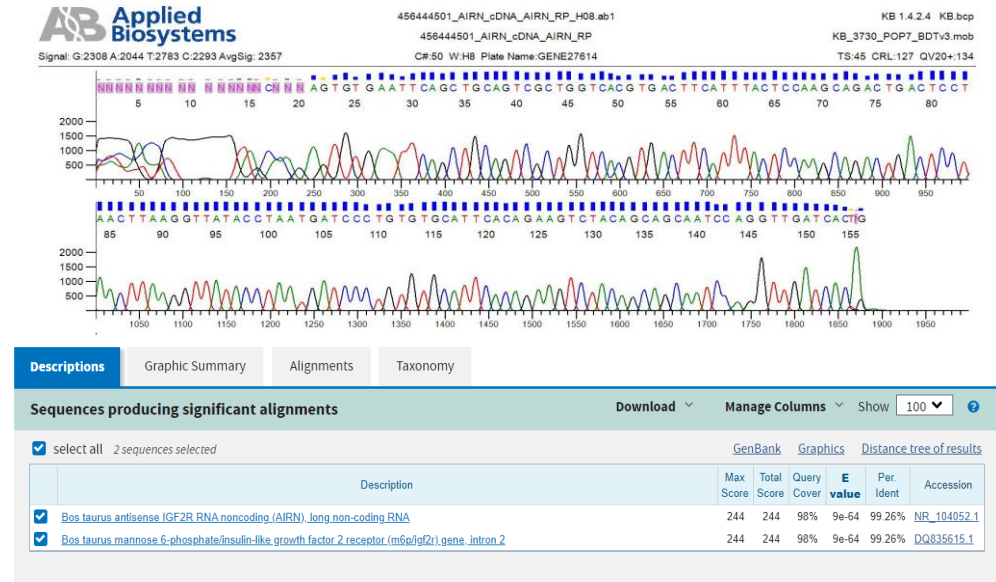
No *IGF2R* transcript detected in bovine ovary DNA as primers were designed to be exon spanning and, therefore, detect cDNA only. *AIRN* is a long non-coding RNA (lncRNA) antisense transcript transcribed from genomic DNA and, therefore, is detected in bovine ovary DNA and liver cDNA sample.

Appendix 4.7 IGF2R/AIRN amplicon sequencing

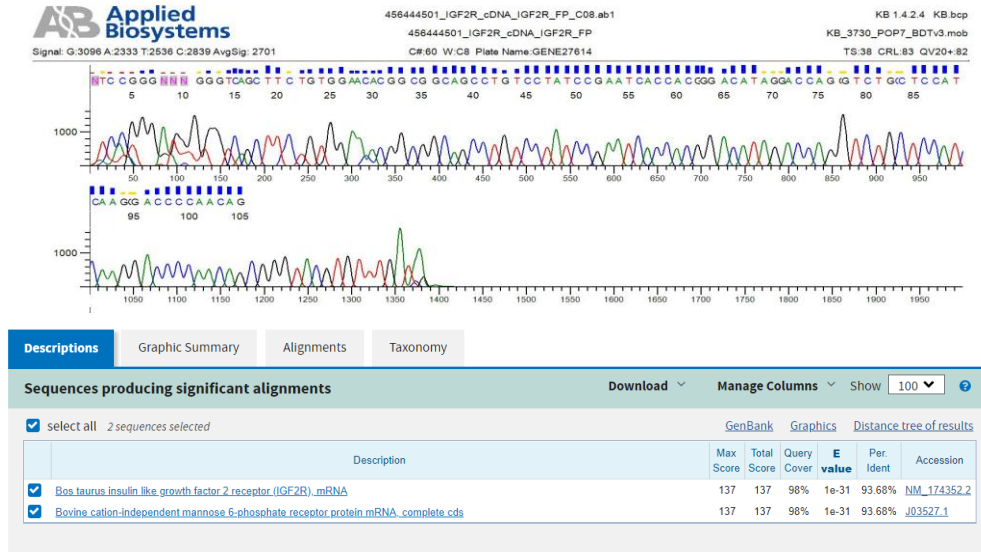
Source Biosciences, Nottingham, UK



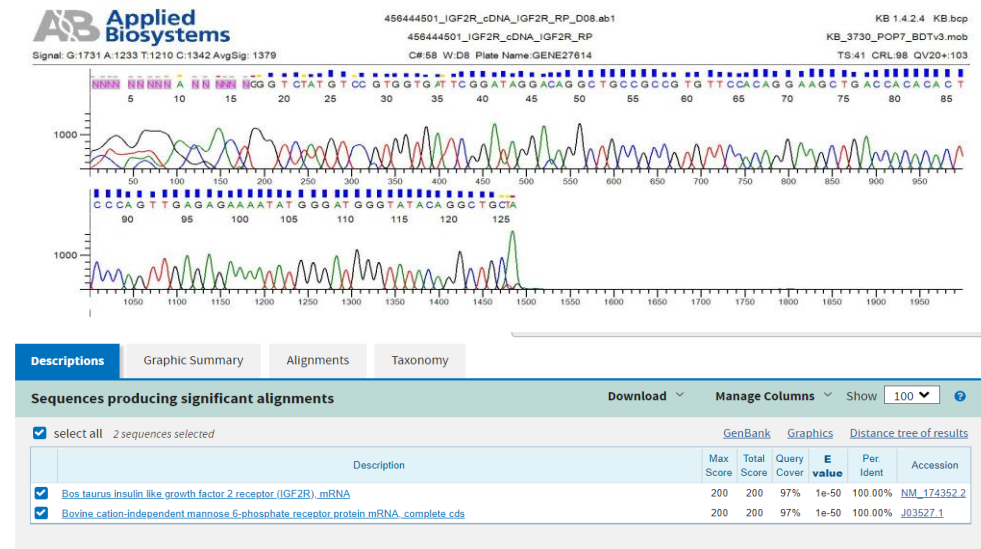
Bovine AIRN forward primer sequence and NCBI Blast output.



Bovine AIRN reverse primer sequence and NCBI Blast output.



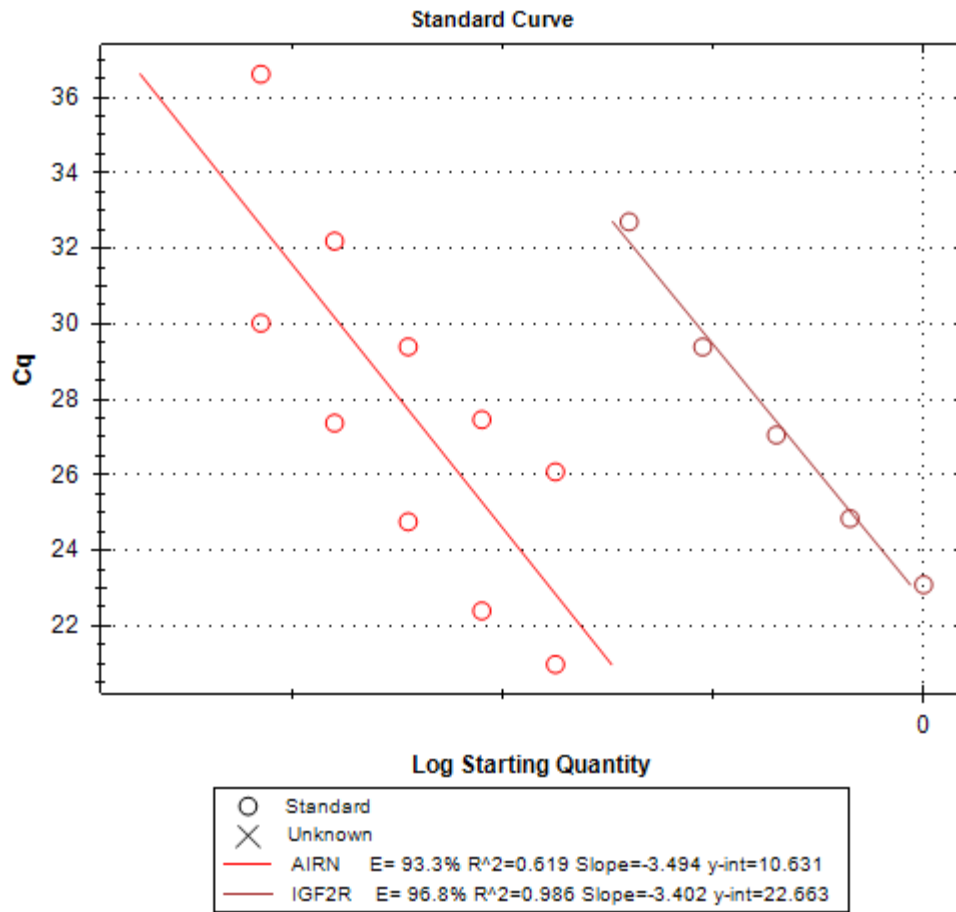
Bovine *IGF2R* forward primer sequence and NCBI Blast output.



Bovine *IGF2R* reverse primer sequence and NCBI Blast output.

Appendix 4.8 Calibration standard curves for qPCR (liver)

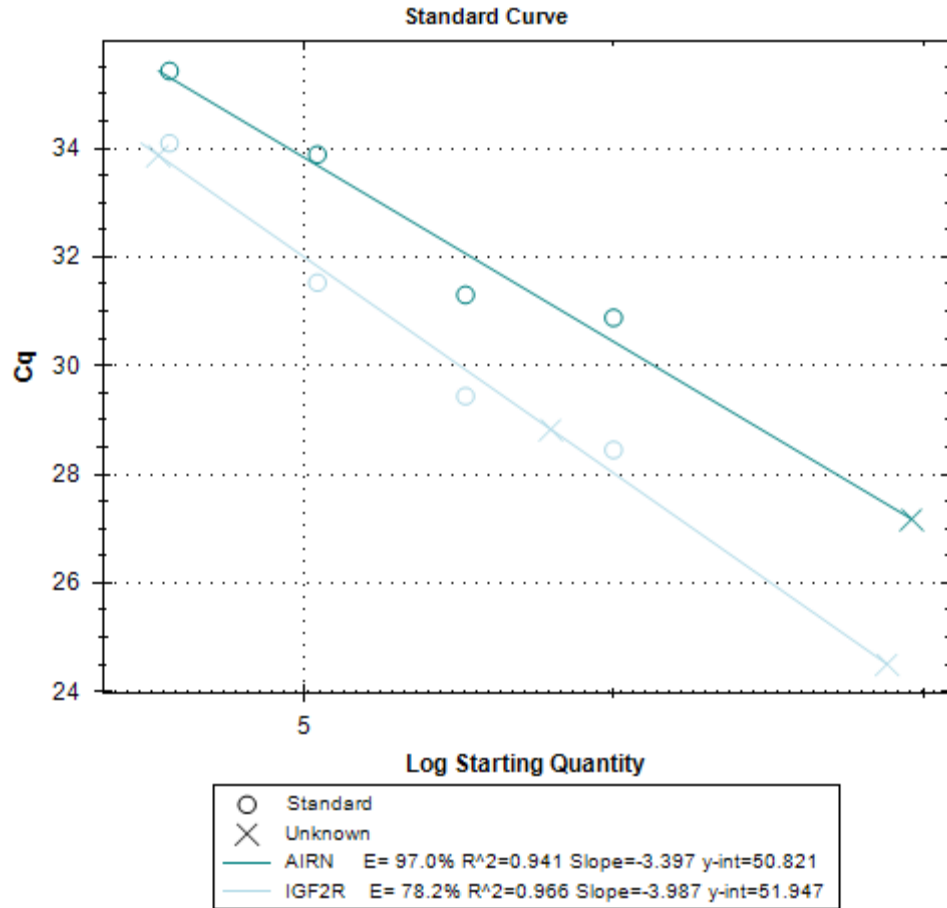
IGF2R/AIRN transcript expression conducted using bovine liver



Slope (R^2) for *AIRN* primers low in bovine liver (0.619) but suitable in blastocyst (0.941; Appendix 4.9). This could be a combination of effects associated with primer design, inaccurate sample/reagent pipetting or analysis of the standard curve.

Appendix 4.9 Calibration standard curves for qPCR (blastocysts)

AIRN transcript expression conducted using bovine blastocysts



Amplification efficiency for *IGF2R* primers low in bovine blastocysts (78.2%) but suitable in liver (96.8%; Appendix 4.8). This could be a combination of effects associated with primer design, inaccurate sample/reagent pipetting and the low abundance of starting material (mRNA transcript) extracted from bovine blastocysts compared with a high abundance extracted from liver.









Appendix 4.10 Position and methylation (%) of each DMS within *IGF2R* intron 2 DMR.

Cluster 1 contains 13 DMS highlighted in yellow. Cluster 2 contains 11 DMS highlighted in green.

MethStart	Av.TE.50	Av.TE.10	Av.meth.diff	Av.meth%
96221369	32.31	13.18	19.13	decreased
96221371	41.76	7.97	33.79	decreased
96221375	34.25	8.94	25.30	decreased
96221396	32.40	8.14	24.26	decreased
96221409	29.19	4.87	24.32	decreased
96221472	34.83	26.47	8.35	decreased
96221474	44.17	30.79	13.38	decreased
96221483	41.42	25.75	15.68	decreased
96221503	36.25	25.23	11.02	decreased
96221507	30.79	21.25	9.55	decreased
96221588	41.26	24.91	16.35	decreased
96221634	11.71	36.87	-25.16	increased
96222398	47.78	30.64	17.15	decreased
96222400	44.53	24.95	19.58	decreased
96223037	50.07	23.74	26.33	decreased
96223047	52.44	29.86	22.58	decreased
96223103	41.34	16.48	24.87	decreased
96223131	42.96	25.00	17.96	decreased
96223135	40.43	23.75	16.68	decreased
96223137	42.01	25.00	17.01	decreased
96223156	34.39	14.58	19.81	decreased
96223184	41.95	22.92	19.03	decreased
96223199	42.50	23.89	18.61	decreased

Appendix 4.11 ClustalW2 multiple sequence alignment: *IGF2R* nucleotide sequence homology (%) between species.

Species	Reference genome	<i>IGF2R</i> location (Chr: bases)	Protein-coding transcripts	Transcripts (bp)	Protein (aa)	<i>IGF2R</i> identity %	Intron 2 %	DMR2 cluster region %	DMR2 cluster 1 %	DMR2 cluster 2 %	DMS cluster 1 %	DMS cluster 2 %
<i>Bos taurus</i>	ARS-UCD1.2	9: 96197493-96300017	1/1	9058	2499	100.0	100.0	100.0	100.0	100.0	100.0	100.0
<i>Ovis aries</i>	Oar_v3.1	8: 82874886-82959397	1/1	7389	2463	91.9	45.8	0.0	0.0	0.0	0.0	0.0
<i>Sus scrofa</i>	Hampshire_pig_v1	LUXS01016444.1: 25529918-26587436	3/3	9008	2488	68.6	74.0	89.4	87.1	88.0	75.0	90.9
				8846	2434							
<i>Homo sapiens</i>	GRCh38.p13	6: 159969099- 160113507	2/6	8837	2431	60.3	52.3	49.5	51.8	47.3	50.0	81.8
				803	-							
				245	-							
				14044	2491							
				762	185							
597	-											
6468	-											
2755	-											
355	-											
<i>Mus musculus</i>	GRCm38.p6	17: 12682406-12769664	1/3	8887	2483	49.7	45.1	0.0	0.0	0.0	0.0	0.0
<i>Rattus rattus</i>	Rnor_6.0	1: 48176106-48264477	1/1	803	-	49.7	44.4	39.1	33.1	44.5	33.3	63.6
				245	-							

% Identity key	
100	
90-100	
80-90	
70-80	
60-70	
50-60	
40-50	
30-40	

Source(s): Ensembl Genome Browser (<https://www.ensembl.org>); ClustalW2 1.2.4, EMBL-EBI (<https://www.ebi.ac.uk/Tools/msa/clustalw2/>). Abbreviation(s): aa, amino acids, bp, base pairs Chr, chromosome; DMR2, differentially methylated region 2; DMS, differentially methylated site (cytosine). Nucleotide sequence percentage similarity with cattle (%).

Appendix 4.12 Multiple sequence alignment of *IGF2R* DMR2 clusters

Multiple sequence alignment of *IGF2R* - DMR2 cluster 1

(ClustalW2 1.2.4, EMBL-EBI; <https://www.ebi.ac.uk/Tools/msa/clustalw2/>)

CLUSTAL O(1.2.4) multiple sequence alignment

```

mouseintron2 ----- 1903
ratintron2 TCTTATAGATCCCAGGACTACCGGCCAACCAGAGATGGCACCCACAAAGGGCTAGGCC 5875
sheepintron2 ----- 1546
humanintron2 TGCGGTAGGCAGGAGGGCTGCCTGTGAAGTGGAGTACCAGGCTTTGTGGCTTCAAGGA 13002
cowintron2 CAGGCTGGGCCCCGTGGCCGCCCGGAGGGGGTGGCCAGGCCGAGCAGCTCAGCGA 4864
pigintron2 AGCGCTGGACCCCGAGGCCCGGGCGGAGTGGGATGCCAGGCTGGCAGCCTCAGGA 4232

mouseintron2 ----- 1903
ratintron2 TTCCCGTTGATCACTAATTGAG----AAAATGCCTTATAGC---TGGATTTTCATGGAG 5927
sheepintron2 ----- 1546
humanintron2 GGCCAAATCATCATGGGCTTGCTTGGGCTTGGAGGTGCGACCTGGTGGGCTGCAGAATG 13062
cowintron2 GGTCCGGTTCCGAGCT---CGGCCGGGCTCGGCCCGGAGCGC--CGAGGGCGGCAGGCCA 4919
pigintron2 GACCGAGTTGGAGCT---CGGCCGGGCTCGGCCCGGACGC--CGAGGGTGGCAGGCCA 4287

mouseintron2 ----- 1903
ratintron2 GTGTTTCCCTCAATTGAGA---CTCCTCTTCTCTAGTGATTCTAGCTTGTGTCTAGGTGA 5984
sheepintron2 ----- 1546
humanintron2 CGACTTGGTGGCCTGACTGAGCAGCATGTAGGCGCTGGTGCAGCCTGGCATGGTGGTAC 13122
cowintron2 GGCCCGGCCGGCC-----TGGCAGCGCGGCTGGTGGGCGGACTCTGGTGAGCGCGG 4971
pigintron2 GGCCGGGCAGGCC-----CGGATCGCGCCTGGTGGACGGGCTCTGGTGAGCGGG 4339

mouseintron2 ----- 1903
ratintron2 CACAAAACCAGCCAGTATAACAGGGGAA-G-TGAAACAATGTCTGATTGATTACCAG 6042
sheepintron2 ----- 1546
humanintron2 CTT-GAG-AGCGTGGCCTAGAGGGCTCCGAGGTGCAGCCTGGCCAGTGTGGTCTGGAGG 13180
cowintron2 CCGA-CGC-CGCAGGGTCTGCAGGACCC---GGCGTGGCCTGGCCGGCGGGCGGTGGCTG 5026
pigintron2 CTTG-GTG-CGCAGGTCTGCAGGACCC---GGCGGGCCTGGCCGGGAGAGCGTGGCCG 4394

mouseintron2 ----- 1903
ratintron2 GGTTTTGGACCGGGTGCTAGGA-----ACTACTAGGCTCTTAGTACT----G 6087
sheepintron2 ----- 1546
humanintron2 GGTCTGGCAAGCGCTATCTGGAGCACTAGAGGTGTGGCCTGTTTTCCG----- 13230
cowintron2 GGGCTGGCGGGCGGGCGGAGCGCTGCCGGACGGGCGCCTGGCGCGCAGGGTCGAGAGG 5086
pigintron2 GGTCCGGCGGGCACGGGCGAGTGGCCGG---GCGGGCCTGGCGCGCAGGGTCTGGAGG 4451

mouseintron2 ----- 1903
ratintron2 AGAATAGGAGTGTGTGATGAGAAGTGGTGGTTGTTAAAAGAGCT-GGTGTAGTATTCT 6146
sheepintron2 ----- 1546
humanintron2 -----GGTGGTCTAGTAGTGTAGCTTGGAGTGCTG-----GGTGGTGTGGC 13273
cowintron2 ACCCGCGCGGCCGGGCTGCAGAGCGTGGCTGGGTCTGACGGGCTCGGGCGAGCGTGGC 5146
pigintron2 ACCCGCGCGGCTGGACTGTGGAGCGTGGCTGGTCTGGCGGGCGGGCGAGCATGGC 4511

```

First cluster of DMS in DMR2 of *IGF2R* intron 2 that were differentially methylated within the trophectoderm (TE) of bovine embryos cultured in low physiological methionine concentration (50 v 10 $\mu\text{mol/L}$).

Start of DMR2 cluster 1 in grey. DMS cluster 1 region nucleotide sequence in red. Hypomethylated cytosine residues in bovine sequence in blue. Hypermethylated cytosine residue in bovine sequence in purple. Cytosine residues conserved between species in green. Nucleotide numbers refer to location on chromosomes.

Multiple sequence alignment (ClustalW2 1.2.4) - DMR2 cluster 2

(ClustalW2 1.2.4, EMBL-EBI; <https://www.ebi.ac.uk/Tools/msa/clustalw2/>)

mouseintron2	-----	1903
ratintron2	CCTGCCCTTCTTTTCTGCAACGCGGCACCTTTTGTAGCG--CGCCCTCCTCCT--GCAACGCGA	6799
sheepintron2	-----	1546
humanintron2	--GGAGCTTGGGGTCTGCAGTGTCTGGAGGCCGAGGCCTGGATGTTGGGGACAG-----	14003
cowintron2	--GGAGACCGTGATCTGGAGGGCCTGGAGCGCACGGTCTGGCGGGTCCGGAGGACCCGG	5882
pigintron2	--GGAGACCGTGGTCTGGAGGACCTGGCGCGTGCGGCCTGGCGGGTCCGGAGGACCCGG	5247
mouseintron2	-----	1903
ratintron2	TACTTTTGTAGTGCGCCCTTCTGCAACGCGCGGTCTGATCATAGAACCCTTCGAATCCT	6859
sheepintron2	-----	1546
humanintron2	---GTCTTGGGAGCTGACTGG---GGGCTGGCGTGGTGGCGGCAGCCCGCAGTCCCT	14055
cowintron2	CGCGATCTGGTGGGCCCGGTGAGCG-CGAGCTGGTCTGGTGGGCCAGCGCGCGGGCCT	5941
pigintron2	CGCGATCTGGCGGGCCCGCGAGCG-CGACTGGTCTGGCGGGCCAGCGAGCGCGGCCT	5306
mouseintron2	-----	1903
ratintron2	CCCTTT--GTGCAGCTTGTACCCCTTAGGATAA---CTCGGAAACCT---CT---G	6905
sheepintron2	-----	1546
humanintron2	GCCT-----GGCC-----CTTGTCTGG-----	14072
cowintron2	GGTCTGGTGGACCCGGCCTGGAGAGCGTGGTCTGGAGGACCCGGCGCGCGGTCTGGCG	6001
pigintron2	GGTCTGGCTGACCCGGCTGGAGAGCGTGGTCTGGAGGACCTGGCGCGCGGTCTGAGC	5366
mouseintron2	-----	1903
ratintron2	AACCTTCCCTTCTCCTCCCTCCCTCCCTCCCTCCCTCCCTCCGCACTCAACCACCGGAA	6965
sheepintron2	-----	1546
humanintron2	--GAGGCCGGGTCTCTGCGGCC-----TCTCGCCGGTGTGCCCCTTGGCCACTGGCG	14124
cowintron2	GGCCTGGCGCGGTCCGGTTGGC-----A--GCGCGCGGTCCGGCGGGCCAGCGCGC	6023
pigintron2	GGCCTGGCGCGGTCCGGCGGGCC-----A--GCGCGCGGTCCGGCGGGCCAGCGCGC	5418
mouseintron2	-----	1903
ratintron2	TCACGCTAAAACTCCGAACCCCTCGGGCAGCGCGCATCTGGCTCGCGCAGTGCCT	7025
sheepintron2	-----	1546
humanintron2	TGCGAGGAA--GCCGGCAGGAGT--GGG-----TGTGCGCCCGCCCGGCTCT	14169
cowintron2	-----CGAGCGCGCGGTCTGGAGGA	6043
pigintron2	GGTCTGGAGGACCCAGCGCGGTCTGGCGGGC-----CCAGCGCGCGGTCTGGTGA	5471
mouseintron2	-----	1903
ratintron2	GGAATCGCGCGCTAAAAATCTCCGAACCCCTGAGCAGCGCGCACCCCTGGCTCACAGTGC	7085
sheepintron2	-----	1546
humanintron2	ACCGCGAGGGATGCAGTGGCCG--CCAGCGTGGCCGTGCGGC-----TG	14212
cowintron2	CCCAGCGCGGTCTGGCGGACCCG--GCCTG--GAGAGCGCGGT-----CT	6084
pigintron2	CCCAGCGCGGTCTGGCGGACCCG--GCCTG--GGGAGCGCGGT-----CT	5512
mouseintron2	-----	1903
ratintron2	CGCGGAACCTTCTGAACCTCCGAACCTCCCTTCTTGTAGCTTGCACCCTCAGGATAG	7145
sheepintron2	-----	1546
humanintron2	GGTCACTCCCTT-CCCGCTCCAGGGCC----TT----TTTCTGCCTCCTTTT----	14256
cowintron2	GGAGGACCCGGC-GCGGCCTGGCGGGCCTGGCGG-----ACGCGCGCTGGTGGCGGG	6138
pigintron2	GGAGGACCCGGC-GCGGCCTGGCGGGCCTGGCGGA-----GCGCGCGCTGGTGGCGGG	5566
mouseintron2	-----	1903
ratintron2	CTCGGAACCTCTAAAGTCTCTTCCCTCCCTCTTG-----CCACACGGCA	7194
sheepintron2	-----	1546
humanintron2	-----CAGGACGTGACCCGCACATTATGAGGGACC	14286
cowintron2	CCCTGCCCCG--AGACCGCGTCTGGCCGGCACGGCGCGCGCAGCCCGGTCTGGAGGACC	6196
pigintron2	CCCAGCGGG--AGACCGCGTCTGGCGGGCCTGGCGCGCACCTGGTCTGGAGGACC	5624

Second cluster of DMS in DMR2 of *IGF2R* intron 2 that were differentially methylated within the trophectoderm (TE) of bovine embryos cultured in low physiological methionine concentration (50 v 10 $\mu\text{mol/L}$).

DMS cluster 2 region nucleotide sequence in red. Hypomethylated cytosine residues in bovine sequence in blue. Cytosine residues conserved between species in green. Nucleotide numbers refer to location on chromosomes.

DMR2 cluster 2 – multiple sequence alignment continued

(ClustalW2 1.2.4, EMBL-EBI; <https://www.ebi.ac.uk/Tools/msa/clustalw2/>)

mouseintron2	-----	1903
ratintron2	CAACCAGAATCACAGCACAAACAGGAATCACATTAATAATCCTCCGAA-----CCTTTGGG	7249
sheepintron2	-----	1546
humanintron2	CGTAGGGCTCTTGACACAGAGG-GGTACCCCTATGTGTGAACAGGTACAGAGTTGGGG	14345
cowintron2	CGGCCTGGAGAGCGCGGCTGGAGGACCCGGCGGGTCTGGTCTGCTGG---GGCCCCGC	6253
pigintron2	CGGCCGGGAGAGCGCGGCTGGAGGACCCGGCGGGTCTGGTCTGGTGG---GGCCCCGC	5681
mouseintron2	-----	1903
ratintron2	CAGCGGCACCCCTGGCTCGCGCAGT-----GCCGCGG-----	7280
sheepintron2	-----	1546
humanintron2	GCTTGGCTTCTGAACTTGCCAGGAAACACCGCATCCCTTTTCTGCAGCGGCCGCC-CCC	14404
cowintron2	CAGTGTGGTCTGGTCTGGCGGCCCGGCTGGAGAGCGTGGTCTGGCGGGCCCGGCGGC	6313
pigintron2	CAGTGTGGTCTGGTCTGGCGGACCCGGCTGGAGAGCGTGGTCTGGCGGGCCCGGCGGC	5741
mouseintron2	-----	1903
ratintron2	-----AATCCTCAGAAATCCCGCTTGCCCGCA-----AACACGGATTGTGCAG	7323
sheepintron2	-----	1546
humanintron2	--CATCCCCACCCGCCCATTT-----CTCTCCCTCCCCAACTGCAG	14445
cowintron2	GGTCTGGAGGACCCGGCGGATCTGGCGGGCCCGGCGAGCGGCCAGCCCATTTGGCG	6373
pigintron2	GGTCTGGAGGACCCGGCGGCTTGCCGGGGCCCGGCGAGCGGCCAGCCCATTTGGCG	5801
mouseintron2	-----	1903
ratintron2	AAATCTCCGGACCCCGTT-----CCCCACAGTAGCTGGTGCA	7364
sheepintron2	-----	1546
humanintron2	CCTTCCGCGCTCCTTGCCCTCGAGCCTCCCTGGGTCCCTGCACCTCCCATGTCCC	14505
cowintron2	CCGTCTCGGGAGCTGG-----CCGTGGGCTGGCTGTGGC	6411
pigintron2	CCGTCTCGGGAGCTGG-----CCGTGGGCTGGCTGTGGC	5839
mouseintron2	-----	1903
ratintron2	GCCCGGAGTAGAACCCCTCCCCCTTTCGAGCGTGGCACACTCGTGTGGATCGCC	7424
sheepintron2	-----	1546
humanintron2	CCACGACTCCTAGGCCTCTCGCGCTTCC-----CCAGGACCCCGCGCA-----TCCT----	14552
cowintron2	CGCCCGCCGCAGTCTCGCCCGGCTTCGT-CCGGGGAGGACGGCCA---GGCT---	6462
pigintron2	CGCCCGCCGCAGTCTCGCCCGGCTTGGT-CCGGGGAGGACGGCCA---GGCT---	5890
mouseintron2	-----	1903
ratintron2	AGTAACCTCTGGAGCCTTACCCTTGCATATAGCAGGACGGCGCGAGGACCTCCCTC	7484
sheepintron2	-----	1546
humanintron2	---GGCCTCTTGCCTCCCGGTCCTCAGCGCCTCCTCGGCCCGCTGCCTCCCGCA	14609
cowintron2	---GGCCGGGTGCC--GCGGGAGTCCGCCGGGGCGCTGCCCGGTGCACCGGGCC	6517
pigintron2	---GGCCGGTTGCCG--CGGTT--GTCTGCCCGGTTCACTGCCCGGTGCATGCGGCC	5943
mouseintron2	-----	1903
ratintron2	CCTTCTCCTCTGTGTGACGCGCA-----TGGCGCTGCGCGGCTCTTGACGGCCCTCG	7539
sheepintron2	-----	1546
humanintron2	CCTTTT---GCGCCTCATGGGCTCCCGGTGCCTTCTGCCCGCCGCTCGCGCGCCCC-	14665
cowintron2	TCTTGCAGTGCCTGGGTGGCAATCGGTCTGGCAGTAGCGGAGGAGGGGTGC-	6576
pigintron2	TGTCCCGAGTGCCTGAGTGGCAGCCGGTCCCGCCGCCAGGTGGAGCGGGCAG-AGG-	6001
mouseintron2	-----	1903
ratintron2	TGTAGTTTGAACCCCTCGTGAGTGCGGGGAAACCGAGTGTGAGTCTCATGCAGCTCG	7599
sheepintron2	-----	1546
humanintron2	-----TCGCCT-CCTCATGCCCCTCGCGCC-----CATACCTCCCCAACC---T	14708
cowintron2	-----AGGAGGCTGGACGGGCGAGCGGGGGGTGGCAGTGGGGCTGACGCTGAGGG	6630
pigintron2	-----AAGAAGCAAGATGGACAGGAGGGGGGATGCGGATGGGGCTGACGCTTAGGG	6055
mouseintron2	-----	1903
ratintron2	GAAACCTTCACCC-----TGGCGCTGAACCTCAAGCGGGGAGCCTTTG-----C	7644
sheepintron2	-----	1546
humanintron2	GTGCCTCTTGCCATCCCGTGTACCACCCGGCATCCTCCGTGCCCATGCG-----C	14761
cowintron2	ACGCCGCTTCCCGAGCGCGCGCCCGGAGCTCG-GCCGGTCCGCTCGGCTCAAGGC	6689
pigintron2	ATGCCGCGCCCGCTCCGCGCGG--CAGAGGTGGCCGATCCCTCTCGGCCCTGGC	6113

Second cluster of DMS in DMR2 of *IGF2R* intron 2 that were differentially methylated within the trophoblast (TE) of bovine embryos cultured in low physiological methionine concentration (50 v 10 µmol/L).

End of DMR2 cluster 2 in grey. DMS cluster 2 region nucleotide sequence in red. Hypomethylated cytosine residues in bovine sequence in blue. Cytosine residues conserved between species in green. Nucleotide numbers refer to location on chromosomes.

Appendix Chapter 5

Appendix 5.1 Working solutions and methodology for RRBS

Msp1 digest:

Msp1 digest working solution

Msp1 digest component	Volume (1 reaction, μL)
Msp1 (NEB R0106T)	4
Smart cut buffer	4
Unmethylated λ -DNA (37.5 μg)	1 (14.7x diluted DNA)
Nuclease-free PCR water	12
DNA sample (5 μg)	20

Msp1 digest mix 2	Volume (1 reaction, μL)
Msp1 (NEB R0106T)	1
Smart cut buffer	1
DNA sample (5 μg)	8

The digestion mixture was incubated at 37°C for 2 h before the addition of 10 μL Msp1 enzyme digest mix 2. The contents were vortexed and centrifuged briefly before the addition of 10 μL Msp1 enzyme and incubation at 37°C for 14 h. After the addition of 10 μL Msp1 enzyme digest mix 2 the contents were vortexed, centrifuged and incubated at 37°C again for 4 h (total 20 h). Samples were incubated at 80°C for 20 min to inactivate Msp1 before another brief centrifugation and storage on ice. The digestion product was purified using Quaquick PCR kit (Qiagen 28104).

End-repair:

End-repair master mix (working solution)

End-repair mix component	Volume (1 reaction, μL)
Large Klenow fragment	1
T4 ligase buffer + ATP	10
End-repair dNTP mix (10 mM each)	4
T4 DNA Polymerase	5
T4 PNK	5
Purified Msp1 cut DNA	28
Nuclease-free PCR water	47

End-repair reaction mix was incubated at 20°C for 30 min. The product was purified using Qiaquick PCR kit. The sample was eluted in 37 μL EB buffer.

dA-tailing:dA-tailing master mix (working solution)

dA-tailing mix component	Volume (1 reaction, μL)
DNA sample	32
NEB2 buffer	5
dATP (1 mM)	10
Klenow fragment exo-	3

dA-tailing reaction mix was incubated at 37°C for 30 min followed by a hold at 4°C. The product was purified using Qiagen MinElute PCR kit and the sample was eluted in 12 μL EB buffer.

Adaptor ligation:Ligation mix working solution

Ligation mix component	Volume (1 reaction, μL)
DNA sample	10
Methylated adapter (NEB, 15 μM)	2.5
Blunt/TA ligase master mix (2X, NEB)	12.5

Methylated adaptor ligation mix was incubated at 20°C for 20 min and 3 μL USER™ (Uracil-Specific Excision Reagent enzyme) was added before incubation at 37°C for 15 min. The product was purified using Qiagen MinElute PCR kit and the sample was eluted in 12 μL EB buffer.

Methylated adaptor ligation product purification

Next, 3 μL loading dye (6X, promega cat no. G1881) was added to 10 μL the purified methylated adaptor ligated product and concentrated using a SpeedVac Vacuum Concentrator at the low heat setting for 10 min to remove residual ethanol. Four microliters of water were added to concentrated samples and they were run on 2% agarose gel containing GelGreen Nucleic acid gel stain (10,000X). Product bands of 200-400 bp in length were excised from the gel to isolate adaptor ligated DNA (this fragment length equates to 80-280 bp plus 124 bp methylated adaptor). The DNA was extracted using Qiagen MinElute gel extraction kit and the sample was eluted in 14 μL EB buffer.

Bisulphite conversion:

Bisulphite conversion of DNA was achieved using the EZ DNA methylation Kit (Zymo) according to the manufacturer's protocol. The sample was incubated with M-dilution buffer mix at 37°C for 15 min. Then, 100 µL CT Conversion Reagent was added.

M-dilution buffer mix working solution

M-dilution buffer mix component	Volume (1 reaction, µL)
DNA sample	4
M-dilution buffer	5
Nuclease-free PCR water	41

The DNA sample contents were mixed and centrifuged prior to bisulphite conversion. The bisulphite conversion protocol took approximately 20 h and the conditions were as follows: 95°C for 30 s, followed by 19 cycles of 60 min at 50°C and a final hold at 4°C. All steps were performed in a PCR thermocycler. Bisulphite converted DNA was purified according to the manufacturer's protocol and samples were eluted in a final volume of 20 µL.

RRBS Library Preparation:Library preparation mix working solution

Library preparation mix component	Volume (1 reaction, µL)
Pfu Turbo Buffer	2.5
dNTP (Turbo)	0.6
Universal primer stock (NEB)	0.75
Pfu Turbo enzyme	0.5
Bisulphite converted DNA sample	1
Nuclease-free PCR water	18.9

The purified DNA was subjected to amplification by PCR using the RRBS Library Preparation master mix. The amplification conditions were as follows: 95°C for 5 min, followed by 12 cycles of 95°C for 15 s, 61°C for 30 s, and 72°C for 7 min with a final hold at 4°C. PCR products were purified using the MiniElute PCR kit (Qiagen) and DNA was eluted in 12 µL nuclease-free PCR water. The speed-vac was used for 5 min (low heat) to remove residual ethanol. Water was added to each sample to make the final volume to 10 µL. DNA samples were transferred to Deep Seq (The University of Nottingham) for bisulphite sequencing analysis.

Appendix 5.2 GO terms enriched in DvOP5 and LvLFF4

Biological Process GO terms enriched in DvOP5

Biological Process GO (DvOP5, n=186)		FDR (q-value)
GO:0010544	Negative Regulation Of Platelet Activation	0.00000
GO:0045199	Maintenance Of Epithelial Cell Apical/Basal Polarity	0.00000
GO:0046533	Negative Regulation Of Photoreceptor Cell Differentiation	0.00000
GO:0010172	Embryonic Body Morphogenesis	0.00000
GO:0021544	Subpallium Development	0.00000
GO:0034653	Retinoic Acid Catabolic Process	0.00000
GO:0071376	Cellular Response To Corticotropin-Releasing Hormone Stimulus	0.00000
GO:0007442	Hindgut Morphogenesis	0.00000
GO:0021543	Pallium Development	0.00000
GO:0021914	Regulation Of Smoothened Signaling Pathway In Ventral Spinal Cord Patterning	0.00000
GO:0034334	Adherens Junction Maintenance	0.00000
GO:0060708	Spongiotrophoblast Differentiation	0.00000
GO:0061314	Notch Signaling Involved In Heart Development	0.00000
GO:0072034	Renal Vesicle Induction	0.00000
GO:0072049	Comma-Shaped Body Morphogenesis	0.00000
GO:0072050	S-Shaped Body Morphogenesis	0.00000
GO:0072162	Metanephric Mesenchymal Cell Differentiation	0.00000
GO:1903936	Cellular Response To Sodium Arsenite	0.00000
GO:0002790	Peptide Secretion	0.00000
GO:0003357	Noradrenergic Neuron Differentiation	0.00000
GO:0003401	Axis Elongation	0.00000
GO:0006222	Ump Biosynthetic Process	0.00000
GO:0006572	Tyrosine Catabolic Process	0.00000
GO:0006657	Cdp-Choline Pathway	0.00000
GO:0007501	Mesodermal Cell Fate Specification	0.00000
GO:0010512	Negative Regulation Of Phosphatidylinositol Biosynthetic Process	0.00000
GO:0010957	Negative Regulation Of Vitamin D Biosynthetic Process	0.00000
GO:0014015	Positive Regulation Of Gliogenesis	0.00000
GO:0015697	Quaternary Ammonium Group Transport	0.00000
GO:0015746	Citrate Transport	0.00000
GO:0016577	Histone Demethylation	0.00000
GO:0021526	Medial Motor Column Neuron Differentiation	0.00000
GO:0021559	Trigeminal Nerve Development	0.00000
GO:0021568	Rhombomere 2 Development	0.00000
GO:0021681	Cerebellar Granular Layer Development	0.00000
GO:0021782	Glial Cell Development	0.00000
GO:0021891	Olfactory Bulb Interneuron Development	0.00000
GO:0021893	Cerebral Cortex Gabaergic Interneuron Fate Commitment	0.00000
GO:0021913	Transcription From RNAIi Promoter In Spinal Cord Interneuron Specification	0.00000
GO:0021937	Cerebellar Purkinje Cell In Regulation Of Granule Cell Precursor Cell Proliferation	0.00000
GO:0021986	Habenula Development	0.00000
GO:0030431	Sleep	0.00000
GO:0030852	Regulation Of Granulocyte Differentiation	0.00000
GO:0031103	Axon Regeneration	0.00000
GO:0032286	Central Nervous System Myelin Maintenance	0.00000
GO:0032401	Establishment Of Melanosome Localization	0.00000
GO:0032770	Positive Regulation Of Monooxygenase Activity	0.00000
GO:0032823	Regulation Of Natural Killer Cell Differentiation	0.00000
GO:0032912	Negative Regulation Of Transforming Growth Factor Beta2 Production	0.00000
GO:0033058	Directional Locomotion	0.00000
GO:0033082	Regulation Of Extrathymic T Cell Differentiation	0.00000
GO:0034124	Regulation Of Myd88-Dependent Toll-Like Receptor Signaling Pathway	0.00000
GO:0035295	Tube Development	0.00000
GO:0042136	Neurotransmitter Biosynthetic Process	0.00000
GO:0042942	D-Serine Transport	0.00000
GO:0043370	Regulation Of Cd4-Positive, Alpha-Beta T Cell Differentiation	0.00000
GO:0045586	Regulation Of Gamma-Delta T Cell Differentiation	0.00000
GO:0045608	Negative Regulation Of Inner Ear Auditory Receptor Cell Differentiation	0.00000
GO:0045659	Negative Regulation Of Neutrophil Differentiation	0.00000
GO:0046885	Regulation Of Hormone Biosynthetic Process	0.00000
GO:0048385	Regulation Of Retinoic Acid Receptor Signaling Pathway	0.00000
GO:0048563	Post-Embryonic Animal Organ Morphogenesis	0.00000
GO:0048871	Multicellular Organismal Homeostasis	0.00000
GO:0050954	Sensory Perception Of Mechanical Stimulus	0.00000
GO:0051136	Regulation Of Nk T Cell Differentiation	0.00000
GO:0060026	Convergent Extension	0.00000
GO:0060067	Cervix Development	0.00000
GO:0060083	Smooth Muscle Contraction Involved In Micturition	0.00000
GO:0060221	Retinal Rod Cell Differentiation	0.00000
GO:0060302	Negative Regulation Of Cytokine Activity	0.00000
GO:0060434	Bronchus Morphogenesis	0.00000
GO:0060675	Ureteric Bud Morphogenesis	0.00000
GO:0060775	Planar Cell Polarity Pathway Involved In Gastrula Mediolateral Intercalation	0.00000
GO:0061771	Response To Caloric Restriction	0.00000
GO:0071657	Positive Regulation Of Granulocyte Colony-Stimulating Factor Production	0.00000
GO:0072011	Glomerular Endothelium Development	0.00000
GO:0072086	Specification Of Loop Of Henle Identity	0.00000
GO:0072108	Mesenchymal To Epithelial Transition In Metanephros Morphogenesis	0.00000
GO:0072190	Ureter Urothelium Development	0.00000
GO:0072289	Metanephric Nephron Tubule Formation	0.00000
GO:0072674	Multinuclear Osteoclast Differentiation	0.00000
GO:0090076	Relaxation Of Skeletal Muscle	0.00000
GO:0090218	Positive Regulation Of Lipid Kinase Activity	0.00000

Biological Process GO continued (DvOP5, n=186)		FDR (q-value)
GO:0097340	Inhibition Of Cysteine-Type Endopeptidase Activity	0.00000
GO:0097535	Lymphoid Lineage Cell Migration Into Thymus	0.00000
GO:0099039	Sphingolipid Translocation	0.00000
GO:1900625	Positive Regulation Of Monocyte Aggregation	0.00000
GO:1901382	Regulation Of Chorionic Trophoblast Cell Proliferation	0.00000
GO:1901991	Negative Regulation Of Mitotic Cell Cycle Phase Transition	0.00000
GO:1902871	Positive Regulation Of Amacrine Cell Differentiation	0.00000
GO:1902963	Metalloendopeptidase Activity In Amyloid Precursor Protein Catabolic Process	0.00000
GO:1903539	Protein Localization To Postsynaptic Membrane	0.00000
GO:1904956	Regulation Of Midbrain Dopaminergic Neuron Differentiation	0.00000
GO:1905167	Positive Regulation Of Lysosomal Protein Catabolic Process	0.00000
GO:1905521	Regulation Of Macrophage Migration	0.00000
GO:1990927	Calcium Ion Regulated Lysosome Exocytosis	0.00000
GO:2000041	Negative Regulation Of Planar Cell Polarity Pathway Involved In Axis Elongation	0.00000
GO:2000392	Regulation Of Lamellipodium Morphogenesis	0.00000
GO:2000563	Positive Regulation Of Cd4-Positive, Alpha-Beta T Cell Proliferation	0.00000
GO:2000675	Negative Regulation Of Type B Pancreatic Cell Apoptotic Process	0.00000
GO:2000981	Negative Regulation Of Inner Ear Receptor Cell Differentiation	0.00000
GO:001656	Metanephros Development	0.00012
GO:0021796	Cerebral Cortex Regionalization	0.00139
GO:0051246	Regulation Of Protein Metabolic Process	0.00139
GO:0072197	Ureter Morphogenesis	0.00139
GO:0009952	Anterior/Posterior Pattern Specification	0.00191
GO:0042474	Middle Ear Morphogenesis	0.00426
GO:0035019	Somatic Stem Cell Population Maintenance	0.00561
GO:0018101	Protein Citrullination	0.00561
GO:0032808	Lacrimal Gland Development	0.00561
GO:0070848	Response To Growth Factor	0.00561
GO:0090084	Negative Regulation Of Inclusion Body Assembly	0.00561
GO:1900748	Positive Regulation Of Vascular Endothelial Growth Factor Signaling Pathway	0.00561
GO:2001046	Positive Regulation Of Integrin-Mediated Signaling Pathway	0.00561
GO:0042472	Inner Ear Morphogenesis	0.00595
GO:0048546	Digestive Tract Morphogenesis	0.00647
GO:0048557	Embryonic Digestive Tract Morphogenesis	0.00647
GO:0048665	Neuron Fate Specification	0.00647
GO:0048856	Anatomical Structure Development	0.00647
GO:0006536	Glutamate Metabolic Process	0.00751
GO:0021520	Spinal Cord Motor Neuron Cell Fate Specification	0.00751
GO:0032330	Regulation Of Chondrocyte Differentiation	0.00751
GO:0060707	Trophoblast Giant Cell Differentiation	0.01514
GO:0090190	Positive Regulation Of Branching Involved In Ureteric Bud Morphogenesis	0.01514
GO:0048646	Anatomical Structure Formation Involved In Morphogenesis	0.01644
GO:0035987	Endodermal Cell Differentiation	0.01726
GO:0001709	Cell Fate Determination	0.01925
GO:0090179	Planar Cell Polarity Pathway Involved In Neural Tube Closure	0.01925
GO:0097320	Plasma Membrane Tubulation	0.01925
GO:0021983	Pituitary Gland Development	0.02056
GO:0030879	Mammary Gland Development	0.02056
GO:0060037	Pharyngeal System Development	0.02160
GO:0001839	Neural Plate Morphogenesis	0.02160
GO:0003170	Heart Valve Development	0.02160
GO:0008595	Anterior/Posterior Axis Specification, Embryo	0.02160
GO:0010518	Positive Regulation Of Phospholipase Activity	0.02160
GO:0014905	Myoblast Fusion Involved In Skeletal Muscle Regeneration	0.02160
GO:0014910	Regulation Of Smooth Muscle Cell Migration	0.02160
GO:0021555	Midbrain-Hindbrain Boundary Morphogenesis	0.02160
GO:0021615	Glossopharyngeal Nerve Morphogenesis	0.02160
GO:0030050	Vesicle Transport Along Actin Filament	0.02160
GO:0030323	Respiratory Tube Development	0.02160
GO:0030858	Positive Regulation Of Epithelial Cell Differentiation	0.02160
GO:0038170	Somatostatin Signaling Pathway	0.02160
GO:0043374	Cd8-Positive, Alpha-Beta T Cell Differentiation	0.02160
GO:0045061	Thymic T Cell Selection	0.02160
GO:0046546	Development Of Primary Male Sexual Characteristics	0.02160
GO:0048341	Paraxial Mesoderm Formation	0.02160
GO:0048570	Notochord Morphogenesis	0.02160
GO:0060033	Anatomical Structure Regression	0.02160
GO:0060363	Cranial Suture Morphogenesis	0.02160
GO:0060676	Ureteric Bud Formation	0.02160
GO:0061138	Morphogenesis Of A Branching Epithelium	0.02160
GO:0061309	Cardiac Neural Crest Cell Development Involved In Outflow Tract Morphogenesis	0.02160
GO:0061312	Bmp Signaling Pathway Involved In Heart Development	0.02160
GO:0071709	Membrane Assembly	0.02160
GO:0072107	Positive Regulation Of Ureteric Bud Formation	0.02160
GO:0072201	Negative Regulation Of Mesenchymal Cell Proliferation	0.02160
GO:0086015	Sa Node Cell Action Potential	0.02160
GO:1900020	Positive Regulation Of Protein Kinase C Activity	0.02160
GO:1903979	Negative Regulation Of Microglial Cell Activation	0.02160
GO:2001137	Positive Regulation Of Endocytic Recycling	0.02160
GO:0042795	Snrna Transcription By Rna Polymerase Ii	0.02262
GO:0001893	Maternal Placenta Development	0.02486
GO:0006646	Phosphatidylethanolamine Biosynthetic Process	0.02486
GO:0016188	Synaptic Vesicle Maturation	0.02486
GO:0021953	Central Nervous System Neuron Differentiation	0.02486
GO:0035239	Tube Morphogenesis	0.02486
GO:0038066	P38Mapk Cascade	0.02486
GO:0048702	Embryonic Neurocranium Morphogenesis	0.02486
GO:0060426	Lung Vasculature Development	0.02486
GO:0060430	Lung Sacculle Development	0.02486
GO:1902732	Positive Regulation Of Chondrocyte Proliferation	0.02486
GO:2000394	Positive Regulation Of Lamellipodium Morphogenesis	0.02486
GO:2000810	Regulation Of Bicellular Tight Junction Assembly	0.02486

Biological Process GO continued (DvOP5, n=186)		FDR (q-value)
GO:0010719	Negative Regulation Of Epithelial To Mesenchymal Transition	0.02715
GO:0043542	Endothelial Cell Migration	0.02715
GO:0060021	Roof Of Mouth Development	0.02750
GO:0071542	Dopaminergic Neuron Differentiation	0.02893
GO:0042476	Odontogenesis	0.03172
GO:0060349	Bone Morphogenesis	0.03172
GO:0023019	Signal Transduction Involved In Regulation Of Gene Expression	0.03909
GO:0035050	Embryonic Heart Tube Development	0.03909
GO:0035909	Aorta Morphogenesis	0.03909
GO:0045668	Negative Regulation Of Osteoblast Differentiation	0.04003
GO:0006909	Phagocytosis	0.04003

Cellular Component GO terms enriched in DvOP5

Cellular Component GO (DvOP5, n=7)		FDR (q-value)
GO:0005610	Laminin-5 Complex	0.00000
GO:0005899	Insulin Receptor Complex	0.00000
GO:0031095	Platelet Dense Tubular Network Membrane	0.00000
GO:0048787	Presynaptic Active Zone Membrane	0.00000
GO:0065010	Extracellular Membrane-Bounded Organelle	0.00000
GO:0044309	Neuron Spine	0.04782
GO:0098839	Postsynaptic Density Membrane	0.04782

Molecular Function GO terms enriched in DvOP5

Molecular Function GO (DvOP5, n=30)		FDR (q-value)
GO:0008401	Retinoic Acid 4-Hydroxylase Activity	0.00000
GO:0044323	Retinoic Acid-Responsive Element Binding	0.00000
GO:0001515	Opioid Peptide Activity	0.00000
GO:0002153	Steroid Receptor Rna Activator Rna Binding	0.00000
GO:0003958	Nadph-Hemoprotein Reductase Activity	0.00000
GO:0004067	Asparaginase Activity	0.00000
GO:0004144	Diacylglycerol O-Acyltransferase Activity	0.00000
GO:0004305	Ethanolamine Kinase Activity	0.00000
GO:0005250	A-Type (Transient Outward) Potassium Channel Activity	0.00000
GO:0008481	Sphinganine Kinase Activity	0.00000
GO:0008934	Inositol Monophosphate 1-Phosphatase Activity	0.00000
GO:0009374	Biotin Binding	0.00000
GO:0015651	Quaternary Ammonium Group Transmembrane Transporter Activity	0.00000
GO:0016520	Growth Hormone-Releasing Hormone Receptor Activity	0.00000
GO:0017050	D-Erythro-Sphingosine Kinase Activity	0.00000
GO:0034988	Fc-Gamma Receptor I Complex Binding	0.00000
GO:0050436	Microfibril Binding	0.00000
GO:0052832	Inositol Monophosphate 3-Phosphatase Activity	0.00000
GO:0052834	Inositol Monophosphate Phosphatase Activity	0.00000
GO:0001972	Retinoic Acid Binding	0.00010
GO:0043565	Sequence-Specific Dna Binding	0.00042
GO:0005089	Rho Guanyl-Nucleotide Exchange Factor Activity	0.00082
GO:0004668	Protein-Arginine Deiminase Activity	0.00404
GO:0032050	Clathrin Heavy Chain Binding	0.00404
GO:0000981	Dna-Binding Transcription Factor Activity, Rna Polymerase Ii-Specific	0.01688
GO:0004994	Somatostatin Receptor Activity	0.01688
GO:0016208	Amp Binding	0.01688
GO:0038036	Sphingosine-1-Phosphate Receptor Activity	0.01908
GO:0048185	Activin Binding	0.01908
GO:0003700	Dna-Binding Transcription Factor Activity	0.02271

Biological Process GO terms enriched in LvLFF4

Biological Process GO (LvLFF4, n=193)		FDR (q-value)
GO:0018101	Protein Citrullination	0.00000
GO:0045199	Maintenance Of Epithelial Cell Apical/Basal Polarity	0.00000
GO:0051918	Negative Regulation Of Fibrinolysis	0.00000
GO:0003170	Heart Valve Development	0.00000
GO:0045061	Thymic T Cell Selection	0.00000
GO:0006021	Inositol Biosynthetic Process	0.00000
GO:0021914	Regulation Of Smoothened Signaling Pathway In Ventral Spinal Cord Patterning	0.00000
GO:0031077	Post-Embryonic Camera-Type Eye Development	0.00000
GO:0034334	Adherens Junction Maintenance	0.00000
GO:0045064	T-Helper 2 Cell Differentiation	0.00000
GO:0045446	Endothelial Cell Differentiation	0.00000
GO:0048793	Pronephros Development	0.00000
GO:0060414	Aorta Smooth Muscle Tissue Morphogenesis	0.00000
GO:0060743	Epithelial Cell Maturation Involved In Prostate Gland Development	0.00000
GO:0061314	Notch Signaling Involved In Heart Development	0.00000
GO:0072034	Renal Vesicle Induction	0.00000
GO:0072676	Lymphocyte Migration	0.00000
GO:0097553	Calcium Ion Transmembrane Import Into Cytosol	0.00000
GO:1902255	Positive Regulation Of Intrinsic Apoptotic Signaling Pathway By P53 Class Mediator	0.00000
GO:1902474	Positive Regulation Of Protein Localization To Synapse	0.00000
GO:1903936	Cellular Response To Sodium Arsenite	0.00000
GO:0000294	Nuclear-Transcribed Mrna Catabolic Process, Endonucleolytic Cleavage-Dependent Decay	0.00000
GO:0001838	Embryonic Epithelial Tube Formation	0.00000
GO:0002415	Immunoglobulin Transcytosis In Epithelial Cells Mediated	0.00000
GO:0002418	Immune Response To Tumor Cell	0.00000
GO:0003253	Cardiac Neural Crest Cell Migration Involved In Outflow Tract Morphogenesis	0.00000
GO:0003335	Corneocyte Development	0.00000
GO:0003401	Axis Elongation	0.00000
GO:0003415	Chondrocyte Hypertrophy	0.00000
GO:0006222	Ump Biosynthetic Process	0.00000
GO:0006534	Cysteine Metabolic Process	0.00000
GO:0006572	Tyrosine Catabolic Process	0.00000
GO:0006972	Hyperosmotic Response	0.00000
GO:0008050	Female Courtship Behavior	0.00000
GO:0010734	Negative Regulation Of Protein Glutathionylation	0.00000
GO:0010899	Regulation Of Phosphatidylcholine Catabolic Process	0.00000
GO:0010957	Negative Regulation Of Vitamin D Biosynthetic Process	0.00000
GO:0015705	Iodide Transport	0.00000
GO:0015746	Citrate Transport	0.00000
GO:0016577	Histone Demethylation	0.00000
GO:0017038	Protein Import	0.00000
GO:0019100	Male Germ-Line Sex Determination	0.00000
GO:0021546	Rhombomere Development	0.00000
GO:0021681	Cerebellar Granular Layer Development	0.00000
GO:0021740	Principal Sensory Nucleus Of Trigeminal Nerve Development	0.00000
GO:0021782	Glial Cell Development	0.00000
GO:0021891	Olfactory Bulb Interneuron Development	0.00000
GO:0021913	Transcription From RNAP II Promoter In Ventral Spinal Cord Interneuron Specification	0.00000
GO:0021937	Cerebellar Purkinje Regulation Of Granule Cell Precursor Cell Proliferation	0.00000
GO:0021986	Habenula Development	0.00000
GO:0030431	Sleep	0.00000
GO:0030852	Regulation Of Granulocyte Differentiation	0.00000
GO:0032232	Negative Regulation Of Actin Filament Bundle Assembly	0.00000
GO:0032286	Central Nervous System Myelin Maintenance	0.00000
GO:0032401	Establishment Of Melanosome Localization	0.00000
GO:0032770	Positive Regulation Of Monooxygenase Activity	0.00000
GO:0032902	Nerve Growth Factor Production	0.00000
GO:0032912	Negative Regulation Of Transforming Growth Factor Beta2 Production	0.00000
GO:0032959	Inositol Trisphosphate Biosynthetic Process	0.00000
GO:0033058	Directional Locomotion	0.00000
GO:0034616	Response To Laminar Fluid Shear Stress	0.00000
GO:0035459	Vesicle Cargo Loading	0.00000
GO:0035926	Chemokine (C-C Motif) Ligand 2 Secretion	0.00000
GO:0035989	Tendon Development	0.00000
GO:0036343	Psychomotor Behavior	0.00000
GO:0036413	Histone H3-R26 Citrullination	0.00000
GO:0042420	Dopamine Catabolic Process	0.00000
GO:0043370	Regulation Of Cd4-Positive, Alpha-Beta T Cell Differentiation	0.00000
GO:0048170	Positive Regulation Of Long-Term Neuronal Synaptic Plasticity	0.00000
GO:0048194	Golgi Vesicle Budding	0.00000
GO:0048385	Regulation Of Retinoic Acid Receptor Signaling Pathway	0.00000
GO:0048562	Embryonic Organ Morphogenesis	0.00000
GO:0048563	Post-Embryonic Animal Organ Morphogenesis	0.00000
GO:0048871	Multicellular Organismal Homeostasis	0.00000
GO:0050779	Rna Destabilization	0.00000
GO:0051046	Regulation Of Secretion	0.00000
GO:0051389	Inactivation Of Mapk Activity	0.00000
GO:0051656	Establishment Of Organelle Localization	0.00000
GO:0055005	Ventricular Cardiac Myofibril Assembly	0.00000
GO:0060023	Soft Palate Development	0.00000
GO:0060026	Convergent Extension	0.00000
GO:0060067	Cervix Development	0.00000
GO:0060073	Micturition	0.00000
GO:0060157	Urinary Bladder Development	0.00000
GO:0060214	Endocardium Formation	0.00000

Biological Process GO continued (LvLFF4, n=193)		FDR (q-value)
GO:0060221	Retinal Rod Cell Differentiation	0.00000
GO:0060421	Positive Regulation Of Heart Growth	0.00000
GO:0060434	Bronchus Morphogenesis	0.00000
GO:0060545	Positive Regulation Of Necroptotic Process	0.00000
GO:0060775	Planar Cell Polarity Pathway Involved In Gastrula Mediolateral Intercalation	0.00000
GO:0061032	Visceral Serous Pericardium Development	0.00000
GO:0061146	Peyer'S Patch Morphogenesis	0.00000
GO:0061771	Response To Caloric Restriction	0.00000
GO:0070141	Response To Uv-A	0.00000
GO:0070563	Negative Regulation Of Vitamin D Receptor Signaling Pathway	0.00000
GO:0071305	Cellular Response To Vitamin D	0.00000
GO:0071477	Cellular Hypotonic Salinity Response	0.00000
GO:0071642	Positive Regulation Of Macrophage Inflammatory Protein 1 Alpha Production	0.00000
GO:0071896	Protein Localization To Adherens Junction	0.00000
GO:0072086	Specification Of Loop Of Henle Identity	0.00000
GO:0072179	Nephric Duct Formation	0.00000
GO:0072190	Ureter Urothelium Development	0.00000
GO:0072289	Metanephric Nephron Tubule Formation	0.00000
GO:0072674	Multinuclear Osteoclast Differentiation	0.00000
GO:0072752	Cellular Response To Rapamycin	0.00000
GO:0090118	Receptor-Mediated Endocytosis Involved In Cholesterol Transport	0.00000
GO:0090164	Asymmetric Golgi Ribbon Formation	0.00000
GO:0097049	Motor Neuron Apoptotic Process	0.00000
GO:0097340	Inhibition Of Cysteine-Type Endopeptidase Activity	0.00000
GO:0098698	Postsynaptic Specialization Assembly	0.00000
GO:0099039	Sphingolipid Translocation	0.00000
GO:1901228	Regulation Of Transcription From Rna Polymerase Ii Promoter Involved In Heart Development	0.00000
GO:1901382	Regulation Of Chorionic Trophoblast Cell Proliferation	0.00000
GO:1901991	Negative Regulation Of Mitotic Cell Cycle Phase Transition	0.00000
GO:1902513	Regulation Of Organelle Transport Along Microtubule	0.00000
GO:1902595	Regulation Of Dna Replication Origin Binding	0.00000
GO:1902991	Regulation Of Amyloid Precursor Protein Catabolic Process	0.00000
GO:1902995	Positive Regulation Of Phospholipid Efflux	0.00000
GO:1903401	L-Lysine Transmembrane Transport	0.00000
GO:1903539	Protein Localization To Postsynaptic Membrane	0.00000
GO:1903984	Positive Regulation Of Trail-Activated Apoptotic Signaling Pathway	0.00000
GO:1905167	Positive Regulation Of Lysosomal Protein Catabolic Process	0.00000
GO:2000276	Negative Regulation Of Oxidative Phosphorylation Uncoupler Activity	0.00000
GO:2000329	Negative Regulation Of T-Helper 17 Cell Lineage Commitment	0.00000
GO:2000392	Regulation Of Lamellipodium Morphogenesis	0.00000
GO:2000563	Positive Regulation Of Cd4-Positive, Alpha-Beta T Cell Proliferation	0.00000
GO:2000675	Negative Regulation Of Type B Pancreatic Cell Apoptotic Process	0.00000
GO:2000677	Regulation Of Transcription Regulatory Region Dna Binding	0.00000
GO:2001257	Regulation Of Cation Channel Activity	0.00000
GO:0006536	Glutamate Metabolic Process	0.00153
GO:0010596	Negative Regulation Of Endothelial Cell Migration	0.00495
GO:0046902	Regulation Of Mitochondrial Membrane Permeability	0.00495
GO:0051246	Regulation Of Protein Metabolic Process	0.00495
GO:0072197	Ureter Morphogenesis	0.00495
GO:1902732	Positive Regulation Of Chondrocyte Proliferation	0.00495
GO:2000394	Positive Regulation Of Lamellipodium Morphogenesis	0.00495
GO:0001709	Cell Fate Determination	0.01114
GO:0001776	Leukocyte Homeostasis	0.01584
GO:0003337	Mesenchymal To Epithelial Transition Involved In Metanephros Morphogenesis	0.01584
GO:0009410	Response To Xenobiotic Stimulus	0.01584
GO:0010757	Negative Regulation Of Plasminogen Activation	0.01584
GO:0015812	Gamma-Aminobutyric Acid Transport	0.01584
GO:0060390	Regulation Of Smad Protein Signal Transduction	0.01584
GO:0061304	Retinal Blood Vessel Morphogenesis	0.01584
GO:0070100	Negative Regulation Of Chemokine-Mediated Signaling Pathway	0.01584
GO:0070508	Cholesterol Import	0.01584
GO:0071371	Cellular Response To Gonadotropin Stimulus	0.01584
GO:0072189	Ureter Development	0.01584
GO:0098719	Sodium Ion Import Across Plasma Membrane	0.01584
GO:2000647	Negative Regulation Of Stem Cell Proliferation	0.01584
GO:2000669	Negative Regulation Of Dendritic Cell Apoptotic Process	0.01584
GO:2001046	Positive Regulation Of Integrin-Mediated Signaling Pathway	0.01584
GO:0014067	Negative Regulation Of Phosphatidylinositol 3-Kinase Signaling	0.02493
GO:0030836	Positive Regulation Of Actin Filament Depolymerization	0.02493
GO:0032330	Regulation Of Chondrocyte Differentiation	0.02493
GO:0034115	Negative Regulation Of Heterotypic Cell-Cell Adhesion	0.02493
GO:0034383	Low-Density Lipoprotein Particle Clearance	0.02493
GO:0070166	Enamel Mineralization	0.02493
GO:2000178	Negative Regulation Of Neural Precursor Cell Proliferation	0.02493
GO:0032331	Negative Regulation Of Chondrocyte Differentiation	0.02549
GO:0042474	Middle Ear Morphogenesis	0.02549
GO:0030878	Thyroid Gland Development	0.04259
GO:0035115	Embryonic Forelimb Morphogenesis	0.04348
GO:0045599	Negative Regulation Of Fat Cell Differentiation	0.04707
GO:0001957	Intramembranous Ossification	0.04941
GO:0002819	Regulation Of Adaptive Immune Response	0.04941
GO:0008595	Anterior/Posterior Axis Specification, Embryo	0.04941
GO:0010172	Embryonic Body Morphogenesis	0.04941
GO:0010518	Positive Regulation Of Phospholipase Activity	0.04941
GO:0010907	Positive Regulation Of Glucose Metabolic Process	0.04941
GO:0021615	Glossopharyngeal Nerve Morphogenesis	0.04941
GO:0030050	Vesicle Transport Along Actin Filament	0.04941
GO:0030859	Polarized Epithelial Cell Differentiation	0.04941
GO:0034653	Retinoic Acid Catabolic Process	0.04941
GO:0035087	Sirna Loading Onto Risc Involved In Rna Interference	0.04941
GO:0035456	Response To Interferon-Beta	0.04941
GO:0035754	B Cell Chemotaxis	0.04941

Biological Process GO continued (LvLFF4, n=193)		FDR (q-value)
GO:0043304	Regulation Of Mast Cell Degranulation	0.04941
GO:0043374	Cd8-Positive, Alpha-Beta T Cell Differentiation	0.04941
GO:0048341	Paraxial Mesoderm Formation	0.04941
GO:0055012	Ventricular Cardiac Muscle Cell Differentiation	0.04941
GO:0060033	Anatomical Structure Regression	0.04941
GO:0060040	Retinal Bipolar Neuron Differentiation	0.04941
GO:0060509	Type I Pneumocyte Differentiation	0.04941
GO:0061309	Cardiac Neural Crest Cell Development Involved In Outflow Tract Morphogenesis	0.04941
GO:0071376	Cellular Response To Corticotropin-Releasing Hormone Stimulus	0.04941
GO:0072107	Positive Regulation Of Ureteric Bud Formation	0.04941
GO:0072207	Metanephric Epithelium Development	0.04941
GO:0072284	Metanephric S-Shaped Body Morphogenesis	0.04941
GO:0072383	Plus-End-Directed Vesicle Transport Along Microtubule	0.04941
GO:0086015	Sa Node Cell Action Potential	0.04941
GO:0090129	Positive Regulation Of Synapse Maturation	0.04941
GO:2000391	Positive Regulation Of Neutrophil Extravasation	0.04941

Cellular Component GO terms enriched in LvLFF4

Cellular Component GO (LvLFF4, n=12)		FDR (q-value)
GO:0033093	Weibel-Palade Body	0.00000
GO:0035976	Transcription Factor Ap-1 Complex	0.00000
GO:0005608	Laminin-3 Complex	0.00000
GO:0005899	Insulin Receptor Complex	0.00000
GO:0017109	Glutamate-Cysteine Ligase Complex	0.00000
GO:0031095	Platelet Dense Tubular Network Membrane	0.00000
GO:0036501	Ufd1-Npl4 Complex	0.00000
GO:0043256	Laminin Complex	0.00000
GO:0048787	Presynaptic Active Zone Membrane	0.00000
GO:0062157	Mitochondrial Atp-Gated Potassium Channel Complex	0.00000
GO:0065010	Extracellular Membrane-Bounded Organelle	0.00000
GO:0097059	Cntrf-Clc1 Complex	0.00000

Molecular Function GO terms enriched in LvLFF4

Molecular Function GO (LvLFF4, n=43)		FDR (q-value)
GO:0004668	Protein-Arginine Deiminase Activity	0.00000
GO:0005332	Gamma-Aminobutyric Acid:Sodium Symporter Activity	0.00000
GO:0016208	Amp Binding	0.00000
GO:0004704	Nf-Kappab-Inducing Kinase Activity	0.00000
GO:0016614	Oxidoreductase Activity, Acting On Ch-OH Group Of Donors	0.00000
GO:0022849	Glutamate-Gated Calcium Ion Channel Activity	0.00000
GO:0044323	Retinoic Acid-Responsive Element Binding	0.00000
GO:0002153	Steroid Receptor Rna Activator Rna Binding	0.00000
GO:0003958	Nadph-Hemoprotein Reductase Activity	0.00000
GO:0004067	Asparaginase Activity	0.00000
GO:0004140	Dephospho-Coa Kinase Activity	0.00000
GO:0004144	Diacylglycerol O-Acyltransferase Activity	0.00000
GO:0004305	Ethanolamine Kinase Activity	0.00000
GO:0004345	Glucose-6-Phosphate Dehydrogenase Activity	0.00000
GO:0004357	Glutamate-Cysteine Ligase Activity	0.00000
GO:0004445	Inositol-Polyphosphate 5-Phosphatase Activity	0.00000
GO:0008481	Sphinganine Kinase Activity	0.00000
GO:0008934	Inositol Monophosphate 1-Phosphatase Activity	0.00000
GO:0009374	Biotin Binding	0.00000
GO:0015111	Iodide Transmembrane Transporter Activity	0.00000
GO:0016520	Growth Hormone-Releasing Hormone Receptor Activity	0.00000
GO:0017050	D-Erythro-Sphingosine Kinase Activity	0.00000
GO:0019911	Structural Constituent Of Myelin Sheath	0.00000
GO:0030298	Receptor Signaling Protein Tyrosine Kinase Activator Activity	0.00000
GO:0034188	Apolipoprotein A-I Receptor Activity	0.00000
GO:0034988	Fc-Gamma Receptor I Complex Binding	0.00000
GO:0036313	Phosphatidylinositol 3-Kinase Catalytic Subunit Binding	0.00000
GO:0052832	Inositol Monophosphate 3-Phosphatase Activity	0.00000
GO:0052834	Inositol Monophosphate Phosphatase Activity	0.00000
GO:0072345	Naadp-Sensitive Calcium-Release Channel Activity	0.00000
GO:0090556	Phosphatidylserine Floppase Activity	0.00000
GO:0098808	Mrna Cap Binding	0.00000
GO:1905573	Ganglioside Gm1 Binding	0.00000
GO:0005089	Rho Guanyl-Nucleotide Exchange Factor Activity	0.00228
GO:0043565	Sequence-Specific Dna Binding	0.00404
GO:0001972	Retinoic Acid Binding	0.00739
GO:0005123	Death Receptor Binding	0.01149
GO:0071889	14-3-3 Protein Binding	0.03797
GO:0004966	Galanin Receptor Activity	0.03797
GO:0004972	Nmda Glutamate Receptor Activity	0.03797
GO:0005222	Intracellular Camp-Activated Cation Channel Activity	0.03797
GO:0034186	Apolipoprotein A-I Binding	0.03797
GO:0047961	Glycine N-Acyltransferase Activity	0.03797

Appendix 5.3 Enriched 'Sequence-specific DNA binding' GO term

Common differentially methylated genes enriched in GO:0043565

GO:0043565 Transcription factor genes in common (n=104)		
ENSOARG00000000046	<i>LHX1</i>	<i>Lim Homeobox 1</i>
ENSOARG00000000266	<i>BCL11B</i>	<i>Baf Chromatin Remodeling Complex Subunit Bcl11B</i>
ENSOARG00000000544	<i>ELF3</i>	<i>E74 Like Ets Transcription Factor 3</i>
ENSOARG00000000992	<i>VSX2</i>	<i>Visual System Homeobox 2</i>
ENSOARG00000002241	<i>CSRNP1</i>	<i>Cysteine And Serine Rich Nuclear Protein 1</i>
ENSOARG00000002366	<i>RXRA</i>	<i>Retinoid X Receptor Alpha</i>
ENSOARG00000002449	<i>SP5</i>	<i>Sp5 Transcription Factor</i>
ENSOARG00000002613	<i>SHOX2</i>	<i>Short Stature Homeobox 2</i>
ENSOARG00000002740	<i>HSF4</i>	<i>Heat Shock Transcription Factor 4</i>
ENSOARG00000002778		
ENSOARG00000003151	<i>FOX11</i>	<i>Forkhead Box I1</i>
ENSOARG00000003363		
ENSOARG00000003437	<i>PITX2</i>	<i>Paired Like Homeodomain 2</i>
ENSOARG00000003669	<i>ZFHX3</i>	<i>Zinc Finger Homeobox 3</i>
ENSOARG00000003822	<i>IRF4</i>	<i>Interferon Regulatory Factor 4</i>
ENSOARG00000003928	<i>HNF4A</i>	<i>Hepatocyte Nuclear Factor 4 Alpha</i>
ENSOARG00000004153	<i>NKX2-5</i>	<i>Nk2 Homeobox 5</i>
ENSOARG00000004347	<i>MSX2</i>	<i>Msh Homeobox 2</i>
ENSOARG00000004745	<i>USF2</i>	<i>Upstream Transcription Factor 2, C-Fos Interacting</i>
ENSOARG00000004750	<i>LHX3</i>	<i>Lim Homeobox 3</i>
ENSOARG00000004863	<i>TBXT</i>	<i>T-Box Transcription Factor T</i>
ENSOARG00000005070	<i>FOXA2</i>	<i>Forkhead Box A2</i>
ENSOARG00000005301	<i>HLF</i>	<i>Hlf Transcription Factor, Par Bzip Family Member</i>
ENSOARG00000005572	<i>DLX4</i>	<i>Distal-Less Homeobox 4</i>
ENSOARG00000005637	<i>ETV4</i>	<i>Ets Variant Transcription Factor 4</i>
ENSOARG00000006012		
ENSOARG00000006034	<i>SIX2</i>	<i>Six Homeobox 2</i>
ENSOARG00000006249	<i>TBX3</i>	<i>T-Box Transcription Factor 3</i>
ENSOARG00000006262	<i>BCL2</i>	<i>Bcl2 Apoptosis Regulator</i>
ENSOARG00000006541	<i>LONP1</i>	<i>Lon Peptidase 1, Mitochondrial</i>
ENSOARG00000006553	<i>SPI1</i>	<i>Spi-1 Proto-Oncogene</i>
ENSOARG00000006704	<i>ETV3</i>	<i>Ets Translocation Variant 3</i>
ENSOARG00000007034	<i>HOXB5</i>	<i>Homeobox B5</i>
ENSOARG00000007078	<i>LHX5</i>	<i>Lim Homeobox 5</i>
ENSOARG00000007106	<i>HOXB3</i>	<i>Homeobox B3</i>
ENSOARG00000007140	<i>HNF4G</i>	<i>Hepatocyte Nuclear Factor 4 Gamma</i>
ENSOARG00000007388	<i>MSX1</i>	<i>Msh Homeobox 1</i>
ENSOARG00000007984	<i>NR4A2</i>	<i>Nuclear Receptor Subfamily 4 Group A Member 2</i>
ENSOARG00000008034	<i>MAF</i>	<i>Maf Bzip Transcription Factor</i>
ENSOARG00000008192	<i>FOXA1</i>	<i>Forkhead Box A1</i>
ENSOARG00000008269	<i>GATA6</i>	<i>Gata Binding Protein 6</i>
ENSOARG00000008350	<i>ISL1</i>	<i>Isl Lim Homeobox 1</i>
ENSOARG00000008922	<i>ANHX</i>	<i>Anomalous Homeobox</i>
ENSOARG00000009439	<i>EVX1</i>	<i>Even-Skipped Homeobox 1</i>
ENSOARG00000009717		
ENSOARG00000009789		
ENSOARG00000009797	<i>HOXA3</i>	<i>Homeobox A3</i>
ENSOARG00000009842	<i>HOXA2</i>	<i>Homeobox A2</i>
ENSOARG00000009878	<i>MEF2A</i>	<i>Myocyte Enhancer Factor 2A</i>
ENSOARG00000010006	<i>POU5F1</i>	<i>Pou Class 5 Homeobox 1</i>
ENSOARG00000010167		
ENSOARG00000010199	<i>EGR3</i>	<i>Early Growth Response 3</i>

GO:0043565 Transcription factor genes in common continued (n=104)		
ENSOARG00000010587	<i>PAX7</i>	Paired Box 7
ENSOARG00000010741	<i>FOXO3</i>	Forkhead Box O3
ENSOARG00000010751	<i>SPDEF</i>	Sam Pointed Domain Containing Ets Transcription Factor
ENSOARG00000011193	<i>FOXE1</i>	Forkhead Box E1
ENSOARG00000011249	<i>VAX2</i>	Ventral Anterior Homeobox 2
ENSOARG00000011324	<i>LMX1A</i>	Lim Homeobox Transcription Factor 1 Alpha
ENSOARG00000011785	<i>PPARD</i>	Peroxisome Proliferator Activated Receptor Delta
ENSOARG00000012314		
ENSOARG00000012459		
ENSOARG00000012571	<i>SOX30</i>	Sry-Box Transcription Factor 30
ENSOARG00000013030	<i>SNAI2</i>	Snail Family Transcriptional Repressor 2
ENSOARG00000013052	<i>GLI2</i>	Gli Family Zinc Finger 2
ENSOARG00000013102	<i>ETS1</i>	Ets Proto-Oncogene 1, Transcription Factor
ENSOARG00000013174	<i>SNAI1</i>	Snail Family Transcriptional Repressor 1
ENSOARG00000013206		
ENSOARG00000013245	<i>DMRT2</i>	Doublesex And Mab-3 Related Transcription Factor 2
ENSOARG00000013693		
ENSOARG00000013742	<i>LHX2</i>	Lim Homeobox 2
ENSOARG00000013779	<i>SOX9</i>	Sry-Box Transcription Factor 9
ENSOARG00000013941	<i>GATA3</i>	Gata Binding Protein 3
ENSOARG00000014119	<i>RARA</i>	Retinoic Acid Receptor Alpha
ENSOARG00000014239	<i>NFATC2</i>	Nuclear Factor Of Activated T Cells 2
ENSOARG00000014473	<i>SOX8</i>	Sry-Box Transcription Factor 8
ENSOARG00000014532	<i>ETS2</i>	Ets Proto-Oncogene 2, Transcription Factor
ENSOARG00000014667	<i>PITX1</i>	Paired Like Homeodomain 1
ENSOARG00000015228	<i>GATA4</i>	Gata Binding Protein 4
ENSOARG00000015328	<i>MTA2</i>	Metastasis Associated 1 Family Member 2
ENSOARG00000015356	<i>ELF4</i>	E74 Like Ets Transcription Factor 4
ENSOARG00000015439	<i>LHX9</i>	Lim Homeobox 9
ENSOARG00000015662	<i>BARHL2</i>	Barh Like Homeobox 2
ENSOARG00000015980	<i>NR5A2</i>	Nuclear Receptor Subfamily 5 Group A Member 2
ENSOARG00000016041	<i>FOXN4</i>	Forkhead Box N4
ENSOARG00000016067	<i>MKX</i>	Mohawk Homeobox
ENSOARG00000016074	<i>ZNF281</i>	Zinc Finger Protein 281
ENSOARG00000016191	<i>PAX6</i>	Paired Box 6
ENSOARG00000016331	<i>HOXC10</i>	Homeobox C10
ENSOARG00000017214	<i>NR4A1</i>	Nuclear Receptor Subfamily 4 Group A Member 1
ENSOARG00000017237	<i>PRDM16</i>	Pr/Set Domain 16
ENSOARG00000017472	<i>HOXD3</i>	Homeobox D3
ENSOARG00000017581	<i>KDM6B</i>	Lysine Demethylase 6B
ENSOARG00000017630	<i>NR2F6</i>	Nuclear Receptor Subfamily 2 Group F Member 6
ENSOARG00000017964	<i>IRX3</i>	Iroquois Homeobox 3
ENSOARG00000018027	<i>IRX6</i>	Iroquois Homeobox 6
ENSOARG00000018238	<i>TEF</i>	Tef Transcription Factor, Par Bzip Family Member
ENSOARG00000018550	<i>EMX2</i>	Empty Spiracles Homeobox 2
ENSOARG00000018722	<i>HDAC4</i>	Histone Deacetylase 4
ENSOARG00000018997	<i>GSX2</i>	Gs Homeobox 2
ENSOARG00000019395	<i>ALX3</i>	Alx Homeobox 3
ENSOARG00000019427	<i>PPARA</i>	Peroxisome Proliferator Activated Receptor Alpha
ENSOARG00000020097	<i>OTX1</i>	Orthodenticle Homeobox 1
ENSOARG00000021060	<i>RORC</i>	Rar Related Orphan Receptor C
ENSOARG00000021129	<i>SIX1</i>	Six Homeobox 1
ENSOARG00000000046	<i>LHX1</i>	Lim Homeobox 1
ENSOARG00000000266	<i>BCL11B</i>	Baf Chromatin Remodeling Complex Subunit Bcl11B
ENSOARG000000000544	<i>ELF3</i>	E74 Like Ets Transcription Factor 3
ENSOARG000000000992	<i>VSX2</i>	Visual System Homeobox 2
ENSOARG000000002241	<i>CSRNP1</i>	Cysteine And Serine Rich Nuclear Protein 1

GO:0043565 Transcription factor genes in common continued (n=104)		
ENSOARG00000002366	<i>RXRA</i>	<i>Retinoid X Receptor Alpha</i>
ENSOARG00000002449	<i>SP5</i>	<i>Sp5 Transcription Factor</i>
ENSOARG00000002613	<i>SHOX2</i>	<i>Short Stature Homeobox 2</i>
ENSOARG00000002740	<i>HSF4</i>	<i>Heat Shock Transcription Factor 4</i>
ENSOARG00000002778		
ENSOARG00000003151	<i>FOXI1</i>	<i>Forkhead Box I1</i>
ENSOARG00000003363	<i>FOXN3</i>	<i>Forkhead box N3</i>
ENSOARG00000003437	<i>PITX2</i>	<i>Paired Like Homeodomain 2</i>
ENSOARG00000003669	<i>ZFH3</i>	<i>Zinc Finger Homeobox 3</i>
ENSOARG00000003822	<i>IRF4</i>	<i>Interferon Regulatory Factor 4</i>
ENSOARG00000003928	<i>HNF4A</i>	<i>Hepatocyte Nuclear Factor 4 Alpha</i>
ENSOARG00000004153	<i>NKX2-5</i>	<i>Nk2 Homeobox 5</i>
ENSOARG00000004347	<i>MSX2</i>	<i>Msh Homeobox 2</i>
ENSOARG00000004745	<i>USF2</i>	<i>Upstream Transcription Factor 2, C-Fos Interacting</i>
ENSOARG00000004750	<i>LHX3</i>	<i>Lim Homeobox 3</i>
ENSOARG00000004863	<i>TBXT</i>	<i>T-Box Transcription Factor T</i>
ENSOARG00000005070	<i>FOXA2</i>	<i>Forkhead Box A2</i>
ENSOARG00000005301	<i>HLF</i>	<i>Hlf Transcription Factor, Par Bzip Family Member</i>
ENSOARG00000005572	<i>DLX4</i>	<i>Distal-Less Homeobox 4</i>
ENSOARG00000005637	<i>ETV4</i>	<i>Ets Variant Transcription Factor 4</i>
ENSOARG00000006012	<i>FOXO1</i>	<i>Forkhead box O1</i>
ENSOARG00000006034	<i>SIX2</i>	<i>Six Homeobox 2</i>
ENSOARG00000006249	<i>TBX3</i>	<i>T-Box Transcription Factor 3</i>
ENSOARG00000006262	<i>BCL2</i>	<i>Bcl2 Apoptosis Regulator</i>
ENSOARG00000006541	<i>LONP1</i>	<i>Lon Peptidase 1, Mitochondrial</i>
ENSOARG00000006553	<i>SPI1</i>	<i>Spi-1 Proto-Oncogene</i>
ENSOARG00000006704	<i>ETV3</i>	<i>Ets Translocation Variant 3</i>
ENSOARG00000007034	<i>HOXB5</i>	<i>Homeobox B5</i>
ENSOARG00000007078	<i>LHX5</i>	<i>Lim Homeobox 5</i>
ENSOARG00000007106	<i>HOXB3</i>	<i>Homeobox B3</i>
ENSOARG00000007140	<i>HNF4G</i>	<i>Hepatocyte Nuclear Factor 4 Gamma</i>
ENSOARG00000007388	<i>MSX1</i>	<i>Msh Homeobox 1</i>
ENSOARG00000007984	<i>NR4A2</i>	<i>Nuclear Receptor Subfamily 4 Group A Member 2</i>
ENSOARG00000008034	<i>MAF</i>	<i>Maf Bzip Transcription Factor</i>
ENSOARG00000008192	<i>FOXA1</i>	<i>Forkhead Box A1</i>
ENSOARG00000008269	<i>GATA6</i>	<i>Gata Binding Protein 6</i>
ENSOARG00000008350	<i>ISL1</i>	<i>Isl Lim Homeobox 1</i>
ENSOARG00000008922	<i>ANHX</i>	<i>Anomalous Homeobox</i>
ENSOARG00000009439	<i>EVX1</i>	<i>Even-Skipped Homeobox 1</i>
ENSOARG00000009717	<i>HOXA5</i>	<i>Homeobox protein Hox-A5</i>
ENSOARG00000009789	<i>HOXA4</i>	<i>Homeobox A4</i>
ENSOARG00000009797	<i>HOXA3</i>	<i>Homeobox A3</i>
ENSOARG00000009842	<i>HOXA2</i>	<i>Homeobox A2</i>
ENSOARG00000009878	<i>MEF2A</i>	<i>Myocyte Enhancer Factor 2A</i>
ENSOARG00000010006	<i>POU5F1</i>	<i>Pou Class 5 Homeobox 1</i>
ENSOARG00000010167	<i>NR2F2</i>	<i>Nuclear receptor subfamily 2, group F, member 2</i>
ENSOARG00000010199	<i>EGR3</i>	<i>Early Growth Response 3</i>
ENSOARG00000010587	<i>PAX7</i>	<i>Paired Box 7</i>
ENSOARG00000010741	<i>FOXO3</i>	<i>Forkhead Box O3</i>
ENSOARG00000010751	<i>SPDEF</i>	<i>Sam Pointed Domain Containing Ets Transcription Factor</i>
ENSOARG00000011193	<i>FOXE1</i>	<i>Forkhead Box E1</i>
ENSOARG00000011249	<i>VAX2</i>	<i>Ventral Anterior Homeobox 2</i>
ENSOARG00000011324	<i>LMX1A</i>	<i>Lim Homeobox Transcription Factor 1 Alpha</i>
ENSOARG00000011785	<i>PPARD</i>	<i>Peroxisome Proliferator Activated Receptor Delta</i>
ENSOARG00000012314	<i>EN1</i>	<i>Engrailed homeobox 1</i>
ENSOARG00000012459	<i>PDX1</i>	<i>Pancreatic and duodenal homeobox 1</i>
ENSOARG00000012571	<i>SOX30</i>	<i>Sry-Box Transcription Factor 30</i>

GO:0043565 Transcription factor genes in common continued (n=104)		
ENSOARG00000013030	<i>SNAI2</i>	<i>Snail Family Transcriptional Repressor 2</i>
ENSOARG00000013052	<i>GLI2</i>	<i>Gli Family Zinc Finger 2</i>
ENSOARG00000013102	<i>ETS1</i>	<i>Ets Proto-Oncogene 1, Transcription Factor</i>
ENSOARG00000013174	<i>SNAI1</i>	<i>Snail Family Transcriptional Repressor 1</i>
ENSOARG00000013206	<i>HLX</i>	<i>H2.0-like homeobox</i>
ENSOARG00000013245	<i>DMRT2</i>	<i>Doublesex And Mab-3 Related Transcription Factor 2</i>
ENSOARG00000013693		
ENSOARG00000013742	<i>LHX2</i>	<i>Lim Homeobox 2</i>
ENSOARG00000013779	<i>SOX9</i>	<i>Sry-Box Transcription Factor 9</i>
ENSOARG00000013941	<i>GATA3</i>	<i>Gata Binding Protein 3</i>
ENSOARG00000014119	<i>RARA</i>	<i>Retinoic Acid Receptor Alpha</i>
ENSOARG00000014239	<i>NFATC2</i>	<i>Nuclear Factor Of Activated T Cells 2</i>
ENSOARG00000014473	<i>SOX8</i>	<i>Sry-Box Transcription Factor 8</i>
ENSOARG00000014532	<i>ETS2</i>	<i>Ets Proto-Oncogene 2, Transcription Factor</i>
ENSOARG00000014667	<i>PITX1</i>	<i>Paired Like Homeodomain 1</i>

PIPS Reflective Statement

Note to examiners:

This statement is included as an appendix to the thesis in order that the thesis accurately captures the PhD training experienced by the candidate as a BBSRC Doctoral Training Partnership student.

The Professional Internship for PhD Students is a compulsory 3-month placement which must be undertaken by DTP students. It is usually centred on a specific project and must not be related to the PhD project. This reflective statement is designed to capture the skills development which has taken place during the student's placement and the impact on their career plans it has had.

My statement:

From June to September 2019, I undertook my professional internship at Delft University of Technology (TU Delft). My project aimed to publicise the efforts and achievements of the 'Data Champions'. The Data Champions are members of the research community at TU Delft who share a passion for knowledge exchange and a desire to build a collaborative and researcher-led community to drive the uptake of Open Science within their departments and institutes.

Currently, there are more than 50 Data Champions who volunteer their discipline-specific expertise, promote 'FAIR data' principles, advocate for good research data management (RDM) and advise academics about the proper handling of research data. In order to reward and recognise their exemplary work, I conducted one-to-one interviews with 11 Data Champions to learn about: i) their personal research; ii) how they effectively engage with researchers; iii) their motivations for joining the Data Champions programme; and, iv) their future goals and aspirations. Following each interview, I wrote, illustrated and published their personal stories as written case studies on the '[Open Working](#)' blog.

The case studies were shared on social media channels (Twitter and LinkedIn), and after receiving positive feedback from my colleagues I was asked to write a 'toolkit' to inspire and educate other institutions about how to implement a community-based model for RDM support. In collaboration with research support staff from TU Delft, the University of Cambridge (UK) and EPFL (Switzerland), the case studies and toolkit were published as an open access book titled '[The Real World of Research Data](#)'.

During my internship, I was invited to participate in a booksprint; a 3-day writing exercise alongside seven authors and editors. '[Engaging Researchers with Data Management: The Cookbook](#)' is a collection of 24 case studies drawn from institutions across the globe that demonstrate how to engage the research community with RDM. These case studies illustrate the variety of innovative strategies that institutions have developed to engage with their researchers about data management. To share our collective experience of the booksprint, I published a [blog article](#) to the Research Data Alliance (RDA) website.

Based on the success of my internship at TU Delft, I was invited to give a keynote talk about '[Community-based models to engage researchers with data management](#)' at the University of Vienna (Austria) in September 2019. In addition, I received an early career researcher grant to present my work at the 'RDA 14th Plenary' held in Helsinki (Finland) the following month (<https://rd-alliance.org/>). After writing about my internship in a Springer Nature article, '[Open Science Opens Doors: How #SciData18 helped me unlock career](#)

[opportunities](#)', I was invited to the 'Better Science through Better Data' #SciData19 Conference' held in London in November to give a [lightning talk](#).

I developed many personal and professional skills during my internship. Whilst both exhilarating and daunting, the opportunity to travel and work in the Netherlands for three months enabled me to leave my comfort zone and experience a new culture (although cycling and learning the Dutch language weren't my forte!)

I enjoyed the social aspect of my role in science communication and took great satisfaction in helping academic researchers share their personal stories with a wider audience. I developed my verbal and written skills whilst interviewing researchers, and was able to gather and assimilate relevant information to write articles to meet strict deadlines. I also found my creative confidence to produce illustrations to accompany my written articles.

I realised the importance of building collaborative networks and cooperating as part of a multidisciplinary team. Scientific research can often be lonely and isolating, with many academics working in silos. By working with the grass roots community of Data Champions, I learned ways to lure researchers from their disciplinary comfort zones and encourage them to work together, and to share knowledge and resources in order to achieve the common goal of 'Better Science'.

From October 2020, I look forward to starting my new position as [4TU.ResearchData](#) Community Manager at TU Delft. The primary focus of my role will be to promote the use of the 4TU.ResearchData repository nationally and internationally, and to stimulate the creation and reuse of research data in specific subject areas.

Appendix references

- Albersen M, Bosma M, Knoers NV, de Ruiter BH, Diekman EF, *et al.* (2013) The intestine plays a substantial role in human vitamin B6 metabolism: a Caco-2 cell model. *PLoS One*. 8(1): e54113
- Anas MK, Lee MB, Zhou C, Hammer MA, Slow S, *et al.* (2008) SIT1 is a betaine/proline transporter that is activated in mouse eggs after fertilization and functions until the 2-cell stage. *Development*. 135: 4123-4130
- Appaji Rao N, Ambili M, Jala VR, Subramanya HS and Savithri HS (2003) Structure-function relationship in serine hydroxymethyltransferase. *Biochim Biophys Acta*. 1647(1-2): 24-29
- Arora K, Sequeira JM, Hernández AI, Alarcon JM and Quadros EV (2017) Behavioral alterations are associated with vitamin B12 deficiency in the transcobalamin receptor/CD320 KO mouse. *PLoS One*. 12: e0177156
- Augspurger NR, Scherer CS, Garrow TA and Baker DH (2005) Dietary S-methylmethionine, a component of foods, has choline-sparing activity in chickens. *J Nutr*. 135(7): 1712-7
- Barić I, Cuk M, Fumić K, Vugrek O, Allen RH, *et al.* (2005) S-Adenosylhomocysteine hydrolase deficiency: a second patient, the younger brother of the index patient, and outcomes during therapy. *J Inherit Metab Dis*. 28: 885-902
- Barišić A, Pereza N, Hodžić A, Ostojić S and Peterlin B (2017) A Single Nucleotide Polymorphism of DNA methyltransferase 3B gene is a risk factor for recurrent spontaneous abortion. *Am J Reprod Immunol*. 78: e12765
- Beagle B, Yang TL, Hung J, Cogger EA, Moriarty DJ, *et al.* (2005) The glycine N-methyltransferase (GNMT) 1289 C->T variant influences plasma total homocysteine concentrations in young women after restricting folate intake. *J Nutr*. 135: 2780-5
- Beaudin AE, Abarinov EV, Noden DM, Perry CA, Chu S, *et al.* (2011) Shmt1 and de novo thymidylate biosynthesis underlie folate-responsive neural tube defects in mice. *Am J Clin Nutr*. 93: 789-98
- Benkhalifa M, Bacrie PC, Dumont M, Junca AM, Belloc S, *et al.* (2008) Imprinting in the human oocyte: homocysteine recycling to methionine through methyltetrahydrofolate homocysteine methyl transferase (MTR) and betaine homocysteine methyl transferase (BHMT 2). *Fertility and Sterility - Abstract*. 90(1): S328
- Benkhalifa M, Montjean D, Cohen-Bacrie P and Ménézo Y (2010) Imprinting: RNA expression for homocysteine recycling in the human oocyte. *Fertil Steril*. 93(5): 1585-90
- Blackburn PR, Tischer A, Zimmermann MT, Kempainen JL, Sastry S, *et al.* (2017) A Novel Kleeftstra Syndrome-associated Variant That Affects the Conserved TPLX Motif within the Ankyrin Repeat of EHMT1 Leads to Abnormal Protein Folding. *J Biol Chem*. 292: 3866-76
- Bó G and Mapletoft RJ (2013) Evaluation and classification of bovine embryos. *Animal Reproduction*. 10(3): 344-348
- Bourc'his D, Xu GL, Lin CS, Bollman B and Bestor TH (2001) Dnmt3L and the establishment of maternal genomic imprints. *Science*. 294: 2536-9
- Bourgis F, Roje S, Nuccio ML, Fisher DB, Tarczynski MC, *et al.* (1999) S-methylmethionine Plays a Major Role in Phloem Sulfur Transport and Is Synthesized by a Novel Type of Methyltransferase. *Plant Cell*. 11(8): 1485-98.
- Boyles AL, Billups AV, Deak KL, Siegel DG, Mehlretter L, *et al.* (2006) Neural tube defects and folate pathway genes: family-based association tests of gene-gene and gene-environment interactions. *Environ Health Perspect*. 114: 1547-52

- Burg M and Ferraris JD (2008) Intracellular Organic Osmolytes: Function and Regulation. *J Biol Chem.* 283(12): 7309–7313
- Cai B, Zhang T, Zhong R, Zou L, Zhu B, *et al.* (2014) Genetic variant in MTRR, but not MTR, is associated with risk of congenital heart disease: an integrated meta-analysis. *PLoS One.* 9: e89609
- Cao L, Wang Y, Zhang R, Dong L, Cui H, *et al.* (2018) Association of neural tube defects with gene polymorphisms in one-carbon metabolic pathway. *Childs Nerv Syst.* 34: 277-84
- Chadwick LH, McCandless SE, Silverman GL, Schwartz S, Westaway D, *et al.* (2000) Betaine-homocysteine methyltransferase-2: cDNA cloning, gene sequence, physical mapping, and expression of the human and mouse genes. *Genomics.* 70(1): 66-73
- Chen M, Huang YL, Huang YC, Shui IM, Giovannucci E, *et al.* (2014) Genetic polymorphisms of the glycine N-methyltransferase and prostate cancer risk in the health professionals follow-up study. *PLoS One.* 9: e94683
- Chen Z, Karaplis AC, Ackerman SL, Pogribny IP, Melnyk S, *et al.* (2001) Mice deficient in methylenetetrahydrofolate reductase exhibit hyperhomocysteinemia and decreased methylation capacity, with neuropathology and aortic lipid deposition. *Hum Mol Genet.* 10: 433-43
- Chien YH, Abdenur JE, Baronio F, Bannick AA, Corrales F, *et al.* (2015) Mudd's disease (MAT I/III deficiency): a survey of data for MAT1A homozygotes and compound heterozygotes. *Orphanet J Rare Dis.* 10: 99
- Christensen KE, Deng L, Leung KY, Arning E, Bottiglieri T, *et al.* (2013) A novel mouse model for genetic variation in 10-formyltetrahydrofolate synthetase exhibits disturbed purine synthesis with impacts on pregnancy and embryonic development. *Hum Mol Genet.* 22: 3705- 19
- Crivello NA, Blusztajn JK, Joseph JA, Shukitt-Hale B and Smith DE (2010) Short-term nutritional folate deficiency in rats has a greater effect on choline and acetylcholine metabolism in the peripheral nervous system than in the brain, and this effect escalates with age. *Nutr Res.* 30(10):722-730
- de Jong L, Meng Y, Dent J and Hekimi S (2004) Thiamine pyrophosphate biosynthesis and transport in the nematode *Caenorhabditis elegans*. *Genetics.* 168(2): 845-54
- Deng L, Elmore CL, Lawrance AK, Matthews RG and Rozen R (2008) Methionine synthase reductase deficiency results in adverse reproductive outcomes and congenital heart defects in mice. *Mol Genet Metab.* 94: 336-42
- Elmore CL, Wu X, Leclerc D, Watson ED, Bottiglieri T, *et al.* (2007) Metabolic derangement of methionine and folate metabolism in mice deficient in methionine synthase reductase. *Mol Genet Metab.* 91: 85-97
- Farquharson J and Adams JF (1976) The forms of vitamin B12 in foods. *Br J Nutr.* 36(1): 127-136
- Friso S, Choi SW, Girelli D, Mason JB, Dolnikowski GG, *et al.* (2002) A common mutation in the 5,10-methylenetetrahydrofolate reductase gene affects genomic DNA methylation through an interaction with folate status. *Proc Natl Acad Sci U S A.* 99: 5606-11
- Fukuwatari T, Wada H and Shibata K (2008) Age-related alterations of B-group vitamin contents in urine, blood and liver from rats. *J Nutr Sci Vitaminol (Tokyo).* 54(5): 357-62
- Ganu R, Garrow T, Koutmos M, Rund L and Schook LB (2013) Splicing variants of the porcine betaine-homocysteine S-methyltransferase gene: implications for mammalian metabolism. *Gene.* 529(2): 228-37

- Ganu RS, Garrow TA, Sodhi M, Rund LA and Schook LB (2011) Molecular characterization and analysis of the porcine betaine homocysteine methyltransferase and betaine homocysteine methyltransferase-2 genes. *Gene*. 473(2): 133-8
- Ganu RS, Ishida Y, Koutmos M, Kolokotronis SO, Roca AL, *et al.* (2015) Evolutionary Analyses and Natural Selection of Betaine-Homocysteine S-Methyltransferase (BHMT) and BHMT2 Genes. *PLoS One*. 10(7): e0134084
- García-Minguillán CJ, Fernandez-Ballart JD, Ceruelo S, Ríos L, Bueno O, Berrocal-Zaragoza MI, Molloy AM, *et al.* (2014) Riboflavin status modifies the effects of methylenetetrahydrofolate reductase (MTHFR) and methionine synthase reductase (MTRR) polymorphisms on homocysteine. *Genes Nutr*. 9(6): 435
- Garrow TA (1996) Purification, kinetic properties, and cDNA cloning of mammalian betaine-homocysteine methyltransferase. *J Biol Chem*. 271(37): 22831-8
- Gong M, Dong W, He T, Shi Z, Huang G, *et al.* (2015) MTHFR 677C>T polymorphism increases the male infertility risk: a meta-analysis involving 26 studies. *PLoS One*. 10: e0121147
- Goodhand KL, Watt RG, Staines ME, Hutchinson JS, and Broadbent PJ (1999) In vivo oocyte recovery and in vitro embryo production from bovine donors aspirated at different frequencies or following FSH treatment. *Theriogenology*. 51(5): 951-61
- Graulet B, Matte JJ, Desrochers A, Doepel L, Palin MF, *et al.* (2007) Effects of dietary supplements of folic acid and vitamin B12 on metabolism of dairy cows in early lactation. *J Dairy Sci*. 90(7): 3442-55
- Guay F, Jacques Matte J, Girard CL, Palin MF, Giguère A, *et al.* (2002) Effects of folic acid and vitamin B12 supplements on folate and homocysteine metabolism in pigs during early pregnancy. *Br J Nutr*. 88(3): 253-63
- Guo DC, Gong L, Regalado ES, Santos-Cortez RL, Zhao R, *et al.* (2015) MAT2A mutations predispose individuals to thoracic aortic aneurysms. *Am J Hum Genet*. 96: 170-7
- Guzmán MA, Navarro MA, Carnicer R, Sarría AJ, Acín S, *et al.* (2006) Cystathionine beta- synthase is essential for female reproductive function. *Hum Mol Genet*. 15: 3168-76
- Halsted CH, Villanueva JA, Devlin AM, Niemelä O, Parkkila S, *et al.* (2002) Folate Deficiency Disturbs Hepatic Methionine Metabolism and Promotes Liver Injury in the Ethanol-Fed Micropig. *Proc Natl Acad Sci U S A*. 99(15): 10072-7
- Hashimoto M, Murata K, Ishida J, Kanou A, Kasuya Y, *et al.* (2016) Severe Hypomyelination and Developmental Defects Are Caused in Mice Lacking Protein Arginine Methyltransferase 1 (PRMT1) in the Central Nervous System. *J Biol Chem*. 291: 2237-45
- Hassan AA, Torkjel MS and Brustad M (2012) Level of selected nutrients in meat, liver, tallow and bone marrow from semi-domesticated reindeer (*Rangifer t. tarandus* L.). *Int J Circumpolar Health*. 71: 17997
- Henderson JW, Ricker RD, Bidlingmeyer BA and Woodward C (2000) Rapid, accurate, sensitive, and reproducible HPLC analysis of amino acids. *Agilent Technologies, assignee. US Pat. No. 5980-1193E*
- Hogeveen M, de Heijer M, Semmekrot BA, Sporcken JM, Ueland PM, *et al.* (2013) Umbilical choline and related methylamines betaine and dimethylglycine in relation to birth weight. *Pediatr. Res*. 73(6): 783-787
- Ikeda S, Kawahara-Miki R, Iwata H, Sugimoto M and Kume S (2017) Role of methionine adenosyltransferase 2A in bovine preimplantation development and its associated genomic regions. *Sci Rep*. 7: 3800
- Ikeda S, Namekawa T, Sugimoto M and Kume S (2010) Expression of methylation pathway enzymes in bovine oocytes and preimplantation embryos. *J Exp Zool A Ecol Genet Physiol*. 313(3): 129-36

- Indyk HE, Persson BS, Caselunghe MC, Moberg A, Filonzi EL, *et al.* (2002) Determination of vitamin B12 in milk products and selected foods by optical biosensor protein-binding assay: method comparison. *J AOAC Int.* 85(1): 72-81
- Jaiswal SK, Sukla KK, Chauhan A, Lakhota AR, Kumar A, *et al.* (2017) Choline metabolic pathway gene polymorphisms and risk for Down syndrome: An association study in a population with folate-homocysteine metabolic impairment. *Eur J Clin Nutr.* 71: 45-50
- James SJ, Melnyk S, Jernigan S, Pavliv O, Trusty T, *et al.* (2010) A functional polymorphism in the reduced folate carrier gene and DNA hypomethylation in mothers of children with autism. *Am J Med Genet B Neuropsychiatr Genet.* 153B: 1209-20
- Johnson AR, Craciunescu CN, Guo Z, Teng YW, Thresher RJ, *et al.* (2010) Deletion of murine choline dehydrogenase results in diminished sperm motility. *FASEB J.* 24: 2752-61
- Johnson WG, Scholl TO, Spychala JR, Buyske S, Stenroos ES, *et al.* (2005) Common dihydrofolate reductase 19-base pair deletion allele: a novel risk factor for preterm delivery. *Am J Clin Nutr.* 81: 664-8
- Kanakkaparambil R, Singh R, Li D, Webb R and Sinclair KD (2009) B-vitamin and homocysteine status determines ovarian response to gonadotropin treatment in sheep. *Biol Reprod.* 80(4): 743-52
- Kelly TL, Neaga OR, Schwahn BC, Rozen R and Trasler JM (2005) Infertility in 5,10-methylenetetrahydrofolate reductase (MTHFR)-deficient male mice is partially alleviated by lifetime dietary betaine supplementation. *Biol Reprod.* 72: 667-77
- Kleppa KE and Stuen S (2003) High serum folate values in lambs experimentally infected with *Anaplasma phagocytophilum*. *Acta Vet Scand.* 44(3-4): 199-202
- Koning AM, Holwerda KM, Weedon-Fekjær SM, Staff AC, Nolte IM, *et al.* (2013) P23 CBS gene variants are associated with conditions characterized by ischemia. *Nitric Oxide.* 31: S44-5
- Kovatscheva EG and Popova JG (1977) [S-Methylmethionine content in plant and animal tissues and stability during storage]. *ahrung.* 21(6): 465-72
- Kwong WY, Adamiak SJ, Gwynn A, Singh R and Sinclair KD (2010) Endogenous folates and single-carbon metabolism in the ovarian follicle, oocyte and pre-implantation embryo. *Reproduction.* 139(4): 705-15
- Laanpere M, Altmäe S, Kaart T, Stavreus-Evers A, Nilsson TK, *et al.* (2011) Folate-metabolizing gene variants and pregnancy outcome of IVF. *Reprod Biomed Online.* 22: 603-14
- Lai SC, Nakayama Y, Sequeira JM, Wlodarczyk BJ, Cabrera RM, *et al.* (2013) The transcobalamin receptor knockout mouse: a model for vitamin B12 deficiency in the central nervous system. *FASEB J.* 27: 2468-75
- Lazaros L, Xita N, Hatzi E, Kaponis A, Makrydimas G, *et al.* (2012) Phosphatidylethanolamine N-methyltransferase and choline dehydrogenase gene polymorphisms are associated with human sperm concentration. *Asian J Androl.* 14: 778-83
- Lee MB, Kooistra M, Zhang B, Slow S, Fortier AL, *et al.* (2012) Betaine homocysteine methyltransferase is active in the mouse blastocyst and promotes inner cell mass development. *J Biol Chem.* 287: 33094-103
- Li E, Bestor TH and Jaenisch R (1992) Targeted mutation of the DNA methyltransferase gene results in embryonic lethality. *Cell.* 69: 915-26
- Li F, Feng Q, Lee C, Wang S, Pelleymounter LL, *et al.* (2008) Human betaine-homocysteine methyltransferase (BHMT) and BHMT2: common gene sequence variation and functional characterization. *Mol Genet Metab.* 94(3): 326-5

- Liao YJ, Liu SP, Lee CM, Yen CH, Chuang PC, *et al.* (2009) Characterization of a glycine N- methyltransferase gene knockout mouse model for hepatocellular carcinoma: Implications of the gender disparity in liver cancer susceptibility. *Int J Cancer*. 124: 816-26
- Liu SP, Li YS, Chen YJ, Chiang EP, Li AF, *et al.* (2007) Glycine N-methyltransferase-/- mice develop chronic hepatitis and glycogen storage disease in the liver. *Hepatology*. 46: 1413-25
- Lonsdale D (2015) Thiamine and magnesium deficiencies: keys to disease. *Med Hypotheses*. 84(2): 129-34
- Lu SC, Alvarez L, Huang ZZ, Chen L, An W, *et al.* (2001) Methionine adenosyltransferase 1A knockout mice are predisposed to liver injury and exhibit increased expression of genes involved in proliferation. *Proc Natl Acad Sci U S A*. 98: 5560-5
- Luka Z, Capdevila A, Mato JM and Wagner C (2006) A glycine N-methyltransferase knockout mouse model for humans with deficiency of this enzyme. *Transgenic Res*. 15: 393-7
- Maclean KN, Sikora J, Kožich V, Jiang H, Greiner LS, *et al.* (2010) A novel transgenic mouse model of CBS-deficient homocystinuria does not incur hepatic steatosis or fibrosis and exhibits a hypercoagulative phenotype that is ameliorated by betaine treatment. *Mol Genet Metab*. 101: 153-62
- Magnes C, Fauland A, Gander E, Narath S, Ratzer M, *et al.* (2014) Polyamines in biological samples: rapid and robust quantification by solid-phase extraction online-coupled to liquid chromatography-tandem mass spectrometry. *J Chromatogr A*. 1331: 44-51
- Martinelli D, Deodato F and Dionisi-Vici C (2011) Cobalamin C defect: natural history, pathophysiology, and treatment. *J Inherit Metab Dis*. 34(1): 127-135
- Matte JJ, Guay F, Le Floc'h N and Girard CL (2010) Bioavailability of dietary cyanocobalamin (vitamin B12) in growing pigs. *J Anim Sci*. 88(12): 3936-44
- McCann MEE, McCracken KJ, Hoey L, Pentieva K, McNulty H, *et al.* (2004) Effect of dietary folic acid supplementation on the folate content of broiler chicken meat - 2004 SPRING MEETING OF THE WPSA UK BRANCH POSTERS. *British Poultry Science*. 45(1): S65-S66
- McLain AL, Szweda PA and Szweda LI (2011) α -Ketoglutarate dehydrogenase: a mitochondrial redox sensor. *Free Radic Res*. 45(1): 29-36
- Miller MW, Duhl DM, Winkes BM, Arredondo-Vega F, Saxon PJ, *et al.* (1994) The mouse lethal nonagouti (a(x)) mutation deletes the S-adenosylhomocysteine hydrolase (Ahcy) gene. *EMBO J*. 13: 1806-16
- Mitchell LM, Robinson JJ, Watt RG, McEvoy TG, Ashworth CJ, *et al.* (2007) Effects of cobalt/vitamin B12 status in ewes on ovum development and lamb viability at birth. *Reprod Fertil Dev*. 19(4): 553-62
- Mládková J, Vaněk V, Buděšínský M, Elbert T, Demianová Z, *et al.* (2012) Double-headed sulfur-linked amino acids as first inhibitors for betaine-homocysteine S-methyltransferase 2. *J Med Chem*. 55(15): 6822-31
- Momb J, Lewandowski JP, Bryant JD, Fitch R, Surman DR, *et al.* (2013) Deletion of Mthfd11 causes embryonic lethality and neural tube and craniofacial defects in mice. *Proc Natl Acad Sci U S A*. 110: 549-54
- Mostowska A, Hozyasz KK and Jagodzinski PP (2006) Maternal MTR genotype contributes to the risk of non-syndromic cleft lip and palate in the Polish population. *Clin Genet*. 69: 512-7
- Mrozikiewicz PM, Bogacz A, Omielańczyk M, Wolski H, Bartkowiak-Wieczorek J, *et al.* (2015) The importance of rs1021737 and rs482843 polymorphisms of cystathionine

- gamma-lyase in the etiology of preeclampsia in the Caucasian population. *Ginekol Pol.* 86: 119-25
- Müller H (1993) The determination of the folic acid content of foods of animal origin using high performance liquid chromatography (HPLC) *Z Lebensm Unters Forsch.* 196(6): 518-21
- Murphy LE, Mills JL, Molloy AM, Qian C, Carter TC, *et al.* (2011) Folate and vitamin B12 in idiopathic male infertility. *Asian J Androl.* 13: 856-61
- Ning N, Zhu J, Du Y, Gao X, Liu C and Li J (2014) Dysregulation of hydrogen sulphide metabolism impairs oviductal transport of embryos. *Nat Commun.* 5: 4107
- Okano M, Bell DW, Haber DA and Li E (1999) DNA methyltransferases Dnmt3a and Dnmt3b are essential for de novo methylation and mammalian development. *Cell.* 99: 247-57
- Ortigue-Marty I, Micol D, Prache S, Dozias D and Girard CL (2005) Nutritional value of meat: the influence of nutrition and physical activity on vitamin B12 concentrations in ruminant tissues. *Reprod Nutr Dev.* 45(4): 453-67
- Pajares MA and Pérez-Sala D (2006) Betaine homocysteine S-methyltransferase: just a regulator of homocysteine metabolism? *Cell Mol Life Sci.* 63(23): 2792-803
- Pangilinan F, Mitchell A, VanderMeer J, Molloy AM, Troendle J, *et al.* (2010) Transcobalamin II receptor polymorphisms are associated with increased risk for neural tube defects. *J Med Genet.* 47: 677-85
- Parle-McDermott A, Pangilinan F, Mills JL, Signore CC, Molloy AM, *et al.* (2005) A polymorphism in the MTHFD1 gene increases a mother's risk of having an unexplained second trimester pregnancy loss. *Mol Hum Reprod.* 11: 477-80
- Pawlak MR, Scherer CA, Chen J, Roshon MJ and Ruley HE (2000) Arginine N-methyltransferase 1 is required for early postimplantation mouse development, but cells deficient in the enzyme are viable. *Mol Cell Biol.* 20: 4859-69
- Pérez Mato I, Sanchez del Pino MM, Chamberlin ME, Mudd SH, Mato JM, *et al.* (2001) Biochemical basis for the dominant inheritance of hypermethioninemia associated with the R264H mutation of the MAT1A gene. A monomeric methionine adenosyltransferase with tripolyphosphatase activity. *J Biol Chem.* 276: 13803-9
- Pérez-Miguelsanz J, Vallecillo N, Garrido F, Reytor E, Pérez-Sala D, *et al.* (2017) Betaine homocysteine S-methyltransferase emerges as a new player of the nuclear methionine cycle. *Biochim Biophys Acta Mol Cell Res.* 1864(7): 1165-1182
- Perry C, Yu S, Chen J, Matharu KS and Stover PJ (2007) Effect of vitamin B6 availability on serine hydroxymethyltransferase in MCF-7 cells. *Arch Biochem Biophys.* 462(1):21-27
- Piedrahita JA, Oetama B, Bennett GD, van Waes J, Kamen BA, *et al.* (1999) Mice lacking the folic acid-binding protein Folbp1 are defective in early embryonic development. *Nat Genet.* 23: 228-32
- Pouteau E, Meirim I, Métairon S and Fay LB (2001) Acetate, propionate and butyrate in plasma: determination of the concentration and isotopic enrichment by gas chromatography/mass spectrometry with positive chemical ionization. *J Mass Spectrom.* 36(7): 798-80
- Powers HJ (2003) Riboflavin (vitamin B-2) and health. *Am J Clin Nutr.* 77(6): 1352-1360
- Prasoon KR, Sunitha T, Srinadh B, Deepika ML, Kumari TM, *et al.* (2016) Paternal transmission of MTHFD1 G1958A variant predisposes to neural tube defects in the offspring. *Dev Med Child Neurol.* 58: 625-31
- Prasoon KR, Tella S, Buragadda S, Tiruvatturu MK and Akka J (2017) Interaction between Maternal and Paternal SHMT C1420T Predisposes to Neural Tube Defects in

- the Fetus: Evidence from Case-Control and Family-Based Triad Approaches. *Birth Defects Res.* 109: 1020-29
- Rouillon A, Surdin-Kerjan Y and Thomas D (1999) Transport of sulfonium compounds. Characterization of the s-adenosylmethionine and s-methylmethionine permeases from the yeast *Saccharomyces cerevisiae*. *J Biol Chem.* 274(40): 28096-105
- Rubini M, Brusati R, Garattini G, Magnani C, Liviero F, *et al.* (2005) Cystathionine beta-synthase c.844ins68 gene variant and non-syndromic cleft lip and palate. *Am J Med Genet A.* 136A: 368-72
- Sabri MI, Soiefer AI, Kisby GE and Spencer PS (1989) Determination of polyamines by precolumn derivatization with 9-fluorenylmethyl chloroformate and reverse-phase high-performance liquid chromatography. *J Neurosci Methods.* 29(1): 27-31
- Sakurai T, Asakura T, Mizuno A, Matsuda M (1992) Absorption and metabolism of pyridoxamine in mice. II. Transformation of pyridoxamine to pyridoxal in intestinal tissues. *J Nutr Sci Vitaminol (Tokyo).* 38(3): 227-233
- Shane B (2008) Folate and vitamin B12 metabolism: overview and interaction with riboflavin, vitamin B6, and polymorphisms. *Food Nutr Bull.* 29(2): S5-16
- Shibata K, Shimizu A and Fukuwatari T (2013) Vitamin B1 Deficiency Does not Affect the Liver Concentrations of the Other Seven Kinds of B-Group Vitamins in Rats. *Nutr Metab Insights.* 6: 1–10
- Shirohzu H, Kubota T, Kumazawa A, Sado T, Chijiwa T, *et al.* (2002) Three novel DNMT3B mutations in Japanese patients with ICF syndrome. *Am J Med Genet.* 112: 31-7
- Sinclair KD, Allegrucci C, Singh R, Gardner DS, Sebastian S, *et al.* (2007) DNA methylation, insulin resistance, and blood pressure in offspring determined by maternal periconceptional B vitamin and methionine status. *Proc Natl Acad Sci U S A.* 104(49): 19351-6
- Smith RM and Osborne-White WS (1973) Folic acid metabolism in vitamin B12-deficient sheep. Depletion of liver folates. *Biochem J.* 136(2): 279-93
- Song J, da Costa KA, Fischer LM, Kohlmeier M, Kwock L, *et al.* (2005) Polymorphism of the PEMT gene and susceptibility to nonalcoholic fatty liver disease (NAFLD). *FASEB J.* 19: 1266-71
- Spiegelstein O, Mitchell LE, Merriweather MY, Wicker NJ, Zhang Q, *et al.* (2004) Embryonic development of folate binding protein-1 (Folbp1) knockout mice: Effects of the chemical form, dose, and timing of maternal folate supplementation. *Dev Dyn.* 231: 221-31
- Stangl GI, Roth-Maier DA and Kirchgessner M (2000) Vitamin B-12 deficiency and hyperhomocysteinemia are partly ameliorated by cobalt and nickel supplementation in pigs. *J Nutr.* 130(12): 3038-44
- Steele W, Allegrucci C, Singh R, Lucas E, Priddle H, *et al.* (2005) Human embryonic stem cell methyl cycle enzyme expression: modelling epigenetic programming in assisted reproduction? *Reprod Biomed Online.* 10(6): 755-66
- Sun S, Gui Y, Jiang Q and Song H (2011) Dihydrofolate reductase is required for the development of heart and outflow tract in zebrafish. *Acta Biochim Biophys Sin (Shanghai).* 43: 957-69
- Swanson DA, Liu ML, Baker PJ, Garrett L, Stitzel M, *et al.* (2001) Targeted disruption of the methionine synthase gene in mice. *Mol Cell Biol.* 21: 1058-65
- Szegedi SS, Castro CC, Koutmos M and Garrow TA (2008) Betaine-homocysteine S-methyltransferase-2 is an S-methylmethionine-homocysteine methyltransferase. *J Biol Chem.* 283(14): 8939-45

- Tang Q, Chen Y, Wu W, Ding H, Xia Y, *et al.* (2017) Idiopathic male infertility and polymorphisms in the DNA methyltransferase genes involved in epigenetic marking. *Sci Rep.* 7: 11219
- Teng YW, Mehedint MG, Garrow TA and Zeisel SH (2011) Deletion of betaine-homocysteine S- methyltransferase in mice perturbs choline and 1-carbon metabolism, resulting in fatty liver and hepatocellular carcinomas. *J Biol Chem.* 286: 36258-67
- Tiwari D, Das CR, Bose PD and Bose S (2017) Associative role of TYMS6bpdel polymorphism and resulting hyperhomocysteinemia in the pathogenesis of preterm delivery and associated complications: A study from Northeast India. *Gene.* 627: 129-36
- Tremain-Boon SG, Hart JC, Wilson PR and Lopez-Villalobos N (2002) Liver copper, selenium and vitamin B12 concentrations in farmed and feral red deer (*Cervus elaphus*). *N Z Vet J.* 50(3): 111-4
- Vasanth Rao P, Garrow TA, John F, Garland D, Millian NS, *et al.* (1998) Betaine-homocysteine methyltransferase is a developmentally regulated enzyme crystallinn in rhesus monkey lens. *J. Biol. Chem.* 46(3): 30669-30674
- Vugrek O, Beluzić R, Nakić N and Mudd SH (2009) S-adenosylhomocysteine hydrolase (AHCY) deficiency: two novel mutations with lethal outcome. *Hum Mutat.* 30: E555-65
- Walkey CJ, Donohue LR, Bronson R, Agellon LB and Vance DE (1997) Disruption of the murine gene encoding phosphatidylethanolamine N-methyltransferase. *Proc Natl Acad Sci U S A.* 94: 12880-5
- Watanabe M, Osada J, Aratani Y, Kluckman K, Reddick R, *et al.* (1995) Mice deficient in cystathionine beta-synthase: animal models for mild and severe homocyst(e)inemia. *Proc Natl Acad Sci U S A.* 92: 1585-9
- Watkins SM, Zhu X and Zeisel SH (2003) Phosphatidylethanolamine-N-methyltransferase activity and dietary choline regulate liver-plasma lipid flux and essential fatty acid metabolism in mice. *J Nutr.* 1333: 3386-91
- Williams DV, G. Levy G and Stobaus T (2007) Composition of Australian red meat 2002. 3. *Nutrient profile Food Aust.* 59(7): 331-341
- Xu J, Clare CE, Brassington AH, Sinclair KD and Barrett DA (2020) Comprehensive and quantitative profiling of B vitamins and related compounds in the mammalian liver. *J Chromatogr B Analyt Technol Biomed Life Sci.* 1136: 121884
- Yang G, Wu L, Jiang B, Yang W, Qi J, *et al.* (2008) H₂S as a physiologic vasorelaxant: hypertension in mice with deletion of cystathionine gamma-lyase. *Science.* 322: 587-90
- Zhang B, Denomme MM, White CR, Leung KY, Lee MB, *et al.* (2015) Both the folate cycle and betaine-homocysteine methyltransferase contribute methyl groups for DNA methylation in mouse blastocysts. *FASEB J.* 29(3): 1069-79
- Zhang Q, Bai B, Liu X, Miao C and Li H (2014) Association of folate metabolism genes MTHFR and MTRR with multiple complex congenital malformation risk in Chinese population of Shanxi. *Transl Pediatr.* 3: 259-67
- Zhao JY, Yang XY, Shi KH, Sun SN, Hou J, *et al.* (2013) A functional variant in the cystathionine β -synthase gene promoter significantly reduces congenital heart disease susceptibility in a Han Chinese population. *Cell Res.* 23: 242-53
- Zhao R, Russell RG, Wang Y, Liu L, Gao F, *et al.* (2001) Rescue of embryonic lethality in reduced folate carrier-deficient mice by maternal folic acid supplementation reveals early neonatal failure of hematopoietic organs. *J Biol Chem.* 276: 10224-8
- Zhu H, Wlodarczyk BJ, Scott M, Yu W, Merriweather M, *et al.* (2007) Cardiovascular abnormalities in Folr1 knockout mice and folate rescue. *Birth Defects Res A Clin Mol Teratol.* 79: 257-68

Zhu X, Mar MH, Song J and Zeisel SH (2004) Deletion of the *Pemt* gene increases progenitor cell mitosis, DNA and protein methylation and decreases calretinin expression in embryonic day 17 mouse hippocampus. *Brain Res Dev Brain Res.* 149: 121-9

Zhu X, Song J, Mar MH, Edwards LJ and Zeisel SH (2003) Phosphatidylethanolamine N- methyltransferase (PEMT) knockout mice have hepatic steatosis and abnormal hepatic choline metabolite concentrations despite ingesting a recommended dietary intake of choline. *Biochem J.* 370: 987-93